Application to FSANZ to Vary Food Standard 1.5.2 to Include the EPA+DHA Canola (*Brassica napus*) Event LBFLFK

Prepared by [redacted]
BASF Australia Ltd

Submitted September 2021

TABLE OF CONTENTS

LIST OF FIGURES

LIST OF TABLES

LIST OF APPENDED ELECTRONIC DOCUMENTS

Appendix 1 Statutory Declaration verifying that that information provided to FSANZ with this submission is true and correct.

Appendix 2 201608-007R, History of safe use for the fatty acids in EPA+DHA canola event LBFLFK. Unpublished Study. BASF Plant Science, Regulatory Research Report Number 201608-007R, 1-57.

Appendix 3 201603-003, Molecular characterization of the EPA+DHA canola event LBFLFK. Unpublished Study. BASF Plant Science, Final Report Number 201603-003, 1-608. (**Contains confidential commercial information)**

Appendix 4 201605-007R, Vector construction and transformation for the generation of the EPA+DHA canola event LBFLFK. Unpublished Study. BASF Plant Science, Regulatory Research Report Number 201605-007R, 1-61. (**Contains confidential commercial information)**

Appendix 5 201601-004, Determination of the levels of newly expressed proteins in EPA+DHA canola event LBFLFK field-grown in the United States during 2016. Unpublished Study. BASF Plant Science, Final Report Number 201601-004, 1-204.

Appendix 6 201601-008, Characterization of plant-produced proteins from immature seed of EPA+DHA canola event LBFLFK. Unpublished Study. BASF Plant Science, Final Report Number 201601-008, 1-224.

Appendix 7 201511-008R, Production and characterization of antibodies specific to the D12D(Ps) protein found in EPA+DHA canola. Unpublished Study. BASF Plant Science, Regulatory Research Report Number 201511-008R, 1-26.

Appendix 8 201601-007R, Production and characterization of antibodies specific to the D6D(Ot) protein found in EPA+DHA canola. Unpublished Study. BASF Plant Science, Regulatory Research Report Number 201601-007R, 1-23.

Appendix 9 201512-004R, Production and characterization of antibodies specific to the D6E(Tp) protein found in EPA+DHA canola. Unpublished Study. BASF Plant Science, Regulatory Research Report Number 201512-004R, 1-32.

Appendix 10 201602-008R, Production and characterization of antibodies specific to the D6E(Pp) protein found in EPA+DHA canola. Unpublished Study. BASF Plant Science, Regulatory Research Report Number 201602-008R, 1-46.

Appendix 11 201602-019R, Production and characterization of antibodies specific to the D5D(Tc) protein found in EPA+DHA canola. Unpublished Study. BASF Plant Science, Regulatory Research Report Number 201602-019R, 1-25.

Appendix 12 201602-006R, Production and characterization of antibodies specific to the O3D(Pir) protein found in EPA+DHA canola. Unpublished Study. BASF Plant Science, Regulatory Research Report Number 201602-006R, 1-38.

Appendix 13 201602-011R, Production and characterization of antibodies specific to the O3D(Pi) protein found in EPA+DHA canola. Unpublished Study. BASF Plant Science, Regulatory Research Report Number 201602-011R, 1-28.

Appendix 14 201602-003R, Production and characterization of antibodies specific to the D5E(Ot) protein found in EPA+DHA canola. Unpublished Study. BASF Plant Science, Regulatory Research Report Number 201602-003R, 1-65.

Appendix 15 201602-017R, Production and characterization of antibodies specific to the D4D(Tc) protein found in EPA+DHA canola. Unpublished Study. BASF Plant Science, Regulatory Research Report Number 201602-017R, 1-49.

Appendix 16 201602-013R, Production and characterization of antibodies specific to the D4D(Pl) protein found in EPA+DHA canola. Unpublished Study. BASF Plant Science, Regulatory Research Report Number 201602-013R, 1-26.

Appendix 17 201602-014R, Production and characterization of the acetohydroxy acid synthase (AtAHAS) [A122TS653N] N-6xHis fusion protein reference substance. Unpublished Study. BASF Plant Science, Regulatory Research Report Number 201602-014R, 1-15.

Appendix 18 201608-001R, History of safe use for the introduced proteins of EPA+DHA canola event LBFLFK. Unpublished Study. BASF Plant Science, Regulatory Research Report Number 201608-001R, 1-76.

Appendix 19 21-RSOS0167-ROW, EPA+DHA canola event LBFLFK newly expressed membrane proteins: Bioinformatics assessment of amino acid sequence identity to known allergens and toxins.

Appendix 20 201604-001, Heat stability of newly expressed proteins produced in immature seed of EPA+DHA canola event LBFLFK. Unpublished Study. BASF Plant Science, Final Report Number 201604-001, 1-50.

Appendix 21 201604-002, pH stability of newly expressed proteins produced in immature seed of EPA+DHA canola event LBFLFK. Unpublished Study. BASF Plant Science, Final Report Number 201604-002, 1-49.

Appendix 22 201601-003, Agronomic and phenotypic characteristics of EPA+DHA canola event LBFLFK field-grown in the United States during 2016 and composition of the harvested seed. Unpublished Study. BASF Plant Science, Final Report Number 201601-003, 1-1583.

Appendix 23 201601-001, Compositional analysis of processed fractions derived from EPA+DHA canola event LBFLFK grown in 2016 United States field trials. Unpublished Study. BASF Plant Science, Final Report Number 201601-001, 1-442.

Appendix 24 201703-009R, Literature review of the bioavailability of EPA and DHA in EPA+DHA canola event LBFLFK. Unpublished Study. BASF Plant Science, Regulatory Research Report Number 201703-009R, 1-15.

Appendix 25 201703-004R, Fatty acid profile of RBD oil from EPA+DHA canola event LBFLFK and various edible oils and fat containing foods. Unpublished Study. BASF Plant Science, Regulatory Research Report Number 201703-004R, 1-112.

Appendix 26 201807-001, Characterization of diet containing EPA+DHA canola event LBFLFK defatted meal and refined, bleached, and deodorized oil after the conclusion of the in-life phase of the repeated-dose 90-day oral toxicity study # 50C0050/18S015. Unpublished Study. BASF Plant Science, Final Report Number 201807-001, 1-219.

LIST OF ABBREVIATIONS AND DEFINITIONS

Abbreviation	Definition
AHAS	Acetohydroxy acid synthase
AHAS(*At*)	Large subunit of acetohydroxy acid synthase from *Arabidopsis thaliana*; refers to the AHAS enzyme large subunit comprising the A122T and S653N amino acid substitutions conferring tolerance to imidazolinone herbicide in the context of EPA+DHA canola
[A122TS653N]	Substitution of an alanine residue (A) with a threonine (T) at amino acid 122 and a serine residue (S) with an asparagine (N) at amino acid 653, relative to the *csr1-2* gene of *Arabidopsis thaliana*
a.i.	Active ingredient
ANOVA	Analysis of variance
ARA	Arachidonic acid
B. napus	*Brassica napus* L.
BAC	Bacterial artificial chromosome
bp	Base pair
C14:0	Myristic acid or Tetradecanoic acid
C16:0	Palmitic acid or Hexadecanoic acid
C16:1n-9	Cis-7 hexadecenoic acid or (7Z)-Hexadec-7-enoic acid
C16:1n-7	Palmitoleic acid or (9Z)-Hexadec-9-enoic acid
C16:3n-3	Hexadecatrienoic acid or (7Z,10Z,13Z)-Hexadeca-7,10,13-trienoic acid
C17:0	Margaric acid or Heptadecanoic acid
C17:1	Margaroleic acid
C18:0	Stearic acid or Octadecanoic acid
C18:1n-7	Cis-vaccenic acid or (11Z)-Octadec-11-enoic acid
C18:1n-9	Oleic acid (OA) or (9Z)-Octadec-9-enoic acid
C18:2n-6	Linoleic acid (LA) or (9Z,12Z)-Octadeca-9,12-dienoic acid
C18:2n-9	(6Z,9Z)-Octadeca-6,9-dienoic acid
C18:3n-3	Alpha-linolenic acid (ALA) or (9Z,12Z,15Z)-Octadeca-9,12,15-trienoic acid
C18:3n-6	Gamma-linolenic acid (GLA) or (6Z,9Z,12Z)-Octadeca-6,9,12-trienoic acid
C18:4n-3	Stearidonic acid (SDA) or (6Z,9Z,12Z,15Z)-Octadeca-6,9,12,15-tetraenoic acid
C20:0	Arachidic acid or Eicosanoic acid

Abbreviation	Definition
C20:1n-9	Gondoic acid or (11Z)-Eicos-11-enoic acid
C20:2n-6	Eicosadienoic acid or (11Z,14Z)-Eicosa-11,14-dienoic acid
C20:2n-9	(8Z,11Z)-Eicosa-8,11-dienoic acid
C20:3n-3	Eicosatrienoic acid (ETrA) or (11Z,14Z,17Z)-Eicosa-11,14,17-trienoic acid
C20:3n-6	Dihomo-gamma-linolenic acid (DGLA)
C20:3n-9	Mead acid or (5Z,8Z,11Z)-Eicosa-5,8,11-trienoic acid
C20:4n-3	Bishomostearidonic acid (ETA) or (8Z,11Z,14Z,17Z)-Eicosa-8,11,14,17-tetraenoic acid
C20:4n-6	Arachidonic acid (ARA)
C20:5n-3	Timnodonic acid (EPA) or (5Z,8Z,11Z,14Z,17Z)-Eicosa-5,8,11,14,17-pentaenoic acid
C22:0	Behenic acid or Docosanoic acid
C22:1n-9	Erucic acid or (13Z)-Docos-13-enoic acid
C22:2n-6	Docosadienoic acid or (13Z,16Z)-Docosa-13,16-dienoic acid
C22:4n-3	(10Z,13Z,16Z,19Z)-Docosa-10,13,16,19-tetraenoic acid
C22:4n-6	Adrenic acid or (7Z,10Z,13Z,16Z)-Docosa-7,10,13,16-tetraenoic acid (DTA)
C22:5n-3	Clupanodonic acid (DPAn-3) or (7Z,10Z,13Z,16Z,19Z)-Docosa-7,10,13,16,19-pentaenoic acid
C22:5n-6	Osbond acid (DPAn-6) or (4Z,7Z,10Z,13Z,16Z)-Docosa-4,7,10,13,16-pentaenoic acid
C22:6n-3	Docosahexaenoic acid (DHA) or (4Z,7Z,10Z,13Z,16Z,19Z)-Docosa-4,7,10,13,16,19-hexaenoic acid
C24:0	Lignoceric acid or Tetracosanoic acid
C24:1n-9	Nervonic acid or (15Z)-Tetracos-15-enoic acid
D12D(*Ps*)	Delta-12 desaturase from *Phytophthora sojae*
D4D(*Pl*)	Delta-4 desaturase from *Pavlova lutheri*
D4D(*Tc*)	Delta-4 desaturase from *Thraustochytrium* sp.
D5D(*Tc*)	Delta-5 desaturase from *Thraustochytrium* sp.
D5E(*Ot*)	Delta-5 elongase from *Ostreococcus tauri*
D6D(*Ot*)	Delta-6 desaturase from *Ostreococcus tauri*
D6E(*Pp*)	Delta-6 elongase from *Physcomitrella patens*
D6E(*Tp*)	Delta-6 elongase from *Thalassiosira pseudonana*
DGLA	Dihomo-gamma-linolenic acid
DHA	Docosahexaenoic acid

Abbreviation	Definition
DPA	Docosapentaenoic acid
DW	Dry weight
ELISA	Enzyme-linked immunosorbent assay
ELO	Elongation
EPA	Eicosapentaenoic acid
FAME(s)	Fatty acid methyl ester(s)
FW	Fresh weight
gDNA	Genomic DNA
GLA	Gamma-linolenic acid
GRAS	Generally Recognised as Safe
HOSU	History of safe use
IDP	Identity Preservation
ILSI	International Life Sciences Institute
kb	Kilobase
kDa	Kilodalton
LA	Linoleic acid
LB	T-DNA left border
LBFLFK	Event name for EPA+DHA canola, also known as Event LBFLFK, LBFLFK canola, LBFLFK event, EPA+DHA canola
LC-MS/MS	Liquid chromatography tandem mass spectrometry
LC-PUFA(s)	Long-chain polyunsaturated fatty acid(s)
LOD	Limit of detection
LOQ	Limit of quantitation
LTM593	Plasmid vector used to transform *Brassica napus* hypocotyl cells to produce EPA+DHA canola event LBFLFK. Also known as LTM593-1qcz.
MW	Molecular weight
NC fusion	Recombinant protein consisting of a fusion of the amino- and carboxy-termini of a protein
NGS	Next generation sequencing
O3D(*Pi*)	Omega-3 desaturase from *Phytophthora infestans*
O3D(*Pir*)	Omega-3 desaturase from *Pythium irregulare*
OA	Oleic acid
OECD	Organisation for Economic Co-operation and Development
ORF(s)	Open reading frame(s)

Abbreviation	Definition
PCR	Polymerase chain reaction
PPP	Plant-produced proteins
RB	T-DNA right border
RBD oil	Refined, bleached, and deodorised oil
SD	Standard deviation
SDS-PAGE	Sodium dodecyl sulfate-polyacrylamide gel electrophoresis
SE	Standard error
SGF	Simulated gastric fluid
SIF	Simulated intestinal fluid
T_0	The parent transformed plant
T_1	The immediate progeny of the T_0 plant
T_2	The immediate progeny of the T_1 plant
T-DNA	Transfer DNA
TFA	Trans fatty acids
TLC	Thin layer chromatography
UTR	Untranslated region

EXECUTIVE SUMMARY

EPA+DHA canola event LBFLFK (OECD Unique ID BPS-BFLFK-2) was produced using *Agrobacterium rhizogenes*-mediated transformation of the conventional canola variety Kumily. LBFLFK canola expresses fatty acid desaturase and elongase proteins and a herbicide resistant acetohydroxy acid synthase protein. Enzyme-encoding genetic sequences and associated expression cassettes were introduced from a number of eukaryotic organisms (*Phytophthora sojae*, *Ostreococcus tauri*, *Thalassiosira pseudonana*, *Physcomitrella patens*, *Thraustochytrium* sp., *Phytophthora infestans*, *Pythium irregulare*, *Pavlova lutheri*, and *Arabidopsis thaliana*) to alter the production of specific fatty acids in canola, resulting in the production of omega-3 long-chain polyunsaturated fatty acids (LC-PUFAs) and tolerance to treatment with the herbicide active ingredient imazamox.

Canola normally produces primarily C18:1n-9 (oleic) and C18:2n-6 (linolenic) fatty acids in seeds through the combined efforts of *de novo* fatty acid synthesis, elongation, and desaturation enzymes. The introduction of seven desaturases and three elongases to develop EPA+DHA canola event LBFLFK causes production of LC-PUFAs including DHA (docosahexaenoic acid, C22:6n-3) and its biosynthetic intermediate EPA (eicosapentaenoic acid, C20:5n-3) from these endogenous fatty acids through an aerobic pathway. LBFLFK canola provides a plant-based and scalable production system for omega-3 fatty acids and will be another source of EPA and DHA for consumers as either a food ingredient or as an aquaculture feed ingredient. The herbicide tolerance trait is conferred through the introduction of a modified acetohydroxy acid synthase (AHAS) protein from the *Arabidopsis thaliana* plant.

To maintain the quality and ensure the segregation of LBFLFK canola seeds, grains, and processed products, an Identity Preservation System (IDP) will be implemented at every step of production and handling. Processing operations will be conducted either at dedicated facilities or at facilities with specific measures in place to ensure segregation from other products. Canola can be manufactured into a variety of products for human and animal consumption or for industrial purposes. As a specialty canola with a fatty acid profile containing the LC-PUFAs EPA and DHA, the oil produced from LBFLFK canola will be sold specifically as a source of dietary omega-3 LC-PUFAs. Refined oil derived from EPA+DHA canola may be used as a dietary supplement to provide an alternate source of omega-3 LC-PUFAs, pending any additional regulatory reviews required for this use. Additionally, the oil will be used as an input to aquafeed operations to provide omega-3 LC-PUFAs to farmed aquatic species. Defatted canola meal produced from LBFLFK canola will be available for use in the same applications as conventional canola meal. The primary application for canola meal is as a feed ingredient for livestock. The defatted meal produced from LBFLFK canola will not be sold as a source of omega-3 LC-PUFAs, as the oil content of the meal will be too low to make a significant contribution to the nutrition of the livestock.

All requisite domestic and international regulatory approvals, including labelling requirements based on nutritional content, will be obtained prior to use of specific products of EPA+DHA canola for food or feed purposes.

BASF Australia Ltd[1] prepared this application to amend the Australia New Zealand Food Standards Code Standard 1.5.2 (Food Produced Using Gene Technology) to allow for the

[1] - here and after referred to as 'BASF'.

inclusion of food derived from genetically modified LBFLFK canola in the Australian and New Zealand food industries. More specifically, BASF requests to allow the use of genetically modified *Brassica napus* (canola) oil derived from the transformation event LBFLFK in the Australian and New Zealand food industries. Information included in the application covers Part 3.1.1 and Part 3.5.1 of the application handbook.

The data package has been provided to FSANZ for LBFLFK canola; however, food products derived from the processed oil are not anticipated to contain novel proteins. A large body of food safety data is available on EPA and DHA LC-PUFAs themselves and health and nutrition claims related to their consumption have been formally assessed, and Standards are in place (*Food Standards Australia New Zealand Act 1991 (Cth)*, Schedule 4, Nutrition and Health Related Claims). Data requirements as per the July 2019 Application Handbook are addressed here below.

Table 1. Gazetted FSANZ Standards for Crop Lines Genetically Modified to Produce Long-Chain Fatty Acids

Crop	Events/Lines Evaluated	FSANZ Application Number
Canola	DHA canola line NS-B50027-4	A1143
Soybean	High oleic acid soybeans lines G94-1,G94-19 and G168; High oleic acid soybean line DP-305423-1; Stearidonic acid containing soybean line MON87769; Herbicide-tolerant, high oleic acid soybean line MON87705	A387; A1018; A1041; A1049
Safflower	Super High Oleic Safflower Lines 26 and 40	A1156

The canola variety used for the introduction of the EPA+DHA canola trait was Kumily, a spring cultivar of *Brassica napus* L. Therefore, this parental variety is used as the conventional counterpart in studies conducted to generate the data provided in this application.

The data and information presented in this submission demonstrate that derived products from LBFLFK are comparable to conventional canola, with the exception of the introduced proteins and the trait-associated changes in the composition of fatty acids. The safety of LBFLFK canola was confirmed based on multiple, well-established lines of evidence including:

- A molecular characterisation of the introduced DNA in LBFLFK canola demonstrated two intact, stable copies of the intended T-DNA insert at two loci within the canola genome.
- An assessment of the newly expressed proteins in LBFLFK canola demonstrated that there are no associated safety concerns.
- A compositional assessment of harvested grain and processed fractions confirmed compositional equivalence with the conventional counterpart, except for the introduced EPA+DHA traits.
- A review of the changes of the fatty acid profile of LBFLFK canola compared to conventional canola and other fatty acids sources, including a nutritional safety and exposure assessment demonstrated the safety of the oil produced.

Molecular Characterisation of EPA+DHA Canola Event LBFLFK

Combination of gene sequencing techniques (next-generation sequencing and Sanger sequencing), polymerase chain reaction, bioinformatic, and genetic segregation analysis has been used for the molecular characterisation of LBFLFK canola. This allowed the following conclusions:

- Next-generation sequencing of total genomic DNA and subsequent bioinformatic analysis demonstrated that LBFLFK has two inserts integrated at two separated loci (Insert1 and Insert2) and confirmed the absence of the transformation vector backbone sequences in event LBFLFK.
- The two inserts are stably integrated in the LBFLFK canola genome.
- Sanger sequencing analyses confirmed that each of the two inserts has the intended 13 gene expression cassettes and was identical to the vector T-DNA except for two single nucleotide changes in Insert1 and one nucleotide change in Insert2 that do not impact the functionality of the proteins produced. Both T-DNA inserts were intact, apart from a short rearrangement of 64 bp in the RB (right border) sequence of Insert1.
- A comparison to the sequence of the insertion site from the parental canola Kumily variety demonstrated that an 8-bp deletion was created at the genome integration site of Insert1 (Locus1) and a 31-bp deletion was created at the genome integration site of Insert2 (Locus2) in Kumily. No canola genomic sequence rearrangements were found at either integration site.
- A bioinformatics analysis identified 11 potential open reading frames that span the junctions between the T-DNA inserts and the flanking genomic DNA. None of the ORFs (open reading frames) created by the insertion showed any significant homology to known allergens, protein toxins, or antinutrients.
- Segregation analysis of F_2 and F_3 LBFLFK offspring showed that Insert1 and Insert2 in LBFLFK are both independently inherited according to Mendelian principles.

Characterisation and Quantification of Newly Expressed Proteins

Eleven proteins were introduced into canola event LBFLFK. This includes ten integral membrane proteins (desaturases and elongases), controlled by seed-specific promoters, that impact the content of omega-3 LC-PUFAs in the seeds. The 10 desaturases and elongases are a delta-12 desaturase from *Phytophthora sojae* (D12D(*Ps*)), a delta-6 desaturase from *Ostreococcus tauri* (D6D(*Ot*)), a delta-6 elongase from *Thalassiosira pseudonana* (D6E(*Tp*)), a delta-6 elongase from *Physcomitrella patens* (D6E(*Pp*)), a delta-5 desaturase from *Thraustochytrium* sp. (D5D(*Tc*)), an omega-3 desaturase from *Pythium irregulare* (O3D(*Pir*)), an omega-3 desaturase from *Phytophthora infestans* (O3D(*Pi*)), a delta-5 elongase from *Ostreococcus tauri* (D5E(*Ot*)), a delta-4 desaturase from *Thraustochytrium* sp. (D4D(*Tc*)), and a delta-4 desaturase from *Pavlova lutheri* (D4D(*Pl*)). The eleventh protein is the soluble, chloroplast-located acetohydroxy acid synthase from *Arabidopsis thaliana*, containing two amino acid substitutions (A122T and S653N). This enzyme, AHAS(*At*) [A122TS653N], under control of a constitutive promoter, confers tolerance to treatment with the herbicide active ingredient imazamox in event LBFLFK.

The safety assessment of crops improved through biotechnology includes a description of the nature and biochemical function of the newly expressed proteins. This typically includes characterisation for identity and amino acid sequence, for apparent molecular weight and immunoreactivity, and for potential glycosylation and enzymatic activity. In general, this involves either isolation of the newly expressed proteins from the plant or production of the protein in a heterologous expression system, depending on the properties of the newly expressed proteins and levels of expression.

Integral membrane proteins, including fatty acid desaturases and elongases that contain multiple transmembrane-spanning domains are difficult to isolate or concentrate. Such intractable proteins are also generally not able to be produced at high levels in heterologous systems. In order to characterise the desaturase and elongase proteins introduced to LBFLFK canola, a membrane protein extract was prepared from developing plant embryos isolated from immature seeds. This membrane protein fraction contains the highest concentration of the elongases and desaturases as active, complete proteins. Characterisation studies of the introduced herbicide tolerant AHAS(*At*) [A122TS653N] protein using plant protein extracts were also performed.

The concentration of each of the 11 newly introduced proteins in seed samples was also assessed. This protein expression data confirmed the presence of all but two of the proteins. The proteins O3D(*Pi*) and D6E(*Pp*) were not quantifiable in any tissue sample of LBFLFK canola. The introduced desaturase and elongases were only quantifiable in seed tissue, which aligns with the use of seed-specific promoters that control expression, and AHAS(*At*) [A122TS653N], driven by a constitutive promoter, was quantifiable in most tissue samples although it was not quantifiable in mature seed.

Safety Assessment of Newly Expressed Proteins

A weight-of-evidence approach, addressing the history of safe use and consumption, amino acid sequence similarity to known toxins, antinutrients, and allergens, digestibility, and degradation with exposure to elevated temperatures, was used to demonstrate the safety of the newly expressed proteins in LBFLFK canola.

The lack of adverse findings identified for these proteins and their donor organisms by a systematic literature search demonstrates a history of safe use based on uses in the food supply or from exposure routes other than intended food use. The protein sequence of each newly expressed protein was found to be structurally and functionally related to other proteins that are safely consumed by humans as food and by animals as feed. The wide distribution of proteins identified suggests that humans and animals have long been exposed, as part of their diet and environment, to similar proteins without adverse effects. As shown by bioinformatic analysis, none of the newly expressed proteins in LBFLFK have significant homology to any known protein toxins, antinutrients, or allergens.

Digestive fate analysis was used to determine the sensitivity of the newly expressed proteins to simulated gastric (SGF) and intestinal (SIF) fluid digestion. Each of the newly expressed proteins present at sufficient levels to be assayed was found to be susceptible to digestion in SGF, SIF, or SGF followed by SIF.

Heat treatment sensitivity was evaluated by enzyme activity and structural integrity. The enzyme activity of D6D(*Ot*), D5D(*Tc*), O3D(*Pir*), and O3D(*Pi*) in response to heat treatment

was not assessed because enzyme activity was not detectable in LBFLFK protein extract. The heat sensitivity of these proteins was assessed by structural integrity only or (in the case of O3D(*Pi*)) was not assessed due to the low amount of protein in LBFLFK protein extract. Each of the newly expressed proteins assayable for structural integrity was heat-labile, and each of the newly expressed proteins assayable for enzymatic activity lost its activity, indicating that the proteins will not remain intact after the conditions of commercial processing used to produce oil and meal.

It is noted that the O3D(*Pi*) and D6E(*Pp*) proteins were not assessed for structural integrity to heat treatment or to digestibility in SGF or SIF as these proteins were not found at detectable levels in LBFLFK protein extract preparations or LBFLFK tissues. However, the extremely low amounts of O3D(*Pi*) and D6E(*Pp*) protein also suggest that they are unlikely to present any safety concern to humans or animals.

Overall, applying a weight-of-evidence approach, all newly expressed proteins in LBFLFK are considered to behave as any other dietary protein and thus do not raise any safety concerns with regard to human or animal health.

Compositional Analysis

Grain samples produced over two growing seasons and the processed fractions oil and meal produced over one growing season were harvested and analysed for composition. This compositional assessment included measurements of proximates, fibres, amino acids, fatty acids, vitamins, minerals, antinutrients, and phytosterols. The components selected for analysis were based primarily on guidance provided in the consensus document for canola from the Organisation for Economic Co-operation and Development (OECD). The composition of LBFLFK canola was compared with the parental canola variety Kumily. Compositional assessment of LBFLFK-derived grain included samples produced from field plots both sprayed and not sprayed with commercial application rates of imazamox herbicide, to demonstrate there is no difference in composition due to the herbicide treatment.

Across-site mean values were compared to the range of means generated from conventional canola reference varieties, the International Life Sciences Institute (ILSI) Crop Composition Database data, and peer-reviewed scientific literature to provide context for the comparative analyses and assess the broader biological relevance of the results. Data suitable for statistical analysis were subjected to mixed model analysis of variance.

As expected, the introduction of the EPA+DHA trait and the associated metabolic pathways in LBFLFK canola resulted in the presence of fatty acids not found in conventional canola. The EPA+DHA trait impacted the amount of fatty acids normally observed in conventional canola varieties in an expected way, with the content of oleic acid also significantly reduced in LBFLFK canola across treatments and seasons relative to the parental control variety Kumily. As expected, the concentrations of measured fatty acids not associated with the introduced enzymatic pathway were not changed in LBFLFK canola.

For the other components measured, the results of the comparative approach demonstrate that LBFLFK canola is equivalent to other commercially available canola varieties. Processing did not alter or impact the nutritional value of oil derived from LBFLFK canola. The overall composition of the crude oil and RBD oil fractions for LBFLFK is comparable to that of

conventional canola oil with the exception of the intended changes in the fatty acids resulting from the introduced EPA+DHA trait.

Nutritional Safety

To establish the safety of the fatty acids in LBFLFK associated with the EPA+DHA trait and the safety of the overall fatty acid profile, a systematic literature search was conducted. This was complemented with a detailed comparative analysis of the fatty acid composition of various edible oils and fat-containing foods. All fatty acids introduced by the EPA+DHA trait are already present in foods that are considered safe for consumption, and the fatty acid profile of LBFLFK oil is similar to other EPA- and DHA-containing oils commonly consumed, such as fish oil.

If oil from LBFLFK is utilised as a food ingredient, it will provide a new and alternative source of omega-3 LC-PUFAs, thereby increasing consumer access and possibly contributing to a general increase in the consumption of omega-3 fatty acids. Increasing evidence and a greater awareness of the health benefits of these sources of omega-3 fatty acids may also contribute to an increase in consumption among consumers who prefer or require more dietary omega-3.

PART 1 GENERAL INFORMATION ON THE APPLICATION

1.1 Applicant Details

(a) Applicant (individual organisation's) name

BASF Australia Ltd

(b) Name of contact person

[redacted]

(c) Address (street and postal)

BASF Australia Ltd
Level 12, 28 Freshwater Place
Melbourne, VIC, 3006
Australia

(d) Telephone numbers

Tel: [redacted]

(e) Email address

[redacted]

(f) Nature of applicant's business

Seeds and traits, biotechnology.

(g) Details of other individuals, companies or organisations associated with the application

Not applicable.

1.2 Purpose of the Application

BASF Australia Ltd requests to vary FSANZ Standard 1.5.2 to allow the use of genetically modified canola (*B. napus*) derived from transformation event LBFLFK in the Australian and New Zealand food industries.

Like other canola varieties, the products of event LBFLFK will be processed into oil and defatted meal fractions. Oil and meal from canola can be manufactured into a variety of products for human and agricultural consumption or for industrial purposes (OECD, 2011b). As a specialty canola with a fatty acid profile containing the LC-PUFAs EPA and DHA, the oil produced from event LBFLFK will be consumed specifically for the purpose of providing dietary omega-3 LC-PUFAs. The oil will be incorporated as an ingredient into various consumer food items to provide individuals with more options for dietary omega-3 LC-PUFAs (see U.S. FDA (2017a) for categories of food where EPA- and DHA-containing oil from event LBFLFK may be incorporated as an ingredient). Refined oil derived from EPA+DHA canola may also be used as a dietary supplement to provide an alternate source of omega-3 LC-PUFAs pending any additional regulatory requirement for these uses. Additionally, the oil will be used as an input to aquafeed operations to provide omega-3 LC-PUFAs to farmed aquatic species. Defatted canola meal produced from LBFLFK canola will be available for use in the same applications as conventional canola meal. The primary application for canola meal is as a feed ingredient for livestock. The defatted meal produced from LBFLFK canola will not be sold as a source of omega-3 LC-PUFAs as the oil content of the meal will be too low to make a significant contribution to the nutrition of the livestock.

Canola varieties containing event LBFLFK will be approved as a single event for food approval in the major canola producing and importing countries of the world. The meal is intended to be traded as aquaculture feed internationally. Therefore, it is anticipated that food products derived from canola containing this event will be present in the Australian and New Zealand food supply.

1.3 Justification for the Application

The LBFLFK transformation event introduced two inserts integrated at two separated loci. Each of the two inserts has the intended 13 gene expression cassettes and was identical to the vector T-DNA except for two single nucleotides in protein coding sequences that do not impact the functionality of the proteins produced. These genes confer two novel traits: (i) a modification of the genome such that the sequences encoding the fatty acid synthesis enzymes are introduced; and (ii) tolerance to the broad spectrum imidazolinone herbicides, such as imazamox. It is anticipated that food products derived from canola containing event LBFLFK canola will be present in the Australian and New Zealand food supply.

Advantages of LBFLFK canola

The novel traits expressed by canola varieties containing event LBFLFK provide several potential benefits over conventional canola varieties and other transgenic canola currently on the market. Currently, the omega-3 LC-PUFAs EPA and DHA are primarily consumed through seafood, including finfish (e.g., salmon, tuna, and trout) and shellfish (e.g., crab, mussels, and oysters) (Blasbalg et al., 2011; Kitessa et al., 2014). Numerous health organisations recommend adult intakes of 250–500 mg combined EPA and DHA per day (Yi et al., 2014; Salem and Eggersdorfer, 2015). While this recommendation is met in some countries, many

countries, including the U.S. and Australia, fall below the recommended average for daily intakes (Gebauer et al., 2006; Kris-Etherton et al., 2009; Flock et al., 2013; Salem and Eggersdorfer, 2015; Meyer, 2016). The primary reason for this deficiency is that the supply of fatty acids from marine animals and other sources is limited. There is a significant challenge in producing and distributing products containing EPA and DHA to consumers in adequate quantity (Salem and Eggersdorfer, 2015). There is also high demand for fish oil as a primary ingredient for farmed fish, especially fatty fish like salmon or trout. This demand is not fully met, to the point where the harvested fish now have a reduced level of omega-3 fatty acids compared to historical levels (Kitessa et al., 2014; Tocher, 2015).

- The herbicide tolerance trait of LBFLFK canola will allow for selective post-emergence weed control during field production. The use of herbicide with the active ingredient imazamox (an imidazolinone) will follow the same agronomic practices as used for Clearfield® canola (registered trademark of BASF under license). Clearfield canola products have been widely adopted in North America (Canola Council of Canada, 2017) and are common in Australia (BASF, 2018; GRDC Grownotes, 2018; Dhammu et al., 2020), and herbicide applications for LBFLFK canola production will follow established weed control practices.
- To maintain the quality and ensure the segregation of LBFLFK canola seeds, grains, and processed products, an Identity Preservation System (IDP) will be implemented at every step of production and handling. Processing operations will be conducted either at dedicated facilities or at facilities with specific measures in place to ensure segregation from other products. Like other canola varieties, the products of LBFLFK canola will be processed into oil and defatted meal fractions. Oil and meal from canola can be manufactured into a variety of products for human and agricultural consumption or for industrial purposes (OECD, 2011b). As a specialty canola with a fatty acid profile containing the LC-PUFAs EPA and DHA, the oil produced from LBFLFK canola will be consumed specifically for the purpose of providing dietary omega-3 LC-PUFAs. The refined oil may also be provided to dietary supplement manufacturers as an alternate source of omega-3 LC-PUFA fatty acids. Additionally, the oil will be used as an input to aquafeed operations to provide omega-3 LC-PUFAs to farmed aquatic species. Defatted canola meal produced from LBFLFK canola will be available for use in the same applications as conventional canola meal. The primary application for canola meal is as a feed ingredient for livestock. The defatted meal produced from LBFLFK canola will not be sold as a source of omega-3 LC-PUFAs as the oil content of the meal will be too low to make a significant contribution to the nutrition of the livestock.

The herbicide tolerance trait will provide a tool to growers for selective breeding and weed control during field production. The herbicide tolerance trait will allow for application of Group 2 herbicides, including Beyond® herbicide (active ingredient imazamox) (registered trademark of BASF under license), during breeding and commercial production of LBFLFK canola.

Note:

(a) Any public health and safety issues related to the proposed change including details of target groups and population groups that may be adversely affected.

(b) Any consumer choice issues related to the proposed change.

(c) Any evidence that the food industry generally or other specific companies have an interest in, or support, the proposed change.

In relation to points (a), (b), and (c) above, the data contained within this submission indicate the general safety of LBFLFK canola-derived foods based on the history of safe use of omega-3 LC-PUFAs in the human diet. From the work conducted, there is no indication that there are public health or safety issues related to the proposed change to Standard 1.5.2 of the Food Standards Code. The section below and Appendix 2, discussing food safety of LBFLFK canola, go into further detail in this respect.

Consumer choice with respect to the proposed change is anticipated to be dealt with by FSANZ via their assessment of the data included in this package. It should be noted that LBFLFK canola when used in breeding systems to deliver canola-derived food products will result in the primary food product—omega-3 LC-PUFA rich oil—which contains novel proteins which are below the limit of detection. As this food item results in an altered nutritional profile, it will require listing in subsection S26-3(2) of Schedule 26 of the Food Standards Code and will require labelling to differentiate it from canola oil derived from non-GM canola varieties. It is noted that this product, if marketed in Australia as a food ingredient, will provide a new and alternative source of long-chain omega-3-fatty acids which will increase consumer access. Consumers will then be able to make informed choices based on labelling requirements as to whether they would prefer products enriched with EPA and DHA.

As LBFLFK *B. napus* is still in the developmental stage with BASF, there is no specific information available to indicate that the food industry has interest in, or supports, the proposed change to the Standard 1.5.2.

EPA+DHA canola, however, will be produced as a specialty canola variety using an identity-preservation (IDP) closed-loop production system. This production will be done in partnership with [redacted] an agriculture and food production company with extensive experience in the production of specialty canola varieties. Therefore, there is interest to support the proposed change specifically from [redacted]

<u>Food safety</u>

The pathway for producing the long-chain omega-3 fatty acid docosahexaenoic acid (DHA) from oleic acid has been assessed by FSANZ previously. No public health or safety concerns were identified associated with the DHA expression from oleic acid expressed in NuSeed canola line NS-B50027-4. In the review of NS-B50027-4 canola, FSANZ stated: *"Based on the data provided in the present Application, and other available information, food derived from DHA canola is considered to be as safe for human consumption as food derived from conventional canola cultivars"* (FSANZ, 2017).

Information provided in this application supports claims that the proteins expressed by the LBFLFK canola event share no characteristics consistent with toxins or allergens. The potential for mammalian toxicity is addressed for these proteins. Compositional and nutritional analyses demonstrate that food derived from canola containing event LBFLFK is as safe and nutritious as food derived from conventional canola varieties.

The status for requests for uses of LBFLFK canola as food and feed in other importing countries is provided in Table 2. Further information on the global submission status can be provided to update FSANZ during the application process.

Table 2. Current Global Submission Status for LBFLFK Canola

Country	Agency	Submission date
US	USDA	November 2017 (approved)
US	FDA	January 2018
Canada	CFIA	February 2018 (approved)
Canada	Health Canada	February 2018 (approved)
South Korea	MFDS	September 2018
South Korea	RDA	September 2018
Japan	MAFF	August 2019
Japan	MHLW	June 2019
China	MARA	September 2019
Mexico	COFEPRIS	September 2020
EU	EFSA	June 2019

1.4 Regulatory Impact Information

Costs and benefits, and impacts on trade

Varying the FSANZ Standards to include LBFLFK will contribute to maintaining stable food prices, consumer choice in the marketplace, and decreased production costs for food products rich in omega-3 LC-PUFAs in the longer term.

LC-PUFAs including EPA and DHA are currently primarily sourced from marine sources, including oil from wild fish. However, these marine sources of LC-PUFAs are not a reliable or sustainable source for the increased demand for commercially reared fish and crustaceans. There is a clear need for alternative sources of EPA and DHA to meet these demands (Salem and Eggersdorfer, 2015; Tocher, 2015; FAO, 2020).

Canola oil can already be used in aquafeed operations to supplement the limited oil available from marine sources (Canola Council of Canada, 2015). However, replacing fish oil with canola or other vegetable oils has reduced the levels of omega-3 available in farmed fish. It has been recommended to substitute fish oil with alternative sources of EPA and DHA to support the aquaculture operations that are the primary consumer of fish oil. LBFLFK canola can provide sustainable and stable access as a source of these omega-3 fatty acids, to better meet demands for LC-PUFAs in aquafeed operations and better ensure consumer access in all markets (Salem and Eggersdorfer, 2015; Tocher, 2015).

The potential trade implications of not including canola event LBFLFK in the FSANZ Standards are significant. To maintain the integrity of the supply of canola products from canola event LBFLFK, production and processing will be conducted under an Identity Preservation System (IDP).

EPA+DHA canola will be a new specialty canola oil produced using an IDP closed-loop production system. There are additional costs associated with IDP production, and growers and other grain handlers are usually paid a premium as an incentive to maintain the required isolation from other production. Production of specialty canola under IDP is familiar to canola

producers, and the additional costs of segregation of LBFLFK grain and oil would be not be expected to be significantly different than current practices.

The US and Canada are major trading partners of Australia, and approved transgenic crops are generally considered to be substantially equivalent to conventional crops in both of these countries. In both Canada and the US, segregation and labelling of products containing the LBFLFK canola oil will be required. Products containing event LBFLFK imported into Australia from the US and Canada, or other trading partners with similar treatments of transgenic crops, may need to be removed from sale without appropriate pre-market approval in the importing destinations. This could expose Australia to disputes with trading partners at the World Trade Organization.

A rejection of the EPA+DHA canola application may have major trade implications, particularly if this product is introduced in other parts of the world, and would result in denying the foreseen benefits of an alternate and more sustainable source of omega-3 fatty acids.

1.5 Information to Support the Application

All of the relevant information to support the application is supplied within this dossier. Suitable literature references are provided in reference lists at the end of the discursive part of this submission and at the end of each of the technical appendices to the dossier.

1.6 Assessment Procedure

We consider that the appropriate assessment for this application is the General Procedure based on prior consideration for pre-market approval of other GM foods in Standard 1.5.2 with altered nutritional profile.

1.7 Confidential Commercial Information

A formal request for confidential commercial information (CCI) has been submitted to FSANZ.

1.8 Other Confidential Information

BASF requests that for documents provided with this application that have privacy information, treat this privacy information as “Other Confidential Information”. This request includes the cover letter and Statutory Declaration (Appendix 1).

1.9 Exclusive Capturable Commercial Benefit (ECCB)

The application is expected to confer an ECCB upon BASF since it will contribute to facilitating commercial activities with LBFLFK canola, once commercially preferred varieties are available, firstly in the North America, possibly followed by other canola producing countries.

1.10 International and Other Standards

The BASF research and development data included in this application were conducted according to international standards. In the safety assessment of biotechnology products, BASF refers primarily to the Codex Alimentarius Commission weight-of-evidence approach (Codex Alimentarius Commission, 2009b), and the relevant Codex Standard is:

Guideline for the conduct of food safety assessment of foods derived from recombinant-DNA plants. CAC/GL 45-2003. Adopted in 2003, Annexes II and III adopted in 2008 (Codex Alimentarius Commission, 2009c).

Other guidelines and recommendations are also considered including those of the World Health Organisation (WHO), the United Nations Food and Agriculture Organisation (FAO), the United States Food and Drug Administration (U.S. FDA), the United States Environment Protection Agency (U.S. EPA), and the European Food Safety Agency (EFSA) (FAO/WHO, 2001; Codex Alimentarius Commission, 2009c; EFSA Panel on Genetically Modified Organisms, 2011; U.S. FDA, 2012; U.S. EPA, 2017).

1.11 Statutory Declaration

Included in the application to FSANZ as an electronic document at Appendix 1.

1.12 Checklist for General Requirements

APPLICATION REQUIREMENT CHECKLIST	CHECK	PAGE NUMBER
Mandatory Requirements (Application Handbook General requirements 3.1.1)		
A Form of application	☒	-
Application in English	☒	-
Executive Summary	☒	Separate file
Relevant Sections of Part 3 clearly identified	☒	-
Pages sequentially numbered	☒	-
Information to support the application	☒	Separate files
Electronic copy (searchable)	☒	-
All references provided	☒	Separate files
B Applicant details	☒	23
C Purpose of application	☒	24
D Justification for application	☒	24
Regulatory impact information	☒	27
Impact on international trade	☒	27
E Information to support the application	☒	28
Data requirements	☒	-
F Assessment procedure	☒	28
General	☒	-
Major	-	-
Minor	-	-
High level health claim variation	-	-
G Confidential commercial information	☒	Separate files
CCI material separated from other application material	☒	-
Formal request including reasons	☒	Separate file

APPLICATION REQUIREMENT CHECKLIST	CHECK	PAGE NUMBER
I Exclusive Capturable Commercial Benefit	☒	28
Justification provided	☒	-
J International and other national standards	☒	28
International standards	☒	-
Other national standards	☒	-
K Statutory Declaration	☒	Separate file
L Checklist/s provided with application	☒	29
3.1.1 Checklist	☒	29
All page number references from application included	☒	-
Any other relevant checklists for Chapters 3.2 – 3.7	☒	29
Foods Produced Using Gene Technology (Application Handbook Section 3.5.1)		
A.1 Nature and identity	☒	31
A.2 History of use of host and donor organisms	☒	31
A.3 Nature of the genetic modification	☒	55
B.1 Characterisation and safety assessment	☒	89
B.2 New proteins	☒	158
B.3 Other (non-protein) new substances	☒	225
B.4 Novel herbicide metabolites in GM herbicide-tolerant plants	☒	225
B.5 Compositional analyses	☒	226
C Nutritional impact of the GM food	☒	298
D Other information	☒	299

PART A TECHNICAL INFORMATION ON THE FOOD PRODUCED USING GENE TECHNOLOGY

A.1 Nature and Identity of the Genetically Modified Food

(a) A description of the GM organism from which the new GM food is derived. The description must include the nature and purpose of the genetic modification

EPA+DHA canola event LBFLFK is a biotechnology-derived canola cultivar of *Brassica napus* L., referred to herein as LBFLFK (OECD unique identifier BPS-BFLFK-2). It contains genes that impact the content of omega-3 long-chain polyunsaturated fatty acids in the seeds and contains a gene that confers tolerance to imidazolinone herbicides. The fatty acid trait is conferred by the introduction of a metabolic pathway consisting of ten genes encoding the following proteins: delta-12 desaturase from *Phytophthora sojae*, delta-6 desaturase from *Ostreococcus tauri*, delta-6 elongase from *Thalassiosira pseudonana*, delta-6 elongase from *Physcomitrella patens*, delta-5 desaturase from *Thraustochytrium* sp., omega-3 desaturase from *Pythium irregulare*, omega-3 desaturase from *Phytophthora infestans*, delta-5 elongase from *Ostreococcus tauri*, delta-4 desaturase from *Thraustochytrium* sp., and delta-4 desaturase from *Pavlova lutheri* to produce eicosapentaenoic acid (EPA) and docosahexaenoic acid (DHA). The herbicide tolerance is conferred by the introduction of an acetohydroxy acid synthase (*AHAS*) gene from *Arabidopsis thaliana* with two amino acid substitutions (A122T, S653N).

(b) The name, line number and OECD Unique identifier of each of the new lines or strains of GM organism from which the food is derived

The transformation event is named “LBFLFK”, and canola transformed with this event will be referred to as LBFLFK canola. The OECD Unique identifier of LBFLFK canola is BPS-BFLFK-2.

(c) The name the food will be marketed under (if known)

This is unknown as this application is related to a commodity crop rather than a specific food or additive.

A.2 History and Use of the Host and Donor Organisms

The taxonomic classifications of the organisms from which the genetic elements of LBFLFK canola are derived are presented in Table 4.

Canola

Oilseed rape belongs to the botanical family Brassicaceae, also commonly known as the mustard or cabbage family. *Brassica napus* L. (n=19, AA and CC genomes) is a natural tetraploid containing the diploid chromosome set of both parents, also known as amphidiploid (OGTR, 2016). Common names used for oil-producing *B. napus* varieties include canola, rape, rapeseed, oilseed rape, and turnip. The taxonomic hierarchy for this member of the mustard family (taxonomic serial number 23060) (ITIS, 2016) is as follows:

Kingdom: Plantae – plants
Subkingdom: Viridiplantae – green plants

Division:	Tracheophyta – vascular plants
Subdivision:	Spermatophytina – seed plants
Class:	Magnoliopsida – flowering plants
Order:	Brassicales
Family:	Brassicaceae – mustard family
Genus:	*Brassica* L. – mustard
Species:	*Brassica napus* L.

Historically, rapeseed oil was used primarily for industrial purposes (lamp oil, soap-making), and it was produced from Brassicaceae species including *B. napus, B. rapa, and B. juncea*. Rapeseed breeding efforts to improve agronomic characteristics and oil content were intensified in Canada after its introduction from Europe in the 1940s. During the 1970s, low erucic acid rapeseed was developed from *B. napus* and *B. rapa* varieties to make rapeseed oil suitable for human consumption. A few years later, a "double-low" cultivar was developed by breeding with low erucic acid and glucosinolate levels (OGTR, 2016). These edible rapeseed varieties, collectively referred to as canola, have since been widely used for edible oil production and animal feed use (OECD, 2011b). Defined quality specifications for canola oil stipulate that the "oil shall contain less than 2% erucic acid in its fatty acid profile and the solid component shall contain less than 30 micromoles of any one or any mixture of 3-butenyl glucosinolate, 4-pentenyl glucosinolate, 2-hydroxy-3-butenyl glucosinolate, and 2-hydroxy-4-pentenyl glucosinolate per gram of air-dry, oil-free solid" (Canola Council of Canada, 2016b).

The food and feed use of low erucic acid rapeseed has been well reviewed (OECD, 2011b). The harvested seeds are processed into two major products: oil and meal. The oil is used primarily for human consumption whereas the protein-containing meal is diverted to animal consumption (Heuzé et al., 2016). Food uses of the protein fractions have not been greatly reported but do represent another potential consumption route for low erucic acid rapeseed. A limited number of Asian countries, including India, consume canola seed as a source of food (USDA-FAS, 2016).

Refined oil from low erucic acid rapeseed is used as an ingredient in a wide variety of consumer food goods and is also sold directly to consumers for home cooking applications. As such, it is the third largest source of vegetable oil (after soybean oil and palm oil) and oil meal (after soybean and cotton) in the world (Heuzé et al., 2016). In Australia, canola oil is used in frying and baking applications and is an ingredient in salad dressings, margarine, and a variety of other products. Canola oil appeals to health-conscious consumers because it has a low percentage of saturated fat and is free of artificial trans-fats. High-oleic acid canola varieties have been developed recently that are used in commercial high-temperature frying applications to replace partially hydrogenated oils (USDA-ERS, 2017). In Canada, low erucic acid rapeseed oil represents more than two-thirds of the vegetable oil consumed. In the United States the usage rate is lower, at approximately 10%, but low erucic acid rapeseed oil is found in a wide variety of food products and is commonly purchased for home use (OECD, 2011b).

Arabidopsis thaliana

Scientific name (common name) and taxonomic classification

Arabidopsis thaliana (*A. thaliana*) (common name: mouse-ear cress), the source organism for the acetohydroxy acid synthase *AHAS(At)* gene, is a member of the mustard (Brassicaceae) family, which includes several cultivated vegetable species such as broccoli, cabbage,

cauliflower, turnip, rapeseed, and radish. *A. thaliana* is a small flowering plant that is widely used as a model organism in plant biology research as its genome is small, has been fully sequenced, and is easily manipulated (Koornneef and Meinke, 2010). The taxonomic classification for *A. thaliana* is as follows (NCBI, 2017a):

Domain:	Eukaryota
Kingdom:	Plantae
Subkingdom:	Viridiplantae
Division:	Streptophyta
Order:	Brassicales
Family:	Brassicaceae
Genus:	*Arabidopsis* Heynh.
Species:	*Arabidopsis thaliana* (L.) Heynh.

Information on naturally occurring toxins, antinutrients, and allergens

A. thaliana is not known to be a source of toxins. As is typical of the Brassicaceae family, *A. thaliana* has been described to contain glucosinolates in varying composition and concentration (Kliebenstein et al., 2001). Glucosinolates are a large group of naturally occurring plant defence compounds that occur in all Brassica-originated feeds and fodders. The primary deleterious effects of ingestion of glucosinolates in animals are reduced palatability and decreased growth and production (Tripathi and Mishra, 2007).

A. thaliana is not considered an allergy-causing plant. Neither the COMPARE database[2], which includes a comprehensive repository of all known allergens with clinical evidence of allergenicity based on standardised criteria, nor the AllergenOnline database[3], which provides access to a peer-reviewed allergen list, retrieved any protein sequences from *A. thaliana* that are known or putative allergens. However, there are sporadic publications reporting potentially allergenic proteins in *A. thaliana*. The lipid transfer protein 1 in *A. thaliana* has been identified as a possible allergen (i.e. recognised by human IgE) (Chardin et al., 2003), and one case of occupational asthma was reported in a laboratory worker due to inhalation exposure to *A. thaliana* pollen (Yates et al., 2008). *A. thaliana* also contains profilins, small proteins which are thought to be responsible for certain types of allergies (Thorn et al., 1997). Finally, one study reported that the Arabidopsis genome encodes Pollen Ole e 1 domain-containing proteins (Hu et al., 2014) that are present in many plants (Jiménez-López et al., 2011).

Available toxicology data for the organism

As indicated in the previous paragraph, *A. thaliana* is not known to be a source of toxins.

Information on the past and present use, if any, in the food supply and exposure route(s) other than intended food use

A. thaliana is generally not consumed as food. However, *A. thaliana* is a member of the mustard family, which includes several routinely consumed vegetables such as broccoli, cabbage, cauliflower, turnip, rapeseed, and radish.

[2] http://comparedatabase.org/about-compare-database/
[3] http://www.allergenonline.org

Ostreococcus tauri

Scientific name (common name) and taxonomic classification

Ostreococcus tauri (*O. tauri*) (common name: none found), the source organism for the delta-6 desaturase *D6D*(*Ot*) and the delta-5 elongase *D5E*(*Ot*) genes, is a unicellular marine green microalga commonly found in all oceans. It is the smallest free-living eukaryote, recognised as a model organism of the marine phytoplankton assemblage, and widely distributed from coastal to oligotrophic waters (Zhang et al., 2013).

The taxonomic classification for *O. tauri* is as follows (Guiry, 2015a; NCBI, 2017b):

Domain:	Eukaryota
Kingdom:	Plantae
Subkingdom:	Viridiplantae
Division:	Chlorophyta
Class:	Mamiellophyceae
Order:	Mamiellales
Family:	Bathycoccaceae
Genus:	*Ostreococcus*
Species:	*Ostreococcus tauri*

Information on naturally occurring toxins, antinutrients, and allergens

O. tauri is not known to produce or contain toxins, allergens, or antinutrients. Neither the COMPARE database nor the AllergenOnline database retrieved any protein sequences from *O*. *tauri* that are known or putative allergens.

Available toxicology data for the organism

As indicated in the previous paragraph, *O. tauri* is not known to be a source of toxins.

Information on the past and present use, if any, in the food supply and exposure route(s) other than intended food use

O. tauri is not directly consumed as food or feed. However, as a green microalga, *O. tauri* is part of the marine phytoplankton community, the lowest tier in the aquatic food web, and is indirectly consumed by fish that ultimately could end up as human food.

Pavlova lutheri

Scientific name (common name) and taxonomic classification

Pavlova lutheri (*P. lutheri*) (common name: none found), the source organism for the delta-4 desaturase *D4D*(*Pl*) gene, is a marine microalga. The taxonomic classification for *P. lutheri* is as follows (Guiry, 2015b; NCBI, 2017c):

Domain: Eukaryota
Kingdom: Chromista
Division: Haptophyta
Class: Pavlovophyceae
Order: Pavlovales
Family: Pavlovaceae
Genus: *Pavlova*
Species: *Pavlova lutheri*

Information on naturally occurring toxins, antinutrients, and allergens

Pavlova lutheri is not known to produce or contain toxins, antinutrients, or allergens. Neither the COMPARE database nor the AllergenOnline database retrieved any protein sequences from *P. lutheri* that are known or putative allergens.

Available toxicology data for the organism

As indicated in the previous paragraph, *P. lutheri* is not known to be a source of toxins.

Information on the past and present use, if any, in the food supply and exposure route(s) other than intended food use

P. lutheri is not consumed directly as food. *P. lutheri* is a marine microalga commonly used in the aquaculture industry to feed marine organisms (Ponis et al., 2006). It has been studied for its fatty acid production and its use as a live feed in bivalve hatcheries (Dhert and Sorgeloos, 1995; Ponis et al., 2003a; Carvalho and Malcata, 2005). *P. lutheri* is frequently used as part of aquafeed diets for carpet shells (Aranda-Burgos et al., 2014), Japanese bay scallop (Semura, 1995), Chilean scallop (Caers et al., 2003), great scallop (Delaunay et al., 1993; Gagné et al., 2012), giant sea scallop (Gouda et al., 2006), king scallop (Laing, 2000; Hawkins et al., 2005), Japanese pearl oyster (Numaguchi, 2000; Tomaru et al., 2002), European flat oysters (Jonsson et al., 1999; González-Araya et al., 2011; González-Araya et al., 2012; Ronquillo et al., 2012; González-Araya et al., 2013), black-lip pearl oyster (Doroudi et al., 2003), pacific oysters (Knauer et al., 1999; Ponis et al., 2003b; Ponis et al., 2008), the bivalve *Venus verrucosa* (Grémare et al., 1998), copepods (Brugnano et al., 2008), giant tiger prawn (D'Souza et al., 2000), sea urchin (Kashenko, 2007), and others. Accordingly, human consumption of *P. lutheri* is expected to be primarily by indirect consumption of shellfish and other marine organisms.

Physcomitrella patens

Scientific name (common name) and taxonomic classification

Physcomitrella patens (*P. patens*) (common name: spreading earth moss), the source organism for the delta-6 elongase *D6E*(*Pp*) gene, is a moss. The taxonomic classification for *P. patens* is as follows (NCBI, 2017d):

Domain:	Eukaryota
Kingdom:	Plantae
Subkingdom	Viridiplantae
Division:	Streptophyta
Class:	Bryopsida
Order:	Funariales
Family:	Funariaceae
Genus:	*Physcomitrella*
Species:	*Physcomitrella patens*

Information on naturally occurring toxins, antinutrients, and allergens

P. patens is not known to produce or contain toxins, antinutrients, or allergens. *P. patens* has been used as an experimental organism for more than 80 years, and its use as a model to explore plant functions has increased in recent years (Cove et al., 2009). *P. patens* is regarded as an advantageous system to produce recombinant biopharmaceuticals (Decker et al., 2014; Reski et al., 2015). For example, oral vaccines produced in this moss are considered suitable for the formulation of orally administered vaccines since no toxic effects are attributed to the ingestion of this moss (Decker et al., 2014; Rosales-Mendoza et al., 2014).

Neither the COMPARE database nor the AllergenOnline database retrieved any protein sequences in *P. patens* that are known or putative allergens.

Available toxicology data for the organism

As indicated in the previous paragraph, *P. patens* is not known to be a source of toxins.

Information on the past and present use, if any, in the food supply and exposure route(s) other than intended food use

P. patens is not consumed as food or feed.

Phytophthora infestans

Scientific name (common name) and taxonomic classification

Phytophthora infestans (*P. infestans*) (common name: Potato late blight fungus), the source organism for the omega-3 desaturase *O3D*(*Pi*) gene, belongs to the oomycetes, a group of fungus-like eukaryotes. The taxonomic classification for *P. infestans* is as follows (NCBI, 2017e):

Domain:	Eukaryota
Kingdom:	Chromista
Superdivision:	Stramenopiles (Heterokonts)
Class:	Oomycetes
Order:	Peronosporales
Genus:	*Phytophthora*
Species:	*Phytophthora infestans*

Information on naturally occurring toxins, antinutrients, and allergens

P. infestans is not known to produce or contain toxins, antinutrients, or allergens. Neither the COMPARE database nor the AllergenOnline database retrieved any protein sequences from *P. infestans* that are known or putative allergens.

Available toxicology data for the organism

As indicated in the previous paragraph, *P. infestans* is not known to be a source of toxins.

Information on the past and present use, if any, in the food supply and exposure route(s) other than intended food use

P. infestans is not consumed as food or feed.

Phytophthora sojae

Scientific name (common name) and taxonomic classification

Phytophthora sojae (*P. sojae*) (common name: soybean stem and root rot agent), the source organism for the delta-12 desaturase *D12D*(*Ps*) gene, belongs to the oomycetes, a group of fungus-like eukaryotes. The taxonomic classification for *P. sojae* is as follows (NCBI, 2017f):

Domain:	Eukaryota
Kingdom:	Chromista
Superdivision:	Stramenopiles (Heterokonts)
Class:	Oomycetes
Order:	Peronosporales
Genus:	*Phytophthora*
Species:	*Phytophthora sojae*

Information on naturally occurring toxins, antinutrients, and allergens

P. sojae is not known to produce or contain toxins, antinutrients, or allergens. Neither the COMPARE database nor the AllergenOnline database retrieved any protein sequences in *P. sojae* that are known or putative allergens.

Available toxicology data for the organism

As indicated in the previous paragraph, *P. sojae* is not known to be a source of toxins.

Information on the past and present use, if any, in the food supply and exposure route(s) other than intended food use

P. sojae is not consumed as food or feed.

Pythium irregulare

Scientific name (common name) and taxonomic classification

Pythium irregulare (*P. irregulare*) (common name: none found), the source organism for the omega-3 desaturase *O3D*(*Pir*) gene, belongs to the oomycetes, a group of fungus-like eukaryotes. The taxonomic classification for *P. irregulare* is as follows (NCBI, 2017g):

Domain: Eukaryota
Kingdom: Chromista
Class: Oomycetes
Order: Pythiales
Family: Pythiaceae
Genus: *Pythium*
Species: *Pythium irregulare*

Information on naturally occurring toxins, antinutrients, and allergens

P. irregulare is not known to produce or contain toxins, antinutrients, or allergens. The suitability of *P. irregulare* as a producer of fatty acids for use in dietary supplements was evaluated, and the authors concluded that *P. irregulare* can be considered a safe source of biomass and EPA-containing oil for use as an ingredient in food, feed, and pharmaceuticals because there is no evidence showing that this species is associated with any disease or production of toxins affecting humans (Wu et al., 2013).

Neither the COMPARE database nor the AllergenOnline database retrieved any protein sequences in *P. irregulare* that are known or putative allergens.

Available toxicology data for the organism

As indicated in the previous paragraph, *P. irregulare* is not known to be a source of toxins.

Information on the past and present use, if any, in the food supply and exposure route(s) other than intended food use

P. irregulare is not consumed as food or feed. However, *P. irregulare* can be considered a safe source of biomass or oil for use as ingredients in food and feed because there is no evidence showing that this species is associated with any disease or production of toxins affecting humans (Wu et al., 2013).

Thalassiosira pseudonana

Scientific name(s) (common name) and taxonomic classification

Thalassiosira pseudonana (*T. pseudonana*) (common name: none found), the source organism for the delta-6 elongase *D6E*(*Tp*) gene, is a marine diatom. Diatoms are one of the most abundant group of phytoplankton (Keller et al., 1989) representing at least 40% of the primary production in oceans (i.e. the synthesis of organic compounds from carbon dioxide) (Rousseaux and Gregg, 2013; Bushey et al., 2014). The taxonomic classification for *T. pseudonana* is as follows (WoRMS, 2015; NCBI, 2017h):

Domain:	Eukaryota
Kingdom:	Chromista
Superdivision:	Stramenopiles (Heterokonts)
Division:	Ochrophyta
Class:	Bacillariophyceae
Order:	Thalassiosirales
Family:	Thalassiosiraceae
Genus:	*Thalassiosira*
Species:	*Thalassiosira pseudonana*

Information on naturally occurring toxins, antinutrients, and allergens

T. pseudonana is not known to produce or contain antinutrients or allergens. *T. pseudonana* has been reported to produce the neurotoxin Beta-N-methylamino-L-alanine (BMAA) (Jiang et al., 2014), which is produced by many representative species of diatoms as well as by cyanobacteria and dinoflagellates (Lage et al., 2015). Nevertheless, *T. pseudonana* is frequently used as part of aquafeed diets (e.g., for bivalves and crustacean larvae) (Brown, 2002). In addition, *T. pseudonana*-derived biosilica has successfully been used to deliver chemotherapeutic drugs to cancer cells, indicating a non-toxic nature (Delalat et al., 2015). *T. pseudonana* has also been shown to produce small quantities of apo-fucoxanthinoid compounds during senescence, a phenomenon known to many diatoms (Shaw et al., 1995). Extracts from *T. pseudonana* displayed no feeding deterrent activity to model copepods in bioassays (Shaw et al., 1994).

Neither the COMPARE database nor the AllergenOnline database retrieved any protein sequences in *T. pseudonana* that are known or putative allergens.

Available toxicology data for the organism

No toxicology data for *T. pseudonana* have been produced. *T. pseudonana* has a history of use as part of aquafeed diets.

Information on the past and present use, if any, in the food supply and exposure route(s) other than intended food use

T. pseudonana is not consumed as food. It is frequently used as part of aquafeed diets for marine organisms such as prawns (D'Souza et al., 2000), pacific oysters (Thompson and Harrison, 1992; Thompson et al., 1996), clams (Li et al., 2002; Liu et al., 2016), copepods (Harris, 1977), and basket cockle (Liu et al., 2009). Accordingly, human consumption of *T. pseudonana* is expected to be indirect via consumption of mussels, clams, and prawns.

Thraustochytrium sp.[4]

Scientific name (common name) and taxonomic classification

Thraustochytrids (common name: none found) are marine protists that belong to the class of Labyrinthulomycetes, which are primarily marine organisms that are considered important components of marine microbial communities. Thraustochytrids are microorganisms that are epibiotic in nature and represent a diverse group of organisms living in marine and estuarine habitats throughout the world, exhibiting a saprotrophic mode of nutrition (Raghukumar, 2002). They were first reported in 1936 (Sparrow, 1936).

The taxonomic classification for *Thraustochytrium* sp., the source organism for the delta-4 desaturase *D4D*(*Tc*) and the delta-5 desaturase *D5D*(*Tc*) genes, is as follows (WoRMS, 2004; NCBI, 2017i):

Domain:	Eukaryota
Kingdom:	Chromista
Superdivision:	Stramenopiles (Heterokonts)
Class:	Labyrinthulomycetes
Order:	Thraustochytriida
Family:	Thraustochytriaceae
Genus:	*Thraustochytrium*

Information on naturally occurring toxins, antinutrients, and allergens

Thraustochytrium sp. is not known to produce or contain toxins, antinutrients, or allergens. A number of Thraustochytrid species serve as sources of DHA used in dietary supplements and for DHA production in industry (Sijtsma and de Swaaf, 2004).

Neither the COMPARE database nor the AllergenOnline database retrieved any protein sequences in *Thraustochytrium* sp. That are known or putative allergens.

Available toxicology data for the organism

As indicated in the previous paragraph, *Thraustochytrium* sp. Is not known to be a source of toxins.

Information on the past and present use, if any, in the food supply and exposure route(s) other than intended food use

Thraustochytrium sp. Is not directly consumed as food. *Thraustochytrium* sp. Cells can be used as a source of naturally occurring carotenoids and as alternative fish feed to Nile tilapia (Atienza et al., 2012). A study regarding the Thraustochytrid *Schizochytrium* sp. Found no reports in the literature of direct human consumption of Thraustochytrids (Hammond et al., 2001). However, indirect human consumption likely occurs as these organisms are consumed by filter-feeding marine invertebrates, including mussels and clams, and by fish that are consumed directly by humans (Bergé and Barnathan, 2005).

[4] The species was not identified at the time of cloning (Qiu et al., 2001).

Regulatory sequences

Expression of the *c-D12D*(*Ps*) coding sequence is driven by p-*napA*(*Bn*), a seed-specific promoter from *Brassica napus* (Ellerström et al., 1996; Rask et al., 1998). The intron-containing 5' untranslated region (UTR) used (i-At5g63190) is from Arabidopsis locus At5g63190 (Sharma et al., 2007; Wang et al., 2008). Polyadenylation and termination of transcription is directed by t-*rbcS*(*Ps*), the E9 3' UTR of the *rbcS* gene from garden pea (*Pisum sativum*) encoding the small subunit of ribulose bisphosphate carboxylase protein (Coruzzi et al., 1984; Smigocki, 1991).

Expression of the *c-D6D*(*Ot*) coding sequence is driven by p-*SBP*(*Vf*), a seed-specific sucrose-binding protein-related gene promoter from faba bean (*Vicia faba*) (Grimes et al., 1992; Heim et al., 2001). The intron-containing 5' UTR (i-At1g65090) is from Arabidopsis locus At1g65090 (Braybrook et al., 2006). Polyadenylation and termination of transcription is directed by t-*CATHD*(*St*), the 3' UTR of potato (*Solanum tuberosum*) cathepsin D inhibitor gene (Hannapel, 1993).

Expression of the *c-D6E*(*Tp*) coding sequence is driven by p-*PXR*(*Lu*), the seed-specific peroxiredoxin like protein gene *PXR* promoter of flax (*Linum usitatissimum*) (Duwenig and Loyall, 2007). The intron-containing 5' UTR (i-At1g62290) is from Arabidopsis locus At1g62290 (Chen et al., 2002). Polyadenylation and termination of transcription is directed by t-*PXR*(*At*), the 3' UTR of *Arabidopsis thaliana* peroxiredoxin (PXR)-like protein gene *PER1* (Haslekås et al., 1998).

Expression of the *c-D6E*(*Pp*) coding sequence is under the control of p-*USP*(*Vf*), the promoter of the gene encoding a seed protein gene of unknown function from faba bean (*Vicia faba*) (Bäumlein et al., 1991). The intron-containing 5' UTR (i-At1g01170) is from Arabidopsis locus At1g01170 (Nakabayashi et al., 2005). Polyadenylation and termination of transcription is directed by t-*CaMV35S*, the 35S 3' UTR derived from the Cauliflower Mosaic Virus (Hajdukiewicz et al., 1994).

There are two expression cassettes for *c-D5D*(*Tc*). For the first, designated D5D(*Tc*)1, expression is driven by p-*CNL*(*Lu*), the seed-specific *conlinin* gene promoter from flax (*Linum usitatissimum*) (Truksa et al., 2003). The intron-containing 5' UTR (i-At5g63190) is from Arabidopsis locus At5g63190 (Sharma et al., 2007; Wang et al., 2008). Polyadenylation and termination of transcription is directed by t-*OCS*, the 3' UTR of the octopine synthase gene (MacDonald et al., 1991).

For the second expression cassette of *c-D5D*(*Tc*), designated D5D(*Tc*)2, expression is driven by p-*SETL*(*Bn*), the seed-specific *Brassica napus SETL* gene promoter (Bauer and Senger, 2010). Transcription termination is directed by t-*SETL*(*Bn*), the terminator of the *Brassica napus SETL*(*Bn*) gene (Bauer and Senger, 2010).

Expression of the *c-O3D*(*Pi*) coding sequence is driven by p-*USP*(*Vf*), the promoter of the gene encoding a seed protein gene of unknown function from faba bean (*Vicia faba*) (Bäumlein et al., 1991). The intron-containing 5' UTR (i-At1g01170) is from Arabidopsis locus At1g01170 (Nakabayashi et al., 2005). Polyadenylation and termination of transcription is directed by t-*CaMV35S*, the 3' UTR derived from the Cauliflower Mosaic Virus ((Hajdukiewicz et al., 1994)).

There are two expression cassettes for *c-O3D*(*Pir*). For the first, designated O3D(*Pir*)1, expression is driven by p-*SETL*(*Bn*), the seed-specific *Brassica napus SETL* gene promoter (Bauer and Senger, 2010). Transcription termination is directed by t-*SETL*(*Bn*), the terminator of the *Brassica napus SETL*(*Bn*) gene (Bauer and Senger, 2010).

For the second expression cassette of *c-O3D*(*Pir*), designated O3D(*Pir*)2, expression is driven by p-*PXR*(*Lu*), the seed-specific peroxiredoxin like protein gene *PXR* promoter of flax (*Linum usitatissimum*) (Duwenig and Loyall, 2007). The intron-containing 5' UTR (i-*AGO4*(*At*)) is from Arabidopsis gene *AGO4*(*At*) (Zilberman et al., 2003). Polyadenylation and termination of transcription is directed by t-*PXR*(*At*), the 3' UTR of *Arabidopsis thaliana* peroxiredoxin (PXR)-like protein gene *PER1* (Haslekås et al., 1998).

Expression of the *c-D5E*(*Ot*) coding sequence is driven by p-*FAE1*(*Bn*), a seed-specific gene promoter for a fatty acid elongase from *Brassica napus* (Han et al., 2001). The intron-containing 5' UTR (i-At1g62290) is from Arabidopsis locus At1g62290 (Chen et al., 2002). Polyadenylation and termination of transcription is directed by t-*FAE1*(*At*), the 3' UTR of a fatty acid elongase gene from *Arabidopsis thaliana* (Rossak et al., 2001).

Expression of the *c-D4D*(*Tc*) coding sequence is driven by p-*ARC5*(*Pv*), the seed-specific *Arcelin-5* (*Arc5*) gene promoter from kidney bean (*Phaseolus vulgaris*) (Goossens et al., 1994; Goossens et al., 1999). Polyadenylation and termination of transcription is directed by the *Phaseolus vulgaris Arc5* gene 3' UTR (Goossens et al., 1994; Goossens et al., 1999).

Expression of the *c-D4D*(*Pl*) coding sequence is driven p-*CNL*(*Lu*), the seed-specific *conlinin* gene promoter from flax (*Linum usitatissimum*) (Truksa et al., 2003). The intron-containing 5' UTR (i-At1g65090) is from Arabidopsis locus At1g65090 (Braybrook et al., 2006). Polyadenylation and termination of transcription is directed by t-*OCS*, the 3' UTR of the octopine synthase gene (MacDonald et al., 1991).

Expression of the *c-AHAS*(*At*) coding sequence is driven by p-*Ubi4*(*Pc*), a ubiquitin promoter from parsley (*Petroselinum crispum*) (Kawalleck et al., 1993). The intron-containing 5' UTR is i-*Ubi4*(*Pc*), from the *Petroselinum crispum* ubiquitin promoter (Kawalleck et al., 1993). Polyadenylation and termination of transcription is directed by t-*AHAS*(*At*), the 3' UTR of the *Arabidopsis thaliana AHAS* large subunit gene (Mazur et al., 1987).

Agrobacterium rhizogenes (Chilton et al., 1982) is a soil-borne, gram-negative bacterium that has been extensively studied since it was identified as an agent capable of transferring DNA into the genome of the root cells of host plants. *A. rhizogenes* is a well-known prokaryotic organism capable of transferring DNA to the eukaryotic cell (de Groot et al., 1998), and this ability has been noted and utilised in *B. napus* (Guerche et al., 1987). This gene transfer ability may have evolved from bacterial conjugal transfer systems which mobilise plasmids for transfer between bacterial cells (Stachel and Zambryski, 1986) and is exploited in biotechnology. Consequently, *A. rhizogenes* is a widely used transformation system in plant biotechnology.

Table 3. Expression Cassettes Contained in the T-DNA of Construct LTM593

Expression cassettes are listed in the same order as they are present in LTM593 (Figure 3). In those instances where the same coding sequence is used twice (*c-D5D*(*Tc*) and *c-O3D*(*Pir*)), a suffix number is added to the expression cassette name to distinguish them.

Expression cassette	Promoter	5' UTR	Coding sequence	Terminator
D6E(*Pp*)	Seed-specific promoter of unknown *Vicia faba* seed protein gene *USP*	Intron-containing 5' UTR of *Arabidopsis thaliana* locus *At1g01170*	*Physcomitrella patens* delta-6 elongase	CaMV35S terminator
D5D(*Tc*)*1*	Seed-specific promoter of *Linum usitatissimum* conlinin gene	Intron-containing 5' UTR of *Arabidopsis thaliana* locus *At5g63190*	*Thraustochytrium* sp. delta-5 desaturase	Octopine synthase terminator
D6D(*Ot*)	Seed-specific promoter of a *Vicia faba* sucrose-binding protein-related gene	Intron-containing 5' UTR of *Arabidopsis thaliana* locus *At1g65090*	*Ostreococcus tauri* delta-*6* desaturase	Terminator of the *Solanum tuberosum* cathepsin D inhibitor gene (*CATHD*(*St*))
D6E(*Tp*)	Seed-specific promotor of *Linum usitatissimum* peroxiredoxin like protein gene	Intron-containing 5' UTR of *Arabidopsis thaliana* locus *At1g62290*	*Thalassiosira pseudonana* delta-6 elongase	Terminator of *Arabidopsis thaliana* peroxiredoxin (PXR)-like protein gene *PER1*(*At*)
D12D(*Ps*)	Seed-specific promoter of *Brassica napus* seed storage protein *napA*	Intron-containing 5' UTR of *Arabidopsis thaliana* locus *At5g63190*	*Phytophthora sojae* delta-12 desaturase	*Pisum sativum rbcS*(*Ps*) E9 terminator
O3D(*Pir*)*1*	Seed-specific promoter of the *Brassica napus SETL* gene	None	*Pythium irregulare* omega-3 desaturase	Terminator of the *Brassica napus SETL* gene
O3D(*Pi*)	Seed-specific promoter of unknown *Vicia faba* seed protein gene *USP*	Intron-containing 5' UTR of *Arabidopsis thaliana* locus *At1g01170*	*Phytophthora infestans* omega-3 desaturase	CaMV35S terminator
D5D(*Tc*)*2*	Seed-specific promoter of the *Brassica napus SETL* gene	None	*Thraustochytrium* sp. delta-5 desaturase	Terminator of the *Brassica napus SETL* gene

Expression cassette	Promoter	5' UTR	Coding sequence	Terminator
D4D(*Tc*)	Seed-specific *Phaseolus vulgaris Arcelin-5* gene promoter	None	*Thraustochytrium* sp. delta-4 desaturase	*Phaseolus vulgaris Arc5* terminator
O3D(*Pir*)*2*	Seed-specific promotor of *Linum usitatissimum* peroxiredoxin like protein gene *PXR*	Intron-containing 5' UTR of *Arabidopsis thaliana* locus *AGO4*(*At*)	*Pythium irregulare* omega-3 desaturase	Terminator of *Arabidopsis thaliana* peroxiredoxin (PXR)-like protein gene *PER1*
D4D(*Pl*)	Seed-specific promoter of *Linum usitatissimum conlinin* gene	Intron-containing 5' UTR of *Arabidopsis thaliana* locus *At1g65090*	*Pavlova lutheri* delta-4 desaturase	Octopine synthase terminator
D5E(*Ot*)	Seed-specific promoter of *Brassica napus* beta-ketoacyl-CoA synthase (*FAE1.1*) gene	Intron-containing 5' UTR of *Arabidopsis thaliana* locus *At1g62290*	*Ostreococcus tauri* delta-5 elongase	*Arabidopsis thaliana* fatty acid elongase (*FAE1*(*At*)) terminator
AHAS(*At*)	Constitutive *Petroselinum crispum* ubiquitin promoter	Intron-containing 5' UTR of *Petroselinum crispum* ubiquitin gene	*Arabidopsis thaliana* acetohydroxy acid synthase	Terminator of *Arabidopsis thaliana* acetohydroxy acid synthase large subunit gene

Genetic elements outside of the T-DNA of LTM593 (vector backbone)

Approximately 16 kb of vector backbone region is located outside of the T-DNA borders of the vector construct LTM593. This backbone region of LTM593 contains a bacterial origin of replication (o-*Ori2*), the replication initiation gene (*c-repE*), and plasmid partition genes (*c-sopA, c-sopB and sopC*) from the *E. coli* F plasmid. With the proteins encoded by *c-repE*, *c-sopA*, and *c-sopB* and the cis-acting sequence *sopC*, in combination with the o-*Ori2* origin of replication, plasmids of up to 300 kb can be stably maintained in *E. coli* (Murotsu et al., 1984; Masson and Ray, 1986; Mori et al., 1986; Shizuya et al., 1992).

The operon *repABC* (*c-repA*, *c-repB*, *c-repC*) is derived from the *Agrobacterium tumefaciens* plasmid pTiC58 (Li and Farrand, 2000). The encoded proteins are responsible for plasmid segregation and replication in Agrobacterium (Oka et al., 1981; Tabata et al., 1989; Gerdes et al., 2000; Pinto et al., 2012). The origin of conjugal transfer (*ori*T) is the place at which plasmid transfer initiates (Marx and Lidstrom, 2001).

In addition, the backbone region of LTM593 also contains a bacterial selectable marker (*KanR*) that comprises a bacterial promoter and coding sequence of transposon Tn*903* that confers kanamycin resistance in *E. coli* (Oka et al., 1981; Naumovski and Friedberg, 1983) and *Agrobacterium* (Gardner et al., 1986) to aid in selection during the cloning process.

(a) For the donor organism(s) from which the genetic elements are derived:

(i) Any known pathogenicity, toxicity or allergenicity of relevance to the food

Canola (*Brassica napus* L.)

The nutritional, antinutritional, and toxicant components of low erucic acid rapeseed (canola) including *B. napus* have been well reviewed (OECD, 2011b). The original breeding efforts in Canada to produce low erucic acid rapeseed led to the development of varieties that produce oil with improved fatty acid composition including low erucic acid, and reduced content of glucosinolates in the meal.

Erucic acid (C22:1) is a fatty acid present in non-canola rapeseed and mustard at up to 30 to 60% of the total fatty acids. Consumption of erucic acid in high amounts is associated with myocardial lipidosis in laboratory monkeys and pigs, and myocardial necrosis followed by fibrosis in rats (FSANZ, 2003). Myocardial lipidosis is reported to reduce heart muscle contractile movement. So far, there is no clear evidence that consumption of high doses of erucic acid correlates with heart failure in humans (FSANZ, 2003). As mentioned previously, the potential safety concerns led to the development of rapeseed varieties that produce an oil with improved fatty acid composition and low erucic acid.

Although glucosinolates are not considered to be antinutrients, their hydrolysis products have antithyroid activity and, due to low palatability, inhibit feed intake in livestock animals (OECD, 2011b). Glucosinolates are sulfur-containing secondary plant metabolites that come in contact with the enzyme myrosinase when the cells of the seed are crushed during processing, releasing sulfur, glucose, and thiocyanates. These metabolites can be toxic to liver and kidneys (Tripathi and Mishra, 2007). Different processing techniques, including heating at different time lengths, have been applied to remove or minimise myrosinase content in rapeseed meal to lessen the harmful effects of glucosinolates on animals. However, since intestinal microflora also produce myrosinase, the potential negative effects of glucosinolates are not always eliminated (Tripathi and Mishra, 2007).

In addition to the aforementioned erucic acid and glucosinolates, which are reduced in canola quality varieties, grain from *B. napus* also contains phenolic compounds and phytic acid. Sinapine, a choline ester of sinapic acid, is the main phenolic compound found in low erucic acid varieties that can easily be excreted after consumption by most animals. However, laying hens cannot readily catabolise it, and it can accumulate in tissues and eggs. Tannins are another phenolic compound that can be found in canola quality varieties of rapeseed, usually at 1 to 3% of oil-free meal. Tannins can reduce digestibility by binding proteins and complex carbohydrates. Phytic acid (myo-inositol hexakisphosphate) is the principal form of stored phosphorus in plant tissues. It chelates minerals such as iron, zinc, phosphate, calcium, potassium, and magnesium. The bioavailability of trace elements such as zinc and iron can thus be reduced by the presence of phytic acid in monogastric animals (OECD, 2011b).

Sensitivity and allergenicity to *Brassica* species have been mostly associated with occupational exposure; however, these are described as rare cases (Trinidade et al., 2010; OECD, 2011b). Rapeseed flour can cause occupational asthma symptoms to workers while preparing animal feed (Alvarez et al., 2001). Rapeseed pollen has been identified as a potential cause for allergic sensitisation due to the presence of cross-reacting homologues of well-known allergens, e.g., calcium-binding proteins, profilins, and high molecular weight

glycoproteins (Focke et al., 1998). Allergic reactions were also identified in children with atopic dermatitis after a labial or open-food challenge with crushed seeds of *Brassica rapa* (Poikonen et al., 2006). However, because rapeseed oil contains little or no protein and therefore is free from allergy-inducing proteins, the implication of these results to the potential allergenicity of canola oil is likely low (Gylling, 2006).

Arabidopsis thaliana

Information on naturally occurring toxins, antinutrients, and allergens

A. thaliana is not known to be a source of toxins. As is typical of the Brassicaceae family, *A. thaliana* has been described to contain glucosinolates in varying composition and concentration (Kliebenstein et al., 2001). Glucosinolates are a large group of naturally occurring plant defence compounds that occur in all Brassica-originated feeds and fodders. The primary deleterious effects of ingestion of glucosinolates in animals are reduced palatability and decreased growth and production (Tripathi and Mishra, 2007).

A. thaliana is not considered an allergy-causing plant. Neither the COMPARE database[5], which includes a comprehensive repository of all known allergens with clinical evidence of allergenicity based on standardised criteria, nor the AllergenOnline database[6], which provides access to a peer-reviewed allergen list, retrieved any protein sequences from *A. thaliana* that are known or putative allergens. However, there are sporadic publications reporting potentially allergenic proteins in *A. thaliana*. The lipid transfer protein 1 in *A. thaliana* has been identified as a possible allergen (i.e. recognised by human IgE) (Chardin et al., 2003), and one case of occupational asthma was reported in a laboratory worker due to inhalation exposure to *A. thaliana* pollen (Yates et al., 2008). *A. thaliana* also contains profilins, small proteins which are thought to be responsible for certain types of allergies (Thorn et al., 1997). Finally, one study reported that the Arabidopsis genome encodes Pollen Ole e 1 domain-containing proteins (Hu et al., 2014) that are present in many plants (Jiménez-López et al., 2011).

Additional information on pathogenicity and the relationship to known pathogens

No reports were identified indicating that this plant causes disease in humans or animals.

Information on the past and present use, if any, in the food supply and exposure route(s) other than intended food use (e.g., possible presence as contaminants)

A. thaliana is not generally consumed as food. However, *A. thaliana* is a member of the mustard family, which includes several routinely consumed vegetables such as broccoli, cabbage, cauliflower, turnip, rapeseed, and radish.

Ostreococcus tauri

Information on naturally occurring toxins, antinutrients, and allergens

O. tauri is not known to produce or contain toxins, allergens, or antinutrients. Neither the COMPARE database[2], which includes a comprehensive repository of all known allergens with clinical evidence of allergenicity based on standardised criteria, nor the AllergenOnline

[5] http://comparedatabase.org/about-compare-database/
[6] http://www.allergenonline.org

database[3], which provides access to a peer-reviewed allergen list, retrieved any protein sequences from *O. tauri* that are known or putative allergens.

Additional information on pathogenicity and the relationship to known pathogens

O. tauri is not known to cause disease in humans or animals.

Information on the past and present use, if any, in the food supply and exposure route(s) other than intended food use (e.g., possible presence as contaminants)

O. tauri is not directly consumed as food or feed. However, as a green microalga, *O. tauri* is part of the marine phytoplankton community, the lowest tier in the aquatic food web, and is indirectly consumed by fish that ultimately could end up as human food.

Pavlova lutheri

Information on naturally occurring toxins, antinutrients, and allergens

Pavlova lutheri is not known to produce or contain toxins, antinutrients, or allergens. Neither the COMPARE database[2], which includes a comprehensive repository of all known allergens with clinical evidence of allergenicity based on standardised criteria, nor the AllergenOnline database[3], which provides access to a peer-reviewed allergen list, retrieved any protein sequences from *P. lutheri* that are known or putative allergens.

Additional information on pathogenicity and the relationship to known pathogens

P. lutheri is not known to cause disease in humans or animals. The *P. lutheri* culture available from the American Type Culture Collection (ATCC) is classified as Biosafety Level 1 (ATCC, 2017a). Organisms classified as Biosafety Level 1 are not known to cause disease in humans or animals based on classification by the U.S. Public Health Service (U.S. HHS et al., 2009) and the World Health Organization (WHO, 2004).

Information on the past and present use, if any, in the food supply and exposure route(s) other than intended food use (e.g., possible presence as contaminants)

P. lutheri is not consumed directly as food. *P. lutheri* is a marine microalga commonly used in the aquaculture industry to feed marine organisms (Ponis et al., 2006). It has been studied for its fatty acid production and its use as a live feed in bivalve hatcheries (Dhert and Sorgeloos, 1995; Brown, 2002; Ponis et al., 2003b; Carvalho and Malcata, 2005). *P. lutheri* is frequently used as part of aquafeed diets for carpet shells (Aranda-Burgos et al., 2014), Japanese bay scallop (Semura, 1995), Chilean scallop (Caers et al., 2003), great scallop (Delaunay et al., 1993; Gagné et al., 2012), giant sea scallop (Gouda et al., 2006), king scallop (Laing, 2000; Hawkins et al., 2005), Japanese pearl oyster (Numaguchi, 2000; Tomaru et al., 2002), European flat oysters (Jonsson et al., 1999; González-Araya et al., 2011; González-Araya et al., 2012; Ronquillo et al., 2012; González-Araya et al., 2013), black-lip pearl oyster (Doroudi et al., 2003), pacific oysters (Knauer et al., 1999; Ponis et al., 2003b; Ponis et al., 2008), the bivalve *Venus verrucosa* (Grémare et al., 1998), copepods (Brugnano et al., 2008), giant tiger prawn (D'Souza et al., 2000), sea urchin (Kashenko, 2007), and others. Accordingly, human consumption of P*. lutheri* would be expected to be primarily by indirect consumption of shellfish and other marine organisms.

Physcomitrella patens

Information on naturally occurring toxins, antinutrients, and allergens

P. patens is not known to produce or contain toxins, antinutrients, or allergens. *P. patens* has been used as an experimental organism for more than 80 years, and its use as a model to explore plant functions has increased in recent years (Cove et al., 2009). *P. patens* is regarded as an advantageous system to produce recombinant biopharmaceuticals (Decker et al., 2014; Reski et al., 2015). For example, oral vaccines produced in this moss are considered suitable for the formulation of orally administered vaccines since no toxic effects are attributed to the ingestion of this moss (Decker et al., 2014; Rosales-Mendoza et al., 2014).

Neither the COMPARE database[2], which includes a comprehensive repository of all known allergens with clinical evidence of allergenicity based on standardised criteria, nor the AllergenOnline database[3], which provides access to a peer-reviewed allergen list, retrieved any protein sequences in *P. patens* that are known or putative allergens.

Additional information on pathogenicity and the relationship to known pathogens

P. patens is not known to cause disease in humans or animals.

Information on the past and present use, if any, in the food supply and exposure route(s) other than intended food use (e.g., possible presence as contaminants)

P. patens is not consumed as food or feed.

Phytophthora infestans

Information on naturally occurring toxins, antinutrients, and allergens

P. infestans is not known to produce or contain toxins, antinutrients, or allergens. Neither the COMPARE database[2], which includes a comprehensive repository of all known allergens with clinical evidence of allergenicity based on standardised criteria, nor the AllergenOnline database[3], which provides access to a peer-reviewed allergen list, retrieved any protein sequences from *P. infestans* that are known or putative allergens.

Additional information on pathogenicity and the relationship to known pathogens

P. infestans is not known to cause disease in humans or animals. All *P. infestans* cultures available from the American Type Culture Collection (ATCC) are classified as Biosafety Level 1 (ATCC, 2017b). Organisms classified as Biosafety Level 1 are not known to cause disease to humans or animals based on classification by the U.S. Public Health Service (U.S. HHS et al., 2009) and the World Health Organization (WHO, 2004).

The genus *Phytophthora* contains a number of species that are known plant pathogens (Sandhu et al., 2005), and *P. infestans* is the cause of late blight, the most economically important disease of potato (Jo et al., 2014).

Like other plant pathogens, *P. infestans* has the ability to manipulate biochemical, physiological, and morphological processes in its host plants through a diverse array of virulence or avirulence molecules, defined as effectors (Kamoun, 2002). Recent characterisation of four oomycete avirulence (*Avr*) genes revealed that they encode effector proteins with a common modular structure, including a N-terminal conserved RXLR (arginine-any amino acid-leucine-arginine) motif. Several lines of evidence initially indicated

that these Avr proteins are secreted by the pathogen and then translocated into the host cell during infection (Morgan and Kamoun, 2007). To date, all experimentally verified *P. infestans Avr* genes encode RXLR effectors (Rodewald and Trognitz, 2013; Anderson et al., 2015).

Information on the past and present use, if any, in the food supply and exposure route(s) other than intended food use (e.g., possible presence as contaminants)

P. infestans is not consumed as food or feed.

Phytophthora sojae

Information on naturally occurring toxins, antinutrients, and allergens

P. sojae is not known to produce or contain toxins, antinutrients, or allergens. Neither the COMPARE database[2], which includes a comprehensive repository of all known allergens with clinical evidence of allergenicity based on standardised criteria, nor the AllergenOnline database[3], which provides access to a peer-reviewed allergen list, retrieved any protein sequences in *P. sojae* that are known or putative allergens.

Additional information on pathogenicity and the relationship to known pathogens

P. sojae is not known to cause disease in humans or animals. All *P. sojae* cultures available from the American Type Culture Collection (ATCC) are classified as Biosafety Level 1 (ATCC, 2017c). Organisms classified as Biosafety Level 1 are not known to cause disease humans or animals based on classification by the U.S. Public Health Service (U.S. HHS et al., 2009) and the World Health Organization (WHO, 2004).

The genus *Phytophthora* contains a number of species that are known plant pathogens (Sandhu et al., 2005). To manipulate host defences, plant pathogenic oomycetes like *P. sojae* secrete and translocate RXLR effectors into plant cells to promote virulence (Birch et al., 2008). These oomycete effector proteins have a common modular structure and contain an RXLR motif following an N-terminal signal peptide, which is thought to allow translocation into plant cells (Fawke et al., 2015).

Information on the past and present use, if any, in the food supply and exposure route(s) other than intended food use (e.g., possible presence as contaminants)

P. sojae is not consumed as food or feed.

Pythium irregulare

Information on naturally occurring toxins, antinutrients, and allergens

P. irregulare is not known to produce or contain toxins, antinutrients, or allergens. The suitability of *P. irregulare* as a producer of fatty acids for use in dietary supplements was evaluated, and the authors concluded that *P. irregulare* can be considered a safe source of biomass and EPA-containing oil for use as an ingredient in food, feed, and pharmaceuticals because there is no evidence showing that this species is associated with any disease or production of toxins affecting humans (Wu et al., 2013).

Neither the COMPARE database[2], which includes a comprehensive repository of all known allergens with clinical evidence of allergenicity based on standardised criteria, nor the AllergenOnline database[3], which provides access to a peer-reviewed allergen list, retrieved any protein sequences in *P. irregulare* that are known or putative allergens.

Additional information on pathogenicity and the relationship to known pathogens

P. irregulare is not known to cause disease in humans or animals. All *P. irregulare* cultures available from the American Type Culture Collection (ATCC) are classified as Biosafety Level 1 (ATCC, 2017d). Organisms classified as Biosafety Level 1 are not known to cause disease humans or animals based on classification by the U.S. Public Health Service (U.S. HHS et al., 2009) and the World Health Organization (WHO, 2004).

The genus *Pythium* has been widely recognised as a plant pathogen, infecting roots and colonizing the vascular tissues of various plants such as soybeans, corn, and other vegetables (Parveen and Sharma, 2014). Plant pathogenic oomycetes like *P. irregulare* secrete and translocate RXLR effectors into plant cells to promote virulence (Birch et al., 2008). These oomycete effector proteins have a common modular structure and contain an RXLR motif following an N-terminal signal peptide, which is thought to allow translocation into plant cells (Fawke et al., 2015).

Information on the past and present use, if any, in the food supply and exposure route(s) other than intended food use (e.g., possible presence as contaminants)

P. irregulare is not consumed as food or feed. However, *P. irregulare* can be considered a safe source of biomass or oil for use as ingredients in food and feed because there is no evidence showing that this species is associated with any disease or production of toxins affecting humans (Wu et al., 2013).

Thalassiosira pseudonana

Information on naturally occurring toxins, antinutrients, and allergens

T. pseudonana is not known to produce or contain antinutrients or allergens. *T. pseudonana* has been reported to produce the neurotoxin Beta-N-methylamino-L-alanine (BMAA) (Jiang et al., 2014), which is produced by many representative species of diatoms as well as by cyanobacteria and dinoflagellates (Lage et al., 2015). Nevertheless, *T. pseudonana* is frequently used as part of aquafeed diets (e.g., for bivalves and crustacean larvae) (Brown, 2002). In addition, T*. pseudonana*-derived biosilica has successfully been used to deliver chemotherapeutic drugs to cancer cells, indicating a non-toxic nature (Delalat et al., 2015). *T. pseudonana* has also been shown to produce small quantities of apo-fucoxanthinoid compounds during senescence, a phenomenon known to many diatoms (Shaw et al., 1995). Extracts from *T. pseudonana* displayed no feeding deterrent activity to model copepods in bioassays (Shaw et al., 1994).

Neither the COMPARE database[2], which includes a comprehensive repository of all known allergens with clinical evidence of allergenicity based on standardised criteria, nor the AllergenOnline database[3], which provides access to a peer-reviewed allergen list, retrieved any protein sequences in *T. pseudonana* that are known or putative allergens.

Additional information on pathogenicity and the relationship to known pathogens

T. pseudonana is not known to cause disease in humans or animals.

Information on the past and present use, if any, in the food supply and exposure route(s) other than intended food use (e.g., possible presence as contaminants)

T. pseudonana is not consumed as food. It is frequently used as part of aquafeed diets for marine organisms such as prawns (D'Souza et al., 2000), pacific oysters (Thompson and Harrison, 1992; Thompson et al., 1996), clams (Li et al., 2002; Liu et al., 2016), copepods (Harris, 1977), and basket cockle (Liu et al., 2009). Accordingly, human consumption of *T. pseudonana* is expected to be indirect via consumption of mussels, clams, and prawns.

Thraustochytrium sp.

Information on naturally occurring toxins, antinutrients, and allergens

Thraustochytrium sp. is not known to produce or contain toxins, antinutrients, or allergens. A number of Thraustochytrid species serve as sources of DHA used in dietary supplements and for DHA production in industry (Sijtsma and de Swaaf, 2004).

Neither the COMPARE database[2], which includes a comprehensive repository of all known allergens with clinical evidence of allergenicity based on standardised criteria, nor the AllergenOnline database[3], which provides access to a peer-reviewed allergen list, retrieve any protein sequences in *Thraustochytrium* sp. that are known or putative allergens.

Additional information on pathogenicity and the relationship to known pathogens

Thraustochytrium sp. is not known to cause disease in humans or animals.

Information on the past and present use, if any, in the food supply and exposure route(s) other than intended food use (e.g., possible presence as contaminants)

Thraustochytrium sp. is not directly consumed as food. *Thraustochytrium* sp. cells can be used as a source of naturally occurring carotenoids and as alternative fish feed to Nile tilapia (Atienza et al., 2012). A study regarding the Thraustochytrid *Schizochytrium* sp. found no reports in the literature of direct human consumption of Thraustochytrids (Hammond et al., 2001). However, indirect human consumption likely occurs as these organisms are consumed by filter-feeding marine invertebrates, including mussels and clams, and by fish that are consumed directly by humans (Bergé and Barnathan, 2005).

(ii) History of use of the organism in the food supply or history of human exposure to the organism through other than intended food use (e.g., as a normal contaminant).

Canola (*Brassica napus* L.)

The host organism, cultivated canola (*B. napus*), is an established agricultural field crop that has been grown for millennia as a source of food and feed and has a long history of safe use. *B. napus* is a member of the subtribe Brassicinae of the tribe Brassiceae of the Cruciferous (Brassicaceae) family, sometimes referred to as the mustard family (OECD, 1997). There are two types of *B. napus*: 1) oil-yielding oleiferous rape, of which one subset with specific quality characteristics is often referred to as "canola" (vernacular name), and 2) the tuber-bearing swede or rutabaga. Canola, the oleiferous type, can also be subdivided into spring and winter forms. Sanskrit writings of 2000 to 1500 BC directly refer to oleiferous *B. napus* forms (sarson types) and mustard. In Europe, domestication is believed to have occurred in the early Middle Ages. Commercial plantings of rapeseed are recorded in the Netherlands as early as the 16th

century. At that time rapeseed oil was used primarily as an oil for lamps. Later it came to be used as a lubricant in steam engines (OECD, 1997).

Although used widely as an edible oil in Asia, only through breeding for improved oil quality and the development of improved processing techniques has rapeseed oil become important in western countries. Since the Second World War, rapeseed production in Europe and Canada has increased dramatically as a result of improved oil and meal quality. Modern techniques of plant transformation and genotype identification using isozymes, restriction fragment length polymorphism (RFLP) markers, or random amplified polymorphic DNA (RAPD) markers will complement classical breeding for the production of other improved lines (Buzza, 2007). China, India, Europe, and Canada are now the top producers, although this crop can be successfully grown in the United States, South America, and Australia, where annual production has increased sharply over the last few years. Today, two species of *Brassica* have commercialised varieties with "double low" characteristics, i.e. low erucic acid content in the fatty acid profile and very low glucosinolate content in the meal, characteristics desirable for high-quality vegetable oil and high-quality animal feed. In North America these species (*B. napus* and *B. rapa*) are considered to be of "canola" quality (OECD, 1997).

B. napus is grown as a winter annual in regions where winter conditions do not result in very low temperatures, which would kill the plants. These biotypes typically require vernalisation before the onset of stem elongation, raceme development, flowering, and seed set. In North America and northern parts of Europe, a spring biotype of *B. napus* that requires no vernalisation prior to flowering is grown. These biotypes are typically lower yielding than the winter annual types, requiring considerably less time to complete their life cycle (OECD, 1997).

Information on the other organisms from which genetic elements are derived, the history of use in the food supply, and history of human exposure to the organisms is described for each individual organism in section A.2(a)(i) above.

Regulatory sequences

The promoter and terminator sequences used in LBFLFK canola are derived from common plants, aquatic organisms, microorganisms, or plant pathogens. These genetic elements constitute a minute component of their respective genomes; no genes that may be implicated in human disease, allergies, or toxic effects have been transferred. Many of these organisms from which these elements are derived are model species in plant science with a history of safe use. These elements are described in section A.3(b)(i).

Donor organisms from which the genetic elements are derived

See section A.2(a)(i) and section B.1(b).

(b) For the host organism into which the genes were transferred:

(i) Its history of safe use for food

The food and feed use of low erucic acid rapeseed has been well reviewed (OECD, 2011b). The harvested seeds are processed into two major products: oil and meal. The oil is used primarily for human consumption whereas the protein-containing meal is diverted to animal consumption (Heuzé et al., 2016). Food uses of the protein fractions have not been greatly reported but do represent another potential consumption route for low erucic acid rapeseed.

A limited number of Asian countries, including India, consume canola seed as a source of food (USDA-FAS, 2016).

Refined oil from low erucic acid rapeseed is used as an ingredient in a wide variety of consumer food goods and is also sold directly to consumers for home cooking applications. As such, it is the third largest source of vegetable oil (after soybean oil and palm oil) and oil meal (after soybean and cotton) in the world (Heuzé et al., 2016). In Australia, canola oil is used in frying and baking applications and is an ingredient in salad dressings, margarine, and a variety of other products. Canola oil appeals to health-conscious consumers because it has a low percentage of saturated fat and is free of artificial trans-fats. High-oleic acid canola varieties have been developed recently that are used in commercial high-temperature frying applications to replace partially hydrogenated oils (USDA-ERS, 2017). In some countries, such as Canada, low erucic acid rapeseed oil represents more than two-thirds of the vegetable oil consumed. In Australia the usage rate is lower; however, canola is the most sought-after soft oil (seed derived oil), represents approximately 45% of our total soft oils usage, and is found in a wide variety of food products and is commonly purchased for home use (AOF, 2019). In the case of animal feed, the meal left over after oil extraction is the primary feed product. In the United States, canola meal is primarily used by the dairy industry while in Australia, it is used primarily to feed poultry, pigs, and to a lesser extent in feedlots and aquaculture (AOF, 2004). Currently, the aquaculture operations industry uses fishmeal and fish oil as sources of EPA and DHA in the feed formulations that are prepared. Fishmeal and fish oil are still considered the most nutritious and digestible ingredients for farmed fish feeds, and most fish oil still goes into aquaculture feeds (FAO, 2016). As demand for fish oil has increased, it is recommended to substitute fishmeal and fish oil in animal feeds with alternative sources of EPA and DHA that could replace fish oil in feed. The Canola Council of Canada has pointed to the possibility of replacing fish oil with canola oil in aquafeed (Canola Council of Canada, 2015). There is a relatively limited supply of fish oil available, but an increasing demand for commercially reared fish and crustaceans. The replacement of fish oil with various vegetable oils has been widely documented, generally with very little impact on the growth performance of fish (Glencross and Turchini, 2011). Canola/rapeseed oil is the most widely used vegetable oils in diets for salmon and trout (Turchini et al., 2013) as it is highly desired due to its relatively low levels of omega-6 fatty acids and helps to maintain the omega-3:omega-6 ratio naturally found in fish. Up to 90% of the fish oil was replaced with canola oil in diets for rainbow trout with no loss in performance (Turchini et al., 2013).

As with any other crop, the nutrient composition of canola can vary due to environmental growing conditions, or due to the genetics or to processing factors. Canola meal needs to be adjusted to each type of animal and its needs (Canola Council of Canada, 2016a). Canola meal is an economical protein source for animals that do not have high energy or lysine requirements (USDA-ERS, 2017). Canola meal has a lower protein content than soybean meal (34 to 38% versus 44 to 49%) and lower content of essential amino acids. Therefore, as a protein feed for all classes of livestock, low erucic acid rapeseed is typically balanced with other protein ingredients (e.g., soybean meal, field peas). Because low erucic acid rapeseed meal typically contains about 30% hulls, it has a high fibre content, which limits its use in monogastric diets to approximately 15% of the total diet. Higher inclusion rates are practical in ruminant rations. Low erucic acid rapeseed meal can be used as the sole protein supplement for ruminants (i.e. approximately 30% of the total diet). De-hulled low erucic acid rapeseed meal has the potential to compete with soybean meal in swine and poultry diets.

However, when used as the only source of protein, it could result in lower animal performance (Heuzé et al., 2016). Low erucic acid rapeseed meal has also been used in aquaculture in many fish species, e.g., salmon, rainbow trout, catfish, and carp and in crustaceans like shrimp. However, the high fibre content in rapeseed meal could limit its nutritional value for carnivorous fish species. By balancing the rapeseed meal content in the diet, it is possible to limit the fibre content to no more than 8% to avoid impairing fish growth performance (Heuzé et al., 2016). The oil from low erucic acid rapeseed may also be used as a feed ingredient, with recommended inclusion rates for livestock at 3 to 4% and aquaculture at 10% to 20% (OECD, 2011b; Ytrestøyl et al., 2014).

(ii) The part of the organism typically used as food

The two primary products of LBFLFK canola used in food and feed, oil and meal respectively, are derived from the seed. The various food (and feed) uses of these products are detailed in section A.2(b)(i) above.

(iii) The types of products likely to include the food or food ingredient

See the information under section A.2(b)(i) above.

(iv) Whether special processing is required to render food derived from the organism safe to eat

Brief summary of canola processing

Several processing steps are involved in making canola oil and meal at a commercial processing facility (Unger, 2015), and these were followed to produce the samples for analysis. An overview of the processing steps is provided in Figure 1. To begin, cleaned and tempered canola grain is rolled or flaked with applied heat followed by crushing and pressing to produce the pressed oil fraction. The pressed oil and meal fractions are then processed separately according to end-product requirements. The canola meal remaining after pressing contains between 14–20% oil (OECD, 2011b). The remaining oil in the meal is extracted using hexane to produce defatted meal and extracted oil.

A physical blend of pressed oil and extracted oil (the combination referred to as crude oil herein) was produced for refining at a ratio of approximately 83:17% of pressed oil: extracted oil. This crude oil was further processed by refining, bleaching, and deodorizing. It is noted that pressed oil alone may also be used commercially. The resulting oil product is referred to as refined, bleached, and deodorised (RBD) oil. Additional details of processing canola into commercial equivalent fractions are provided in Unger (2015).

Figure 1. Flow Diagram for Preparation of Oil and Meal from Canola

Process steps are indicated in the right most column, and resulting products of the processing are indicated to the left.

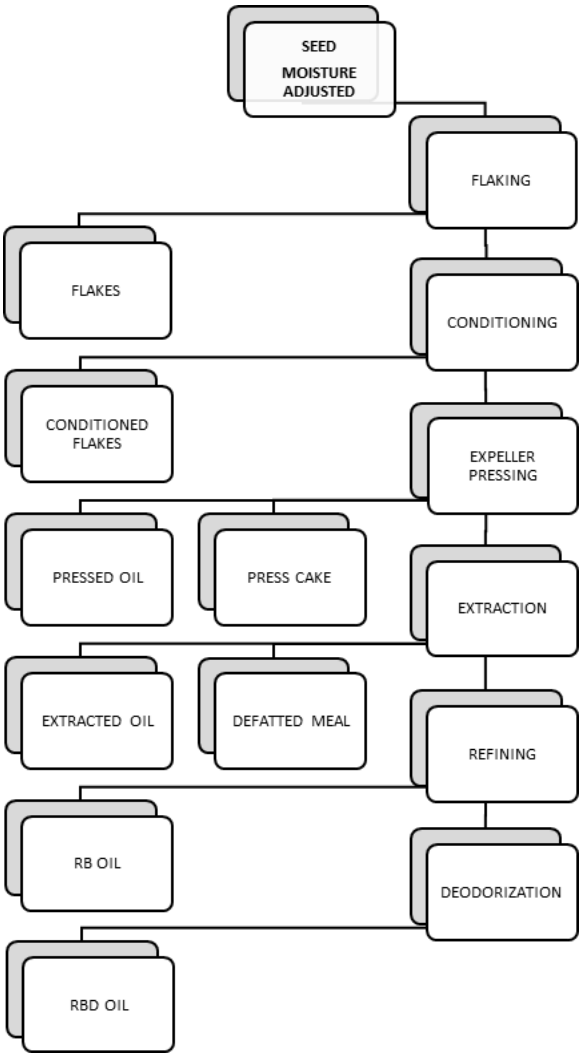

A.3 The Nature of the Genetic Modification

(a) A description of the method used to transform the host organism

Agrobacterium-mediated transformation of hypocotyl segments followed a modified De Block protocol (De Block et al., 1989). The host plant for EPA+DHA canola event LBFLFK is a canola cultivar of *Brassica napus* (L.). The transformation process used the commercial canola variety Kumily.

Hypocotyl segments of Kumily seedlings were inoculated with disarmed *Agrobacterium rhizogenes* strain SHA001 (Mankin et al., 2007) containing transformation plasmid vector LTM593 (see section A.3(b) below). After three days of co-cultivation, explants were transferred to plant growth medium containing the antibiotic carbenicillin to prevent Agrobacterium growth. Following seven days of recovery, the explants were transferred to selection medium containing imazethapyr (an imidazolinone herbicide) and cultured for two

weeks for selective regeneration of shoots. Herbicide-resistant shootlets were placed on medium facilitating shoot elongation and root development, and rooted shoots were transferred to soil for growth and further analysis. Transgenic plants (T_0 plants) regenerated via Agrobacterium-mediated transformation and tissue culture and subsequent T_1 and T_2 generations produced by selfing were characterised by molecular analyses, fatty acid profiles, agronomic evaluations, and herbicide efficacy analyses. Those plants that produced higher levels of EPA and DHA in the seed, that were imidazolinone herbicide tolerant, free of any vector backbone from LTM593, and that displayed normal phenotypic characteristics were advanced for further development. Based on its superior characteristics, event LBFLFK was selected as an elite candidate and evaluated further. A schematic overview of the transformation and development process of EPA+DHA canola event LBFLFK is depicted in Figure 2.

Figure 2. Schematic Depicting the Process of Canola Transformation and Development of EPA+DHA Canola Event LBFLFK

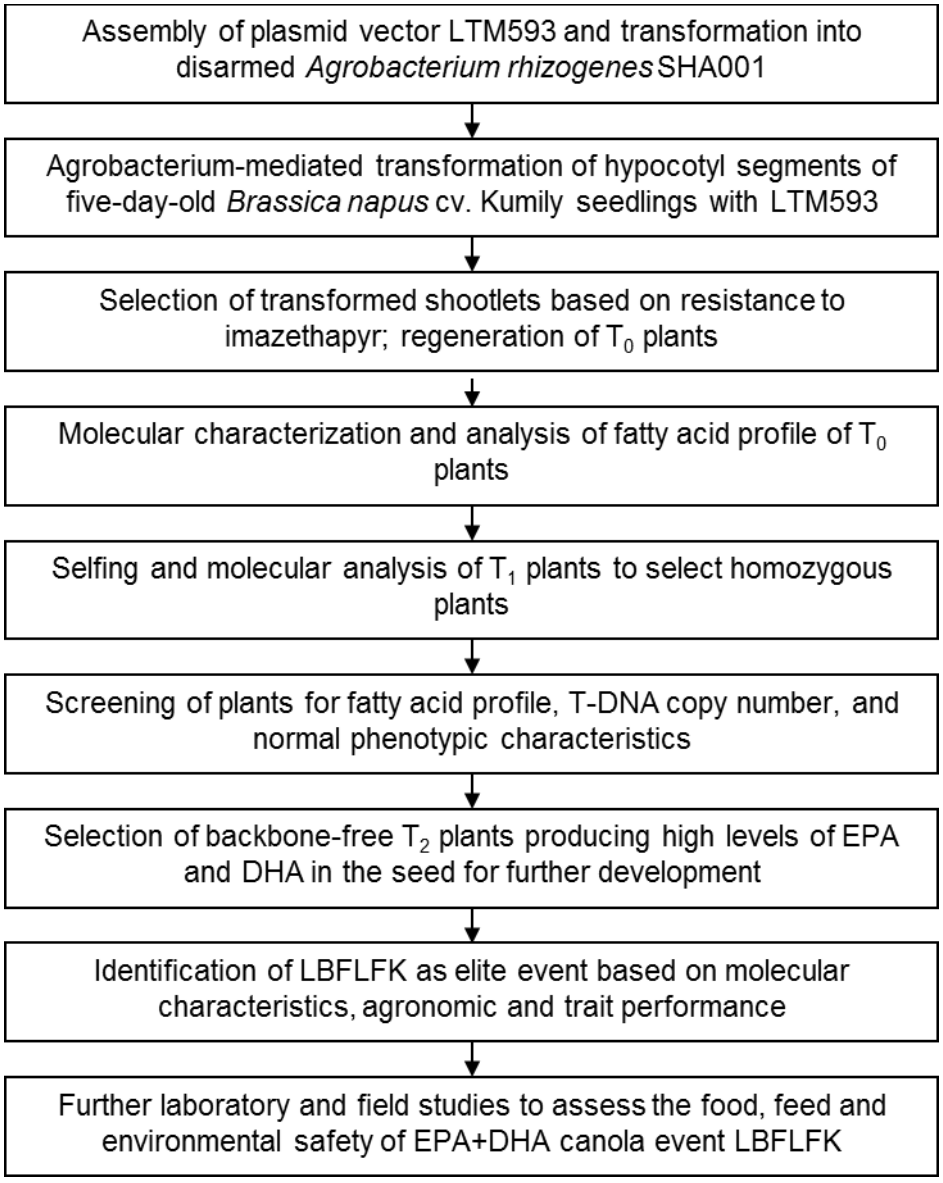

See Table 4 below and section A.3(b)(i) for a description of the vector.

(b) A description of the construct and the transformation vectors used, including:

(i) The size, source and function of all the genetic components including marker genes, regulatory and other elements; and

The construct LTM593 contains 13 expression cassettes. There are 12 fatty acid synthesis cassettes encoding 10 different fatty acid desaturases and elongases, of which D5D(*Tc*) and O3D(*Pir*) coding sequences are present twice, in two different expression cassettes (Figure 3). These, combined with the *Brassica napus* native fatty acid synthesis enzymes, enable

synthesis of EPA and DHA in the canola seeds. The T-DNA of vector LTM593 also encodes a mutant AHAS(*At*) protein with two amino acid substitutions (A122T and S653N) to confer tolerance to imidazolinone herbicides (Tan et al., 2005). This section describes the components of vector LTM593 that were used to generate EPA+DHA canola event LBFLFK.

The map of plasmid LTM593 is shown in Figure 3. The location, size, origin, and function of the genetic elements included in the plasmid are described in Table 4.

Figure 3. Circular Map of Plasmid LTM593

Plasmid LTM593 (also indicated as LTM593-1qcz) was used in Agrobacterium-mediated transformation to generate EPA+DHA canola event LBFLFK. Coding sequences are indicated by boxes with an arrowhead, with the orientation of the arrow showing the transcription direction. Arcs with arrowheads in the inner circle indicate the 13 expression cassettes, which are named after the respective coding sequences. In those instances where the same coding sequence is used twice (*c-D5D*(*Tc*) and *c-O3D*(*Pir*)), a suffix number is added to the cassette name in the inner circle.

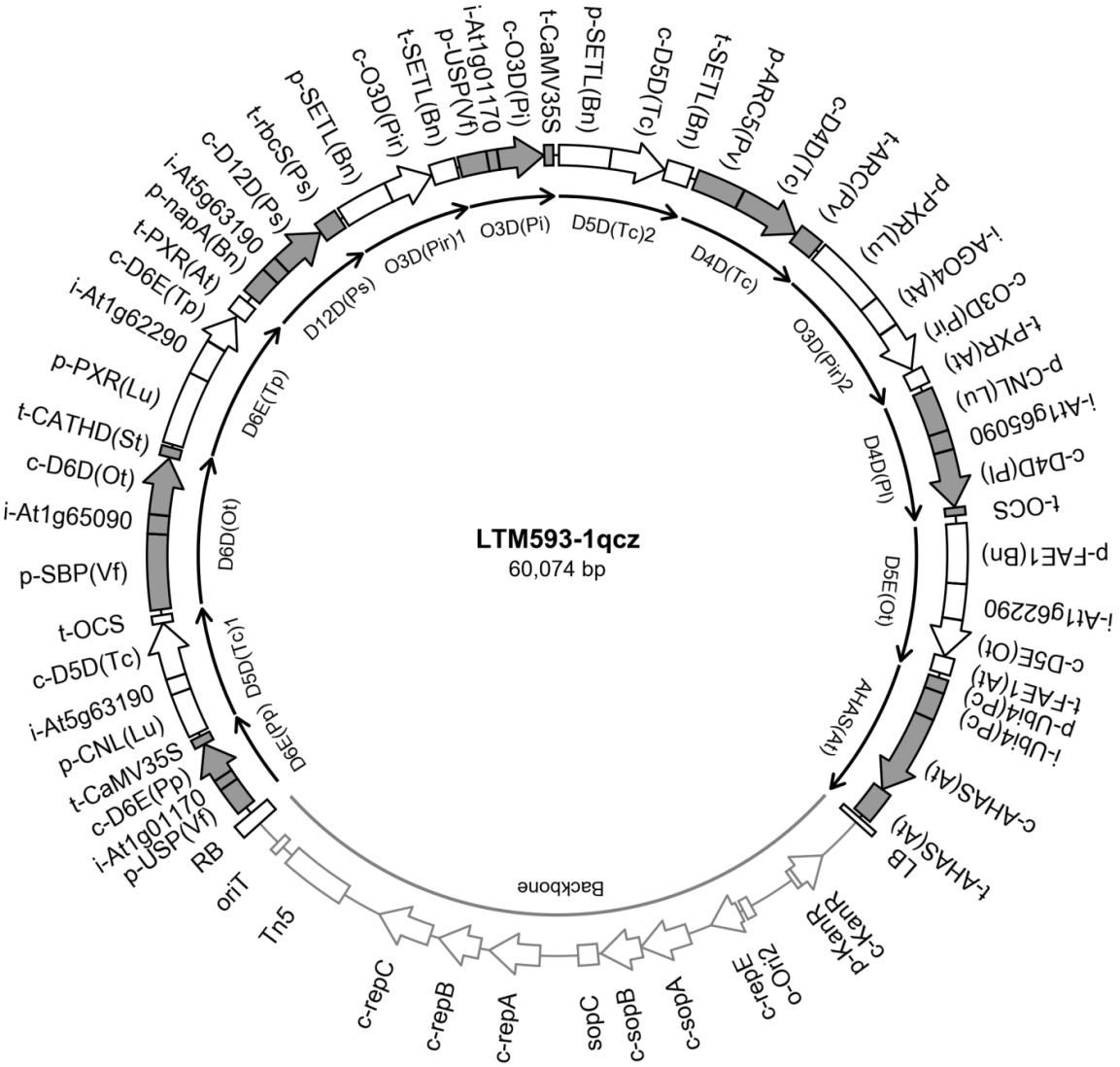

Genetic elements inside the T-DNA of LTM593

In this section, the fatty acid desaturases and elongases are listed in order of the introduced biosynthesis pathway—first the coding sequences, then the associated regulatory sequences.

D12D(*Ps*) coding sequence (*Phytophthora sojae*)

The D12D(*Ps*) coding sequence (*c-D12D*(*Ps*)) encodes the delta-12 desaturase protein, a polypeptide of 398 amino acids, approximately 46 kDa in size. The D12D(*Ps*) protein creates a double bond at the 12th position from the carboxyl end of oleic acid (OA) and catalyses the conversion of OA to linoleic acid (LA).

D6D(*Ot*) coding sequence (*Ostreococcus tauri*)

The D6D(*Ot*) coding sequence (*c-D6D*(*Ot*)) encodes the delta-6 desaturase protein, a polypeptide of 456 amino acids, approximately 52 kDa in size. The D6D(*Ot*) protein creates a double bond at the sixth position from the carboxyl end of LA and catalyses the conversion of LA to γ-linolenic acid (GLA).

D6E(*Tp*) coding sequence (*Thalassiosira pseudonana*)

The D6E(*Tp*) coding sequence (*c-D6E*(*Tp*)) encodes the delta-6 elongase protein, a polypeptide of 272 amino acids, approximately 32 kDa in size. The D6E(*Tp*) protein adds two carbon-hydrogen groups to the carboxyl end of GLA and catalyses the conversion of GLA to dihomo-gamma-linolenic acid (DGLA). The *c-D6E*(*Tp*) sequence introduced using LTM593 includes a sequence substitution such that the translated protein has one amino acid difference compared to the published protein sequence from the donor organism. The *c-D6E*(*Tp*) sequence encodes for a serine at position 196 while the published sequence from the donor organism encodes a proline at position 196. This P196S substitution does not occur in any known conserved domains responsible for the functionality of the D6E(*Tp*) protein (Leonard et al., 2004; Meyer et al., 2004).

D6E(*Pp*) coding sequence (*Physcomitrella patens*)

The D6E(*Pp*) coding sequence (*c-D6E*(*Pp*)) encodes the delta-6 elongase protein, a polypeptide of 290 amino acids, approximately 33 kDa in size. The D6E(*Pp*) protein adds two carbon-hydrogen groups to the carboxyl end of GLA and catalyses the conversion of GLA to DGLA.

D5D(*Tc*) coding sequence (*Thraustochytrium* sp.)

The D5D(*Tc*) coding sequence (*c-D5D*(*Tc*)) encodes the delta-5 desaturase protein, a polypeptide of 439 amino acids, approximately 50 kDa in size. The D5D(*Tc*) protein creates a double bond at the fifth position from the carboxyl end of DGLA and catalyses the conversion of DGLA to arachidonic acid (ARA). The *c-D5D*(*Tc*) sequence is present in two different expression cassettes in the T-DNA of LTM593.

O3D(*Pi*) coding sequence (*Phytophthora infestans*)

The O3D(*Pi*) coding sequence (*c-O3D*(*Pi*)) encodes the omega-3 desaturase protein, a polypeptide of 361 amino acids, approximately 41 kDa in size. The O3D(*Pi*) protein creates a double bond at the third position from the omega (methyl) end of ARA and catalyses the conversion of ARA to EPA.

O3D(*Pir*) coding sequence (*Pythium irregulare*)

The O3D(*Pir*) coding sequence (*c-O3D*(*Pir*)) encodes the omega-3 desaturase protein, a polypeptide of 363 amino acids, approximately 40 kDa in size. The O3D(*Pir*) protein creates a double bond at the third position from the omega (methyl) end of ARA and catalyses the conversion of ARA to EPA. The *c-O3D*(*Pir*) coding sequence is present in two different expression cassettes in the T-DNA of LTM593.

D5E(*Ot*) coding sequence (*Ostreococcus tauri*)

The D5E(*Ot*) coding sequence (*c-D5E*(*Ot*)) encodes the delta-5 elongase protein, a polypeptide of 300 amino acids, approximately 34 kDa in size. The D5E(*Ot*) protein adds two carbon-hydrogen groups to the carboxyl end of EPA and catalyses the conversion of EPA to docosapentaenoic acid (DPA).

D4D(*Tc*) coding sequence (*Thraustochytrium* sp.)

The D4D(*Tc*) coding sequence (*c-D4D*(*Tc*)) encodes the delta-4 desaturase protein, a polypeptide of 519 amino acids, approximately 59 kDa in size. The D4D(*Tc*) protein creates a double bond at the fourth position from the carboxyl end of DPA and catalyses the conversion of DPA to DHA.

D4D(*Pl*) coding sequence (*Pavlova lutheri*)

The D4D(*Pl*) coding sequence (*c-D4D*(*Pl*)) encodes the delta-4 desaturase protein, a polypeptide of 445 amino acids, approximately 49 kDa in size. The D4D(*Pl*) protein creates a double bond at the fourth position from the carboxyl end of DPA and catalyses the conversion of DPA to DHA.

AHAS(*At*) coding sequence (*Arabidopsis thaliana*)

The AHAS(*At*) coding sequence (*c-AHAS*(*At*)) encodes the large subunit of acetohydroxy acid synthase, a polypeptide of 670 amino acids, approximately 73 kDa in size. The AHAS(*At*) protein will catalyse the first step in the biosynthesis of branched-chain amino acids (Figure 4). The *c-AHAS*(*At*) sequence introduced using LTM593 includes sequence substitutions such that the translated protein has an alanine residue with a threonine at amino acid position 122 (A122T) and a serine residue with an asparagine at amino acid position 653 (S653N). These amino acid substitutions impair imidazolinone binding to the AHAS(*At*) large subunit protein, rendering plants containing the protein tolerant to treatment with imidazolinone herbicides (Haughn and Somerville, 1990; Tan et al., 2005).

Regulatory sequences

For a description of the regulatory sequences used, see section A.2.

Figure 4. Enzymatic Reactions Catalysed by Acetohydroxy Acid Synthase (AHAS)

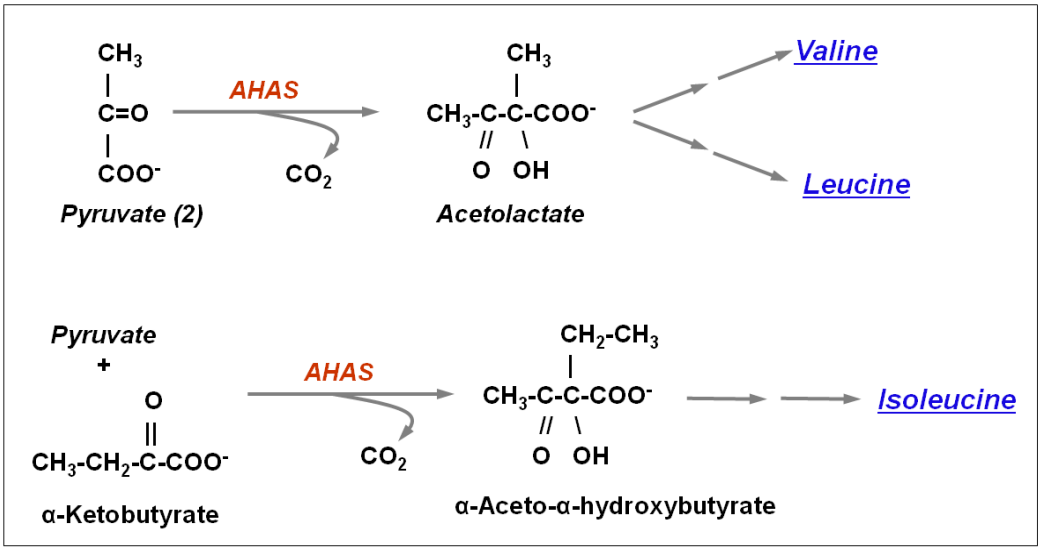

Table 4. Genetic Elements Comprising the LTM593 Vector Used in LBFLFK *B. napus*

Prefixes used in the table are as follows: p-, promoter; i-, intron-containing 5' untranslated region (UTR); *c*-, coding sequence; t-, transcription terminator; o-, origin of replication. In those instances where the same coding sequence is used twice (*c-D5D*(*Tc*) and *c-O3D*(*Pir*)), a suffix number is added to the name of the coding region.

Genetic element	Location in construct (size in base pairs)	Origin and function (reference)
T-DNA		
RB	1 – 328 (328)	*Agrobacterium tumefaciens*, octopine-type Ti plasmid pTi15955, right T-DNA border region, identical to section of GenBank®[7] nucleotide accession number AF242881 (Barker et al., 1983).
intervening sequence	329 – 508 (180)	Region required for cloning of genetic elements.
p-*USP*(*Vf*)	509 – 1192 (684)	*Vicia faba*, promoter region of unknown seed protein gene *USP* (Bäumlein et al., 1991), identical to section of GenBank nucleotide accession number HJ187156, and highly homologous to section of GenBank nucleotide accession number X56240.
i-*At1g01170*	1,193 – 1,444 (252)	*Arabidopsis thaliana*, intron-containing 5' UTR of locus At1g01170 (Nakabayashi et al., 2005).
intervening sequence	1,445 – 1,446 (2)	Region required for cloning of genetic elements.
***c-D6E*(*Pp*)**	1,447 – 2,319 (873)	*Physcomitrella patens*, delta-6 elongase (originally named as polyunsaturated fatty acid specific elongation enzyme 1, *PSE1*), codon optimised based on GenBanknucleotide accession number AF428243 (Zank et al., 2000; Zank et al., 2002).

[7] GenBank is a registered trademark of the United States Department of Health and Human Service.

Genetic element	Location in construct (size in base pairs)	Origin and function (reference)
t-*CaMV35S*	2,320 – 2,535 (216)	Cauliflower mosaic virus, CaMV35S terminator region, identical to section of GenBank nucleotide accession number AF234316 (Hajdukiewicz et al., 1994).
intervening sequence	2,536 – 2,627 (92)	Region required for cloning of genetic elements.
p-*CNL*(*Lu*)	2,628 – 3,691 (1064)	*Linum usitatissimum*, seed-specific promoter of *conlinin* gene (Truksa et al., 2003), identical to section of GenBank nucleotide accession number HJ187156.
i-*At5g63190*	3,692 – 4,068 (377)	*Arabidopsis thaliana*, intron-containing 5' UTR of locus At5g63190 (Sharma et al., 2007; Wang et al., 2008).
intervening sequence	4,069 – 4,071 (3)	Region required for cloning of genetic elements.
***c-D5D*(*Tc*)1**	4,072 – 5,391 (1,320)	*Thraustochytrium* sp., delta-5 desaturase, codon optimised based on GenBank nucleotide accession number AF489588 (Qiu et al., 2001).
t-*OCS*	5,392 – 5,583 (192)	*Agrobacterium tumefaciens*, octopine-type Ti plasmid pTi15955, terminator of octopine synthase gene (MacDonald et al., 1991), identical to section of the GenBank nucleotide accession number NC_002377.
intervening sequence	5,584 – 5,718 (135)	Region required for cloning of genetic elements.
p-*SBP*(*Vf*)	5,719 – 7,517 (1,799)	*Vicia faba*, promoter of a sucrose-binding protein-related gene (Grimes et al., 1992; Heim et al., 2001), active at late seed development stage, identical to GenBank nucleotide accession number LQ576466.
i-*At1g65090*	7,518 – 7,972 (455)	*Arabidopsis thaliana*, intron-containing 5' UTR of locus At1g65090 (Braybrook et al., 2006).
intervening sequence	7,973 – 7,981 (9)	Region required for cloning of genetic elements.
***c-D6D*(*Ot*)**	7,982 – 9,352 (1,371)	*Ostreococcus tauri*, delta-6 desaturase, codon optimised based on GenBank nucleotide accession number AY746357 (Domergue et al., 2005).
intervening sequence	9,353 – 9,379 (27)	Region required for cloning of genetic elements.
t-*CATHD*(*St*)	9,380 – 9,614 (235)	*Solanum tuberosum*, terminator of cathepsin D inhibitor gene (Hannapel, 1993), identical to section of GenBank nucleotide accession number HJ187168.
intervening sequence	9,615 – 9,692 (78)	Region required for cloning of genetic elements.
p-*PXR*(*Lu*)	9,693 – 11,419 (1,727)	*Linum usitatissimum*, seed-specific promotor of peroxiredoxin like protein gene *PXR* (Duwenig and Loyall, 2007), identical to GenBank nucleotide accession number HL700593.
i-*At1g62290*	11,420 – 12,265 (846)	*Arabidopsis thaliana*, intron-containing 5' UTR of locus At1g62290 (Chen et al., 2002).

Genetic element	Location in construct (size in base pairs)	Origin and function (reference)
intervening sequence	12,266 – 12,278 (13)	Region required for cloning of genetic elements.
***c-D6E*(*Tp*)**	12,279 – 13,097 (819)	*Thalassiosira pseudonana*, delta-6 elongase (Armbrust et al., 2004), codon optimised based on GenBank nucleotide accession number XM_002288445.
intervening sequence	13,098 – 13,152 (55)	Region required for cloning of genetic elements.
t-*PXR*(*At*)	13,153 – 13,552 (400)	*Arabidopsis thaliana*, terminator of peroxiredoxin (PXR)-like protein gene *PER1* (GenBank nucleotide accession number HL700651, At1g48130, (Haslekås et al., 1998)).
intervening sequence	13,553 – 13,721 (169)	Region required for cloning of genetic elements.
p-*napA*(*Bn*)	13,722 – 14,385 (664)	*Brassica napus*, seed-specific promoter of seed storage protein napin A/B gene (Ellerström et al., 1996; Rask et al., 1998), identical to GenBank nucleotide accession number LQ576463.
i-*At5g63190*	14,386 – 14,762 (377)	*Arabidopsis thaliana*, intron-containing 5' UTR of locus At5g63190 (Sharma et al., 2007; Wang et al., 2008).
intervening sequence	14,763 – 14,768 (6)	Region required for cloning of genetic elements.
***c-D12D*(*Ps*)**	14,769 – 15,965 (1,197)	*Phytophthora sojae*, delta-12 desaturase, codon optimised based on GenBank accession number GY508423 (Cirpus and Bauer, 2006).
intervening sequence	15,966 – 15,983 (18)	Region required for cloning of genetic elements.
t-*rbcS*(*Ps*)	15,984 – 16,541 (558)	*Pisum sativum*, terminator of RuBisCO small subunit gene (*rbcS*) E9 (Coruzzi et al., 1984; Smigocki, 1991), identical to section of GenBank nucleotide accession number AY572837.
intervening sequence	16,542 – 16,633 (92)	Region required for cloning of genetic elements.
p-*SETL*(*Bn*)	16,634 – 17,867 (1,234)	*Brassica napus*, seed-specific promoter of *SETL*(*Bn*) gene (Bauer and Senger, 2010), identical to a section of GenBank nucleotide accession number HC307781.
intervening sequence	17,868 – 17,869 (2)	Region required for cloning of genetic elements.
***c-O3D*(*Pir*)1**	17,870 – 18,961 (1,092)	*Pythium irregulare*, omega-3 desaturase, codon optimised based on GenBank nucleotide accession number FB753541 (Cheng et al., 2010).
intervening sequence	18,962 – 18,982 (21)	Region required for cloning of genetic elements.

Genetic element	Location in construct (size in base pairs)	Origin and function (reference)
t-*SETL*(*Bn*)	18,983 – 19,596 (614)	*Brassica napus*, terminator of *SETL*(*Bn*) gene (Bauer and Senger, 2010), identical to GenBank nucleotide accession number HC307782.
intervening sequence	19,597 – 19,674 (78)	Region required for cloning of genetic elements.
p-*USP*(*Vf*)	19,675 – 20,358 (684)	*Vicia faba*, promoter region of unknown seed protein gene *USP* (Bäumlein et al., 1991), identical to section of GenBank nucleotide accession number HJ187156, and highly homologous to section of GenBank nucleotide accession number X56240.
i-*At1g01170*	20,359 – 20,610 (252)	*Arabidopsis thaliana*, intron-containing 5' UTR of locus At1g01170 (Nakabayashi et al., 2005).
intervening sequence	20,611 – 20,620 (10)	Region required for cloning of genetic elements.
***c-O3D*(*Pi*)**	20,621 – 21,706 (1086)	*Phytophthora infestans*, omega-3 desaturase, codon optimised based on GenBank nucleotide accession number XM_002902553 (Wu et al., 2005).
intervening sequence	21,707 – 21,714 (8)	Region required for cloning of genetic elements.
t-*CaMV35S*	21,715 – 21,930 (216)	Cauliflower mosaic virus, CaMV35S terminator region, identical to section of GenBank nucleotide accession number AF234316 (Hajdukiewicz et al., 1994).
intervening sequence	21,931 – 22,065 (135)	Region required for cloning of genetic elements.
p-*SETL*(*Bn*)	22,066 – 23,299 (1234)	*Brassica napus*, seed-specific promoter of *SETL*(*Bn*) gene (Bauer and Senger, 2010), identical to a section of GenBank nucleotide accession number HC307781.
intervening sequence	23,300 – 23,301 (2)	Region required for cloning of genetic elements.
c-D5D*(*Tc*)*2	23,302 – 24,621 (1,320)	*Thraustochytrium* sp., delta-5 desaturase, codon optimised based on GenBank nucleotide accession number AF489588 (Qiu et al., 2001).
intervening sequence	24,622 – 24,642 (21)	Region required for cloning of genetic elements.
t-*SETL*(*Bn*)	24,643 – 25,256 (614)	*Brassica napus*, terminator of *SETL*(*Bn*) gene (Bauer and Senger, 2010), identical to GenBank nucleotide accession number HC307782.
intervening sequence	25,257 – 25,402 (146)	Region required for cloning of genetic elements.

Genetic element	Location in construct (size in base pairs)	Origin and function (reference)
p-*ARC5*(*Pv*)	25,403 – 26,553 (1,151)	*Phaseolus vulgaris*, seed–specific *Arcelin-5* gene promoter, identical to GenBank nucleotide accession number JC056714, and homologous to GenBank nucleotide accession number Z50202 (Goossens et al., 1994; Goossens et al., 1999).
intervening sequence	26,554 – 26,563 (10)	Region required for cloning of genetic elements.
***c*-*D4D*(*Tc*)**	26,564 – 28,123 (1,560)	*Thraustochytrium* sp., delta-4 desaturase, codon optimised based on GenBank nucleotide accession number GN042654 (Qiu et al., 2001).
intervening sequence	28,124 – 28,136 (13)	Region required for cloning of genetic elements.
t-*ARC*(*Pv*)	28,137 – 28,736 (600)	*Phaseolus vulgaris*, terminator of *Arc5* gene, identical to section of GenBank nucleotide accession number Z50202 (Goossens et al., 1994; Goossens et al., 1999).
intervening sequence	28,737 – 28,828 (92)	Region required for cloning of genetic elements.
p-*PXR*(*Lu*)	28,829 – 30,555 (1,727)	*Linum usitatissimum*, seed-specific promotor of peroxiredoxin like protein gene *PXR* (Duwenig and Loyall, 2007), identical to GenBank nucleotide accession number HL700593.
i-*AGO4*(*At*)	30,556 – 31,313 (758)	*Arabidopsis thaliana*, intron-containing 5' UTR of gene *AGO4*(*At*) (Zilberman et al., 2003).
intervening sequence	31,314 – 31,328 (15)	Region required for cloning of genetic elements.
***c*-*O3D*(*Pir*)2**	31,329 – 32,420 (1,092)	*Pythium irregulare*, omega-3 desaturase, codon optimised based on GenBank nucleotide accession number FB753541 (Cheng et al., 2010).
intervening sequence	32,421 – 32,476 (56)	Region required for cloning of genetic elements.
t-*PXR*(*At*)	32,477 – 32,876 (400)	*Arabidopsis thaliana*, terminator of peroxiredoxin (PXR)-like protein gene *PER1* (GenBank nucleotide accession number HL700651, At1g48130 (Haslekås et al., 1998)).
intervening sequence	32,877 – 33,011 (135)	Region required for cloning of genetic elements.
p-*CNL*(*Lu*)	33,012 – 34,075 (1064)	*Linum usitatissimum*, seed-specific promoter of *conlinin* gene (Truksa et al., 2003), identical to section of GenBank nucleotide accession number HJ187156.
i-*At1g65090*	34,076 – 34,530 (455)	*Arabidopsis thaliana*, intron-containing 5' UTR of locus At1g65090 (Braybrook et al., 2006).

Genetic element	Location in construct (size in base pairs)	Origin and function (reference)
intervening sequence	34,531 – 34,539 (9)	Region required for cloning of genetic elements.
***c-D4D*(*Pl*)**	34,540 – 35,877 (1338)	*Pavlova lutheri*, delta-4 desaturase, codon optimised based on GenBank nucleotide accession number AY332747 (Tonon et al., 2003).
intervening sequence	35,878 – 35,898 (21)	Region required for cloning of genetic elements.
t-*OCS*	35,899 – 36,090 (192)	*Agrobacterium tumefaciens*, octopine-type Ti plasmid pTi15955, terminator of octopine synthase gene (MacDonald et al., 1991), identical to section of the GenBank nucleotide accession number NC_002377.
intervening sequence	36,091 – 36,283 (193)	Region required for cloning of genetic elements.
p-*FAE1*(*Bn*)	36,284 – 37,713 (1,430)	*Brassica napus*, promoter of fatty acid elongase (*FAE1.1*) gene, identical to section of GenBank nucleotide accession number HC474755, and highly homologous to section of GenBank nucleotide accession number AF275254 (Han et al., 2001).
i-*At1g62290*	37,714 – 38,560 (847)	*Arabidopsis thaliana*, intron-containing 5' UTR of locus At1g62290 (aspartyl protease family protein) (Chen et al., 2002).
intervening sequence	38,561 – 38,567 (7)	Region required for cloning of genetic elements.
***c-D5E*(*Ot*)**	38,568 – 39,470 (903)	*Ostreococcus tauri*, delta-5 elongase (Crowe et al., 1994), codon optimised based on GenBank nucleotide accession number CS020159.
intervening sequence	39,471 – 39,486 (16)	Region required for cloning of genetic elements.
t-*FAE1*(*At*)	39,487 – 39,886 (400)	*Arabidopsis thaliana*, terminator of fatty acid elongase gene (*FAE1*) (Rossak et al., 2001), identical to section of GenBank nucleotide accession number HV571989.
intervening sequence	39,887 – 40,004 (118)	Region required for cloning of genetic elements.
p-*Ubi4*(*Pc*)	40,005 – 40,398 (394)	*Petroselinum crispum*, ubiquitin (Pcubi4-2) promoter, identical to section of GenBank nucleotide accession number X64345 (Kawalleck et al., 1993).
i-*Ubi4*(*Pc*)	40,399 – 40,986 (588)	*Petroselinum crispum*, ubiquitin gene intron in the 5' UTR, identical to section of GenBank nucleotide accession number JC289689, and highly homologous to section of GenBank nucleotide accession number X64345 (Kawalleck et al., 1993).
intervening sequence	40,987 – 40,993 (7)	Region required for cloning of genetic elements.

Genetic element	Location in construct (size in base pairs)	Origin and function (reference)
***c-AHAS*(*At*)**	40,994 – 43,006 (2,013)	*Arabidopsis thaliana*, acetohydroxy acid synthase large-subunit (Mazur et al., 1987) with S653N substitution and A122T substitution, highly homologous to GenBank nucleotide accession number NM_114714.
t-*AHAS*(*At*)	43,007 – 43,786 (780)	*Arabidopsis thaliana*, terminator of *AHAS*(*At*) gene (Mazur et al., 1987), highly homologous to a segment in GenBank nucleotide accession number CP002686.
intervening sequence	43,787 – 43,874 (88)	Region required for cloning of genetic elements.
LB	43,875 – 44,010 (136)	*Agrobacterium tumefaciens*, octopine-type Ti plasmid pTi15955, left T-DNA border region, identical to section of GenBank nucleotide accession number AF242881 (Barker et al., 1983).
Vector backbone		
intervening sequence	44,011 – 45,141 (1,131)	Bases 44170 to 44835 is a partial chloramphenicol acetyltransferase gene, including its promoter and partial coding sequence, identical to section of GenBank nucleotide accession number HQ245711.
c-KanR	Complement 45,142 – 45,957 (816)	*E. coli*, aminoglycoside 3'-phosphotransferase of kanamycin resistance transposon Tn*903* (Oka et al., 1981; Naumovski and Friedberg, 1983), identical to a section of GenBank nucleotide accession number V00359.
p-*KanR*	Complement 45,958 – 46,078 (121)	*E. coli*, promoter for aminoglycoside 3'-phosphotransferase gene of kanamycin resistance transposon Tn*903* (Naumovski and Friedberg, 1983), identical to a section of GenBank nucleotide accession number NZ_CP009789.
intervening sequence	46,079 – 47,230 (1152)	Region required for cloning of genetic elements.
o-*Ori2*	47,231 – 47,447 (217)	*E. coli*, replication origin (ori-2) of the F plasmid (Murotsu et al., 1984), identical to section of GenBank nucleotide accession number AP001918.
intervening sequence	47,448 – 47,540 (93)	Native intergenic sequence from the *E. coli* F plasmid.
c-repE	47,541 – 48,296 (756)	*E. coli*, *repE* gene of the F plasmid.
intervening sequence	48,297 – 48,874 (578)	Native intergenic sequence between *c-repE* and *c-sopA*.
c-sopA	48,875 – 50,050 (1,176)	*E. coli*, *sopA* gene of the F plasmid (Mori et al., 1986).
c-sopB	50,050 – 51,021 (972)	*E. coli*, *sopB* gene of the F plasmid.

Genetic element	Location in construct (size in base pairs)	Origin and function (reference)
intervening sequence	51,022 – 51,093 (72)	Native intergenic sequence between *sopB* and *sopC.*
sopC	51,094 – 51,567 (474)	*E. coli*, partial *sopC* region of the F plasmid required for plasmid partition (Helsberg and Eichenlaub, 1986; Mori et al., 1986).
intervening sequence	51,568 – 52,480 (913)	Sequence flanking the *repABC* operon from pTiC58, contains the promoter of operon *repABC* (Li and Farrand, 2000).
c-repA	52,481 – 53,698 (1,218)	*Agrobacterium tumefaciens*, *repA* gene from pTiC58 replicon (Li and Farrand, 2000).
intervening sequence	53,699 – 53,927 (229)	Native intergenic sequence in the *repABC* operon.
c-repB	53,928 – 54,938 (1,011)	*Agrobacterium tumefaciens*, *repB* gene from pTiC58 replicon (Li and Farrand, 2000).
intervening sequence	54,939 – 55,152 (214)	Native intergenic sequence in the *repABC* operon.
c-*repC*	55,153 – 56,472 (1,320)	*Agrobacterium tumefaciens*, *repC* gene from pTiC58 replicon (Li and Farrand, 2000).
intervening sequence	56,473 – 57,429 (957)	Region required for cloning of genetic elements.
Tn*5*	57,430 – 58,991 (1,562)	*E. coli*, transposon Tn*5* sequence (Beck et al., 1982), not required for the functionality of LTM593.
intervening sequence	58,992 – 59,286 (295)	Region required for cloning of genetic elements.
oriT	59,287 – 59,455 (169)	*Agrobacterium tumefaciens*, origin of conjugal transfer from pRK310 (Marx and Lidstrom, 2001).
intervening sequence	59,456 – 60,074 (619)	Region required for cloning of genetic elements.

(ii) A detailed map of the location and orientation of all the genetic components contained within the construct and vector, including the location of relevant restriction sites

The genetic elements of vector LTM593 are represented on the vector map (see Figure 3) and are further described in Table 4. LTM593 is 60,074 bp in length (Figure 3) and contains one T-DNA of 44,010 bp (Table 4). The T-DNA is delineated by left border and right border sequences that are derived from the *Agrobacterium tumefaciens* octopine-type plant tumour-inducing plasmid pTi15955 (Barker et al., 1983). The T-DNA contains 13 expression cassettes, with the *AHAS*(*At*) gene and 10 different fatty acid synthesis genes, of which two, D5D(*Tc*) and O3D(*Pir*), are present twice, each time in a different expression cassette. The origin, function, and position of each genetic element present in LTM593 are listed in Table 4, including a description of the prefixes used (e.g., p-, *c*-, t-, etc.). The coding sequences are described individually below followed by a description of the corresponding regulatory elements for each coding sequence.

The backbone region outside of the T-DNA contains genetic elements for the maintenance and selection of the plasmid in bacteria. Genetic elements present in the backbone region of vector LTM593 are summarised in section A.3(c) and also presented in Table 4.

The locations of restriction sites are not provided as restriction enzymes were not employed in the Next Generation Sequencing/Junction Sequence Analysis.

(c) A full molecular characterisation of the genetic modification in the new organism, including:

(i) Identification of all transferred genetic material and whether it has undergone any rearrangements

<u>The characterisation and description of the inserted genetic materials</u>

A comprehensive molecular characterisation of the genetic modification in EPA+DHA canola event LBFLFK was performed. The molecular characterisation consisted of a combination of different sequencing techniques, polymerase chain reaction (PCR), bioinformatic analysis, and genetic segregation studies and determined:

- the number of insertion sites and the number of inserts at each insertion site.
- the organisation and integrity of the inserts at each insertion site and whether genomic rearrangements have occurred upon integration.
- the characterisation of the DNA sequence of all inserted DNA, including flanking regions in the host genome.
- the absence of transformation vector backbone sequences in the LBFLFK genome.
- the identification of open reading frames (ORFs) created by the insertions with contiguous plant genomic DNA.
- the stability of the genetic modification through three generations and the pattern of inheritance.

A schematic representation of the methodology and the basis of the molecular characterisation of LBFLFK canola is illustrated in Figure 5. See section A.3(c)(iv) and Figure 6 for further information on the rearrangements present in the transferred the genetic material.

Figure 5. Molecular Characterisation Strategy

The left text boxes identify the major experimental and analytical processes that were used to achieve the LBFLFK molecular characterisation endpoints, which are listed in the right text boxes.

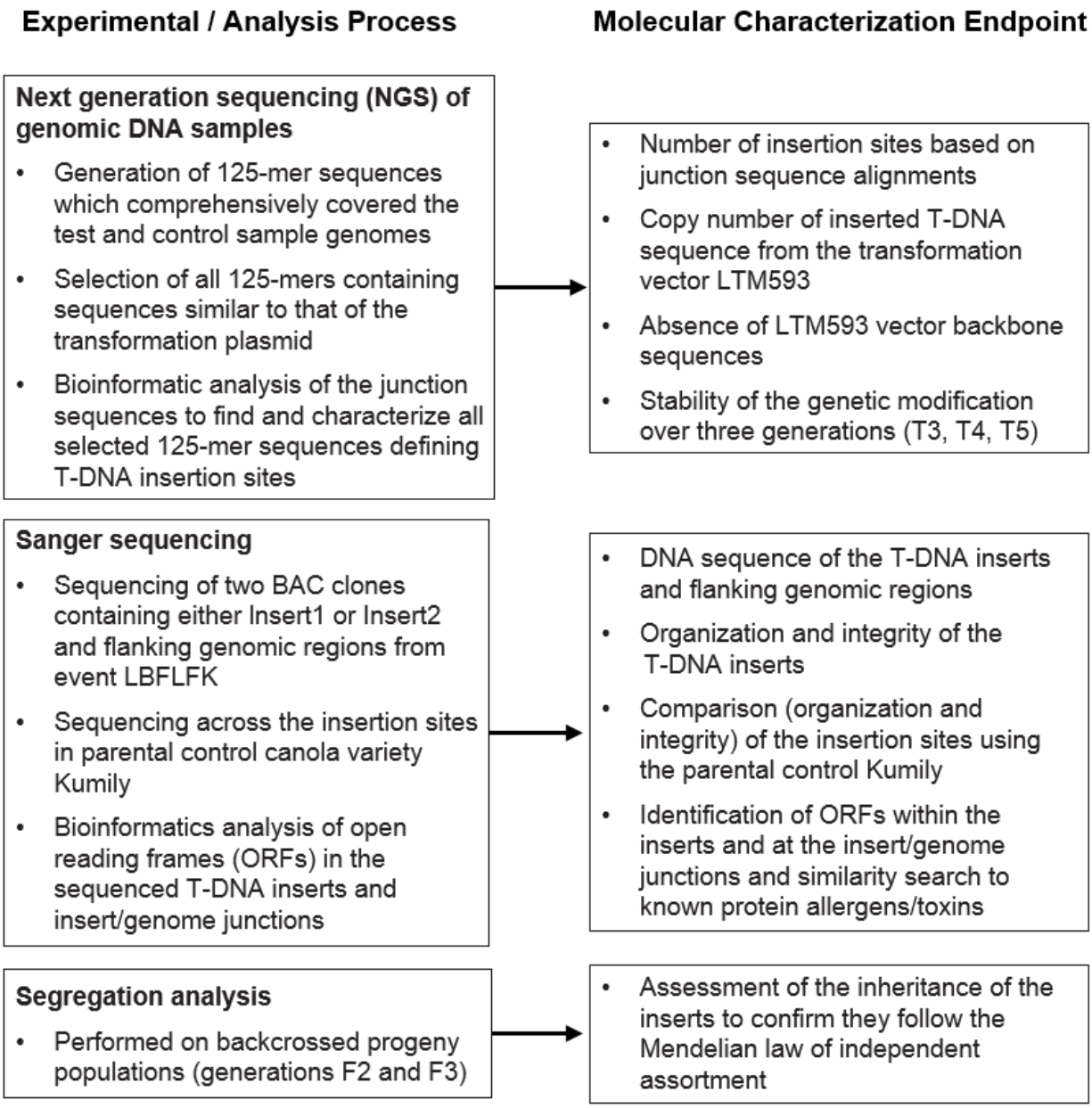

For next-generation sequencing (NGS), genomic DNA (gDNA) was isolated from three generations of LBFLFK (generations T3, T4, and T5). Using an Illumina® HiSeq™ 2500 system, hundreds of millions of randomly-distributed sequence reads of approximately 125 DNA bp were produced. The sequence reads were mapped to the transformation vector LTM593 using bioinformatics tools. The reads that had sequence similarity to LTM593 were selected and characterised. The number of inserts and insertion sites were then determined by analysing the selected sequence reads for novel sequence junctions containing sequence from both LTM593 and the canola genome. In addition, the presence or absence of unintended vector backbone sequences was demonstrated by a lack of sequence reads that matched the LTM593 backbone. The stability of inserted DNA over multiple generations (generations T3, T4, and T5) was demonstrated by comparing the novel junctions and distribution of sequencing reads over the T-DNA insert sequences in those three generations.

To determine the DNA sequences of the inserted material and the flanking regions of the host canola genome, locus-specific PCR and Sanger sequencing were used. To isolate each locus, LBFLFK gDNA was used to prepare a bacterial artificial chromosome (BAC) library. Two BAC clones were identified that separately contained Insert1 and Insert2 along with flanking genomic DNA sequences on each side of the inserts. DNA isolated from these two BACs was used for PCR and sequencing analysis of the two inserts of event LBFLFK along with approximately 1 kb of all flanking sequences. The resulting sequences demonstrated the organisation and integrity of the T-DNA inserts. To assess whether rearrangements or deletions had occurred in the canola genome at the insertion sites, sequences corresponding to each LBFLFK insertion site were isolated and analysed using the gDNA of the parental control variety Kumily and applying PCR followed by Sanger sequencing.

The sequence results from both loci in event LBFLFK were further analysed using bioinformatics to identify ORFs within the inserts and at the junctions between the T-DNA inserts and the canola genome. The deduced amino acid sequences of these ORFs were compared against known protein allergens and toxins.

Finally, segregation analysis of second (F_2) and third filial generation (F_3) offspring after a cross of LBFLFK with Kumily was conducted to demonstrate the stable and independent inheritance (according to Mendelian principles) of the two inserts.

The materials and methods used for achieving the endpoints of the molecular characterisation of LBFLFK are summarised in Table 5. For further details of the materials and methods used, refer to Appendix 3 (CCI).

Table 5. Materials and Methods Used to Achieve Specific Endpoints in the Molecular Characterisation of Canola Event LBFLFK

Characterisation Endpoint	Material	Method
• Number of T-DNA inserts • Number of insertion sites	gDNA LBFLFK, T3 generation	NGS/bioinformatics to map sequence reads and identify split-read clusters partially aligning to T-DNA in LTM593 and partially aligning to host gDNA
• Number of insertion sites	gDNA Kumily	NGS/bioinformatics to identify false positive junctions (genomic canola sequences that are also present in the T-DNA construct)
• Confirm absence of vector backbone	gDNA LBFLFK, T3 generation	NGS/bioinformatics to check alignment of sequence reads with vector backbone sequence)
• Confirm absence of vector backbone	gDNA Kumily spiked LTM593 plasmid DNA	NGS/bioinformatics to demonstrate sufficient sensitivity of NGS/bioinformatics pipeline
• Sequence of T-DNA inserts and flanking regions (organisation and integrity)	BAC containing LBFLFK Insert1 and LBFLFK Insert2, generated from T3 leaf material	Sanger sequencing for locus-specific PCR and sequence analysis
• Check for rearrangements at insertion sites	gDNA Kumily	PCR/Sanger DNA sequencing of Locus1 and Locus2
• Similarity of unintended ORFs to known toxins and allergens	BACs containing LBFLFK Insert1 and LBFLFK Insert2	Bioinformatics analysis of DNA sequence obtained by Sanger sequencing
• Stability of genetic modification over multiple generations	gDNA LBFLFK, generations T3, T4, T5	NGS/bioinformatics to confirm no generational changes in split reads
• Mendelian inheritance	Seeds of F_2 and F_3 generations	Segregation analysis by locus-specific PCR

Seven desaturases and three elongases were introduced into LBFLFK canola, resulting in the production of omega-3 LC-PUFAs, specifically DHA and its biosynthetic intermediate EPA, from canola endogenous fatty acids. In addition, a herbicide tolerance trait is conferred through the introduction of a modified acetohydroxy acid synthase (AHAS) protein from *A. thaliana*. The coding sequences in the T-DNA of plasmid vector LTM593 are derived from different eukaryotic organisms (Table 6).

Table 6. Designation and Donor Organisms of the Newly Expressed Proteins in LTM593

The fatty acid desaturases and elongases are listed in order of the introduced biosynthesis pathway (Figure 4).

Coding sequence designation	Enzyme full name	Enzyme abbreviation	Donor organism
c-D12D(*Ps*)	Delta-12 desaturase (*Ps*)	D12D(*Ps*)	*Phytophthora sojae*
c-D6D(*Ot*)	Delta-6 desaturase (*Ot*)	D6D(*Ot*)	*Ostreococcus tauri*
c-D6E(*Tp*)	Delta-6 elongase (*Tp*)	D6E(*Tp*)	*Thalassiosira pseudonana*
c-D6E(*Pp*)	Delta-6 elongase (*Pp*)	D6E(*Pp*)	*Physcomitrella patens*
c-D5D(*Tc*)	Delta-5 desaturase (*Tc*)	D5D(*Tc*)	*Thraustochytrium* sp.
c-O3D(*Pir*)	Omega-3 desaturase (*Pir*)	O3D(*Pir*)	*Pythium irregulare*
c-O3D(*Pi*)	Omega-3 desaturase (*Pi*)	O3D(*Pi*)	*Phytophthora infestans*
c-D5E(*Ot*)	Delta-5 elongase (*Ot*)	D5E(*Ot*)	*Ostreococcus tauri*
c-D4D(*Tc*)	Delta-4 desaturase (*Tc*)	D4D(*Tc*)	*Thraustochytrium* sp.
c-D4D(*Pl*)	Delta-4 desaturase (*Pl*)	D4D(*Pl*)	*Pavlova lutheri*
c-AHAS(*At*)	Acetohydroxy acid synthase	AHAS(*At*)	*Arabidopsis thaliana*

To achieve the optimal translation rate, the sequences encoding the fatty acid synthesis enzymes were optimised for codon usage in *B. napus*. In addition, the nucleotide sequences were modified to remove the following elements: (i) additional open reading frames (ORFs) longer than 90 bp in sense and anti-sense directions, (ii) ORFs within 30 bp after the start codon in sense direction, (iii) internal TATA-boxes, chi sequences and ribosomal entry sites, (iv) AT-rich or GC-rich sequence stretches, (v) RNA instability motifs, (vi) RNA secondary structures and repeat sequences and (vii) possible cryptic intron splice donor and acceptor sites in higher eukaryotes. Regarding the AHAS(*At*) coding sequence, a few nucleotide changes were introduced to eliminate unwanted restriction sites. These changes did not result in a change to the amino acid sequence of the protein. In addition, the coding sequence contains two mutations that result in the desired amino acid substitutions [A122T] and [S653N] that confer herbicide tolerance. In the following, the fatty acid desaturases and elongases are listed in order of the introduced biosynthesis pathway (Figure 4).

To demonstrate that the nucleotide sequences in LTM593 would have the same translated amino acid sequences of the encoded proteins as those found in the donor organisms, pairwise amino acid sequence alignment using ClustalW was applied (Thompson et al., 1994). A comparison between the deduced amino acid sequences of the fatty acid desaturases and elongases present in LTM593 and the respective amino acid sequences from the donor organisms established that no changes were introduced in the plasmid for all but one coding sequence (see amino acid sequence alignments in Appendix 4 (CCI)). The *c-D6E*(*Tp*) sequence encodes for a serine at position 196 while the published sequence (Armbrust et al.,

2004) from the donor organism encodes a proline at position 196. This [P196S] substitution does not occur in any known conserved domains responsible for the functionality of the D6E(*Tp*) protein (Leonard et al., 2004; Meyer et al., 2004). Pairwise amino acid sequence alignment between the deduced amino acid sequence of AHAS(*At*) present in LTM593 and the respective amino acid sequence from Arabidopsis showed that only the intended amino acid changes [A122T] and [S653N] were introduced.

The coding sequences are described individually below followed by a description of the corresponding regulatory elements for each coding sequence.

Coding sequences

D12D(Ps) coding sequence

The D12D(*Ps*) coding sequence (*c-D12D*(*Ps*)) encodes the delta-12 desaturase protein, a polypeptide of 398 amino acids approximately 46 kDa in size. The *c-D12D*(Ps) sequence (Cirpus and Bauer, 2006) is derived from the common oomycete (water mould) species *Phytophthora sojae*. The D12D(*Ps*) protein creates a double bond at the 12th position from the carboxyl end of oleic acid (OA) and catalyses the conversion of OA to linoleic acid (LA).

D6D(Ot) coding sequence

The D6D(*Ot*) coding sequence (*c-D6D*(*Ot*)) encodes the delta-6 desaturase protein, a polypeptide of 456 amino acids approximately 52 kDa in size. The *c-D6D*(*Ot*) sequence (Domergue et al., 2005) is derived from the unicellular marine green alga species *Ostreococcus tauri*. The D6D(*Ot*) protein creates a double bond at the sixth position from the carboxyl end of LA and catalyses the conversion of LA to gamma-linolenic acid (GLA).

D6E(Tp) coding sequence

The D6E(*Tp*) coding sequence (*c-D6E*(*Tp*)) encodes the delta-6 elongase protein, a polypeptide of 272 amino acids approximately 32 kDa in size. The *c-D6E*(*Tp*) sequence (Armbrust et al., 2004) is derived from the unicellular marine diatom alga species *Thalassiosira pseudonana*. The D6E(*Tp*) protein adds two carbon-hydrogen groups to the carboxyl end of GLA and catalyses the conversion of GLA to dihomo-gamma-linolenic acid (DGLA). The *c-D6E*(*Tp*) sequence introduced using LTM593 includes a sequence substitution such that the translated protein has one amino acid difference compared to the published protein sequence from the donor organism. The *c-D6E*(*Tp*) sequence encodes for a serine at position 196 while the published sequence from the donor organism encodes a proline at position 196. This [P196S] substitution does not occur in any known conserved domains responsible for the functionality of the D6E(*Tp*) protein (Leonard et al., 2004; Meyer et al., 2004).

D6E(Pp) coding sequence

The D6E(*Pp*) coding sequence (*c-D6E*(*Pp*)) encodes the delta-6 elongase protein, a polypeptide of 290 amino acids approximately 33 kDa in size. The *c-D6E*(*Pp*) sequence (Zank et al., 2000; Zank et al., 2002) is derived from the moss species *Physcomitrella patens*. The D6E(*Pp*) protein adds two carbon-hydrogen groups to the carboxyl end of GLA and catalyses the conversion of GLA to DGLA.

D5D(Tc) coding sequence

The D5D(*Tc*) coding sequence (*c-D5D*(*Tc*)) encodes the delta-5 desaturase protein, a polypeptide of 439 amino acids approximately 50 kDa in size. The *c-D5D*(*Tc*) sequence (Qiu et al., 2001) is derived from the marine protist *Thraustochytrium* sp. The D5D(*Tc*) protein creates a double bond at the fifth position from the carboxyl end of DGLA and catalyses the conversion of DGLA to arachidonic acid (ARA). The *c-D5D*(*Tc*) sequence is present in two different expression cassettes in the T-DNA of LTM593.

O3D(Pir) coding sequence

The O3D(*Pir*) coding sequence (*c-O3D*(*Pir*)) encodes the omega-3 desaturase protein, a polypeptide of 363 amino acids approximately 40 kDa in size. The *c-O3D*(*Pir*) sequence (Cheng et al., 2010) is from the common oomycete (water mould) species *Pythium irregulare*. The O3D(*Pir*) protein creates a double bond at the third position from the omega (methyl) end of ARA and catalyses the conversion of ARA to EPA. The *c-O3D*(*Pir*) coding sequence is present in two different expression cassettes in the T-DNA of LTM593.

O3D(Pi) coding sequence

The O3D(*Pi*) coding sequence (*c-O3D*(*Pi*)) encodes the omega-3 desaturase protein, a polypeptide of 361 amino acids approximately 41 kDa in size. The *c-O3D*(*Pi*) sequence (Wu et al., 2005) is from the common oomycete (water mould) species *Phytophthora infestans*. The O3D(*Pi*) protein creates a double bond at the third position from the omega (methyl) end of ARA and catalyses the conversion of ARA to EPA.

D5E(Ot) coding sequence

The D5E(*Ot*) coding sequence (*c-D5E*(*Ot*)) encodes the delta-5 elongase protein, a polypeptide of 300 amino acids approximately 34 kDa in size. The *c-D5E*(*Ot*) sequence (Zank et al., 2005) is from the unicellular marine green alga species *O. tauri*. The D5E(*Ot*) protein adds two carbon-hydrogen groups to the carboxyl end of EPA and catalyses the conversion of EPA to docosapentaenoic acid (DPA).

D4D(Tc) coding sequence

The D4D(*Tc*) coding sequence (*c-D4D*(*Tc*)) encodes the delta-4 desaturase protein, a polypeptide of 519 amino acids approximately 59 kDa in size. The *c-D4D*(*Tc*) sequence (Qiu et al., 2001) is from the marine protist *Thraustochytrium* sp. The D4D(*Tc*) protein creates a double bond at the fourth position from the carboxyl end of DPA and catalyses the conversion of DPA to DHA.

D4D(Pl) coding sequence

The D4D(*Pl*) coding sequence (*c-D4D*(*Pl*)) encodes the delta-4 desaturase protein, a polypeptide of 445 amino acids approximately 49 kDa in size. The *c-D4D*(*Pl*) sequence (Tonon et al., 2003) is from the unicellular marine photosynthetic alga species *Pavlova lutheri*. The D4D(*Pl*) protein creates a double bond at the fourth position from the carboxyl end of DPA and catalyses the conversion of DPA to DHA.

AHAS(At) coding sequence

The AHAS(*At*) coding sequence (*c-AHAS*(*At*)) encodes the large subunit of acetohydroxy acid synthase, a polypeptide of 670 amino acids approximately 73 kDa in size. The *c-AHAS*(*At*) sequence (Mazur et al., 1987) is derived from the plant species *A. thaliana*. The AHAS(*At*) protein catalyses the first step in the biosynthesis of branched-chain amino acids (Figure 4). The *c-AHAS*(*At*) sequence introduced using LTM593 includes sequence substitutions such that the translated protein has an alanine residue with a threonine at amino acid position 122 [A122T] and a serine residue with an asparagine at amino acid position 653 [S653N]. These amino acid substitutions impair imidazolinone binding to the AHAS(*At*) large subunit protein, rendering plants containing the protein tolerant to treatment with imidazolinone herbicides (Haughn and Somerville, 1990; Tan et al., 2005).

Regulatory sequences

For a description of the regulatory sequences used, see section A.2.

(ii) A determination of the number of insertion sites, and the number of copies at each insertion site

The organisation of the inserted genetic material at each insertion site, including copy number and absence of vector backbone

Background information about the use of next-generation sequencing (NGS)

Safety assessments of biotechnology-derived crops include a detailed molecular characterisation of the inserted DNA (Codex Alimentarius Commission, 2009b). Historically, molecular characterisation has relied on Southern blot analysis along with targeted sequencing of PCR products spanning any inserted DNA to establish the number of loci and T-DNA inserts as well as to determine the absence of vector backbone. Improvements in sequencing technologies, such as the use of next generation sequencing (NGS) (Shendure and Ji, 2008; Zhang et al., 2011), have enabled alternative methods for molecular characterisation that do not require Southern blot analysis. Genomic DNA from LBFLFK and Kumily was sequenced using an NGS approach. NGS in combination with bioinformatics analysis is used to address molecular characterisation endpoints in an equivalent way to those achieved with Southern blot-based methods.

The usefulness of NGS data as an alternative to Southern blots in the characterisation of DNA insertions has been shown previously (Kovalic et al., 2012; Zastrow-Hayes et al., 2015). There are multiple advantages to using NGS and bioinformatics, most notably the robustness, simplicity, and consistency of the method compared with Southern blot studies, which require a customised experimental design for every transformation event. New sequencing-based methods overcome many technical challenges inherent in Southern blot analyses (e.g., false positive hybridisation bands resulting from incomplete digestion or star activity and the need for radioactively-labelled probes) and provide higher reproducibility because they are less dependent on complex lab-based procedures.

Quality of the NGS analysis method

The computational pipeline used to analyse NGS data combined bioinformatics tools and parsing algorithms to assess the number of T-DNA inserts, the absence of a transformation vector backbone, and the stability of the inserted T-DNA over three generations.

NGS of a gDNA library results in millions of short DNA sequences (reads) that are derived from all possible positions of the gDNA. The term "read depth" indicates the number of reads that map to a given genomic position. It has been demonstrated that a ≥ 75X read depth of a genome is adequate to provide comprehensive coverage (Kovalic et al., 2012).

Six single-copy endogenous reference genes were used for read uniformity analysis and to demonstrate that the gDNA was sequenced without bias. The minimum average read depth was 160X across both the T-DNA and each of the six single-copy endogenous reference genes for all samples. One hundred percent read breadth with at least 50X read depth for T-DNA in LBFLFK samples and for the six single-copy endogenous reference genes in all analysed gDNA samples was also obtained. Additionally, 100% coverage of vector LTM593 in a Kumily sample spiked with 0.1X equivalent copies of the vector plasmid DNA further demonstrated the sensitivity of the NGS analysis.

Determination of the number of insertion sites and insert copy number

The number of insertion sites of LTM593 DNA in LBFLFK was assessed in T3 seed by NGS technology and subsequent bioinformatics analysis.

Any genomic insertion of DNA sequence from the transformation vector will produce two junctions between the plant genome sequence and the T-DNA insert, one at the 5´ end and one at the 3´ end of the inserted T-DNA. These junction sequences (also called "split-reads") are partially aligned to the host genome and partially aligned to the T-DNA sequence of the transformation vector (Kovalic et al., 2012). Therefore, the number of insertion sites can be deduced from the number of unique junction sequence classes found.

It is noted that, because the LTM593 transformation vector T-DNA contains sequences derived from the canola genome (i.e. the seed-specific promoters), false positive (not unique) junction sequences were identified using Kumily gDNA. These false-positive junctions, found in all LBFLFK and Kumily sequence samples, were eliminated as a step of the NGS bioinformatics pipeline.

Four unique classes of split-read clusters that partially aligned to the T-DNA of vector LTM593 and partially aligned to the host genome sequences were identified in LBFLFK. Two of the four classes of unique junctions aligned partially to the left border (LB) of the vector LTM593 T-DNA, and the other two classes aligned partially to the right border (RB) of the vector LTM593 T-DNA. This indicates the presence of two T-DNA insertion sites in event LBFLFK. The insertion sites were mapped to different chromosomes, demonstrating that two inserts are integrated at two separate loci in LBFLFK.

In addition to the four unique junctions between T-DNA and canola genome sequences, another sequence junction was identified that was produced by a rearrangement of RB sequences of the LTM593 T-DNA in Insert1. This indicated that a minor rearrangement of the RB sequence had occurred during T-DNA insertion. No additional junctions were identified, indicating that each T-DNA insertion site in LBFLFK consists of a single copy of the T-DNA from LTM593 without rearrangements of the introduced gene expression cassette sequences.

These junction sequences, including the RB rearrangement in Insert1, were also confirmed by Sanger DNA sequence analysis (see section A.3(c)(iii)).

No other rearrangements besides the RB rearrangement in Insert1 were present in either insert. Both T-DNA Insert1 and Insert2 contained all 13 intended gene expression cassettes. The cassette sequences were determined to be identical to the T-DNA sequence of LTM593 except for two single nucleotide changes in Insert1 and one nucleotide change in Insert2. In Insert1, one cytosine to adenine nucleotide change was in the coding sequence of the delta-12 desaturase gene, *c-D12D*(*Ps*), which resulted in a phenylalanine to leucine amino acid substitution [F83L] in the D12D(*Ps*) protein. Another cytosine to adenine nucleotide change was found in Insert1 in the promoter sequence p-*PXR*(*Lu*), which is part of an expression cassette containing the *c-O3D*(*Pir*) coding sequence. This nucleotide change does not result in an amino acid substitution. Lastly, there was a guanine to thymine nucleotide change in Insert2 that is in the coding sequence of the delta-4 desaturase gene, *c-D4D*(*Pl*). This change resulted in an alanine to serine amino acid substitution [A102S] in the D4D(*Pl*) protein. The two amino acid changes have no impact on the function or activity of the respective proteins (section B.2).

As detailed in section A.3(c)(i) above and in section A.3(c)(iii) below, NGS analysis and full DNA sequencing of the LBFLFK canola transgenic locus revealed that the inserted genetic material contains two inserts (Insert1 and Insert2) integrated at two separated loci. The arrangement of the LBFLFK canola transgenic locus is shown in Figure 6 below. Sanger sequencing analysis was utilised to generate the complete DNA sequence of the two inserts and the respective flanking genomic sequences in LBFLFK.

Absence of vector backbone

The NGS and bioinformatics also confirmed that event LBFLFK contained no vector backbone sequences as no matching sequences were detected in the gDNA.

(iii) Full DNA sequence of each insertion site, including junction regions with the host DNA

The DNA sequence of the LBFLFK canola transgenic locus and the corresponding insertion locus was determined via Sanger sequencing. This is discussed in further detail under section A.3(c) above.

Figure 6 details the arrangement of the insertion sites and the junction regions relative to the host DNA.

Locus1 and Locus2 were individually isolated, cloned, and analysed using Sanger sequencing. A BAC library was generated from event LBFLFK gDNA, and the BAC clones were screened for the presence of LBFLFK T-DNA insert sequences. A BAC clone containing the complete Insert1 with flanking gDNA and another BAC clone containing the complete Insert2 with flanking gDNA were isolated. The DNA from these BACs was independently subjected to locus-specific PCR followed by Sanger DNA sequence analysis. The obtained DNA sequences demonstrated the organisation and integrity of the two T-DNA inserts, including any rearrangements or nucleotide changes as compared to the vector LTM593 T-DNA.

The obtained LBFLFK insert and flanking sequences were assembled based on the sequences of overlapping PCR products. Every base pair in the consensus sequences was independently determined at least four times, and a Quality Value (QV, similar to *phred*)

(Ewing and Green, 1998) of 70 or more was confirmed for each base pair, correlating to an expected error probability of at most 1 bp in 10,000,000 bp.

Sequence and integrity of the insertion sites

The sequence of the insertion sites in Kumily were analysed in order to reveal any effects due to the insertion of the T-DNAs in event LBFLFK on the canola genome. PCR was performed on genomic Kumily DNA across the insertion sites (Locus1 and Locus2) using a forward primer corresponding to the genomic sequence flanking the RB and a reverse primer corresponding to the genomic sequence flanking the LB of the respective T-DNA inserts. The PCR products were sequenced, and the resulting Kumily sequences were subjected to homology searches against the *B. napus* genome sequence from cultivar Darmor-*bzh* (Chalhoub et al., 2014; Centre National de Séquençage, 2017).

LBFLFK Insert1 was determined to be integrated into chromosome "Cnn random," and LBFLFK Insert2 was determined to be integrated into the "C03" chromosome. A comparison of the sequences obtained from Kumily with those from the 3' and 5' flanking regions of the two T-DNA inserts in LBFLFK revealed an 8-bp deletion of the canola genome at the integration site of Insert1 and a 31-bp deletion at the integration site of Insert2. Short sequence deletions are common occurrences during Agrobacterium-mediated T-DNA integration (Gheysen et al., 1991). The remaining flanking sequences in LBFLFK were identical to Kumily, and no genomic sequence rearrangements were found at either genomic integration site.

(iv) A map depicting the organisation of the inserted genetic material at each insertion site

Figure 6 depicts a diagram of the T-DNA inserts and flanking regions at Locus1 (Panel A) and at Locus2 (Panel B) of event LBFLFK. The corresponding expression cassettes are defined in Panel C. T-DNA Insert1 and Insert2 have a length of 43,818 bp and 43,779 bp, respectively. Compared to the 44,010-bp long T-DNA sequence in vector LTM593, Insert1 had a 184-bp truncation of the 5´ end of the RB and a 72-bp truncation of the 3´ end of the LB. In addition, the first 64 bp in the RB of Insert1 was determined to be a rearrangement of short T-DNA RB-derived repeats as seen also from the NGS analysis. Insert2 had a 184-bp truncation of the 5´ end of the RB with a 53-bp truncation of the 3´ end of the LB.

The organisation of the LBFLFK transgenic locus within the *B. napus* genome, as confirmed by NGS and DNA sequencing of the transgenic locus and corresponding insertion loci, is described above in sections A.3(c)(i)–(iii).

Figure 6. Diagrams of Insert1 and Insert2 and Flanking Regions in LBFLFK

Organisation of LBFLFK expression cassettes and genomic flanking regions in Locus1 (panel A) and Locus2 (panel B). The flanking regions are depicted as open arrows. The grey numbered arrows represent the T-DNA expression cassettes (numbered 1–13). The open boxes represent the right border (RB) at the 5´ end and the left border (LB) at the 3´ end of the T-DNA, respectively, as labelled. Thick black lines indicate regions where the T-DNA sequence differs from the sequence of the transformation vector LTM593 with the nucleotide changes indicated. "C to A" indicates a cytosine to adenine change, and "G to T" indicates a guanine to thymine change. The insertion of Insert1 introduced an 8-bp deletion in the host genome (not shown); the insertion of Insert2 introduced a 31-bp deletion (not shown). Panel C lists the genetic elements that make up the individual expression cassettes.

A

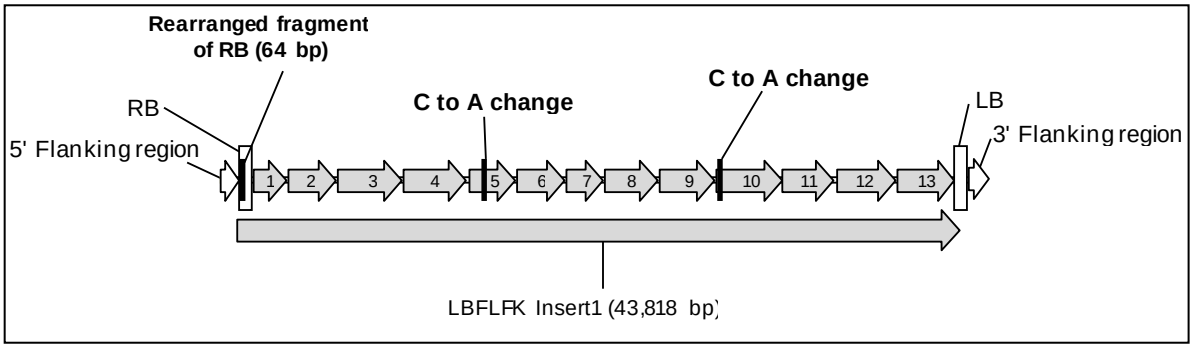

B

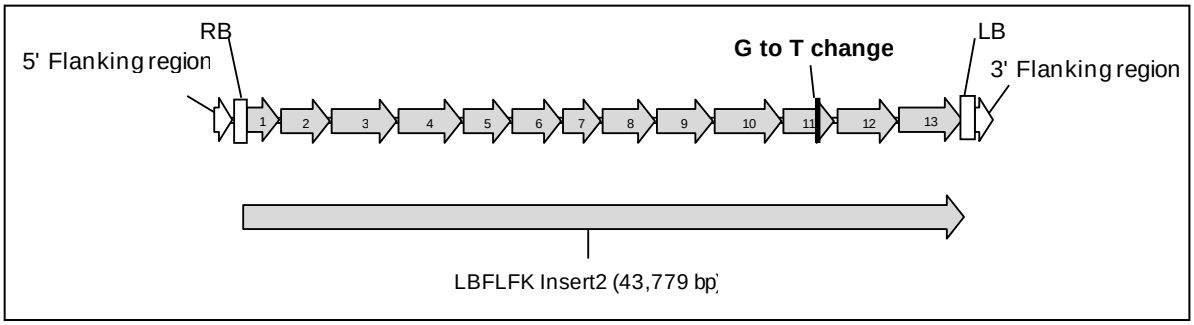

C

Cassette #	Promoter	Intron	CDS	Terminator
1	p-*USP(Vf)*	i-*At1g01170*	c-*D6E(Pp)*	t-*CaMV35S*
2	p-*CNL(Lu)*	i-*At5g63190*	c-*D5D(Tc)1*	t-*OCS*
3	p-*SBP(Vf)*	i-*At1g65090*	c-*D6D(Ot)*	t-*CATHD(St)*
4	p-*PXR(Lu)*	i-*At1g62290*	c-*D6E(Tp)*	t-*PXR(At)*
5	p-*napA(Bn)*	i-*At5g63190*	c-*D12D(Ps)*	t-*rbcS(Ps)*
6	p-*SETL(Bn)*		c-*O3D(Pir)1*	t-*SETL(Bn)*
7	p-*USP(Vf)*	i-*At1g01170*	c-*O3D(Pi)*	t-*CaMV35S*
8	p-*SETL(Bn)*		c-*D5D(Tc)2*	t-*SETL(Bn)*
9	p-*ARC5(Pv)*		c-*D4D(Tc)*	t-*ARC(Pv)*
10	p-*PXR(Lu)*	i-*AGO4(At)*	c-*O3D(Pir)2*	t-*PXR(At)*
11	p-*CNL(Lu)*	i-*At1g65090*	c-*D4D(PI)*	t-*OCS*
12	p-*FAE1(Bn)*	i-*At1g62290*	c-*D5E(Ot)*	t-*FAE1(At)*
13	p-*Ubi4(Pc)*	i-*Ubi4(Pc)*	c-*AHAS(At)*	t-*AHAS(At)*

(v) Identification of any unintended open reading frames created by the T-DNA insertions

A bioinformatic analysis based on the DNA sequence obtained for both T-DNA inserts via Sanger sequencing was conducted to predict the presence of any potential ORFs created at the genomic junctions that could lead to the expression of any unintended proteins. Amino acid sequence alignments were made to determine whether any of the putative polypeptides from any identified ORFs show homology to any known protein allergen, toxin, or antinutrient.

In the context of this analysis, an ORF was defined as any contiguous nucleic acid sequence that contains a string of 30 translated codons between two in-frame termination codons (i.e. TAA, TAG, or TGA) from any of the six potential reading frames (three forward and three reverse reading frames). The deduced amino acid sequences were used as input sequences for the alignments.

A total of 11 ORFs were identified at the four junctions between the canola genome and the T-DNA inserts: one at the Insert1 5´ end, three at the Insert1 3´ end, three at the Insert2 5´ end, and four at the Insert2 3´ end.

To determine the similarity of the identified ORFs to known allergens, the Food Allergy Research and Resource Program (FARRP) Allergen Protein Database[8] was used. It was determined that none of the ORFs created by the insertions shared > 35% identity over 80 amino acids with a known allergen, none had a sequence of eight or more consecutive identical amino acids with a known allergen, and none had any significant overall homology to a known allergen.

Additionally, the National Center for Biotechnology Information (NCBI) GenBank non-redundant peptide sequence database (NCBI Resource Coordinators, 2016) was searched by applying the Basic Local Alignment Search algorithm for protein-to-protein comparisons (BLASTP, NCBI Version 2.6.0+ Jan. 10, 2017) (Altschul et al., 1997) to determine the similarity of the identified ORFs to known toxins and antinutrients. None of the ORFs created by the insertion showed significant homology to known protein toxins as defined in the U.S. Code of Federal Regulations (U.S. EPA, 2017) or showed significant homology to known antinutrients of canola (OECD, 2011b), maize (OECD, 2002a), rice (OECD, 2016), soybean (OECD, 2012), sugar beet (OECD, 2002b), or sugarcane (OECD, 2011a).

[8] http://www.allergenonline.org

(d) A description of how the line or strain from which food is derived was obtained from the original transformant (i.e. provide a family tree or describe the breeding process) including which generations have been used for each study

The breeding history of LBFLFK is shown in Figure 7, and the seeds lots used in the regulatory studies are listed in Table 7.

Figure 7. Breeding History of LBFLFK

T_0 corresponds to the transformed plant, and F_1 corresponds to the first filial generation of offspring of a cross between event LBFLFK and the parental canola variety Kumily. The # index in T# and F# indicate further generations resulting from self-pollination. T4A and T4B were independently propagated from the same pool of T3 seed.

⊗ designates self-pollination; × designates backcrossing.

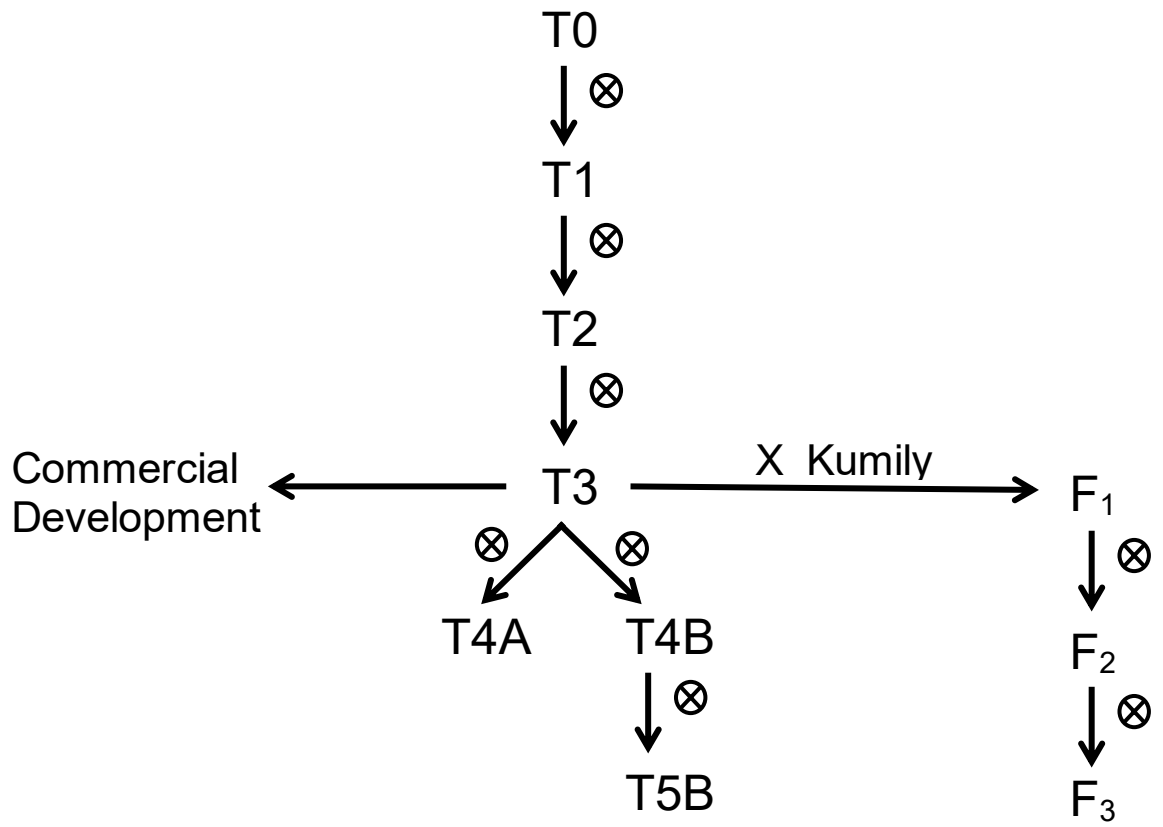

Table 7. LBFLFK Canola Starting Seed Used in Regulatory Studies

Generation	Regulatory Study
T3	Next Generation (NGS) and Sanger sequencing, BAC clone production for molecular characterisation Agronomic and phenotypic characterisation (Winter 2014/15 field trials) Nutrient composition (Winter 2014/15 field trials) Immature seed production for protein characterisation
T4A	Newly expressed protein levels in field produced plant tissues Nutrient composition (Spring 2015 field trial)
T4B	NGS for molecular characterisation (T-DNA insert generational stability)
T5B	NGS for molecular characterisation (T-DNA insert generational stability)
F_2	Mendelian inheritance
F_3	Mendelian inheritance

(e) Evidence of the stability of the genetic changes, including:

(i) The pattern of inheritance of the transferred gene(s) and the number of generations over which this has been monitored; and

Stability of the T-DNA inserts across multiple generations

The stability of inserted T-DNA in LBFLFK across three generations was evaluated using NGS combined with bioinformatic analysis. Two additional generations of event LBFLFK (T4 and T5) were assessed to determine the genetic stability of the two inserts over multiple generations. Read depth distribution patterns across the entire T-DNA were similar in all three analysed generations of LBFLFK, and the same four unique genome/insert junctions were found in all generations. This indicates that the T-DNA inserts were stably inherited.

(ii) The pattern of inheritance and expression of the phenotype over several generations and, where appropriate, across different environments

Mendelian inheritance of the T-DNA inserts

During development of LBFLFK, genotypic segregation data were recorded to assess the inheritance pattern using Chi-square statistical analysis over two generations. The analysis is based on comparing the observed segregation ratio to the segregation ratio that is expected according to Mendelian laws for two independent loci, as found in LBFLFK canola.

The inheritance of the two LBFLFK T-DNA insertion loci was assessed in F_2 and F_3 generations using segregating F_2 and F_3 seed material derived from hemizygous parental plants. Figure 8 shows the full breeding history of LBFLFK and details the generation of materials for the segregation analysis. The zygosity of plants in the T3, F_1, and F_2 generations was assessed via real-time TaqMan® end-point PCR assays. T3 plants were crossed to the parental variety Kumily to produce hemizygous F_1 seeds. After zygosity was confirmed, the F_1 plants were self-pollinated to produce segregating F_2 seeds. These F_2 seeds were pooled, and the resulting seed lot was randomly sampled for segregation analysis. A subset of the F_2 seeds was planted, and hemizygous F_2 plants were selected for self-pollination to produce segregating F_3 seeds. These F_3 seeds were also pooled, and the resulting seed lot was again sampled at random for segregation analysis. The expected ratios for two independently segregating loci are described in Table 8.

Figure 8. Schematic Presentation of the Breeding Tree for Event LBFLFK for the Purpose of Segregation Analysis

T3 represents the T3 generation. F# are the filial generations.
⊗ designates self-pollination; × designates backcrossing.

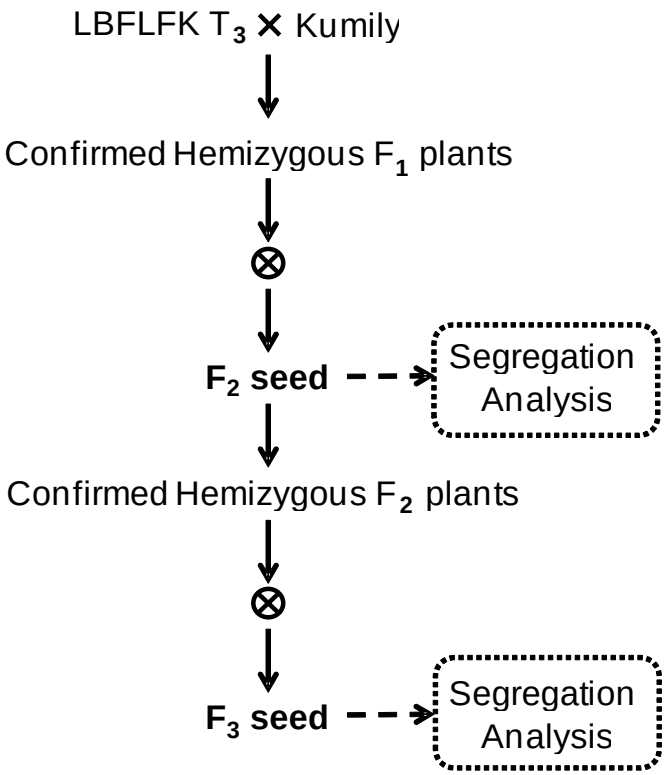

Table 8. Expected Genotype Distribution in the F_2 and F_3 Generations if Inheritance Follows Mendelian Principles

Genotype	AABB	AABb	AAbb	AaBB	AaBb	Aabb	aaBB	aaBb	aabb
Expected segregation ratio	1/16	2/16	1/16	2/16	4/16	2/16	1/16	2/16	1/16

A Pearson's Chi-square (χ^2) analysis was used to statistically compare the observed segregation ratios of the LBFLFK inserts to the expected Mendelian ratios. The Chi-square is calculated as:

$$\chi^2 = \sum \frac{(\text{Observed Value} - \text{Expected Value})^2}{\text{Expected Value}}$$

A significance level of 0.05 for accepting the hypothesis that inheritance followed Mendelian inheritance was used for all statistical tests. A p-value ≥ 0.05 indicates, at a 95% confidence level, that there is no statistically significant evidence for non-Mendelian segregation.

F_2 seeds were randomly picked and subjected to genotyping by locus-specific PCR and subsequent data analysis. Chi-square analysis was carried out with the data obtained from 768 F_2 seeds, and a p-value of 0.543 was obtained (Table 9). Based on this p-value, the hypothesis that segregation is in accordance to Mendel's laws was accepted.

F_3 seeds were randomly selected and subjected to genotyping PCR and subsequent data analysis. Chi-square analysis was carried out with the data obtained from 763 F_3 seeds, and a p-value of 0.974 was obtained (Table 10). Based on this p-value, the hypothesis that segregation is in accordance with Mendel's laws was accepted.

In conclusion, Locus1 and Locus2 segregate as predicted by Mendelian laws, indicating that Insert1 and Insert2 are inherited independently at an equal frequency.

Table 9. Results of the Segregation Analysis of Single F_2 Seeds

Genotypes were successfully determined for 768 out of 792 randomly picked F_2 seeds. The observed frequencies were compared with the expected frequencies using the Chi-Square procedure. According to the obtained p-value, the analysed seed population was segregating as expected.

Genotypes	Number of Seeds (Observed)	Segregation Ratio *	Number of Seeds (Expected)	(Observed – Expected)^2 / Expected
AaBb	200	4/16 or 0.25	192	0.333
AABb	76	2/16 or 0.125	96	4.167
AaBB	98	2/16 or 0.125	96	0.042
Aabb	97	2/16 or 0.125	96	0.010
aaBb	105	2/16 or 0.125	96	0.844
AABB	45	1/16 or 0.0625	48	0.188
AAbb	54	1/16 or 0.0625	48	0.750
aaBB	50	1/16 or 0.0625	48	0.083
aabb	43	1/16 or 0.0625	48	0.521
Total	768		**Chi-Square**	6.938
			p-value	0.543

* Expected frequency according to Mendelian Laws

Table 10. Results of the Segregation Analysis of Single F_3 Seeds

Genotypes were successfully determined for 763 out of 792 randomly picked F_3 seeds. The observed frequencies were compared with the expected frequencies using the Chi-Square procedure. According to the obtained p-value, the analysed seed population was segregating as expected.

Genotypes	Number of Seeds (Observed)	Segregation Ratio *	Number of Seeds (Expected)	(Observed – Expected)^2 / Expected
AaBb	189	4/16 or 0.25	190.75	0.016
AABb	98	2/16 or 0.125	95.375	0.072
AaBB	84	2/16 or 0.125	95.375	1.357
Aabb	100	2/16 or 0.125	95.375	0.224
aaBb	100	2/16 or 0.125	95.375	0.224
AABB	48	1/16 or 0.0625	47.688	0.002
AAbb	49	1/16 or 0.0625	47.688	0.036
aaBB	45	1/16 or 0.0625	47.688	0.151
aabb	50	1/16 or 0.0625	47.688	0.112
Total	763		**Chi-Square**	2.195
			p-value	0.974

* Expected frequency according to Mendelian Laws

Expression of the phenotype across different environments

Levels of expression of the newly expressed proteins

The safety assessment of crops improved through biotechnology typically includes the quantification of the newly expressed proteins to determine the level and site of expression. This also demonstrates that they are expressed as expected in the appropriate tissues and at levels that are consistent with the associated regulatory sequences driving the expression of the corresponding gene (Codex Alimentarius Commission, 2009b).

As described earlier, eleven proteins were introduced into EPA+DHA canola event LBFLFK. The ten desaturases and elongases introduced are controlled by seed-specific promoters, and the soluble, chloroplast-located acetohydroxy acid synthase AHAS(*At*) [A122TS653N] is under the control of a constitutive promoter.

The amounts of each of the newly expressed proteins in EPA+DHA canola tissues were measured by validated quantitative immunoassays. Eleven immunoassays were developed and validated for the purpose of quantifying each of the newly expressed proteins in canola plant tissues. Each protein was measured with either an enzyme-linked immunosorbent assay (ELISA) or a capillary-based quantitative western blot method. The choice of protein quantification method was dependent on the sensitivity, specificity, and reproducibility that was obtainable. Due to the intractable nature of the newly expressed membrane proteins, specific detergents and denaturing reagents were necessary for the extraction of the elongase and desaturase proteins from tissue samples (Bushey et al., 2014). The concentrations of some of these components can interfere with antibody-antigen interactions and were therefore incompatible with ELISA-based methods, which are sensitive to these effects. For such intractable newly expressed proteins, quantitative western blot methods were used.

ELISAs were used to determine the amounts of D12D(*Ps*), D6E(*Pp*), D5D(*Tc*), and D5E(*Ot*) present in the samples. Quantitative western blot methods were used to determine the amounts of D6D(*Ot*), D6E(*Tp*), O3D(*Pir*), O3D(*Pi*), D4D(*Pl*), D4D(*Tc*), and AHAS(*At*) [A122TS653N] present in the samples.

For the AHAS(*At*) [A122TS653N] protein, a quantitative western blot method was applied to allow the use of a single antibody with a preferred specificity compared to the endogenous AHAS protein.

The materials and methods used to determine the concentration of the newly expressed proteins are presented in Appendix 5.

Mean protein levels for each tissue type were determined on a fresh weight (FW) basis and converted to a dry weight (DW) basis after adjusting for the moisture content. The expression levels of each of the newly expressed proteins on a FW and DW basis for both LBFLFK (sprayed) and LBFLFK (non-sprayed) samples are presented in Appendix 5.

Analysed canola tissues included whole plants at different maturity stages, leaf tissue, root tissue, immature seed, mature seed, and pollen. Quantification of the newly expressed elongases and desaturases did not occur in any tissue sample type other than seed, which aligns with the seed-specific promoters that control expression. As intended, each of the newly expressed integral membrane proteins under the control of a seed-specific promoter, with the exception of D6E(*Pp*) and O3D(*Pi*), was quantified[9] in immature and mature seed across field sites. The level of expression for the integral membrane proteins was below the limit of quantitation (< LOQ) in all other tissues analysed. The newly expressed AHAS(*At*) [A122TS653N] protein, driven by a constitutive promoter, was quantifiable in every tissue except mature seed[10].

(f) An analysis of the expressed RNA transcripts, where RNA interference has been used

RNA interference has not been used to develop this food product.

Conclusion on the molecular characterisation

The molecular characterisation efforts described above allow the following conclusions to be made:

- NGS of total genomic DNA and subsequent bioinformatics analysis demonstrated that LBFLFK has two inserts integrated at two separated loci and confirmed the absence of LTM593 vector backbone sequences in the genome of LBFLFK.
- Repeating the analysis for three generations demonstrated that the two inserts are stably integrated in the LBFLFK genome.
- Sanger sequencing analyses confirmed that each of the two inserts has the intended 13 gene expression cassettes. All cassettes were found to be identical to the LTM593 T-DNA except for two single nucleotide changes in Insert1 and one nucleotide change

[9] D5D(*Tc*) and D5E(*Ot*) were only quantified in mature seed samples.
[10] The AHAS(*At*) [A122TS653N] protein was quantified in a single LBFLFK mature seed sample but was otherwise < LOQ in all mature seed samples.

in Insert2. Both T-DNA inserts were intact, apart from a short rearrangement of 64 bp in the RB sequence of Insert1.

- A comparison to the sequence of the insertion site from the parental variety Kumily demonstrated that an 8-bp deletion was created at the genome integration site of Insert1 (Locus1) and a 31-bp deletion was created at the genome integration site of Insert2 (Locus2) in Kumily. No genomic sequence rearrangements were found at either integration site.
- Eleven ORFs were identified that span the junctions between the T-DNA inserts and the flanking genomic DNA. None of the ORFs created by the insertion showed significant homology to known allergens, protein toxins, and antinutrients.

Segregation analysis of F_2 and F_3 LBFLFK offspring showed that Insert1 and Insert2 in LBFLFK are both independently inherited according to Mendelian principles.

PART B CHARACTERISATION AND SAFETY ASSESSMENT OF NEW SUBSTANCES

B.1 Characterisation and Safety Assessment of New Substances

(a) A full description of the biochemical function and phenotypic effects of all new substances (e.g., a protein or an untranslated RNA) that are expressed in the new GM organism, including their levels and site of accumulation, particularly in edible portions

Characterisation of the newly expressed protein

Eleven proteins are newly expressed in EPA+DHA canola event LBFLFK. These include ten integral membrane proteins, desaturase and elongase enzymes, which together impact the content of omega-3 long-chain polyunsaturated fatty acids in the seeds. The eleventh protein is the soluble, chloroplast-located AHAS(*At*) [A122TS653N] enzyme that confers tolerance to treatment with an imidazolinone herbicide.

The safety assessment of crops improved through biotechnology includes a description of the nature and biochemical function of the newly expressed proteins (Codex Alimentarius Commission, 2009b). This typically includes characterisation for identity and amino acid sequence, apparent molecular weight and immunoreactivity, and an assessment of potential glycosylation and enzymatic activity. In general, depending on the properties of the newly expressed proteins and the levels of expression in the genetically modified plant, this may require either the isolation of the newly expressed proteins from the plant or production in a heterologous expression system.

Integral membrane proteins, containing multiple transmembrane-spanning domains, are generally intractable, meaning they are difficult to isolate, concentrate, and quantify from tissues or difficult to produce at high levels in heterologous systems (Madduri et al., 2012; Bushey et al., 2014). The protein characterisations of the integral membrane desaturase and elongase proteins were performed with a membrane fraction purified from crude extracts of developing embryos that were isolated from immature seeds of event LBFLFK. This detergent-free membrane fraction (referred to herein as “plant-produced proteins” or PPP) contains active and full-length elongases and desaturases from the plant. It is noted that there was also sufficient AHAS(*At*) [A122TS653N] present in PPP to perform several of the characterisation studies, but further enrichment by immunopurification from PPP was needed for glycosylation analysis and confirmation of protein identity. Additionally, AHAS(*At*) [A122TS653N] molecular weight, immunoreactivity, and enzyme activity were demonstrated using both leaf protein extracts and PPP. Feedback regulation of AHAS(*At*) [A122TS653N] activity by branched chain amino acids and a decreased sensitivity to imazamox were confirmed using leaf protein extracts.

(b) Information about prior history of human consumption of the new substances, if any, or their similarity to substances previously consumed in food

The safe use of the newly expressed proteins and their donor organisms was evaluated by a systematic literature search that identified relevant documents related to dietary or environmental exposure or toxicity of the newly expressed proteins or donor organisms. In addition, the amino acid sequence of each newly expressed protein was compared to the

amino acid sequences of proteins present in consumed food or feed to identify sequence identity to proteins that are safely consumed by humans as food and by animals as feed.

History of safe use for delta-12 desaturase (*Ps*)

Phytophthora sojae, the donor organism for the D12D(*Ps*) gene, belongs to the oomycetes, a group of fungus-like eukaryotes. *P. sojae* is not known to produce or contain toxins or antinutrients. Likewise, *P. sojae* has not been reported to cause disease in humans or animals. *P. sojae* is not consumed as food or feed. For more information on *P. sojae*, refer to section A.2(a)(i).

Delta-12 desaturases are found in commodity crops, including soybean (Heppard et al., 1996), cotton (Liu et al., 1999; Pirtle et al., 2001; Zhang et al., 2009), peanut (Jung et al., 2000; López et al., 2000), and flax (Krasowska et al., 2007), but are not found in mammals, which are dependent on dietary intake of delta-12 desaturated fatty acids. No reports of adverse effects due to exposure to delta-12 desaturases have been reported.

Amino acid sequence identity of D12D(*Ps*) with other desaturases present in consumed food or feed was assessed. The proteins identified with the highest sequence identity to D12D(*Ps*) originated from vascular plants and mosses, and from fungi. The protein found to have the most identity to D12D(*Ps*) is from *Hordeum vulgare* (barley, 46.7% identity) followed closely by *Oryza brachyantha* (ancestor of rice, 46.4% identity) and *Zea mays* (corn, 46.3% identity). The fungal protein is from *Mortierella alpina* (45% identity), which is used to produce arachidonic acid-rich oil for human consumption that is Generally Recognised as Safe (GRAS) (U.S. FDA, 2001). This protein from *Mortierella alpina* has been shown to have delta-12 desaturase activity (Huang et al., 1999).

Taken together, D12D(*Ps*) is structurally and functionally related to other desaturases that are safely consumed by humans as food and by animals as feed. The lack of adverse findings of D12D(*Ps*) substantiates its HOSU and consumption.

History of safe use for delta-6 desaturase (*Ot*)

Ostreococcus tauri, the donor organism for the D6D(*Ot*) gene, is a unicellular marine green microalga commonly found in oceans. *O. tauri* is not known to produce or contain toxins or antinutrients. Likewise, *O. tauri* has not been reported to cause disease in humans or animals. *O. tauri* is not directly consumed as food or feed. However, *O. tauri* is part of the marine phytoplankton community, the lowest tier in the aquatic food web, and is indirectly consumed by fish, which ultimately could end up as human food. For more information on *O. tauri*, refer to section A.2(a)(i).

Delta-6 desaturases are generally found in all vertebrates, lower plants, insects, and some other invertebrates (Cook and McMaster, 2002). No reports of adverse effects due to exposure to delta-6 desaturases have been reported.

Amino acid sequence identity of D6D(*Ot*) with other desaturases present in consumed food or feed was assessed. The proteins identified with the highest sequence identity to D6D(*Ot*) originated from molluscs *Lingula anatina* (lamp shell, 27.4% identity) and *Octopus vulgaris* (common octopus, 27.3% identity). Other similar sequences, which are all ~25% identical to D6D(*Ot*), originate from diverse sources, including fish (*Tachysurus fulvidraco*, yellowhead catfish), plants (*Oryza sativa*, rice), and birds (*Meleagris gallopavo*, turkey). While specific

delta-6 desaturase activity has not been identified in these sources, the protein from *Octopus vulgaris* has been shown to have delta-5 desaturase activity (Monroig et al., 2012b).

Taken together, D6D(*Ot*) is structurally and functionally related to other desaturases that are safely consumed by humans as food and by animals as feed. The lack of adverse findings of D6D(*Ot*) substantiates its HOSU and consumption.

History of safe use for delta-6 elongase (*Tp*)

Thalassiosira pseudonana, the donor organism for the D6E(*Tp*) gene, is a marine diatom. *T. pseudonana* is not known to produce or contain antinutrients. *T. pseudonana* has been reported to produce the neurotoxin beta-N-methylamino-L-alanine (Jiang et al., 2014), which is produced by many species of diatoms as well as by cyanobacteria and dinoflagellates (Lage et al., 2015). Nevertheless, *T. pseudonana* is frequently used as part of aquafeed diets (e.g., for bivalves and crustacean larvae) (Brown, 2002). In addition, *T. pseudonana*-derived biosilica has been successfully used to deliver chemotherapeutic drugs to cancer cells, indicating a non-toxic nature (Delalat et al., 2015). Extracts from *T. pseudonana* displayed no feeding deterrent activity to model copepods in bioassays (Shaw et al., 1994). *T. pseudonana* has not been reported to cause disease in humans or animals. *T. pseudonana* is not consumed as food. It is frequently used as part of aquafeed diets for marine organisms such as prawns (D'Souza et al., 2000), pacific oysters (Thompson and Harrison, 1992; Thompson et al., 1996), clams (Li et al., 2002; Liu et al., 2016), copepods (Harris, 1977), and basket cockle (Liu et al., 2009). Accordingly, human consumption of *T. pseudonana* is expected to be indirect via consumption of mussels, clams, and prawns. For more information on *T. pseudonana*, refer to section A.2(a)(i).

Delta-6 elongases are found in plant and fungal species (Beaudoin et al., 2000a; Beaudoin et al., 2000b; Zank et al., 2000). No reports of adverse effects due to exposure to delta-6 elongases have been reported.

Amino acid sequence identity of D6E(*Tp*) with other elongases present in consumed food or feed was assessed. All but one of the identified sequences, a mollusc, came from fish. The proteins found to have the highest sequence identity to D6E(*Tp*) originated from *Notothenia coriiceps* (Black rockcod, 33.2% identity), *Oreochromis niloticus* (Nile tilapia, 33.1% identity), and *Salmo salar* (Atlantic salmon, 32.5% identity). The Nile tilapia and Atlantic salmon are used extensively in aquaculture around the world. The selected sequences from *Salmo salar* and *Oreochromis niloticus* are not the same as the proteins that have been experimentally verified as delta-6-elongases, which are 25.1% and 27.1% identical to D6E(*Tp*), respectively (Hastings et al., 2004; Agaba et al., 2005).

Taken together, D6E(*Tp*) is structurally and functionally related to other elongases that are safely consumed by humans as food and by animals as feed. The lack of adverse findings of D6E(*Tp*) substantiates its HOSU and consumption.

History of safe use for delta-6 elongase (*Pp*)

Physcomitrella patens, the donor organism for the D6E(*Pp*) gene, is a moss. *P. patens* is not known to produce or contain toxins or antinutrients. Likewise, *P. patens* has not been reported to cause disease in humans or animals and has been considered a safe source for production of biopharmaceuticals (Decker et al., 2014; Rosales-Mendoza et al., 2014; Reski et al., 2015). *P. patens* is not consumed as food or feed. For more information on *P. patens*, refer to section A.2(a)(i).

Delta-6 elongases are found in plant and fungal species (Beaudoin et al., 2000a; Beaudoin et al., 2000b; Zank et al., 2000). No reports of adverse effects due to exposure to delta-6 elongases have been reported.

Amino acid sequence identity of D6E(*Pp*) with other elongases present in consumed food or feed was assessed. Most of the proteins identified originated from mammals and birds and from fish. However, the proteins found to have the highest sequence identities to D6E(*Pp*) were elongases from *Thraustochytrium* (40.4% identity) and *Mortierella alpina* (36% identity). Several *Thraustochytrium* species are used for industrial production of DHA (Sijtsma and de Swaaf, 2004). *Mortierella alpina* is used to produce arachidonic acid-rich oil for human consumption that is GRAS (U.S. FDA, 2001). All other related sequences were found to have identities to D6E(*Pp*) around 32–33% and included proteins from species such as *Equus asinus* (donkey, 33.8% identity), *Oreochromis niloticus* (Nile tilapia, 33% identity), and *Salmo salar* (Atlantic salmon, 32.3% identity). The Nile tilapia and Atlantic salmon are used extensively in aquaculture around the world. The elongase from *Mortierella alpina* (Parker-Barnes et al., 2000) has been shown to have delta-6 elongase activity.

Taken together, D6E(*Pp*) is structurally and functionally related to other elongases that are safely consumed by humans as food and by animals as feed. The lack of adverse findings of D6E(*Pp*) substantiates its HOSU and consumption.

History of safe use for delta-5 desaturase (*Tc*)

Thraustochytrids are marine protists that belong to the class of Labyrinthulomycetes, which are primarily marine organisms that are considered important components of marine microbial communities. Thraustochytrids are microorganisms that are epibiotic in nature and represent a diverse group of organisms living in marine and estuarine habitats throughout the world, exhibiting a saprotrophic mode of nutrition (Raghukumar, 2002). *Thraustochytrium* sp. are not known to produce or contain toxins or antinutrients. *Thraustochytrium* sp. have not been reported to cause disease in humans or animals. *Thraustochytrium* sp. are not directly consumed as food. However, indirect human consumption likely occurs as these organisms are consumed by filter-feeding marine invertebrates, including mussels and clams, and by fish that are consumed directly by humans (Bergé and Barnathan, 2005). In addition, several Thraustochytrids serve as sources of DHA used in dietary supplements. For more information on Thraustochytrids, refer to section A.2(a)(i).

Delta-5 desaturases are found in algae, protozoa, fungi, plants, and animals including humans (Meesapyodsuk and Qiu, 2012). No reports of adverse effects due to exposure to delta-5 desaturases have been reported.

Amino acid sequence identity of D5D(*Tc*) with other desaturases present in consumed food or feed was assessed. Most of the proteins identified originated from vascular plants and mosses, and from fish. However, the protein found to have the most identity to D5D(*Tc*) is a desaturase from *Thraustochytrium aureum* (58.1% identity). Several *Thraustochytrium* species are used for industrial production of DHA (Sijtsma and de Swaaf, 2004). The *Thraustochytrium* protein has been shown to be a functional delta-5 desaturase (Kobayashi et al., 2011). All other sequences were found to have identities to D5D(*Tc*) around 26–27%. These sequences include proteins from major crops such as *Brassica napus* (canola, 26.1% identity), *Capsicum annuum* (bell pepper, 26.8% identity), *Sesamum indicum* (sesame, 26.2% identity), and sequences from farmed fish such as *Salmo salar* (Atlantic salmon, 26.2% identity) and *Oreochromis niloticus* (Nile tilapia, 26.2% identity). Plants are not known to possess delta-5 desaturase activity, and the plant proteins mentioned above are predicted to be delta-8 desaturases. The protein from *Salmo salar* was found to have delta-6 desaturase activity (Monroig et al., 2010).

Taken together, D5D(*Tc*) is structurally and functionally related to other desaturases that are safely consumed by humans as food and by animals as feed. The lack of adverse findings of D5D(*Tc*) substantiates its HOSU and consumption.

History of safe use for omega-3 desaturase (*Pir*)

Pythium irregulare, the donor organism for the O3D(*Pir*) gene, belongs to the oomycetes, a group of fungus-like eukaryotes. *P. irregulare* is not known to produce or contain toxins or antinutrients. Likewise, *P. irregulare* has not been reported to cause disease in humans or animals. *P. irregulare* is not consumed as food or feed. However, *P. irregulare* is considered a safe source of biomass or oil for use as ingredients in food and feed (Wu et al., 2013). *P. irregulare* has not been reported to cause disease in humans or animals. For more information on *P. irregulare*, refer to section A.2(a)(i).

Omega-3 desaturases are found in all photosynthetic organisms. Humans and other mammals are dependent on dietary intake of omega-3 fatty acids because of the lack of endogenous enzymes for omega-3 desaturation (Simopoulos, 2016). No reports of adverse effects due to exposure to omega-3 desaturases have been reported.

Amino acid sequence identity of O3D(*Pir*) with other desaturases present in consumed food or feed was assessed. The protein found to have the highest sequence identity to O3D(*Pir*) is from the mollusc *Octopus bimaculoides* (California two-spot octopus, 39% identity). All other proteins identified are from major agricultural crops such as *Cucumis melo* (muskmelon, 34.6% identity), *Cicer arietinum* (chickpea, 33.8% identity), and *Linum usitatissimum* (flax seed, 33.5% identity). The protein from *Linum usitatissimum* has been proven to be an omega-3 desaturase (Khadake et al., 2011).

Taken together, O3D(*Pir*) is structurally and functionally related to other desaturases that are safely consumed by humans as food and by animals as feed. The lack of adverse findings of O3D(*Pir*) substantiates its HOSU and consumption.

History of safe use for omega-3 desaturase (*Pi*)

Phytophthora infestans, the donor organism for the O3D(*Pi*) gene, belongs to the oomycetes, a group of fungus-like eukaryotes. *P. infestans* is not known to produce or contain toxins or

antinutrients. Likewise, *P. infestans* has not been reported to cause disease in humans or animals. *P. infestans* is not consumed as food or feed. For more information on *P. infestans*, refer to section A.2(a)(i).

Omega-3 desaturases are found in all photosynthetic organisms. Humans and other mammals are dependent on dietary intake of omega-3 fatty acids because of the lack of endogenous enzymes for omega-3 desaturation (Simopoulos, 2016). No reports of adverse effects due to exposure to omega-3 desaturases have been reported.

Amino acid sequence identity of O3D(*Pi*) with other desaturases present in consumed food or feed was assessed. The proteins found to have the highest sequence identity are from the mollusc *Octopus bimaculoides* (California two-spot octopus, 37.4% identity) and from *Aphanizomenon flos-aquae* (34.6% identity), which is a cyanobacteria found around the world and used to produce dietary supplements (Spolaore et al., 2006). Other proteins identified are from major agricultural crops such as *Solanum lycopersicum* (tomato, 33.4% identity), *Oryza sativa* (rice, 33.2% identity), and *Brassica napus* (canola, 32.2% identity). The *Solanum lycopersicum* protein has been shown to be an omega-3 desaturase (Wang et al., 2014a).

Taken together, O3D(*Pi*) is structurally and functionally related to other desaturases that are safely consumed by humans as food and by animals as feed. The lack of adverse findings of O3D(*Pi*) substantiates its HOSU and consumption.

History of safe use for delta-5 elongase (*Ot*)

Ostreococcus tauri, the donor organism for the D5E(*Ot*) gene, is a unicellular marine green microalga commonly found in oceans. *O. tauri* is not known to produce or contain toxins or antinutrients. Likewise, *O. tauri* has not been reported to cause disease in humans or animals. *O. tauri* is not directly consumed as food or feed. However, *O. tauri* is part of the marine phytoplankton community, the lowest tier in the aquatic food web, and is indirectly consumed by fish, which ultimately could end up as human food. For more information on *O. tauri*, refer to section A.2(a)(i).

Delta-5 elongases are found in animals, including humans (Wang et al., 2014b; Wang et al., 2014c), microalgae (Robert et al., 2009; Petrie et al., 2010), and liverworts (Kajikawa et al., 2006). No reports of adverse effects due to exposure to delta-5 elongases have been reported.

Amino acid sequence identity of D5E(*Ot*) with other elongases present in consumed food or feed was assessed. Most of the proteins identified originated from fish. The protein found to have the highest sequence identity to D5E(*Ot*) is from *Cyprinus carpio* (common carp, 32.1% identity). Other species with proteins similar to D5E(*Ot*) included *Salmo salar* (Atlantic salmon, 31.2% identity), *Mortierella alpina* (30.8% identity), which is used to produce arachidonic acid-rich oil for human consumption that is GRAS (U.S. FDA, 2001), and *Octopus vulgaris* (30.4% identity). The protein from *Octopus vulgaris* has been shown to have both delta-6 and delta-5 elongase activity (Monroig et al., 2012a)

Taken together, D5E(*Ot*) is structurally and functionally related to other elongases that are safely consumed by humans as food and by animals as feed. The lack of adverse findings of D5E(*Ot*) substantiates its HOSU and consumption.

History of safe use for delta-4 desaturase (*Tc*)

Thraustochytrids are marine protists that belong to the class of Labyrinthulomycetes, which are primarily marine organisms that are considered important components of marine microbial communities. Thraustochytrids are microorganisms that are epibiotic in nature and represent a diverse group of organisms living in marine and estuarine habitats throughout the world, exhibiting a saprotrophic mode of nutrition (Raghukumar, 2002). *Thraustochytrium* sp. are not known to produce or contain toxins or antinutrients. Likewise, *Thraustochytrium* sp. have not been reported to cause disease in humans or animals. *Thraustochytrium* sp. are not directly consumed as food. However, indirect human consumption likely occurs as these organisms are consumed by filter-feeding marine invertebrates, including mussels and clams, and by fish that are consumed directly by humans (Bergé and Barnathan, 2005). In addition, several Thraustochytrids serve as sources of DHA used in dietary supplements. For more information on Thraustochytrids, refer to section A.2(a)(i).

Delta-4 desaturases are found in marine microalga and protists (Qiu et al., 2001; Tonon et al., 2003; Pereira et al., 2004; Guo et al., 2013). No reports of adverse effects due to exposure to delta-4 desaturases have been reported.

Amino acid sequence identity of D4D(*Tc*) with other desaturases present in consumed food or feed was assessed. Most of the proteins identified originated from mammals and birds. However, the protein found to have the highest sequence identity to D4D(*Tc*) is from *Thraustochytrium aurem* (70.9% identity). Several *Thraustochytrium* species are used for industrial production of DHA (Sijtsma and de Swaaf, 2004). All other related sequences were found to have identities to D4D(*Tc*) of less than 30% and included species such as the fungus *Mortierella alpina* (29.8% identity), which is used to produce arachidonic acid-rich oil for human consumption that is GRAS (U.S. FDA, 2001), the plant *Prunus mume* (Chinese plum, 24.2% identity), and the mammal *Bos taurus* (cow, 24% identity). Plants are not known to possess delta-4 desaturase activity, but the protein from *Mortierella alpina* (Tavares et al., 2011) has been shown to have delta-5 desaturase activity.

Taken together, D4D(*Tc*) is structurally and functionally related to other desaturases that are safely consumed by humans as food and by animals as feed. The lack of adverse findings of D4D(*Tc*) substantiates its HOSU and consumption.

History of safe use for delta-4 desaturase (*Pl*)

Pavlova lutheri, the donor organism for the D4D(*Pl*) gene, is a marine microalga. *P. lutheri* is not known to produce or contain toxins or antinutrients. Likewise, *P. lutheri* has not been reported to cause disease in humans or animals. *P. lutheri* is not consumed directly as food or feed. However, *P. lutheri* is used as part of aquafeed diets, so it could be indirectly consumed by humans. For more information on *P. lutheri*, refer to section A.2(a)(i).

Delta-4 desaturases are found in marine microalga and protists (Qiu et al., 2001; Tonon et al., 2003; Pereira et al., 2004; Guo et al., 2013). No reports of adverse effects due to exposure to delta-4 desaturases have been reported.

Amino acid sequence identity of D4D(*Pl*) with other desaturases present in consumed food or feed was assessed. Most of the proteins identified originated from fish and from vascular plants and mosses. However, the proteins found to have the highest identity to D4D(*Pl*) are from the red alga *Pyropia yezoensis* (Japanese nori, 27.9% identity) and from the plants *Zea mays* (27.8% identity), *Sorghum bicolor* (27.5% identity), and *Setaria italica* (27.2% identity). Plants are not known to possess delta-4 desaturase activity, and the plant proteins mentioned above are predicted to be delta-8 desaturases. All other sequences were found to have identities to D4D(*Pl*) in the range of 24–26%, including a protein from *Dicentrarchus labrax* (European sea bass, 24.2% identity) that has been shown to be an active delta-6 desaturase (González-Rovira et al., 2009).

Taken together, D4D(*Pl*) is structurally and functionally related to other desaturases that are safely consumed by humans as food and by animals as feed. The lack of adverse findings of D4D(*Pl*) substantiates its HOSU and consumption.

History of safe use for acetohydroxy acid synthase (*At*) [A122TS653N]

Arabidopsis thaliana, the donor organism for the acetohydroxy acid synthase *AHAS*(*At*) gene, is a member of the mustard (Brassicaceae) family. *A. thaliana* is not known to produce or contain toxins. As is typical of the Brassicaceae family, *A. thaliana* has been described to contain glucosinolates in varying composition and concentration (Kliebenstein et al., 2001). Glucosinolates are a large group of naturally occurring plant defence compounds that occur in all Brassica-originated feeds and fodders. The primary deleterious effects of ingestion of glucosinolates in animals are reduced palatability and decreased growth/production (Tripathi and Mishra, 2007). *A. thaliana* has not been reported to cause disease in humans or animals. *A. thaliana* is a member of the mustard family, which includes several routinely consumed vegetables such as broccoli, cabbage, cauliflower, turnip, rapeseed, and radish. For more information on *A. thaliana*, refer to section A.2(a)(i).

AHAS enzymes are ubiquitous in all plants and microbes and have been isolated from numerous organisms (Mazur et al., 1987). There are several naturally occurring mutations in plant *AHAS* genes that confer herbicide tolerance. The most commonly occurring mutations that confer resistance to AHAS inhibitors are substitutions of alanine, proline, tryptophan, and serine at positions 122, 197, 574, and 653, respectively (relative to the Arabidopsis AHAS sequence) (Duggleby and Pang, 2000; Tan et al., 2005).

The AHAS(*At*) [A122TS653N] protein expressed in LBFLFK is encoded by a gene from *Arabidopsis thaliana* and harbors two amino acid substitutions, A122T and S653N, that confer

tolerance to imidazolinone herbicides (Tan et al., 2005). Several commercialised crops have herbicide tolerance conferred by alleles of the *ahas* gene (e.g., Clearfield canola, Clearfield wheat, Clearfield sunflower, Clearfield lentils). The safety of mutant, herbicide-tolerant AHAS enzymes expressed in crops has been extensively investigated and reported (Mathesius et al., 2009; Chukwudebe et al., 2012). No reports of adverse effects due to exposure to AHAS enzymes have been reported.

Amino acid sequence identity of AHAS(*At*) [A122TS653N] with other AHAS enzymes present in consumed food or feed was assessed. The proteins found to have the highest sequence identity to AHAS(*At*) [A122TS653N] originated from vascular plants and mosses and included commonly consumed crops such as *Brassica napus* (canola, 88.2% identity), *Cicer arietinum* (chickpea, 78.2% identity), *Malus domestica* (apple, 78.9% identity), and *Helianthus annuus* (sunflower, 77.6% identity). The protein from *Helianthus annuus* has been shown to be an active AHAS enzyme (Kolkman et al., 2004).

Taken together, AHAS(*At*) [A122TS653N] is structurally and functionally related to other AHAS enzymes that are safely consumed by humans as food and by animals as feed. The lack of adverse findings of AHAS(*At*) [A122TS653N] substantiates its HOSU and consumption.

(c) Information on whether any new protein has undergone any unexpected post-translational modification in the new host

To characterise each of the newly expressed proteins in LBFLFK canola, a series of biochemical experiments was conducted to determine for each protein: (1) the deduced amino acid sequence, (2) the protein quantity in analysed tissues, (3) the apparent molecular weight, (4) the immunoreactivity, (5) the identity, (6) the glycosylation, and (7) the enzymatic activity.

The results of the biochemical and functional characterisation for each introduced protein are described in this section. A summary of these characterisation studies is provided in Table 22 (after the individual protein summaries). For each newly expressed protein, the characterisation data are described followed by a brief summary of the findings. The materials and methods used are further described in Appendix 6.

Delta-12 desaturase (*Ps*)

Structure and function

The delta-12 desaturase (*Ps*) protein D12D(*Ps*), newly expressed in EPA+DHA canola event LBFLFK, is encoded by a coding sequence isolated from the oomycete *Phytophthora sojae*. The deduced D12D(*Ps*) protein consists of 398 amino acids with a calculated molecular mass of 45.6 kDa. The D12D(*Ps*) amino acid sequence, as depicted in Figure 9, shows features that are characteristic of a methyl-end integral membrane desaturase. Depicted are the predicted transmembrane helices, three histidine boxes containing eight conserved histidine residues, and the conserved histidine following the C-terminal transmembrane helix.

EPA+DHA canola event LBFLFK contains two T-DNA inserts that encode the D12D(*Ps*) protein. The two D12D(*Ps*) coding sequences differ by a single nucleotide, resulting in a deduced protein that has a [F83L] substitution, referred to as D12D(*Ps*) [F83L], that is predicted to reside in the first transmembrane-spanning domain of the desaturase (Figure 9). The D12D(*Ps*) [F83L] protein also consists of 398 amino acids but has a calculated molecular mass of 45.5 kDa. *In vivo* experiments in yeast showed that both proteins, D12D(*Ps*) and D12D(*Ps*) [F83L], catalyse the desaturation reaction required to convert C18:1n-9 into C18:2n-6 (Yilmaz et al., 2017) and have similar conversion efficiencies.

A series of biochemical experiments were performed to characterise the two D12D(*Ps*) proteins that were newly expressed in EPA+DHA canola event LBFLFK. The characteristics assessed in these experiments are generally applicable to both D12D(*Ps*) and D12D(*Ps*) [F83L].

Figure 9. Deduced Amino Acid Sequence for Delta-12 Desaturase (*Ps*) in EPA+DHA Canola Event LBFLFK

Using the one letter amino acid code for the D12D(*Ps*) protein in event LBFLFK, the position of predicted transmembrane helices and other characteristic protein motifs are indicated. ▒, ▒,= indicates transmembrane helices as predicted by SCAMPI2 (Peters et al., 2016), TMHMM v.2.0 (Krogh et al., 2001), and SOSUI v 1.11 (Hirokawa et al., 1998), respectively. The sequence contains three histidine-box motifs (▒) with eight conserved histidine residues (H) typical for desaturases (Shanklin et al., 1994) and an additional conserved histidine (H), all of which participate in the coordination of the diiron active centre (Bai et al., 2015; Wang et al., 2015). EPA+DHA canola event LBFLFK carries two T-DNA inserts that encode the D12D(*Ps*) protein, one with the amino acid sequence as shown below and one with the amino acid sequence carrying a phenylalanine to leucine substitution at position 83 (D12D(*Ps*) [F83L]), indicated by **F**.

```
1   MAILNPEADS AANLATDSEA KQRQLAEAGY THVEGAPAPL PLELPHFSLR DLRAAIPKHC
61  FERSFVTSTY YMIKNVLTCA ALFYAATFID RAGAAAYVLW PVYWFFQGSY LTGVWVIAHE
        ========================     ========================

121 CGHQAYCSSE VVNNLIGLVL HSALLVPYHS WRISHRKHHS NTGSCENDEV FVPVTRSVLA

181 SSWNETLEDS PLYQLYRIVY MLVVGWMPGY LFFNATGPTK YWGKSRSHFN PYSAIYADRE
              ========================

241 RWMIVLSDIF LVAMLAVLAA LVHTFSFNTM VKFYVVPYFI VNAYLVLITY LQHTDTYIPH
      ========================     ========================

301 FREGEWNWLR GALCTVDRSF GPFLDSVVHR IVDTHVCHHI FSKMPFYHCE EATNAIKPLL
361 GKFYLKDTTP VPVALWRSYT HCKFVEDDGK VVFYKNKL
```

Apparent molecular weight and immunoreactivity

Western blot analysis using an anti-D12D(*Ps*) protein antibody was used to show immunoreactivity of the D12D(*Ps*) and the D12D(*Ps*) [F83L] proteins in PPP isolated from EPA+DHA canola event LBFLFK (Figure 10). To demonstrate the specificity of the antibody, a D12D(*Ps*) NC fusion reference protein was included as positive control (Figure 10, lane 1). An immunoreactive band was observed in the LBFLFK PPP samples at a molecular weight that was in good agreement with the calculated molecular mass of the D12D(*Ps*) and D12D(*Ps*) [F83L] proteins of 45.6 kDa and 45.5 kDa, respectively (Figure 10, lanes 3 and 4). No signal was detected in PPP isolated from Kumily, the parental control that does not contain the D12D(*Ps*) coding sequences (Figure 10, lane 2).

Figure 10. Western Blot Analysis of Delta-12 Desaturase (*Ps*) in EPA+DHA Canola Event LBFLFK

LBFLFK PPP and Kumily PPP were separated by SDS-PAGE and evaluated by western blot analysis. The membrane was probed with a 1:8,000 dilution of the D12D(*Ps*)-specific antibody and probed with a secondary horseradish peroxidase (HRP)-conjugated antibody. Approximate molecular weight markers loaded in lanes labelled MW are shown on the left and right side of the blot. The calculated molecular mass of the D12D(*Ps*) and the D12D(*Ps*) [F83L] protein encoded by the coding sequences introduced in EPA+DHA canola event LBFLFK is 45.6 kDa and 45.5 kDa, respectively. The calculated molecular mass of the D12D(*Ps*) NC fusion protein used as a positive control for the D12D(*Ps*)-specific antibody is 21.5 kDa.

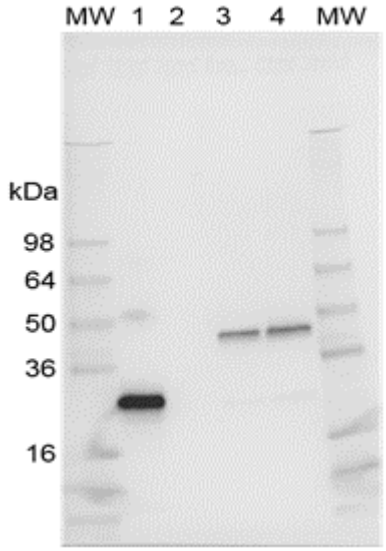

	Lane 1	Lane 2	Lane 3	Lane 4
Sample	D12D(*Ps*) NC fusion protein	Kumily PPP	LBFLFK PPP	LBFLFK PPP
Amount Loaded	32 ng	20 µg	10 µg	20 µg

Identity

Mass spectrometry was used to perform tryptic peptide mapping analysis against the deduced amino acid sequence of the D12D(*Ps*) protein to confirm the identity of the D12D(*Ps*) and the D12D(*Ps*) [F83L] proteins in PPP isolated from EPA+DHA canola event LBFLFK. To minimise the probability of a false positive identification, the current recommendations of the Human Proteome Project Mass Spectrometry Data Interpretation Guidelines 2.1 were followed (Deutsch et al., 2016). Specifically, true positive identification of a protein requires analysis of one sample and identification of at least two peptides consisting of at least nine amino acids, and one of the peptides may not be fully nested within another. The analysis of three different samples identified 15 peptides (Table 11) that matched the expected deduced amino acid sequence of the D12D(*Ps*) protein with ≥ 95% probability of positive identification and covered 51% of the entire protein sequence (Figure 11). Eleven of the peptides listed in Table 11 contained at least nine amino acids and were not fully nested within another (peptides 3 to 15 except 7 and 10). The confidence of having accurately identified the D12D(*Ps*) proteins is further increased by the replicate identification of these 11 peptides in multiple samples and the identification of peptide 7 and 10 that are fully nested within peptide 8 and 13, respectively. These peptides, except peptide 9, map to both the D12D(*Ps*) amino acid sequence as well as to the D12D(*Ps*) [F83L] sequence while peptide 9 only maps to the D12D(*Ps*) protein. The

D12D(*Ps*) proteins were therefore identified in PPP isolated from EPA+DHA canola event LBFLFK.

Table 11. Tryptic Peptides Identified for Delta-12 Desaturase (*Ps*) in EPA+DHA Canola Event LBFLFK using LC-MS/MS Analysis

Number	Peptide Sequence	Amino Acid Length	Replicate 1	Replicate 2	Replicate 3
1	EGEWNWLR	8	X	X	X
2	GALCTVDR	8	X	X	X
3	DTTPVPVALWR	11	X	X	X
4	SFVTSTYYMIK	11	X	X	X
5	SFGPFLDSVVHR	12	X	X	X
6	IVDTHVCHHIFSK	13		X	X
7	SHFNPYSAIYADR	13	X	X	X
8	SHFNPYSAIYADRER	15	X	X	X
9	NVLTCAALFYAATFIDR	17		X	X
10	HHSNTGSCENDEVFVPVTR	19	X	X	X
11	MPFYHCEEATNAIKPLLGK	19	X	X	X
12	AILNPEADSAANLATDSEAK	20	X	X	X
13	KHHSNTGSCENDEVFVPVTR	20	X	X	X
14	SVLASSWNETLEDSPLYQLYR	21	X	X	X
15	QLAEAGYTHVEGAPAPLPLELPHFSLR	27	X	X	X

PPP isolated from event LBFLFK were digested with trypsin and Lys-C followed by LC-MS/MS. Listed are peptides representing the D12D(*Ps*) and D12D(*Ps*) [F83L] protein, identified with 95% confidence using Mascot server v2.5.1 (Matrix Science Ltd, London, UK).

Figure 11. Peptide Mass Coverage by LC-MS/MS Analysis for Delta-12 Desaturase (*Ps*) in EPA+DHA Canola Event LBFLFK

The amino acid sequence of the D12D(*Ps*) protein (Panel A) and the D12D(*Ps*) [F83L] protein (Panel B, [F83L] highlighted in black) encoded by the two T-DNA inserts in EPA+DHA canola event LBFLFK, represented as the one letter amino acid code. PPP isolated from event LBFLFK were digested with trypsin and Lys-C followed by LC-MS/MS in order to identify peptides representing the D12D(*Ps*) and D12D(*Ps*) [F83L] protein. Peptides listed in Table 11 were mapped (**bold underlined**) onto the deduced protein sequences, covering approximately 51% of the full-length D12D(*Ps*) protein and 46% of the full-length D12D(*Ps*) [F83L] protein.

A

1 M**AILNPEADS AANLATDSEA K**QR**QLAEAGY THVEGAPAPL PLELPHFSLR** DLRAAIPKHC

61 FER**SFVTSTY YMIKNVLTCA ALFYAATFID R**AGAAAYVLW PVYWFFQGSY LTGVWVIAHE

121 CGHQAYCSSE VVNNLIGLVL HSALLVPYHS WRISHR**KHHS NTGSCENDEV FVPVTRSVLA**

181 **SSWNETLEDS PLYQLYR**IVY MLVVGWMPGY LFFNATGPTK YWGKSR**SHFN PYSAIYADRE**

241 **R**WMIVLSDIF LVAMLAVLAA LVHTFSFNTM VKFYVVPYFI VNAYLVLITY LQHTDTYIPH

301 FR**EGEWNWLR GALCTVDRSF GPFLDSVVHR IVDTHVCHHI FSKMPFYHCE EATNAIKPLL**

361 **GK**FYLK**DTTP VPVALWR**SYT HCKFVEDDGK VVFYKNKL

B

1 M**AILNPEADS AANLATDSEA K**QR**QLAEAGY THVEGAPAPL PLELPHFSLR** DLRAAIPKHC

61 FER**SFVTSTY YMIK**NVLTCA AL**L**YAATFID RAGAAAYVLW PVYWFFQGSY LTGVWVIAHE

121 CGHQAYCSSE VVNNLIGLVL HSALLVPYHS WRISHR**KHHS NTGSCENDEV FVPVTRSVLA**

181 **SSWNETLEDS PLYQLYR**IVY MLVVGWMPGY LFFNATGPTK YWGKSR**SHFN PYSAIYADRE**

241 **R**WMIVLSDIF LVAMLAVLAA LVHTFSFNTM VKFYVVPYFI VNAYLVLITY LQHTDTYIPH

301 FR**EGEWNWLR GALCTVDRSF GPFLDSVVHR IVDTHVCHHI FSKMPFYHCE EATNAIKPLL**

361 **GK**FYLK**DTTP VPVALWR**SYT HCKFVEDDGK VVFYKNKL

Glycosylation analysis

Both newly expressed D12D(*Ps*) proteins (D12D(*Ps*) and D12D(*Ps*) [F83L]) have the same two potential N-glycosylation sites at $_{184}$NETL$_{187}$ and $_{214}$NATG$_{217}$ (Gavel and von Heijne, 1990; Zielinska et al., 2010) and several potential O-glycosylation sites (any serine or threonine). The glycosylation status of the newly expressed D12D(*Ps*) proteins was analysed using a strategy that first separated all proteins present in the LBFLFK PPP into two fractions (glycosylated proteins and non-glycosylated proteins) and then determined which fraction contained the D12D(*Ps*) proteins by western blot analysis with a D12D(*Ps*)-specific antibody as described in Appendix 7.

Together, these data demonstrated that the D12D(*Ps*) proteins present in PPP isolated from EPA+DHA canola event LBFLFK are not glycosylated.

Enzymatic activity

The functional activities of the newly expressed D12D(*Ps*) proteins (D12D(*Ps*) and D12D(*Ps*) [F83L]) in PPP isolated from EPA+DHA canola event LBFLFK were tested using an *in vitro* assay previously reported for the D12D(*Ps*) enzyme present in membranes isolated from yeast expression strains (Yilmaz et al., 2017). The D12D(*Ps*) was previously shown to desaturate C18:1n-9 to C18:2n-6 when the substrate fatty acid was covalently bound to a lipid, e.g., phosphatidylcholine (PC) (Yilmaz et al., 2017). Therefore, endogenous lysophosphatidylcholine acyl transferase (LPCAT) present in PPP was used to synthesise [^{14}C]-18:1n-9-PC *in situ* by transesterification of [^{14}C]-18:1n-9 from CoA to lysophosphatidylcholine (LPC) (Yilmaz et al., 2017). Specifically, in this assay, PPP (isolated from LBFLFK or Kumily) was incubated with [^{14}C]-18:1n-9-CoA, unlabelled C16:0-lysophosphatidylcholine, and NADH. The resulting fatty acid products were isolated, converted to FAMEs, resolved on a TLC plate, and identified by electronic autoradiography. In the reaction containing LBFLFK PPP (Figure 12, Panel B, lane B and C), a [^{14}C]-FAME was identified that migrates similar to the [^{14}C]-18:2n-6-ME standard (Figure 12, Panel B, lane E), in agreement with the expected product according to the reaction shown in Panel A of Figure 12. This product was not detected when the transfer of [^{14}C]-18:1n-9-CoA to LPC was prevented (Yilmaz et al., 2017). This product was also not detected in the reaction containing parental control Kumily PPP (Figure 12, Panel B, lane A), which does not contain the D12D(*Ps*) coding sequence. Kumily PPP was expected to contain the endogenous *Brassica napus* endoplasmic reticulum D12D (Lee et al., 2013). The absence of [^{14}C]-18:2n-6 product in the reaction containing Kumily PPP indicates a significantly lower endogenous D12D activity relative to the newly expressed D12D(*Ps*).

The substrate specificity and activity of the D12D(*Ps*) [F83L] protein, as determined by *in vivo* fatty acid feeding experiments in yeast, was comparable to reported values for the D12D(*Ps*) protein (Yilmaz et al., 2017). Therefore, the results obtained from the presented *in vitro* assays demonstrate the enzymatic activity of the D12D(*Ps*) and/or D12D(*Ps*) [F83L] proteins present in the LBFLFK PPP, that is consistent with the previously proposed enzymatic reaction shown in Panel A of Figure 12.

Figure 12. *In Vitro* Enzymatic Activity of Delta-12 Desaturases (*Ps*) in EPA+DHA Canola Event LBFLFK

Panel A. D12D(*Ps*) desaturates the fatty acid substrate C18:1n-9 to the fatty acid product C18:2n-6 when the substrate is covalently bound to a lipid e.g., phosphatidylcholine, PC (Yilmaz et al., 2017). In the enzymatic assay, endogenous lysophosphatidylcholine acyl transferase (LPCAT) is used to synthesise [^{14}C]-18:1n-9-PC by transferring [^{14}C]-18:1n-9 from CoA to lysophosphatidylcholine (LPC). Panel B. PPP (20 µg total protein) were incubated in a buffer solution with [^{14}C]-18:1n-9-CoA substrate, unlabelled C16:0-lysophosphatidylcholine, and NADH. Total lipids were extracted, converted to fatty acid methyl esters (FAME), and separated using a 10% $AgNO_3$ TLC plate with a 1:1 ratio of toluene/heptane solvent as the mobile phase. Shown below is an autoradiographic image of the TLC plate of the resolved [^{14}C]-methyl esters (ME). Kumily PPP were used as a control. Lane A, Kumily PPP (control). Lane B and Lane C, LBFLFK PPP loaded in duplicate. Lane D, [^{14}C]-18:1n-9-ME standard (substrate). Lane E, [^{14}C]-18:2n-6-ME standard (product).

A.

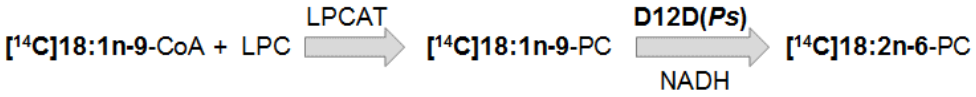

B.

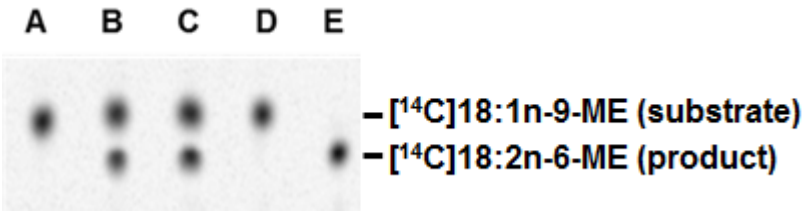

Summary of delta-12 desaturase (*Ps*) characterisation

EPA+DHA canola event LBFLFK contains two T-DNA inserts with the respective D12D(*Ps*) coding sequences differing in one nucleotide. This nucleotide difference results in the two newly expressed proteins D12D(*Ps*) and D12D(*Ps*) [F83L]. The *in silico* predicted protein structure was described and the enzyme function was presented based on published *in vivo* experiments in yeast. Furthermore, a series of biochemical experiments was performed to characterise the D12D(*Ps*) proteins newly expressed in event LBFLFK.

Structure / Function: Bioinformatic analysis indicates the protein is a methyl-end integral membrane desaturase, and *in vivo* yeast experiments confirmed this enzymatic function for both D12D(*Ps*) and D12D(*Ps*) [F83L]. The enzymes convert C18:1n-9 into C18:2n-6.

Immunoreactivity / Molecular weight: Western blot analysis confirmed the D12D(*Ps*) proteins were immunoreactive to an anti-D12D(*Ps*) antibody and the apparent molecular weight was in good agreement to the calculated molecular mass of the D12D(*Ps*) proteins. The antibody used to detect the D12D(*Ps*) proteins is expected to detect both D12D(*Ps*) and D12D(*Ps*) [F83L] with similar sensitivity; therefore this result applied to both D12D(*Ps*) proteins.

Identity: Tryptic peptide mapping using LC-MS/MS positively identified 10 distinct peptides (> 9 amino acids) corresponding to the deduced amino acid sequence of both D12D(*Ps*)

proteins and one peptide (> 9 amino acids) specific to just the D12D(*Ps*) without the F83L substitution. D12D(*Ps*) proteins were therefore identified in EPA+DHA canola event LBFLFK.

Glycosylation: The D12D(*Ps*) proteins were found to be not glycosylated. The antibody used to detect the D12D(*Ps*) proteins is expected to detect both D12D(*Ps*) and D12D(*Ps*) [F83L] with similar sensitivity; therefore, this result applied to both D12D(*Ps*) proteins.

Enzyme activity: Delta-12 desaturation activity, i.e. the introduction of a double bond in C18:1n-9 generating C18:2n-6, was demonstrated.

Delta-6 desaturase (*Ot*)

Structure and function

The delta-6 desaturase (*Ot*) protein D6D(*Ot*), newly expressed in EPA+DHA canola event LBFLFK, is encoded by a coding sequence isolated from the marine green microalga *Ostreococcus tauri*. The deduced D6D(*Ot*) protein consists of 456 amino acids with a calculated molecular mass of 51.7 kDa. The D6D(*Ot*) amino acid sequence, as depicted in Figure 13, shows the features that are characteristic for a front-end integral membrane desaturase. Depicted are the N-terminally fused cytochrome b_5 domain containing the characteristic HPGG motif, the predicted transmembrane helices, three histidine boxes containing seven conserved histidine residues, a conserved glutamine in histidine box 3, and the conserved histidine following the C-terminal transmembrane helix. *In vivo* experiments in yeast showed that this D6D(*Ot*) protein catalyses the desaturation reaction required to convert C18:2n-6 into C18:3n-6 (Domergue et al., 2005; Yilmaz et al., 2017).

Figure 13. Deduced Amino Acid Sequence for Delta-6 Desaturase (*Ot*) in EPA+DHA Canola Event LBFLFK

Using the one letter amino acid code for the D6D(*Ot*) protein in event LBFLFK, the position of predicted transmembrane helices and other characteristic protein motifs are indicated. ▒, ▒,= indicates transmembrane helices as predicted by Scampi 2 (Peters et al., 2016), TMHMM v.2.0 (Krogh et al., 2001), and SOSUI v 1.11 (Hirokawa et al., 1998), respectively. The sequence contains three histidine-box motifs (▒) with seven conserved histidine residues (H) typical for desaturases (Shanklin et al., 1994) and an additional conserved histidine (H), all of which participate in the coordination of the diiron active centre (Bai et al., 2015; Wang et al., 2015). Additionally, the sequence contains a conserved glutamine (Q) in the third histidine box that is essential for activity (Sayanova et al., 2001). Underlined is the cytochrome b_5 domain as annotated by PFAM v31 (Finn et al., 2016), containing the characteristic HPGG motif (Sperling and Heinz, 2001) highlighted in grey.

```
1   MCVETENNDG IPTVEIAFDG ERERAEANVK LSAEKMEPAA LAKTFARRYV VIEGVEYDVT
61  DFKHPGGTVI FYALSNTGAD ATEAFKEFHH RSRKARKALA ALPSRPAKTA KVDDAEMLQD
121 FAKWRKELER DGFFKPSPAH VAYRFAELAA MYALGTYLMY ARYVVSSVLV YACFFGARCG
                                    ==========
181 WVQHEGGHSS LTGNIWWDKR IQAFTAGFGL AGSGDMWNSM HNKHHATPQK VRHDMDLDTT
    ==
241 PAVAFFNTAV EDNRPRGFSK YWLRLQAWTF IPVTSGLVLL FWMFFLHPSK ALKGGKYEEL
301 VWMLAAHVIR TWTIKAVTGF TAMQSYGLFL ATSWVSGCYL FAHFSTSHTH LDVVPADEHL
361 SWVRYAVDHT IDIDPSQGWV NWLMGYLNCQ VIHHLFPSMP QFRQPEVSRR FVAFAKKWNL
421 NYKVMTYAGA WKATLGNLDN VGKHYYVHGQ HSGKTA
```

Apparent molecular weight and immunoreactivity

Western blot analysis using an anti-D6D(*Ot*) protein antibody was used to show immunoreactivity of the D6D(*Ot*) protein in PPP isolated from EPA+DHA canola event LBFLFK (Figure 14). To demonstrate the specificity of the antibody, a D6D(*Ot*) full-length reference protein was included as positive control (Figure 14, lane 1). An immunoreactive band was observed in the LBFLFK PPP samples at a molecular weight that was in good agreement with the calculated molecular mass of the D6D(*Ot*) protein of 51.7 kDa (Figure 14, lanes 3 and 4). No signal was detected in PPP isolated from Kumily, the parental control that does not contain the D6D(*Ot*) coding sequence (Figure 14, lane 2). Another immunoreactive band was also observed at approximately 36 kDa in the LBFLFK PPP (Figure 14, lanes 3 and 4) that was not observed in Kumily PPP (Figure 14, lane 2), likely the result of degradation of the D6D(*Ot*) protein in the PPP sample.

Figure 14. Western Blot Analysis of Delta-6 Desaturase (*Ot*) in EPA+DHA Canola Event LBFLFK

LBFLFK PPP and Kumily PPP were separated by SDS-PAGE and evaluated by western blot analysis. The membrane was probed with a 1:4000 dilution of the D6D(*Ot*)-specific antibody and probed with a secondary HRP-conjugated antibody. Approximate molecular weight markers loaded in lanes MW are shown on the left and right side of the blot. The calculated molecular mass of the D6D(*Ot*) protein from the coding sequence introduced in EPA+DHA canola event LBFLFK is 51.7 kDa. The calculated molecular mass of the D6D(*Ot*) full-length reference standard protein used as a positive control for the D6D(*Ot*)-specific antibody is 51.7 kDa.

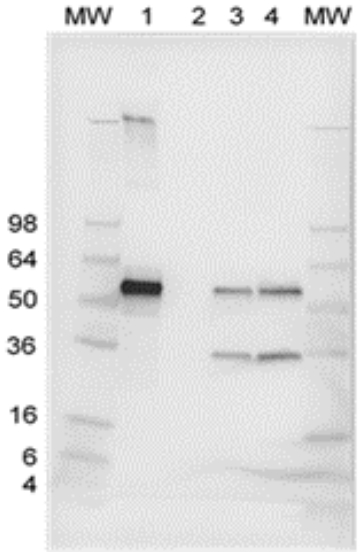

	Lane 1	Lane 2	Lane 3	Lane 4
Sample	D6D(*Ot*) full-length protein	Kumily PPP	LBFLFK PPP	LBFLFK PPP
Amount Loaded	40 ng	20 µg	10 µg	20 µg

Identity

Mass spectrometry was used to perform tryptic peptide mapping analysis against the deduced amino acid sequence of the D6D(*Ot*) protein to confirm the identity of the D6D(*Ot*) protein in PPP isolated from EPA+DHA canola event LBFLFK. To minimise the probability of a false positive identification, the current recommendations of the Human Proteome Project Mass

Spectrometry Data Interpretation Guidelines 2.1 were followed (Deutsch et al., 2016). Specifically, true positive identification of a protein requires analysis of one sample and identification of at least two peptides consisting of at least nine amino acids, and one of the peptides may not be fully nested within another. The analysis of three different samples identified 15 peptides (Table 12) that matched the expected deduced amino acid sequence of the D6D(*Ot*) protein with ≥ 95% probability of true positive identification and covered 23% of the entire protein sequence (Figure 15). Eleven of the peptides listed in Table 12 contained at least nine amino acids and were not fully nested within another (peptides 3 to 8, 11 to 13, 15). The confidence of having accurately identified the D6D(*Ot*) protein is further increased by the replicate identification of eight of these peptides (3–8, 12,13) in multiple samples and the identification of peptides 9 and 14 that are fully nested within peptides 10 and 15, respectively. The D6D(*Ot*) protein was therefore identified in PPP isolated from EPA+DHA canola event LBFLFK.

Table 12. Tryptic Peptides Identified for Delta-6 Desaturase (*Ot*) in EPA+DHA Canola Event LBFLFK using LC-MS/MS Analysis

Peptide	Peptide Sequence	Amino Acid Length	Replicate 1	Replicate 2	Replicate 3
1	KWNLNYK	7		X	X
2	MEPAALAK	8		X	
3	VMTYAGAWK	9		X	X
4	ALAALPSRPAK	11	X	X	X
5	HYYVHGQHSGK	11		X	X
6	VDDAEMLQDFAK	12	X	X	X
7	DGFFKPSPAHVAYR	14	X	X	X
8	YEELVWMLAAHVIR	14		X	X
9	YVVIEGVEYDVTDFK	15		X	X
10	RYVVIEGVEYDVTDFK	16			X
11	FAELAAMYALGTYLMYAR	18	X		
12	HPGGTVIFYALSNTGADATEAFK	23	X	X	X
13	IQAFTAGFGLAGSGDMWNSMHNK	23		X	X
14	HDMDLDTTPAVAFFNTAVEDNRPR	24	X	X	X
15	VRHDMDLDTTPAVAFFNTAVEDNR PR	26			X

PPP isolated from event LBFLFK were digested with trypsin and Lys-C followed by LC-MS/MS. Listed are peptides representing the D6D(*Ot*) protein, identified with 95% confidence using Mascot server v2.5.1 (Matrix Science Ltd, London, UK).

Figure 15. Peptide Mass Coverage by LC-MS/MS Analysis for Delta-6 Desaturase (*Ot*) in EPA+DHA Canola Event LBFLFK

The deduced amino acid sequence of the D6D(*Ot*) protein, newly expressed in EPA+DHA canola event LBFLFK, represented as the one letter amino acid code. PPP isolated from event LBFLFK were digested with trypsin and Lys-C followed by LC-MS/MS in order to identify peptides representing the D6D(*Ot*) protein. Peptides listed in Table 12 were mapped (**bold underlined**) onto the deduced protein sequence, covering approximately 23% of the full-length D6D(*Ot*) protein.

1 MCVETENNDG IPTVEIAFDG ERERAEANVK LSAEK**MEPAA LAK**TFAR**RYV VIEGVEYDVT**
61 **DFKHPGGTVI FYALSNTGAD ATEAFK**EFHH RSRKARK**ALA ALPSRPAK**TA K**VDDAEMLQD**
121 **FAK**WRKELER **DGFFKPSPAH VAYRFAELAA MYALGTYLMY AR**YVVSSVLV YACFFGARCG
181 WVQHEGGHSS LTGNIWWDKR **IQAFTAGFGL AGSGDMWNSM HNK**HHATPQK VR**HDMDLDTT**
241 **PAVAFFNTAV EDNRPR**GFSK YWLRLQAWTF IPVTSGLVLL FWMFFLHPSK ALKGGK**YEEL**
301 **VWMLAAHVIR** TWTIKAVTGF TAMQSYGLFL ATSWVSGCYL FAHFSTSHTH LDVVPADEHL
361 SWVRYAVDHT IDIDPSQGWV NWLMGYLNCQ VIHHLFPSMP QFRQPEVSRR FVAFAK**KWNL**
421 **NYKVMTYAGA WK**ATLGNLDN VGK**HYYVHGQ HSGK**TA

Glycosylation analysis

The D6D(*Ot*) protein has no potential N-glycosylation sites (Gavel and von Heijne, 1990; Zielinska et al., 2010) but several potential O-glycosylation sites (any serine or threonine). The glycosylation status of the newly expressed D6D(*Ot*) protein was analysed using a strategy that first separated all proteins present in the LBFLFK PPP into two fractions (glycosylated proteins and non-glycosylated proteins) and then determined which fraction contained the D6D(*Ot*) protein by western blot analysis with a D6D(*Ot*)-specific antibody as described in Appendix 8.

Together, these data demonstrated that the D6D(*Ot*) protein present in PPP isolated from EPA+DHA canola event LBFLFK was not glycosylated.

Enzymatic activity

The functional activity of the newly expressed D6D(*Ot*) enzyme in PPP isolated from EPA+DHA canola event LBFLFK was tested using an *in vitro* assay previously reported for the D6D(*Ot*) enzyme present in membranes isolated from yeast expression strains (Yilmaz et al., 2017). *In vivo* and *in vitro* experiments using yeast expression strains showed that the D6D(*Ot*) uses acyl-CoA substrates (e.g., C18:2n-6 bound to coenzyme A) but does not efficiently use phospholipid substrates (Domergue et al., 2005; Yilmaz et al., 2017). Therefore, in the assay, PPP (isolated from LBFLFK or Kumily) were incubated with [^{14}C]-18:2n-6-CoA and NADH. The resulting fatty acid products were isolated, converted to FAMEs, resolved on a TLC plate, and identified by electronic autoradiography. In the reaction containing either Kumily or LBFLFK PPP (Figure 16, Panel B, lanes D-F), no [^{14}C]-FAME was identified that migrates similar to the [^{14}C]-18:3n-6-ME standard (Figure 16, Panel B, lane B), indicating the expected product according to the reaction shown in Panel A of Figure 16 was not formed. However, in the reaction containing membranes isolated from yeast expressing the D6D(*Ot*) protein, a [^{14}C]-FAME was identified that migrates similar to the [^{14}C]-18:3n-6-ME standard (Figure 16, Panel B, lanes C and B, respectively), indicating the assay was run appropriately to allow formation of the product by the D6D(*Ot*).

The presence of C18:3n-6 in event LBFLFK seeds, and the fact that in event LBFLFK only the newly expressed D6D(*Ot*) enzyme exhibits the D6D activity required to convert C18:2n-6 into C18:3n-6, indicates D6D(*Ot*) is active in seed of LBFLFK. The difficulty in demonstrating

in vitro activity of the D6D(*Ot*) may result from the central role of acyl-CoAs in lipid metabolism. Many competing enzyme activities rely on acyl-CoA substrates (Waku, 1992; Bates et al., 2009). The high flux of nascent acyl-CoAs into phospholipids via LPCAT was established (Bates et al., 2009) and enables the *in vitro* activity assay of phospholipid dependent desaturases (Yilmaz et al., 2017). In contrast, an assay of acyl-CoA dependent desaturases would be highly affected by the relative activity of enzymes competing for the same acyl-CoA substrate. Combining the results in Figure 16 and the fatty acids found in the seed, it is likely the relative activity of the acyl-CoA dependent D6D(*Ot*) desaturase to all other competing enzymes (such as LPCAT and thioesterases) is higher in yeast membranes compared to LBFLFK PPP; however, the D6D(*Ot*) has the intended *in vivo* activity in seeds of event LBFLFK.

Figure 16. *In Vitro* Enzymatic Activity of Delta-6 Desaturase (*Ot*) in EPA+DHA Canola Event LBFLFK

Panel A. D6D(*Ot*) desaturates the fatty acid substrate C18:2n-6 to the fatty acid product C18:3n-6 (Domergue et al., 2005; Yilmaz et al., 2017). *In vivo* and *in vitro* experiments indicate that the D6D(*Ot*) enzyme desaturates fatty acids covalently attached to coenzyme A while *in vitro* experiments further show that this enzyme does not efficiently desaturate fatty acids covalently bound to phosphatidylcholine (PC) (Domergue et al., 2005; Yilmaz et al., 2017). Panel B. PPP (50 µg total protein) were incubated in a buffer solution with [^{14}C]-18:2n-6-CoA substrate and NADH. Total lipids were extracted, converted to fatty acid ethyl esters (FAMEs), and separated using a reverse phase thin layer chromatography plate with acetonitrile as the mobile phase. Shown below is an autoradiographic image of the TLC plate of the resolved [^{14}C]-methylesters (ME). Kumily PPP was used as a control. Lane A, C18:2n-6-ME substrate. Lane B, C18:3n-6-ME product. Lane C, yeast membranes containing D6D(*Ot*) (control). Lane D, Kumily PPP (control). Lanes E and F, LBFLFK PPP in duplicate.

A.

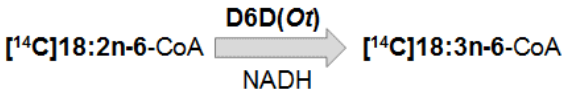

B.

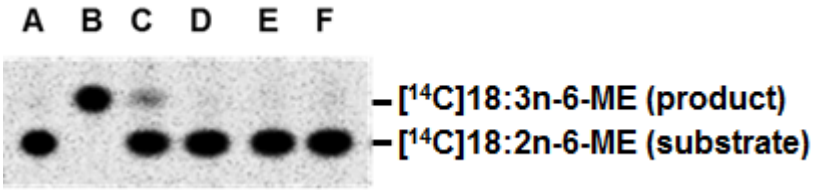

Summary of delta-6 desaturase (*Ot*) characterisation

EPA+DHA canola event LBFLFK contains two T-DNA inserts encoding two identical copies of the D6D(*Ot*) protein. The *in silico* predicted protein structure was described and the enzyme function was presented based on published *in vivo* experiments in yeast. Furthermore, a series of biochemical experiments was performed to characterise the D6D(*Ot*) protein newly expressed in event LBFLFK.

Structure / Function: Bioinformatic analysis indicated the protein is a front-end integral membrane desaturase, and *in vivo* yeast experiments confirmed this enzymatic function. The enzyme converts C18:2n-6 into C18:3n-6.

Immunoreactivity / Molecular weight: Western blot analysis confirmed the protein was immunoreactive to an anti-D6D(*Ot*) antibody. The apparent molecular weight was in good agreement to the calculated molecular mass of the D6D(*Ot*) protein.

Identity: Tryptic peptide mapping using LC-MS/MS positively identified 11 distinct peptides (> 9 amino acids) corresponding to the deduced amino acid sequence of the D6D(*Ot*) protein. The D6D(*Ot*) was therefore identified in EPA+DHA canola event LBFLFK.

Glycosylation: The D6D(*Ot*) protein was found to be not glycosylated.

Enzyme activity: Delta-6 desaturation activity, i.e. the introduction of a double bond in C18:2n-6 generating C18:3n-6, was not detected using the *in vitro* enzyme assay in LBFLFK PPP, likely due to relatively high activity of enzymes competing for the C18:2n-6-CoA substrate in LBFLFK PPP compared to yeast membranes. However, the presence of C18:3n-6 in event LBFLFK seeds, and the fact that in event LBFLFK only the newly expressed D6D(*Ot*) enzyme exhibits the D6D activity required to convert C18:2n-6 into C18:3n-6, demonstrates the D6D(*Ot*) has the intended *in vivo* activity in seeds of event LBFLFK.

Delta-6 elongase (*Tp*)

Structure and function

The delta-6 elongase (*Tp*) protein, D6E(*Tp*), newly expressed in EPA+DHA canola event LBFLFK is encoded by a coding sequence isolated from the marine diatom *Thalassiosira pseudonana*. The deduced D6E(*Tp*) protein consists of 272 amino acids with a calculated molecular mass of 31.8 kDa. The D6E(*Tp*) amino acid sequence, as depicted in Figure 17, shows the features that are characteristic of ELO-type elongases. Depicted are the predicted transmembrane helices and all four of the signature ELO-motifs. *In vivo* experiments in yeast showed that this D6E(*Tp*) protein catalyses the elongation reaction required to convert C18:3n-6 into C20:3n-6 (Meyer et al., 2004; Yilmaz et al., 2017).

Figure 17. Deduced Amino Acid Sequence for Delta-6 Elongase (*Tp*) in EPA+DHA Canola Event LBFLFK

Using the one letter amino acid code for the D6E(*Tp*) protein in event LBFLFK, the position of predicted transmembrane helices and other characteristic protein motifs are indicated. , , = indicates transmembrane helices as predicted by Scampi 2 (Peters et al., 2016), TMHMM v.2.0 (Krogh et al., 2001), and SOSUI v 1.11 (Hirokawa et al., 1998), respectively. The sequence contains four motifs ( ) highly conserved among elongases (Leonard et al., 2004; Meyer et al., 2004; Jakobsson et al., 2006), including the characteristic HXXHH histidine box embedded in the fourth membrane helix that is critical for enzymatic activity (Denic and Weissman, 2007; Hernandez-Buquer and Blacklock, 2013). Highly conserved residues are highlighted in black.

```
1   MDAYNAAMDK IGAAIIDWSD PDGKFRADRE DWWLCDFRSA ITIALIYIAF VILGSAVMQS
                                      ========================

61  LPAMDPYPIK FLYNVSQIFL CAYMTVEAGF LAYRNGYTVM PCNHFNVNDP PVANLLWLFY
                ==========================              ==============

121 ISKVWDFWDTIFIVLGKKWR QLSFLHVYHH TTIFLFYWLN ANVLYDGDIF LTILLNGFIH
    ==========                                  ====================

181 TVMYTYYFIC MHTKDSKTGK SLPIWWKSSL TAFQLIQFTI MMSQATYLVF HGCDKVSLRI
    ====                    ========================              =

241 TIVYFVYILS LFFLFAQFFV QSYMAPKKKK SA
    ======================
```

Apparent molecular weight and immunoreactivity

Western blot analysis using an anti-D6E(*Tp*) protein antibody was used to show immunoreactivity of the D6E(*Tp*) protein in PPP isolated from EPA+DHA canola event LBFLFK (Figure 18). To demonstrate the specificity of the antibody, a D6E(*Tp*) NC fusion reference protein was included as positive control (Figure 18, lane 1). An immunoreactive band was observed in the LBFLFK PPP samples at a molecular weight that was in good agreement with the calculated molecular mass of the D6E(*Tp*) protein of 31.8 kDa, Figure 18, lanes 3 and 4). No signal was detected in the PPP isolated from Kumily, the parental control that does not contain the D6E(*Tp*) coding sequence (Figure 18, lane 2).

Figure 18. Western Blot Analysis of Delta-6 Elongase (*Tp*) in EPA+DHA Canola Event LBFLFK

LBFLFK PPP and Kumily PPP were separated by SDS-PAGE and evaluated by western blot analysis. The membrane was probed with a 1:1,000 dilution of the D6E(*Tp*)-specific antibody and probed with a secondary HRP-conjugated antibody. Approximate molecular weight markers loaded in lanes MW are shown on the left and right side of the blot. The calculated molecular mass of the D6E(*Tp*) protein from the coding sequence introduced in EPA+DHA canola event LBFLFK is 31.8 kDa. The calculated molecular mass of the D6E(*Tp*) NC fusion protein used as a positive control for the D6E(*Tp*)-specific antibody is 16.6 kDa.

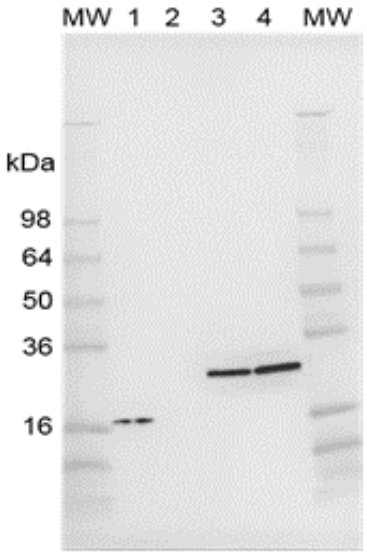

	Lane 1	Lane 2	Lane 3	Lane 4
Sample	D6E(*Tp*) NC fusion protein	Kumily PPP	LBFLFK PPP	LBFLFK PPP
Amount Loaded	30 ng	20 µg	10 µg	20 µg

Identity

Mass spectrometry was used to perform tryptic peptide mapping against the deduced amino acid sequence of the D6E(*Tp*) protein to confirm the identity of the D6E(*Tp*) protein in PPP isolated from EPA+DHA canola event LBFLFK. To minimise the probability of a false positive identification, the current recommendations of the Human Proteome Project Mass Spectrometry Data Interpretation Guidelines 2.1 were followed (Deutsch et al., 2016). Specifically, true positive identification of a protein required the identification of two or more peptides consisting of at least nine amino acids, and one of the peptides may not be fully nested within another. The analysis of three different samples identified four peptides (Table 13) that matched the expected deduced amino acid sequence of the D6E(*Tp*) protein with ≥ 95% probability of true positive identification and covered 12% of the entire protein sequence (Figure 19). Two of the peptides listed in Table 13 contained at least nine amino acids and were not fully nested within another (peptides 3 and 4). The confidence of having accurately identified the D6E(*Tp*) protein is further increased by the replicate identification of these two peptides in multiple samples and the identification of peptide 2 that is fully nested within peptide 3. The D6E(*Tp*) protein was therefore identified in PPP isolated from EPA+DHA canola event LBFLFK.

Table 13. Tryptic Peptides Identified for Delta-6 Elongase (*Tp*) in EPA+DHA Canola Event LBFLFK using LC-MS/MS Analysis

Number	Peptide Sequence	Amino Acid Length	Replicate 1	Replicate 2	Replicate 3
1	SLPIWWK	7	X	X	X
2	EDWWLCDFR	9			X
3	ADREDWWLCDFR	12	X	X	X
4	IGAAIIDWSDPDGK	14	X	X	X

PPP isolated from event LBFLFK were digested with trypsin and Lys-C followed by LC-MS/MS. Listed are peptides representing the D6E(*Tp*) protein, identified with 95% confidence using Mascot server v2.5.1 (Matrix Science Ltd, London, UK).

Figure 19. Peptide Mass Coverage by LC-MS/MS Analysis for Delta-6 Elongase (*Tp*) in EPA+DHA Canola Event LBFLFK

The deduced amino acid sequence of the D6E(*Tp*) protein, newly expressed in EPA+DHA canola event LBFLFK, represented as the one letter amino acid code. PPP isolated from event LBFLFK were digested with trypsin and Lys-C followed by LC-MS/MS in order to identify peptides representing the D6E(*Tp*) protein. Peptides listed in Table 13 were mapped (**bold underlined**) onto the deduced protein sequence, covering approximately 12% of the full-length D6E(*Tp*) protein.

```
1   MDAYNAAMDK IGAAIIDWSD PDGKFRADRE DWWLCDFRSA ITIALIYIAF VILGSAVMQS
61  LPAMDPYPIK FLYNVSQIFL CAYMTVEAGF LAYRNGYTVM PCNHFNVNDP PVANLLWLFY
121 ISKVWDFWDT IFIVLGKKWR QLSFLHVYHH TTIFLFYWLN ANVLYDGDIF LTILLNGFIH
181 TVMYTYYFIC MHTKDSKTGK SLPIWWKSSL TAFQLLQFTI MMSQATYLVF HGCDKVSLRI
241 TIVYFVYILS LFFLFAQFFV QSYMAPKKKK SA
```

Glycosylation analysis

The D6E(*Tp*) protein has no potential N-glycosylation sites (Gavel and von Heijne, 1990; Zielinska et al., 2010) but does have several potential O-glycosylation sites (any serine or threonine). The glycosylation status of the newly expressed D6E(*Tp*) protein was analysed using a strategy that first separated all proteins present in the LBFLFK PPP into two fractions (glycosylated proteins and non-glycosylated proteins) and then determined which fraction contained the D6E(*Tp*) protein by western blot analysis with a D6E(*Tp*)-specific antibody as described in Appendix 9.

Together, these data demonstrated that the D6E(*Tp*) protein present in PPP isolated from EPA+DHA canola event LBFLFK was not glycosylated.

Enzymatic activity

EPA+DHA canola event LBFLFK contains newly expressed D6E proteins from two different organisms: D6E(*Tp*) from *Thalassiosira pseudonana* (described in this section) and D6E(*Pp*) from *Physcomitrella patens* (described below). The functional activity assays for the D6Es from both organisms are identical and were demonstrated using membranes isolated from yeast expression strains (Yilmaz et al., 2017). Therefore, in the PPP isolated from EPA+DHA canola event LBFLFK, the presence of either D6E was tested using this *in vitro* assay; however, the relative contributions of the individual D6Es to the total D6E activity cannot be determined. Specifically, PPP were incubated with the two D6E co-substrates, [^{14}C]-malonyl-CoA and unlabelled C18:3n-6-CoA, in the presence of NADPH. The resulting fatty acid products were isolated, converted to FAMEs, resolved on a TLC plate, and identified

by electronic autoradiography. In the reaction containing LBFLFK PPP, a [^{14}C]-FAME was isolated (Figure 20, Panel B, lane C and D) that migrates similar to the [^{14}C]-20:3n-6-ME standard (Figure 20, Panel B, lane A), in agreement with the expected product according to the reaction shown in Panel A of Figure 20. This product was not detected in the reaction containing Kumily PPP (Figure 20, Panel B, lane B), which does not contain D6E(*Tp*) or D6E(*Pp*) coding sequences.

Together the results obtained from these *in vitro* assays demonstrate D6E activity in the LBFLFK PPP isolated from EPA+DHA canola, that is not observed in Kumily PPP. The observed D6E activity is consistent with the previously (Yilmaz et al., 2017) proposed enzymatic reaction shown in Panel A of Figure 20.

Figure 20. *In Vitro* Enzymatic Activity of Delta-6 Elongases in EPA+DHA Canola Event LBFLFK

Panel A. D6E(*Tp*) and D6E(*Pp*) both catalyse the transfer of two carbons from [^{14}C]-malonyl-CoA to C18:3n-6-CoA generating [^{14}C]-20:3n-6-β-keto-CoA, which in the presence of NADPH can be converted to [^{14}C]-20:3n-6-CoA by the endogenous canola elongation complex enzymes. Panel B. PPP (320 µg total protein) were incubated in a buffer solution with [^{14}C]-malonyl-CoA, unlabeled-C18:3n-6-CoA, and NADPH. Depicted is an autoradiographic image of a TLC plate showing separated [^{14}C]-methylesters (MEs) prepared from the total lipids that were extracted from the enzymatic reactions. The resulting fatty acid methyl esters (FAME) from the D6E assay were separated using a reverse phase thin layer chromatography plate with acetonitrile as the mobile phase. Lane A, [^{14}C]-20:3n-6-ME standard. Lane B, Kumily PPP (control). Lanes C and D, LBFLFK PPP in duplicate. The [^{14}C]-labelled malonyl-ME (derived from the substrate [^{14}C]-malonyl-CoA) does not get retained during the extraction process and is therefore not present on the TLC plate. The [^{14}C]-compound observed in lanes C and D that is denoted by an asterisk (*) is derived from the [^{14}C]-20:3n-6-β-keto-CoA product during the isolation of the FAMEs (Yilmaz et al., 2017).

A.

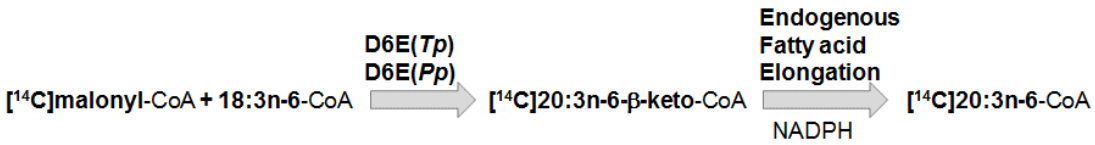

B.

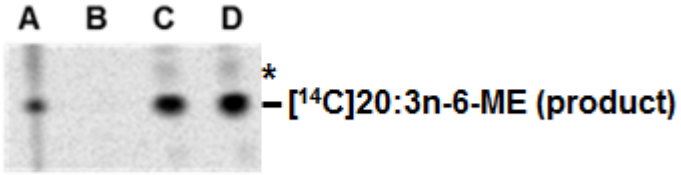

<u>Summary of delta-6 elongase (*Tp*) characterisation</u>

EPA+DHA canola event LBFLFK contains two T-DNA inserts encoding two identical copies of the D6E(*Tp*) protein. The *in silico* predicted protein structure was described and the enzyme function was presented based on published *in vivo* experiments in yeast. Furthermore, a series of biochemical experiments was performed to characterise the D6E(*Tp*) protein newly expressed in event LBFLFK.

Structure / Function: Bioinformatic analysis indicates the protein is an ELO-type integral membrane elongase, and *in vivo* yeast experiments confirmed this enzymatic function. The enzyme catalyses the decarboxylation Claisen-like condensation of two carbons from malonyl-CoA to C18:3n-6-CoA generating C20:3n-6-β-keto-CoA, which is then converted to C20:3n-6-CoA by endogenous enzymes.

Immunoreactivity / Molecular weight: Western blot analysis confirmed the protein was immunoreactive to an anti-D6E(*Tp*) antibody. The apparent molecular weight was in good agreement to the calculated molecular mass of the D6E(*Tp*) protein.

Identity: Tryptic peptide mapping using LC-MS/MS positively identified two distinct peptides (> 9 amino acids) corresponding to the deduced amino acid sequence of the D6E(*Tp*) protein. The D6E(*Tp*) was therefore identified in EPA+DHA canola event LBFLFK.

Glycosylation: The D6E(*Tp*) protein was found to be not glycosylated.

Enzyme activity: Delta-6 elongation activity, i.e. condensation of two carbons from malonyl-CoA to C18:3n-6-CoA generating C20:3n-6-β-keto-CoA, which was ultimately converted to C20:5n-6-CoA by endogenous canola enzymes, was detected in LBFLFK PPP. The detected D6E activity could result from either D6E(*Tp*) or D6E(*Pp*).

Delta-6 elongase (*Pp*)

Structure and function

The delta-6 elongase (*Pp*) protein, D6E(*Pp*), newly expressed in EPA+DHA canola event LBFLFK, is encoded by a coding sequence isolated from the moss *Physcomitrella patens*. The deduced D6E(*Pp*) protein consists of 290 amino acids with a calculated molecular mass of 33.4 kDa. The D6E(*Pp*) amino acid sequence, as depicted in Figure 21, shows the features that are characteristic of ELO-type elongases. Depicted are the predicted transmembrane helices and all four of the signature ELO-motifs. *In vivo* experiments in yeast showed that this D6E(*Pp*) protein catalyses the elongation reaction required to convert C18:3n-6 into C20:3n-6 (Zank et al., 2000; Zank et al., 2002; Domergue et al., 2003; Yilmaz et al., 2017). Additionally, this D6E(*Pp*) was functional upon expression in the seeds of *Nicotiana tabacum*, *Linum usitatissimum*, and *Brassica juncea*, as shown by the successful synthesis of C20:4n-6 and C20:5n-3 in these plants (Abbadi et al., 2004; Wu et al., 2005).

Figure 21. Deduced Amino Acid Sequence for Delta-6 Elongase (*Pp*) in EPA+DHA Canola Event LBFLFK

Using the one letter amino acid code for the D6E(*Pp*) protein in event LBFLFK, the position of predicted transmembrane helices and other characteristic protein motifs are indicated. , , = indicates transmembrane helices as predicted by Scampi 2 (Peters et al., 2016), TMHMM v.2.0 (Krogh et al., 2001), and SOSUI v 1.11 (Hirokawa et al., 1998), respectively. The sequence contains four motifs ( ) highly conserved among elongases (Leonard et al., 2004; Meyer et al., 2004; Jakobsson et al., 2006), including the characteristic HXXHH histidine box embedded in the fourth membrane helix that is critical for enzymatic activity (Denic and Weissman, 2007; Hernandez-Buquer and Blacklock, 2013). Highly conserved residues are highlighted in black.

```
1   MEVVERFYGE LDGKVSQGVN ALLGSFGVEL TDTPTTKGLP LVDSPTPIVL GVSVYLTIVI
                                                  ================
61  GGLLWIKARD LKPRASEPFL LQALVLVHNL FCFALSLYMC VGIAYQAITW RYSLWGNAYN
    =======                 ========================
121 PKHKEMAILV YLFYMSKYVE FMDTVIMILK RSTRQISFLH VYHHSSISLI WWAIAHHAPG
          ========================     ========================
181 GEAYWSAALN SGVHVLMYAY YFLAACLRSS PKLKNKYLFW GRYLTQFQMF QFMLNLVQAY
              ========================
241 YDMKTNAPYP QWLIKILFYY MISLLFLFGN FYVQKYIKPS DGKQKGAKTE
                        ========================
```

Apparent molecular weight and immunoreactivity

Western blot analysis using an anti-D6E(*Pp*) protein antibody was used to show immunoreactivity of the D6E(*Pp*) protein in PPP isolated from EPA+DHA canola event LBFLFK (Figure 22). To demonstrate the specificity of the antibody, a D6E(*Pp*) NC fusion reference protein was included as positive control (Figure 22, lane 1). An immunoreactive band near the calculated mass of the D6E(*Pp*) protein was not observed in the LBFLFK PPP samples (Figure 22, lanes 3 and 4). Likewise, no signal was detected in the PPP isolated from Kumily, the parental control that does not contain the *D6E*(*Pp*) coding sequence, (Figure 22, lane 2) however two non-specific bands were seen in both Kumily and LBFLFK PPP at ~68 kDa and 110 kDa.

Figure 22. Western Blot Analysis of Delta-6 Elongase (*Pp*) in EPA+DHA Canola Event LBFLFK

LBFLFK PPP and Kumily PPP were separated by SDS-PAGE and evaluated by western blot analysis. The membrane was probed with a 1:90 dilution of the D6E(*Pp*)-specific antibody and probed with a secondary HRP-conjugated antibody. Approximate molecular weight markers loaded in lanes MW are shown on the left and right side of the blot. The calculated molecular mass of the D6E(*Pp*) protein from the coding sequence introduced in EPA+DHA canola event LBFLFK is 33.4 kDa. The calculated molecular mass of the D6E(*Pp*) NC fusion protein used as a positive control for the D6E(*Pp*)-specific antibody is 16.8 kDa.

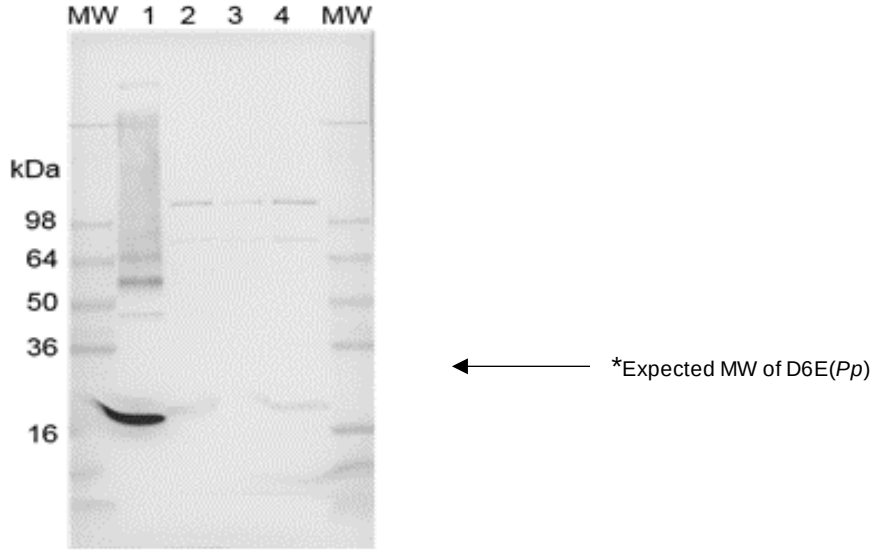

	Lane 1	Lane 2	Lane 3	Lane 4
Sample	D6E(*Pp*) NC fusion protein	Kumily PPP	LBFLFK PPP	LBFLFK PPP
Amount Loaded	50 ng	20 µg	10 µg	20 µg

Identity

Mass spectrometry was used to perform tryptic peptide mapping analysis against the deduced amino acid sequence of the D6E(*Pp*) protein to confirm the identity of the D6E(*Pp*) protein in PPP isolated from EPA+DHA canola event LBFLFK. To minimise the probability of a false positive identification, the current recommendations of the Human Proteome Project Mass Spectrometry Data Interpretation Guidelines 2.1 were followed (Deutsch et al., 2016). Specifically, true positive identification of a protein required the identification of two or more peptides consisting of at least nine amino acids, and one of the peptides may not be fully nested within another. The analysis of three different samples did not identify any peptides that were specific to the deduced D6E(*Pp*) protein sequence and that met the qualifications specified by the Human Proteome Guidelines (Deutsch et al., 2016). The D6E(*Pp*) protein was therefore not identified in PPP isolated from EPA+DHA canola event LBFLFK.

Glycosylation analysis

The glycosylation status of the D6E(*Pp*) protein in PPP isolated from EPA+DHA canola event LBFLFK was not determined since no signal near the calculated molecular weight of D6E(*Pp*) was observed in PPP by western blot analysis (see Figure 22). For more details, please see Appendix 10.

Enzymatic activity

EPA+DHA canola event LBFLFK contains newly expressed D6Es from two different organisms: D6E(*Tp*) from *Thalassiosira pseudonana* (described above), and D6E(*Pp*) from *Physcomitrella patens* (described in this section). The functional activity assays for the D6Es from both organisms are identical and were demonstrated using membranes isolated from yeast expression strains (Yilmaz et al., 2017). Therefore, in the PPP isolated from EPA+DHA canola event LBFLFK, the presence of either D6E protein was tested using this *in vitro* assay (Yilmaz et al., 2017); however, the relative contributions of the individual D6E proteins to the total D6E activity cannot be determined. The results described in the section on D6E(*Tp*) above demonstrate D6E activity in the LBFLFK PPP isolated from EPA+DHA canola. This D6E activity was not observed in Kumily PPP, which does not contain D6E(*Tp*) or D6E(*Pp*) coding sequences. The observed D6E activity is consistent with the previously proposed enzymatic reaction (Yilmaz et al., 2017) shown in Panel A of Figure 20 and could be attributed to either (or both) the D6E(*Tp*) protein or the D6E(*Pp*) protein.

Summary of delta-6 elongase (*Pp*) characterisation

EPA+DHA canola event LBFLFK contains two T-DNA inserts encoding two identical copies of the D6E(*Pp*) protein. The *in silico* predicted protein structure was described and the enzyme function was presented based on published *in vivo* experiments in yeast. Furthermore, a series of biochemical experiments was performed to characterise the D6E(*Pp*) protein newly expressed in event LBFLFK. In summary:

Structure / Function: Bioinformatic analysis indicates the protein is an ELO-type integral membrane elongase, and *in vivo* yeast experiments confirmed this enzymatic function. The enzyme catalyses the decarboxylation Claisen-like condensation of two carbons from malonyl-CoA to C18:3n-6-CoA generating C20:3n-6-β-keto-CoA, which is then converted to C20:3n-6-CoA by endogenous enzymes.

Immunoreactivity / Molecular weight: The D6E(*Pp*)-specific antibody could not detect a protein in agreement with the calculated molecular mass of the D6E(*Pp*); therefore the immunoreactivity and molecular weight of this protein could not be determined.

Identity: Tryptic peptide mapping using LC-MS/MS did not identify the D6E(*Pp*) protein.

Glycosylation: The D6E(*Pp*)-specific antibody could not detect a protein in agreement with the calculated molecular mass of the D6E(*Pp*); therefore the glycosylation status of this protein could not be determined.

Enzyme activity: Delta-6 elongation activity, i.e. condensation of two carbons from malonyl-CoA to C18:3n-6-CoA generating C20:3n-6-β-keto-CoA, which was ultimately converted to C20:5n-6-CoA by endogenous canola enzymes, was detected in LBFLFK PPP. The detected D6E activity could result from either D6E(*Tp*) or D6E(*Pp*).

Delta-5 desaturase (*Tc*)

Structure and function

The delta-5 desaturase (*Tc*) protein, D5D(*Tc*), newly expressed in EPA+DHA canola event LBFLFK is encoded by a coding sequence isolated from the marine protist *Thraustochytrium*

sp. The deduced D5D(*Tc*) protein consists of 439 amino acids with a calculated molecular mass of 49.8 kDa. The D5D(*Tc*) amino acid sequence, as depicted in Figure 23, shows the features that are characteristic for a front-end integral membrane desaturase. Depicted are the N-terminally fused cytochrome b_5 domain containing the characteristic HPGG motif, the predicted transmembrane helices, three histidine boxes containing seven conserved histidine residues, a conserved glutamine in histidine box 3, and the conserved histidine following the C-terminal transmembrane helix. *In vivo* experiments in yeast showed that this D5D(*Tc*) protein catalyses the desaturation reaction required to convert C20:3n-6 into C20:4n-6 (Qiu et al., 2001; Yilmaz et al., 2017). Furthermore, this D5D(*Tc*) was functional upon expression in the seeds of *Brassica juncea*, as shown by the successful synthesis of C20:4n-6 and C20:5n-3 (Wu et al., 2005).

Figure 23. Deduced Amino Acid Sequence for Delta-5 Desaturase (*Tc*) in EPA+DHA Canola Event LBFLFK

Using the one letter amino acid code for the D5D(*Tc*) protein in event LBFLFK, the position of predicted transmembrane helices and other characteristic protein motifs are indicated. ▒,▒,= indicates transmembrane helices as predicted by Scampi 2 (Peters et al., 2016), TMHMM v.2.0 (Krogh et al., 2001), and SOSUI v 1.11 (Hirokawa et al., 1998), respectively. The sequence contains three histidine-box motifs (□) with seven conserved histidine residues (H) typical for desaturases (Shanklin et al., 1994) and an additional conserved histidine (H), all of which participate in the coordination of the diiron active centre (Bai et al., 2015; Wang et al., 2015). Additionally, the sequence contains a conserved glutamine (Q) in the third histidine box that is essential for activity (Sayanova et al., 2001). Underlined is the cytochrome b_5 domain as annotated by PFAM v31 (Finn et al., 2016), containing the characteristic HPGG motif (Sperling and Heinz, 2001) highlighted in grey highlighted in grey.

```
1   MGKGSEGRSA AREMTAEANG DKRKTILIEG VLYDATNFKH PGGSIINFLT EGEAGVDATQ
61  AYREFHQRSG KADKYLKSLP KLDASKVESR FSAKEQARRD AMTRDYAAFR EELVAEGYFD
121 PSIPHMIYRV VEIVALFALS FWLMSKASPT SLVLGVVMNG IAQGRCGWVM HEMGHGSFTG
      ========================  ======================
181 VIWLDDRMCE FFYGVGCGMS GHYWKNQHSK HHAAPNRLEH DVDLNTLPLV AFNERVVRKV
241 KPGSLLALWL RVQAYLFAPV SCLLIGLGWT LYLHPRYMLR TKRHMEFVWI FARYIGWFSL
          ========================              ================
301 MGALGYSPGT SVGMYLCSFG LGCIYIFLQF AVSHTHLPVT NPEDQLHWLE YAADHTVNIS
    =======     ======================
361 TKSWLVTWWM SNLNFQIFHH LFPTAPQFRF KEISPRVEAL FKRHNLPYYD LPYTSAVSTT
421 FANLYSVGHS VGADTKKQD
```

Apparent molecular weight and immunoreactivity

Western blot analysis using an anti-D5D(*Tc*) protein antibody was used to show immunoreactivity of the D5D(*Tc*) protein in PPP isolated from EPA+DHA canola event LBFLFK (Figure 24). To demonstrate the specificity of the antibody, a D5D(*Tc*) full-length reference protein was included as positive control (Figure 24, lane 1). An immunoreactive band was observed in the LBFLFK PPP samples at a molecular weight that was in good agreement with the calculated molecular mass of the D5D(*Tc*) protein of 49.8 kDa (Figure 24, lanes 3 and 4). No signal was detected in PPP isolated from Kumily, the parental control that does not contain the D5D(*Tc*) coding sequence (Figure 24, lane 2). The immunoreactive proteins observed at approximately 20 kDa in the LBFLFK PPP (Figure 24, lanes 3 and 4) are

not observed in Kumily PPP (Figure 24, lane 2), and likely resulted from degradation of the D5D(*Tc*) protein.

Figure 24. Western Blot Analysis of Delta-5 Desaturase (Tc) in EPA+DHA Canola Event LBFLFK

LBFLFK PPP and Kumily PPP were separated by SDS-PAGE and evaluated by western blot analysis. The membrane was probed with a 1:500 dilution of the D5D(*Tc*)-specific antibody and probed with a secondary HRP-conjugated antibody. Approximate molecular weight markers loaded in lanes MW are shown on the left and right side of the blot. The calculated molecular mass of the D5D(*Tc*) protein encoded by the coding sequence introduced in EPA+DHA canola event LBFLFK is 49.8 kDa. The calculated molecular mass of the D5D(*Tc*) full-length reference standard protein used as a positive control for the D5D(*Tc*)-specific antibody is 49.8 kDa.

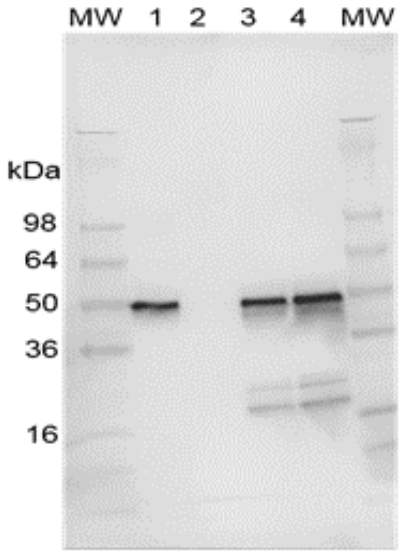

	Lane 1	Lane 2	Lane 3	Lane 4
Sample	D5D(*Tc*) full-length protein	Kumily PPP	LBFLFK PPP	LBFLFK PPP
Amount Loaded	8 ng	20 µg	10 µg	20 µg

Identity

Mass spectrometry was used to perform tryptic peptide mapping analysis against the deduced amino acid sequence of the D5D(*Tc*) protein to confirm the identity of the D5D(*Tc*) protein in PPP isolated from EPA+DHA canola event LBFLFK. To minimise the probability of a false positive identification, the current recommendations of the Human Proteome Project Mass Spectrometry Data Interpretation Guidelines 2.1 were followed (Deutsch et al., 2016). Specifically, true positive identification of a protein requires analysis of one sample and identification of at least two peptides consisting of at least nine amino acids, and one of the peptides may not be fully nested within another. The analysis of three different samples identified eight peptides (Table 14) that matched the expected deduced amino acid sequence of the D5D(*Tc*) protein with ≥ 95% probability of true positive identification and covered 31% of the entire protein sequence (Figure 25). Seven of the peptides listed in Table 14 contained at least nine amino acids and were not fully nested within another (peptides 2–8). The confidence of having accurately identified the D5D(*Tc*) protein is further increased by the

replicate identification of six peptides (2–7) in multiple samples. The D5D(*Tc*) protein was therefore identified in PPP isolated from EPA+DHA canola event LBFLFK.

Table 14. Tryptic Peptides Identified for Delta-5 Desaturase (*Tc*) in EPA+DHA Canola Event LBFLFK using LC-MS/MS Analysis

Number	Peptide Sequence	Amino Acid Length	Replicate 1	Replicate 2	Replicate 3
1	FKEISPR	7	X	X	
2	HMEFVWIFAR	10	X		X
3	VKPGSLLALWLR	12	X	X	X
4	TILIEGVLYDATNFK	15	X	X	X
5	LEHDVDLNTLPLVAFNER	18	X	X	X
6	ASPTSLVLGVVMNGIAQGR	19	X	X	X
7	HPGGSIINFLTEGEAGVDATQAYR	24	X	X	X
8	HNLPYYDLPYTSAVSTTFANLYSVGHS VGADTK	33			X

PPP isolated from event LBFLFK were digested with trypsin and Lys-C followed by LC-MS/MS. Listed are peptides representing the D5D(*Tc*) protein, identified with 95% confidence using Mascot server v2.5.1 (Matrix Science Ltd, London, UK).

Figure 25. Peptide Mass Coverage by LC-MS/MS Analysis for Delta-5 Desaturase (*Tc*) in EPA+DHA Canola Event LBFLFK

The deduced amino acid sequence of the D5D(*Tc*) protein, newly expressed in EPA+DHA canola event LBFLFK, represented as the one letter amino acid code is shown. PPP isolated from event LBFLFK were digested with trypsin and Lys-C followed by LC-MS/MS in order to identify peptides representing the D5D(*Tc*) protein. Peptides listed in Table 14 were mapped (**bold underlined**) onto the deduced protein sequence, covering approximately 31% of the full-length D5D(*Tc*) protein.

```
  1  MGKGSEGRSA AREMTAEANG DKRKTILIEG VLYDATNFKH PGGSIINFLT EGEAGVDATQ
 61  AYREFHQRSG KADKYLKSLP KLDASKVESR FSAKEQARRD AMTRDYAAFR EELVAEGYFD
121  PSIPHMIYRV VEIVALFALS FWLMSKASPT SLVLGVVMNG IAQGRCGWVM HEMGHGSFTG
181  VIWLDDRMCE FFYGVGCGMS GHYWKNQHSK HHAAPNRLEH DVDLNTLPLV AFNERVVRKV
241  KPGSLLALWL RVQAYLFAPV SCLLIGLGWT LYLHPRYMLR TKRHMEFVWI FARYIGWFSL
301  MGALGYSPGT SVGMYLCSFG LGCIYIFLQF AVSHTHLPVT NPEDQLHWLE YAADHTVNIS
361  TKSWLVTWWM SNLNFQIEHH LFPTAPQFRF KEISPRVEAL FKRHNLPYYD LPYTSAVSTT
421  FANLYSVGHS VGADTKKQD
```

Glycosylation analysis

The D5D(*Tc*) protein has one potential N-glycosylation site at $_{358}$NIST$_{361}$ (Gavel and von Heijne, 1990; Zielinska et al., 2010) and several potential O-glycosylation sites (any serine or threonine). The glycosylation status of the newly expressed D5D(*Tc*) protein was analysed using a strategy that first separated all proteins present in the LBFLFK PPP into two fractions (glycosylated proteins and non-glycosylated proteins) and then determined which fraction contained the D5D(*Tc*) protein by western blot analysis with a D5D(*Tc*)-specific antibody as described in Appendix 11.

Therefore, these data demonstrated that the D5D(*Tc*) protein present in PPP isolated from EPA+DHA canola event LBFLFK was not glycosylated.

Enzymatic activity

The functional activity of the newly expressed D5D(*Tc*) enzyme in PPP isolated from EPA+DHA canola event LBFLFK was tested using an *in vitro* assay previously reported for the D5D(*Tc*) enzyme present in membranes isolated from yeast expression strains (Yilmaz et al., 2017). *In vivo* and *in vitro* experiments using yeast expression strains, as well as bioinformatic analysis, all indicate that the D5D(*Tc*) uses acyl-CoA substrates (e.g., C20:3n-6 bound to coenzyme A) (Li et al., 2016; Senger et al., 2016; Yilmaz et al., 2017). Therefore, in the assay PPP (isolated from LBFLFK or Kumily) were incubated with [^{14}C]-20:3n-6-CoA and NADH. The resulting fatty acid products were isolated, converted to FAMEs, resolved on a TLC plate, and identified by electronic autoradiography. In the reaction containing either Kumily or LBFLFK PPP (Figure 26, Panel B, lanes D–F), no [^{14}C]-FAME was identified that migrates similar to the [^{14}C]-20:4n-6-ME standard (Figure 26, Panel B, lane B), indicating the expected product according to the reaction shown in Panel A of Figure 26 was not formed. However, in the reaction containing membranes isolated from yeast expressing the D5D(*Tc*) protein, a [^{14}C]-FAME was identified that migrates similar to the [^{14}C]-20:4n-6-ME standard, indicating the assay was run appropriately to allow formation of the product by the D5D(*Tc*) (Figure 26, Panel B, lanes C and B, respectively).

The presence of C20:4n-6 in event LBFLFK seeds, indicates D5D(*Tc*) is active in seed of LBFLFK. The difficulty in demonstrating *in vitro* activity of the D5D(*Tc*) may result from the central role of acyl-CoAs in lipid metabolism. Many competing enzyme activities rely on acyl-CoA substrates (Waku, 1992; Bates et al., 2009). The high flux of nascent acyl-CoAs into phospholipids via LPCAT was established (Bates et al., 2009), and enables the activity assay of phospholipid dependent desaturases (Yilmaz et al., 2017). In contrast, an assay of acyl-CoA dependent desaturases would be highly affected by the relative activity of enzymes competing for the same acyl-CoA substrate. Combining the results in Figure 16 and the fatty acids found in the seeds, it is likely the relative activity of the acyl-CoA dependent D6D(*Ot*) desaturase to all other competing enzymes (such as LPCAT and thioesterases) is higher in yeast membranes compared to LBFLFK PPP; however, the D5D(*Tc*) has the intended *in vivo* activity in seeds of event LBFLFK.

Figure 26. *In Vitro* Enzymatic Activity of Delta-5 Desaturase (*Tc*) in EPA+DHA Canola Event LBFLFK

Panel A. D5D(*Tc*) desaturates the fatty acid substrate C20:3n-6 to the fatty acid product C20:4n-6 (Yilmaz et al., 2017). *In vivo* and *in vitro* experiments using yeast expression strains, as well as bioinformatic analysis, all indicate that the D5D(*Tc*) enzyme desaturates fatty acids covalently attached to coenzyme A (Li et al., 2016; Senger et al., 2016; Yilmaz et al., 2017). Panel B. PPP (50 µg total protein) were incubated in a buffer solution with [^{14}C]-labelled C20:3n-6-CoA substrate and NADH. Total lipids were extracted, converted to fatty acid methyl esters (FAMEs), and separated using a reverse phase thin layer chromatography plate with acetonitrile as the mobile phase. Shown below is an autoradiographic image of the TLC plate of the resolved [^{14}C]-methyl esters (ME). Lane A, C20:3n-6-ME (substrate standard). Lane B, C20:4n-6-ME (product standard). Lane C, yeast membranes containing D5D(*Tc*) (control). Lane D, Kumily PPP. Lane E and F, LBFLFK PPP in duplicate.

A.

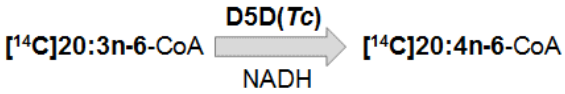

B.

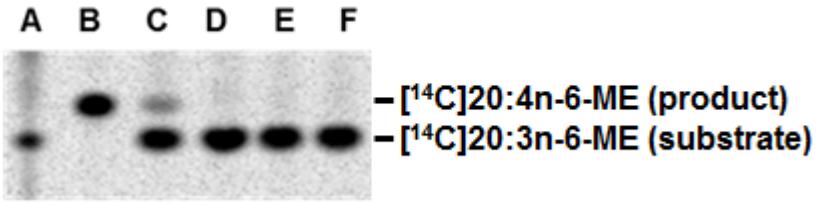

Summary of delta-5 desaturase (*Tc*) characterisation

EPA+DHA canola event LBFLFK contains two T-DNA inserts encoding four identical copies of the D5D(*Tc*) protein. The *in silico* predicted protein structure was described and the enzyme function was presented based on published *in vivo* experiments in yeast. Furthermore, a series of biochemical experiments was performed to characterise the D5D(*Tc*) protein newly expressed in event LBFLFK.

Structure / Function: Bioinformatic analysis indicates the protein is a front-end integral membrane desaturase, and *in vivo* yeast experiments confirmed this enzymatic function. The enzyme converts C20:3n-6 into C20:4n-6.

Immunoreactivity / Molecular weight: Western blot analysis confirmed the protein was immunoreactive to an anti-D5D(*Tc*) antibody. The apparent molecular weight was in good agreement to the calculated molecular mass of the D5D(*Tc*) protein.

Identity: Tryptic peptide mapping using LC-MS/MS positively identified seven distinct peptides (> 9 amino acids) corresponding to the deduced amino acid sequence of the D5D(*Tc*) protein. The D5D(*Tc*) was therefore identified in EPA+DHA canola event LBFLFK.

Glycosylation: The D5D(*Tc*) protein was found to be not glycosylated.

Enzyme activity: Delta-5 desaturation activity, i.e. the introduction of a double bond in C20:3n-6 generating C20:4n-6, was not detected using the *in vitro* enzyme assay in LBFLFK PPP, likely due to the activity of enzymes competing for the C20:3n-6-CoA substrate in

LBFLFK PPP. However, the presence of C20:4n-6 in event LBFLFK seeds indicates the D5D(*Tc*) has the intended *in vivo* activity in seeds of event LBFLFK.

Omega-3 desaturase (*Pir*)

Structure and function

The omega-3 desaturase (*Pir*) protein, O3D(*Pir*), newly expressed in EPA+DHA canola event LBFLFK, is encoded by a coding sequence from the oomycete *Pythium irregulare*. The deduced O3D(*Pir*) protein consists of 363 amino acids with a calculated molecular mass of 40.4 kDa. The O3D(*Pir*) amino acid sequence, as depicted in Figure 27, shows the features that are characteristic for a methyl-end integral membrane desaturase. Depicted are the predicted transmembrane helices, three histidine boxes containing eight conserved histidine residues, and the conserved histidine following the C-terminal transmembrane helix. *In vivo* experiments in yeast showed that this O3D(*Pir*) protein catalyses the reaction required to convert C20:4n-6 into C20:5n-3 (Yilmaz et al., 2017).

Figure 27. Deduced Amino Acid Sequence for Omega-3 Desaturase (*Pir*) in EPA+DHA Canola Event LBFLFK

Using the one letter amino acid code for the O3D(*Pir*) protein in event LBFLFK, the position of predicted transmembrane helices and other characteristic protein motifs are indicated. , ,= indicates transmembrane helices as predicted by Scampi 2 (Peters et al., 2016), TMHMM v.2.0 (Krogh et al., 2001), and SOSUI v 1.11 (Hirokawa et al., 1998), respectively. The sequence contains three histidine-box motifs ( ) with eight conserved histidine residues (H) typical for desaturases (Shanklin et al., 1994) and an additional conserved histidine (H), all of which participate in the coordination of the diiron active centre (Bai et al., 2015; Wang et al., 2015).

```
1   MASTSAAQDA APYEFPSLTE IKRALPSECF EASVPLSLYY TARSLALAGS LAVALSYARA
                                                ================
61  LPLVQANALL DATLCTGYVL LOGIVFWGFF TVGHDCGHGA FSRSHVLNFS VGTLMHSIIL
    ========    ========================
121 TPFESWKLSH RHHHKNTGNI DKDEIFYPQR EADSHPVSRH LVMSLGSAWF AYLFAGFPPR
                                            ========================
181 TMNHFNPWEA MYVRRVAAVI ISLGVLFAFA GLYSYLTFVL GFTTMAIYYF GPLFIFATML
    =               ========================    ====================
241 VVTTFLHHND EETPWYADSE WTYVKGNLSS VDRSYGALID NLSHNIGTHQ IHHLFPIIPH
    ====
301 YKLNDATAAF AKAFPELVRK NAAPIIPTFF RMAAMYAKYG VVDTDAKTFT LKEAKAAAKT
361 KSS
```

Apparent molecular weight and immunoreactivity

Western blot analysis using an anti-O3D(*Pir*) antibody was used to show immunoreactivity of the O3D(*Pir*) protein in PPP isolated from EPA+DHA canola event LBFLFK (Figure 28). To demonstrate the specificity of the antibody, an O3D(*Pir*) NC fusion reference protein was included as positive control (Figure 28, lane 1). An immunoreactive band was observed in the LBFLFK PPP samples at a molecular weight that was in good agreement with the calculated molecular mass of the O3D(*Pir*) protein of 40.4 kDa (Figure 28, lanes 3 and 4). No signal was

detected in PPP isolated from Kumily, the parental control that does not contain the *O3D*(*Pir*) coding sequence (Figure 28, lane 2). The immunoreactive proteins observed at approximately 18 kDa in the LBFLFK PPP (Figure 28, lanes 3 and 4) were not observed in Kumily PPP (Figure 28, lane 2) and likely result from degradation of the O3D(*Pir*) protein.

Figure 28. Western Blot Analysis of Omega-3 Desaturase (*Pir*) in EPA+DHA Canola Event LBFLFK

LBFLFK PPP and Kumily PPP were separated by SDS-PAGE and evaluated by western blot analysis. The membrane was probed with a 1:6,000 dilution of the O3D(*Pir*)-specific antibody and probed with a secondary HRP-conjugated antibody. Approximate molecular weight markers loaded in lanes MW are shown on the left and right side of the blot. The calculated molecular mass of the O3D(*Pir*) protein encoded by the coding sequence introduced in EPA+DHA canola event LBFLFK is 40.4 kDa. The calculated molecular mass of the O3D(*Pir*) NC fusion protein used as a positive control for the O3D(*Pir*)-specific antibody is 18.2 kDa.

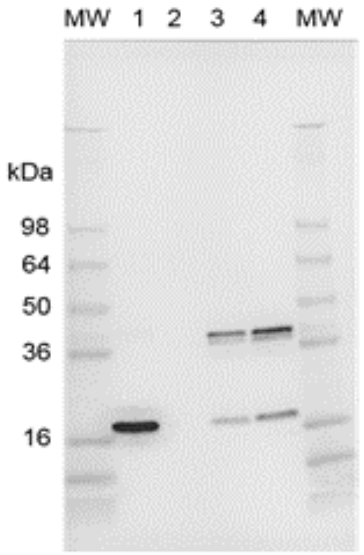

	Lane 1	Lane 2	Lane 3	Lane 4
Sample	O3D(*Pir*) NC fusion protein	Kumily PPP	LBFLFK PPP	LBFLFK PPP
Amount Loaded	10 ng	20 µg	10 µg	20 µg

Identity

Mass spectrometry was used to perform tryptic peptide mapping analysis against the deduced amino acid sequence of the O3D(*Pir*) protein to confirm the identity of the O3D(*Pir*) protein in PPP isolated from EPA+DHA canola event LBFLFK. To minimise the probability of a false positive identification, the current recommendations of the Human Proteome Project Mass Spectrometry Data Interpretation Guidelines 2.1 were followed (Deutsch et al., 2016). Specifically, true positive identification of a protein requires analysis of one sample and identification of at least two peptides consisting of at least nine amino acids, and one of the peptides may not be fully nested within another. The analysis of three different samples identified 12 peptides (Table 15) that matched the expected deduced amino acid sequence of the O3D(*Pir*) protein with ≥ 95% probability of positive identification and covered 37% of the entire protein sequence (Figure 29). Eight of the peptides listed in Table 15 contained at least

nine amino acids and were not fully nested within another (peptides 4–12 except 6). The confidence of having accurately identified the O3D(*Pir*) is further increased by the replicate identification of eight of these peptides (4–11) in multiple samples and the identification of peptide 2 and 6 that are fully nested within peptide 9 and 7, respectively. The O3D(*Pir*) protein was therefore identified in PPP isolated from EPA+DHA canola event LBFLFK.

Table 15. Tryptic Peptides Identified for Omega-3 Desaturase (*Pir*) in EPA+DHA Canola Event LBFLFK using LC-MS/MS Analysis

Number	Peptide Sequence	Amino Acid Length	Replicate 1	Replicate 2	Replicate 3
1	AFPELVR	7	X	X	X
2	DEIFYPQR	8	X	X	X
3	GNLSSVDR	8		X	X
4	YGVVDTDAK	9	X	X	X
5	LNDATAAFAK	10	X	X	X
6	NAAPIIPTFFR	11	X	X	X
7	KNAAPIIPTFFR	12	X	X	X
8	TMNHFNPWEAMYVR	14	X	X	X
9	NTGNIDKDEIFYPQR	15	X	X	X
10	SLALAGSLAVALSYAR	16	X	X	X
11	ALPSECFEASVPLSLYYTAR	20	X	X	X
12	SHVLNFSVGTLMHSIILTPFESWK	24			X

PPP isolated from event LBFLFK was digested with trypsin and Lys-C followed by LC-MS/MS. Listed are peptides representing the O3D(*Pir*) protein, identified with 95% confidence using Mascot server v2.5.1 (Matrix Science Ltd, London, UK).

Figure 29. Peptide Mass Coverage by LC-MS/MS Analysis for Omega-3 Desaturase (*Pir*) in EPA+DHA Canola Event LBFLFK

The deduced amino acid sequence of the O3D(*Pir*) protein, newly expressed in EPA+DHA canola event LBFLFK, represented as the one letter amino acid code. PPP isolated from event LBFLFK were digested with trypsin and Lys-C followed by LC-MS/MS to identify peptides representing the O3D(*Pir*) protein. Peptides listed in Table 15 were mapped (**bold underlined**) onto the deduced O3D(*Pir*) protein sequence, covering approximately 37% of the full-length O3D(*Pir*) protein.

```
1   MASTSAAQDA APYEFPSLTE IKRALPSECF EASVPLSLYY TARSLALAGS LAVALSYARA
61  LPLVQANALL DATLCTGYVL LQGIVFWGFF TVGHDCGHGA FSRSHVLNFS VGTLMHSIIL
121 TPFESWKLSH RHHHKNTGNI DKDEIFYPQR EADSHPVSRH LVMSLGSAWF AYLFAGFPPR
181 TMNHFNPWEA MYVRRVAAVI ISLGVLFAFA GLYSYLTFVL GFTTMAIYYF GPLFIFATML
241 VVTTFLHHND EETPWYADSE WTYVKGNLSS VDRSYGALID NLSHNIGTHQ IHHLFPIIPH
301 YKLNDATAAF AKAFPELVRK NAAPIIPTFF RMAAMYAKYG VVDTDAKTFT LKEAKAAAKT
361 KSS
```

Glycosylation analysis

The O3D(*Pir*) protein has three potential N-glycosylation sites at $_{108}$NFSV$_{111}$, $_{267}$NLSS$_{270}$, and $_{281}$NLSH$_{284}$ (Gavel and von Heijne, 1990; Zielinska et al., 2010) and several potential O-glycosylation sites (any serine or threonine). The glycosylation status of the newly expressed O3D(*Pir*) protein was analysed using a strategy that first separated all proteins present in the LBFLFK PPP into two fractions (glycosylated proteins and non-glycosylated proteins) and then determined which fraction contained the O3D(*Pir*) protein by western blot analysis with a O3D(*Pir*)-specific antibody as described in Appendix 12.

Together, these data demonstrated that the O3D(*Pir*) protein present in PPP isolated from EPA+DHA canola event LBFLFK was not glycosylated.

Enzymatic activity

EPA+DHA canola event LBFLFK contains newly expressed omega-3 desaturases (O3Ds) from two different organisms: O3D(*Pir*) from *Pythium irregulare* (described in this section) and O3D(*Pi*) from *Phytophthora infestans* (described below). The functional activity assays for both O3Ds are identical and were demonstrated using membranes isolated from yeast expression strains (Yilmaz et al., 2017). Therefore, in the PPP isolated from EPA+DHA canola event LBFLFK, this *in vitro* assay tests for the presence of either O3D protein. Both O3Ds appear to desaturate C20:4n-6 to C20:5n-3 when the substrate fatty acid was covalently bound to a lipid e.g., phosphatidylcholine (PC) (Yilmaz et al., 2017). Therefore, endogenous lysophosphatidylcholine acyl transferase (LPCAT) present in PPP was used to synthesise [^{14}C]-20:4n-6-PC *in situ* by transesterification of [^{14}C]-20:4n-6 from CoA to lysophosphatidylcholine (LPC) (Yilmaz et al., 2017). Specifically, in this assay, PPP (isolated from LBFLFK or Kumily) were incubated with [^{14}C]-20:4n-6-CoA, unlabelled C16:0-lysophosphatidylcholine, and NADH. The resulting fatty acid products were isolated, converted to FAMEs, resolved on a TLC plate, and identified by electronic autoradiography. In the reaction containing either Kumily or LBFLFK PPP (Figure 30, Panel B, lanes C–E), no [^{14}C]-FAME was identified that migrates similar to the [^{14}C]-20:5n-3-ME standard (Figure 30, Panel B, lane B), indicating the expected product according to the reaction shown in Panel A of Figure 30 was not formed. The absence of detectable omega-3 desaturase activity may result from the developmental stage of the immature seeds used for the preparation of the LBFLFK PPP, as more mature seed isolated from EPA+DHA canola event LBFLFK was shown to have detectable O3D activity.

Figure 30. *In Vitro* Enzymatic Activity of Omega-3 Desaturases in EPA+DHA Canola Event LBFLFK

Panel A. O3D(*Pir*) and O3D(*Pi*) both appear to desaturate the fatty acid substrate C20:4n-6 to the fatty acid product C20:5n-3 when the substrate is covalently bound to a lipid, e.g., phosphatidylcholine (PC) (Yilmaz et al., 2017). In the enzymatic assay, endogenous lysophosphatidylcholine acyl transferase (LPCAT) is used to synthesise C20:4n-6-PC by transferring C20:4n-6 from CoA to lysophosphatidylcholine (LPC). Panel B. PPP (100 µg total protein) were incubated in a buffer solution with [^{14}C]-20:4n-6-CoA, unlabelled C16:0-lysophosphatidylcholine (LPC), and NADH. Total lipids were extracted, converted to fatty acid methyl esters (FAME), and separated using a 10% $AgNO_3$ thin layer chromatography plate with a 1:1 ratio of toluene/heptane solvent as the mobile phase. Shown below is an autoradiographic image of the TLC plate of the resolved [^{14}C]-methyl esters (ME). Kumily PPP was used as a control. Lane A, C20:4n-6-ME standard. Lane B, C20:5n-3-ME standard. Lane C, Kumily PPP (control). Lanes D and E, LBFLFK PPP in duplicate.

A.

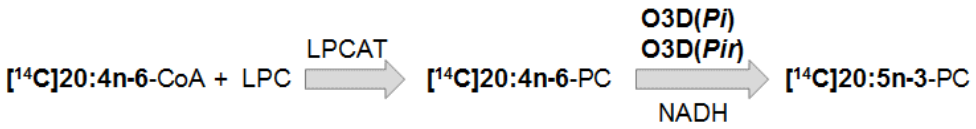

B.

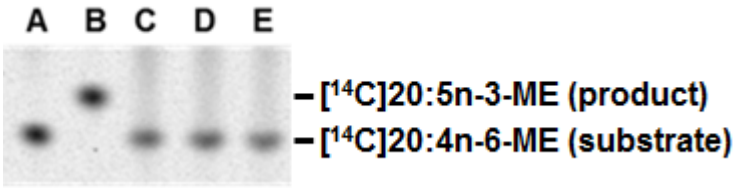

Summary of omega-3 desaturase (*Pir*) characterisation

EPA+DHA canola event LBFLFK contains two T-DNA inserts encoding four identical copies of the O3D(*Pir*) protein. The *in silico* predicted protein structure was described and the enzyme function was presented based on published *in vivo* experiments in yeast. Furthermore, a series of biochemical experiments was performed to characterise the O3D(*Pir*) protein newly expressed in event LBFLFK.

Structure / Function: Bioinformatic analysis indicates the protein is a methyl-end integral membrane desaturase, and *in vivo* yeast experiments confirmed this enzymatic function. The enzyme converts C20:4n-6 into C20:5n-3.

Immunoreactivity / Molecular weight: Western blot analysis confirmed the protein was immunoreactive to an anti-O3D(*Pir*) antibody. The apparent molecular weight was in good agreement to the calculated molecular mass of the O3D(*Pir*) protein.

Identity: Tryptic peptide mapping using LC-MS/MS positively identified eight distinct peptides (> 9 amino acids) corresponding to the deduced amino acid sequence of the O3D(*Pir*) protein. The O3D(*Pir*) was therefore identified in EPA+DHA canola event LBFLFK.

Glycosylation: The O3D(*Pir*) protein was found to be not glycosylated.

Enzyme activity: Omega-3 desaturation activity, i.e. the introduction of a double bond in C20:4n-6 generating C20:5n-3, was not detected using the *in vitro* enzyme assay in LBFLFK

PPP. However, the presence of the C20:5n-3 in event LBFLFK seeds indicates *in vivo* O3D activity in seeds of event LBFLFK, which could result from either O3D(*Pir*) or O3D(*Pi*).

Omega-3 desaturase (*Pi*)

Structure and function

The omega-3 desaturase (*Pi*) protein O3D(*Pi*), newly expressed in EPA+DHA canola event LBFLFK, is encoded by a coding sequence from the oomycete *Phytophthora infestans*. The deduced O3D(*Pi*) protein consists of 361 amino acids with a calculated molecular mass of 40.8 kDa. The O3D(*Pi*) amino acid sequence, as depicted in Figure 31, shows the features that are characteristic for a methyl-end integral membrane desaturase. Depicted are the predicted transmembrane, three histidine boxes containing eight conserved histidine residues, and the conserved histidine following the C-terminal transmembrane helix. *In vivo* experiments in yeast showed that this O3D(*Pi*) protein catalyses the reaction required to convert C20:4n-6 into C20:5n-3 (Yilmaz et al., 2017).

Figure 31. Deduced Amino Acid Sequence for Omega-3 Desaturase (*Pi*) in EPA+DHA Canola Event LBFLFK

Using the one letter amino acid code for the O3D(*Pi*) protein in event LBFLFK, the position of predicted transmembrane helices and other characteristic protein motifs are indicated. , ,= indicates transmembrane helices as predicted by Scampi 2 (Peters et al., 2016), TMHMM v.2.0 (Krogh et al., 2001), and SOSUI v 1.11 (Hirokawa et al., 1998), respectively. The sequence contains three histidine-box motifs ( ) with eight conserved histidine residues (H) typical for desaturases (Shanklin et al., 1994) and an additional conserved histidine (H), all of which participate in the coordination of the diiron active centre (Bai et al., 2015; Wang et al., 2015).

```
1   MATKEAYVFP TLTEIKRSLP KDCFEASVPL SLYYTVRCLV IAVALTFGLN YARALPEVES
                                  ========================
61  FWALDAALCT GYILLQGIVF WGFFTVGHDA GHGAFSRYHL LNFVVGTFMH SLILTPFESW
      ========================
121 KLTHRHHHKN TGNIDRDEVF YPQRKADDHP LSRNLILALG AAWLAYLVEG FPPRKVNHFN
                                    ========================
181 PFEPLFVRQV SAVVISLLAH FFVAGLSIYL SLQLGLKTMA IYYYGPVFVF GSMLVITTFL
                ========================    ====================
241 HHNDEETPWY ADSEWTYVKG NLSSVDRSYG ALIDNLSHNI GTHQIHHLFP IIPHYKLKKA
    ===
301 TAAFHQAFPE LVRKSDEPII KAFFRVGRLY ANYGVVDQEA KLFTLKEAKA ATEAAAKTKS
361 T
```

Apparent molecular weight and immunoreactivity

Western blot analysis using an anti-O3D(*Pi*) protein antibody was used to show immunoreactivity of the O3D(*Pi*) protein in PPP isolated from EPA+DHA canola event LBFLFK (Figure 32). To demonstrate the specificity of the antibody, an O3D(*Pi*) NC fusion reference protein was included as positive control (Figure 32, lane 1). An immunoreactive band near the calculated mass of the O3D(*Pi*) protein of 40.8 kDa was not observed in the LBFLFK PPP samples (Figure 32, lanes 3 and 4). Likewise, no signal was detected in the PPP isolated from

Kumily, the parental control that does not contain the O3D(*Pi*) coding sequence (Figure 32, lane 2). The immunoreactive proteins observed at approximately 98 kDa and slightly smaller than 98 kDa in the LBFLFK PPP and in Kumily PPP (Figure 32, lane 2, lane 4, faint in lane 3), are likely a result from non-specific protein recognition of endogenous canola proteins by the anti-O3D(*Pi*) antibody.

Figure 32. Western Blot Analysis of Omega-3 Desaturase (*Pi*) in EPA+DHA Canola Event LBFLFK

LBFLFK PPP and Kumily PPP were separated by SDS-PAGE and evaluated by western blot analysis. The membrane was probed with a 1:1,000 dilution of the O3D(*Pi*)-specific antibody and probed with a secondary HRP-conjugated antibody. Approximate molecular weight markers loaded in lanes MW are shown on the left and right side of the blot. The calculated molecular mass of the O3D(*Pi*) protein encoded by the coding sequence introduced in EPA+DHA canola event LBFLFK is 40.8 kDa. The calculated molecular mass of the O3D(*Pi*) used as a positive control for the O3D(*Pi*)-specific antibody NC fusion protein is 22.6 kDa.

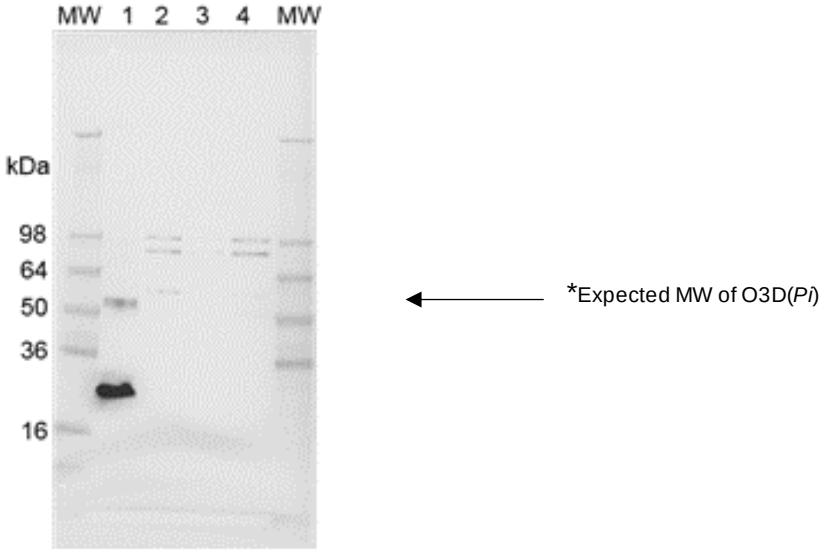

	Lane 1	Lane 2	Lane 3	Lane 4
Sample	O3D(*Pi*) NC fusion protein	Kumily PPP	LBFLFK PPP	LBFLFK PPP
Amount Loaded	10 ng	20 µg	10 µg	20 µg

Identity

Mass spectrometry was used to perform tryptic peptide mapping analysis against the deduced amino acid sequence of the O3D(*Pi*) protein to confirm the identity of the O3D(*Pi*) protein in PPP isolated from EPA+DHA canola event LBFLFK. To minimise the probability of a false positive identification, the current recommendations of the Human Proteome Project Mass Spectrometry Data Interpretation Guidelines 2.1 were followed (Deutsch et al., 2016). Specifically, true positive identification of a protein requires analysis of one sample and identification of at least two peptides consisting of at least nine amino acids, and one of the peptides may not be fully nested within another. The analysis of three different samples identified no peptides that uniquely matched the expected deduced amino acid sequence of the O3D(*Pi*) protein with ≥ 95% probability of positive identification. Peptides 1 and 3 listed in

Table 15 mapped not only to the O3D(*Pir*) protein, but also to O3D(*Pi*) (Figure 33). However, peptide 1 cannot be a result of the tryptic or Lys-C digest of O3D(*Pi*) as it is not preceded by lysine (as in the O3D(*Pir*) protein), and both peptides do not meet the minimum requirements of the Human Proteome Project Mass Spectrometry Data Interpretation Guidelines 2.1 for protein identification due to their length (< 9 amino acids). The O3(*Pi*) protein was therefore not identified in PPP isolated from EPA+DHA canola event LBFLFK.

Figure 33. Peptide Mass Coverage by LC-MS/MS Analysis for Omega-3 Desaturase (*Pi*) in EPA+DHA Canola Event LBFLFK

The deduced amino acid sequence of the O3D(*Pi*) protein, newly expressed in EPA+DHA canola event LBFLFK, represented as the one letter amino acid code. PPP isolated from event LBFLFK was digested with trypsin and Lys-C followed by LC-MS/MS to identify peptides representing the O3D(*Pi*) protein. Peptides 1 and 3 listed in Table 15 were mapped onto the deduced O3D(*Pi*) protein sequence (☐) and **bold underlined**, respectively. Peptide 1 (☐) cannot be a result of the digest of O3D(*Pi*) as it is not preceded by lysine. Peptide 3 (bold) is not unique as it also maps to the O3D(*Pir*) sequence (Figure 27).

```
1   MATKEAYVFP TLTEIKRSLP KDCFEASVPL SLYYTVRCLV IAVALTFGLN YARALPEVES
61  FWALDAALCT GYILLQGIVF WGFFTVGHDA GHGAFSRYHL LNFVVGTFMH SLILTPFESW
121 KLTHRHHHKN TGNIDRDEVF YPQRKADDHP LSRNLILALG AAWLAYLVEG FPPRKVNHFN
181 PFEPLFVRQV SAVVISLLAH FFVAGLSIYL SLQLGLKTMA IYYYGPVFVF GSMLVITTFL
241 HHNDEETPWY ADSEWTYVKG NLSSVDRSYG ALIDNLSHNI GTHQIHHLFP IIPHYKLKKA
301 TAAFHQAFPE LVRKSDEPII KAFFRVGRLY ANYGVVDQEA KLFTLKEAKA ATEAAAKTKS
361 T
```

Glycosylation analysis

The glycosylation status of the O3D(*Pi*) protein in PPP isolated from EPA+DHA canola event LBFLFK was not determined since no signal near the calculated molecular weight of O3D(*Pi*) was observed in PPP by western blot analysis (see Figure 32). For more details, see Appendix 13.

Enzymatic activity

EPA+DHA canola event LBFLFK contains newly expressed O3Ds from two different organisms: O3D(*Pir*) from *Pythium irregulare* (described above), and O3D(*Pi*) from *Phytophthora infestans* (described in this section). The functional activity assays for both O3Ds are identical and were demonstrated using membranes isolated from yeast expression strains (Yilmaz et al., 2017). Therefore, in the PPP isolated from EPA+DHA canola event LBFLFK, this *in vitro* assay tests for the presence of either O3D protein. The results described earlier for O3D(*Pir*) show that the PPP fraction isolated from EPA+DHA canola event LBFLFK did not contain detectable O3D enzyme activity (Figure 30). The absence of detectable omega-3 desaturase activity may result from the developmental stage of immature seeds that were used for the preparation of LBFLFK PPP, as more mature seed isolated form EPA+DHA canola event LBFLFK were shown to have detectable O3D activity.

Summary of omega-3 desaturase (*Pi*) characterisation

EPA+DHA canola event LBFLFK contains two T-DNA inserts encoding two identical copies of the O3D(*Pi*) protein. The *in silico* predicted protein structure was described and the enzyme function was presented based on published *in vivo* experiments in yeast. Furthermore, a series of biochemical experiments was performed to characterise the O3D(*Pi*) protein newly expressed in event LBFLFK.

Structure / Function: Bioinformatic analysis indicates the protein is a methyl-end integral membrane desaturase, and *in vivo* yeast experiments confirmed this enzymatic function. The enzyme converts C20:4n-6 into C20:5n-3.

Immunoreactivity / Molecular weight: The O3D(*Pi*)-specific antibody could not detect a protein in agreement with the calculated molecular mass of the O3D(*Pi*); therefore the immunoreactivity and molecular weight of this protein could not be determined.

Identity: Tryptic peptide mapping using LC-MS/MS did not identify the O3D(*Pi*) protein.

Glycosylation: The O3D(*Pi*)-specific antibody could not detect a protein in agreement with the calculated molecular mass of the O3D(*Pi*); therefore the glycosylation status of this protein could not be determined.

Enzyme activity: Omega-3 desaturation activity, i.e. the introduction of a double bond in C20:4n-6 generating C20:5n-3, was not detected using the *in vitro* enzyme assay in LBFLFK PPP. However, the presence of the C20:5n-3 in event LBFLFK seeds indicates *in vivo* O3D activity in seeds of event LBFLFK, which could result from either O3D(*Pir*) or O3D(*Pi*).

Delta-5 elongase (*Ot*)

Structure and function

The delta-5 elongase (*Ot*) protein D5E(*Ot*), newly expressed in EPA+DHA canola event LBFLFK, is encoded by a coding sequence isolated from the marine green microalga *Ostreococcus tauri*. The deduced D5E(*Ot*) protein consists of 300 amino acids with a calculated molecular mass of 34.2 kDa. The D5E(*Ot*) amino acid sequence, as depicted in Figure 34, shows the features that are characteristic of ELO-type elongases. Depicted are the predicted transmembrane helices and all four signature ELO-motifs. *In vivo* experiments in yeast showed that this D5E(*Ot*) protein catalyses the elongation reaction required to convert C20:5n-3 into C22:5n-3 (Meyer et al., 2004; Yilmaz et al., 2017).

Figure 34. Deduced Amino Acid Sequence for Delta-5 Elongase (*Ot*) in EPA+DHA Canola Event LBFLFK

Using the one letter amino acid code for the D5E(*Ot*) protein in event LBFLFK, the position of predicted transmembrane helices and other characteristic protein motifs are indicated. ,,= indicates transmembrane helices as predicted by Scampi 2 (Peters et al., 2016), TMHMM v.2.0 (Krogh et al., 2001), and SOSUI v 1.11 (Hirokawa et al., 1998), respectively. The sequence contains four motifs ( ) highly conserved among elongases (Leonard et al., 2004; Meyer et al., 2004; Jakobsson et al., 2006), including the characteristic HXXHH histidine box embedded in the fourth membrane helix that is critical for enzymatic activity (Denic and Weissman, 2007; Hernandez-Buquer and Blacklock, 2013). Highly conserved residues are highlighted in black.

```
1   MSASGALLPA IAFAAYAYAT YAYAFEWSHA NGIDNVDARE WIGALSLRLP AIATTMYLLF
    ==========================

61  CLVGPRLMAK REAFDPKGFM LAYNAYQTAF NVVVLGMFAR EISGLGQPVW GSTMPWSDRK
                          ========================

121 SFKILLGVWL HYNNKYLELL DTVFMVARKK TKQLSFLHVY HHSALLIWAWW LVCHLMATND
                                                ========================

181 CIDAYFGAAC NSFIHIVMYS YYLMSALGIR CPWKRYITQA QMLQFVIVFA HAVFVLRQKH
          ========================      ========================

241 CPVTLPWAQM FVMTNMLVLF GNFYLKAYSN KSRGDGASSV KPAETTRAPS VRRTRSRKID
      ========================
```

Apparent molecular weight and immunoreactivity

Western blot analysis using an anti-D5E(*Ot*) protein antibody was used to show immunoreactivity of the D5E(*Ot*) protein in PPP isolated from EPA+DHA canola event LBFLFK (Figure 35). The D5E(*Ot*) NC fusion reference protein, included as positive control (Figure 35, lane 1), displayed an immune-reactive band in good agreement with its calculated molecular mass of 22.2 kDa as well as minor immunoreactive bands correlating to a likely dimer (44 kDa) and degradation products (12 kDa). An immunoreactive band was observed in the LBFLFK PPP samples at a molecular weight that was in good agreement with the calculated molecular mass of the D5E(*Ot*) protein of 34.2 kDa (Figure 35, lanes 3 and 4). No signal was detected in PPP isolated from Kumily, the parental control that does not contain the *D5E*(*Ot*) coding sequence (Figure 35, lane 2).

Figure 35. Western Blot Analysis of Delta-5 Elongase (*Ot*) in EPA+DHA Canola Event LBFLFK

LBFLFK PPP and Kumily PPP were separated by SDS-PAGE and evaluated by western blot analysis. The membrane was probed with a 1:6000 dilution of the D5E(*Ot*)-specific antibody and probed with a secondary HRP-conjugated antibody. Approximate molecular weight markers loaded in lanes labelled MW are shown on the left and right side of the blot. The calculated molecular mass of the D5E(*Ot*) protein from the coding sequence introduced in EPA+DHA canola event LBFLFK is 34.2 kDa. The calculated molecular mass of the D5E(*Ot*) NC fusion protein used as a positive control for the D5E(*Ot*)-specific antibody is 22.2 kDa.

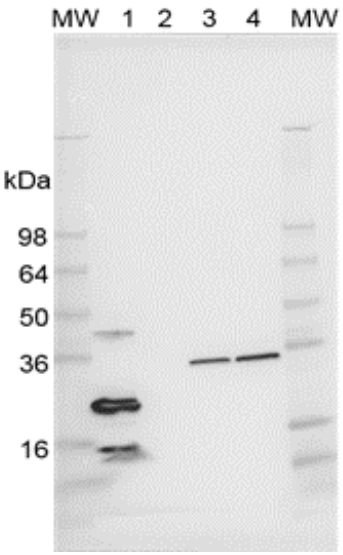

	Lane 1	Lane 2	Lane 3	Lane 4
Sample	D5E(*Ot*) NC fusion protein	Kumily PPP	LBFLFK PPP	LBFLFK PPP
Amount Loaded	30 ng	20 µg	10 µg	20 µg

Identity

Mass spectrometry was used to perform tryptic peptide mapping analysis against the deduced amino acid sequence of the D5E(*Ot*) protein to confirm the identity of the D5E(*Ot*) protein in PPP isolated from EPA+DHA canola event LBFLFK. To minimise the probability of a false positive identification, the current recommendations of the Human Proteome Project Mass Spectrometry Data Interpretation Guidelines 2.1 were followed (Deutsch et al., 2016). Specifically, true positive identification of a protein requires analysis of one sample and identification of at least two peptides consisting of at least nine amino acids, and one of the peptides may not be fully nested within another. The analysis of three different samples identified six peptides (Table 16) that matched the expected deduced amino acid sequence of the D5E(*Ot*) protein with ≥ 95% probability of true positive identification and covered 19% of the entire protein sequence (Figure 36). Four of the peptides listed in Table 16 contained at least nine amino acids and were not fully nested within another (peptides 1, 2, 4, and 6). The confidence of having accurately identified the D5E(*Ot*) protein is further increased by the replicate identification of those four peptides in multiple samples and the identification of peptide 3 and 5 that are fully nested within peptide 4 and 6, respectively. The D5E(*Ot*) protein was therefore identified in PPP isolated from EPA+DHA canola event LBFLFK.

Table 16. Tryptic Peptides Identified for Delta-5 Elongase (*Ot*) in EPA+DHA Canola Event LBFLFK using LC-MS/MS Analysis

Number	Peptide Sequence	Amino Acid Length	Replicate 1	Replicate 2	Replicate 3
1	EWIGALSLR	9	X	X	X
2	YLELLDTVFMVAR	13	X	X	X
3	GDGASSVKPAETTR	14	X	X	
4	SRGDGASSVKPAETTR	16	X	X	X
5	EISGLGQPVWGSTMPWSDR	19			X
6	EISGLGQPVWGSTMPWSDRK	20		X	X

PPP isolated from event LBFLFK was digested with trypsin and Lys-C followed by LC-MS/MS. Listed are peptides representing the D5E(*Ot*) protein, identified with 95% confidence using Mascot server v2.5.1 (Matrix Science Ltd, London, UK).

Figure 36. Peptide Mass Coverage by LC-MS/MS Analysis for Delta-5 Elongase (*Ot*) in EPA+DHA Canola Event LBFLFK

The deduced amino acid sequence of the D5E(*Ot*), protein newly expressed in EPA+DHA canola event LBFLFK, represented as the one letter amino acid code. PPP isolated from event LBFLFK were digested with trypsin and Lys-C followed by LC-MS/MS in order to identify peptides representing the D5E(*Ot*) protein. Peptides listed in Table 16 were mapped (**bold underlined**) onto the deduced protein sequence, covering approximately 19% of the full-length D5E(*Ot*) protein.

1 MSASGALLPA IAFAAYAYAT YAYAFEWSHA NGIDNVDAR**E WIGALSLR**LP AIATTMYLLF
61 CLVGPRLMAK REAFDPKGFM LAYNAYQTAF NVVVLGMFAR **EISGLGQPVW GSTMPWSDRK**
121 SFKILLGVWL HYNNK**YLELL DTVFMVAR**KK TKQLSFLHVY HHALLIWAWW LVCHLMATND
181 CIDAYFGAAC NSFIHIVMYS YYLMSALGIR CPWKRYITQA QMLQFVIVFA HAVFVLRQKH
241 CPVTLPWAQM FVMTNMLVLF GNFYLKAYSN K**SRGDGASSV KPAETTR**APS VRRTRSRKID

Glycosylation analysis

The D5E(*Ot*) protein has one potential N-glycosylation site at $_{270}$NKSR$_{273}$ (Gavel and von Heijne, 1990; Zielinska et al., 2010) and several potential O-glycosylation sites (any serine or threonine). The glycosylation status of the newly expressed D5E(*Ot*) protein was analysed using a strategy that first separated all proteins present in the LBFLFK PPP into two fractions (glycosylated proteins and non-glycosylated proteins) and then determined which fraction contained the D5E(*Ot*) protein by western blot analysis with a D5E(*Ot*)-specific antibody as described in Appendix 14.

Together, these data demonstrated that the D5E(*Ot*) protein present in PPP isolated from EPA+DHA canola event LBFLFK is not glycosylated.

Enzymatic activity

The functional activity of the newly expressed D5E(*Ot*) enzyme in PPP isolated from EPA+DHA canola event LBFLFK was tested using an *in vitro* assay previously reported for the D5E(*Ot*) enzyme present in membranes isolated from yeast expression strains (Yilmaz et al., 2017). Specifically, PPP (isolated from LBFLFK or Kumily) were incubated with the two D5E(*Ot*) co-substrates, [^{14}C]-malonyl-CoA and unlabelled C20:5n-3-CoA, in the presence of NADPH. The resulting fatty acid products were isolated, converted to FAMEs, resolved on a TLC plate, and identified by electronic autoradiography. In the reaction containing LBFLFK

PPP (Figure 37, Panel B, lanes C and D), a [^{14}C]-FAME was identified that migrates similar to the [^{14}C]-22:5n-3-ME standard (Figure 37, Panel B, lane A), in agreement with the expected product according to the reaction shown in Panel A of Figure 37. This product was not detected in the reaction containing parental control Kumily PPP (Figure 37, panel B, lane B), which does not contain the *D5E*(*Ot*) coding sequence.

Together the results obtained from these *in vitro* assays demonstrate the enzymatic activity of the D5E(*Ot*) protein in the LBFLFK PPP isolated from EPA+DHA canola that is consistent with the previously proposed enzymatic reaction shown in Panel A of Figure 37.

Figure 37. *In Vitro* Enzymatic Activity of Delta-5 Elongase (*Ot*) in EPA+DHA Canola Event LBFLFK

Panel A. D5E(*Ot*) catalyses the transfer of two carbons from [^{14}C]-malonyl-CoA to C20:5n-3-CoA generating [^{14}C]-22:5n-3-β-keto-CoA, which in the presence of NADPH can be converted to [^{14}C]-22:5n-3-CoA by the endogenous canola elongation complex enzymes. Panel B. PPP (320 µg total protein) were incubated in a buffer solution with [^{14}C]-malonyl CoA and unlabeled-C20:5n-3-CoA and NADPH. Depicted is an autoradiographic image of a TLC plate showing separated [^{14}C]-methylesters (MEs) prepared from the total lipids that were extracted from the enzymatic reactions. The resulting fatty acid methyl esters (FAME) from the D5E(*Ot*) assay were separated using a reverse phase thin layer chromatography plate with acetonitrile as the mobile phase. Lane A, [^{14}C]-22:5n-3-ME standard. Lane B, Kumily PPP (control). Lanes C and D, LBFLFK PPP in duplicate. The [^{14}C]-labelled malonyl-ME (derived from the substrate [^{14}C]-malonyl-CoA) does not get retained during the extraction process and is therefore not present on the TLC plate. The [^{14}C]-compound observed in lanes C and D that is denoted by an asterisk (*) is derived from the [^{14}C]-22:5n-3-β-keto-CoA product during the isolation of the FAMEs (Yilmaz et al., 2017).

A.

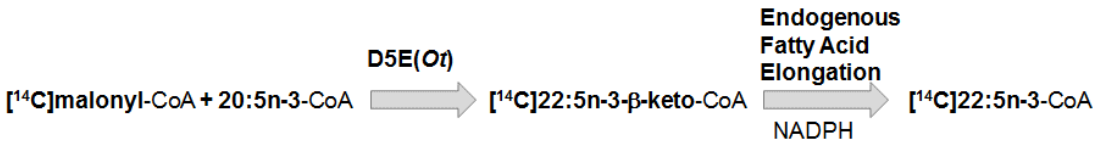

B.

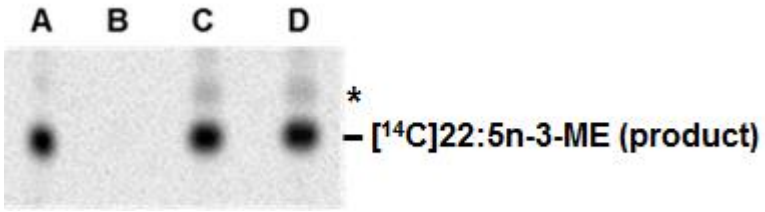

<u>Summary of delta-5 elongase (*Ot*) characterisation</u>

EPA+DHA canola event LBFLFK contains two T-DNA inserts encoding two identical copies of the D5E(*Ot*) protein. The *in silico* predicted protein structure was described and the enzyme function was presented based on published *in vivo* experiments in yeast. Furthermore, a series of biochemical experiments was performed to characterise the D5E(*Ot*) protein newly expressed in event LBFLFK.

Structure / Function: Bioinformatic analysis indicates the protein is an ELO-type membrane integral elongase, and *in vivo* yeast experiments confirmed this enzymatic function. The

enzyme catalyses the decarboxylation Claisen-like condensation of two carbons from malonyl-CoA to C20:5n-3-CoA generating C22:5n-3-β-keto-CoA, which is then converted to C22:5n-3-CoA by endogenous enzymes.

Immunoreactivity / Molecular weight: Western blot analysis confirmed the protein was immunoreactive to an anti-D5E(*Ot*) antibody. The apparent molecular weight was in good agreement to the calculated molecular mass of the D5E(*Ot*) protein.

Identity: Tryptic peptide mapping using LC-MS/MS positively identified four distinct peptides (> 9 amino acids) corresponding to the deduced amino acid sequence of the D5E(*Ot*) protein. The D5E(*Ot*) was therefore identified in EPA+DHA canola event LBFLFK.

Glycosylation: The D5E(*Ot*) protein was found to be not glycosylated.

Enzyme activity: Delta-5 elongation activity, i.e. condensation of two carbons from malonyl-CoA to C20:5n-3-CoA generating C22:5n-3-β-keto-CoA, which was ultimately converted to C22:5n-3-CoA by endogenous canola enzymes, was detected in LBFLFK PPP.

Delta-4 desaturase (*Tc*)

Structure and function

The delta-4 desaturase (*Tc*) protein, D4D(*Tc*), newly expressed in EPA+DHA canola event LBFLFK is encoded by a coding sequence isolated from the marine protist *Thraustochytrium* sp. The deduced D4D(*Tc*) protein consists of 519 amino acids with a calculated molecular mass of 59 kDa. The D4D(*Tc*) amino acid sequence, as depicted in Figure 38, shows the features that are characteristic for a front-end integral membrane desaturase. Depicted are the N-terminally fused cytochrome b_5 domain containing the characteristic HPGG motif, the predicted transmembrane helices, three histidine boxes containing seven conserved histidine residues, a conserved glutamine in histidine box 3, and the conserved histidine following the C-terminal transmembrane helix. *In vivo* experiments in yeast showed that this D4D(*Tc*) protein catalyses the desaturation reaction required to convert C22:5n-3 into C22:6n-3 (Yilmaz et al., 2017).

Figure 38. Deduced Amino Acid Sequence for Delta-4 Desaturase (*Tc*) in EPA+DHA Canola Event LBFLFK

Using the one letter amino acid code for the D4D(*Tc*) protein in event LBFLFK, the position of predicted transmembrane helices and other characteristic protein motifs are indicated. ▒, ▒,= indicates transmembrane helices as predicted by Scampi 2 (Peters et al., 2016), TMHMM v.2.0 (Krogh et al., 2001), and SOSUI v 1.11 (Hirokawa et al., 1998), respectively. The sequence contains three histidine-box motifs (▒) with seven conserved histidine residues (H) typical for desaturases (Shanklin et al., 1994) and an additional conserved histidine (H), all of which participate in the coordination of the diiron active centre (Bai et al., 2015; Wang et al., 2015). Additionally, the sequence contains a conserved glutamine (Q) in the third histidine box that is essential for activity (Sayanova et al., 2001). Underlined is the cytochrome b_5 domain as annotated by PFAM v31 (Finn et al., 2016), containing the characteristic HPGG motif (Sperling and Heinz, 2001) highlighted in grey highlighted in grey.

```
1   MTVGYDEEIP FEQVRAHNKP DDAWCAIHGH VYDVTKFASV HPGGDIILLA AGKEATVLYE
61  TYHVRGVSDA VLRKYRIGKL PDGQGGANEK EKRTLSGLSS ASYYTWNSDF YRVMRERVVA
121 RLKERGKARR GGYELWIKAF LLLVGFWSSL YWMCTLDPSF GAILAAMSLG VFAAFVGTCI

181 QHDGNHGAFA QSRWVNKVAG WTLDMIGASG MTWEFQHVLG HHPYTNLIEE ENGLQKVSGK

241 KMDTKLADQE SDPDVFSTYP MMRLHPWHQK RWYHRFQHIY GPFIFGFMTI NKVVTQDVGV
301 VLRKRLFQID AECRYASPMY VARFWIMKAL TVLYMVALPC YMQGPWHGLK LFAIAHFTCG

                    ======================          ========

361 EVLATMFIVN HIIEGVSYAS KDAVKGTMAP PKTMHGVTPM NNTRKEVEAE ASKSGAVVKS

    ===============

421 VPLDDWAAVQ CQTSVNWSVG SWFWNHFSGG LNHQIEHHLF PGLSHETYYH IQDVVQSTCA
481 EYGVPYQHEP SLWTAYWKML EHLRQLGNEE THESWQRAA
```

Apparent molecular weight and immunoreactivity

Western blot analysis using an anti-D4D(*Tc*) protein antibody was used to show immunoreactivity of the D4D(*Tc*) protein in PPP isolated from EPA+DHA canola event LBFLFK (Figure 39). To demonstrate the specificity of the antibody, a D4D(*Tc*) NC fusion reference protein was included as positive control (Figure 39, lane 1). An immunoreactive band was observed in the LBFLFK PPP samples at a molecular weight that was in good agreement with the calculated molecular mass of the D4D(*Tc*) protein of 59.0 kDa (Figure 39, lanes 3 and 4). No signal was detected in PPP isolated from Kumily, the parental control that does not contain the D4D(*Tc*) coding sequence (Figure 39, lane 2).

Figure 39. Western Blot Analysis of Delta-4 Desaturase (*Tc*) in EPA+DHA Canola Event LBFLFK

LBFLFK PPP and Kumily PPP were separated by SDS-PAGE and evaluated by western blot analysis. The membrane was probed with a 1:4,000 dilution of the D4D(*Tc*)-specific antibody and probed with a secondary HRP-conjugated antibody. Approximate molecular weight markers loaded in lanes labelled MW are shown on the left and right side of the blot. The calculated molecular mass of the D4D(*Tc*) protein encoded by the coding sequence introduced in EPA+DHA canola event LBFLFK is 59.0 kDa. The calculated molecular mass of the D4D(*Tc*) NC fusion protein used as a positive control for the D4D(*Tc*)-specific antibody is 46.7 kDa (apparent molecular weight slightly higher than 50 kDa).

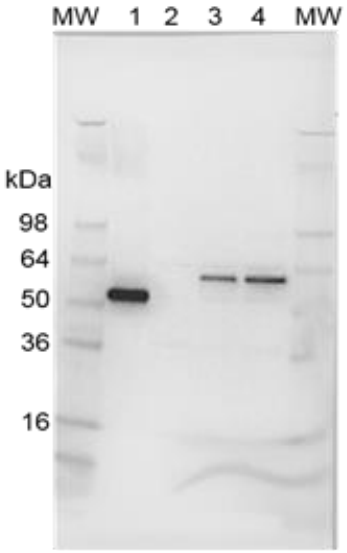

	Lane 1	Lane 2	Lane 3	Lane 4
Sample	D4D(*Tc*) NC fusion protein	Kumily PPP	LBFLFK PPP	LBFLFK PPP
Amount Loaded	6 ng	20 µg	10 µg	20 µg

Identity

Mass spectrometry was used to perform tryptic peptide mapping analysis against the deduced amino acid sequence of the D4D(*Tc*) protein to confirm the identity of the D4D(*Tc*) protein in PPP isolated from EPA+DHA canola event LBFLFK. To minimise the probability of a false positive identification, the current recommendations of the Human Proteome Project Mass Spectrometry Data Interpretation Guidelines 2.1 were followed (Deutsch et al., 2016). Specifically, true positive identification of a protein requires analysis of one sample and identification of at least two peptides consisting of at least nine amino acids, and one of the peptides may not be fully nested within another. The analysis of three different samples identified 10 peptides (Table 17) that matched the expected deduced amino acid sequence of the D4D(*Tc*) protein with ≥ 95% probability of positive identification and covered 23% of the entire protein sequence (Figure 40). Nine peptides listed in Table 17 contained at least nine amino acids and were not fully nested within another (peptide 2–10). The confidence of having accurately identified the D4D(*Tc*) protein is further increased by the replicate identification of seven peptides (3–9) in multiple samples. The D4D(*Tc*) protein was therefore identified in PPP isolated from EPA+DHA canola event LBFLFK.

Table 17. Tryptic Peptides Identified for Delta-4 Desaturase (*Tc*) in EPA+DHA Canola Event LBFLFK using LC-MS/MS Analysis

Number	Peptide Sequence	Amino Acid Length	Replicate 1	Replicate 2	Replicate 3
1	GVSDAVLR	7	X	X	X
2	LFQIDAECR	9		X	
3	YASPMYVAR	9	X	X	
4	VVTQDVGVVLR	11	X	X	X
5	EATVLYETYHVR	12		X	X
6	QLGNEETHESWQR	13		X	X
7	IGKLPDGQGGANEK	14	X		X
8	TVGYDEEIPFEQVR	14	X	X	X
9	FASVHPGGDIILLAAGK	17	X	X	X
10	AHNKPDDAWCAIHGHVYDVTK	21			X

PPP isolated from event LBFLFK was digested with trypsin and Lys-C followed by LC-MS/MS. Listed are peptides representing the D4D(*Tc*) protein, identified with 95% confidence using Mascot server v2.5.1 (Matrix Science Ltd, London, UK).

Figure 40. Peptide Mass Coverage by LC-MS/MS Analysis for Delta-4 Desaturase (*Tc*) in EPA+DHA Canola Event LBFLFK

The deduced amino acid sequence of the D4D(*Tc*) protein, newly expressed in EPA+DHA canola event LBFLFK, represented as the one letter amino acid code. PPP isolated from event LBFLFK were digested with trypsin and Lys-C followed by LC-MS/MS in order to identify peptides representing the D4D(*Tc*) protein. Peptides listed in Table 17 were mapped (**bold underlined**) onto the deduced D4D(*Tc*) protein sequence, covering approximately 23% of the full-length D4D(*Tc*) protein.

1 M**TVGYDEEIP FEQVRAHNKP DDAWCAIHGH VYDVTKFASV HPGGDIILLA AGKEATVLYE**

61 **TYHVRGVSDA VLR**KYR**IGKL PDGQGGANEK** EKRTLSGLSS ASYYTWNSDF YRVMRERVVA

121 RLKERGKARR GGYELWIKAF LLLVGFWSSL YWMCTLDPSF GAILAAMSLG VFAAFVGTCI

181 QHDGNHGAFA QSRWVNKVAG WTLDMIGASG MTWEFQHVLG HHPYTNLIEE ENGLQKVSGK

241 KMDTKLADQE SDPDVFSTYP MMRLHPWHQ*K* RWYHRFQHIY GPFIFGFMTI NK**VVTQDVGV**

301 **VLR**KRLFQID AECR**YASPMY VAR**FWIMKAL TVLYMVALPC YMQGPWHGLK LFAIAHFTCG

361 EVLATMFIVN HIIEGVSYAS KDAVKGTMAP PKTMHGVTPM NNTRKEVEAE ASKSGAVVKS

421 VPLDDWAAVQ CQTSVNWSVG SWFWNHFSGG LNHQIEHHLF PGLSHETYYH IQDVVQSTCA

481 EYGVPYQHEP SLWTAYWKML EHLR**QLGNEE THESWQRAA**

Glycosylation analysis

The D4D(*Tc*) has two potential N-glycosylation sites at $_{401}$NNTR$_{404}$ and $_{436}$NWSV$_{439}$ (Gavel and von Heijne, 1990; Zielinska et al., 2010) and has several potential O-glycosylation sites (any serine or threonine). The glycosylation status of the newly expressed D4D(*Tc*) protein was analysed using a strategy that first separated all proteins present in the LBFLFK PPP into

two fractions (glycosylated proteins and non-glycosylated proteins) and then determined which fraction contained the D4D(*Tc*) protein by western blot analysis with a D4D(*Tc*)-specific antibody as described in Appendix 15.

Together, these data demonstrated that the D4D(*Tc*) protein present in PPP isolated from EPA+DHA canola event LBFLFK is not glycosylated.

Enzymatic activity

EPA+DHA canola event LBFLFK contains newly expressed D4Ds from two different organisms: D4D(*Pl*) and D4D(*Pl*) [A102S] from *Pavlova lutheri* (described below), and D4D(*Tc*) from *Thraustochytrium* sp. (described in this section). The functional activity assays for the D4Ds from both organisms are identical and were demonstrated using membranes isolated from yeast expression strains (Yilmaz et al., 2017). Therefore, in the PPP isolated from EPA+DHA canola event LBFLFK, the presence of all D4Ds was tested using this *in vitro* assay; however, the relative contributions of the individual D4Ds to the total D4D activity cannot be determined. D4D(*Tc*) was previously shown to desaturate C22:5n-3 to C22:6n-3 when the substrate fatty acid was covalently bound to a lipid, e.g., phosphatidylcholine (PC), but the D4D(*Pl*) may accept the substrate C22:5n-3-CoA (Yilmaz et al., 2017). Endogenous lysophosphatidylcholine acyl transferase (LPCAT) present in PPP was used to synthesise [^{14}C]-22:5n-3-PC *in situ* by transesterification of [^{14}C]-22:5n-3 from CoA to lysophosphatidylcholine (LPC) (Yilmaz et al., 2017). Specifically, PPP were incubated with [^{14}C]-22:5n-3-CoA, unlabelled C16:0-lysophosphatidylcholine, and NADH. The resulting fatty acid products were isolated, converted to FAMEs, resolved on a TLC plate, and identified by electronic autoradiography. In the reaction containing LBFLFK PPP (Figure 41, Panel B, lanes B and C), a [^{14}C]-FAME was identified that migrates similar to the [^{14}C]-22:6n-3-ME standard (Figure 41, Panel B, lane E), in agreement with the expected product according to the reaction shown in Panel A of Figure 41. This product was also not detected in the reaction containing parental control Kumily PPP (Figure 41, Panel B, lane C), which does not contain the D4D(*Pl*), D4D(*Pl*) [A102S], or D4D(*Tc*) proteins.

The results obtained from these *in vitro* assays demonstrate D4D activity in the LBFLFK PPP isolated from EPA+DHA canola, that is not observed in Kumily PPP. The observed D4D activity is consistent with the previously proposed enzymatic reaction (Yilmaz et al., 2017) shown in Panel A of Figure 41, and could be attributed to any or all of the D4D(*Pl*), D4D(*Pl*) [A102S], and D4D(*Tc*) proteins.

Figure 41. *In Vitro* Enzymatic Activity of Delta-4 Desaturases in EPA+DHA Canola Event LBFLFK

Panel A. D4D(*Tc*) desaturates the fatty acid substrate C22:5n-3 to the fatty acid product C22:6n-3 when the substrate is covalently bound to a lipid (e.g., phosphatidylcholine, PC), but the D4D(*Pl*) enzyme may accept the substrate C22:5n-3-CoA (Yilmaz et al., 2017). In the enzymatic assay, endogenous lysophosphatidylcholine acyl transferase (LPCAT) is used to synthesise [^{14}C]-22:5n-3-PC by transferring [^{14}C]-22:5n-3 from CoA to lysophosphatidylcholine (LPC). Panel B. PPP (40 µg total protein) were incubated in a buffer solution with [^{14}C]-22:5n-3-CoA substrate, unlabelled C16:0-lysophosphatidylcholine, and NADH. Total lipids were extracted, converted to fatty acid methyl esters (FAME), and separated using a 10% $AgNO_3$ thin layer chromatography plate with a 1:1 ratio of toluene/heptane solvent as the mobile phase. Shown below is an autoradiographic image of the TLC plate of the resolved [^{14}C]-methyl esters (ME). Kumily PPP was used as a control. Lane A, C22:5n-3-ME standard (substrate). Lane B, C22:6n-3-ME standard (product). Lane C, Kumily PPP (control). Lane D and E, LBFLFK PPP loaded in duplicate.

A.

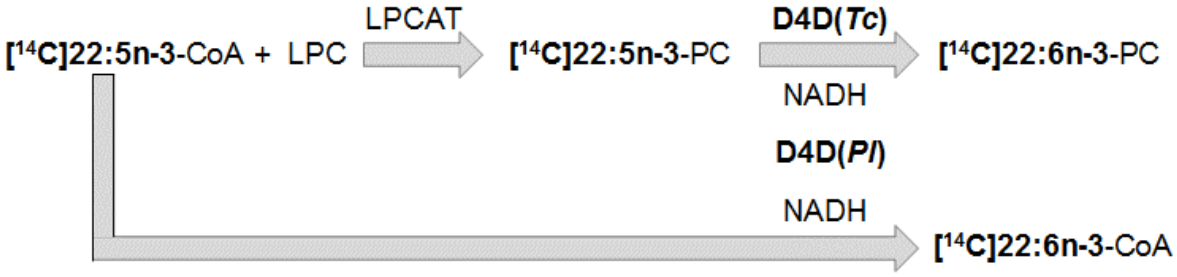

B.

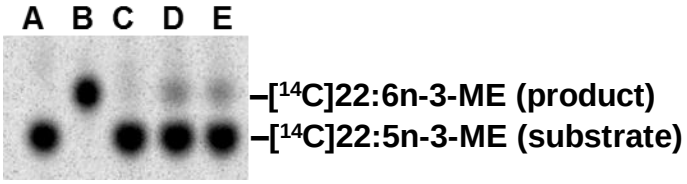

<u>Summary of delta-4 desaturase (*Tc*) characterisation</u>

EPA+DHA canola event LBFLFK contains two T-DNA inserts encoding two identical copies of the D4D(*Tc*) protein. The *in silico* predicted protein structure was described and the enzyme function was presented based on published *in vivo* experiments in yeast. Furthermore, a series of biochemical experiments was performed to characterise the D4D(*Tc*) protein newly expressed in event LBFLFK.

Structure / Function: Bioinformatic analysis indicates the protein is a front-end integral membrane desaturase, and *in vivo* yeast experiments confirmed this enzymatic function. The enzyme converts C22:5n-3 into C22:6n-3.

Immunoreactivity / Molecular weight: Western blot analysis confirmed the protein was immunoreactive to an anti-D4D(*Tc*) antibody. The apparent molecular weight was in good agreement to the calculated molecular mass of the D4D(*Tc*) protein.

Identity: Tryptic peptide mapping using LC-MS/MS positively identified nine distinct peptides (> 9 amino acids) corresponding to the deduced amino acid sequence of the D4D(*Tc*) protein. The D4D(*Tc*) was therefore identified.

Glycosylation: The D4D(*Tc*) protein was found to be not glycosylated.

Enzyme activity: Delta-4 desaturation activity, i.e. the introduction of a double bond in C22:5n-3 generating C22:6n-3, was detected in LBFLFK PPP. The observed D4D activity could be attributed to any or all of the D4D(*Pl*), D4D(Pl) [A102S], or D4D(*Tc*) proteins.

Delta-4 desaturase (*Pl*)

Structure and function

The delta-4 desaturase (*Pl*) protein, D4D(*Pl*), newly expressed in EPA+DHA canola event LBFLFK is encoded by a coding sequence isolated from the marine microalga *Pavlova lutheri*. The deduced D4D(*Pl*) protein consists of 445 amino acids with a calculated molecular mass of 49.1 kDa. The D4D(*Pl*) amino acid sequence, as depicted in Figure 42, shows the features that are characteristic for a front-end integral membrane desaturase. Depicted are the N-terminally fused cytochrome b_5 domain containing the characteristic HPGG motif, the predicted transmembrane helices, three histidine boxes containing seven conserved histidine residues, a conserved glutamine in histidine box 3, and the conserved histidine following the C-terminal transmembrane helix.

EPA+DHA canola event LBFLFK contains two T-DNA inserts that encode the D4D(*Pl*) protein. The two D4D(*Pl*) coding sequences differ by a single nucleotide resulting in a deduced protein that has a [A102S] substitution, referred to as D4D(*Pl*) [A102S], that is predicted to reside in a linker region between the cytochrome b_5 domain and the first transmembrane spanning domain of the desaturase. The D4D(*Pl*) [A102S] protein also consists of 445 amino acids with a calculated molecular mass of 49.1 kDa. *In vivo* experiments in yeast showed that both proteins, the D4D(*Pl*) and the D4D(*Pl*) [A102S], catalyse the desaturation reaction required to convert C22:5n-3 into C22:6n-6 (Yilmaz et al., 2017) and have similar conversion efficiencies.

A series of biochemical experiments were performed to characterise the two D4D(*Pl*) proteins that were newly expressed in EPA+DHA canola event LBFLFK. The characteristics assessed in these experiments are generally applicable to D4D(*Pl*) and D4D(*Pl*) [A102S].

Figure 42. Deduced Amino Acid Sequence for Delta-4 Desaturase (*Pl*) in EPA+DHA Canola Event LBFLFK

Using the one letter amino acid code for the D4D(*Pl*) protein in event LBFLFK, the position of predicted transmembrane helices and other characteristic protein motifs are indicated. ▒, ▒,= indicates transmembrane helices as predicted by Scampi 2 (Peters et al., 2016), TMHMM v.2.0 (Krogh et al., 2001), and SOSUI v 1.11 (Hirokawa et al., 1998), respectively. The sequence contains three histidine-box motifs (▯) with seven conserved histidine residues (H) typical for desaturases (Shanklin et al., 1994) and an additional conserved histidine (H), all of which participate in the coordination of the diiron active centre (Bai et al., 2015; Wang et al., 2015). Additionally, the sequence contains a conserved glutamine (Q) in the third histidine box that is essential for activity (Sayanova et al., 2001). Underlined is the cytochrome b_5 domain as annotated by PFAM v31 (Finn et al., 2016), containing the characteristic HPGG motif (Sperling and Heinz, 2001) highlighted in grey highlighted in grey. EPA+DHA canola event LBFLFK carries two T-DNA inserts that encode the D4D(*Pl*) protein, one with the amino acid sequence as shown below and one with the amino acid sequence with a substitution of alanine by serine at position 102 (D4D(*Pl*) [A102S]), indicated by **A**.

```
1   MPPSAASEGG VAELRAAEVA SYTRKAVDER PDLTIVGDAV YDAKAFRDEH PGGAHFVSLF
61  GGRDATEAFM EYHRRAWPKA RMSKFFVGSL DASEKPTQAD SAYLRLCAEV NALLPKGSGG
121 FAPPSYWLKA AALVVAAVSI EGYMLLRGKT LLLSVFLGLV FAWIGLNIQH DANHGALSRH
                    ========================
181 SVINYCLGYA QDWIGGNMVL WLQEHVVMHH LHTNDVDADP DQKAHGVLRL KPTDGWMPWH
     ========================
241 ALQQLYILPG EAMYAFKLLF LDALELLAWR WEGEKISPLA RALFAPAVAC KLGFWARFVA
      ========================                ====================
301 LPLWLQPTVH TALCICATVC TGSFYLAFFF FISHNFDGVG SVGPKGSLPR SATFVQRQVE
    ==          ========================
361 TSSNVGGYWL GVLNGGLNFQ IEHHLFPRLH HSYYAQIAPV VRTHIEKLGF KYRHFPTVGS
421 NLSSMLQHMG KMGTRPGAEK GGKAE
```

Apparent molecular weight and immunoreactivity

Western blot analysis using an anti-D4D(*Pl*) protein antibody was used to show immunoreactivity of the D4D(*Pl*) and D4D(*Pl*) [A102S] proteins in PPP isolated from EPA+DHA canola event LBFLFK (Figure 43). To demonstrate the specificity of the antibody, a D4D(*Pl*) NC fusion reference protein was included as positive control (Figure 43, lane 1). An immunoreactive band was observed in the LBFLFK PPP samples at a molecular weight that was in good agreement with the calculated molecular mass of the D4D(*Pl*) and D4D(*Pl*) [A102S] proteins of 49.1 kDa (Figure 43, lanes 3 and 4). No signal was detected in PPP isolated from Kumily, the parental control that does not contain the *D4D*(*Pl*) coding sequences (Figure 43, lane 2).

Figure 43. Western Blot Analysis of Delta-4 Desaturase (*Pl*) in EPA+DHA Canola Event LBFLFK

LBFLFK PPP and Kumily PPP were separated by SDS-PAGE and evaluated by western blot analysis. The membrane was probed with a 1:4,000 dilution of the D4D(*Pl*)-specific antibody and probed with a secondary HRP-conjugated antibody. Approximate molecular weight markers loaded in lanes labelled MW are shown on the left and right side of the blot. The calculated molecular mass of the D4D(*Pl*) and D4D(*Pl*) [A102S] protein encoded by the coding sequences introduced in EPA+DHA canola event LBFLFK is 49.1 kDa. The calculated molecular mass of the D4D(*Pl*) NC fusion protein used as a positive control for the D4D(*Pl*)-specific antibody is 24.4 kDa.

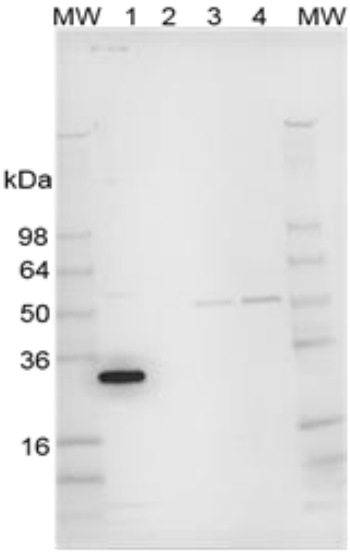

	Lane 1	Lane 2	Lane 3	Lane 4
Sample	D4D(*Pl*) NC fusion protein	Kumily PPP	LBFLFK PPP	LBFLFK PPP
Amount Loaded	7.5 ng	20 µg	10 µg	20 µg

Identity

Tryptic peptide mapping analysis using mass spectrometry against the deduced amino acid sequence of the D4D(*Pl*) protein was used to confirm the identity of the D4D(*Pl*) and the D4D(*Pl*) [A102S] proteins in PPP isolated from EPA+DHA canola event LBFLFK. To minimise the probability of a false positive identification, the current recommendations of the Human Proteome Project Mass Spectrometry Data Interpretation Guidelines 2.1 were followed (Deutsch et al., 2016). Specifically, true positive identification of a protein requires analysis of one sample and identification of at least two peptides consisting of at least nine amino acids, and one of the peptides may not be fully nested within another. The analysis of three different samples identified three peptides (Table 18) that matched the expected deduced amino acid sequence of the D4D(*Pl*) protein with ≥ 95% probability of positive identification and covered 9% of the entire protein sequence (Figure 44). All three peptides listed in Table 18 contained at least nine amino acids and were not fully nested within another. These three peptides map to both the D4D(*Pl*) sequence as well as to the D4D(*Pl*) [A102S] sequence. The confidence having accurately identified the D4D(*Pl*) proteins is further increased by the replicate identification of these three peptides in multiple samples. The D4D(*Pl*) proteins were therefore identified in EPA+DHA canola event LBFLFK.

Table 18. Tryptic Peptides Identified for Delta-4 Desaturase (*Pl*) in EPA+DHA Canola Event LBFLFK using LC-MS/MS Analysis

Number	Peptide Sequence	Amino Acid Length	Replicate 1	Replicate 2	Replicate 3
1	AAEVASYTR	9	X	X	X
2	LHHSYYAQIAPVVR	14	X	X	X
3	AFRDEHPGGAHFVSLFGGR	19	X	X	

PPP isolated from event LBFLFK were digested with trypsin and Lys-C followed by LC-MS/MS. Listed are peptides representing the D4D(*Pl*) and D4D(*Pl*) [A102S] protein, identified with 95% confidence using Mascot server v2.5.1 (Matrix Science Ltd, London, UK).

Figure 44. Peptide Mass Coverage by LC-MS/MS Analysis for Delta-4 Desaturase (Pl) in EPA+DHA Canola Event LBFLFK

The amino acid sequence of the D4D(*Pl*) protein and the D4D(*Pl*) [A102] protein, encoded by T-DNAs introduced in EPA+DHA canola event LBFLFK, represented as the one letter amino acid code. The [A102S] substitution in one of the two proteins is highlighted in black. PPP isolated from event LBFLFK were digested with trypsin and Lys-C followed by LC-MS/MS in order to identify peptides representing the D4D(*Pl*) and D4D(*Pl*) [A102S] protein. Peptides listed in Table 18 were mapped (**bold underlined**) onto the deduced protein sequences, covering approximately 9% of the full-length D4D(*Pl*) protein.

```
1   MPPSAASEGG VAELR<u>**AAEVA SYTR**</u>KAVDER PDLTIVGDAV YDAK<u>**AFRDEH PGGAHFVSLF**</u>

61  <u>**GGR**</u>DATEAFM EYHRRAWPKA RMSKFFVGSL DASEKPTQAD SAYLRLCAEV NALLPKGSGG

121 FAPPSYWLKA AALVVAAVSI EGYMLLRGKT LLLSVFLGLV FAWIGLNIQH DANHGALSRH

181 SVINYCLGYA QDWIGGNMVL WLQEHVVMHH LHTNDVDADP DQKAHGVLRL KPTDGWMPWH

241 ALQQLYILPG EAMYAFKLLF LDALELLAWR WEGEKISPLA RALFAPAVAC KLGFWARFVA

301 LPLWLQPTVH TALCICATVC TGSFYLAFFF FISHNFDGVG SVGPKGSLPR SATFVQRQVE

361 TSSNVGGYWL GVLNGGLNFQ IEHHLFPR<u>**LH HSYYAQIAPV VR**</u>THIEKLGF KYRHFPTVGS

421 NLSSMLQHMG KMGTRPGAEK GGKAE
```

Glycosylation analysis

Both newly expressed D4D(*Pl*) proteins (D4D(*Pl*) and D4D(Pl) [A102S]) have the same potential N-glycosylation site at $_{421}$NLSS$_{424}$ (Gavel and von Heijne, 1990; Zielinska et al., 2010) and several potential O-glycosylation sites (any serine or threonine). The glycosylation status of the newly expressed D4D(*Pl*) proteins was analysed using a strategy that first separated the proteins present in the LBFLFK PPP into two fractions (glycosylated proteins and non-glycosylated proteins) and then determined which fraction contained the D4D(*Pl*) and D4D(*Pl*) [A102S] proteins by western blot analysis with a D4D(*Pl*)-specific antibody as described in Appendix 16.

Together, these data demonstrated that the D4D(*Pl*) proteins present in PPP isolated from EPA+DHA canola event LBFLFK were not glycosylated.

Enzymatic activity

EPA+DHA canola event LBFLFK contains newly introduced D4Ds from two different organisms: D4D(*Pl*) and D4D(*Pl*) [A102S] from *Pavlova lutheri* (described in this section) and D4D(*Tc*) from *Thraustochytrium* sp. (described above). The functional activity assays for the D4Ds from both organisms are identical and were demonstrated using membranes isolated from yeast expression strains (Yilmaz et al., 2017). Therefore, in the PPP isolated from EPA+DHA canola event LBFLFK, the presence of all D4Ds was tested using this *in vitro* assay; however, the relative contributions of the individual D4Ds to the total D4D activity cannot be determined.

The results described for the enzymatic activity of D4D(*Tc*) above demonstrate D4D activity in the LBFLFK PPP isolated from EPA+DHA canola. This D4D activity was not observed in Kumily PPP, which does not contain D4D(*Pl*), D4D(*Pl*) [A102S], or D4D(*Tc*). The observed D4D activity is consistent with the previously proposed enzymatic reaction (Yilmaz et al., 2017) shown in Panel A of Figure 41 and could be attributed to any or all of the D4D(*Pl*), D4D(*Pl*) [A102S], and D4D(*Tc*) proteins. In yeast *in vivo* feeding experiments, the D4D(*Pl*) [A102S] protein was shown to have substrate specificity and activity comparable to what was reported for the D4D(*Pl*) protein (Yilmaz et al., 2017).

Summary of delta-4 desaturase (*Pl*) characterisation

EPA+DHA canola event LBFLFK contains two T-DNA inserts with the respective *D4D*(*Pl*) coding sequences differing in one nucleotide. This nucleotide difference results in the two newly expressed proteins D4D(*Pl*) and D4D(*Pl*) [A102S]. The *in silico* predicted protein structure was described and the enzyme function was presented based on published *in vivo* experiments in yeast. Furthermore, a series of biochemical experiments was performed to characterise the D4D(*Pl*) proteins newly expressed in event LBFLFK.

Structure / Function: Bioinformatic analysis indicates the protein is a front-end integral membrane desaturase, and *in vivo* yeast experiments confirmed this enzymatic function for both D4D(*Pl*) and D4D(*Pl*) [A102S]. The enzyme converts C22:5n-3 into C22:6n-3.

Immunoreactivity / Molecular weight: Western blot analysis confirmed the proteins were immunoreactive to an anti-D4D(*Pl*) antibody. The apparent molecular weight was in good agreement to the calculated molecular mass of the D4D(*Pl*) proteins. The antibody used to detect the D4D(*Pl*) proteins is expected to detect both D4D(*Pl*) and D4D(*Pl*) [A102S] with similar sensitivity; therefore this result applied to both D4D(*Pl*) proteins.

Identity: Tryptic peptide mapping using LC-MS/MS positively identified three distinct peptides (> 9 amino acids) corresponding to the deduced amino acid sequence of both D4D(*Pl*) proteins. D4D(*Pl*) proteins were therefore identified in EPA+DHA canola event LBFLFK.

Glycosylation: The D4D(*Pl*) proteins were found to be not glycosylated. The antibody used to detect the D4D(*Pl*) proteins is expected to detect both D4D(*Pl*) and D4D(*Pl*) [A102S] with similar sensitivity; therefore this result applied to both D4D(*Pl*) proteins.

Enzyme activity: Delta-4 desaturation activity, i.e. the introduction of a double bond in C22:5n-3 generating C22:6n-3, was detected in LBFLFK PPP. The observed D4D activity could be attributed to the D4D(*Pl*), D4D(Pl) [A102S], or D4D(*Tc*) proteins.

Acetohydroxy acid synthase (*At*) [A122TS653N]

Structure and function

The acetohydroxy acid synthase protein, AHAS(*At*) [A122TS653N], newly expressed in EPA+DHA canola event LBFLFK, is the large subunit of acetohydroxy acid synthase, consisting of 670 amino acids with a calculated molecular mass of 72.6 kDa in size as depicted in Figure 45. During transport into the chloroplast, the chloroplast transit peptide is removed to produce the mature AHAS(*At*) [A122TS653N] enzyme which likely interacts with the endogenous *Brassica napus* small subunit enabling proper feedback regulation for AHAS. The amino terminus of the mature AHAS(*At*) [A122TS653N] protein was determined by mass spectrometric peptide mapping to be a valine at position 65. The mature AHAS(*At*) [A122TS653N] protein in EPA+DHA canola event LBFLFK consists of 606 amino acids with a calculated molecular mass of 66.1 kDa. The sequence introduced into LBFLFK includes nucleotide sequence substitutions such that the translated protein has an alanine residue changed to a threonine at amino acid position 122 (A122T) and a serine residue changed to an asparagine at amino acid position 653 (S653N). These amino acid changes in the plant AHAS protein are known to reduce its binding affinity towards imidazolinone herbicides and thereby result in tolerance to these herbicides while maintaining normal biosynthetic function, including proper feedback regulation (Tan et al., 2005).

Figure 45. Deduced Amino Acid Sequence for Acetohydroxy Acid Synthase (*At*) [A122TS653N] in EPA+DHA Canola Event LBFLFK

Shown is the one letter amino acid sequence of the AHAS(*At*) [A122TS653N] protein in event LBFLFK. Residues 1–64 (Underlined) represent the chloroplast transit peptide with the mature AHAS(*At*) [A122TS653N] protein starting at valine 65. Amino acid substitutions are A122T and S653N are shown in **bold underlined** font.

```
1   MAAATTTTTT SSSISFSTKP SPSSSKSPLP ISRFSLPFSL NPNKSSSSSR RRGIKSSSPS
61  SISAVLNTTT NVTTTPSPTK PTKPETFISR FAPDQPRKGA DILVEALERQ GVETVFAYPG
121 G[T]SMEIHQAL TRSSSIRNVL PRHEQGGVFA AEGYARSSGK PGICIATSGP GATNLVSGLA
181 DALLDSVPLV AITGQVPRRM IGTDAFQETP IVEVTRSITK HNYLVMDVED IPRIIEEAFF
241 LATSGRPGPV LVDVPKDIQQ QLAIPNWEQA MRLPGYMSRM PKPPEDSHLE QIVRLISESK
301 KPVLYVGGGC LNSSDELGRF VELTGIPVAS TLMGLGSYPC DDELSLHMLG MHGTVYANYA
361 VEHSDLLLAF GVRFDDRVTG KLEAFASRAK IVHIDIDSAE IGKNKTPHVS VCGDVKLALQ
421 GMNKVLENRA EELKLDFGVW RNELNVQKQK FPLSFKTFGE AIPPQYAIKV LDELTDGKAI
481 ISTGVGQHQM WAAQFYNYKK PRQWLSSGGL GAMGFGLPAA IGASVANPDA IVVDIDGDGS
541 FIMNVQELAT IRVENLPVKV LLLNNQHLGM VMQWEDRFYK ANRAHTFLGD PAQEDEIFPN
601 MLLFAAACGI PAARVTKKAD LREAIQTMLD TPGPYLLDVI CPHQEHVLPM IP[N]GGTFNDV
661 ITEGDGRIKY
```

Apparent molecular weight and immunoreactivity

Western blot analysis using an anti-AHAS(*At*) [A122TS653N] protein antibody was used to show immunoreactivity of the AHAS(*At*) [A122TS653N] protein in PPP isolated from EPA+DHA canola event LBFLFK (Figure 46). To demonstrate the specificity of the antibody, an AHAS(At) [A122TS653N] reference protein was included as positive control (Figure 46, lane 1). An immunoreactive band was observed in the LBFLFK PPP samples at a molecular weight that is in good agreement with the calculated molecular mass of the AHAS(At) [A122TS653N] protein of 66.1 kDa (Figure 46, lane 3 and 4). There is also a strong non-specific cross-reactivity with an unknown protein at ~98 kDa in both Kumily and LBFLFK PPP (Figure 46, lanes 2, 3 and 4), which is a notably higher molecular weight than estimated

for endogenous AHAS(*Bn*) protein (~66 kDa). While the cross-reactivity of the utilised antibody to the AHAS(*Bn*) protein could be expected to result in an immunoreactive band in the Kumily PPP samples at a molecular weight that is in agreement with the calculated molecular weight estimated for endogenous AHAS(*Bn*) protein (~66 kDa), the absence of such a band is likely a result of the much lower concentration of AHAS(*Bn*) in Kumily vs total combined concentration of AHAS(*At*) [A122TS653N] and AHAS(*Bn*) in LBFLFK (section B.2(a)(ii)).

Figure 46. Western Blot Analysis of Acetohydroxy Acid Synthase (*At*) [A122TS653N] in EPA+DHA Canola Event LBFLFK

PPP isolated from EPA+DHA canola event LBFLFK and parental control Kumily were separated by SDS-PAGE and evaluated by western blot analysis. The membrane was probed with a 1:1,000 dilution of the AHAS(*At*) [A122TS653N]-specific antibody and probed with a secondary HRP-conjugated antibody. Approximate molecular weight markers loaded in lanes MW are shown on the left and right side of the blot. The calculated molecular mass of the AHAS(*At*) [A122TS653N] protein encoded by the coding sequence introduced in EPA+DHA canola event LBFLFK is 66.1 kDa. The calculated molecular mass of the reference standard, which also contains a 6x histidine tag and short linker sequence is 68.1 kDa.

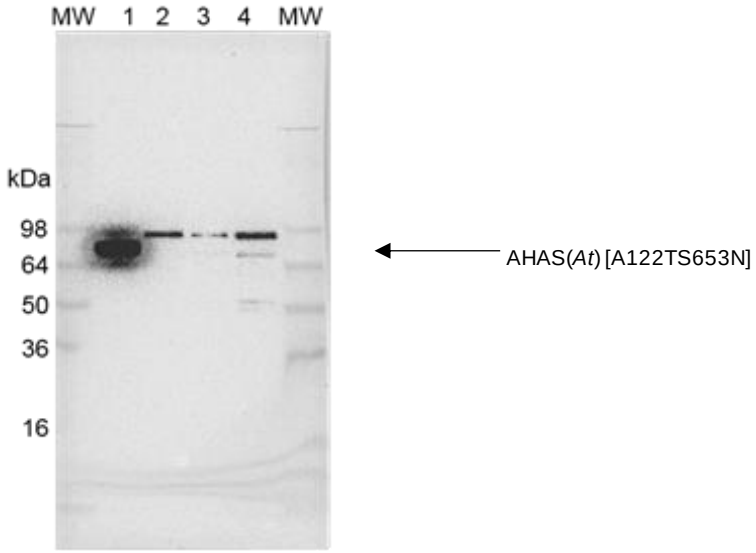

	Lane 1	Lane 2	Lane 3	Lane 4
Sample	AHAS(*At*) [A122TS653N]	Kumily PPP	LBFLFK PPP	LBFLFK PPP
Amount Loaded	5 ng	20 µg	10 µg	20 µg

Identity

Mass spectrometry was used to perform tryptic peptide mapping analysis against the deduced amino acid sequence of the AHAS(*At*) [A122TS653N] protein to confirm the identity of the AHAS(*At*) [A122TS653N] protein in PPP isolated from EPA+DHA canola event LBFLFK. Due to low quantity in LBFLFK PPP, the AHAS(*At*) [A122TS653N] protein was immunopurified from LBFLFK PPP for this analysis. To minimise the probability of a false positive identification, the current recommendations of the Human Proteome Project Mass Spectrometry Data Interpretation Guidelines 2.1 were followed (Deutsch et al., 2016). Specifically, true positive identification of a protein requires analysis of one sample and identification of at least two

peptides consisting of at least nine amino acids, and one of the peptides may not be fully nested within another. The analysis identified seven peptides (Table 19) that matched the expected deduced amino acid sequence of the AHAS(*At*) [A122TS653N] protein with ≥ 95% probability of true positive identification and covered 15% of the entire protein sequence (Figure 47). These peptides were specific to the newly expressed AHAS(*At*) [A122TS653N] protein, and not the endogenous AHAS(*Bn*) protein. Six of the peptides listed in Table 19 contained at least nine amino acids and were not fully nested within another (peptides 2–7). The AHAS(*At*) [A122TS653N] protein was therefore identified in PPP isolated from EPA+DHA canola event LBFLFK.

Table 19. Tryptic Peptides Identified for Acetohydroxy Acid Synthase (*At*) [A122TS653N] in EPA+DHA Canola Event LBFLFK using LC-MS/MS Analysis

Number	Peptide Sequence	Amino Acid Length
1	FAPDQPR	7
2	VLDELTDGK	9
3	TFGEAIPPQYAIK	13
4	HNYLVMDVEDIPR	13
5	MPKPPEDSHLEQIVR	15
6	DIQQQLAIPNWEQAMR	16
7	KPVLYVGGGCLNSSDELGR	19

AHAS(*At*) [A122TS653N] was enriched by immunopurification from PPP isolated from event LBFLFK and digested with trypsin and Lys-C followed by LC-MS/MS. Listed are peptides representing the AHAS(*At*) [A122TS653N], identified with 95% confidence using Mascot server v2.5.1 (Matrix Science Ltd, London, UK).

Figure 47. Peptide Mass Coverage by LC-MS/MS Analysis for Acetohydroxy Acid Synthase (*At*) [A122TS653N] in EPA+DHA Canola Event LBFLFK

The deduced amino acid sequence of the AHAS(*At*) [A122TS653N] protein, newly expressed in the EPA+DHA canola event LBFLFK, represented as the one letter amino acid code. Immunopurified AHAS(*At*) [A122TS653N] protein from PPP isolated from event LBFLFK was digested with trypsin and Lys-C followed by LC-MS/MS in order to identify peptides representing the AHAS(*At*) [A122TS653N] protein. Peptides listed in Table 19 were mapped (**bold underlined**) onto the deduced protein sequence covering approximately 15% of the total protein.

```
1   MAAATTTTTT SSSISFSTKP SPSSSKSPLP ISRFSLPFSL NPNKSSSSSR RRGIKSSSPS
61  SISAVLNTTT NVTTTPSPTK PTKPETFISR FAPDQPRKGA DILVEALERQ GVETVFAYPG
121 GTSMEIHQAL TRSSSIRNVL PRHEQGGVFA AEGYARSSGK PGICIATSGP GATNLVSGLA
181 DALLDSVPLV AITGQVPRRM IGTDAFQETP IVEVTRSITK HNYLVMDVED IPRIIEEAFF
241 LATSGRPGPV LVDVPKDIQQ QLAIPNWEQA MRLPGYMSRM PKPPEDSHLE QIVRLISESK
301 KPVLYVGGGC LNSSDELGRF VELTGIPVAS TLMGLGSYPC DDELSLHMLG MHGTVYANYA
361 VEHSDLLLAF GVRFDDRVTG KLEAFASRAK IVHIDIDSAE IGKNKTPHVS VCGDVKLALQ
421 GMNKVLENRA EELKLDFGVW RNELNVQKQK FPLSFKTFGE AIPPQYAIKV LDELTDGKAI
481 ISTGVGQHQM WAAQFYNYKK PRQWLSSGGL GAMGFGLPAA IGASVANPDA IVVDIDGDGS
541 FIMNVQELAT IRVENLPVKV LLLNNQHLGM VMQWEDRFYK ANRAHTFLGD PAQEDEIFPN
601 MLLFAAACGI PAARVTKKAD LREAIQTMLD TPGPYLLDVI CPHQEHVLPM IPNGGTFNDV
661 ITEGDGRIKY
```

Glycosylation analysis

The AHAS(*At*) [A122TS653N] protein has five potential N-glycosylation sites at $_{43}$NKSS$_{47}$, $_{67}$NTTT$_{70}$, $_{71}$NVTT$_{74}$, $_{312}$NSSD$_{315}$, and $_{404}$KTP$_{407}$ (Gavel and von Heijne, 1990; Zielinska et al., 2010) and has several potential O-glycosylation sites (any serine or threonine). The glycosylation status of the newly expressed AHAS(*At*) [A122TS653N] protein was determined

through biotinylation of the carbohydrate moieties of the proteins in the IP product from LBFLFK PPP and determined which fraction contained the AHAS(*At*) [A122TS653N] protein by western blot analysis with an AHAS(*At*) [A122TS653N]-specific antibody as described in Appendix 17.

Together, these data demonstrated that the AHAS(*At*) [A122TS653N] protein present in PPP isolated from EPA+DHA canola event LBFLFK was not glycosylated.

Enzymatic activity

The AHAS enzymatic reaction specifically catalyses the formation of acetolactate from two pyruvate molecules utilizing the cofactors flavin-adenine dinucleotide (FAD), thiamine pyrophosphate (TPP), and magnesium (Figure 4).

Enzymatic activity is assessed spectrophotometrically by the amount of acetolactate formed by the reaction. This activity assay cannot differentiate the production of acetolactate produced by the newly expressed AHAS(*At*) [A122TS653N] or the endogenous AHAS(*Bn*) protein. It is also known that AHAS activity is highest in young plant tissue (Singh and Shaner, 1995; Duggleby and Pang, 2000). Therefore, the enzymatic activity was measured in both leaf tissue and PPP.

Leaf Tissue: LBFLFK leaf showed a specific activity of 0.999 nmol/min/mg while the Kumily leaf samples showed a specific activity of 0.646 nmol/min/mg.

AHAS activities in LBFLFK and Kumily leaf tissues were measured in the presence of increasing concentrations of the herbicide imazamox (1 µM to 100 µM) as shown in Figure 48 (Table 20). LBFLFK leaf tissue samples showed a greater tolerance to increasing imazamox concentrations with 41% activity remaining at 100 µM imazamox compared to the activity in Kumily leaf tissue with 19%. The event LBFLFK leaf tissue has both the newly expressed AHAS(*At*) [A122TS653N] and the endogenous genes that produce AHAS(*Bn*) proteins with low tolerance to imazamox. Kumily leaf tissue only expresses the endogenous AHAS(*Bn*) proteins.

AHAS activities in LBFLFK and Kumily leaf tissues were also measured in the presence of increasing concentrations of the AHAS feedback inhibitors leucine and valine (Singh and Shaner, 1995; Duggleby and Pang, 2000) (5 µM–1 mM) as shown in Figure 49 (Table 21). LBFLFK and Kumily leaf tissues showed similar sensitivity to increasing leucine and valine concentrations with 62% and 57% activities remaining at 1 mM, respectively. This result indicates that the newly expressed AHAS(*At*) [A122TS653N] protein maintained the same amount of feedback inhibition from leucine and valine as the endogenous AHAS(*Bn*) proteins.

Plant-Produced Proteins: AHAS enzyme activity was observed in the LBFLFK and Kumily PPP. The AHAS activity in LBFLFK PPP showed AHAS specific activity of 0.764 nmol/min/mg while the Kumily PPP showed a specific activity of 0.678 nmol/min/mg. Similar specific activities are not unexpected since the parental canola variety Kumily has endogenous genes that produces AHAS(*Bn*) proteins and total activity assays cannot distinguish introduced from endogenous enzyme. Studies using PPP isolated from LBFLFK and Kumily in the presence of imazamox did not demonstrate the same inhibitory effects as seen in extract from leaves. This discrepancy may be related to high concentration of lipids present in the PPP matrix and

the relatively low AHAS protein concentration—the inhibitor may bind to the lipids and not the enzyme.

Figure 48. Inhibition of Leaf AHAS Activity in EPA+DHA Canola Event LBFLFK and the Parental Control Variety Kumily by Imidazolinone Herbicide, Imazamox

Leaf extracts from event LBFLFK and the parental variety Kumily were incubated in a buffer containing pyruvate and using thiamine pyrophosphate (TPP) as a co-enzyme with Mg^{2+} and flavin adenine dinucleotide (FAD) as a cofactor. Acetolactate produced by AHAS is converted to acetoin in the presence of acid, and acetoin is detected colorimetrically (A_{530} nm) after interaction with creatine and naphthol. Inhibition was measured with the inclusion of imazamox in the assay buffer at increasing concentrations and reported below as % activity remaining compared to samples without imazamox. Squares (■) represent Kumily leaf extract samples and circles (●) represent LBFLFK leaf extract samples.

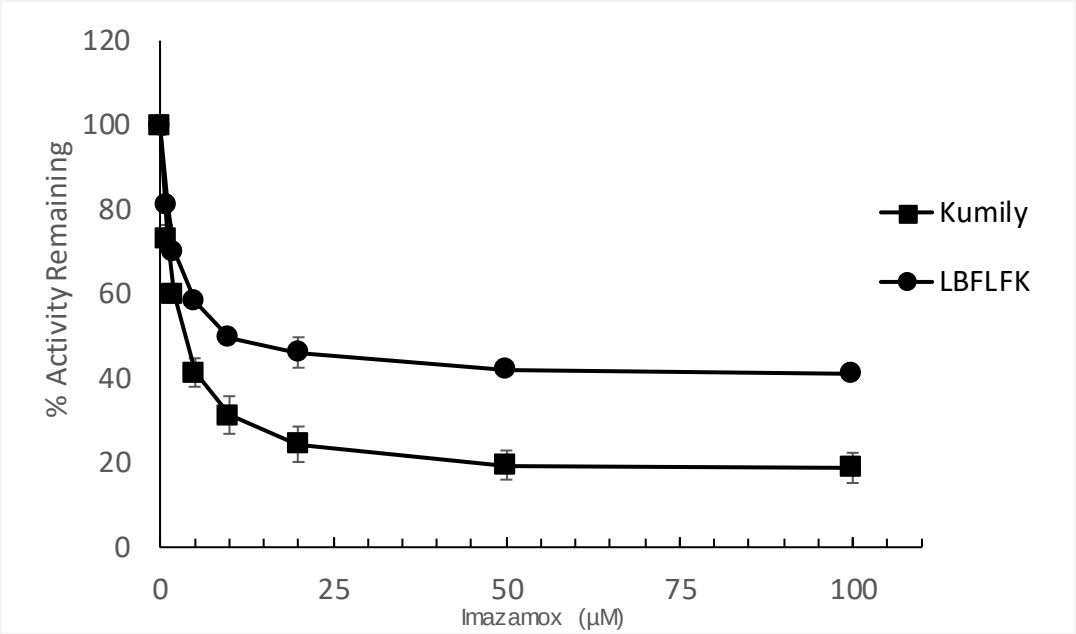

Table 20. Specific Activity Percent Activity Remaining Values for Inhibition of Leaf AHAS Activity in EPA+DHA Canola Event LBFLFK and the Parental Control Variety Kumily by Imidazolinone Herbicide, Imazamox

		0 µM imazamox	1 µM imazamox	2 µM imazamox	5 µM imazamox	10 µM imazamox	20 µM imazamox	50 µM imazamox	100 µM imazamox	Leaf Total Protein Conc. (mg/ml)
Kumily	Average Specific Activity of 3 Replicates (nmol/mg/min)	0.754 ± 0.005[1]	0.551 ± 0.018	0.452 ± 0.003	0.312 ± 0.011	0.236 ± 0.011	0.184 ± 0.008	0.147 ± 0.005	0.142 ± 0.005	6.589
	Percent Activity Remaining	---	73.2 ± 3.18	60.0 ± 0.65	41.4 ± 3.38	31.3 ± 4.46	24.4 ± 4.20	19.5 ± 3.45	18.8 ± 3.57	
LBFLFK	Average Specific Activity of 3 Replicates (nmol/mg/min)	1.162 ± 0.028	0.944 ± 0.003	0.815 ± 0.006	0.677 ± 0.006	0.576 ± 0.003	0.536 ± 0.019	0.490 ± 0.006	0.477 ± 0.003	6.053
	Percent Activity Remaining	---	81.2 ± 0.34	70.1 ± 0.68	58.3 ± 0.81	49.6 ± 0.55	46.1 ± 3.61	42.2 ± 1.12	41.1 ± 0.67	

[1] Standard deviation

Figure 49. Feedback Inhibition of Leaf AHAS Activity in EPA+DHA Canola Event LBFLFK and the Parental Control Variety Kumily by Valine and Leucine

Leaf extracts from event LBFLFK and the parental variety Kumily were incubated in a buffer containing pyruvate and using thiamine pyrophosphate (TPP) as a co-enzyme with Mg^{2+} and flavin adenine dinucleotide (FAD) as a cofactor. Acetolactate produced by AHAS is converted to acetoin in the presence of acid, and acetoin is detected colorimetrically (A_{530} nm) after interaction with creatine and naphthol. Inhibition was measured with the inclusion of leucine and valine in the assay buffer at increasing concentrations and reported below as % activity remaining compared to samples without leucine and valine. Squares (■) represent Kumily leaf extract samples and circles (●) represent LBFLFK leaf extract samples.

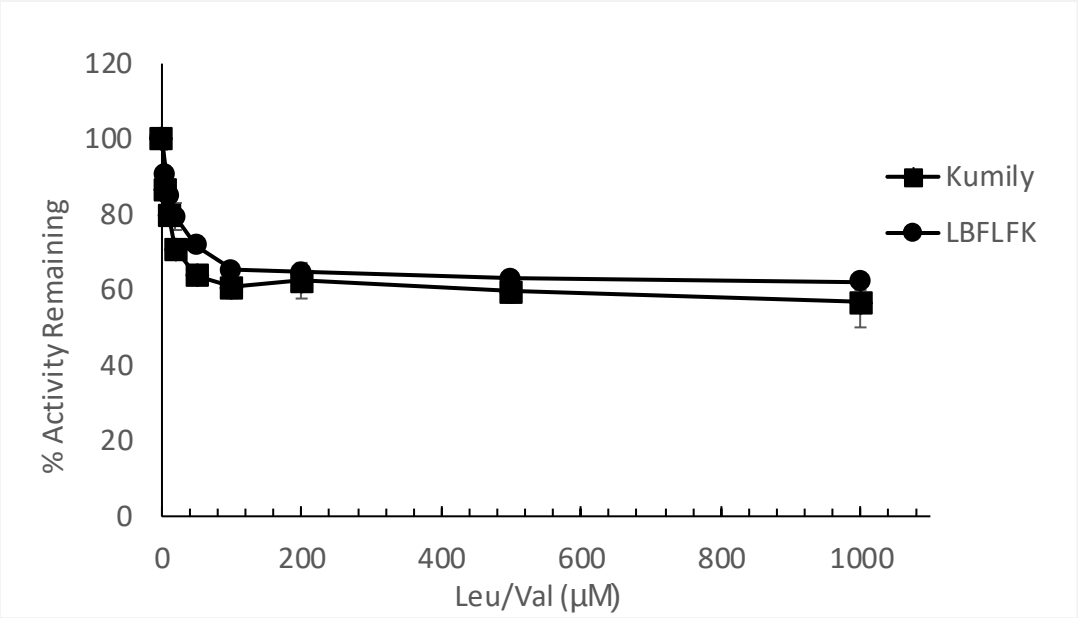

Table 21. Specific Activity Percent Activity Remaining Values for Feedback Inhibition of Leaf AHAS Activity in EPA+DHA Canola Event LBFLFK and the Parental Control Variety Kumily by Valine and Leucine

		0 µM Leu/Val	5 µM Leu/Val	10 µM Leu/Val	20 µM Leu/Val	50 µM Leu/Val	100 µM Leu/Val	200 µM Leu/Val	500 µM Leu/Val	1000 µM Leu/Val	Leaf Total Protein Conc. (mg/ml)
Kumily	Average Specific Activity of 3 Replicates (nmol/mg/min)	0.297 ± 0.008[1]	0.258 ± 0.005	0.238 ± 0.002	0.211 ± 0.005	0.190 ± 0.002	0.180 ± 0.005	0.186 ± 0.009	0.177 ± 0.005	0.169 ± 0.011	10.048
	Percent Activity Remaining	---	86.6 ± 1.97	80.0 ± 0.81	71.0 ± 2.40	63.9 ± 1.01	60.6 ± 2.81	62.5 ± 4.72	59.5 ± 2.86	56.9 ± 6.79	
LBFLFK	Average Specific Activity of 3 Replicates (nmol/mg/min)	0.507 ± 0.008	0.460 ± 0.003	0.431 ± 0.006	0.403 ± 0.014	0.364 ± 0.006	0.331 ± 0.005	0.329 ± 0.006	0.319 ± 0.006	0.315 ± 0.007	10.446
	Percent Activity Remaining	---	90.6 ± 0.69	84.9 ± 1.48	79.5 ± 3.57	71.7 ± 1.52	65.2 ± 1.47	64.8 ± 1.68	62.9 ± 2.00	62.1 ± 2.11	

[1] Standard deviation

Summary of AHAS(*At*) [A122TS653N] characterisation

EPA+DHA canola event LBFLFK contains two T-DNA inserts encoding two identical copies of the AHAS(*At*) [A122TS653N] protein. A series of biochemical experiments was performed to characterise the AHAS(*At*) [A122TS653N] protein newly expressed in event LBFLFK.

Structure / Function: The AHAS(*At*) [A122TS653N] protein represents the large subunit of the plastidial localised acetohydroxy acid synthase. The chloroplast transit peptide is removed upon import into the chloroplast, which results in mature AHAS(*At*) [A122TS653N] enzyme.

Immunoreactivity / Molecular weight: Western blot analysis confirmed the protein was immunoreactive to an anti-AHAS(*At*) [A122TS653N] antibody. The apparent molecular weight was in good agreement to the calculated molecular mass of the mature AHAS(*At*) [A122TS653N] protein lacking 64 amino acids of the N-terminus of the immature protein.

Identity: Tryptic peptide mapping using LC-MS/MS positively identified six distinct peptides (> 9 amino acids) corresponding to the deduced amino acid sequence of the AHAS(*At*) [A122TS653N] protein. The AHAS(*At*) [A122TS653N] was therefore identified.

Glycosylation: The AHAS(*At*) [A122TS653N] protein was found to be not glycosylated.

Enzyme activity: The enzymatic activity of the AHAS protein was demonstrated in LBFLFK PPP via an *in vitro* assay for the AHAS protein confirming normal biosynthetic function of the AHAS(*At*) [A122TS653N] enzyme. Additionally, AHAS activity assessed in LBFLFK leaf tissue extracts displayed a greater tolerance to the herbicide imazamox compared to Kumily leaf extracts and thereby confirmed the altered binding of AHAS to imazamox due to the two amino acid substitutions. Both LBFLFK and Kumily leaf extracts showed similar feedback inhibition when incubated with the amino acids leucine and valine, which confirms that the amino acid substitutions in the AHAS(*At*) [A122TS653N] protein did not impact the feedback regulation by branched-chain amino acids.

Table 22. Characteristics of the Newly Expressed Proteins in PPP Isolated from EPA+DHA Canola Event LBFLFK

Protein	Apparent Molecular Weight (kDa)	Immuno-reactivity	Identity	Newly Expressed Protein Concentration Mean ± SD		Observed Activity	Glycosylation Status
				Wet Weight (µg/ml)	Dry Weight (µg/g)		
D12D(*Ps*)	41.8	Confirmed	Confirmed	7.88 ± 0.38	175.05 ± 27.69	Yes	Negative
D6D(*Ot*)	55.6	Confirmed	Confirmed	38.12 ± 2.09	793.36 ± 153.44	ND	Negative
D6E(*Tp*)	25.0	Confirmed	Confirmed	657.57 ± 107.49	16386.31 ± 2192.83	Yes	Negative
D6E(*Pp*)	ND	ND	ND	ND	NA		NA
D5D(*Tc*)	46.8	Confirmed	Confirmed	6.82 ± 0.81	395.11 ± 103.03	ND	Negative
O3D(*Pir*)	38.1	Confirmed	Confirmed	156.67 ± 13.67	4029.87 ± 117.09	ND	Negative
O3D(*Pi*)	ND	ND	ND	ND	NA		NA
D5E(*Ot*)	30.8	Confirmed	Confirmed	8.88 ± 0.11	220.42 ± 5.08	Yes	Negative
D4D(*Tc*)	63.1	Confirmed	Confirmed	34.74 ± 1.79	593.63 ± 13.88	Yes	Negative
D4D(*Pl*)	50.7	Confirmed	Confirmed	11.24 ± 0.40	194.54 ± 64.81		Negative
AHAS(*At*) [A122TS653N]	79.2	Confirmed	Confirmed	0.54 ± 0.04	24.28 ± 1.29	Yes	Negative

ND = Not detected or below detection limit, NA = Not applicable (assay not performed)
Characterisation experiments of AHAS(*At*) [A122TS653N] in leaf extracts confirmed the immunoreactivity of a protein with an apparent molecular weight of 79.2 kDa, with observable enzyme activity and protein concentrations of 1.07 ± 0.67 µg/ml (wet weight) and 7.41 ± 1.67 µg/ml (dry weight).

(d) Where any ORFs have been identified (in subparagraph A.3 (c) (v) of this Guideline (3.5.1), bioinformatics analyses to indicate the potential for allergenicity and toxicity of the ORFs.

As indicated in section A.3(c)(v) of this application, a total of 11 ORFs were identified at the four junctions between the canola genome and the T-DNA inserts: one at the Insert1 5´ end, three at the Insert1 3´ end, three at the Insert2 5´ end, and four at the Insert2 3´ end.

To determine the similarity of the identified ORFs to known allergens, the Food Allergy Research and Resource Program (FARRP) Allergen Protein Database[11] was used. It was determined that none of the ORFs created by the insertions shared > 35% identity over 80 amino acids with a known allergen, none had a sequence of eight or more consecutive identical amino acids with a known allergen, and none had any significant overall homology to a known allergen.

Additionally, the National Center for Biotechnology Information (NCBI) GenBank non-redundant peptide sequence database (NCBI Resource Coordinators, 2016) was searched by applying the Basic Local Alignment Search algorithm for protein-to-protein comparisons (BLASTP, NCBI Version 2.6.0+ Jan. 10, 2017) (Altschul et al., 1997) to determine the similarity of the identified ORFs to known toxins and antinutrients. None of the ORFs created by the insertion showed significant homology to known protein toxins as defined in the U.S. Code of Federal Regulations (U.S. EPA, 2017) or showed significant homology to known antinutrients of canola (OECD, 2011b), maize (OECD, 2002a), rice (OECD, 2016), soybean (OECD, 2012), sugar beet (OECD, 2002b), or sugarcane (OECD, 2011a).

B.2 New Proteins

The safety assessment of agricultural products produced through biotechnology includes an evaluation of the safety of the newly expressed proteins (Codex Alimentarius Commission, 2009b). This assessment is accomplished by applying a weight-of-evidence approach to the data generated from *in silico* and experimental studies. A weight-of-evidence approach is used because no single assay or biochemical characteristic can identify a protein as a hazard and, scientifically, it is not possible to prove a lack of hazard with complete certainty (Delaney et al., 2008).

The weight-of-evidence approach for the safety assessment of newly expressed proteins prioritises the testing into two tiers (Delaney et al., 2008). Tier I testing (potential hazard identification) includes establishing a history of safe use (HOSU) and consumption (provided in section B.1(b) of this application), amino acid sequence similarity between the newly expressed protein and known protein toxins and antinutrients (section B.2(a)(i)), biological function of the protein in the plant (section A.3(b)(i)), stability to heat or conditions of commercial processing (section B.2(a)(ii)), degradation in appropriate representative gastric and intestinal model systems (section B.2(a)(ii)), and expression level (section A.3(e)(ii) and Table 22 in section B.1(c)). Tier II testing (hazard classification), which may be performed on a case-by-case basis if the first tier does not provide sufficient evidence to make a determination of safety, might include acute or repeated dose toxicity testing of the newly expressed proteins or hypothesis-based studies.

[11] http://www.allergenonline.org

Bioinformatic analysis of the amino acid sequence of each newly expressed protein was performed to determine the similarity of the amino acid sequence of the newly expressed proteins to known protein toxins or antinutrients. Nucleotide sequences from both LBFLFK Insert1 and LBFLFK Insert2 (section A.3(c)(iii)) were translated into amino acid sequences, and bioinformatic analyses were performed on both LBFLFK Insert1 and LBFLFK Insert2 sequences.

Proteins are subjected to a variety of conditions during commercial processing that can have a major impact on their function (Kilara et al., 1986; Meade et al., 2005). Thus, heat stability of the newly expressed proteins is evaluated to determine the impact of commercial processing conditions on enzyme activity and structural integrity. Additionally, proteolytic enzymes in the gastrointestinal tract impact the structural integrity and functional activity of most dietary proteins. Thus, the stability of the newly expressed proteins to degradation in simulated gastric fluid (SGF) containing pepsin and simulated intestinal fluid (SIF) containing pancreatin is determined.

Specifically, for LBFLFK, heat stability and digestibility studies of the newly expressed proteins were performed with a membrane fraction purified from crude extracts of developing embryos that were isolated from immature seeds of LBFLFK. This detergent-free membrane fraction, referred to as “plant-produced proteins” (PPP), contains the newly expressed elongases and desaturases. The digestive fate assessment of AHAS(*At*) [A122TS653N] was performed with AHAS(*At*) [A122TS653N] protein present in LBFLFK PPP and LBFLFK leaf isolates.

Safety assessments for each of the introduced proteins are provided in the following sections. The safe use of each protein and respective donor organism was evaluated by a systematic literature search that identified relevant documents related to dietary exposure (i.e. presence in food or feed) or toxicity of the newly expressed protein or donor organism. To establish a history of consumption, each protein sequence was used to identify similarity to other proteins that are safely consumed via the GenBank non-redundant protein sequence database.

Additional details on the materials and methods used can be found in (Appendix 18).

(a) Information on the potential toxicity of any new proteins, including:

(i) A bioinformatic comparison of the amino acid sequence of each of the new proteins to known protein toxins and anti-nutrients (e.g., protease inhibitors, lectins)

(ii) Information on the stability of the protein to proteolysis in appropriate gastrointestinal model systems

<u>Delta-12 desaturase (*Ps*)</u>

Bioinformatic analysis – toxins for delta-12 desaturase (*Ps*)

Bioinformatic analysis was used to determine whether the amino acid sequence of D12D(*Ps*) had significant sequence similarity to known protein toxins or antinutrients. The amino acid sequences from both LBFLFK Insert1 and LBFLFK Insert2 were used for bioinformatic analysis. For D12D(*Ps*), LBFLFK Insert1 includes a nucleotide change in the coding region, which results in the F83L amino acid substitution (section A.3(c)(ii)). D12D(*Ps*) did not show

significant homology to proteins that are toxic to humans (Appendix 19). D12D(*Ps*) did not show significant homology to known antinutrients (OECD, 2002a, b, 2011a, b, 2012, 2016).

Stability to heat of delta-12 desaturase (*Ps*)

A heat stability analysis on D12D(*Ps*) was performed to assess the effects of different temperatures on enzyme activity and protein structural integrity. LBFLFK PPP samples containing the D12D(*Ps*) protein were incubated at 30, 50, 70, and 90°C for 5 and 20 min while a separate LBFLFK PPP sample was maintained on ice (0°C) and served as a baseline control (see Appendix 20 for details). Additional controls included Kumily PPP to represent the parental control line that does not contain the newly expressed proteins and the PPP storage buffer alone.

The effect of heat treatment on the relative activity of the D12D(*Ps*) protein was evaluated using a fatty acid desaturase assay (Yilmaz et al., 2017), and the results are presented in Table 23. The desaturase assay does not discriminate between the intended D12D(*Ps*) and the D12D(*Ps*) [F83L]. The D12D(*Ps*) enzyme activity was unaffected after 5 and 20 min at 30°C. However, the D12D(*Ps*) proteins were completely inactivated (< LOD, Table 23) within 5 min at 50°C. The same result was obtained after longer treatment (20 min) and at temperatures > 50°C.

The effect of heat treatment on the structural integrity of the D12D(*Ps*) protein was evaluated by western blot analysis, and the results are presented in Figure 50. The antibody used does not discriminate between the intended D12D(*Ps*) and the D12D(*Ps*) [F83L]. The western blot analysis demonstrated that the LBFLFK sample without heat treatment contained a distinct single band with an apparent molecular weight of ~48 kDa in good agreement with the calculated molecular weight of the D12D(*Ps*) protein (Figure 50, lane 3). While this single band of ~48 kDa was present at all temperatures and times tested, its signal decreased and protein aggregation intensified after 5 min at temperatures ≥ 50°C as indicated by a smear appearing at molecular weights > 48 kDa. This result is typical of proteins subjected to heat, especially for membrane proteins (Nury and Meunier, 1990; Lohner and Esser, 1991; Yan et al., 2004; Lee et al., 2005b; Harris and Booth, 2012; Roman and González Flecha, 2014). In the Kumily sample (Figure 50, lane 2), a very small amount of non-specific binding was detected that runs at approximately the same molecular weight as the D12D(*Ps*) protein. This non-specific binding could be a cross-reaction to a protein in *Brassica napus*. Finally, no cross-reaction was found with the PPP storage buffer (Figure 50, lane 1).

These results show that D12D(*Ps*) loses enzyme activity (Table 23) and undergoes structural change in the form of aggregation (Figure 50) within 5 min at ≥ 50°C. Therefore, the D12D(*Ps*) protein is not likely to remain intact or functional after commercial processing.

Table 23. Relative Enzyme Activity of D12D(*Ps*) after Heat Treatment of 5 and 20 Minutes

	30°C		50°C		70°C		90°C	
Protein	**5 min**	**20 min**	**5 min**	**20 min**	**5 min**	**20 min**	**5 min**	**20 min**
D12D(*Ps*)	104%	96%	< LOD	< LOD	< LOD	< LOD	< LOD	< LOD

Note: Results are % activity remaining compared to an LBFLFK sample that was not subjected to heat treatment prior to the enzyme activity assay.

LOD (Limit of Detection) = 38667 volume unit (VU)

Figure 50. Western Blot Analysis of the D12D(*Ps*) Protein in LBFLFK after Heat Treatment

The effect of heat treatment on the structural integrity of the D12D(*Ps*) protein was analysed via western blot. The D12D(*Ps*) protein consists of 398 amino acids with a calculated molecular mass of 45.6 kDa (migrates at ~48 kDa).

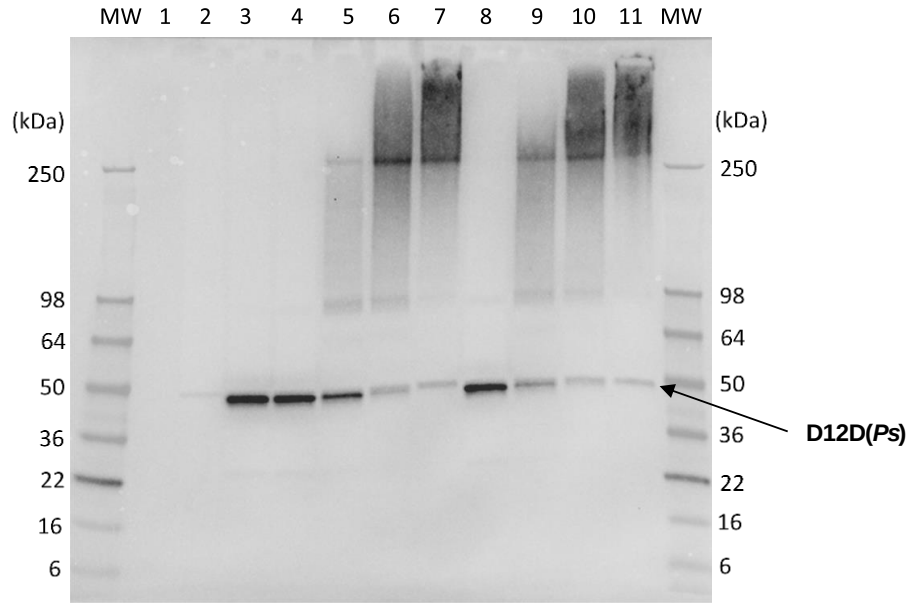

Lane	Sample	Incubation Temperature (°C)	Incubation Time (min)
1	PPP Storage Buffer	0	-
2	Kumily PPP	0	-
3	LBFLFK PPP	0	-
4	LBFLFK PPP	30	5
5	LBFLFK PPP	50	5
6	LBFLFK PPP	70	5
7	LBFLFK PPP	90	5
8	LBFLFK PPP	30	20
9	LBFLFK PPP	50	20
10	LBFLFK PPP	70	20
11	LBFLFK PPP	90	20

Digestive fate (*SGF/SIF*) *for delta-12 desaturase* (*Ps*)

The sensitivity of D12D(*Ps*) to SGF and SIF digestion was also assessed. The digestibility of the D12D(*Ps*) protein was evaluated by visual analysis of protein degradation in a time course on a western blot. The antibody used was raised against a D12D(*Ps*) NC fusion protein and does not discriminate between the intended D12D(*Ps*) and the D12D(*Ps*) [F83L]. A separate western blot was run to estimate the LOD of the D12D(*Ps*) protein. The LOD of the D12D(*Ps*) protein was 0.054 nanograms (ng) D12D(*Ps*), corresponding to 300 ng LBFLFK PPP. This D12D(*Ps*) amount corresponds to 9.6% and 10.8% of the total D12D(*Ps*) protein loaded in each lane of the SGF and SIF gels, respectively (Appendix 21).

Following exposure to SGF, western blot analysis demonstrated that the intensity of a ~48 kDa protein band, which aligns with the calculated molecular weight of the full-length D12D(*Ps*) protein, dropped below the D12D(*Ps*) LOD within 0.5 min (Figure 51, lane 5). This result indicates ≥ 90.4% digestion of the full-length D12D(*Ps*) protein within 0.5 min with SGF. The band migrating at ~24 kDa, which likely represents a fragment of D12D(*Ps*), was also digested within 0.5 min. Controls for the SGF assay without pepsin showed only minor degradation of the D12D(*Ps*) protein over the 60-min time course as deduced from the signal intensities of the bands at ~48 kDa and 24 kDa (G-con, Figure 51, lanes 2–3). This result indicates that digestion of the D12D(*Ps*) protein was primarily due to pepsin proteolytic activity and not instability of the D12D(*Ps*) protein in the test system. As expected, controls with pepsin but without D12D(*Ps*) protein (SGF alone, Figure 51, lanes 12 and 13) showed no unspecific detection of pepsin by the D12D(*Ps*)-specific antibody, which would be expected to result in a black band at ~50 kDa.

Following exposure to SIF, western blot analysis demonstrated that the intensity of an ~48 kDa band in good agreement with the calculated molecular weight of the full-length D12D(*Ps*) protein dropped below the D12D(*Ps*) LOD within 0.5 min (Figure 52, lane 5). This result indicates ≥ 89.2% digestion of the full-length D12D(*Ps*) protein within 0.5 min with SIF. Controls for the SIF assay without pancreatin showed only minor change of the D12D(*Ps*) protein over the 60-min time course as deduced from the signal intensities of the bands at ~48 kDa and 24 kDa (I-con, Figure 52, lanes 2–3). This result indicates that digestion of the D12D(*Ps*) protein was primarily due to pancreatin proteolytic activity and not instability of the D12D(*Ps*) protein in the test system. As found for the D12D(*Ps*) SGF assay, controls with pancreatin but without D12D(*Ps*) protein (SIF alone, Figure 52, lanes 12 and 13) showed no unspecific detection of pancreatin by the D12D(*Ps*)-specific antibody, which would be expected to result in a black band(s) between 4 and 64 kDa.

These results demonstrate that the D12D(*Ps*) is susceptible to digestion and rapidly degraded in SGF and SIF.

Figure 51. Western Blot Analysis of the D12D(*Ps*) Protein in LBFLFK Subjected to SGF

A western blot used to analyse the digestibility of the D12D(*Ps*) protein with SGF. In each lane, 3.125 µg of LBFLFK PPP was loaded, which corresponds to 0.56 ng D12D(*Ps*) protein (LOD = 0.054 ng D12D(*Ps*)). The D12D(*Ps*) protein consists of 398 amino acids with a calculated molecular mass of 45.6 kDa (migrates at ~48 kDa, indicated by the arrow). Lanes 1 and 14 are molecular weight markers with kDa values shown on the left. G-con: Buffer control (no pepsin). SGF alone: Negative control (no test protein).

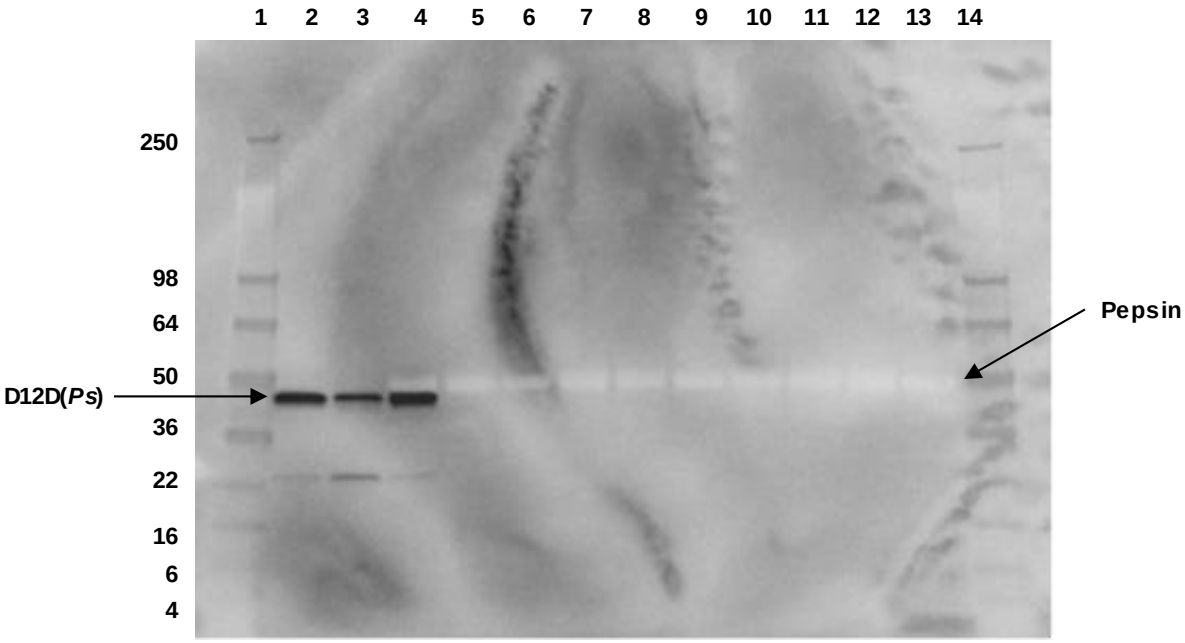

Lane	Sample	Incubation Time (min)
1	molecular weight marker	-
2	G-con	0
3	G-con	60
4	SGF	0
5	SGF	0.5
6	SGF	2
7	SGF	5
8	SGF	10
9	SGF	20
10	SGF	30
11	SGF	60
12	SGF alone	0
13	SGF alone	60
14	molecular weight marker	-

Figure 52. Western Blot Analysis of the D12D(*Ps*) Protein in LBFLFK Subjected to SIF

A western blot used to analyse the digestibility of the D12D(*Ps*) protein with SIF. In each lane, 2.813 µg of LBFLFK PPP was loaded, which corresponds to 0.50 ng D12D(*Ps*) protein (LOD = 0.054 ng D12D(*Ps*)). The D12D(*Ps*) protein consists of 398 amino acids with a calculated molecular mass of 45.6 kDa (migrates at ~48 kDa, indicated by the arrow). Lanes 1 and 14 are molecular weight markers with kDa values shown on the left of blot. I-con: Buffer control (no pancreatin). SIF alone: Negative control (no test protein).

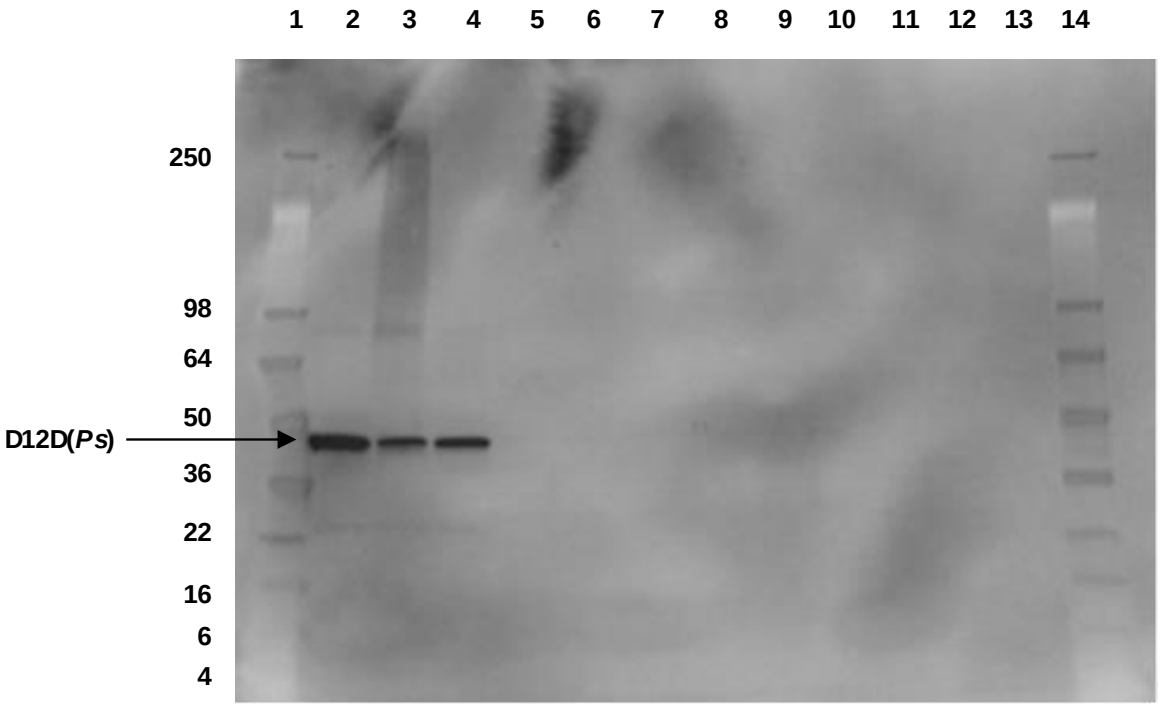

Lane	Sample	Incubation Time (min)
1	molecular weight marker	-
2	I-con	0
3	I-con	60
4	SIF	0
5	SIF	0.5
6	SIF	2
7	SIF	5
8	SIF	10
9	SIF	20
10	SIF	30
11	SIF	60
12	SIF alone	0
13	SIF alone	60
14	molecular weight marker	-

Delta-6 desaturase (*Ot*)

Bioinformatic analysis – toxins for delta-6 desaturase (*Ot*)

Bioinformatic analysis was used to determine whether the amino acid sequence of D6D(*Ot*) had significant sequence similarity to known protein toxins or antinutrients. D6D(*Ot*) did not show significant homology to proteins that are toxic to humans (Appendix 19). D6D(*Ot*) did not show significant homology to known antinutrients (OECD, 2002a, b, 2011a, b, 2012, 2016).

Stability to heat of delta-6 desaturase (*Ot*)

A heat stability analysis of D6D(*Ot*) was performed to assess the effects of different temperatures on protein structural integrity. The enzyme activity of D6D(*Ot*) in response to heat was not assessed because enzyme activity was not detectable in LBFLFK PPP. Sample treatment of the D6D(*Ot*) protein was identical to that of D12D(*Ps*) (Appendix 20).

The effect of heat treatment on the structural integrity of the D6D(*Ot*) protein was evaluated by western blot analysis, and the results are presented in Figure 53. The western blot analysis demonstrated that the LBFLFK sample without heat treatment contained a distinct band with an apparent molecular weight of ~56 kDa in good agreement with the calculated molecular weight of the D6D(*Ot*) protein (Figure 53, lane 3). The band detected at ~36 kDa likely represents a D6D(*Ot*) fragment. While the bands corresponding to D6D(*Ot*) (~56 kDa) and its fragment (~36 kDa) were present at all temperatures and times tested, their signals decreased and protein aggregation intensified after 5 min at temperatures ≥ 50°C as indicated by a smear appearing at molecular weights > 56 kDa. Appearance of aggregates is typical of proteins subjected to heat, especially for membrane proteins (Nury and Meunier, 1990; Lohner and Esser, 1991; Yan et al., 2004; Lee et al., 2005b; Harris and Booth, 2012; Roman and González Flecha, 2014). Finally, no cross-reaction was found with the PPP storage buffer and Kumily sample in Figure 53, lanes 1 and 2, respectively.

These results show that D6D(*Ot*) undergoes structural change in the form of aggregation (Figure 53) within 5 min at ≥ 50°C. Therefore, the D6D(*Ot*) protein is heat-labile and not likely to remain intact after commercial processing.

Figure 53. Western Blot Analysis of the D6D(*Ot*) Protein in LBFLFK after Heat Treatment

The effect of heat treatment on the structural integrity of the D6D(*Ot*) protein was analysed via western blot. The D6D(*Ot*) protein consists of 456 amino acids with a calculated molecular mass of 51.7 kDa (migrates at ~56 kDa).

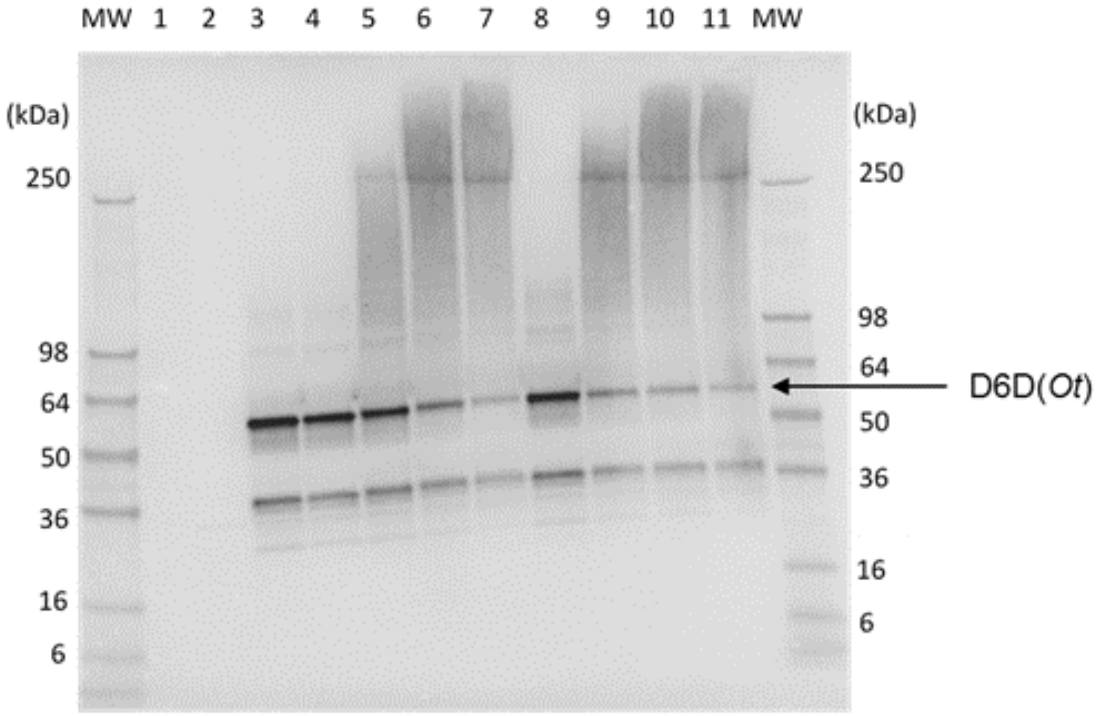

Lane	Sample	Incubation Temperature (°C)	Incubation Time (min)
1	PPP Storage Buffer	0	-
2	Kumily PPP	0	-
3	LBFLFK PPP	0	-
4	LBFLFK PPP	30	5
5	LBFLFK PPP	50	5
6	LBFLFK PPP	70	5
7	LBFLFK PPP	90	5
8	LBFLFK PPP	30	20
9	LBFLFK PPP	50	20
10	LBFLFK PPP	70	20
11	LBFLFK PPP	90	20

Digestive fate (*SGF/SIF*) *for delta-6 desaturase* (*Ot*)

The sensitivity of D6D(*Ot*) to SGF and SIF digestion was also assessed. The digestibility of the D6D(*Ot*) protein was evaluated by visual analysis of protein degradation in a time course on a western blot with an antibody raised against D6D(*Ot*) full-length protein. A separate western blot was run to estimate the LOD of the D6D(*Ot*) protein. The LOD of the D6D(*Ot*) protein was 0.014 ng D6D(*Ot*), corresponding to 15.625 ng LBFLFK PPP. This D6D(*Ot*) amount corresponds to 1.6% and 1.7% of the total D6D(*Ot*) protein loaded in each lane of the SGF and SIF gels, respectively (Appendix 21).

Following exposure to SGF, western blot analysis demonstrated that the intensity of a ~56 kDa band in good agreement with the calculated molecular weight of the full-length D6D(*Ot*) protein dropped below the D6D(*Ot*) LOD within 0.5 min (Figure 54, lane 5). This result indicates ≥ 98.4% digestion of the full-length D6D(*Ot*) protein within 0.5 min with SGF. The bands migrating at ~36 and 22 kDa, which are likely to represent fragments of D6D(*Ot*), were also digested within 0.5 min. Controls for the SGF assay without pepsin showed only minor degradation of the protein over the 60-min time course (G-con, Figure 54, lanes 2–3), which indicates that digestion of the D6D(*Ot*) protein was largely due to pepsin proteolytic activity and not instability of the protein in the test system. As expected, controls with pepsin but without D6D(*Ot*) (SGF alone, Figure 54, lanes 12 and 13) showed no unspecific detection of pepsin by the D6D(*Ot*)-specific antibody, which would be expected to result in a black band at ~50 kDa.

Following exposure to SIF, western blot analysis demonstrated that the intensity of a ~56 kDa band in good agreement with the calculated molecular weight of the full-length D6D(*Ot*) protein dropped below the D6D(*Ot*) LOD within 0.5 min (Figure 55, lane 5). This result indicates ≥ 98.3% digestion of the full-length D6D(*Ot*) protein within 0.5 min with SIF. The bands migrating at ~36 and 22 kDa, which are likely to represent fragments of D6D(*Ot*), were also digested within 0.5 min. Controls for the SIF assay without pancreatin showed only minor change of the D6D(*Ot*) protein over the 60-min time course as deduced from the signal intensities of the bands at ~56 kDa and 36 kDa (I-con, Figure 55, lanes 2–3). This result indicates that digestion of the D6D(*Ot*) protein was primarily due to pancreatin proteolytic activity and not instability of the D6D(*Ot*) protein in the test system. As found for the D6D(*Ot*) SGF assay, controls with pancreatin but without D6D(*Ot*) protein (SIF alone, Figure 55, lanes 12 and 13) showed no unspecific detection of pancreatin by the D6D(*Ot*)-specific antibody, which would be expected to result in a black band(s) between 4 and 64 kDa.

These results demonstrate that the D6D(*Ot*) is susceptible to digestion and rapidly degraded in SGF and SIF.

Figure 54. Western Blot Analysis of the D6D(*Ot*) Protein in LBFLFK Subjected to SGF

A western blot used to analyse the digestibility of the D6D(*Ot*) protein with SGF. In each lane, 1.042 µg of LBFLFK PPP was loaded, which corresponds to 0.90 ng D6D(*Ot*) protein (LOD = 0.014 ng D6D(*Ot*)). The D6D(*Ot*) protein consists of 456 amino acids with a calculated molecular mass of 51.7 kDa (migrates at ~56 kDa, indicated by the arrow). Lanes 1 and 14 are molecular weight markers with kDa values shown on the left. G-con: Buffer control (no pepsin). SGF alone: Negative control (no test protein).

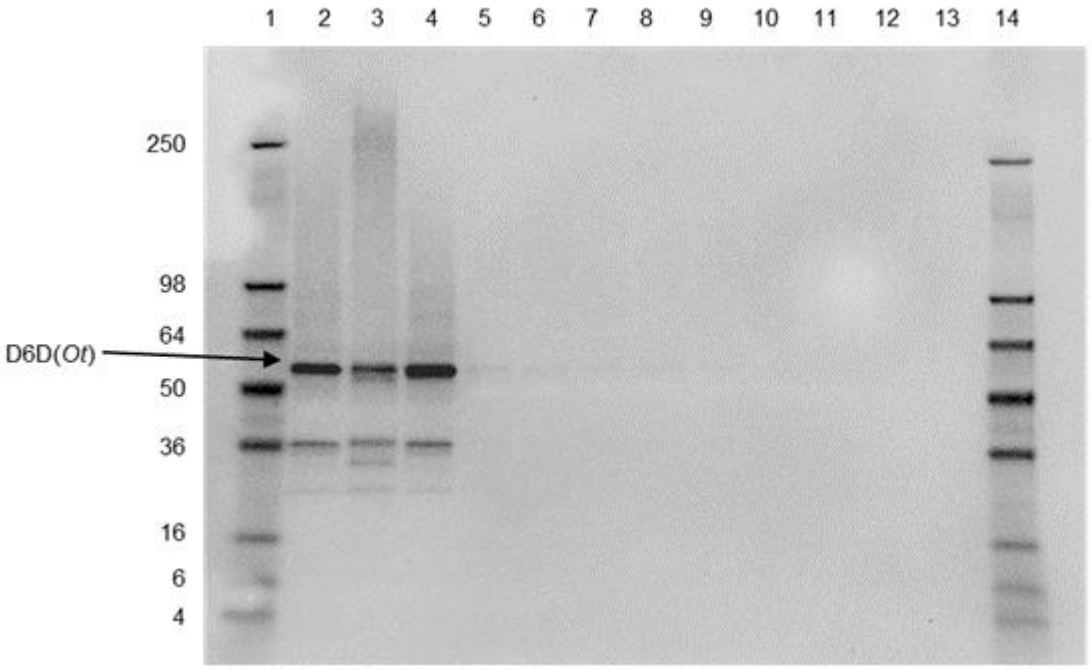

Lane	Sample	Incubation Time (min)
1	molecular weight marker	-
2	G-con	0
3	G-con	60
4	SGF	0
5	SGF	0.5
6	SGF	2
7	SGF	5
8	SGF	10
9	SGF	20
10	SGF	30
11	SGF	60
12	SGF alone	0
13	SGF alone	60
14	molecular weight marker	-

Figure 55. Western Blot Analysis of the D6D(*Ot*) Protein in LBFLFK Subjected to SIF

A western blot used to analyse the digestibility of the D6D(*Ot*) protein with SIF. In each lane, 0.94 µg of LBFLFK PPP was loaded, which corresponds to 0.81 ng D6D(*Ot*) protein (LOD = 0.014 ng D6D(*Ot*)). The D6D(*Ot*) protein consists of 456 amino acids with a calculated molecular mass of 51.7 kDa (migrates at ~56 kDa, indicated by the arrow). Lanes 1 and 14 are molecular weight markers with kDa values shown on the left of blot. I-con: Buffer control (no pancreatin). SIF alone: Negative control (no test protein).

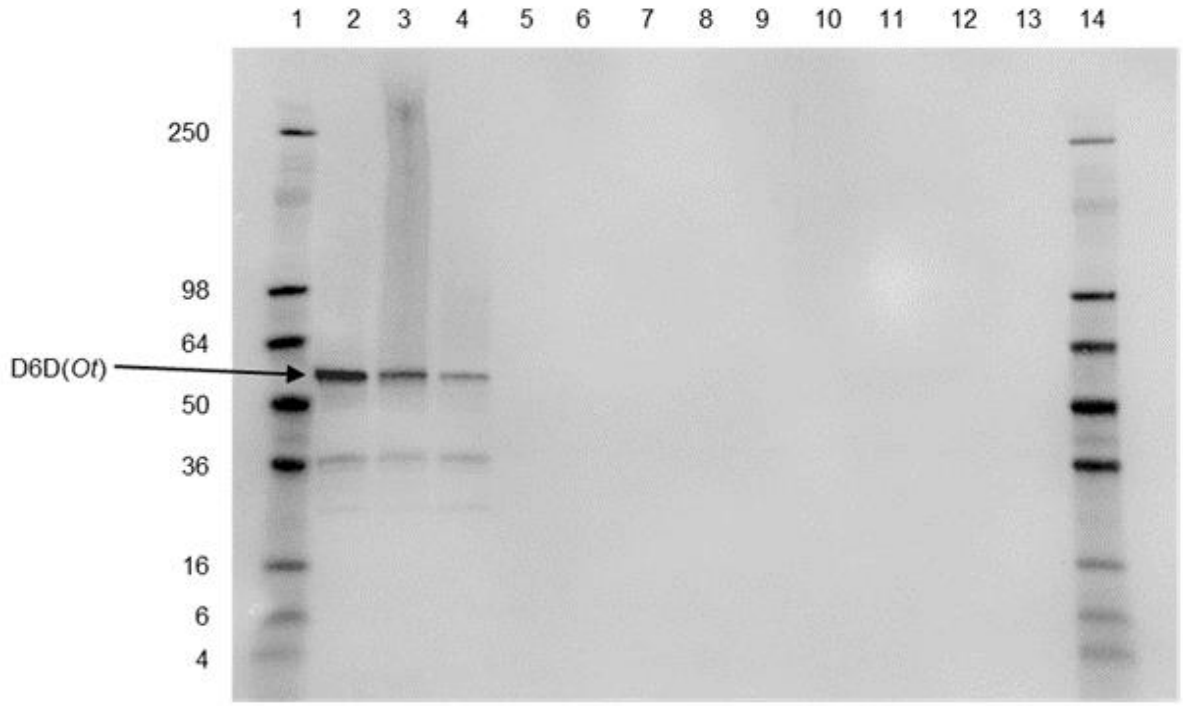

Lane	Sample	Incubation Time (min)
1	molecular weight marker	-
2	I-con	0
3	I-con	60
4	SIF	0
5	SIF	0.5
6	SIF	2
7	SIF	5
8	SIF	10
9	SIF	20
10	SIF	30
11	SIF	60
12	SIF alone	0
13	SIF alone	60
14	molecular weight marker	-

Delta-6 elongase (*Tp*)

Bioinformatic analysis – toxins for delta-6 elongase (Tp)

Bioinformatic analysis was used to determine whether the amino acid sequence of D6E(*Tp*) had significant sequence similarity to known protein toxins or antinutrients. D6E(*Tp*) did not show significant homology to proteins that are toxic to humans (Appendix 19). D6E(*Tp*) did not show significant homology to known antinutrients (OECD, 2002a, b, 2011a, b, 2012, 2016).

Stability to heat of delta-6 elongase (*Tp*)

A heat stability analysis of D6E(*Tp*) was performed to assess the effect of different temperatures on enzyme activity and protein structural integrity. Sample treatment of the D6E(*Tp*) protein was identical to that of D12D(*Ps*) (Appendix 20). The enzyme activity assay cannot distinguish between the individual D6-elongase enzymes D6E(*Tp*) and D6E(*Pp*) in LBFLFK PPP.

The effect of heat treatment on the relative activity of the D6E protein was evaluated using a fatty acid elongase assay (Yilmaz et al., 2017), and the results are presented in Table 24. The relative activity was partially retained (56% and 47%) at 30 °C after 5 min and 20 min. However, the D6E proteins were largely inactivated (< LOQ) at 50°C within 5 min and completely inactivated (< LOD) after longer treatment (20 min). The complete inactivation was also observed for all temperatures tested > 50°C within 5 min.

The effect of heat treatment on the structural integrity of the D6E(*Tp*) protein was evaluated by western blot analysis, and the results are presented in Figure 56. The western blot analysis demonstrated that the LBFLFK sample without heat treatment contained a distinct band with an apparent molecular weight of ~25 kDa, which is in good agreement to the calculated molecular weight of the D6E(*Tp*) protein. A band detected at ~76 kDa in LBFLFK PPP (Figure 56, lanes 3–11) is likely a result of unspecific detection of Bovine Serum Albumin (BSA), as it also detected in both control samples (Figure 56, lanes 1–2). BSA is an assay component and has a calculated molecular weight of 66.4 kDa. While the D6E(*Tp*) band of ~25 kDa was present at most temperatures and times tested, its signal decreased and protein aggregation intensified after 5 min at temperatures ≥ 70°C as indicated by a smear appearing at molecular weights > 250 kDa. This result is typical of proteins subjected to heat, especially for membrane proteins (Nury and Meunier, 1990; Lohner and Esser, 1991; Yan et al., 2004; Lee et al., 2005b; Harris and Booth, 2012; Roman and González Flecha, 2014).

These results show that D6E enzyme activity is lost at ≥ 50°C (Table 24) and undergoes significant structural change in the form of aggregation (Figure 56) at ≥ 70°C within 5 min. These results demonstrate that D6E(*Tp*) protein is heat-labile and the enzymatic activity is unlikely to remain after commercial processing.

Table 24. Relative Enzyme Activity of D6E after Heat Treatment of 5 and 20 Minutes

Protein	30°C		50°C		70°C		90°C	
	5 min	20 min	5 min	20 min	5 min	20 min	5 min	20 min
D6E	56%	47%	< LOQ	< LOD	< LOD	< LOD	< LOD	< LOD

Note: Results are % activity remaining compared to an LBFLFK sample that was not subjected to heat treatment prior to the enzyme activity assay.
LOQ (Limit of Quantitation) = 73.95 CPM; LOD (Limit of Detection) = 49.47 CPM

Figure 56. Western Blot Analysis of the D6E(*Tp*) Protein in LBFLFK after Heat Treatment

The effect of heat treatment on the structural integrity of the D6E(*Tp*) protein was analysed via western blot. The D6E(*Tp*) protein consists of 272 amino acids with a calculated molecular mass of 31.8 kDa (migrates at ~25 kDa).

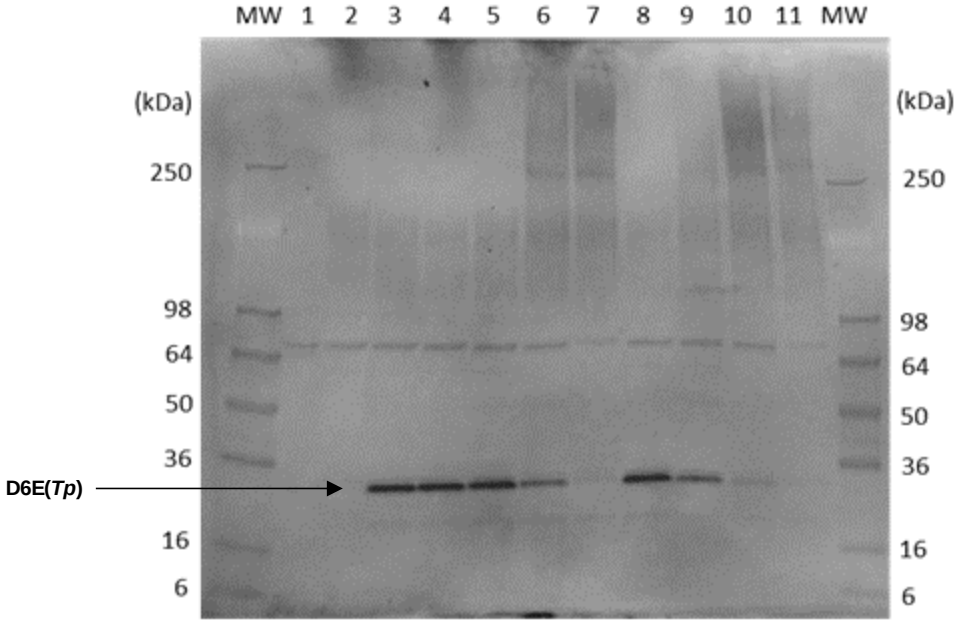

Lane	Sample	Incubation Temperature (°C)	Incubation Time (min)
1	PPP Storage Buffer	0	-
2	Kumily PPP	0	-
3	LBFLFK PPP	0	-
4	LBFLFK PPP	30	5
5	LBFLFK PPP	50	5
6	LBFLFK PPP	70	5
7	LBFLFK PPP	90	5
8	LBFLFK PPP	30	20
9	LBFLFK PPP	50	20
10	LBFLFK PPP	70	20
11	LBFLFK PPP	90	20

Digestive fate (*SGF/SIF*) *for delta-6 elongase* (*Tp*)

The sensitivity of D6E(*Tp*) to SGF and SIF digestion was also assessed. Due to limited digestion by SGF (see this section and Figure 59), a sequential digestion with SGF followed by SIF was performed. The digestibility of the D6E(*Tp*) protein was evaluated by visual analysis of protein degradation in a time course on a western blot with an antibody raised against D6E(*Tp*) N-terminal peptide. Two separate western blots were run to estimate the LOD of the D6E(*Tp*) protein. One of them had the samples treated at 40°C for 30 min to align with the treatment used for SGF digestion samples; the other one had the samples treated at 76°C for 10 min to align with the treatment used for SIF digestion samples. Due to the propensity of D6E(*Tp*) protein to aggregate upon temperature treatment at 76°C and the tendency to degrade at low pH (≤ pH 3.0), samples from the acidic SGF digestion were not visible when treated the same as SIF samples at 76°C. Therefore, the SGF samples were treated at a lower temperature (40°C) to minimise the aggregation as well as the acid degradation of the protein and remain visible (at Time (T) = 0 min) on western blot analysis. The LODs of the D6E(*Tp*) protein for both sample treatments were the same 2.63 ng D6E(*Tp*) corresponding to 176.2 ng LBFLFK PPP. This D6E(*Tp*) amount corresponds to 1.0% and 1.1% of the total D6E(*Tp*) protein loaded in each lane of the SGF and SIF gels, respectively. In the case of sequential digestion (SGF followed by SIF digestion), it corresponds to 1.0% and 0.7% of the total D6E(*Tp*) protein loaded in each lane of the SGF and the following SIF digestion, respectively (Appendix 21).

Following exposure to SGF, western blot analysis demonstrated that a smaller fragment around 16 kDa appeared after 0.5 min of digestion (Figure 57, lane 5). While the bands corresponding to the full-length D6E(*Tp*) protein (~25 kDa) and the degradation fragment (~16 kDa) were present at most of the time points monitored, the signals decreased significantly at the end of the time course (60 min, Figure 57, lanes 5–11). Controls for the SGF assay without pepsin showed only minor change of the D6E(*Tp*) protein over the 60-min time course as deduced from the signal intensities of the bands at ~25 kDa (G-con, Figure 57, lanes 2–3). This result indicates that digestion of the D6E(*Tp*) protein was primarily due to pepsin proteolytic activity and not instability of the D6E(*Tp*) protein in the test system. As expected, controls with pepsin but without D6E(*Tp*) protein (SGF alone, Figure 57, lanes 12 and 13) showed no unspecific detection of pepsin by the D6E(*Tp*)-specific antibody, which would be expected to result in a black band at ~50 kDa.

Following exposure to SIF, western blot analysis demonstrated that the intensity of a ~25 kDa band in good agreement with the calculated molecular weight of the full-length D6E(*Tp*) protein dropped below the D6E(*Tp*) LOD within 0.5 min (Figure 58, lane 5). This result indicates ≥ 98.9% digestion of the full-length D6E(*Tp*) protein within 0.5 min with SIF. Furthermore, three smaller fragments around 20, 16, and 6 kDa appeared after 0.5 min of digestion (Figure 58, lane 5) and were digested in SIF pancreatin within 20 min (Figure 58, lane 9). Controls for the SIF assay without pancreatin showed only minor change of the D6E(*Tp*) protein over the 60-min time course as deduced from the signal intensities of the bands at ~25 kDa (I-con, Figure 58, lanes 2–3). This result indicates that digestion of the D6E(*Tp*) protein was primarily due to pancreatin proteolytic activity and not instability of the D6E(*Tp*) protein in the test system. As found for the D6E(*Tp*) SGF assay, controls with pancreatin but without D6E(*Tp*) protein (SIF alone, Figure 58, lanes 12 and 13) showed no unspecific detection of pancreatin by the D6E(*Tp*)-specific antibody, which would be expected to result in a black band(s) between 4 and 64 kDa.

Digestibility of D6E(*Tp*) was assessed in sequential digestion of SGF followed by SIF (Figure 59). Also, in this experiment, the D6E(*Tp*) protein remained detectable after 30 min incubation with SGF (Figure 59, lanes 6–8) but was degraded rapidly within 0.5 min upon incubation with SIF (Figure 59, lanes 9–10). This result indicates ≥ 99.3% digestion of the full-length D6E(*Tp*) protein with 30 min SGF digestion followed by 0.5 min SIF digestion. Controls in this assessment were consistent with the stand-alone SGF and SIF assessments shown above.

This result suggests that the D6E(*Tp*) protein is integrated into the membrane such that its potential protease cleavage sites are not immediately accessible to pepsin in SGF. The lipases present in SIF may potentially break down the lipid membranes making the D6E(*Tp*) protein accessible to proteases for digestion. A similar result was obtained with D5E(*Ot*) protein, suggesting that these two elongases share similar susceptibilities to SGF/SIF digestion. Based on the above results, the D6E(*Tp*) is susceptible to digestion when subjected to sequential digestion in SGF followed by SIF.

Figure 57. Western Blot Analysis of the D6E(*Tp*) Protein in LBFLFK Subjected to SGF

A western blot used to analyse the digestibility of the D6E(*Tp*) protein with SGF. In each lane, 18.35 µg of LBFLFK PPP was loaded, which corresponds to 274 ng D6E(*Tp*) protein (LOD = 2.63 ng D6E(*Tp*)). The samples were treated at 40°C (temperature used for SGF) prior to being loaded on a gel. The D6E(*Tp*) protein consists of 272 amino acids with a calculated molecular mass of 31.8 kDa (migrates at ~25 kDa, indicated by the arrow). Lanes 1 and 14 are molecular weight markers with kDa values shown on the left. G-con: Buffer control (no pepsin). SGF alone: Negative control (no test protein).

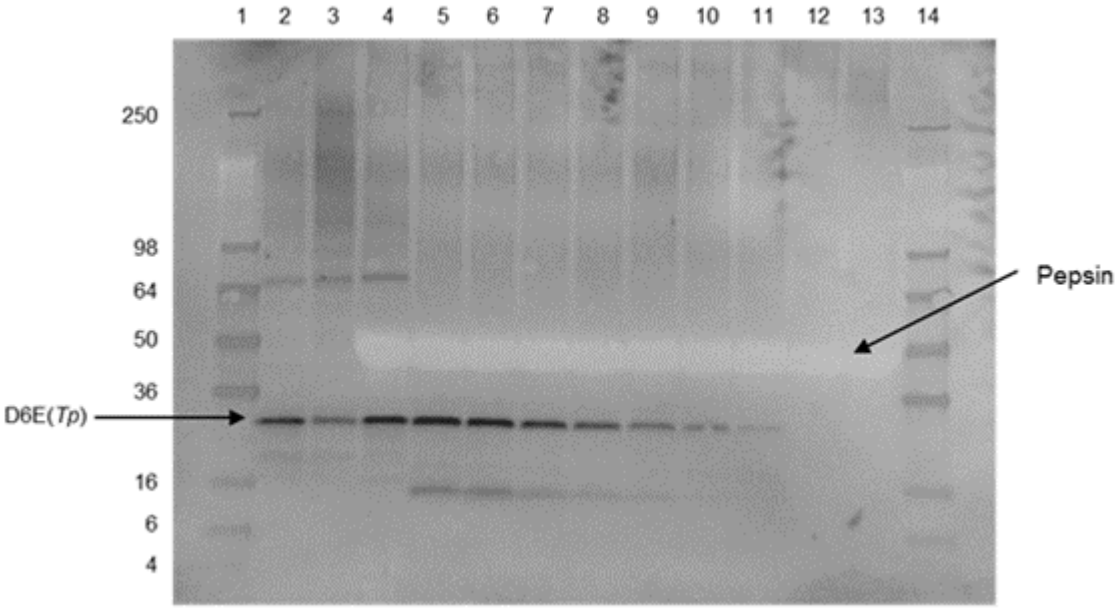

Lane	Sample	Incubation Time (min)
1	molecular weight marker	-
2	G-con	0
3	G-con	60
4	SGF	0
5	SGF	0.5
6	SGF	2
7	SGF	5
8	SGF	10
9	SGF	20
10	SGF	30
11	SGF	60
12	SGF alone	0
13	SGF alone	60
14	molecular weight marker	-

Figure 58. Western Blot Analysis of the D6E(*Tp*) Protein in LBFLFK Subjected to SIF

A western blot used to analyse the digestibility of the D6E(*Tp*) protein with SIF. In each lane, 16.52 µg of LBFLFK PPP was loaded, which corresponds to 247 ng D6E(*Tp*) protein (LOD = 2.63 ng D6E(*Tp*)). The samples were treated at 76°C (temperature used for SIF) prior to being loaded on a gel. The D6E(*Tp*) protein consists of 272 amino acids with a calculated molecular mass of 31.8 kDa (migrates at ~25 kDa, indicated by the arrow). Lanes 1 and 14 are molecular weight markers with kDa values shown on the left of blot. I-con: Buffer control (no pancreatin). SIF alone: Negative control (no test protein).

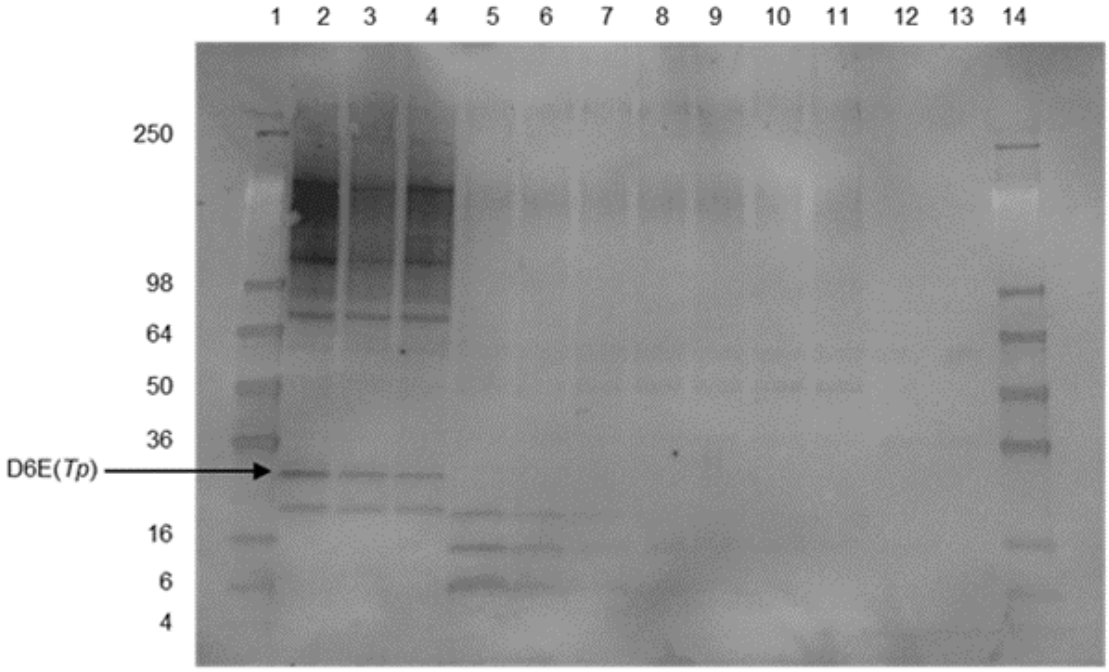

Lane	Sample	Incubation Time (min)
1	molecular weight marker	-
2	I-con	0
3	I-con	60
4	SIF	0
5	SIF	0.5
6	SIF	2
7	SIF	5
8	SIF	10
9	SIF	20
10	SIF	30
11	SIF	60
12	SIF alone	0
13	SIF alone	60
14	molecular weight marker	-

Figure 59. Western Blot Analysis of the D6E(*Tp*) Protein in LBFLFK Subjected to Sequential Digestion of SGF followed by SIF

A western blot used to analyse the digestibility of the D6E(*Tp*) protein with sequential digestion of SGF followed by SIF. In each lane of SGF, 18.35 µg of LBFLFK PPP was loaded, which corresponds to 274 ng D6E(*Tp*) protein (LOD = 2.63 ng D6E(*Tp*)). In each lane of SIF, 24.77 µg of LBFLFK PPP was loaded, which corresponds to 370 ng D6E(*Tp*) protein. The D6E(*Tp*) protein consists of 272 amino acids with a calculated molecular mass of 31.8 kDa (migrates at ~25 kDa, indicated by the arrow). Lanes 1 and 15 are molecular weight markers with kDa values shown on the left of blot. SD G-con: SGF buffer control (no pepsin). SD I-con: SIF buffer control (no pancreatin). SD SGF alone: SGF negative control (contains pepsin but contains no test protein). SD SIF alone: SIF negative control (contains pancreatin but contains no test protein).

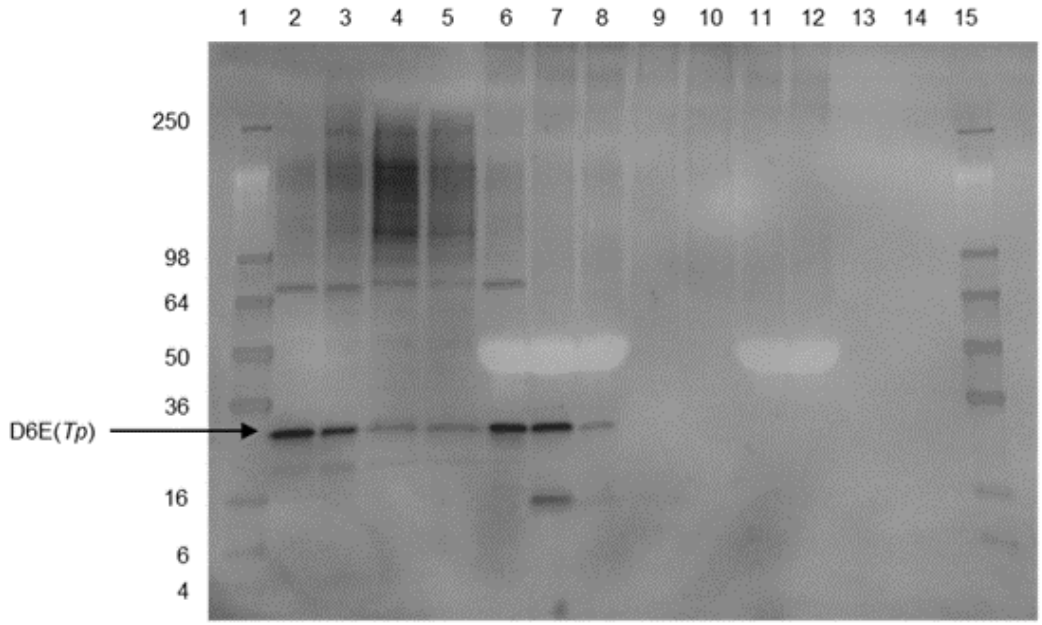

Lane	Sample	Incubation Time (min)	Incubation Temperature (°C)
1	molecular weight marker	-	-
2	SD G-con	0.5	40
3	SD G-con	30	40
4	SD I-con	0.5	76
5	SD I-con	30	76
6	SD SGF	0	40
7	SD SGF	0.5	40
8	SD SGF	30	40
9	SD SGF → SIF	0.5	76
10	SD SGF → SIF	30	76
11	SD SGF alone	0.5	40
12	SD SGF alone	30	40
13	SD SIF alone	0.5	76
14	SD SIF alone	30	76
15	molecular weight marker	-	-

Delta-6 elongase (*Pp*)

Bioinformatic analysis – toxins for delta-6 elongase (Pp)

Bioinformatic analysis was used to determine whether the amino acid sequence of D6E(*Pp*) had significant sequence similarity to known protein toxins or antinutrients. D6E(*Pp*) did not show significant homology to proteins that are toxic to humans (Appendix 19). D6E(*Pp*) did not show significant homology to known antinutrients (OECD, 2002a, b, 2011a, b, 2012, 2016).

Stability to heat of delta-6 elongase (*Pp*)

A heat stability analysis of D6E(*Pp*) was performed to assess the effect of different temperatures on enzyme activity. Sample treatment of the D6E(*Pp*) protein was identical to that of D12D(*Ps*) (Appendix 20). The effect of heat treatment on the relative activity of the D6E proteins was evaluated using a fatty acid elongase assay (Yilmaz et al., 2017). The results are the same as shown for the D6E(*Tp*) protein and presented in Table 24 as the elongase assay does not distinguish between the individual delta-6 elongase enzymes D6E(*Tp*) and D6E(*Pp*) in LBFLFK PPP. For LOD and LOQ of delta-6 elongase enzyme activity, see Appendix 20. The D6E(*Pp*) protein was not assessed for structural integrity upon heat treatment because the D6E(*Pp*) protein was not detected in LBFLFK PPP and LBFLFK tissues. The low amount of D6E(*Pp*) protein is unlikely to present a safety concern to humans or animals.

Digestive fate (*SGF/SIF*) *for delta-6 elongase* (*Pp*)

The D6E(*Pp*) protein was not assessed for digestibility in SGF or SIF because the D6E(*Pp*) protein was not detected in LBFLFK PPP and LBFLFK tissues. The low amount of D6E(*Pp*) protein is unlikely to present a safety concern to humans or animals.

Delta-5 desaturase (*Tc*)

Bioinformatic analysis – toxins for delta-5 desaturase (Tc)

Bioinformatic analysis was used to determine whether the amino acid sequence of D5D(*Tc*) had significant sequence similarity to known protein toxins or antinutrients. D5D(*Tc*) did not show significant homology to proteins that are toxic to humans (Appendix 19). D5D(*Tc*) did not show significant homology to known antinutrients (OECD, 2002a, b, 2011a, b, 2012, 2016).

Stability to heat of delta-5 desaturase (*Tc*)

A heat stability analysis of D5D(*Tc*) was performed to assess the effect of different temperatures on protein structural integrity. The enzyme activity of D5D(*Tc*) in response to heat treatment was not assessed because enzyme activity was not detectable in LBFLFK PPP. Sample treatment of the D5D(*Tc*) protein was identical to that of D12D(*Ps*) (see Appendix 20).

The effect of heat treatment on the structural integrity of the D5D(*Tc*) protein was evaluated by western blot analysis, and the results are presented in Figure 60. The western blot analysis demonstrated that the LBFLFK sample without heat treatment contained a distinct band with an apparent molecular weight of ~50 kDa, which is in good agreement with the calculated molecular weight of the D5D(*Tc*) protein (Figure 60, lane 3). While the band corresponding to D5D(*Tc*) (~50 kDa) was present at all temperatures and times tested, its signal decreased and

protein aggregation intensified after 20 min at temperatures ≥ 50°C as indicated by a smear appearing at molecular weights > 50 kDa. This result is typical of proteins subjected to heat, especially for membrane proteins (Nury and Meunier, 1990; Lohner and Esser, 1991; Yan et al., 2004; Lee et al., 2005b; Harris and Booth, 2012; Roman and González Flecha, 2014). There is a small amount of non-specific cross-reactivity to a protein in the Kumily control (Figure 60, lane 2) that runs at approximately the same weight as the D5D(*Tc*) protein. Finally, no cross-reaction was found with the PPP storage buffer (Figure 60, lane 1).

These results show that D5D(*Tc*) undergoes structural change in the form of aggregation (Figure 60) within 20 min at ≥ 50°C. These results demonstrate that D5D(*Tc*) protein is heat-labile and not likely to remain intact after commercial processing.

Figure 60. Western Blot Analysis of the D5D(*Tc*) Protein in LBFLFK after Heat Treatment

The effect of heat treatment on the structural integrity of the D5D(*Tc*) protein was analysed via western blot. The D5D(*Tc*) protein consists of 439 amino acids with a calculated molecular mass of 48.8 kDa (migrates at ~50 kDa).

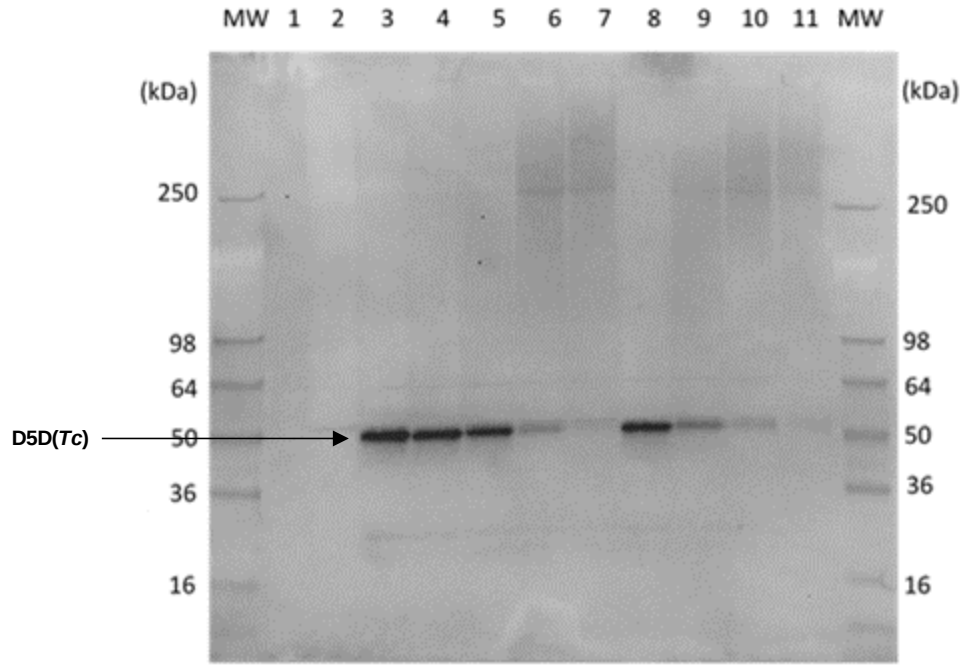

Lane	Sample	Incubation Temperature (°C)	Incubation Time (min)
1	PPP Storage Buffer	0	-
2	Kumily PPP	0	-
3	LBFLFK PPP	0	-
4	LBFLFK PPP	30	5
5	LBFLFK PPP	50	5
6	LBFLFK PPP	70	5
7	LBFLFK PPP	90	5
8	LBFLFK PPP	30	20
9	LBFLFK PPP	50	20
10	LBFLFK PPP	70	20
11	LBFLFK PPP	90	20

Digestive fate (*SGF/SIF*) *for delta-5 desaturase* (*Tc*)

The sensitivity of D5D(*Tc*) to SGF and SIF digestion was also assessed. The digestibility of the D5D(*Tc*) protein was evaluated by visual analysis of protein degradation in a time course on a western blot with an antibody raised against D5D(*Tc*) full-length protein. A separate western blot was run to estimate the LOD of the D5D(*Tc*) protein. The LOD of the D5D(*Tc*) protein was 0.139 ng D5D(*Tc*), corresponding to 900 ng LBFLFK PPP. This D5D(*Tc*) amount corresponds to 9.6% and 10.6% of the total D5D(*Tc*) protein loaded in each lane of the SGF and SIF gels, respectively (Appendix 21).

Following exposure to SGF, western blot analysis demonstrated that the intensity of a ~50 kDa band in good agreement with the calculated molecular weight of the full-length D5D(*Tc*) protein dropped below the D5D(*Tc*) LOD within 0.5 min (Figure 61, lane 5). This result indicates ≥ 90.4% digestion of the full-length D5D(*Tc*) protein within 0.5 min with SGF. Controls for the SGF assay without pepsin showed no change over the 60-min time course as deduced from the signal intensities of the bands at ~50 kDa (G-con, Figure 61, lanes 2–3). This indicates that digestion of the D5D(*Tc*) protein was primarily due to pepsin proteolytic activity and not instability of the D5D(*Tc*) protein in the test system. As expected, controls with pepsin but without D5D(*Tc*) protein (SGF alone, Figure 61, lanes 12 and 13) showed no unspecific detection of pepsin by the D5D(*Tc*)-specific antibody, which would be expected to result in a black band at ~50 kDa.

Following exposure to SIF, western blot analysis demonstrated that the intensity of a ~50 kDa band in good agreement with the calculated molecular weight of the full-length D5D(*Tc*) protein dropped below the D5D(*Tc*) LOD within 0.5 min (Figure 62, lane 5). This result indicates ≥ 89.4% digestion of the full-length D5D(*Tc*) protein within 0.5 min with SIF. Controls for the SIF assay without pancreatin showed a minor signal decrease in the D5D(*Tc*) protein over the 60-min time course (I-con, Figure 62, lanes 2–3), which indicates that digestion of the D5D(*Tc*) protein was largely due to pancreatin proteolytic activity and not instability of the D5D(*Tc*) protein in the test system. As found for the D5D(*Tc*) SGF assay, controls with pancreatin but without D5D(*Tc*) protein (SIF alone, Figure 62, lanes 12 and 13) showed no unspecific detection of pancreatin by the D5D(*Tc*)-specific antibody, which would be expected to result in a black band(s) between 4 and 64 kDa.

These results demonstrate that the D5D(*Tc*) is susceptible to digestion and rapidly degraded in SGF and SIF.

Figure 61. Western Blot Analysis of the D5D(*Tc*) Protein in LBFLFK Subjected to SGF

A western blot used to analyse the digestibility of the D5D(*Tc*) protein with SGF. In each lane, 9.38 µg of LBFLFK PPP were loaded, which corresponds to 1.45 ng D5D(*Tc*) protein (LOD = 0.139 ng D5D(*Tc*)). The D5D(*Tc*) protein consists of 439 amino acids with a calculated molecular mass of 48.8 kDa (migrates at ~50 kDa, indicated by the arrow). Lanes 1 and 14 are molecular weight markers with kDa values shown on the left. G-con: Buffer control (no pepsin). SGF alone: Negative control (no test protein).

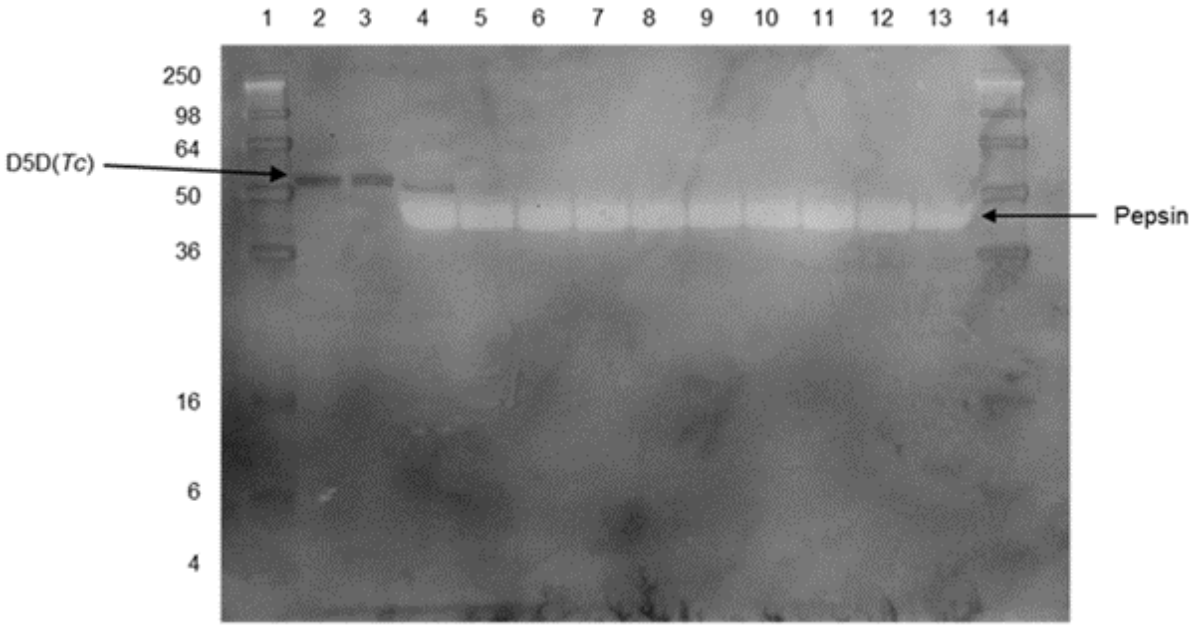

Lane	Sample	Incubation Time (min)
1	molecular weight marker	-
2	G-con	0
3	G-con	60
4	SGF	0
5	SGF	0.5
6	SGF	2
7	SGF	5
8	SGF	10
9	SGF	20
10	SGF	30
11	SGF	60
12	SGF alone	0
13	SGF alone	60
14	molecular weight marker	-

Figure 62. Western Blot Analysis of the D5D(*Tc*) Protein in LBFLFK Subjected to SIF

A western blot used to analyse the digestibility of the D5D(*Tc*) protein with SIF. In each lane, 8.44 µg of LBFLFK PPP were loaded, which corresponds to 1.31 ng D5D(*Tc*) protein (LOD = 0.139 ng D5D(*Tc*)). The D5D(*Tc*) protein consists of 439 amino acids with a calculated molecular mass of 48.8 kDa (migrates at ~50 kDa, indicated by the arrow). Lanes 1 and 14 are molecular weight markers with kDa values shown on the left of blot. I-con: Buffer control (no pancreatin). SIF alone: Negative control (no test protein).

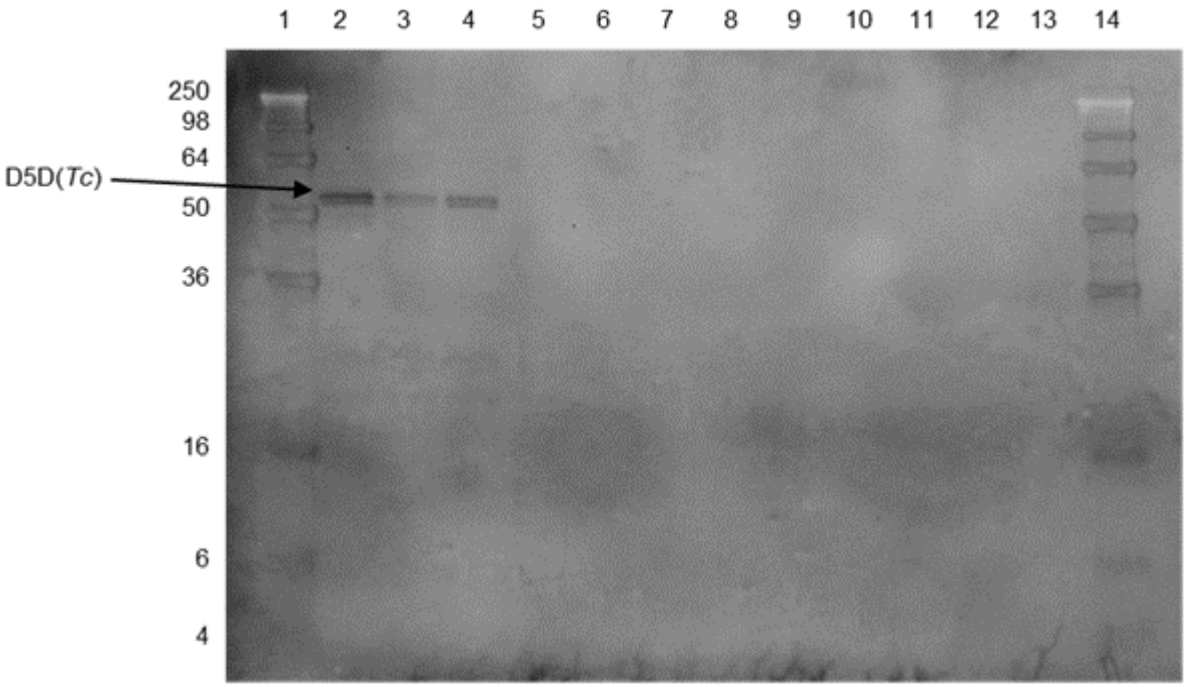

Lane	Sample	Incubation Time (min)
1	molecular weight marker	-
2	I-con	0
3	I-con	60
4	SIF	0
5	SIF	0.5
6	SIF	2
7	SIF	5
8	SIF	10
9	SIF	20
10	SIF	30
11	SIF	60
12	SIF alone	0
13	SIF alone	60
14	molecular weight marker	-

Omega-3 desaturase (*Pir*)

Bioinformatic analysis – toxins for omega-3 desaturase (*Pir*)

Bioinformatic analysis was used to determine whether the amino acid sequence of O3D (*Pir*) had significant sequence similarity to known protein toxins or antinutrients. O3D(*Pir*) did not show significant homology to proteins that are toxic to humans (Appendix 19). O3D(*Pir*) did not show significant homology to known antinutrients (OECD, 2002a, b, 2011a, b, 2012, 2016).

Stability to heat of omega-3 desaturase (*Pir*)

A heat stability analysis of O3D(*Pir*) was performed to assess the effects of different temperatures on protein structural integrity. The enzyme activity of O3D(*Pir*) in response to heat treatment was not assessed because O3D enzyme activity was not detectable in LBFLFK PPP. Sample treatment of the O3D(*Pir*) protein was identical to that of D12D(*Ps*) (Appendix 20).

The effect of heat treatment on the structural integrity of the O3D(*Pir*) protein was evaluated by western blot analysis, and the results are presented in Figure 63. The western blot analysis demonstrated that the LBFLFK sample without heat treatment contained a distinct band with an apparent molecular weight of ~38 kDa, which is in good agreement with the calculated molecular weight of the O3D(*Pir*) protein (Figure 63, lane 3). Bands detected at ~28 kDa and ~20 kDa are likely degradation fragments of the O3D(*Pir*) protein. While the band corresponding to O3D(*Pir*) (~38 kDa) was present at all temperatures and times tested, its signal decreased and protein aggregation intensified after 5 min at temperatures ≥ 50°C as indicated by a smear appearing at molecular weights > 38 kDa (Figure 63, lanes 4–11). This result is typical of proteins subjected to heat, especially for membrane proteins (Nury and Meunier, 1990; Lohner and Esser, 1991; Yan et al., 2004; Lee et al., 2005b; Harris and Booth, 2012; Roman and González Flecha, 2014). Finally, no cross-reaction was found with the PPP storage buffer and Kumily sample in Figure 63, lanes 1 and 2, respectively.

The results show that O3D(*Pir*) undergoes structural change in the form of aggregation, (Figure 63) within 5 min at ≥ 50°C. These results demonstrate that O3D(*Pir*) protein is heat-labile and not likely to remain intact after commercial processing.

Figure 63. Western Blot Analysis of the O3D(*Pir*) Protein in LBFLFK after Heat Treatment

The effect of heat treatment on the structural integrity of the O3D(*Pir*) protein was analysed via western blot. The O3D(*Pir*) protein consists of 363 amino acids with a calculated molecular mass of 40.4 kDa (migrates at ~38 kDa).

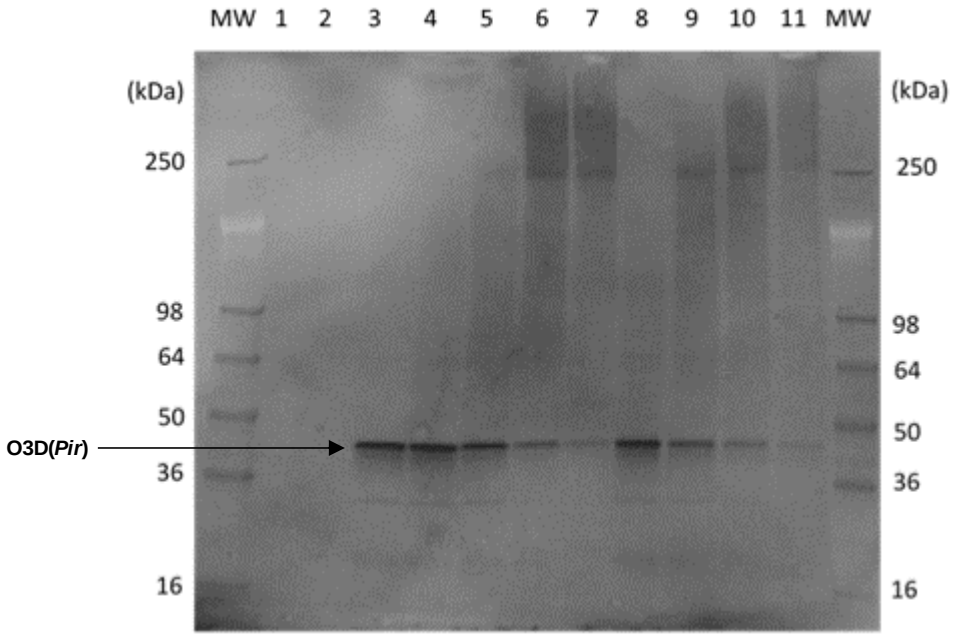

Lane	Sample	Incubation Temperature (°C)	Incubation Time (min)
1	PPP Storage Buffer	0	-
2	Kumily PPP	0	-
3	LBFLFK PPP	0	-
4	LBFLFK PPP	30	5
5	LBFLFK PPP	50	5
6	LBFLFK PPP	70	5
7	LBFLFK PPP	90	5
8	LBFLFK PPP	30	20
9	LBFLFK PPP	50	20
10	LBFLFK PPP	70	20
11	LBFLFK PPP	90	20

Digestive fate (*SGF/SIF*) *for omega-3 desaturase* (*Pir*)

The sensitivity of O3D(*Pir*) to SGF and SIF digestion was also assessed. The digestibility of the O3D(*Pir*) protein was evaluated by visual analysis of protein degradation in a time course on a western blot with an antibody raised against O3D(*Pir*) NC fusion protein. A separate western blot was run to estimate the LOD of the O3D(*Pir*) protein. The LOD of the O3D(*Pir*) protein was 1.423 ng O3D(*Pir*), corresponding to 400 ng LBFLFK PPP. This O3D(*Pir*) amount corresponds to 3.2% and 3.6% of the total O3D(*Pir*) protein loaded in each lane of the SGF and SIF gels, respectively (see Figure 64).

Following exposure to SGF, western blot analysis demonstrated that the intensity of a ~38 kDa band in good agreement with the calculated molecular weight of the full-length O3D(*Pir*)

protein dropped below the O3D(*Pir*) LOD within 0.5 min (Figure 64, lane 5). This result indicates ≥ 96.8% digestion of the full-length O3D(*Pir*) protein within 0.5 min with SGF. A degradation fragment that migrates at ~15 kDa was generated within 0.5 min digestion (Figure 64, lane 5) and gradually disappeared within 30 min (lane 10). Controls for the SGF assay without pepsin showed only minor change of the O3D(*Pir*) protein over the 60-min time course as deduced from the signal intensities of the bands at ~38 kDa (G-con, Figure 64, lanes 2–3). This result indicates that digestion of the O3D(*Pir*) protein was primarily due to pepsin proteolytic activity and not instability of the O3D(*Pir*) protein in the test system. As expected, controls with pepsin but without O3D(*Pir*) protein (SGF alone, Figure 64, lanes 12 and 13) showed no unspecific detection of pepsin by the O3D(*Pir*)-specific antibody, which would be expected to result in a black band at ~50 kDa.

Following exposure to SIF, western blot analysis demonstrated that the intensity of a ~38 kDa band in good agreement with the calculated molecular weight of the full-length O3D(*Pir*) protein dropped below the O3D(*Pir*) LOD within 0.5 min (Figure 65, lane 5). This result indicates ≥ 96.4% digestion of the full-length O3D(*Pir*) protein within 0.5 min with SIF. The band migrating at ~20 kDa, which are likely to represent a fragment of the O3D(*Pir*), was also digested within 0.5 min. Controls for the SIF assay without pancreatin showed minor change of the O3D(*Pir*) protein over the 60-min time course as deduced from the signal intensities of the bands at ~38 kDa (I-con, Figure 65, lanes 2 to 3). This result indicates that digestion of the O3D(*Pir*) protein was primarily due to pancreatin proteolytic activity and not instability of the O3D(*Pir*) protein in the test system. As found for the O3D(*Pir*) SGF assay, controls with pancreatin but without O3D(*Pir*) protein (SIF alone, Figure 65, lanes 12 and 13) showed no unspecific detection of pancreatin by the O3D(*Pir*)-specific antibody, which would be expected to result in a black band(s) between 4 and 64 kDa.

These results demonstrate that the O3D(*Pir*) is susceptible to digestion and rapidly degraded in SGF and SIF.

Figure 64. Western Blot Analysis of the O3D(*Pir*) Protein in LBFLFK Subjected to SGF

A western blot used to analyse the digestibility of the O3D(*Pir*) protein with SGF. In each lane, 12.5 µg of LBFLFK PPP were loaded, which corresponds to 44.47 ng O3D(*Pir*) protein (LOD = 1.423 ng O3D(*Pir*)). The O3D(*Pir*) protein consists of 363 amino acids with a calculated molecular mass of 40.4 kDa (migrates at ~38 kDa, indicated by the arrow). Lanes 1 and 14 are molecular weight markers with kDa values shown on the left. G-con: Buffer control (no pepsin). SGF alone: Negative control (no test protein).

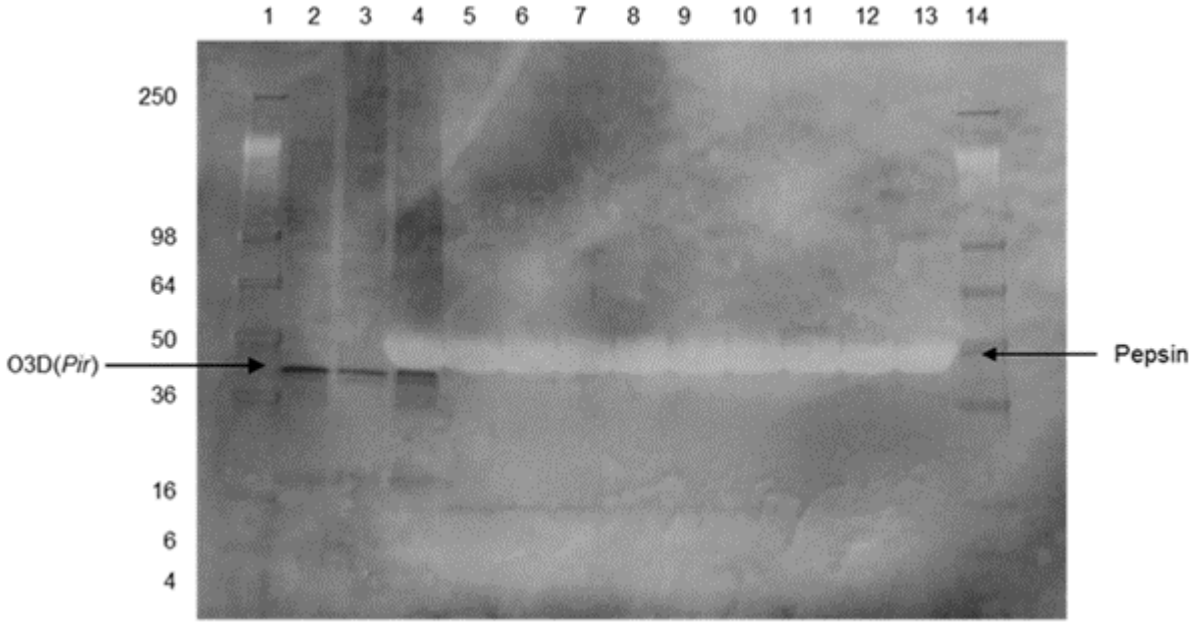

Lane	Sample	Incubation Time (min)
1	molecular weight marker	-
2	G-con	0
3	G-con	60
4	SGF	0
5	SGF	0.5
6	SGF	2
7	SGF	5
8	SGF	10
9	SGF	20
10	SGF	30
11	SGF	60
12	SGF alone	0
13	SGF alone	60
14	molecular weight marker	-

Figure 65. Western Blot Analysis of the O3D(*Pir*) Protein in LBFLFK Subjected to SIF

A western blot used to analyse the digestibility of the O3D(*Pir*) protein with SIF. In each lane, 11.25 µg of LBFLFK PPP were loaded, which corresponds to 40.02 ng O3D(*Pir*) protein (LOD = 1.423 ng O3D(*Pir*)). The O3D(*Pir*) protein consists of 363 amino acids with a calculated molecular mass of 40.4 kDa (migrates at ~38 kDa, indicated by the arrow). Lanes 1 and 14 are molecular weight markers with kDa values shown on the left of blot. I-con: Buffer control (no pancreatin). SIF alone: Negative control (no test protein).

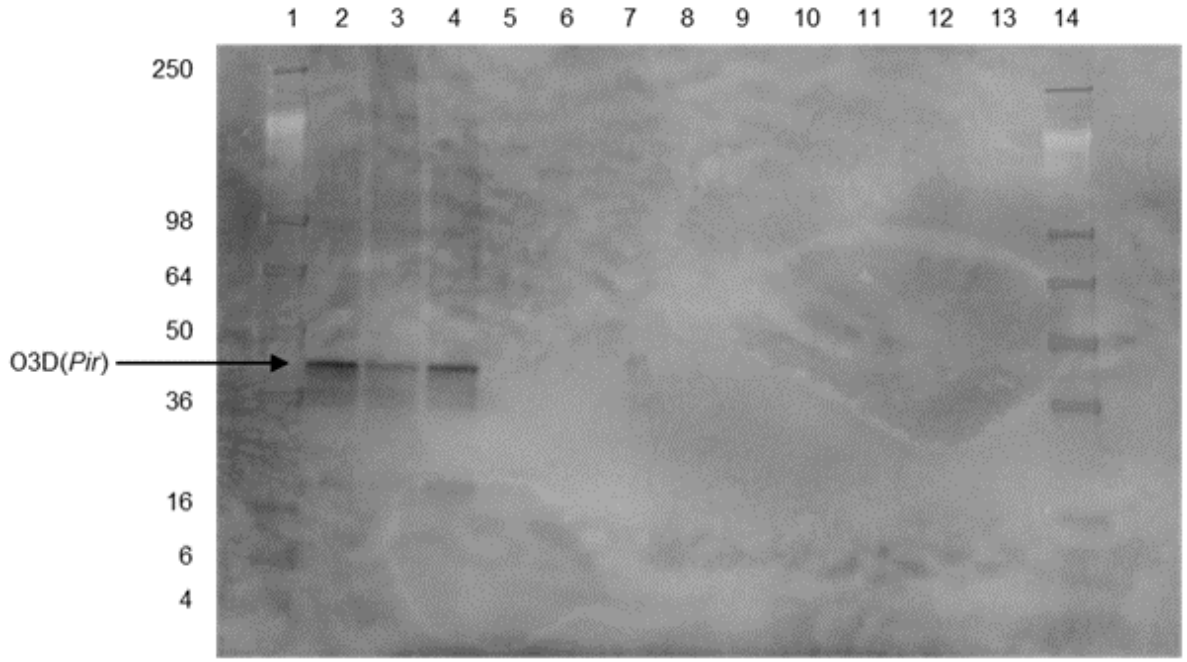

Lane	Sample	Incubation Time (min)
1	molecular weight marker	-
2	I-con	0
3	I-con	60
4	SIF	0
5	SIF	0.5
6	SIF	2
7	SIF	5
8	SIF	10
9	SIF	20
10	SIF	30
11	SIF	60
12	SIF alone	0
13	SIF alone	60
14	molecular weight marker	-

Omega-3 desaturase (*Pi*)

Bioinformatic analysis – toxins for omega-3 desaturase (Pi)

Bioinformatic analysis was used to determine whether the amino acid sequence of O3D(*Pi*) had significant sequence similarity to known protein toxins or antinutrients. O3D(*Pi*) did not show significant homology to proteins that are toxic to humans (Appendix 19). O3D(*Pi*) did not show significant homology to known antinutrients (OECD, 2002a, b, 2011a, b, 2012, 2016).

Stability to heat of omega-3 desaturase (*Pi*)

The enzyme activity of O3D(*Pi*) in response to heat treatment was not assessed because O3D enzyme activity was not detectable in LBFLFK PPP. The O3D(*Pi*) protein was also not assessed for structural integrity following heat treatment because the O3D(*Pi*) protein was not detected in LBFLFK PPP and LBFLFK tissues. The low amount of O3D(*Pi*) protein is unlikely to present a safety concern to humans or animals.

Digestive fate (*SGF/SIF*) *for omega-3 desaturase* (*Pi*)

The O3D(*Pi*) protein was not assessed for digestibility in SGF or SIF because the O3D(*Pi*) protein was not detected in LBFLFK PPP and LBFLFK tissues. The low amount of O3D(*Pi*) protein is unlikely to present a safety concern to humans or animals.

Delta-5 elongase (*Ot*)

Bioinformatic analysis – toxins for delta-5 elongase (*Ot*)

Bioinformatic analysis was used to determine whether the amino acid sequence of D5E(*Ot*) had significant sequence similarity to known protein toxins or antinutrients. D5E(*Ot*) did not show significant homology to proteins that are toxic to humans (Appendix 19). D5E(*Ot*) did not show significant homology to known antinutrients (OECD, 2002a, b, 2011a, b, 2012, 2016).

Stability to heat of delta-5 elongase (*Ot*)

A heat stability analysis of D5E(*Ot*) was performed to assess the effect of different temperatures on enzyme activity and protein structural integrity. Sample treatment of the D5E(*Ot*) protein was identical to that of D12D(*Ps*) (Appendix 20).

The effect of heat treatment on the relative activity of the D5E(*Ot*) protein was evaluated using a fatty acid elongase assay (Yilmaz et al., 2017), and the results are presented in Table 25. The relative activity was partially retained (64% and 25%) at 30°C after 5 min and 20 min. However, the D5E(*Ot*) protein was inactivated to < LOQ at 50°C within 5 min and completely inactivated to < LOD after longer treatment (20 min).

The effect of heat treatment on the structural integrity of the D5E(*Ot*) protein was evaluated by western blot analysis, and the results are presented in Figure 66. The western blot analysis demonstrated that the LBFLFK sample without heat treatment contained a distinct band with an apparent molecular weight of ~31 kDa, which is in good agreement with the calculated molecular weight of the D5E(*Ot*) protein, along with a non-specific cross-reaction band at ~50 kDa (Figure 66, lane 3). Aggregation was detected at temperatures ≥ 50°C as a smear and was exacerbated with increasing time and temperature. At the same time, the signal intensity of the bands at ~31 kDa, representing the monomeric full-length D5E(*Ot*), decreased

after 20 min at temperatures ≥ 50°C. This result is typical of proteins subjected to heat, especially for membrane proteins (Nury and Meunier, 1990; Lohner and Esser, 1991; Yan et al., 2004; Lee et al., 2005b; Harris and Booth, 2012; Roman and González Flecha, 2014) . The non-specific cross-reaction band was shown in all samples (~50 kDa, Figure 66, lanes 2–11) except the PPP storage buffer (Figure 66, lane 1), suggesting that the cross-reaction protein was from PPP.

These results show that D5E(*Ot*) loses enzyme activity (Table 25) and undergoes structural change in the form of aggregation (Figure 66) at ≥ 50°C. These results demonstrate that D5E(*Ot*) protein is heat-labile and not likely to remain intact or functional after commercial processing.

Table 25. Relative Enzyme Activity of D5E(*Ot*) after Heat Treatment of 5 and 20 Minutes

	30°C		50°C		70°C		90°C	
Protein	**5 min**	**20 min**	**5 min**	**20 min**	**5 min**	**20 min**	**5 min**	**20 min**
D5E(*Ot*)	64%	25%	< LOQ	< LOD	< LOD	< LOD	< LOD	< LOQ

Note: Results are % activity remaining compared to an LBFLFK sample that was not subjected to heat treatment prior to the enzyme activity assay.
LOQ (Limit of Quantitation) = 66.90 CPM
LOD (Limit of Detection) = 47.00 CPM

Figure 66. Western Blot Analysis of the D5E(*Ot*) Protein in LBFLFK after Heat Treatment

The effect of heat treatment on the structural integrity of the D5E(*Ot*) protein was analysed via western blot. The D5E(*Ot*) protein consists of 300 amino acids with a calculated molecular mass of 34.2 kDa (migrates at ~31 kDa).

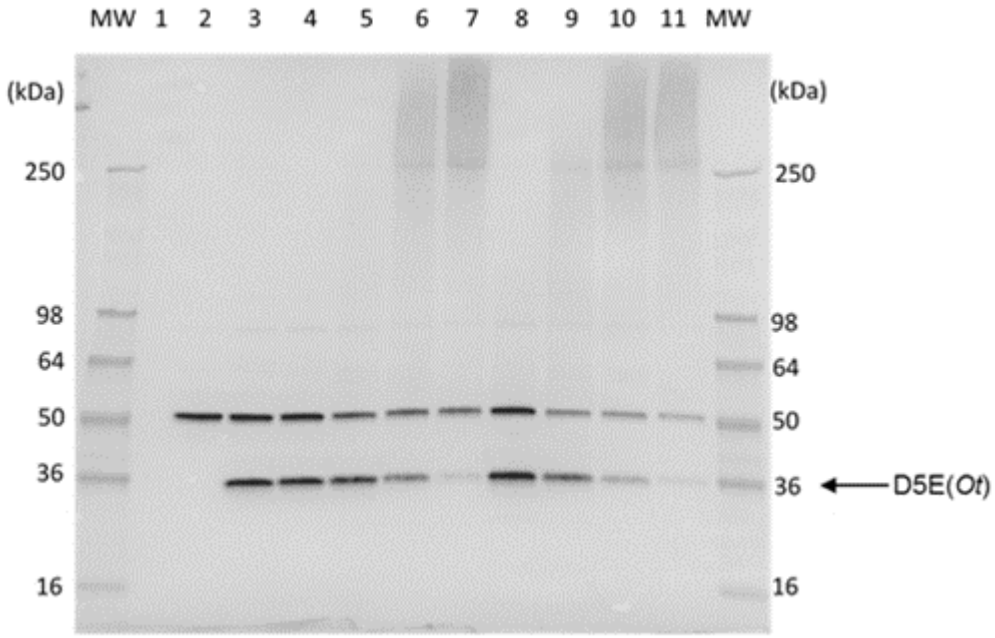

Lane	Sample	Incubation Temperature (°C)	Incubation Time (min)
1	PPP Storage buffer	0	-
2	Kumily PPP	0	-
3	LBFLFK PPP	0	-
4	LBFLFK PPP	30	5
5	LBFLFK PPP	50	5
6	LBFLFK PPP	70	5
7	LBFLFK PPP	90	5
8	LBFLFK PPP	30	20
9	LBFLFK PPP	50	20
10	LBFLFK PPP	70	20
11	LBFLFK PPP	90	20

Digestive fate (*SGF/SIF*) *for delta-5 elongase* (*Ot*)

The sensitivity of D5E(*Ot*) to SGF and SIF digestion was also assessed. Due to limited digestion by SGF (see below and Figure 69), a sequential digestion with SGF followed by SIF was performed. The digestibility of the D5E(*Ot*) protein was evaluated by visual analysis of protein degradation in a time course on a western blot with an antibody raised against D5E(*Ot*) NC fusion protein. A separate western blot was run to estimate the LOD of the D5E(*Ot*) protein. The LOD of the D5E(*Ot*) protein was 0.006 ng D5E(*Ot*), corresponding to 30 ng LBFLFK PPP. This D5E(*Ot*) amount corresponds to 1.0% and 1.1% of the total D5E(*Ot*) protein loaded in each lane of the SGF and SIF gels, respectively. In the case of sequential digestion (SGF followed by SIF digestion), it corresponds to 1.0% and 0.7% of the total D5E(*Ot*) protein loaded in each lane of the SGF and the following SIF digestion, respectively (Appendix 21).

Following exposure to SGF, western blot analysis demonstrated that two smaller fragments (~18 and ~26 kDa) appeared in the first 0.5 min, suggesting that the D5E(*Ot*) protein was partially digested (Figure 67, lane 5). All bands including the full-length D5E(*Ot*) protein, which migrated at ~31 kDa, were faintly detectable throughout the 60-min incubation with SGF (Figure 67, lanes 5–11). Controls for the SGF assay without pepsin showed only minor change of the D5E(*Ot*) protein over the 60-min time course as deduced from the signal intensities of the bands at ~31 kDa (G-con, Figure 67, lanes 2 to 3). This result indicates that digestion of the D5E(*Ot*) protein was primarily due to pepsin proteolytic activity and not instability of the D5E(*Ot*) protein in the test system. As expected, controls with pepsin but without D5E(*Ot*) protein (SGF alone, Figure 67, lanes 12 and 13) showed no unspecific detection of pepsin by the D5E(*Ot*)-specific antibody, which would be expected to result in a black band at ~50 kDa. Nonetheless, pepsin was faintly visible throughout the blot due to the large amount of pepsin protein loaded (Figure 67, lanes 4–13). The ~50 kDa non-specific cross-reaction band that was also observed in the heat stability blot (Figure 67) co-migrated with pepsin, making it difficult to distinguish at T = 0 (Figure 67, lane 4).

Following exposure to SIF, western blot analysis demonstrated that the full-length D5E(*Ot*) protein (~31 kDa) dropped below the LOD within 0.5 min (Figure 68, lane 5). This result indicates ≥ 98.9% digestion of the full-length D5E(*Ot*) protein within 0.5 min with SIF. Controls for the SIF assay without pancreatin showed only minor change of the D5E(*Ot*) protein over the 60-min time course as deduced from the signal intensities of the bands at ~31 kDa (I-con, Figure 68, lanes 2–3). This result indicates that digestion of the D5E(*Ot*) protein was primarily due to pancreatin proteolytic activity and not instability of the D5E(*Ot*) protein in the test system. Finally, controls with pancreatin but without D5E(*Ot*) protein (SIF alone, Figure 68, lanes 12 and 13) showed a weak cross-reaction (~60 kDa) to pancreatin with the antibody. This cross-reaction band was faintly detectable for 60 min with SIF (Figure 68, lanes 4–11).

Digestibility of D5E(*Ot*) was assessed in sequential digestion of SGF followed by SIF (Figure 69). Also in this experiment, the D5E(*Ot*) protein remained partially intact for 30 min with SGF (Figure 69, lane 8) but was degraded rapidly within 0.5 min upon incubation with SIF (Figure 69, lanes 9–10). This result indicates ≥ 99.3% digestion of the full-length D5E(*Ot*) protein with 30 min SGF digestion followed by 0.5 min SIF digestion. Controls in this assessment were consistent with the stand-alone SGF and SIF assessments shown above.

This result suggests that the D5E(*Ot*) protein is integrated to the membrane such that its potential protease cleavage sites are not immediately accessible to pepsin in SGF. The lipases present in SIF may potentially break down the lipid membranes, making the D5E(*Ot*) protein accessible to proteases for digestion. A similar result was obtained with D6E(*Tp*) protein, suggesting that these two elongases share similar susceptibilities to digestion. Based on the above results, the D5E(*Ot*) is susceptible to digestion when subjected to sequential digestion in SGF followed by SIF.

Figure 67. Western Blot Analysis of the D5E(*Ot*) Protein in LBFLFK Subjected to SGF

A western blot used to analyse the digestibility of the D5E(*Ot*) protein with SGF. In each lane, 3.13 µg of LBFLFK PPP were loaded, which corresponds to 0.63 ng D5E(*Ot*) protein (LOD = 0.006 ng D5E(*Ot*)). The D5E(*Ot*) protein consists of 300 amino acids with a calculated molecular mass of 34.2 kDa (migrates at ~31 kDa, indicated by the arrow). Lanes 1 and 14 are molecular weight markers with kDa values shown on the left. G-con: Buffer control (no pepsin). SGF alone: Negative control (no test protein).

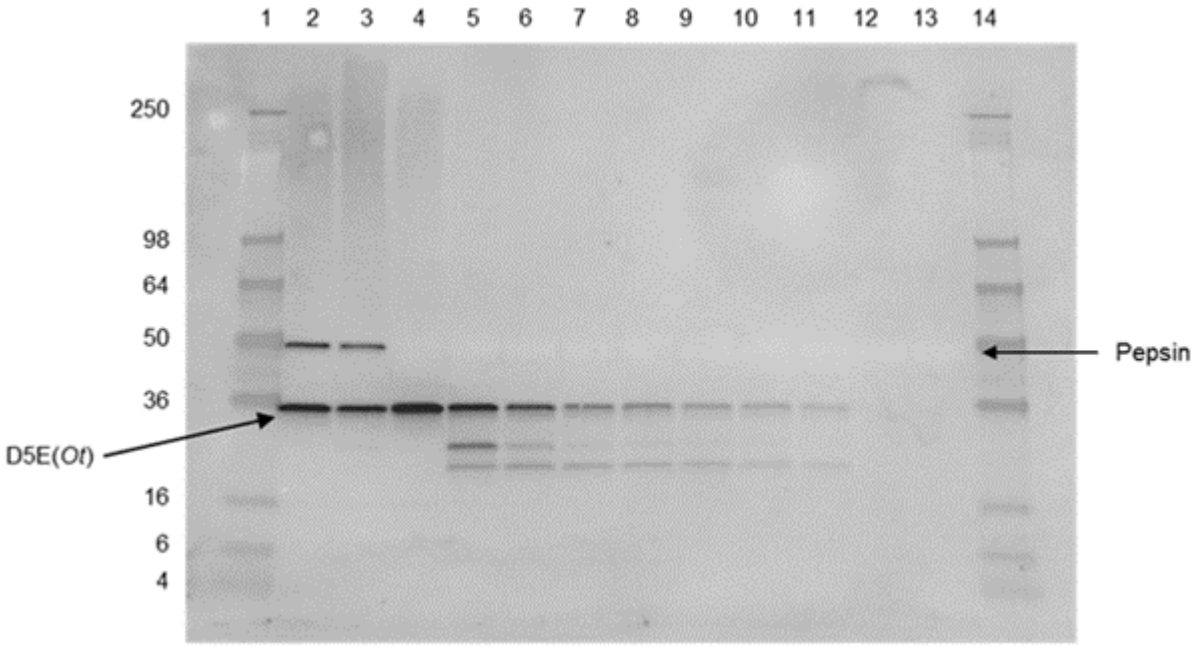

Lane	Sample	Incubation Time (min)
1	molecular weight marker	-
2	G-con	0
3	G-con	60
4	SGF	0
5	SGF	0.5
6	SGF	2
7	SGF	5
8	SGF	10
9	SGF	20
10	SGF	30
11	SGF	60
12	SGF alone	0
13	SGF alone	60
14	molecular weight marker	-

Figure 68. Western Blot Analysis of the D5E(*Ot*) Protein in LBFLFK Subjected to SIF

A western blot used to analyse the digestibility of the D5E(*Ot*) protein with SIF. In each lane, 2.81 µg of LBFLFK PPP were loaded, which corresponds to 0.57 ng D5E(*Ot*) protein (LOD = 0.006 ng D5E(*Ot*)). The D5E(*Ot*) protein consists of 300 amino acids with a calculated molecular mass of 34.2 kDa (migrates at ~31 kDa, indicated by the arrow). Lanes 1 and 14 are molecular weight markers with kDa values shown on the left of blot. I-con: Buffer control (no pancreatin). SIF alone: Negative control (no test protein).

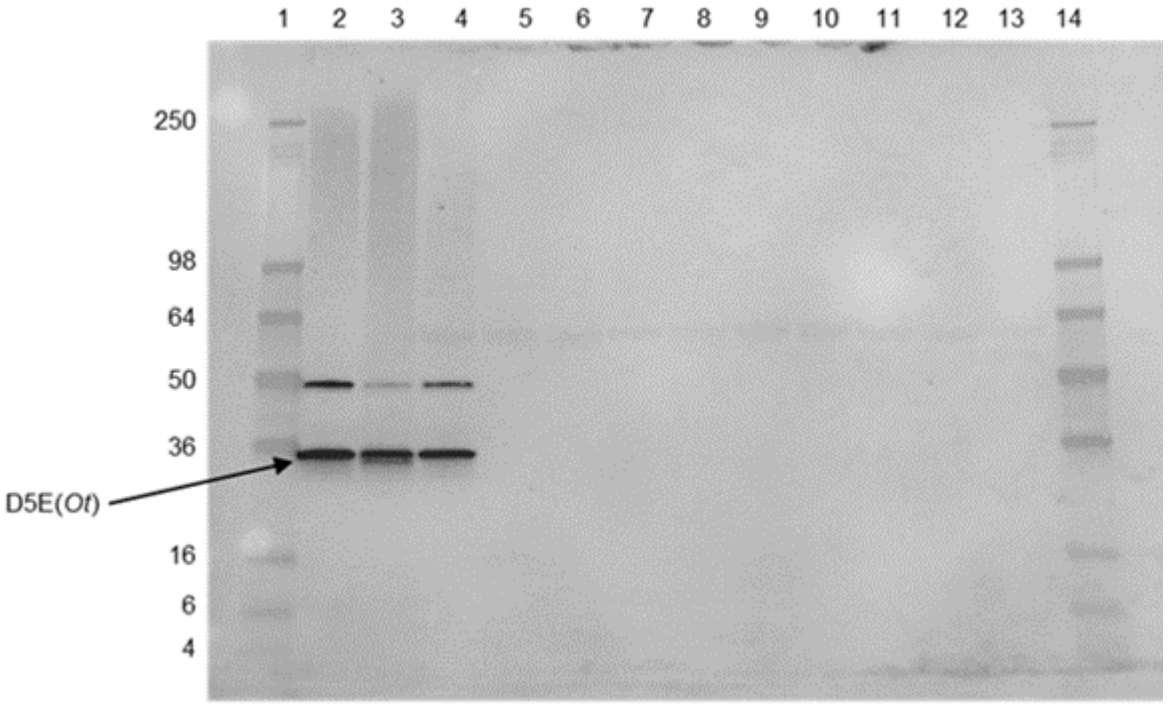

Lane	Sample	Incubation Time (min)
1	molecular weight marker	-
2	I-con	0
3	I-con	60
4	SIF	0
5	SIF	0.5
6	SIF	2
7	SIF	5
8	SIF	10
9	SIF	20
10	SIF	30
11	SIF	60
12	SIF alone	0
13	SIF alone	60
14	molecular weight marker	-

Figure 69. Western Blot Analysis of the D5E(*Ot*) Protein in LBFLFK Subjected to Sequential Digestion of SGF followed by SIF

A western blot used to analyse the digestibility of the D5E(*Ot*) protein with sequential digestion of SGF followed by SIF. In each lane of SGF, 3.13 µg of LBFLFK PPP were loaded, which corresponds to 0.63 ng D5E(*Ot*) protein (LOD = 0.006 ng D5E(*Ot*)). In each lane of SIF, 4.22 µg of LBFLFK PPP were loaded, which corresponds to 0.85 ng D5E(*Ot*) protein. The D5E(*Ot*) protein consists of 300 amino acids with a calculated molecular mass of 34.2 kDa (migrates at ~31 kDa, indicated by the arrow). Lanes 1 and 15 are molecular weight markers with kDa values shown on the left of blot. SD G-con: SGF buffer control (no pepsin). SD I-con: SIF buffer control (no pancreatin). SD SGF alone: SGF negative control (contains pepsin but contains no test protein). SD SIF alone: SIF negative control (contains pancreatin but contains no test protein).

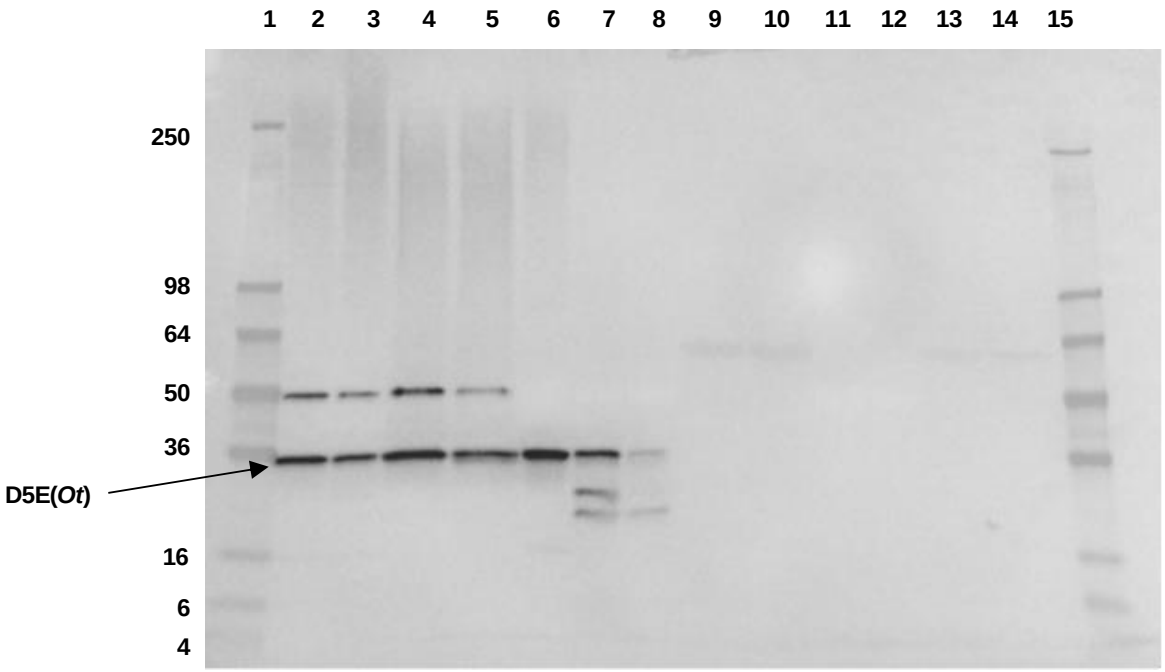

Lane	Sample	Incubation Time (min)
1	molecular weight marker	-
2	SD G-con	0.5
3	SD G-con	30
4	SD I-con	0.5
5	SD I-con	30
6	SD SGF	0
7	SD SGF	0.5
8	SD SGF	30
9	SD SGF → SIF	0.5
10	SD SGF → SIF	30
11	SD SGF alone	0.5
12	SD SGF alone	30
13	SD SIF alone	0.5
14	SD SIF alone	30
15	molecular weight marker	-

Delta-4 desaturase (*Tc*)

Bioinformatic analysis – toxins for delta-4 desaturase (*Tc*)

Bioinformatic analysis was used to determine whether the amino acid sequence of D4D(*Tc*) had significant sequence similarity to known protein toxins or antinutrients. D4D(*Tc*) did not show significant homology to proteins that are toxic to humans (Appendix 19). D4D(*Tc*) did not show significant homology to known antinutrients (OECD, 2002a, b, 2011a, b, 2012, 2016).

Stability to heat of delta-4 desaturase (*Tc*)

A heat stability analysis of D4D(*Tc*) was performed to assess the effect of different temperatures on enzyme activity and protein structural integrity. Sample treatment of the D4D(*Tc*) protein was identical to that of D12D(*Ps*) (Appendix 20). The enzyme activity assay cannot distinguish between the individual D4-desaturase enzymes D4D(*Tc*), D4D(*Pl*), and D4D(*Pl*) [A102S] in LBFLFK PPP.

The effect of heat treatment on the relative activity of the D4D proteins was evaluated using a fatty acid desaturase assay (Yilmaz et al., 2017), and the results are presented in Table 26. The results demonstrate that the D4D proteins in LBFLFK PPP retained enzymatic activity at 30°C after 5 and 20 min when compared to the baseline D4D enzymatic activity observed for the LBFLFK PPP incubated at 0°C. However, the D4D proteins were largely inactivated (< LOQ) at ≥ 50°C within 5 min and completely inactivated (< LOD) after longer treatment (20 min) at 90°C.

The effect of heat treatment on the structural integrity of the D4D(*Tc*) protein was evaluated by western blot analysis, and the results are presented in Figure 70. The western blot analysis demonstrated that the LBFLFK sample without heat treatment contained a distinct single band with an apparent molecular weight of ~63 kDa, which is in good agreement with the calculated molecular weight of the full-length D4D(*Tc*) protein (Figure 70, lane 3). While the band corresponding to D4D(*Tc*) was present at all temperatures and times tested, its signal decreased and protein aggregation intensified after 20 min at temperatures ≥ 50°C as indicated by a smear appearing at molecular weight > 63 kDa. This result is typical of proteins subjected to heat, especially for membrane proteins (Nury and Meunier, 1990; Lohner and Esser, 1991; Yan et al., 2004; Lee et al., 2005b; Harris and Booth, 2012; Roman and González Flecha, 2014). Finally, no cross-reaction was found with the PPP storage buffer and Kumily sample in Figure 70, lanes 1 and 2, respectively.

These results show that D4D enzyme activity is lost (Table 26) and undergoes structural change in the form of aggregation (Figure 70) at ≥ 50°C within 20 min. These results demonstrate that D4D(*Tc*) protein is heat-labile and the enzymatic activity is unlikely to remain after commercial processing.

Table 26. Relative Enzyme Activity of D4D after Heat Treatment of 5 and 20 Minutes

	30°C		50°C		70°C		90°C	
Protein	**5 min**	**20 min**	**5 min**	**20 min**	**5 min**	**20 min**	**5 min**	**20 min**
D4D	103%	92%	< LOQ	< LOQ	< LOQ	< LOQ	< LOQ	< LOD

Note: Results are % activity remaining compared to an LBFLFK sample that was not subjected to heat treatment prior to the enzyme activity assay.
LOQ (Limit of Quantitation) = 104770 VU
LOD (Limit of Detection) = 39509 VU

Figure 70. Western Blot Analysis of the D4D(*Tc*) Protein in LBFLFK after Heat Treatment

The effect of heat treatment on the structural integrity of the D4D(*Tc*) protein was analysed via western blot. The D4D(*Tc*) protein consists of 519 amino acids with a calculated molecular mass of 59.1 kDa (migrates at ~63 kDa).

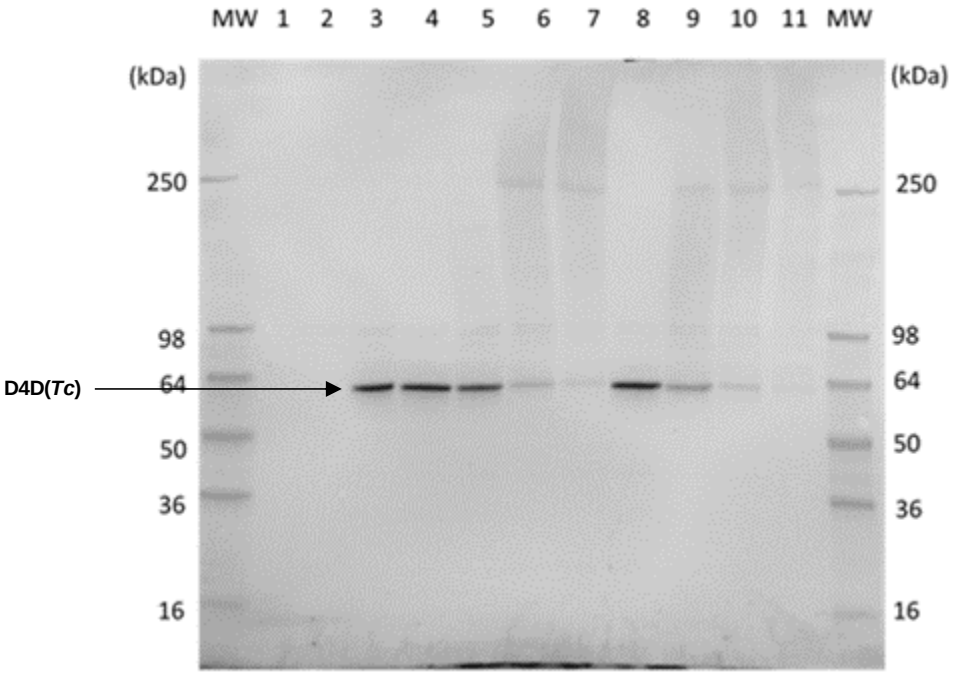

Lane	Sample	Incubation Temperature (°C)	Incubation Time (min)
1	PPP Storage Buffer	0	-
2	Kumily PPP	0	-
3	LBFLFK PPP	0	-
4	LBFLFK PPP	30	5
5	LBFLFK PPP	50	5
6	LBFLFK PPP	70	5
7	LBFLFK PPP	90	5
8	LBFLFK PPP	30	20
9	LBFLFK PPP	50	20
10	LBFLFK PPP	70	20
11	LBFLFK PPP	90	20

Digestive fate (*SGF/SIF*) *for delta-4 desaturase* (*Tc*)

The sensitivity of D4D(*Tc*) to SGF and SIF digestion was also assessed. The digestibility of the D4D(*Tc*) protein was evaluated by visual analysis of protein degradation in a time course on a western blot with an antibody raised against D4D(*Tc*) NC fusion protein. The LOD of the D4D(*Tc*) protein was 0.099 ng D4D(*Tc*), corresponding to 125 ng LBFLFK PPP. This D4D(*Tc*) amount corresponds to 12.1% and 13.4% of the total D4D(*Tc*) protein loaded in each lane of the SGF and SIF gels, respectively (Appendix 21).

Following exposure to SGF, western blot analysis demonstrated that the intensity of a ~63 kDa band in good agreement with the calculated molecular weight of the full-length D4D(*Tc*) protein dropped below the D4D(*Tc*) LOD within 0.5 min (Figure 71, lane 5). This result indicates ≥ 87.9% digestion of the full-length D4D(*Tc*) protein within 0.5 min with SGF. Controls for the SGF assay without pepsin showed only minor change of the D4D(*Tc*) protein over the 60-min time course as deduced from the signal intensities of the bands at ~63 kDa (G-con, Figure 71, lanes 2–3). This indicates that digestion of the D4D(*Tc*) protein was primarily due to pepsin proteolytic activity and not instability of the D4D(*Tc*) protein in the test system. As expected, controls with pepsin but without D4D(*Tc*) protein (SGF alone, Figure 71, lanes 12 and 13) showed no unspecific detection of pepsin by the D4D(*Tc*)-specific antibody, which would be expected to result in a black band at ~50 kDa.

Following exposure to SIF, western blot analysis demonstrated that the intensity of a ~63 kDa band in good agreement with the calculated molecular weight of the full-length D4D(*Tc*) protein dropped below the D4D(*Tc*) LOD within 0.5 min (Figure 72, lane 5). This result indicates ≥ 86.6% digestion of the full-length D4D(*Tc*) protein within 0.5 min with SIF. Controls for the SIF assay without pancreatin showed no change of the protein over the 60-min time course (I-con, Figure 72, lanes 2–3), which indicates that digestion of the D4D(*Tc*) protein was largely due to pancreatin proteolytic activity and not instability of the D4D(*Tc*) protein in the test system. As found for the D4D(*Tc*) SGF assay, controls with pancreatin but without D4D(*Tc*) protein (SIF alone, Figure 72, lanes 12 and 13) showed no unspecific detection of pancreatin by the D4D(*Tc*)-specific antibody, which would be expected to result in a black band(s) between 4 and 64 kDa.

These results demonstrate that the D4D(*Tc*) is susceptible to digestion and rapidly degraded in SGF and SIF.

Figure 71. Western Blot Analysis of the D4D(*Tc*) Protein in LBFLFK Subjected to SGF

A western blot used to analyse the digestibility of the D4D(*Tc*) protein with SGF. In each lane, 1.042 µg of LBFLFK PPP were loaded, which corresponds to 0.82 ng D4D(*Tc*) protein (LOD = 0.099 ng D4D(*Tc*)). The D4D(*Tc*) protein consists of 519 amino acids with a calculated molecular mass of 59.1 kDa (migrates at ~63 kDa, indicated by the arrow). Lanes 1 and 14 are molecular weight markers with kDa values shown on the left of blot. G-con: Buffer control (no pepsin). SGF alone: Negative control (no test protein).

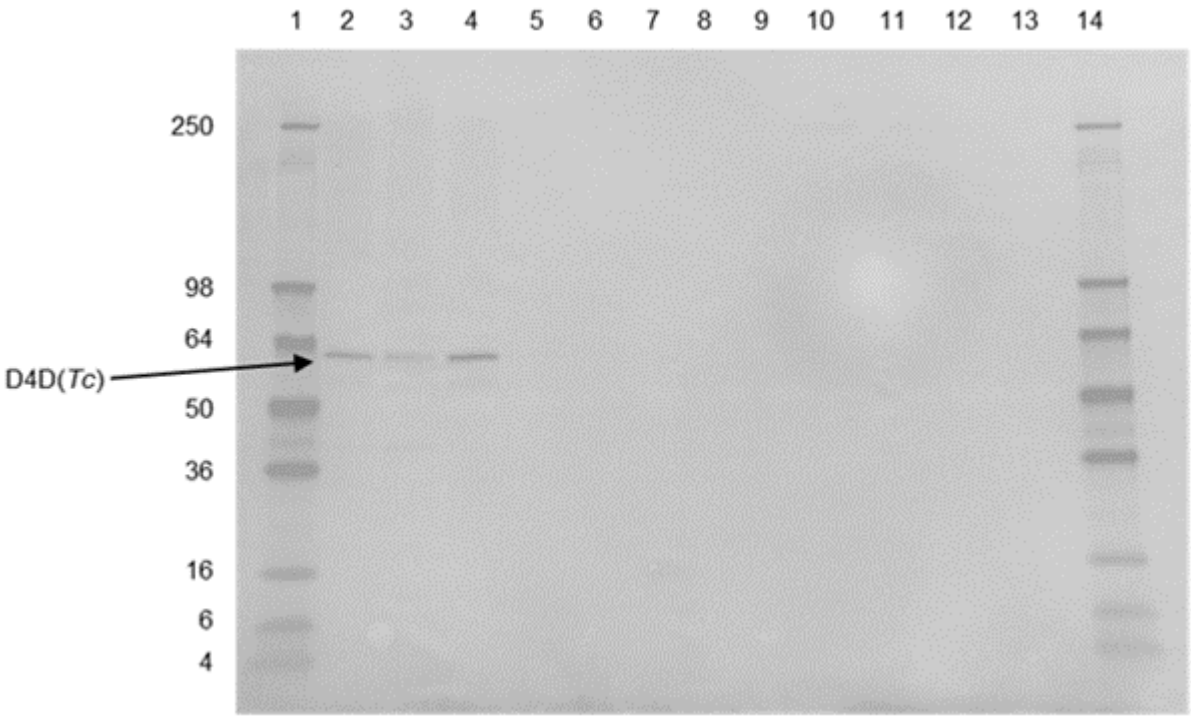

Lane	Sample	Incubation Time (min)
1	molecular weight marker	-
2	G-con	0
3	G-con	60
4	SGF	0
5	SGF	0.5
6	SGF	2
7	SGF	5
8	SGF	10
9	SGF	20
10	SGF	30
11	SGF	60
12	SGF alone	0
13	SGF alone	60
14	molecular weight marker	-

Figure 72. Western Blot Analysis of the D4D(*Tc*) Protein in LBFLFK Subjected to SIF

A western blot used to analyse the digestibility of the D4D(*Tc*) protein with SIF. In each lane, 0.94 µg of LBFLFK PPP were loaded, which corresponds to 0.74 ng D4D(*Tc*) protein (LOD = 0.099 ng D4D(*Tc*)). The D4D(*Tc*) protein consists of 519 amino acids with a calculated molecular mass of 59.1 kDa (migrates at ~63 kDa, indicated by the arrow). Lanes 1 and 14 are molecular weight markers with kDa values shown on the left of blot. I-con: Buffer control (no pancreatin). SIF alone: Negative control (no test protein).

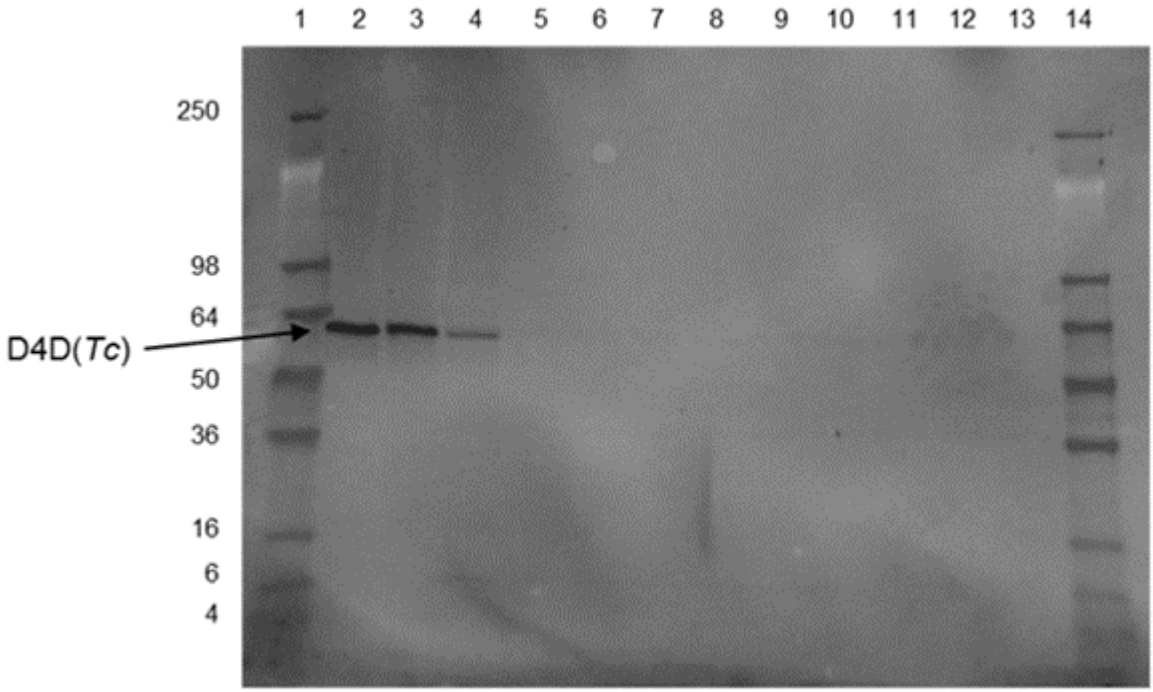

Lane	Sample	Incubation Time (min)
1	molecular weight marker	-
2	I-con	0
3	I-con	60
4	SIF	0
5	SIF	0.5
6	SIF	2
7	SIF	5
8	SIF	10
9	SIF	20
10	SIF	30
11	SIF	60
12	SIF alone	0
13	SIF alone	60
14	molecular weight marker	-

Delta-4 desaturase (*Pl*)

Bioinformatic analysis – toxins for delta-4 desaturase (*Pl*)

Bioinformatic analysis was used to determine whether the amino acid sequence of D4D(*Pl*) had significant sequence similarity to known protein toxins or antinutrients. The amino acid sequences from both LBFLFK Insert1 and LBFLFK Insert2 were used for bioinformatic analysis. For D4D(*Pl*), LBFLFK Insert2 includes a nucleotide change in the coding region, which results in the A102S amino acid substitution (section A.3(c)(ii)). D4D(*Pl*) did not show significant homology to proteins that are toxic to humans (Appendix 19). D4D(*Pl*) did not show significant homology to known antinutrients (OECD, 2002a, b, 2011a, b, 2012, 2016).

Stability to heat of delta-4 desaturase (*Pl*)

A heat stability analysis of D4D(*Pl*) was performed to assess the effect of different temperatures on enzyme activity and protein structural integrity. Sample treatment of the D4D(*Pl*) protein was identical to that of D12D(*Ps*) (Appendix 20). The effect of heat treatment on the relative activity of the D4D proteins was evaluated using a fatty acid desaturase assay (Yilmaz et al., 2017). The results are the same as shown for D4D(*Tc*) and presented in Table 26 as the desaturase assay does not distinguish between the individual delta-4 desaturase enzymes D4D(*Pl*), D4D(*Tc*), and D4D(*Pl*) [A102S] in LBFLFK PPP. For LOD and LOQ of D4D enzyme activity, see Appendix 20.

The effect of heat treatment on the structural integrity of the D4D(*Pl*) protein was evaluated by western blot analysis, and the results are presented in Figure 73. The antibody used does not discriminate between the intended D4D(*Pl*) and the D4D(*Pl*) [A102S]. The western blot analysis demonstrated that the LBFLFK sample without heat treatment contained a distinct band with an apparent molecular weight of ~51 kDa, which is in good agreement with the calculated molecular weight of the D4D(*Pl*) protein (Figure 73, lane 3). While the band corresponding to D4D(*Pl*) was present at all temperatures and times tested, the signal of the full-length D4D(*Pl*) protein was decreased at 50°C and significantly decreased with increasing temperatures (Figure 73, lanes 4–11). A higher molecular weight smear was detected at temperatures ≥ 70°C, suggesting that the decreased signal of the full-length D4D(*Pl*) protein at 50°C was likely due to aggregation. This result is typical of proteins subjected to heat, especially for membrane proteins (Nury and Meunier, 1990; Lohner and Esser, 1991; Yan et al., 2004; Lee et al., 2005b; Harris and Booth, 2012; Roman and González Flecha, 2014). Finally, no cross-reaction was found with the PPP storage buffer and Kumily sample in Figure 73, lanes 1 and 2, respectively.

These results show that D4D enzyme activity is lost at ≥ 50°C (Table 26) and undergoes structural change in the form of aggregation at ≥ 70°C within 5 min (Figure 73). These results demonstrate that D4D(*Pl*) protein is heat-labile and the enzymatic activity is unlikely to remain after commercial processing.

Figure 73. Western Blot Analysis of the D4D(*PI*) Protein in LBFLFK after Heat Treatment

The effect of heat treatment on the structural integrity of the D4D(*PI*) protein was analysed via western blot. The D4D(*PI*) protein consists of 445 amino acids with a calculated molecular mass of 49.2 kDa (migrates at ~51 kDa).

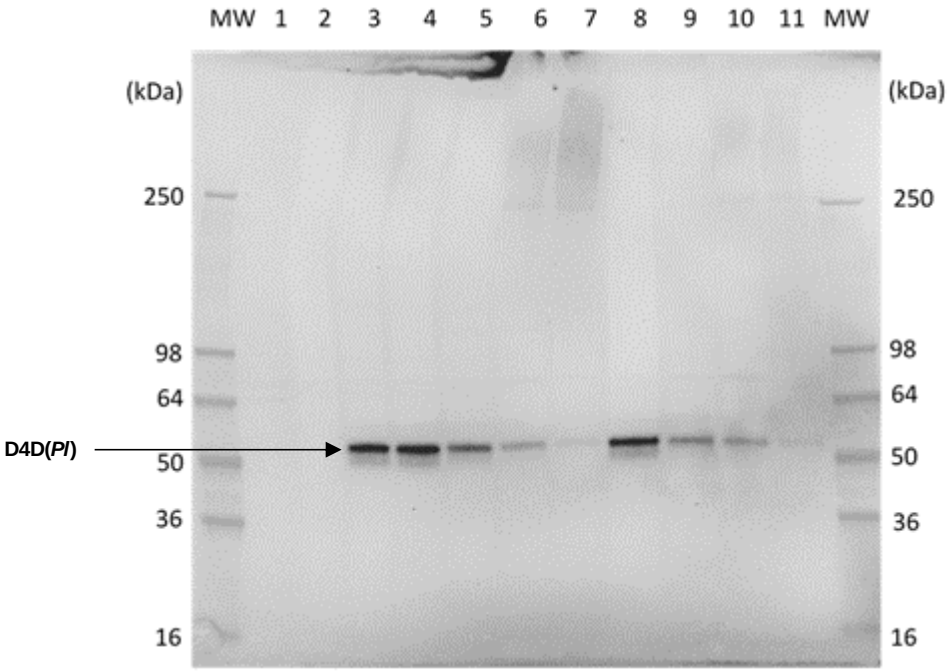

Lane	Sample	Incubation Temperature (°C)	Incubation Time (min)
1	PPP Storage Buffer	0	-
2	Kumily PPP	0	-
3	LBFLFK PPP	0	-
4	LBFLFK PPP	30	5
5	LBFLFK PPP	50	5
6	LBFLFK PPP	70	5
7	LBFLFK PPP	90	5
8	LBFLFK PPP	30	20
9	LBFLFK PPP	50	20
10	LBFLFK PPP	70	20
11	LBFLFK PPP	90	20

Digestive fate (*SGF/SIF*) *for delta-4 desaturase* (*PI*)

The sensitivity of D4D(*PI*) to SGF and SIF digestion was also assessed. The digestibility of the D4D(*PI*) protein was evaluated by visual analysis of protein degradation in a time course on a western blot. The antibody used was raised against D4D(*PI*) NC fusion protein and does not discriminate between the intended D4D(*PI*) and the D4D(*PI*) [A102S]. The LOD of the D4D(*PI*) protein was 0.102 ng D4D(*PI*), corresponding to 400 ng LBFLFK PPP. This D4D(*PI*) amount corresponds to 3.2% and 3.6% of the total D4D(*PI*) protein loaded in each lane of the SGF and SIF gels, respectively (Appendix 21). The two higher molecular weight bands

migrating at ~70 and ~80 kDa were likely to be cross-reactive proteins as these sizes are less than the size of its dimer (~100 kDa).

Following exposure to SGF, western blot analysis demonstrated that the intensity of a ~51 kDa band in good agreement with the calculated molecular weight of the full-length D4D(*Pl*) protein dropped below the D4D(*Pl*) LOD within 0.5 min (Figure 74, lane 5). This result indicates ≥ 96.8% digestion of the full-length D4D(*Pl*) protein within 0.5 min with SGF. Controls for the SGF assay without pepsin showed only minor degradation of the D4D(*Pl*) protein over the 60-min time course as deduced from the signal intensities of the bands at ~51 kDa (G-con, Figure 74, lanes 2–3). This indicates that digestion of the D4D(*Pl*) protein was primarily due to pepsin proteolytic activity and not instability of the D4D(*Pl*) protein in the test system. As expected, controls with pepsin but without D4D(*Pl*) protein (SGF alone, Figure 74, lanes 12 and 13) showed no unspecific detection of pepsin by the D4D(*Pl*)-specific antibody, which would be expected to result in a black band at ~50 kDa.

Following exposure to SIF, western blot analysis demonstrated that the intensity of a ~51 kDa band in good agreement with the calculated molecular weight of the full-length D4D(*Pl*) protein dropped below the D4D(*Pl*) LOD within 0.5 min (Figure 75, lane 5). This result indicates ≥ 96.4% digestion of the full-length D4D(*Pl*) protein within 0.5 min with SIF. Controls for the SIF assay without pancreatin showed reduced signal of the full-length D4D(*Pl*) protein over the 60-min time course (I-con, Figure 75, lanes 2–3) indicating that the protein is not stable in the test system. As found for the D4D(*Pl*) SGF assay, controls with pancreatin but without D4D(*Pl*) protein (SIF alone, Figure 75, lanes 12 and 13) showed no unspecific detection of pancreatin by the D4D(*Pl*)-specific antibody, which would be expected to result in a black band(s) between 4 and 64 kDa.

These results demonstrate that the D4D(*Pl*) is susceptible to digestion and rapidly degraded in SGF and SIF.

Figure 74. Western Blot Analysis of the D4D(*PI*) Protein in LBFLFK Subjected to SGF

A western blot used to analyse the digestibility of the D4D(*PI*) protein with SGF. In each lane, 12.5 µg of LBFLFK PPP were loaded, which corresponds to 3.19 ng D4D(*PI*) protein (LOD = 0.102 ng D4D(*PI*)). The D4D(*PI*) protein consists of 445 amino acids with a calculated molecular mass of 49.2 kDa (migrates at ~51 kDa, indicated by the arrow). Lanes 1 and 14 are molecular weight markers with kDa values shown on the left of blot. G-con: Buffer control (no pepsin). SGF alone: Negative control (no test protein).

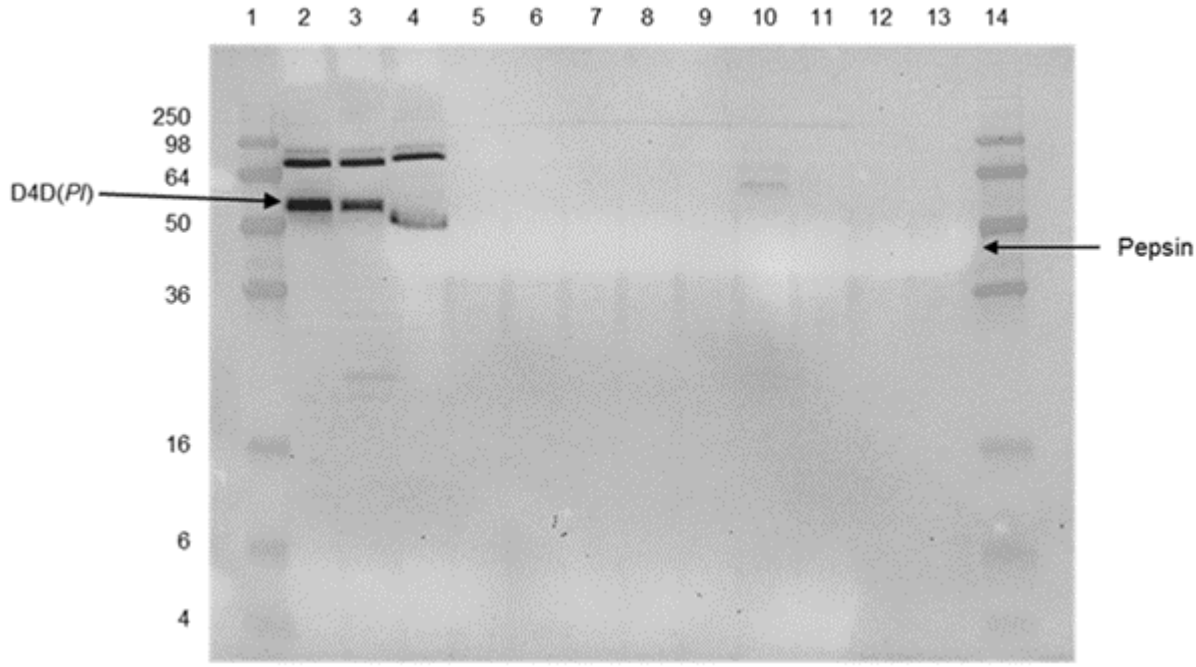

Lane	Sample	Incubation Time (min)
1	molecular weight marker	-
2	G-con	0
3	G-con	60
4	SGF	0
5	SGF	0.5
6	SGF	2
7	SGF	5
8	SGF	10
9	SGF	20
10	SGF	30
11	SGF	60
12	SGF alone	0
13	SGF alone	60
14	molecular weight marker	-

Figure 75. Western Blot Analysis of the D4D(*PI*) Protein in LBFLFK Subjected to SIF

A western blot used to analyse the digestibility of the D4D(*PI*) protein with SIF. In each lane, 11.25 µg of LBFLFK PPP were loaded, which corresponds to 2.87 ng D4D(*PI*) protein (LOD = 0.102 ng D4D(*PI*)). The D4D(*PI*) protein consists of 445 amino acids with a calculated molecular mass of 49.2 kDa (migrates at ~51 kDa, indicated by the arrow). Lanes 1 and 14 are molecular weight markers with kDa values shown on the left of blot. I-con: Buffer control (no pancreatin). SIF alone: Negative control (no test protein).

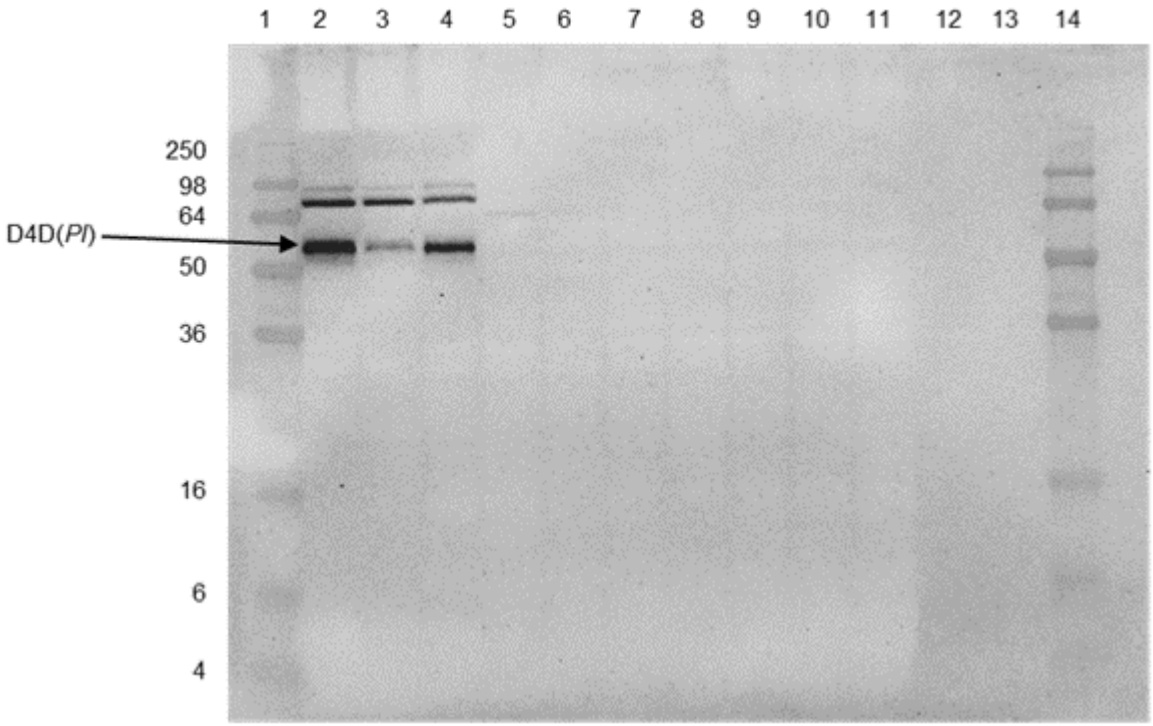

Lane	Sample	Incubation Time (min)
1	molecular weight marker	-
2	I-con	0
3	I-con	60
4	SIF	0
5	SIF	0.5
6	SIF	2
7	SIF	5
8	SIF	10
9	SIF	20
10	SIF	30
11	SIF	60
12	SIF alone	0
13	SIF alone	60
14	molecular weight marker	-

Acetohydroxy acid synthase (*At*) [A122TS653N]

Bioinformatic analysis – toxins for acetohydroxy acid synthase (*At*) *[A122TS653N]*

Bioinformatic analysis was used to determine whether the amino acid sequence of AHAS(*At*) [A122TS653N] had significant sequence similarity to known protein toxins or antinutrients. AHAS(*At*) [A122TS653N] did not show significant homology to proteins that are toxic to humans (Appendix 19). AHAS(*At*) [A122TS653N] did not show significant homology to known antinutrients (OECD, 2002a, b, 2011a, b, 2012, 2016).

Stability to heat of acetohydroxy acid synthase (*At*) *[A122TS653N]*

A heat stability analysis of AHAS(*At*) [A122TS653N] was performed to assess the effect of different temperatures on enzyme activity and protein structural integrity. Sample treatment of the AHAS(*At*) [A122TS653N] protein was identical to that of D12D(*Ps*) (Appendix 20). The enzyme activity assay cannot distinguish between the newly expressed AHAS(*At*) [A122TS653N] protein and the endogenous canola AHAS protein (AHAS(*Bn*)) in LBFLFK PPP.

The effect of heat treatment on the relative activity of the AHAS proteins was evaluated using the enzyme activity assay (Singh et al., 1988), and the results are presented in Table 27. The results demonstrate that the AHAS proteins retained enzymatic activity at 30°C after 5 and 20 min. However, the AHAS proteins were largely inactivated (< LOQ) at 50°C within 5 min and completely inactivated (< LOD) after longer treatment (20 min) and/or higher temperatures (≥ 70°C). Though this assay cannot distinguish the AHAS enzyme activity between endogenous AHAS(*Bn*) protein and the newly expressed AHAS(*At*) [A122TS653N] protein, these results demonstrate that increasing temperatures caused a loss of AHAS enzyme activity.

The effect of heat treatment on the structural integrity of the AHAS(*At*) [A122TS653N] protein was evaluated by western blot analysis, and the results are presented in Figure 76. The antibody generated against the full-length protein is not expected to distinguish between the AHAS(*At*) [A122TS653N] protein and the endogenous AHAS(*Bn*) protein. The western blot analysis demonstrated that the LBFLFK sample without heat treatment contained a distinct band with an apparent molecular weight of ~79 kDa, which is in good agreement with the calculated molecular weight of the AHAS(*At*) [A122TS653N] and AHAS(*Bn*) proteins (Figure 76, lane 3). While the band corresponding to the AHAS proteins was present at all temperatures and times tested, the signal decreased with increasing time and temperature (Figure 76, lanes 4–11). The bands migrating at ≤ 60 kDa and ~90 kDa are likely to represent fragments of the AHAS proteins and cross-reactivity, respectively. The band detected in the Kumily control (Figure 76, lane 2) is likely to be the endogenous AHAS(*Bn*).

These results show that AHAS enzyme activity is lost at ≥ 50°C (Table 27) and undergoes structural change in the form of decreasing signal intensity (Figure 76). These results demonstrate that AHAS(*At*) [A122TS653N] protein is heat-labile and the enzymatic activity is unlikely to remain after commercial processing.

Table 27. Relative Enzyme Activity of AHAS after Heat Treatment of 5 and 20 Minutes

	30°C		50°C		70°C		90°C	
Protein	**5 min**	**20 min**	**5 min**	**20 min**	**5 min**	**20 min**	**5 min**	**20 min**
AHAS	95%	73%	< LOQ	< LOD	< LOD	< LOD	< LOD	< LOD

Note: Results are % activity remaining compared to an LBFLFK sample that was not subjected to heat treatment prior to the enzyme activity assay.
LOQ (Limit of Quantitation) = 0.0341 mM
LOD (Limit of Detection) = 0.0129 mM

Figure 76. Western Blot Analysis of the AHAS Protein in LBFLFK after Heat Treatment

The effect of heat treatment on the structural integrity of the AHAS(*At*) [A122TS653N] protein was analysed via western blot. The AHAS(*At*) [A122TS653N] protein consists of 606 amino acids with a calculated molecular mass of 66.1 kDa (migrates at ~79 kDa).

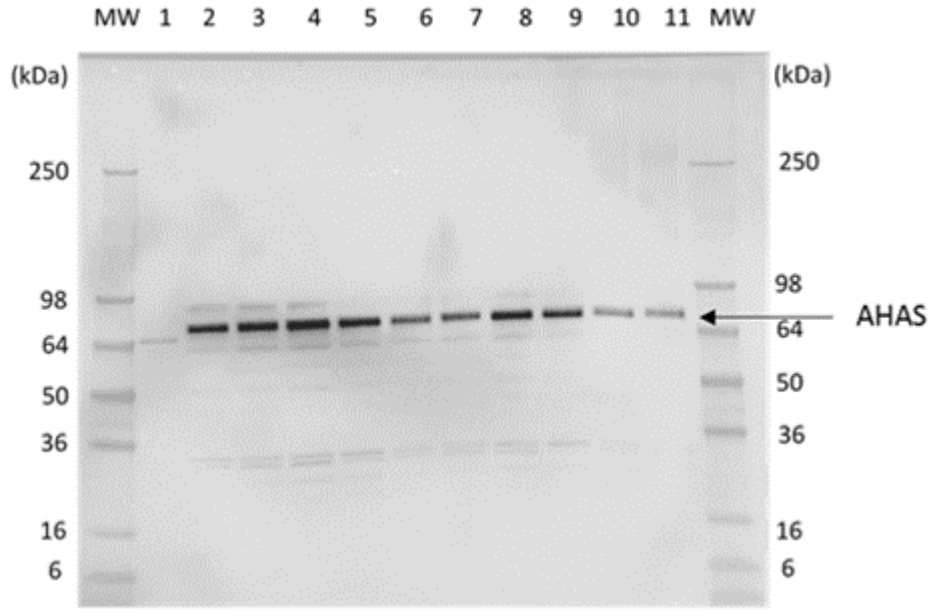

Lane	Sample	Incubation Temperature (°C)	Incubation Time (min)
1	PPP Storage Buffer	0	-
2	Kumily PPP	0	-
3	LBFLFK PPP	0	-
4	LBFLFK PPP	30	5
5	LBFLFK PPP	50	5
6	LBFLFK PPP	70	5
7	LBFLFK PPP	90	5
8	LBFLFK PPP	30	20
9	LBFLFK PPP	50	20
10	LBFLFK PPP	70	20
11	LBFLFK PPP	90	20

Digestive fate (*SGF/SIF*) *for acetohydroxy acid synthase* (*At*) *[A122TS653N]*

The sensitivity of AHAS(*At*) [A122TS653N] to SGF and SIF digestion was also assessed. Unlike the other newly expressed proteins in LBFLFK, AHAS(*At*) [A122TS653N] is a soluble protein. Thus, its digestibility in SGF and SIF was assessed in both PPP and leaf tissue. The digestibility of the AHAS(*At*) [A122TS653N] protein was evaluated by visual analysis of protein degradation in a time course on a western blot with an antibody raised against AHAS(*At*) [A122TS653N] full-length protein. The AHAS protein present in LBFLFK is a mixture of the newly expressed Arabidopsis AHAS(*At*) [A122TS653N] protein and the endogenous canola AHAS protein AHAS(*Bn*). Since the antibody used is not expected to distinguish between the two AHAS proteins, it is not possible to provide a relative amount of each. Thus, the digestive fate results represent the digestion of both AHAS proteins.

Following exposure to SGF, western blot analysis demonstrated that an ~79 kDa band in good agreement with the calculated molecular weight of the full-length AHAS proteins was digested within 0.5 min regardless of matrix (both LBFLFK PPP and LBFLFK leaf tissue; Figure 77 and Figure 78, lane 5). Similarly, the bands migrating at ≤ 60 kDa and ~90 kDa, which likely represent AHAS protein fragments and cross-reactivity to other proteins, respectively, were also digested within 0.5 min. In both matrices, controls for the SGF assay without pepsin showed only minor decreases of the AHAS proteins' signal over the 60-min time course as deduced from the signal intensities of the bands at ~79 kDa (G-con, Figure 77 and Figure 78, lanes 2–3). This indicates that digestion of the AHAS proteins was primarily due to pepsin proteolytic activity and not instability of the AHAS proteins in the test system. As expected, controls with pepsin but without AHAS proteins (SGF alone, Figure 77 and Figure 78, lanes 12 and 13) showed no unspecific detection of pepsin by the AHAS-specific antibody, which would be expected to result in a black band at ~50 kDa.

Following exposure to SIF, the AHAS proteins responded differently depending on the matrix. Using leaf tissue, western blot analysis demonstrated that the intensity of an ~79 kDa band in good agreement with the calculated molecular weight of the full-length AHAS proteins dropped below the detection limit within 0.5 min (Figure 80, lane 5). The AHAS proteins disappeared in the 60 min I-Con (buffer control without pancreatin) sample, indicating that the proteins are unstable in the test system (Figure 80, lanes 2 and 3). The multi-bands migrating between 33 and 64 kDa are cross-reactions to pancreatin as shown in the controls with pancreatin but without AHAS proteins (SIF alone, Figure 80, lanes 12 and 13). The results show that the AHAS proteins in leaf tissue are sensitive to SIF with or without pancreatin. On the other hand, when using PPP, the AHAS proteins (~79 kDa) remained stable over the 60-min time course either in the presence of pancreatin (Figure 79, lanes 4–11) or in the absence of pancreatin (Figure 79, lanes 2–3). Consequently, digestibility of the AHAS proteins in PPP was assessed in a sequential digestion of SGF followed by SIF (Figure 81). Consistent with the results for SGF digestion alone, the AHAS proteins were degraded rapidly (within 0.5 min) with SGF (Figure 81, lane 7) and thus, no AHAS proteins were remaining for further digestion with SIF (Figure 81, lanes 9–10). Controls in this assessment were consistent with the stand-alone SGF and SIF assessments shown in Figure 77 and Figure 79. These results demonstrate that the AHAS proteins are susceptible to digestion in SGF and, when leaf tissue is used, also to digestion in SIF.

Figure 77. Western Blot Analysis of the AHAS Protein in LBFLFK PPP Subjected to SGF

A western blot used to analyse the digestibility of the AHAS(*At*) [A122TS653N] and AHAS(*Bn*) proteins with SGF. In each lane, 10.4 µg of LBFLFK PPP were loaded. The mature AHAS(*At*) [A122TS653N] protein consists of 606 amino acids with a calculated molecular mass of 66.1 kDa and the mature AHAS(*Bn*) proteins consists of 602 amino acids with a calculated molecular mass of 65.8 kDa with both proteins migrating ~79 kDa. Lanes 1 and 14 are molecular weight markers with kDa values shown on the left of blot. G-con: Buffer control (no pepsin). SGF alone: Negative control (no test protein).

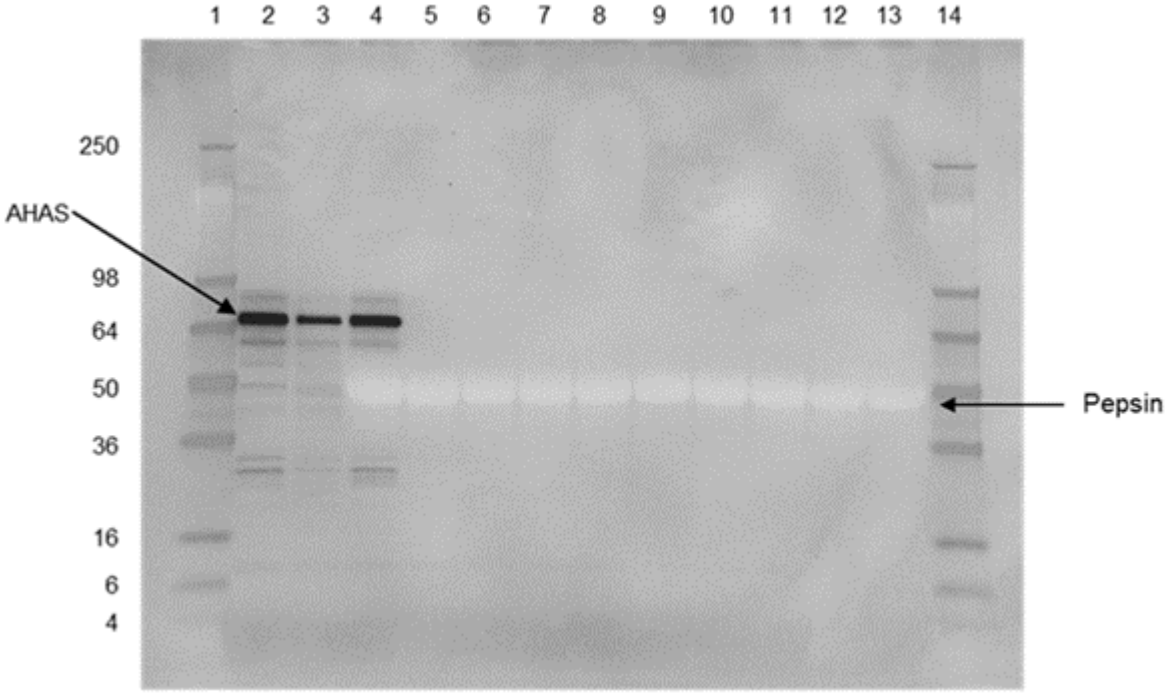

Lane	Sample	Incubation Time (min)
1	molecular weight marker	-
2	G-con	0
3	G-con	60
4	SGF	0
5	SGF	0.5
6	SGF	2
7	SGF	5
8	SGF	10
9	SGF	20
10	SGF	30
11	SGF	60
12	SGF alone	0
13	SGF alone	60
14	molecular weight marker	-

Figure 78. Western Blot Analysis of the AHAS Protein in LBFLFK Leaf Tissue Subjected to SGF

A western blot used to analyse the digestibility of the AHAS(*At*) [A122TS653N] and AHAS(*Bn*) proteins with SGF. In each lane, 14.2 µg of LBFLFK leaf tissue extract were loaded. The mature AHAS(*At*) [A122TS653N] protein consists of 606 amino acids with a calculated molecular mass of 66.1 kDa, and the mature AHAS(*Bn*) protein consists of 602 amino acids with a calculated molecular mass of 65.8 kDa, with both proteins migrating at ~79 kDa. Lanes 1 and 14 are molecular weight markers with kDa values shown on the left of blot. G-con: Buffer control (no pepsin). SGF alone: Negative control (no test protein).

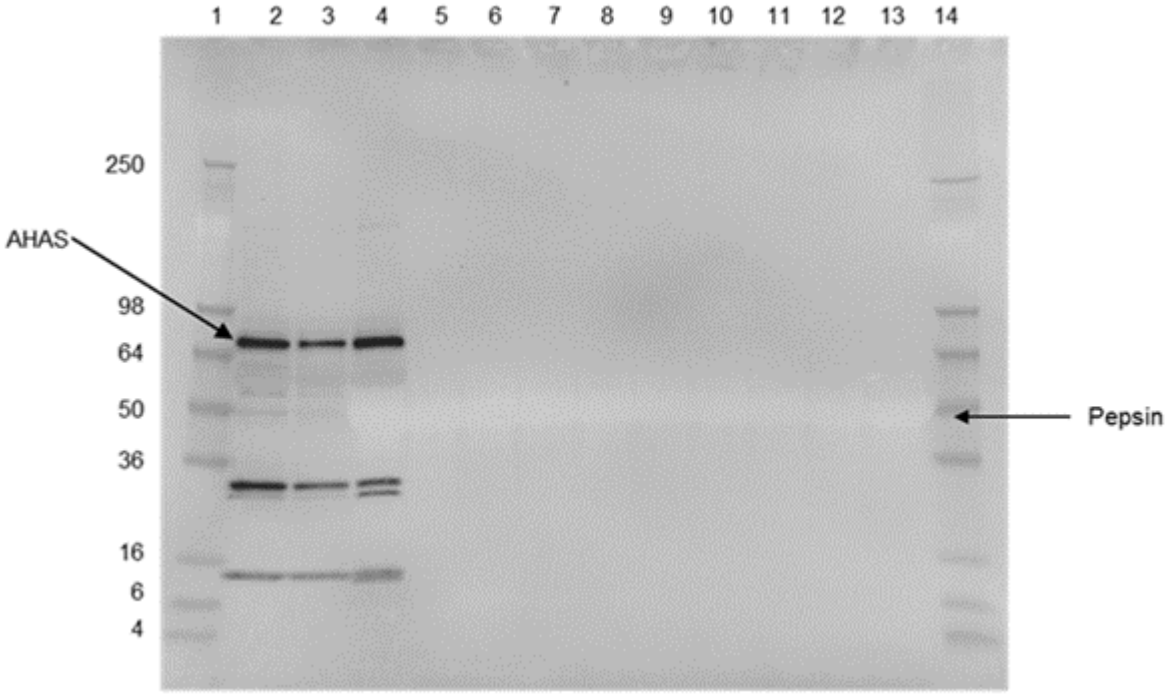

Lane	Sample	Incubation Time (min)
1	molecular weight marker	-
2	G-con	0
3	G-con	60
4	SGF	0
5	SGF	0.5
6	SGF	2
7	SGF	5
8	SGF	10
9	SGF	20
10	SGF	30
11	SGF	60
12	SGF alone	0
13	SGF alone	60
14	molecular weight marker	-

Figure 79. Western Blot Analysis of the AHAS Protein in LBFLFK PPP Subjected to SIF

A western blot used to analyse the digestibility of the AHAS(*At*) [A122TS653N] and AHAS(*Bn*) proteins with SIF. In each lane 9.38 µg of LBFLFK PPP were loaded. The mature AHAS(*At*) [A122TS653N] protein consists of 606 amino acids with a calculated molecular mass of 66.1 kDa, and the mature AHAS(*Bn*) protein consists of 602 amino acids with a calculated molecular mass of 65.8 kDa, with both proteins migrating at ~79 kDa. Lanes 1 and 14 are molecular weight markers with kDa values shown on the left of blot. I-con: Buffer control (no pancreatin). SIF alone: Negative control (no test protein).

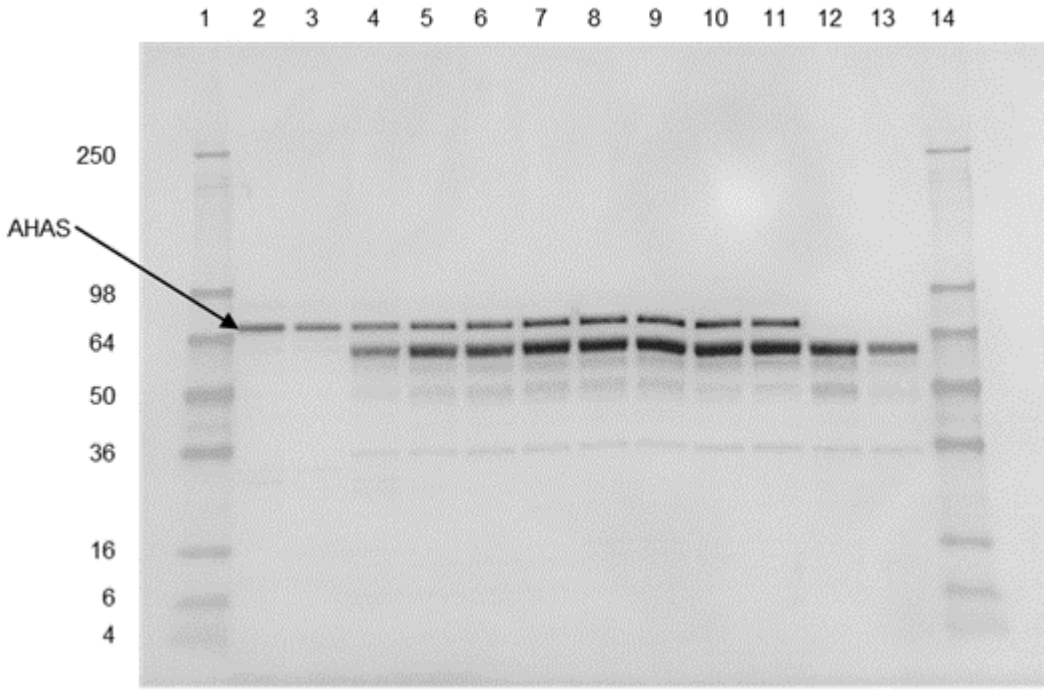

Lane	Sample	Incubation Time (min)
1	molecular weight marker	-
2	I-con	0
3	I-con	60
4	SIF	0
5	SIF	0.5
6	SIF	2
7	SIF	5
8	SIF	10
9	SIF	20
10	SIF	30
11	SIF	60
12	SIF alone	0
13	SIF alone	60
14	molecular weight marker	-

Figure 80. Western Blot Analysis of the AHAS Protein in LBFLFK Leaf Tissue Subjected to SIF

A western blot used to analyse the digestibility of the AHAS(*At*) [A122TS653N] and AHAS(*Bn*) proteins with SIF. In each lane, 12.8 µg of LBFLFK leaf tissue extract were loaded. The mature AHAS(*At*) [A122TS653N] protein consists of 606 amino acids with a calculated molecular mass of 66.1 kDa, and the mature AHAS(*Bn*) protein consists of 602 amino acids with a calculated molecular mass of 65.8 kDa, with both proteins migrating at ~79 kDa. Lanes 1 and 14 are molecular weight markers with kDa values shown on the left of blot. I-con: Buffer control (no pancreatin). SIF alone: Negative control (no test protein).

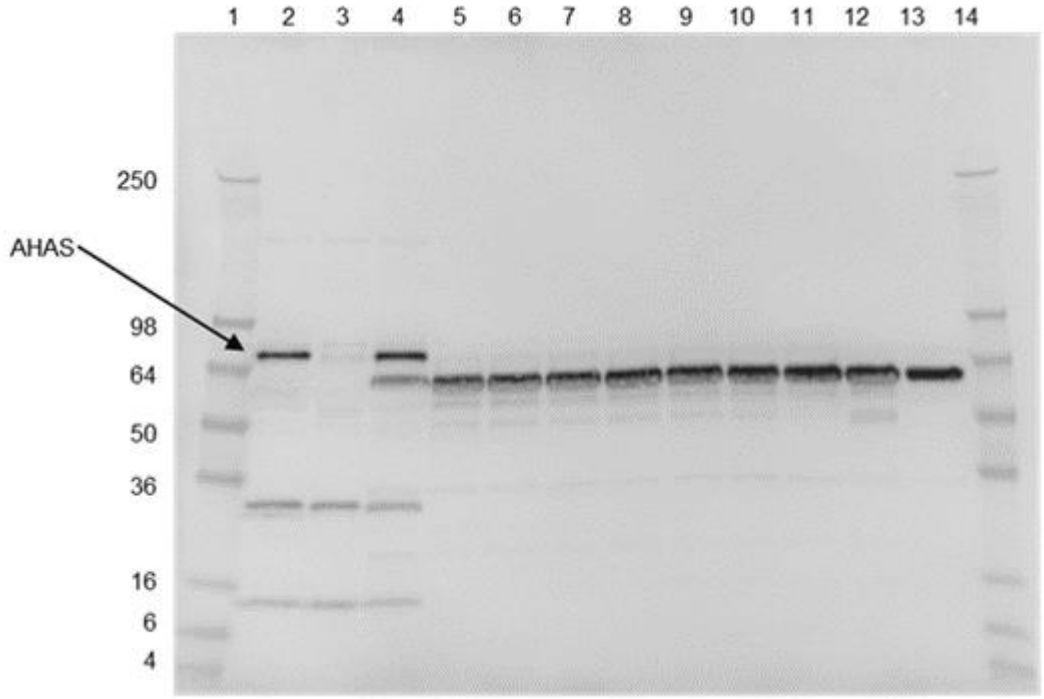

Lane	Sample	Incubation Time (min)
1	molecular weight marker	-
2	I-con	0
3	I-con	60
4	SIF	0
5	SIF	0.5
6	SIF	2
7	SIF	5
8	SIF	10
9	SIF	20
10	SIF	30
11	SIF	60
12	SIF alone	0
13	SIF alone	60
14	molecular weight marker	-

Figure 81. Western Blot Analysis of the AHAS Protein in LBFLFK PPP Subjected to Sequential Digestion of SGF followed by SIF

A western blot used to analyse the digestibility of the AHAS(*At*) [A122TS653N] and AHAS(*Bn*) proteins with sequential digestion of SGF followed by SIF. In each lane of SGF, 10.4 µg of LBFLFK PPP were loaded. In each lane of SIF, 14.1 µg of LBFLFK PPP were loaded. The mature AHAS(*At*) [A122TS653N] protein consists of 606 amino acids with a calculated molecular mass of 66.1 kDa, and the mature AHAS(*Bn*) protein consists of 602 amino acids with a calculated molecular mass of 65.8 kDa, with both proteins migrating at ~79 kDa. Lanes 1 and 15 are molecular weight markers with kDa values shown on the left of blot. SD G-con: SGF buffer control (no pepsin). SD I-con: SIF buffer control (no pancreatin). SD SGF alone: SGF negative control (contains pepsin but contains no test protein). SD SIF alone: SIF negative control (contains pancreatin but contains no test protein).

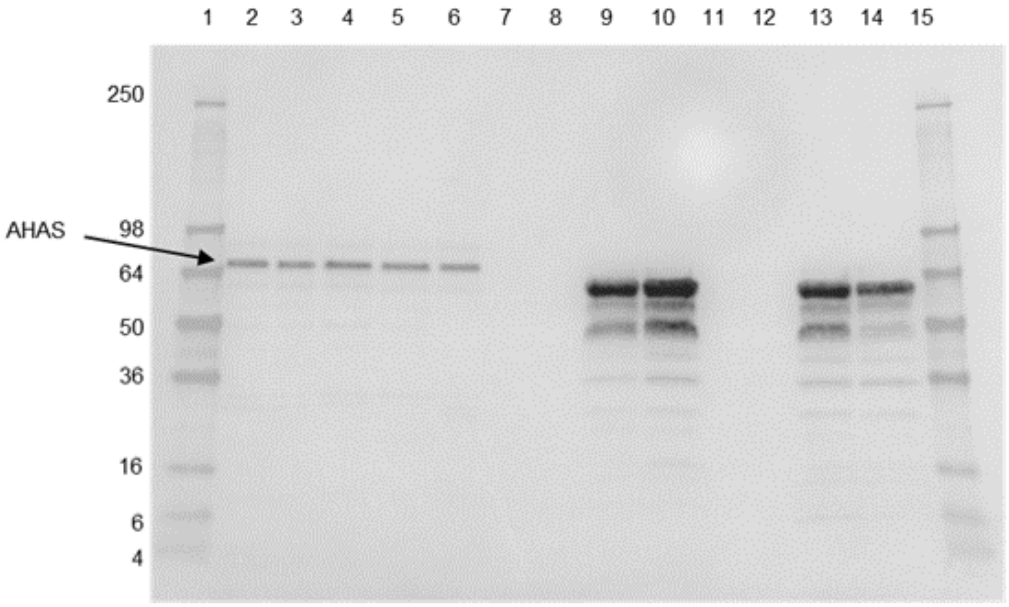

Lane	Sample	Incubation Time (min)
1	molecular weight marker	-
2	SD G-con	0.5
3	SD G-con	30
4	SD I-con	0.5
5	SD I-con	30
6	SD SGF	0
7	SD SGF	0.5
8	SD SGF	30
9	SD SGF → SIF	0.5
10	SD SGF → SIF	30
11	SD SGF alone	0.5
12	SD SGF alone	30
13	SD SIF alone	0.5
14	SD SIF alone	30
15	molecular weight marker	-

Conclusions on the toxicity assessment

A weight-of-evidence approach, which addressed HOSU and consumption, amino acid sequence similarity to known toxins or antinutrients, stability to heat (such as during commercial processing), and digestive fate, was used to demonstrate the safety of the newly

expressed proteins in LBFLFK (Table 28). The biological function and expression level of the proteins in the plant are found in section A.3(b)(i), and section A.3(e)(ii) and Table 22 in section B.1(c) respectively.

The lack of adverse findings identified by a systematic literature search for the newly expressed proteins and their donor organisms demonstrates their HOSU. Moreover, the protein sequence of each newly expressed protein was found to be structurally and functionally related to other proteins that are safely consumed by humans as food and by animals as feed. The wide distribution of proteins identified suggests that humans and animals have been exposed as part of their diet and environment to proteins similar to the desaturases and elongases present in LBFLFK for many years without adverse effects.

The observation that the amino acid sequences for desaturases and elongases are not highly conserved, especially when comparing different taxonomic groups, is an expected result for this class of proteins. For example, D6E(*Pp*) was found to be 36% identical to a sequence from *Mortierella alpina* that has been shown to have delta-6 elongase activity, and D4D(*Tc*) was shown to be 35.4% identical to an experimentally verified delta-4 desaturase from *Euglena gracilis*. A similar percent identity (around 32%) was observed between the integral membrane protein delta-9 stearoyl-CoA desaturases from mammals and other organisms (including crop plants) when determined using a protein sequence similarity network approach (Atkinson et al., 2009; Li et al., 2016). It is also worth noting that an integral membrane protein delta-9 desaturase from the fungus *Aspergillus nidulans* was shown to have 30–56% identity with desaturases present in food crops, and these data were used to conclude that similar proteins have been safely consumed by humans (Madduri et al., 2012). Furthermore, regioselectivity (i.e. whether a double bond is introduced at the delta-5 or delta-6 position) and substrate specificity (e.g., chain length of substrate) of desaturases and elongases can be altered by modifying only a few amino acids (López Alonso et al., 2003; Denic and Weissman, 2007; Lim et al., 2014). These findings explain why desaturases and elongases identified in food or feed sometimes have (or are predicted to have) different regioselectivity than the target sequence to which they are related. However, regardless of regioselectivity and substrate specificity, no reports of adverse effects have been identified due to exposure to any desaturase or elongase.

None of the newly expressed proteins in LBFLFK were shown by bioinformatic analysis to have significant homology to known protein toxins or antinutrients.

As discussed before, heat treatment sensitivity was evaluated by enzyme activity and structural integrity. The enzyme activity of D6D(*Ot*), D5D(*Tc*), O3D(*Pi*), and O3D(*Pir*) in response to heat treatment was not assessed because enzyme activity was not detectable in LBFLFK PPP. The heat sensitivity of these proteins was assessed by structural integrity only or not assessed (O3D(*Pi*)) due to the low amount of protein in LBFLFK PPP. Each of the newly expressed proteins assayed for structural integrity were heat-labile, and each of the newly expressed proteins assayed for enzymatic activity lost its activity, suggesting that enzyme activity is unlikely to remain after commercial processing.

Digestive fate analysis was used to determine the sensitivity of the newly expressed proteins to SGF and SIF digestion. Each of the newly expressed proteins assayed were found to be susceptible to digestion in SGF, SIF, or SGF followed by SIF.

The O3D(*Pi*) and D6E(*Pp*) proteins were not assessed for structural integrity to heat treatment or to digestibility in SGF or SIF because these proteins were not detected in LBFLFK PPP or LBFLFK tissues. The low amount of O3D(*Pi*) and D6E(*Pp*) proteins is unlikely to present a safety concern to humans or animals.

Overall, applying a weight-of-evidence approach, all newly expressed proteins in LBFLFK are considered to behave as any other dietary protein and thus do not raise any safety concerns with regard to human or animal health.

Table 28. Summary of Endpoints Related to the Safety Assessment of the Newly Expressed Proteins in LBFLFK

Protein	HOSU of the donor organism	HOSU of the newly expressed protein	Related to other proteins present in consumed food or feed	Similarity to known toxins and antinutrients based on bioinformatic analysis	Sensitive to heat treatment		Susceptible to digestion
					Loss of enzyme activity	Loss of structural integrity	
D12D(*Ps*)	Yes	Yes	Yes	No	Yes	Yes	Yes (SGF and SIF)
D6D(*Ot*)	Yes	Yes	Yes	No	NA[1]	Yes	Yes (SGF and SIF)
D6E(*Tp*)	Yes	Yes	Yes	No	Yes	Yes	Yes (SIF; SGF followed by SIF)
D6E(*Pp*)	Yes	Yes	Yes	No		NA[2]	NA[2]
D5D(*Tc*)	Yes	Yes	Yes	No	NA[1]	Yes	Yes (SGF and SIF)
O3D(*Pir*)	Yes	Yes	Yes	No	NA[1]	Yes	Yes (SGF and SIF)
O3D(*Pi*)	Yes	Yes	Yes	No		NA[2]	NA[2]
D5E(*Ot*)	Yes	Yes	Yes	No	Yes	Yes	Yes (SIF; SGF followed by SIF)
D4D(*Tc*)	Yes	Yes	Yes	No	Yes	Yes	Yes (SGF and SIF)
D4D(*Pl*)	Yes	Yes	Yes	No	Yes	Yes	Yes (SGF and SIF)
AHAS(*At*) [A122TS653N]	Yes	Yes	Yes	No	Yes	Yes	Yes (Leaf: SGF and SIF) Yes (PPP: SGF; SGF followed by SIF)

NA = not assessed

[1] Enzyme activity was not assessed because enzyme activity was not detectable in LBFLFK PPP (section B.1(c)).

[2] Loss of structural integrity to heat treatment or digestibility in SGF or SIF was not assessed because these proteins were not detected in LBFLFK PPP (section B.1(c)) and LBFLFK tissues (section A.3(e)(ii)).

(iii) An animal toxicity study if the bioinformatics comparison and biochemical studies indicate either a relationship with known protein toxins/anti-nutrients or resistance to proteolysis

The safety assessment of agricultural products produced through biotechnology includes an evaluation of the safety of the newly expressed proteins (Codex Alimentarius Commission, 2009b). This assessment is accomplished by applying a weight-of-evidence approach to the data generated from *in silico* and experimental studies. A weight-of-evidence approach is used because no single assay or biochemical characteristic can identify a protein as a hazard and, scientifically, it is not possible to prove a lack of hazard with complete certainty (Delaney et al., 2008).

Tier I testing (potential hazard identification) includes establishing a history of safe use (HOSU) and consumption (provided in section B.1(b) of this application), amino acid sequence similarity between the newly expressed protein and known protein toxins and antinutrients (section B.2(a)(i)), biological function of the protein in the plant (section A.3(b)(i)), stability to heat or conditions of commercial processing (section B.2(a)(ii)), degradation in appropriate representative gastric and intestinal model systems (section B.2(a)(ii)), and expression level (section A.3(e)(ii) and Table 22 in section B.1(c)) and dietary intake (Part C(a)). Tier II testing (hazard classification), which may be performed on a case-by-case basis if the first tier does not provide sufficient evidence to make a determination of safety, might include acute or repeated dose toxicity testing of the newly expressed proteins or hypothesis-based studies.

The safe use of the newly expressed proteins and their donor organisms was evaluated by a systematic literature search that identified relevant documents related to dietary or environmental exposure or toxicity of the newly expressed proteins or donor organisms. In addition, the amino acid sequence of each newly expressed protein was compared to the amino acid sequences of proteins present in consumed food or feed to identify sequence identity to proteins that are safely consumed by humans as food and by animals as feed. Based on Tier I testing, safety of the newly expressed proteins from LBFLFK canola was considered to have been demonstrated and no further acute toxicity or repeat-dose testing was considered necessary for the proteins.

(b) Information on the potential allergenicity of any new proteins, including:

(i) Source of the new protein

The safety assessment of agricultural products produced through biotechnology includes an evaluation of the potential allergenicity of the newly expressed proteins. This assessment is accomplished by applying a weight-of-evidence approach since no single criterion is sufficiently predictive of allergenicity or non-allergenicity. The weight-of-evidence approach includes an evaluation of the potential allergenicity associated with the source of the newly expressed protein (donor organism), the extent of similarity of the protein amino acid sequence to known allergens, the resistance to digestion by pepsin, and the effect of the conditions of commercial processing on the presence of the protein in the final food product (Codex Alimentarius Commission, 2009b).

Canola itself is not considered a major allergenic food source as it is not included on the list of allergens potentially present in food that require labelling in Australia (Standard 1.2.3 of the Food Standards Code). The allergenicity of the donor organisms was evaluated by a

systematic literature search that identified relevant documents related to dietary exposure (i.e. presence in food or feed) or allergenicity of the donor organism and by searching lists of allergens in available allergen databases.

Bioinformatic analysis of the amino acid sequence of each newly expressed protein was performed to determine the similarity of the amino acid sequence of the newly expressed proteins to known or putative allergens including food, respiratory, venom/salivary, or contact allergenic proteins. Nucleotide sequences from both LBFLFK Insert1 and LBFLFK Insert2 (section A.3(c)) were translated into amino acid sequences, and bioinformatic analysis was performed on both LBFLFK Insert1 and LBFLFK Insert2 sequences.

Proteins are subjected to a variety of conditions during commercial processing that can have a major impact on their function (Kilara et al., 1986; Meade et al., 2005). Thus, heat stability of the newly expressed proteins is evaluated to determine the impact of commercial processing conditions on enzyme activity and structural integrity.

A shared property of numerous allergenic proteins is their resistance to degradation (Astwood et al., 1996; Vieths et al., 1999; Vassilopoulou et al., 2006). Dietary proteins that are resistant to digestion are deemed more likely to elicit an immune response as their structures are preserved from degradation, allowing the allergen to survive and to provoke the immune system when absorbed by the small intestine (Metcalfe et al., 1996; Taylor, 2002; Moreno et al., 2005; Castro-Sánchez and Martín-Villa, 2013). Consequently, protein digestibility by stomach pepsin is used as a relevant parameter to assess the allergenic potential of newly expressed proteins. Based on knowledge of the relation of dietary allergens and gastrointestinal digestion, a digestion assay in simulated gastric fluid (SGF) containing pepsin has been developed for assessing the allergenic capacity of newly expressed proteins. This widely used SGF assay was standardised by the International Life Science Institute (ILSI) based on an international, multi-laboratory ring study (Thomas et al., 2004). The ring study concluded that the standardised SGF assay is robust, and the results are reproducible in different laboratories. Although the correlation of protein stability in pepsin and the likelihood of a protein being an allergen is not absolute (Fu et al., 2002; Díaz-Perales et al., 2003; Lee et al., 2005a), the SGF assay is the most commonly used method to assess newly expressed proteins for allergenicity.

Proteins that pass the stomach with little or no degradation could still be degraded by intestinal enzymes, reducing the likelihood of absorption of larger protein fragments in the small intestine. Consequently, protein digestibility in simulated intestinal fluid (SIF) containing pancreatin is used in addition to the SGF assay (Yagami et al., 2000; Okunuki et al., 2002; Huang et al., 2010) as an additional parameter to assess the allergenic potential of newly expressed proteins. Pancreatin is a mixture of enzymes that contains amylases, lipases, and proteases produced by the pancreas. This mixture of enzymes not only digests proteins but also lipids and carbohydrates. The stand-alone SIF assay (not preceded by the SGF assay) omits the exposure of the newly expressed protein to the acidic denaturing condition of the stomach and does not fully mimic the digestion condition *in vivo*. It has been shown that allergens from avocado, banana, potato, melon, and peach, which were degraded in the SGF assay within 8 minutes (min), were not completely degraded in the SIF assay for up to 16 hours of incubation (Yagami et al., 2000). The stand-alone SIF assay may provide additional information within the weight-of-evidence approach for allergenicity assessment of newly expressed proteins. Furthermore, if protein fragments are observed in the SGF assay, a

sequential digestion (pepsin digestion followed by pancreatin digestion) to more closely mimic the *in vivo* conditions for protein digestion may also be appropriate (Hammond, 2007).

Specifically, for LBFLFK, heat stability and digestibility studies of the newly expressed proteins were performed with a membrane fraction purified from crude extracts of developing embryos that were isolated from immature seeds of LBFLFK. This detergent-free membrane fraction, referred to as "plant-produced proteins" (PPP), contains the newly expressed elongases and desaturases. The digestive fate assessment of AHAS(*At*) [A122TS653N] was performed with AHAS(*At*) [A122TS653N] protein present in LBFLFK PPP and LBFLFK leaf isolates. The results of these studies for each introduced protein are summarised above in section B.2(a)(ii). More details on the results are provided in Appendix 21.

(ii) A bioinformatics comparison of the amino acid sequence of the novel protein to known allergens

Delta-12-desaturase (*Ps*)

Donor organism

The allergenicity of *Phytophthora* sojae (*P. sojae*), the donor organism for the *D12D*(*Ps*) gene, was evaluated by a systematic literature search that identified relevant documents related to dietary exposure (i.e. presence in food or feed) or allergenicity of the donor organism. In addition, both the COMPARE Allergen Database[12], which includes a comprehensive repository of all known allergens with clinical evidence of allergenicity based on standardised criteria, and the Food Allergy Research and Resource Program (FARRP) Allergen Protein Database[13], which provides access to a peer-reviewed allergen list, were analysed for any amino acid sequences from *P. sojae*. No evidence indicating that *P. sojae* produces or contains known or putative allergens or elicits an allergenic response has been identified. For more information on *P. sojae*, refer to section A.2(a).

Bioinformatic analysis – allergens

Bioinformatic analysis was used to determine whether the amino acid sequence of D12D(*Ps*) had significant sequence similarity to known or putative allergens. The amino acid sequences from both LBFLFK Insert1 and LBFLFK Insert2 were used for bioinformatic analysis. For D12D(*Ps*), LBFLFK Insert1 includes a nucleotide change in the coding region, which results in the F83L amino acid substitution (section A.3(c)(ii)). D12D(*Ps*) did not share > 35% identity over 80 amino acids, a sequence with 100% identity over eight amino acids (Silvanovich et al., 2005), or significant homology (Silvanovich et al., 2009) to any amino acid sequence in the FARRP Allergen Protein Database.

Delta-6 desaturase (*Ot*)

Donor organism

The allergenicity of *Ostreococcus tauri,* the donor organism for the *D6D*(*Ot*) gene, was evaluated by a systematic literature search that identified relevant documents related to dietary exposure (i.e. presence in food or feed) or allergenicity of the donor organism. In

12 http://comparedatabase.org/about-compare-database/

13 http://www.allergenonline.org

addition, both the COMPARE Allergen Database, which includes a comprehensive repository of all known allergens with clinical evidence of allergenicity based on standardised criteria, and the Food Allergy Research and Resource Program (FARRP) Allergen Protein Database, which provides access to a peer-reviewed allergen list, were analysed for any amino acid sequences from *O. tauri*. No evidence indicating that *O. tauri* produces or contains known or putative allergens or elicits an allergenic response has been identified. For more information on *O. tauri*, refer to section A.2(a).

Bioinformatic analysis – allergens

Bioinformatic analysis was used to determine whether the amino acid sequence of D6D(*Ot*) had significant sequence similarity to known or putative allergens. D6D(*Ot*) did not share > 35% identity over 80 amino acids, a sequence with 100% identity over eight amino acids (Silvanovich et al., 2005), or significant homology (Silvanovich et al., 2009) to any amino acid sequence in the FARRP Allergen Protein Database.

Delta-6 elongase (*Tp*)

Donor organism

The allergenicity of *Thalassiosira pseudonana*, the donor organism for the *D6E*(*Tp*) gene, was evaluated by a systematic literature search that identified relevant documents related to dietary exposure (i.e. presence in food or feed) or allergenicity of the donor organism. In addition, both the COMPARE Allergen Database, which includes a comprehensive repository of all known allergens with clinical evidence of allergenicity based on standardised criteria, and the Food Allergy Research and Resource Program (FARRP) Allergen Protein Database, which provides access to a peer-reviewed allergen list, were analysed for any amino acid sequences from *T. pseudonana*. No evidence indicating that *T. pseudonana* produces or contains known or putative allergens or elicits an allergenic response has been identified. For more information on *T. pseudonana*, refer to section A.2(a).

Bioinformatic analysis – allergens

Bioinformatic analysis was used to determine whether the amino acid sequence of D6E(*Tp*) had significant sequence similarity to known or putative allergens. D6E(*Tp*) did not share > 35% identity over 80 amino acids, a sequence with 100% identity over eight amino acids (Silvanovich et al., 2005), or significant homology (Silvanovich et al., 2009) to any amino acid sequence in the FARRP Allergen Protein Database.

Delta-6 elongase (*Pp*)

Donor organism

The allergenicity of *Physcomitrella patens*, the donor organism for the *D6E*(*Pp*) gene, was evaluated by a systematic literature search that identified relevant documents related to dietary exposure (i.e. presence in food or feed) or allergenicity of the donor organism. In addition, both the COMPARE Allergen Database, which includes a comprehensive repository of all known allergens with clinical evidence of allergenicity based on standardised criteria, and the Food Allergy Research and Resource Program (FARRP) Allergen Protein Database, which provides access to a peer-reviewed allergen list, were analysed for any amino acid sequences from *P. patens*. No evidence indicating that *P. patens* produces or contains known

or putative allergens or elicits an allergenic response has been identified. For more information on *P. patens*, refer to section A.2(a).

Bioinformatic analysis – allergens

Bioinformatic analysis was used to determine whether the amino acid sequence of D6E(*Pp*) had significant sequence similarity to known or putative allergens. D6E(*Pp*) did not share > 35% identity over 80 amino acids, a sequence with 100% identity over eight amino acids (Silvanovich et al., 2005), or significant homology (Silvanovich et al., 2009) to any amino acid sequence in the FARRP Allergen Protein Database.

Delta-5 desaturase (*Tc*)

Donor organism

The allergenicity of *Thraustochytrium* sp., the donor organism for the *D5D*(*Tc*) gene, was evaluated by a systematic literature search that identified relevant documents related to dietary exposure (i.e. presence in food or feed) or allergenicity of the donor organism. In addition, both the COMPARE Allergen Database, which includes a comprehensive repository of all known allergens with clinical evidence of allergenicity based on standardised criteria, and the Food Allergy Research and Resource Program (FARRP) Allergen Protein Database, which provides access to a peer-reviewed allergen list, were analysed for any amino acid sequences from *Thraustochytrium* sp. No evidence indicating that *Thraustochytrium* sp. produce or contain known or putative allergens or elicits an allergenic response has been identified. For more information on *Thraustochytrium* sp., refer to section A.2(a).

Bioinformatic analysis – allergens

Bioinformatic analysis was used to determine whether the amino acid sequence of D5D(*Tc*) had significant sequence similarity to known or putative allergens. D5D(*Tc*) did not share > 35% identity over 80 amino acids, a sequence with 100% identity over eight amino acids (Silvanovich et al., 2005), or significant homology (Silvanovich et al., 2009) to any amino acid sequence in the FARRP Allergen Protein Database.

Omega-3 desaturase (*Pir*)

Donor organism

The allergenicity of *Pythium irregulare,* the donor organism for the *O3D*(*Pir*) gene, was evaluated by a systematic literature search that identified relevant documents related to dietary exposure (i.e. presence in food or feed) or allergenicity of the donor organism. In addition, both the COMPARE Allergen Database, which includes a comprehensive repository of all known allergens with clinical evidence of allergenicity based on standardised criteria, and the Food Allergy Research and Resource Program (FARRP) Allergen Protein Database, which provides access to a peer-reviewed allergen list, were analysed for any amino acid sequences from *P. irregulare*. No evidence indicating that *P. irregulare* produces or contains known or putative allergens or elicits an allergenic response has been identified. For more information on *P. irregulare*, refer to section A.2(a).

Bioinformatic analysis – allergens

Bioinformatic analysis was used to determine whether the amino acid sequence of O3D (*Pir*) had significant sequence similarity to known or putative allergens. O3D(*Pir*) did not share > 35% identity over 80 amino acids, a sequence with 100% identity over eight amino acids (Silvanovich et al., 2005), or significant homology (Silvanovich et al., 2009) to any amino acid sequence in the FARRP Allergen Protein Database.

Omega-3 desaturase (*Pi*)

Donor organism

The allergenicity of *Phytophthora infestans*, the donor organism for the *O3D*(*Pi*) gene, was evaluated by a systematic literature search that identified relevant documents related to dietary exposure (i.e. presence in food or feed) or allergenicity of the donor organism. In addition, both the COMPARE Allergen Database, which includes a comprehensive repository of all known allergens with clinical evidence of allergenicity based on standardised criteria, and the Food Allergy Research and Resource Program (FARRP) Allergen Protein Database, which provides access to a peer-reviewed allergen list, were analysed for any amino acid sequences from *P. infestans*. No evidence indicating that *P. infestans* produces or contains known or putative allergens or elicits an allergenic response has been identified. For more information on *P. infestans*, refer to section A.2(a).

Bioinformatic analysis – allergens

Bioinformatic analysis was used to determine whether the amino acid sequence of O3D (*Pi*) had significant sequence similarity to known or putative allergens. O3D (*Pi*) did not share > 35% identity over 80 amino acids, a sequence with 100% identity over eight amino acids (Silvanovich et al., 2005), or significant homology (Silvanovich et al., 2009) to any amino acid sequence in the FARRP Allergen Protein Database.

Delta-5 elongase (*Ot*)

Donor organism

The allergenicity of *Ostreococcus tauri,* the donor organism for the *D5E*(*Ot*) gene, was evaluated by a systematic literature search that identified relevant documents related to dietary exposure (i.e. presence in food or feed) or allergenicity of the donor organism. In addition, both the COMPARE Allergen Database, which includes a comprehensive repository of all known allergens with clinical evidence of allergenicity based on standardised criteria, and the Food Allergy Research and Resource Program (FARRP) Allergen Protein Database, which provides access to a peer-reviewed allergen list, were analysed for any amino acid sequences from *O. tauri*. No evidence indicating that *O. tauri* produces or contains known or putative allergens or elicits an allergenic response has been identified. For more information on *O. tauri*, refer to section A.2(a).

Bioinformatic analysis – allergens

Bioinformatic analysis was used to determine whether the amino acid sequence of D5E(*Ot*) had significant sequence similarity to known or putative allergens. D5E(*Ot*) did not share > 35% identity over 80 amino acids, a sequence with 100% identity over eight amino acids

(Silvanovich et al., 2005), or significant homology (Silvanovich et al., 2009) to any amino acid sequence in the FARRP Allergen Protein Database.

Delta-4 desaturase (*Tc*)

Donor organism

The allergenicity of *Thraustochytrium* sp.*,* the donor organism for the *D4D*(*Tc*) gene, was evaluated by a systematic literature search that identified relevant documents related to dietary exposure (i.e. presence in food or feed) or allergenicity of the donor organism. In addition, both the COMPARE Allergen Database, which includes a comprehensive repository of all known allergens with clinical evidence of allergenicity based on standardised criteria, and the Food Allergy Research and Resource Program (FARRP) Allergen Protein Database, which provides access to a peer-reviewed allergen list, were analysed for any amino acid sequences from *Thraustochytrium* sp. No evidence indicating that *Thraustochytrium* sp. produce or contain known or putative allergens or elicit an allergenic response has been identified. For more information on *Thraustochytrium* sp., refer to section A.2(a).

Bioinformatic analysis – allergens

Bioinformatic analysis was used to determine whether the amino acid sequence of D4D(*Tc*) had significant sequence similarity to known or putative allergens. D4D(*Tc*) did not share > 35% identity over 80 amino acids, a sequence with 100% identity over eight amino acids (Silvanovich et al., 2005), or significant homology (Silvanovich et al., 2009) to any amino acid sequence in the FARRP Allergen Protein Database.

Delta-4 desaturase (*Pl*)

Donor organism

The allergenicity of *Pavlova lutheri,* the donor organism for the *D4D*(*Pl*) gene, was evaluated by a systematic literature search that identified relevant documents related to dietary exposure (i.e. presence in food or feed) or allergenicity of the donor organism. In addition, both the COMPARE Allergen Database, which includes a comprehensive repository of all known allergens with clinical evidence of allergenicity based on standardised criteria, and the Food Allergy Research and Resource Program (FARRP) Allergen Protein Database, which provides access to a peer-reviewed allergen list, were analysed for any amino acid sequences from *P. lutheri*. No evidence indicating that *P. lutheri* produces or contains known or putative allergens or elicits an allergenic response has been identified. For more information on *P. lutheri*, refer to section A.2(a).

Bioinformatic analysis – allergens

Bioinformatic analysis was used to determine whether the amino acid sequence of D4D(*Pl*) had significant sequence similarity to known or putative allergens. The amino acid sequences from both LBFLFK Insert1 and LBFLFK Insert2 were used for bioinformatic analysis. For D4D(*Pl*), LBFLFK Insert2 includes a nucleotide change in the coding region, which results in the A102S amino acid substitution. D4D(*Pl*) did not share > 35% identity over 80 amino acids, a sequence with 100% identity over eight amino acids (Silvanovich et al., 2005), or significant homology (Silvanovich et al., 2009) to any amino acid sequence in the FARRP Allergen Protein Database.

Acetohydroxy acid synthase (*At*) [A122TS653N]

Donor organism

The allergenicity of *Arabidopsis thaliana*, the donor organism for the *AHAS*(*At*) gene, was evaluated by a systematic literature search that identified relevant documents related to dietary exposure (i.e. presence in food or feed) or allergenicity of the donor organism. In addition, both the COMPARE Allergen Database (Health and Environmental Sciences Institute, 2017), which includes a comprehensive repository of all known allergens with clinical evidence of allergenicity based on standardised criteria, and the Food Allergy Research and Resource Program (FARRP) Allergen Protein Database, which provides access to a peer-reviewed allergen list, were analysed for any amino acid sequences from *A. thaliana*. No evidence indicating that *A. thaliana* produces or contains known or putative allergens or elicits an allergenic response was identified from these analyses. However, a few sporadic publications indicating the presence of potentially allergenic proteins in *A. thaliana* have been reported. The lipid transfer protein 1 in *A. thaliana* has been identified as a possible allergen (i.e. recognised by human IgE) (Chardin et al., 2003), and one case of occupational asthma was reported in a laboratory worker due to inhalation exposure to *A. thaliana* pollen (Yates et al., 2008). *A. thaliana* also contains profilins, small proteins that are thought to be responsible for certain types of allergies (Thorn et al., 1997). Finally, one study reported that the Arabidopsis genome encodes Pollen Ole e 1 domain-containing proteins (Hu et al., 2014) that are present in many plants (Jiménez-López et al., 2011). Nonetheless, *A. thaliana* is a member of the mustard (Brassicaceae) family, which includes several cultivated vegetable species such as broccoli, cabbage, cauliflower, turnip, rapeseed, and radish, indicating repeated exposure of humans and animals in the diets and environment. For more information on *A. thaliana*, refer to section A.2(a).

Bioinformatic analysis – allergens

Bioinformatic analysis was used to determine whether the amino acid sequence of AHAS(*At*) [A122TS653N] had significant sequence similarity to known or putative allergens. AHAS(*At*) [A122TS653N] did not share > 35% identity over 80 amino acids, a sequence with 100% identity over eight amino acids (Silvanovich et al., 2005), or significant homology (Silvanovich et al., 2009) to any amino acid sequence in the FARRP Allergen Protein Database.

Conclusions on the allergenicity assessment

A weight-of-evidence approach, which addressed the potential allergenicity associated with the source of the newly expressed protein (donor organism), the extent of similarity of the protein's amino acid sequence to known allergens, the resistance to digestion by pepsin, and the effect of the conditions of commercial processing on the presence of the protein in the final food product (Codex Alimentarius Commission, 2009b), was used to assess the potential allergenicity of the newly expressed proteins in LBFLFK (Table 28).

No evidence indicating that any of the donor organisms contain known or putative allergens or elicit an allergenic response was identified by a systematic literature search or by searching lists of allergens in available allergen databases.

None of the newly expressed proteins in LBFLFK were shown by bioinformatic analysis to have significant homology to proteins that are known or putative allergens, including food, respiratory, venom/salivary, or contact allergenic proteins.

Heat treatment sensitivity was evaluated by enzyme activity and structural integrity. The enzyme activity of D6D(*Ot*), D5D(*Tc*), O3D(*Pi*), and O3D(*Pir*) in response to heat treatment was not assessed because enzyme activity was not detectable in LBFLFK PPP. The heat sensitivity of these proteins was assessed by structural integrity only or not assessed (O3D(*Pi*)) due to the low amount of protein in LBFLFK PPP. Each of the newly expressed proteins assayed for structural integrity were heat-labile, and each of the newly expressed proteins assayed for enzymatic activity lost its activity, suggesting that enzyme activity is unlikely to remain after commercial processing (section B.2(a)(ii)).

Digestive fate analysis was used to determine the sensitivity of the newly expressed proteins to SGF and SIF digestion. Each of the newly expressed proteins assayed were found to be susceptible to digestion in SGF, SIF, or SGF followed by SIF.

The O3D(*Pi*) and D6E(*Pp*) proteins were not assessed for structural integrity to heat treatment or to digestibility in SGF or SIF because these proteins were not detected in LBFLFK PPP or LBFLFK tissues. The low amount of O3D(*Pi*) and D6E(*Pp*) proteins is unlikely to present a safety or allergenic risk to humans or animals.

Overall, applying a weight-of-evidence approach, all newly expressed proteins in LBFLFK are considered unlikely to be food allergens.

(iii) The new protein's structural properties, including, but not limited to, its susceptibility to enzymatic degradation (e.g., proteolysis), heat and/or acid stability

Please refer to sections B.2(a) and B.2(b) above for information on enzymatic degradation and heat and acid stability for the proteins considered in this submission.

(iv) Specific serum screening where a new protein is derived from a source known to be allergenic or has sequence homology with a known allergen

As discussed in sections A.2(a) and B.1(b), the proteins expressed by LBFLFK canola are derived from organisms with a HOSU, and these proteins show no evidence of being allergenic based on extensive literature searches, bioinformatic analysis, tests for heat stability, and analysis of the proteolytic profile of each in SGF, SIF, or SGF followed by SIF. There is no evidence of allergenicity or sequence homology with known allergens that suggest specific serum screening of any of the new proteins expressed by LBFLFK canola is necessary.

(v) Information on whether the new protein(s) have a role in the elicitation of gluten-sensitive enteropathy, in cases where the introduced genetic material is obtained from wheat, rye, barley, oats, or related cereal grains.

Not applicable. The introduced genetic material is not obtained from wheat, rye, barley, oats, or related cereal grains.

Refer to section B.1(a). Note that microbially produced proteins were not utilised, only samples expressed *in planta* and extracted to form the PPP were utilised for protein characterisation and safety assessment. Therefore, evidence that microbially produced proteins are biochemically, structurally, and functionally equivalent to that expressed in the food produced using gene technology is not required.

B.3 Other (Non-Protein) New Substances

(a) The identity and biological function of the substance

The fatty acid biosynthetic pathway introduced in LBFLFK canola intentionally impacted the content of omega-3 LC-PUFAs due to the introduction of the EPA+DHA trait and changed the fatty acid profile in the grain of LBFLFK canola. Fatty acid levels in grain of LBFLFK canola are reported in section B.5(a).

(b) Whether the substance has previously been safely consumed in food

All fatty acids with altered levels are already present in foods that are considered safe for consumption; therefore, no further assessment is considered necessary.

(c) Potential dietary exposure to the substance

ANZ Food Standards Code Schedule 4 – Nutrition, health and related claims contains entries for long chain Omega-3 fatty acids, including DHA. The conditions for permitted general level health claims Part 3 – Other notes EPA and DHA as having the specific health effect of "Contributes to heart health" when part of a "Diet containing 500mg of EPA and DHA per day". For the Australian and New Zealand populations, an example nutritional and dietary intake assessment is available for DHA canola (FSANZ, 2017). The nutrients of interest in these assessments were n-3 LC-PUFAs. The only nutrient reference values that are established are for n-3 LC-PUFAs, rather than specifically for DHA (FSANZ, 2017). Therefore, it can be concluded that none of the substances in LBFLFK canola are new to the New Zealand and Australia population and should be a part of everyday dietary intake. Thus, a potential dietary exposure assessment to LBFLFK canola is not warranted. LBFLFK canola will provide an alternative source of EPA and DHA for existing markets.

(d) Where RNA interference has been used:

Not applicable. RNA interference has not been used.

(i) The role of any endogenous target gene and any changes to the food as a result of silencing that gene

Not applicable. RNA interference has not been used.

(ii) The expression levels of the RNA transcript

Not applicable. RNA interference has not been used.

(iii) The specificity of the RNA interference

Not applicable. RNA interference has not been used.

B.4 Novel Herbicide Metabolites in GM Herbicide-Tolerant Plants

The AHAS(*At*) protein catalyses the first step in the biosynthesis of branched-chain amino acids. The amino acid substitutions impair imidazolinone binding to the AHAS(*At*) large subunit protein, rendering plants containing the protein tolerant to treatment with imidazolinone herbicides (Haughn and Somerville, 1990).

The AHAS(*At*) [A122TS653N] protein expressed in LBFLFK canola is encoded by a gene from *A. thaliana* and harbours two amino acid substitutions, [A122T] and [S653N], that confer tolerance to imidazolinone herbicides (Tan et al., 2005). Several commercialised crops have herbicide tolerance conferred by alleles of the *ahas* gene (e.g., Clearfield canola, Clearfield wheat, Clearfield sunflower, Clearfield lentils).

The herbicide tolerance trait of LBFLFK canola will allow for selective post-emergence weed control during field production. The use of herbicide with the active ingredient imazamox (an imidazolinone), such as Beyond herbicide, will follow the same agronomic practices as used for Clearfield canola. The first imidazolinone tolerant canola (also known as Smart canola or Clearfield) was released in Australia in 2000. These varieties have been widely adopted (Cowling, 2007), and herbicide applications for LBFLFK canola will follow established weed control practice.

B.5 Compositional Analyses of the Food Produced Using Gene Technology

(a) The levels of relevant key nutrients, toxicants and anti-nutrients in the food produced using gene technology compared with the levels in appropriate comparator (usually the non-GM counterpart). A statistical analysis of the data must be provided.

Nutrient composition of the harvested grain

As part of the food, feed, and environmental safety assessment of EPA+DHA canola event LBFLFK, a comparative assessment of grain components of LBFLFK was performed. For this assessment, LBFLFK, along with the parental control variety Kumily and conventional canola (*Brassica napus*) reference varieties, were grown and harvested under the same conditions at multiple locations. The purpose of the comparison, performed following Codex guidelines (Codex Alimentarius Commission, 2009b), was to establish that nutritional components were not altered in a manner that would have an adverse impact on human and animal health or the environment.

Canola grain harvested from field-grown plots was used for compositional analysis. This includes plots of LBFLFK sprayed with Beyond herbicide (sprayed), LBFLFK (non-sprayed), Kumily, and six conventional reference varieties (Q2, 46A65, IMC105, IMC302, Wizzard, and Orinoco). Data from two growing seasons (Table 29), winter 2014/15 and spring 2015, were generated. Harvested mature seed from five of the winter trials and from seven of the spring trials were used for compositional analysis, with comparisons both within and across seasons. All four plot replicates of a field entry at each location were analysed. Additional information on the study design can be found in Appendix 22.

Table 29. Field Trial Locations used for Compositional Analysis of Harvested Seed

Field Trial ID	City, State	Trial Season
3SRBLY1	[redacted]	Winter 2014/15
3SRJV		Winter 2014/15
3SRKT		Winter 2014/15
3SROM		Winter 2014/15
3SRRH		Winter 2014/15
3NRLS		Spring 2015
3NRGE		Spring 2015
3NRCB		Spring 2015
3NRNW-1		Spring 2015
3NRMA-2		Spring 2015
3NREP		Spring 2015
3NRLS		Spring 2015

The components selected for analysis were based primarily on the guidance provided in the consensus document for canola from the Organisation for Economic Co-operation and Development (OECD, 2011b). A total of 112 components were measured in canola grain (Table 30).

Across-site statistical analyses for the detection of genotype-by-environment (referred to in this document as entry-by-site) interactions and for differences between LBFLFK and Kumily were carried out for all compositional assessments. Some data were transformed to avoid strong deviations from analysis of variance (ANOVA) assumptions. Linear mixed model ANOVA methods were used for performing mean comparisons between the LBFLFK entries (sprayed or non-sprayed) and Kumily. A significance level of $\alpha = 0.05$ (confidence level = 95%) was used for all statistical tests. Individual site analyses were performed if a statistically significant entry-by-site interaction was observed. Data meeting at least one of the following three criteria were considered not suitable for ANOVA.

- The characteristic has 6 or less distinct values.
- The mode of the characteristic has more than 40% frequency.
- More than 40% of the site-entry combinations had null variance.

Across-site mean values were compared to 1) the range of means generated from the reference varieties, 2) the International Life Sciences Institute (ILSI) Crop Composition Database data (ILSI, 2016), and 3) peer-reviewed scientific literature to provide context for the comparative analyses and assess the broader biological relevance of the results.

Additional details of the materials and methods for compositional analysis, including the statistics used for data comparisons, the results of by-site individual site analysis performed, and a table presenting the reference data from the ILSI Crop Composition database and peer-reviewed scientific literature, are provided in Appendix 22.

Table 30. Measured Canola Grain Components

Amino Acids[1]		
Alanine	Leucine	Threonine
Arginine	Isoleucine	Tryptophan
Aspartic Acid	Methionine	Tyrosine
Cystine	Phenylalanine	Valine
Glutamic Acid	Proline	Hydroxyproline
Glycine	Serine	Total Lysine
Histidine		
Antinutrients[1]		
Progoitrin	Gluconapoleiferin	4-Hydroxyglucobrassicin
Glucoalyssin	Gluconasturtiin	Phytic Acid
Glucobrassicin	Glucoraphanin	Tannins
Glucobrassicanapin	Neoglucobrassicin	Sinapine
Glucoiberin	Epi-Progoitrin	Coumaric Acid
Gluconapin	Total Glucosinolates[4]	Ferulic Acid
Fatty Acids[2]		
C14:0	C18:2n-9	C20:4n-6
C16:0	C18:2 trans	C20:5n-3
C16:1n-7	C18:3n-3	C22:0
C16:1n-9	C18:3n-6	C22:1n-9
C16:1 trans	C18:4n-3	C22:2n-6
C16:3n-3	C20:0	C22:4n-3
C17:0	C20:1n-9	C22:4n-6
C17:1	C20:2n-6	C22:5n-3
C18:0	C20:2n-9	C22:5n-6
C18:1n-7	C20:3n-3	C22:6n-3
C18:1n-9	C20:3n-6	C24:0
C18:1 trans	C20:3n-9	C24:1n-9
C18:2n-6	C20:4n-3	Total trans fatty acids
Minerals[1]		
Calcium	Phosphorus	Potassium
Copper	Magnesium	Sodium
Iron	Manganese	Zinc
Proximates and Fibres[1]		
Acid detergent fibre	Ash	Moisture[3]
Crude fibre	Crude fat	Protein
Neutral detergent fibre		
Sterols[1]		
24-Methylene cholesterol	Cholesterol	Delta-7 avenasterol
Beta-sitosterol	Clerosterol	Delta-7 stigmastenol
Brassicasterol	Delta-5 avenasterol	Sitostanol
Campestanol	Delta-5,23 stigmastadienol	Stigmasterol
Campesterol	Delta-5,24 stigmastadienol	Total phytosterols
Vitamins[1]		
Vitamin K1	Beta-tocopherol	Delta-tocopherol
Alpha-tocopherol	Gamma-tocopherol	Total tocopherols

[1] Data are reported on a dry weight basis.
[2] Data are reported as percent of total fatty acids.
[3] Data are reported as percent of fresh weight.
[4] Data are obtained by calculation.

Proximates and fibres

Proximates and fibres are major components of canola grain that impact processing and the application of processed products as a food and animal feed (OECD, 2011b). The proximates and fibre components analysed were moisture, crude fat, protein, ash, crude fibre, acid detergent fibre, and neutral detergent fibre. These components were measured on a percent dry weight basis except for moisture, which was measured on a percent fresh weight basis.

Winter 2014/15 season

For all proximate and fibre components across all locations for the 2014/15 season (Table 31), no statistically significant differences were observed between LBFLFK and Kumily. Only neutral detergent fibre had a statistically significant entry-by-site interaction for this season, with statistically significant differences at three locations and LBFLFK sometimes above the range of the references, but with no consistent trend seen across locations. The across-site means for all proximate and fibre components for LBFLFK were within the range of the reference varieties.

Spring 2015 season

For the 2015 season, statistically significant differences, though small in magnitude, were observed for acid detergent fibre, crude fibre, and neutral detergent fibre (Table 32). LBFLFK was statistically significantly lower than Kumily for acid detergent fibre, crude fibre, and neutral detergent fibre. There were no statistically significant entry-by-site interactions for this season. The results for all proximate and fibre components for LBFLFK (sprayed and non-sprayed) were within the range of the reference varieties.

Table 31. Proximates and Fibre – Across-Site Summary Statistics – Winter 2014/15

Component (% dry weight)	Control (Kumily)	LBFLFK (sprayed)[1]	Control minus LBFLFK (sprayed)	Reference Variety Range	LBFLFK (non-sprayed)[2]	Control minus LBFLFK (non-sprayed)
	Mean (SE) min–max	Mean (SE) min–max	Difference (SE) (p-value)[3]	min–max	Mean (SE) min–max	Difference (SE) (p-value)[3]
Acid detergent fibre	13.50 (0.27) 12.85–13.97	13.93 (0.27) 12.82–15.28	-0.43 (0.34) (0.231)	11.09–14.52	13.87 (0.27) 13.45–14.15	-0.37 (0.34) (0.307)
Ash	4.73 (0.21) 4.22–5.09	4.70 (0.21) 4.08–5.52	0.023 (0.13) (0.869)	3.59–5.77	4.62 (0.21) 4.10–5.35	0.11 (0.13) (0.451)
Crude fat	35.11 (1.83) 30.98–42.46	34.46 (1.83) 31.23–40.59	0.65 (0.44) (0.176)	27.82–44.56	35.42 (1.83) 32.41–41.72	-0.31 (0.44) (0.498)
Crude fibre	13.56 (0.28) 13.07–14.05	13.21 (0.28) 12.08–14.12	0.35 (0.4) (0.387)	11.07–14.80	13.03 (0.28) 12.03–13.5	0.54 (0.4) (0.186)
Moisture[4]	8.39 (0.21) 7.77–8.91	8.36 (0.21) 7.92–8.96	0.029 (0.087) (0.742)	7.59–9.45	8.29 (0.21) 7.60–8.83	0.11 (0.087) (0.246)
Neutral detergent fibre	16.92 (0.36) 16.10–18.40	16.84 (0.36) 15.85–18.70	0.07 (0.51) (0.886)	14.97–18.02	17.03 (0.36) 16.77–17.55	-0.11 (0.5) (0.833)
Protein	26.53 (1.43) 20.75–28.34	26.60 (1.43) 21.54–28.88	-0.07 (0.36) (0.849)	21.45–32.03	26.41 (1.43) 20.51–28.45	0.12 (0.36) (0.748)

[1] LBFLFK (sprayed) received standard herbicide treatments for weed control plus Beyond herbicide spray (35 g a.i./ha) at the 3–4 leaf stage.
[2] LBFLFK (non-sprayed) received standard herbicide treatments for weed control but no Beyond herbicide spray.
[3] Difference test p-value: * indicates p≤ 0.05; means are averages of five locations with four plot replications at each location.
[4] Moisture content in fresh weight.

Table 32. Proximates and Fibres – Across-Site Summary Statistics – Spring 2015

Component (% dry weight)	Control (Kumily)	LBFLFK (sprayed)[1]	Control minus LBFLFK (sprayed)	Reference Variety Range	LBFLFK (non-sprayed)[2]	Control minus LBFLFK (non-sprayed)
	Mean (SE) min–max	Mean (SE) min–max	Difference (SE) (p-value)[3]	min–max	Mean (SE) min–max	Difference (SE) (p-value)[3]
Acid detergent fibre	11.73 (0.3) 10.95–13.1	11.32 (0.3) 10.39–13.1	0.41 (0.2) (0.046)*	9.14–11.95	11.29 (0.3) 10.41–12.18	0.43 (0.2) (0.034)*
Ash	4.57 (0.16) 4.13–5.38	4.50 (0.16) 3.93–5.24	0.076 (0.064) (0.238)	3.92–5.53	4.55 (0.16) 4.09–5.15	0.021 (0.064) (0.749)
Crude fat	38.95 (0.96) 34.02–42.17	38.45 (0.96) 31.95–45.08	0.49 (0.64) (0.444)	31.29–44.23	38.6 (0.96) 35.22–41.90	0.34 (0.64) (0.595)
Crude fibre	10.37 (0.19) 9.46–11.00	9.39 (0.19) 8.90–10.24	0.99 (0.17) (< 0.001)*	7.57–10.95	9.39 (0.19) 8.70–9.83	0.98 (0.17) (< 0.001)*
Moisture[4]	7.33 (0.14) 6.64–7.73	7.30 (0.14) 6.70–7.66	0.03 (0.05) (0.559)	6.37–8.10	7.25 (0.14) 6.57–7.66	0.088 (0.05) (0.108)
Neutral detergent fibre	15.26 (0.26) 14.45–16.3	14.55 (0.26) 13.65–15.40	0.72 (0.29) (0.031)*	12.45–15.7	14.51 (0.26) 13.80–15.72	0.76 (0.29) (0.024)*
Protein	26.21 (0.56) 24.50–28.18	26.17 (0.56) 24.57–27.78	0.042 (0.17) (0.802)	22.53–31.24	26.29 (0.56) 24.13–28.18	-0.075 (0.17) (0.655)

[1] LBFLFK (sprayed) received standard herbicide treatments for weed control plus Beyond herbicide spray (35 g a.i./ha) at the 3–4 leaf stage.
[2] LBFLFK (non-sprayed) received standard herbicide treatments for weed control but no Beyond herbicide spray.
[3] Difference test p-value: * indicates p≤ 0.05; means are averages of seven locations with four plot replications at each location.
[4] Moisture content in fresh weight.

Across seasons and biological relevance

Comparing the results of the 2014/15 and the 2015 seasons, no differences between LBFLFK and Kumily were observed for moisture, crude fat, protein, and ash, and the values for these components were within the ranges of the reference varieties.

Statistically significant differences, small in magnitude, were only observed in the 2015 season for acid detergent fibre, crude fibre, and neutral detergent fibre for LBFLFK compared to Kumily. No trends were observed across seasons for these components. Furthermore, the proximate components of LBFLFK were within the ranges of the reference varieties across sites within a season and were within the range presented by either the peer-reviewed literature or ILSI Crop Composition Database values. Because these LBFLFK proximate and fibre component values were within the range of natural variation, the observed differences are considered not biologically relevant.

Amino acids

Amino acids are minor components of canola seed that impact the use of canola meal as a feedstock for livestock, poultry, and fish (OECD, 2011b). Nineteen amino acid components were analysed and reported on a percent dry weight basis (Table 30).

Winter 2014/15 season

For the 2014/15 season, no statistically significant differences were observed between LBFLFK and Kumily (Table 33), and no statistically significant entry-by-site interactions were present. The means for all 19 amino acids for LBFLFK were within the ranges of the reference varieties.

Spring 2015 season

For the 2015 season, alanine, aspartic acid, leucine, methionine, tyrosine, and valine showed statistically significant differences, though small in magnitude. Except for aspartic acid, which was statistically higher in both LBFLFK treatments compared to Kumily (Table 34), these differences were inconsistent. The results for all 19 amino acids measured in LBFLFK were within the ranges of the reference varieties.

Across seasons and biological relevance

Comparing the results of the 2014/15 and the 2015 seasons, no differences between LBFLFK and Kumily were observed for 13 amino acids (arginine, cystine, glutamic acid, glycine, histidine, hydroxyproline, isoleucine, phenylalanine, proline, serine, threonine, total lysine, and tryptophan). The values for these components were also within the ranges of the reference varieties.

Statistically significant differences, small in magnitude, were observed in the 2015 season for alanine, aspartic acid, leucine, methionine, tyrosine, and valine. No across-season trends were observed. Furthermore, all amino acid components of LBFLFK were also within the range presented by the ILSI Crop Composition Database values; therefore, the observed differences are considered not biologically relevant.

Table 33. Amino Acids – Across-Site Summary Statistics – Winter 2014/15

Component (% dry weight)	Control (Kumily)	LBFLFK (sprayed)[1]	Control minus LBFLFK (sprayed)	Reference Variety Range	LBFLFK (non-sprayed)[2]	Control minus LBFLFK (non-sprayed)
	Mean (SE) min–max	Mean (SE) min–max	Difference (SE) (p-value)[3]	min–max	Mean (SE) min–max	Difference (SE) (p-value)[3]
Alanine	1.13 (0.052) 0.91–1.21	1.15 (0.052) 0.99–1.22	-0.017 (0.018) (0.367)	0.94–1.33	1.15 (0.052) 0.92–1.22	-0.01 (0.018) (0.591)
Arginine	1.57 (0.09) 1.20–1.70	1.57 (0.09) 1.25–1.71	0.001 (0.027) (0.971)	1.29–1.96	1.55 (0.09) 1.19–1.71	0.013 (0.027) (0.64)
Aspartic acid	2.09 (0.11) 1.66–2.35	2.14 (0.11) 1.79–2.31	-0.052 (0.034) (0.126)	1.55–2.43	2.15 (0.11) 1.75–2.41	-0.058 (0.034) (0.089)
Cystine	0.62 (0.053) 0.43–0.73	0.62 (0.053) 0.43–0.73	0.0015 (0.011) (0.9)	0.49–0.82	0.62 (0.053) 0.41–0.72	0.0015 (0.011) (0.9)
Glutamic acid	4.44 (0.31) 3.24–4.9	4.47 (0.31) 3.31–5.03	-0.032 (0.071) (0.664)	3.55–5.8	4.47 (0.31) 3.19–4.99	-0.03 (0.071) (0.678)
Glycine	1.28 (0.065) 1.02–1.38	1.28 (0.065) 1.05–1.38	-0.0008 (0.018) (0.966)	1.06–1.56	1.28 (0.065) 1.01–1.39	-0.0006 (0.018) (0.975)
Histidine	0.70 (0.044) 0.52–0.77	0.69 (0.044) 0.53–0.76	0.012 (0.0099) (0.24)	0.57–0.88	0.69 (0.044) 0.52–0.76	0.011 (0.0099) (0.297)
Hydroxyproline	0.21 (0.008) 0.19–0.22	0.2 (0.008) 0.17–0.21	0.0075 (0.01) (0.467)	0.17–0.26	0.21 (0.008) 0.19–0.23	-0.0035 (0.01) (0.734)
Isoleucine	1.04 (0.054) 0.81–1.14	1.03 (0.054) 0.84–1.11	0.0083 (0.015) (0.591)	0.85–1.27	1.02 (0.054) 0.81–1.08	0.02 (0.015) (0.196)

Component (% dry weight)	Control (Kumily)	LBFLFK (sprayed)[1]	Control minus LBFLFK (sprayed)	Reference Variety Range	LBFLFK (non-sprayed)[2]	Control minus LBFLFK (non-sprayed)
	Mean (SE) min–max	Mean (SE) min–max	Difference (SE) (p-value)[3]	min–max	Mean (SE) min–max	Difference (SE) (p-value)[3]
Leucine	1.77 (0.094) 1.38–1.93	1.74 (0.094) 1.40–1.88	0.029 (0.026) (0.254)	1.45–2.21	1.73 (0.094) 1.35–1.89	0.034 (0.026) (0.183)
Methionine	0.53 (0.032) 0.41–0.58	0.52 (0.032) 0.41–0.58	0.005 (0.0077) (0.533)	0.43–0.64	0.52 (0.032) 0.39–0.57	0.008 (0.0077) (0.328)
Phenylalanine	1.03 (0.051) 0.83–1.12	1.02 (0.051) 0.84–1.1	0.0063 (0.015) (0.669)	0.84–1.25	1.02 (0.051) 0.81–1.11	0.01 (0.015) (0.481)
Proline	1.55 (0.1) 1.16–1.67	1.52 (0.1) 1.16–1.7	0.032 (0.024) (0.183)	1.29–1.98	1.52 (0.1) 1.10–1.68	0.035 (0.024) (0.152)
Serine	1.08 (0.052) 0.88–1.17	1.07 (0.052) 0.89–1.15	0.0091 (0.02) (0.659)	0.89–1.34	1.08 (0.052) 0.86–1.2	0.0023 (0.02) (0.911)
Threonine	1.10 (0.051) 0.9–1.18	1.09 (0.051) 0.91–1.17	0.01 (0.016) (0.529)	0.91–1.31	1.10 (0.051) 0.89–1.19	0.0066 (0.016) (0.687)
Total Lysine	1.64 (0.11) 1.22–1.82	1.7 (0.11) 1.31–1.9	-0.059 (0.039) (0.135)	1.34–2.05	1.61 (0.11) 1.17–1.79	0.028 (0.039) (0.482)
Tryptophan	0.39 (0.021) 0.30–0.41	0.38 (0.021) 0.30–0.41	0.0065 (0.0056) (0.282)	0.31–0.48	0.38 (0.021) 0.30–0.40	0.006 (0.0056) (0.318)
Tyrosine	0.73 (0.035) 0.59–0.80	0.73 (0.035) 0.60–0.79	-0.002 (0.011) (0.853)	0.61–0.88	0.74 (0.035) 0.60–0.80	-0.0095 (0.011) (0.379)
Valine	1.35 (0.07) 1.05–1.46	1.34 (0.07) 1.10–1.46	0.005 (0.019) (0.794)	1.09–1.61	1.33 (0.07) 1.06–1.42	0.018 (0.019) (0.35)

[1] LBFLFK (sprayed) received standard herbicide treatments for weed control plus Beyond herbicide spray (35 g a.i./ha) at the 3–4 leaf stage.
[2] LBFLFK (non-sprayed) received standard herbicide treatments for weed control but no Beyond herbicide spray.
[3] Difference test p-value: * indicates p≤ 0.05; means are averages of five locations with four plot replications at each location.

Table 34. Amino Acids – Across-Site Summary Statistics – Spring 2015

Component (% dry weight)	Control (Kumily)	LBFLFK (sprayed)[1]	Control minus LBFLFK (sprayed)	Reference Variety Range	LBFLFK (non-sprayed)[2]	Control minus LBFLFK (non-sprayed)
	Mean (SE) min–max	Mean (SE) min–max	Difference (SE) (p-value)[3]	min–max	Mean (SE) min–max	Difference (SE) (p-value)[3]
Alanine	1.14 (0.025) 1.06–1.22	1.14 (0.025) 1.06–1.21	-0.001 (0.007) (0.867)	0.99–1.33	1.15 (0.025) 1.03–1.23	-0.015 (0.007) (0.033)*
Arginine	1.61 (0.044) 1.49–1.76	1.60 (0.044) 1.48–1.71	0.011 (0.014) (0.431)	1.32–1.95	1.61 (0.044) 1.42–1.76	0.001 (0.014) (0.944)
Aspartic acid	2.06 (0.083) 1.83–2.33	2.14 (0.083) 1.86–2.41	-0.076 (0.017) (< 0.001)*	1.55–2.5	2.17 (0.083) 1.83–2.51	-0.11 (0.017) (< 0.001)*
Cystine	0.58 (0.016) 0.49–0.64	0.57 (0.016) 0.49–0.61	0.012 (0.0091) (0.197)	0.52–0.78	0.57 (0.016) 0.49–0.63	0.013 (0.0091) (0.16)
Glutamic acid	4.44 (0.081) 4.13–4.90	4.42 (0.081) 4.23–4.64	0.027 (0.039) (0.497)	3.87–5.68	4.46 (0.081) 4.13–4.73	-0.01 (0.039) (0.791)
Glycine	1.30 (0.028) 1.22–1.40	1.29 (0.028) 1.21–1.38	0.006 (0.009) (0.515)	1.12–1.54	1.30 (0.028) 1.18–1.4	-0.007 (0.009) (0.428)
Histidine	0.69 (0.012) 0.65–0.74	0.68 (0.012) 0.65–0.72	0.011 (0.0082) (0.181)	0.62–0.87	0.69 (0.012) 0.64–0.72	0.0032 (0.0082) (0.696)
Hydroxyproline	0.19 (0.0039) 0.17–0.20	0.18 (0.0039) 0.17–0.20	0.0036 (0.0054) (0.515)	0.15–0.21	0.18 (0.0039) 0.17–0.19	0.0079 (0.0054) (0.162)
Isoleucine	1.04 (0.025) 0.96–1.13	1.03 (0.025) 0.96–1.10	0.012 (0.011) (0.268)	0.89–1.26	1.04 (0.025) 0.94–1.11	0.0031 (0.011) (0.777)

Component (% dry weight)	Control (Kumily)	LBFLFK (sprayed)[1]	Control minus LBFLFK (sprayed)	Reference Variety Range	LBFLFK (non-sprayed)[2]	Control minus LBFLFK (non-sprayed)
	Mean (SE) min–max	Mean (SE) min–max	Difference (SE) (p-value)[3]	min–max	Mean (SE) min–max	Difference (SE) (p-value)[3]
Leucine	1.79 (0.042) 1.66–1.96	1.75 (0.042) 1.64–1.88	0.034 (0.012) (0.007)*	1.53–2.18	1.77 (0.042) 1.58–1.92	0.019 (0.012) (0.119)
Methionine	0.51 (0.0092) 0.47–0.55	0.50 (0.0092) 0.48–0.52	0.011 (0.0057) (0.065)	0.46–0.61	0.50 (0.0092) 0.47–0.54	0.012 (0.0057) (0.043)*
Phenylalanine	1.05 (0.029) 0.94–1.15	1.04 (0.029) 0.96–1.12	0.0074 (0.012) (0.526)	0.88–1.27	1.05 (0.029) 0.93–1.15	-0.0012 (0.012) (0.92)
Proline	1.55 (0.029) 1.44–1.72	1.52 (0.029) 1.46–1.62	0.031 (0.02) (0.127)	1.37–1.97	1.53 (0.029) 1.45–1.64	0.017 (0.02) (0.412)
Serine	1.10 (0.023) 1.04–1.19	1.09 (0.023) 1.03–1.16	0.012 (0.009) (0.185)	0.95–1.31	1.10 (0.023) 1.00–1.19	-0.001 (0.009) (0.95)
Threonine	1.12 (0.023) 1.05–1.20	1.11 (0.023) 1.04–1.17	0.0084 (0.011) (0.459)	0.97–1.3	1.11 (0.023) 1.01–1.19	0.0016 (0.011) (0.887)
Total Lysine	1.55 (0.023) 1.50–1.63	1.55 (0.023) 1.48–1.60	-0.0014 (0.019) (0.942)	1.42–1.92	1.55 (0.023) 1.46–1.66	0.0036 (0.019) (0.855)
Tryptophan	0.38 (0.0083) 0.34–0.40	0.37 (0.0083) 0.35–0.40	0.0061 (0.0052) (0.249)	0.33–0.46	0.37 (0.0083) 0.34–0.4	0.0046 (0.0052) (0.377)
Tyrosine	0.706 (0.018) 0.64–0.76	0.711 (0.018) 0.65–0.77	-0.005 (0.003) (0.134)	0.60–0.85	0.715 (0.018) 0.64–0.77	-0.008 (0.003) (0.018)*
Valine	1.34 (0.03) 1.26–1.45	1.34 (0.03) 1.25–1.41	-0.004 (0.008) (0.586)	1.14–1.62	1.35 (0.03) 1.21–1.46	-0.016 (0.008) (0.042)*

[1] LBFLFK (sprayed) received standard herbicide treatments for weed control plus Beyond herbicide spray (35 g a.i./ha) at the 3–4 leaf stage.
[2] LBFLFK (non-sprayed) received standard herbicide treatments for weed control but no Beyond herbicide spray.
[3] Difference test p-value: * indicates p≤ 0.05; means are averages of seven locations with four plot replications at each location.

Fatty acids levels

Canola is produced as a crop primarily for its oil, having a low content of saturated fatty acids, a high content of monounsaturated fatty acids, and a low content (< 2% of total fatty acids) of erucic acid (C22:1n-9) (OECD, 2011b). EPA+DHA canola event LBFLFK has an intentional change to the fatty acid profile compared to other canola varieties, producing long-chain polyunsaturated fatty acids, including EPA (C20:5n-3) and DHA (C22:6n-3), as a consequence of the introduced metabolic pathway. Therefore, an expanded panel of fatty acids was assessed to account for this intentional change. In total, 39 fatty acid components were analysed (Table 30). Comparisons of fatty acids were performed using relative percent data values (percentage of the total fatty acid content of an individual sample), which is the standard approach for assessing fatty acid levels in vegetable oils (OECD, 2011b).

Winter 2014/15 season

No comparative statistical analysis could be performed for the fatty acids C16:3n-3[14], C18:2 trans, C22:1n-9 (erucic acid), and C22:2n-6, which were below the LOQ across all sample entries.

In addition, no comparative statistical analysis could be performed for the fatty acids C16:1 trans, C18:2n-9, C18:3n-6, C18:4n-3, C20:2n-9, C20:3n-3, C20:3n-6, C20:3n-9, C20:4n-3, C20:4n-6, C20:5n-3 (EPA), C22:4n-3, C22:4n-6, C22:5n-3, C22:5n-6, and C22:6n-3 (DHA), which were measured in LBFLFK samples but were generally below the LOQ in Kumily and reference variety samples. The presence of these fatty acids in LBFLFK is attributable to the EPA+DHA trait (Table 35).

The fatty acids that could be subjected to statistical analysis to determine the difference in composition for LBFLFK as compared to Kumily were C16:0, C16:1n-7, C18:0, C18:1n-7, C18:1n-9, C18:2n-6, C18:3n-3, C20:0, C20:1n-9, C22:0, C24:0, C24:1n-9, and total trans fatty acids (Table 36). Of these, the fatty acids C16:1n-7, C18:0, C18:1n-9, C18:2n-6, C18:3n-3, C20:0, C20:1n-9, C22:0, C24:0, C24:1n-9, and total trans fatty acids showed statistically significant differences when compared to Kumily. Except for C20:0 and C24:0, statistically significant entry-by-site interactions were observed for all the fatty acids listed. The mean values for C16:1n-7, C18:3n-3, C22:0, and C24:1n-9 in LBFLFK were within the range of the reference varieties.

Spring 2015 season

No comparative statistical analysis could be performed for the fatty acids C16:3n-3, C18:2 trans, C22:1n-9 (erucic acid), and C22:2n-6 as they were again below the LOQ across all sample entries.

In addition, no comparative statistical analysis could be performed for the fatty acids C16:1 trans, C18:1 trans, C18:2n-9, C18:3n-6, C18:4n-3, C20:2n-9, C20:3n-3, C20:3n-6, C20:3n-9, C20:4n-3, C20:4n-6, C20:5n-3 (EPA), C22:4n-3, C22:4n-6, C22:5n-3, C22:5n-6, and C22:6n-3 (DHA), which were measured in LBFLFK samples but were generally below the LOQ in Kumily and reference variety samples. The presence of these fatty acids in LBFLFK is attributable to the EPA+DHA trait (Table 37).

[14] C16:3n-3 was detected at a very low level in one sample of LBFLFK (sprayed), which was likely a false signal – data not shown.

The fatty acids that could be subjected to statistical analysis to determine the difference in composition for LBFLFK as compared to Kumily were C16:0, C16:1n-7, C18:0, C18:1n-7, C18:1n-9, C18:2n-6, C18:3n-3, C20:0, C20:1n-9, C22:0, C24:0, C24:1n-9, and total trans fatty acids (Table 38). The fatty acids C16:1n-7, C18:0, C18:1n-7, C18:1n-9, C18:2n-6, C18:3n-3, C20:0, C20:1n-9, C22:0, C24:0, C24:1n-9, and total trans fatty acids showed statistically significant differences in LBFLFK compared to Kumily. Except for C20:0 and total trans fatty acids, statistically significant entry-by-site interactions were observed for all the fatty acids listed. The mean values for C16:1n-7, C18:1n-7, C18:3n-3, C20:0, and C22:0 in LBFLFK were within the range of the reference varieties. The values of C18:1n-7 in LBFLFK were both higher and lower than those of Kumily at different sites, and so there was not a clear trend for this analyte.

Across seasons and biological relevance

The introduction of the EPA+DHA trait and the associated enzymatic pathway in LBFLFK results in the presence of fatty acids not normally found in conventional canola, as expected. In addition, the enzymatic pathway uses endogenous fatty acids as substrates to produce EPA and DHA, which impacts the content of some fatty acids that are normally present in conventional canola varieties. Therefore, the across-season comparison of fatty acids provided here is discussed below in three parts: canola endogenous fatty acids not impacted by the trait, canola endogenous fatty acids impacted by the trait, and EPA+DHA trait-associated fatty acids.

Canola endogenous fatty acids not impacted by the trait

Among the fatty acids that were above the LOQ in both LBFLFK and Kumily and therefore suitable for statistical analysis, only C16:0 did not show any statistically significant differences in either season. The means of C16:0 for both LBFLFK and Kumily were slightly above the upper limit of the reference range but within the ranges of natural variation based on the ILSI Crop Composition Database and peer-reviewed literature values. The fatty acid C18:1n-7 only showed statistically significant differences in the spring 2015 data set, and a by-site analysis demonstrated both higher and lower values compared to the control at different sites. Therefore, the differences seen with these two fatty acids are not considered to be biologically relevant.

Values for the fatty acids C14:0, C16:1n-9, C17:0, C17:1, and C20:2n-6 in LBFLFK in both seasons and for C18:1 trans in one season were not suitable for statistical comparative analysis. However, mean values for these fatty acids were generally within the range of the reference varieties. These components represent a relatively minor fraction of the fatty acid profile, and means were within the ranges of natural variation based on the peer-reviewed literature and the ILSI Crop Composition Database, hence LBFLFK is considered equivalent to conventional canola for these fatty acids.

It is noted that the fatty acid C22:1n-9 (erucic acid) was consistently below the LOQ across all samples for LBFLFK and Kumily for both seasons. Canola varieties must have levels of this antinutrient below 2% (OECD, 2011b).

Canola endogenous fatty acids impacted by the trait

Statistically significant differences were observed across both seasons when comparing LBFLFK with Kumily for C16:1n-7, C18:0, C18:1n-9, C18:2n-6, C18:3n-3, C20:0, C20:1n-9,

C22:0, C24:0, C24:1n-9, and total trans fatty acids (Table 36 and Table 38). These differences are attributed to the introduction of the EPA+DHA trait in LBFLFK. In both seasons, LBFLFK had statistically significantly lower C16:1n-7, C18:1n-9, C18:3n-3, C20:0, C20:1n-9, C22:0, C24:0, and C24:1n-9 compared to Kumily. LBFLFK had statistically significantly higher C18:0, C18:2n-6, and total trans fatty acids than Kumily. The mean values for C16:1n-7, C18:3n-3, C20:0, C22:0, and C24:1n-9 were still generally within the reference ranges and within the range of natural variation based on the ILSI Crop Composition Database and/or peer-reviewed literature. The measurement for C24:0 was outside the respective reference range but within the range of natural variation based on the peer-reviewed literature and ILSI Crop Composition Database values.

In LBFLFK across both seasons, the mean values for C18:1n-9 (oleic acid, decreased), C18:2n-6 (linoleic acid, increased), and total trans fatty acids (slightly increased) were consistently outside of the reference ranges and outside the range of natural variation based on the peer-reviewed literature and the ILSI Crop Composition Database values.

Oleic acid and linoleic acid are primary precursors for the production of the long-chain polyunsaturated fatty acids in EPA+DHA canola. Oleic acid, the starting substrate fatty acid for the newly introduced fatty acid synthesis pathway, is statistically significantly lower in LBFLFK across treatments and seasons relative to Kumily. The conversion of oleic acid into longer chain and more highly unsaturated fatty acids also likely has a secondary effect on the overall levels of C18:0, which were higher in LBFLFK treatments across seasons than Kumily and the reference ranges. Additionally, the higher relative linoleic acid content is attributable to the newly expressed delta-12 desaturase from *Phytophthora sojae* (D12D(*Ps*)) that produces this fatty acid from oleic acid (Yilmaz et al., 2017).

The trend of increased total trans fatty acids across seasons in LBFLFK, primarily in the form of C18:1 trans, represents only a marginal and low amount of the total fatty acids (0.3%). This increase in trans fatty acids is minor compared to the amount of trans fatty acids produced as a result of conventional commercial processing of canola seeds to refined, bleached, and deodorised oil, with the introduction of trans isomers coming primarily from deodorisation (Unger, 2015). Additionally, this minor increase in trans fats is not surprising as isomerisation of fatty acids to trans fats occurs spontaneously and at a faster rate with fatty acids with higher degrees of unsaturation like those produced in LBFLFK (Wolff, 1993; Chardigny, 1996).

EPA+DHA trait-associated fatty acids

The fatty acids C16:1 trans, C18:2n-9, C18:3n-6, C18:4n-3, C20:2n-9, C20:3n-3, C20:3n-6, C20:3n-9, C20:4n-3, C20:4n-6, C20:5n-3 (EPA), C22:4n-3, C22:4n-6, C22:5n-3, C22:5n-6, and C22:6n-3 (DHA) were consistently below the LOQ in Kumily and the reference varieties across both seasons (Table 35 and Table 37). The presence of these fatty acids in LBFLFK but not in Kumily and reference varieties is expected and attributed to the introduction of the EPA+DHA trait in LBFLFK (Yilmaz et al., 2017).

Table 35. Fatty Acids Consistently Quantified only in LBFLFK – Across-Site Comparison – Winter 2014/15

Component (% of total fatty acids)	LBFLFK (sprayed)[1]	LBFLFK (non-sprayed)[2]
	Mean (SE) min–max	Mean (SE) min–max
C16:1 trans	0.068 (0.0031) 0.065–0.073	0.066 (0.0038) 0.060–0.070
C18:2n-9	0.90 (0.089) 0.82–1.03	0.91 (0.071) 0.84–1.01
C18:3n-6	1.75 (0.42) 1.12–2.17	1.70 (0.44) 0.97–2.09
C18:4n-3	0.26 (0.039) 0.20–0.29	0.25 (0.044) 0.18–0.29
C20:2n-9	0.22 (0.042) 0.17–0.28	0.23 (0.038) 0.19–0.26
C20:3n-3	0.064 (0.0063) 0.057–0.073	0.062 (0.0076) 0.052–0.073
C20:3n-6	3.56 (0.79) 2.25–4.19	3.56 (0.77) 2.29–4.19
C20:3n-9	0.062 (0.012) 0.048–0.070	0.064 (0.0099) 0.052–0.077
C20:4n-3	1.77 (0.39) 1.15–2.11	1.80 (0.37) 1.27–2.12
C20:4n-6	2.26 (0.36) 1.89–2.72	2.19 (0.39) 1.66–2.62
C20:5n-3	7.21 (1.26) 4.98–7.94	7.21 (1.34) 4.83–7.96
C22:4n-3	0.51 (0.12) 0.32–0.64	0.51 (0.1) 0.36–0.61
C22:4n-6	0.46 (0.11) 0.29–0.56	0.44 (0.11) 0.27–0.54
C22:5n-3	2.94 (0.53) 2.05–3.44	2.93 (0.46) 2.16–3.38
C22:5n-6	0.089 (0.027) 0.051–0.12	0.085 (0.022) 0.048–0.11
C22:6n-3	1.02 (0.18) 0.73–1.18	1.02 (0.18) 0.71–1.15

Means are averages of five locations with four plot replications at each location.
[1] LBFLFK (sprayed) received standard herbicide treatments for weed control plus Beyond herbicide spray (35 g a.i./ha) at the 3–4 leaf stage.
[2] LBFLFK (non-sprayed) received standard herbicide treatments for weed control but no Beyond herbicide spray.

Table 36. Fatty Acids – Across-Site Summary Statistics – Winter 2014/15

Component (% of total fatty acids)	Control (Kumily)	LBFLFK (sprayed)[1]	Control minus LBFLFK (sprayed)	Reference Variety Range	LBFLFK (non-sprayed)[2]	Control minus LBFLFK (non-sprayed)
	Mean (SE) min–max	Mean (SE) min–max	Difference (SE) (p-value)[3]	min–max	Mean (SE) min–max	Difference (SE) (p-value)[3]
C14:0	0.063 (0.0072) 0.052–0.073	0.071 (0.0027) 0.068–0.075	NA	0.04–0.08	0.067 (0.0054) 0.060–0.073	NA
C16:0	4.87 (0.091) 4.49–5.16	4.84 (0.091) 4.61–5.06	0.032 (0.036) (0.41)	3.04–4.72	4.81 (0.091) 4.59–5.04	0.059 (0.036) (0.142)
C16:1n-7	0.31 (0.0075) 0.28–0.34	0.21 (0.0075) 0.20–0.22	0.098 (0.0085) (< 0.001)*	0.20–0.33	0.20 (0.0075) 0.19–0.22	0.10 (0.0085) (< 0.001)*
C16:1n-9	0.053 (0.01) 0.037–0.065	0.060 (0.012) 0.042–0.075	NA	0.030–0.087	0.058 (0.0086) 0.045–0.068	NA
C17:0	0.047 (0.0021) 0.045–0.05	0.046 (0.0042) 0.04–0.05	NA	< LOQ–0.048	0.048 (0.0045) 0.042–0.052	NA
C17:1	0.050 (0.0021) 0.048–0.052	< LOQ	NA	< LOQ–0.060	< LOQ	NA
C18:0	1.97 (0.043) 1.86–2.06	2.54 (0.043) 2.37–2.68	-0.58 (0.038) (< 0.001)*	1.78–2.22	2.49 (0.043) 2.38–2.62	-0.53 (0.038) (< 0.001)*
C18:1n-7	3.34 (0.054) 3.16–3.50	3.40 (0.054) 3.31–3.56	-0.052 (0.033) (0.154)	2.77–3.56	3.35 (0.054) 3.16–3.48	-0.012 (0.033) (0.728)
C18:1n-9	54.61 (1.29) 53.64–55.50	25.5 (1.29) 22.53–31.04	29.11 (1.17) (< 0.001)*	55.59–76.02	25.94 (1.29) 22.62–32.26	28.67 (1.17) (< 0.001)*

Component (% of total fatty acids)	Control (Kumily)	LBFLFK (sprayed)[1]	Control minus LBFLFK (sprayed)	Reference Variety Range	LBFLFK (non-sprayed)[2]	Control minus LBFLFK (non-sprayed)
	Mean (SE) min–max	Mean (SE) min–max	Difference (SE) (p-value)[3]	min–max	Mean (SE) min–max	Difference (SE) (p-value)[3]
C18:1 trans	< LOQ < LOQ–0.08	0.16 (0.054) 0.07–0.20	NA	< LOQ–0.07	0.17 (0.041) 0.10–0.20	NA
C18:2n-6	20.07 (0.52) 19.03–21.00	28.79 (0.52) 27.35–30.28	-8.72 (0.38) (< 0.001)*	5.68–23.45	28.39 (0.52) 27.21–29.86	-8.32 (0.38) (< 0.001)*
C18:3n-3	7.49 (0.33) 6.55–8.38	4.83 (0.33) 4.12–5.65	2.67 (0.11) (< 0.001)*	1.69–8.39	4.91 (0.33) 4.14–6.16	2.58 (0.11) (< 0.001)*
C20:0	0.66 (0.031) 0.59–0.69	0.52 (0.031) 0.44–0.63	0.13 (0.039) (0.001)*	0.55–0.79	0.60 (0.031) 0.56–0.63	0.052 (0.039) (0.183)
C20:1n-9	0.97 (0.021) 0.93–1.00	0.64 (0.021) 0.59–0.72	0.33 (0.022) (< 0.001)*	0.93–1.34	0.65 (0.021) 0.59–0.73	0.33 (0.022) (< 0.001)*
C20:2n-6	0.056 (0.0033) 0.052–0.060	0.10 (0.0011) 0.098–0.10	NA	0.034–0.08	0.099 (0.0014) 0.098–0.10	NA
C22:0	0.34 (0.0074) 0.30–0.37	0.26 (0.0074) 0.24–0.26	0.086 (0.0081) (< 0.001)*	0.24–0.44	0.25 (0.0074) 0.25–0.26	0.088 (0.0081) (< 0.001)*
C24:0	0.20 (0.013) 0.13–0.24	0.093 (0.013) 0.061–0.12	0.11 (0.012) (< 0.001)*	0.13–0.38	0.093 (0.013) 0.074–0.12	0.11 (0.012) (< 0.001)*
C24:1n-9	0.13 (0.0045) 0.10–0.15	0.086 (0.0045) 0.078–0.091	0.045 (0.0044) (< 0.001)*	0.084–0.16	0.086 (0.0045) 0.08–0.091	0.045 (0.0044) (< 0.001)*
Total trans fatty acids	0.11 (0.018) 0.093–0.14	0.32 (0.018) 0.24–0.36	-0.21 (0.019) (< 0.001)*	0.077–0.13	0.34 (0.018) 0.26–0.37	-0.23 (0.019) (< 0.001)*

NA indicates not suitable for statistical analysis.
[1] LBFLFK (sprayed) received standard herbicide treatments for weed control plus Beyond herbicide spray (35 g a.i./ha) at the 3–4 leaf stage.
[2] LBFLFK (non-sprayed) received standard herbicide treatments for weed control but no Beyond herbicide spray.
[3] Difference test p-value: * indicates p≤ 0.05; means are averages of five locations with four plot replications at each location.

Table 37. Fatty Acids Consistently Quantified only in LBFLFK – Across-Site Comparison – Spring 2015

Component (% of total fatty acids)	LBFLFK (sprayed)[1]	LBFLFK (non-sprayed)[2]
	Mean (SE) min–max	Mean (SE) min–max
C16:1 trans	0.057 (0.0043) 0.050–0.060	0.053 (0.0022) 0.050–0.055
C18:1 trans	0.12 (0.019) 0.10–0.15	0.13 (0.022) 0.10–0.15
C18:2n-9	1.12 (0.15) 0.96–1.38	1.12 (0.15) 0.96–1.40
C18:3n-6	1.60 (0.16) 1.44–1.82	1.62 (0.16) 1.46–1.85
C18:4n-3	0.26 (0.038) 0.21–0.33	0.26 (0.039) 0.22–0.34
C20:2n-9	0.33 (0.06) 0.27–0.43	0.33 (0.062) 0.26–0.44
C20:3n-3	0.067 (0.0093) 0.060–0.082	0.066 (0.0089) 0.060–0.080
C20:3n-6	4.06 (0.38) 3.65–4.53	4.08 (0.31) 3.74–4.50
C20:3n-9	0.079 (0.016) 0.060–0.10	0.077 (0.016) 0.057–0.10
C20:4n-3	1.92 (0.27) 1.54–2.37	1.92 (0.25) 1.55–2.35
C20:4n-6	1.87 (0.25) 1.62–2.19	1.87 (0.25) 1.57–2.23
C20:5n-3	6.27 (0.46) 5.47–6.98	6.26 (0.49) 5.32–6.93
C22:4n-3	0.68 (0.12) 0.54–0.90	0.72 (0.1) 0.60–0.91
C22:4n-6	0.45 (0.042) 0.38–0.50	0.45 (0.046) 0.38–0.51
C22:5n-3	2.75 (0.15) 2.51–3.00	2.74 (0.17) 2.44–2.97
C22:5n-6	0.072 (0.017) 0.05–0.10	0.072 (0.015) 0.055–0.098
C22:6n-3	0.77 (0.12) 0.59–0.96	0.76 (0.11) 0.61–0.95

Means are averages of seven locations with four plot replications at each location.
[1] LBFLFK (sprayed) received standard herbicide treatments for weed control plus Beyond herbicide spray (35 g a.i./ha) at the 3–4 leaf stage.
[2] LBFLFK (non-sprayed) received standard herbicide treatments for weed control but no Beyond herbicide spray.

Table 38. Fatty Acids – Across-Site Summary Statistics – Spring 2015

Component (% of total fatty acids)	Control (Kumily)	LBFLFK (sprayed)[1]	Control minus LBFLFK (sprayed)	Reference Variety Range	LBFLFK (non-sprayed)[2]	Control minus LBFLFK (non-sprayed)
	Mean (SE) min–max	Mean (SE) min–max	Difference (SE) (p-value)[3]	min–max	Mean (SE) min–max	Difference (SE) (p-value)[3]
C14:0	0.061 (0.0069) 0.052–0.075	0.064 (0.0038) 0.060–0.070	NA	0.04–0.07	0.064 (0.0049) 0.060–0.073	NA
C16:0	4.54 (0.11) 4.12–5.13	4.57 (0.11) 4.20–5.12	-0.031 (0.018) (0.114)	2.91–4.46	4.56 (0.11) 4.20–5.07	-0.022 (0.018) (0.248)
C16:1n-7	0.29 (0.011) 0.25–0.38	0.19 (0.011) 0.17–0.23	0.10 (0.007) (< 0.001)*	0.18–0.28	0.19 (0.011) 0.17–0.23	0.10 (0.007) (< 0.001)*
C16:1n-9	0.040 (0.0057) 0.032–0.050	0.048 (0.0049) 0.040–0.055	NA	0.030–0.062	0.047 (0.0044) 0.04–0.052	NA
C17:0	0.048 (0.0028) 0.042–0.050	0.048 (0.0037) 0.042–0.052	NA	0.032–0.048	0.049 (0.0028) 0.042–0.050	NA
C17:1	0.053 (0.0035) 0.050–0.060	< LOQ	NA	0.040–0.060	< LOQ	NA
C18:0	2.18 (0.061) 1.95–2.33	2.77 (0.061) 2.52–3.06	-0.59 (0.021) (< 0.001)*	1.73–2.23	2.74 (0.061) 2.52–3.00	-0.56 (0.021) (< 0.001)*
C18:1n-7	3.50 (0.1) 3.28–4.13	3.46 (0.1) 3.21–3.98	0.042 (0.021) (0.047)*	2.57–3.47	3.44 (0.1) 3.21–3.98	0.057 (0.021) (0.007)*
C18:1n-9	54.83 (0.74) 49.59–56.69	26.41 (0.74) 23.31–28.18	28.43 (0.42) (< 0.001)*	55.21–76.44	26.27 (0.74) 23.01–27.98	28.56 (0.42) (< 0.001)*

Component (% of total fatty acids)	Control (Kumily)	LBFLFK (sprayed)[1]	Control minus LBFLFK (sprayed)	Reference Variety Range	LBFLFK (non-sprayed)[2]	Control minus LBFLFK (non-sprayed)
	Mean (SE) min–max	Mean (SE) min–max	Difference (SE) (p-value)[3]	min–max	Mean (SE) min–max	Difference (SE) (p-value)[3]
C18:2n-6	19.29 (0.47) 17.98–21.88	27.89 (0.47) 26.09–29.61	-8.6 (0.6) (< 0.001)*	5.81–23.23	28.07 (0.47) 25.97–29.86	-8.78 (0.6) (< 0.001)*
C18:3n-3	8.01 (0.21) 7.17–9.08	5.37 (0.21) 4.88–6.08	2.64 (0.1) (< 0.001)*	1.97–8.52	5.37 (0.21) 4.90–6.06	2.64 (0.1) (< 0.001)*
C20:0	0.7 (0.017) 0.64–0.78	0.66 (0.017) 0.60–0.73	0.044 (0.005) (< 0.001)*	0.57–0.80	0.65 (0.017) 0.59–0.72	0.048 (0.005) (< 0.001)*
C20:1n-9[4]	1.03[4] 1.00–1.08	0.70[4] 0.68–0.73	1.47[4] (< 0.001)*	1.00–1.45	0.7[4] 0.68–0.73	1.47[4] (< 0.001)*
C20:2n-6	0.071 (0.019) 0.05–0.1	0.10 (0) 0.10–0.10	NA	0.045–0.12	0.10 (0) 0.10–0.10	NA
C22:0	0.34 (0.011) 0.29–0.41	0.26 (0.011) 0.22–0.30	0.085 (0.0046) (< 0.001)*	0.23–0.45	0.26 (0.011) 0.22–0.30	0.085 (0.0046) (< 0.001)*
C24:0	0.19 (0.0078) 0.16–0.24	0.13 (0.0078) 0.11–0.15	0.067 (0.0043) (< 0.001)*	0.15–0.31	0.12 (0.0078) 0.10–0.15	0.069 (0.0043) (< 0.001)*
C24:1n-9	0.13 (0.0079) 0.094–0.19	0.082 (0.0079) 0.066–0.11	0.046 (0.005) (< 0.001)*	0.084–0.18	0.083 (0.0079) 0.064–0.11	0.045 (0.005) (< 0.001)*
Total trans fatty acids	0.062 (0.0065) 0.055–0.070	0.27 (0.0065) 0.25–0.32	-0.21 (0.0091) (< 0.001)*	< LOQ–0.10	0.28 (0.0065) 0.26–0.30	-0.22 (0.0091) (< 0.001)*

NA indicates not suitable for statistical analysis.
[1] LBFLFK (sprayed) received standard herbicide treatments for weed control plus Beyond herbicide spray (35 g a.i./ha) at the 3–4 leaf stage.
[2] LBFLFK (non-sprayed) received standard herbicide treatments for weed control but no Beyond herbicide spray.
[3] Difference test p-value: * indicates p≤ 0.05; means are averages of seven locations with four plot replications at each location.
[4] Data were log-transformed. Means and differences were back-transformed. Difference column data are the ratio, rather than the difference, of the two means. Back-transformed SE is not provided.

Vitamins and minerals

Vitamins and minerals are minor components of canola that primarily impact the utility of canola meal. The use of pre-mixes in least cost rations lessens the importance of these components, except for phosphorous bound in phytic acid (OECD, 2011b). Fat-soluble vitamin K1 and tocopherols (including vitamin E) are found in processed edible oils and contribute to human health and nutrition. Tocopherols (alpha-, beta-, gamma-, delta-, and total tocopherols), vitamin K1, and nine mineral components in LBFLFK were compared to Kumily and conventional canola varieties.

Winter 2014/15 season

For the vitamins analysed in the 2014/15 season (Table 39), delta-tocopherol was statistically significantly lower and vitamin K1 was statistically significantly higher in LBFLFK (sprayed only) compared to Kumily, though the differences were small in magnitude. No statistically significant differences were observed for any of the other vitamins for LBFLFK compared to Kumily. There were no statistically significant entry-by-site interactions. All vitamin components in grain from LBFLFK were within the ranges of the reference varieties.

For minerals analysed in the 2014/15 season (Table 40), calcium and magnesium were statistically significantly lower in LBFLFK compared to Kumily, though the differences were small in magnitude.

Copper, manganese, and zinc did not meet the criteria required for statistical analysis. There were no statistically significant entry-by-site interactions for this season. Mineral components measured for LBFLFK were within or slightly outside the range of the reference varieties.

Spring 2015 season

For the vitamins analysed in the 2015 season (Table 41), vitamin K1 was statistically significantly higher in LBFLFK compared to Kumily, with the differences small in magnitude. No statistically significant differences were observed for any of the other vitamins for LBFLFK compared to Kumily, and all measured values were within or close to the range of the reference varieties.

For the minerals analysed in the 2015 season (Table 42), calcium and magnesium were again statistically significantly lower in LBFLFK compared to Kumily, with the differences small in magnitude. Phosphorus was statistically significantly higher in LBFLFK (non-sprayed) compared to Kumily, but this difference was also small in magnitude.

Copper, iron, manganese, sodium, and zinc did not meet the criteria required for statistical analysis. The calcium content in LBFLFK was only slightly lower than the lower limit of the reference variety range. All other minerals measured for LBFLFK were within the range of the reference varieties.

Across seasons and biological relevance

Comparing the vitamin and mineral results of the 2014/15 and the 2015 seasons, no differences were observed between LBFLFK and Kumily for alpha-tocopherol, beta-tocopherol, gamma-tocopherol, total tocopherols, copper, iron, manganese, potassium, sodium, and zinc. The values for these components were all within the range of the reference varieties.

A statistically significantly lower delta-tocopherol content was observed for LBFLFK (sprayed) compared to Kumily only in the 2014/15 season (Table 39). A statistically significantly higher phosphorous content was only observed for LBFLFK (non-sprayed) compared to Kumily in the 2015 season (Table 42). For both delta-tocopherol and phosphorous, no trends were observed across seasons, and all values were within the range of the reference varieties. Therefore, these differences in values for these components are considered not biologically relevant.

A statistically significant but slight increase in vitamin K1 content was observed for LBFLFK compared to Kumily (Table 39 and Table 41). However, these increased vitamin K1 values were well within the range of reference varieties for each season and within ILSI Crop Composition Database and peer-reviewed literature values. Therefore, these observed differences are considered not biologically relevant.

Though differences were small in magnitude, calcium and magnesium were both statistically significantly lower for LBFLFK compared to Kumily across both seasons. Though these minerals were marginally lower than the reference range in one season, the values for both were well within the range of the ILSI Crop Composition Database values; therefore, the differences in values for these components are considered not biologically relevant.

In summary, vitamin and mineral values in LBFLFK were within the range of natural variation for canola, and all observed differences are therefore considered not biologically relevant.

Table 39. Vitamins – Across-Site Summary Statistics – Winter 2014/15

Analytical Component (mg/100 g dry weight)	Control (Kumily)	LBFLFK (sprayed)[1]	Control minus LBFLFK (sprayed)	Reference Variety Range	LBFLFK (non-sprayed)[2]	Control minus LBFLFK (non-sprayed)
	Mean (SE) min–max	Mean (SE) min–max	Difference (SE) (p-value)[3]	min–max	Mean (SE) min–max	Difference (SE) (p-value)[3]
Alpha-tocopherol	16.84 (1.45) 10.50–19.80	15.94 (1.45) 11.12–17.45	0.9 (0.69) (0.2)	11.05–25.30	15.88 (1.45) 10.59–17.77	0.97 (0.7) (0.177)
Beta-tocopherol	0.31 (0.045) 0.13–0.42	0.32 (0.045) 0.17–0.40	-0.0068 (0.024) (0.783)	0.13–0.55	0.32 (0.045) 0.14–0.40	-0.009 (0.024) (0.716)
Delta-tocopherol	0.73 (0.045) 0.61–0.84	0.63 (0.045) 0.52–0.73	0.1 (0.034) (0.017)*	0.41–1.07	0.67 (0.045) 0.57–0.79	0.064 (0.034) (0.099)
Gamma-tocopherol	26.96 (0.8) 25.93–28.15	27.01 (0.8) 23.75–29.75	-0.05 (0.92) (0.958)	19.10–27.93	26.98 (0.8) 25.45–29.75	-0.015 (0.92) (0.987)
Total tocopherols	44.88 (1.71) 38.00–49.27	43.91 (1.71) 40.75–48.17	0.98 (1.43) (0.514)	31.27–49.18	43.88 (1.71) 38.27–48.70	1.01 (1.45) (0.506)
Vitamin K1	0.088 (0.01) 0.067–0.110	0.097 (0.01) 0.075–0.130	-0.0091 (0.0034) (0.027)*	0.038–0.110	0.091 (0.01) 0.075–0.12	-0.0039 (0.0034) (0.28)

[1] LBFLFK (sprayed) received standard herbicide treatments for weed control plus Beyond herbicide spray (35 g a.i./ha) at the 3–4 leaf stage.
[2] LBFLFK (non-sprayed) received standard herbicide treatments for weed control but no Beyond herbicide spray.
[3] Difference test p-value: * indicates p≤ 0.05; means are averages of five locations with four plot replications at each location.

Table 40. Minerals – Across-Site Summary Statistics – Winter 2014/15

Component (% dry weight)	Control (Kumily)	LBFLFK (sprayed)[1]	Control minus LBFLFK (sprayed)	Reference Variety Range	LBFLFK (non-sprayed)[2]	Control minus LBFLFK (non-sprayed)
	Mean (SE) min–max	Mean (SE) min–max	Difference (SE) (p-value)[3]	min–max	Mean (SE) min–max	Difference (SE) (p-value)[3]
Calcium	0.33 (0.022) 0.25–0.40	0.30 (0.022) 0.22–0.36	0.027 (0.0081) (0.01)*	0.27–0.47	0.29 (0.022) 0.24–0.34	0.037 (0.0081) (0.002)*
Copper	0.00031 (7.4e-05) 0.0002–0.0004	0.00030 (7.1e-05) 0.0002–0.0004	NA	0.0002–0.0004	0.00028 (3.4e-05) 0.00022–0.0003	NA
Iron	0.010 (0.0034) 0.0046–0.019	0.010 (0.0034) 0.0053–0.028	-0.0002 (0.0028) (0.953)	0.0034–0.024	0.010 (0.0034) 0.0053–0.022	0.0002 (0.0028) (0.955)
Magnesium	0.33 (0.0081) 0.31–0.35	0.31 (0.0081) 0.28–0.33	0.016 (0.0038) (0.002)*	0.32–0.38	0.31 (0.0081) 0.29–0.33	0.016 (0.0038) (0.003)*
Manganese	0.0052 (0.00047) 0.0047–0.0057	0.0064 (0.0033) 0.0040–0.0120	NA	0.0030–0.0062	0.0052 (0.00057) 0.0045–0.0060	NA
Phosphorus	0.73 (0.043) 0.61–0.86	0.74 (0.043) 0.61–0.89	-0.006 (0.015) (0.694)	0.60–0.94	0.75 (0.043) 0.63–0.88	-0.013 (0.015) (0.389)
Potassium	1.08 (0.05) 0.96–1.28	1.07 (0.05) 0.98–1.23	0.0088 (0.021) (0.676)	0.68–1.41	1.06 (0.05) 0.99–1.19	0.017 (0.021) (0.41)
Sodium	0.0044 (0.0011) < LOQ–0.0055	0.0047 (0.0011) < LOQ–0.0096	-0.0002 (0.0009) (0.799)	< LOQ–0.015	0.0042 (0.0011) < LOQ–0.0062	0.0002 (0.0009) (0.824)
Zinc	0.0032 (0.00035) 0.0030–0.0037	0.0036 (0.00042) 0.003–0.004	NA	0.003–0.004	0.0036 (0.00037) 0.003–0.004	NA

NA indicates not suitable for statistical analysis.
[1] LBFLFK (sprayed) received standard herbicide treatments for weed control plus Beyond herbicide spray (35 g a.i./ha) at the 3–4 leaf stage.
[2] LBFLFK (non-sprayed) received standard herbicide treatments for weed control but no Beyond herbicide spray.
[3] Difference test p-value: * indicates p≤ 0.05; means are averages of five locations with four plot replications at each location.

Table 41. Vitamins – Across-Site Summary Statistics – Spring 2015

Component (mg/100 g dry weight)	Control (Kumily)	LBFLFK (sprayed)[1]	Control minus LBFLFK (sprayed)	Reference Variety Range	LBFLFK (non-sprayed)[2]	Control minus LBFLFK (non-sprayed)
	Mean (SE) min–max	Mean (SE) min–max	Difference (SE) (p-value)[3]	min–max	Mean (SE) min–max	Difference (SE) (p-value)[3]
Alpha-tocopherol[4]	9.98[4] 9.14–11.11	10.42[4] 9.23–13.25	0.96[4] (0.142)	9.33–16.32	10.12[4] 8.82–12.42	0.99[4] (0.629)
Beta-tocopherol[4]	0.20[4] 0.12–0.37	0.20[4] 0.11–0.43	0.99[4] (0.970)	< LOQ–0.55	0.16[4] 0.12–0.55	1.21[4] (0.343)
Delta-tocopherol[4]	0.61[4] 0.49–0.77	0.63[4] 0.52–0.79	0.97[4] (0.759)	0.34–0.80	0.62[4] 0.41–1.00	0.98[4] (0.859)
Gamma-tocopherol	23.42 (1.21) 19.75–25.45	24.01 (1.21) 19.52–30.7	-0.59 (0.94) (0.545)	13.9–23.93	22.7 (1.21) 17.8–27	0.72 (0.94) (0.460)
Total tocopherols	34.34 (1.6) 29.51–37.25	35.38 (1.6) 31.14–45.00	-1.04 (1.21) (0.408)	23.85–41.94	33.82 (1.6) 27.80–40.76	0.52 (1.21) (0.677)
Vitamin K1[4]	0.11[4] 0.091–0.21	0.12[4] 0.099–0.18	0.92[4] (0.01)*	0.059–0.15	0.13[4] 0.11–0.19	0.90[4] (0.002)*

[1] LBFLFK (sprayed) received standard herbicide treatments for weed control plus Beyond herbicide spray (35 g a.i./ha) at the 3–4 leaf stage.
[2] LBFLFK (non-sprayed) received standard herbicide treatments for weed control but no Beyond herbicide spray.
[3] Difference test p-value: * indicates p≤ 0.05; means are averages of seven locations with four plot replications at each location.
[4] Data were log-transformed. Means and differences were back-transformed. Difference column data are the ratio, rather than the difference, of the two means. Back-transformed SE is not provided.

Table 42. Minerals – Across-Site Summary Statistics – Spring 2015

Component (% dry weight)	Control (Kumily)	LBFLFK (sprayed)[1]	Control minus LBFLFK (sprayed)	Reference Variety Range	LBFLFK (non-sprayed)[2]	Control minus LBFLFK (non-sprayed)
	Mean (SE) min–max	Mean (SE) min–max	Difference (SE) (p-value)[3]	min–max	Mean (SE) min–max	Difference (SE) (p-value)[3]
Calcium	0.32 (0.018) 0.25–0.42	0.29 (0.018) 0.23–0.37	0.03 (0.0057) (< 0.001)*	0.30–0.52	0.29 (0.018) 0.22–0.35	0.034 (0.0057) (< 0.001)*
Copper	0.00027 (5.4e-05) 0.0002–0.00035	0.00028 (4e-05) 0.0002–0.00032	NA	0.00017–0.0005	0.00027 (3.5e-05) 0.0002–0.0003	NA
Iron	0.0080 (0.0011) 0.007–0.010	0.0075 (0.00092) 0.006–0.0085	NA	0.004–0.014	0.0079 (0.0011) 0.0062–0.0092	NA
Magnesium	0.34 (0.0075) 0.31–0.38	0.32 (0.0075) 0.30–0.35	0.018 (0.0023) (< 0.001)*	0.32–0.40	0.33 (0.0075) 0.30–0.37	0.012 (0.0023) (< 0.001)*
Manganese	0.0044 (0.00072) 0.003–0.0052	0.0044 (0.00079) 0.003–0.0052	NA	0.002–0.005	0.0044 (0.00072) 0.003–0.005	NA
Phosphorus	0.80 (0.032) 0.69–0.92	0.81 (0.032) 0.71–0.90	-0.018 (0.011) (0.129)	0.73–1.07	0.82 (0.032) 0.73–0.92	-0.026 (0.011) (0.035)*
Potassium	0.98 (0.049) 0.88–1.25	0.98 (0.049) 0.85–1.26	0.0034 (0.0097) (0.727)	0.65–1.18	1 (0.049) 0.87–1.27	-0.014 (0.0097) (0.15)
Sodium	0.0021 (0.0015) < LOQ–0.005	< LOQ < LOQ–0.0047	NA	< LOQ–0.0065	< LOQ < LOQ–0.0042	NA
Zinc	0.0036 (0.00045) 0.003–0.0042	0.0039 (0.00028) 0.0032–0.004	NA	0.0030–0.0042	0.0040 (0.00038) 0.0032–0.0045	NA

NA indicates not suitable for statistical analysis.
[1] LBFLFK (sprayed) received standard herbicide treatments for weed control plus Beyond herbicide spray (35 g a.i./ha) at the 3–4 leaf stage.
[2] LBFLFK (non-sprayed) received standard herbicide treatments for weed control but no Beyond herbicide spray.
[3] Difference test p-value: * indicates p≤ 0.05; means are averages of seven locations with four plot replications at each location.

Antinutrients

Antinutrients are those components present in canola that may have a negative impact on either animal or human health (OECD, 2011b). Glucosinolates (twelve individual analytes and a calculated total glucosinolate value), phytic acid, tannins, and representative phenolic acids (sinapine as a derivative of sinapic acid, coumaric acid, and ferulic acid) in LBFLFK were compared to Kumily and conventional canola varieties. Though not specifically recommended by the OECD consensus document, coumaric acid and ferulic acid were included in the analysis as additional representatives of phenolic acid occurring in canola grain.

Winter 2014/15 season

For antinutrients in the 2014/15 season (Table 43), statistically significant differences were observed for glucoalyssin, glucobrassicin, glucobrassicanapin, gluconapin (sprayed only), and sinapine for LBFLFK compared to Kumily. Total glucosinolates were statistically significantly higher for LBFLFK (non-sprayed) compared to Kumily. Only glucobrassicin had a statistically significant entry-by-site interaction for this season. The glucosinolates epi-progoitrin, glucoiberin, gluconapoleiferin, and glucoraphanin did not meet the criteria required for statistical analysis.

Coumaric acid content was below LOQ in grain from LBFLFK, hence the values for this component were not suitable for statistical analysis. Tannin content was below the LOQ across all samples.

For all antinutrient components, the mean LBFLFK values were within the range of the reference varieties except for neoglucobrassicin, where the mean values were slightly higher than the upper limit of the range of the reference varieties, and coumaric acid, where the mean values (below LOQ) were below the lower limit of the range of the reference varieties.

Spring 2015 season

For antinutrients in the 2015 season (Table 44), statistically significant differences were observed for glucobrassicin, gluconapin, total glucosinolates, and sinapine for LBFLFK compared to Kumily.

Coumaric acid was statistically significantly lower in LBFLFK (non-sprayed) and was the only component in this data set to have a statistically significant entry-by-site interaction for this season. The glucosinolates epi-progoitrin, glucoiberin, gluconapoleiferin, glucoraphanin, and neoglucobrassicin did not meet the criteria required for statistical analysis. Tannin content was below the LOQ across all samples.

For all antinutrient components, the mean values of LBFLFK were within the range of the reference varieties except for coumaric acid, where the mean value (below LOQ) for LBFLFK (sprayed) was below the range of the reference varieties.

Across seasons and biological relevance

Comparing the antinutrient results of the 2014/15 and the 2015 seasons, no differences were observed between LBFLFK and Kumily for phytic acid, ferulic acid, and the glucosinolates 4-hydroxyglucobrassicin, epi-progoitrin, gluconapoleiferin, gluconasturtiin, neoglucobrassicin, and progoitrin. In both seasons, glucoiberin, glucoraphanin, and tannins were consistently below LOQ for all measurements.

Coumaric acid showed a statistically significant difference only for LBFLFK (non-sprayed) in the 2015 season whereas the other values were below LOQ for LBFLFK across both seasons and could not be subjected to statistical analysis. Therefore, any differences in values for coumaric acid in LBFLFK as compared to Kumily are considered not biologically relevant.

Sinapine was statistically significantly lower for LBFLFK compared to Kumily in both the 2014/15 and 2015 seasons. However, because mean values of sinapine were within the range of the reference varieties and ILSI Crop Composition Database values, these differences are within the range of natural variability and are considered not biologically relevant.

Glucoalyssin and glucobrassicanapin were statistically significantly lower in LBFLFK as compared to Kumily in the 2014/15 season only. No trends were observed across seasons, and the means were within the range of the reference varieties. Therefore, differences in values for these components in LBFLFK are considered not biologically relevant.

Gluconapin content across seasons was statistically significantly higher, though the difference was small in magnitude, for LBFLFK as compared to Kumily, except for LBFLFK (non-sprayed) in the 2014/15 season. No trends were observed across seasons, and the means were within the range of the reference varieties. Therefore, differences in values for this component in LBFLFK are considered not biologically relevant.

Glucobrassicin was statistically significantly higher in LBFLFK compared to Kumily consistently across both the 2014/15 and 2015 seasons. Mean values of glucobrassicin, however, were within the within-season range represented by the reference varieties and within the range of ILSI Crop Composition Database values. Furthermore, the contribution of glucobrassicin to the total glucosinolates content in canola is small, and as the values were within the range of natural variation, the observed differences are considered not biologically relevant.

The calculated measure of total glucosinolates in LBFLFK was statistically significantly higher than Kumily in the 2015 season, and a similar difference was seen in the comparison of LBFLFK (non-sprayed) to Kumily in the 2014/15 season. However, the mean values for LBFLFK were within the range of the reference varieties. Additionally, the measured total glucosinolates values for LBFLFK meet the quality standards for canola (OECD, 2011b) and are within the range of values found in peer-reviewed literature and the ILSI Crop Composition Database values. Therefore, these differences are within the range of natural variation, considered not biologically relevant, and do not introduce any new safety concerns compared to conventional canola.

In summary, all antinutrient values for LBFLFK were within the range of natural variation, and observed differences are considered not biologically relevant.

Table 43. Antinutrients – Across-Site Summary Statistics – Winter 2014/15

Component (unit)	Control (Kumily)	LBFLFK (sprayed)[1]	Control minus LBFLFK (sprayed)	Reference Variety Range	LBFLFK (non-sprayed)[2]	Control minus LBFLFK (non-sprayed)
	Mean (SE) min–max	Mean (SE) min–max	Difference (SE) (p-value)[3]	min–max	Mean (SE) min–max	Difference (SE) (p-value)[3]
Phytic acid (% dry weight)	2.02 (0.13) 1.53–2.46	1.98 (0.13) 1.6–2.38	0.044 (0.064) (0.492)	1.52–2.77	2.07 (0.13) 1.73–2.36	-0.047 (0.064) (0.468)
Tannins (% dry weight)	< LOQ	< LOQ	NA	< LOQ	< LOQ	NA
4-hydroxyglucobrassicin (µmol/g dry weight)	2.14 (0.19) 1.76–2.5	2.05 (0.19) 1.48–2.72	0.091 (0.15) (0.559)	1.53–4.48	2.3 (0.19) 1.84–2.68	-0.17 (0.15) (0.295)
Epi-progoitrin (µmol/g dry weight)	< LOQ < LOQ–0.055	< LOQ < LOQ–0.055	NA	< LOQ–0.092	< LOQ < LOQ–0.068	NA
Glucoalyssin (µmol/g dry weight)	0.69 (0.076) 0.45–0.89	0.62 (0.076) 0.45–0.81	0.07 (0.03) (0.027)*	0.077–0.71	0.62 (0.076) 0.39–0.82	0.077 (0.03) (0.015)*
Glucobrassicin (µmol/g dry weight)	0.26 (0.11) 0.11–0.37	0.59 (0.11) 0.22–0.96	-0.33 (0.072) (0.002)*	< LOQ–0.90	0.56 (0.11) 0.18–0.83	-0.3 (0.072) (0.003)*
Glucobrassicanapin (µmol/g dry weight)	0.24 (0.034) 0.13–0.33	0.21 (0.034) 0.11–0.29	0.032 (0.012) (0.028)*	0.053–0.32	0.19 (0.034) 0.099–0.29	0.047 (0.012) (0.004)*
Glucoiberin (µmol/g dry weight)	< LOQ	< LOQ	NA	< LOQ	< LOQ	NA
Gluconapin (µmol/g dry weight)	1.40 (0.14) 0.94–1.79	1.72 (0.14) 1.53–1.92	-0.32 (0.088) (0.006)*	0.96–3.51	1.55 (0.14) 1.02–1.95	-0.15 (0.088) (0.121)

Component (unit)	Control (Kumily)	LBFLFK (sprayed)[1]	Control minus LBFLFK (sprayed)	Reference Variety Range	LBFLFK (non-sprayed)[2]	Control minus LBFLFK (non-sprayed)
	Mean (SE) min–max	Mean (SE) min–max	Difference (SE) (p-value)[3]	min–max	Mean (SE) min–max	Difference (SE) (p-value)[3]
Gluconapoleiferin (µmol/g dry weight)	0.051 (0.03) < LOQ–0.095	< LOQ < LOQ–0.073	NA	< LOQ–0.54	< LOQ < LOQ–0.085	NA
Gluconasturtiin (µmol/g dry weight)	0.32 (0.061) 0.12–0.44	0.27 (0.061) 0.12–0.44	0.05 (0.04) (0.217)	< LOQ–0.62	0.27 (0.061) 0.12–0.41	0.049 (0.04) (0.222)
Glucoraphanin (µmol/g dry weight)	< LOQ	< LOQ	NA	< LOQ	< LOQ	NA
Neoglucobrassicin (µmol/g dry weight)	0.25 (0.072) < LOQ–0.41	0.24 (0.072) < LOQ–0.41	0.011 (0.023) (0.637)	< LOQ–0.22	0.28 (0.072) < LOQ–0.47	-0.034 (0.023) (0.135)
Progoitrin (µmol/g dry weight)	2.83 (0.2) 2.41–3.36	2.85 (0.2) 2.27–3.37	-0.014 (0.13) (0.915)	0.87–5.39	2.84 (0.2) 2.27–3.38	-0.004 (0.13) (0.976)
Total glucosinolates[4] (µmol/g dry weight)	6.95 (0.41) 5.81–7.80	7.44 (0.41) 6.39–8.54	-0.49 (0.28) (0.084)	4.55–11.57	7.54 (0.41) 6.1–8.44	-0.59 (0.28) (0.041)*
Coumaric acid (µg/g dry weight)	13.09 (4.56) < LOQ–17.61	< LOQ	NA	10.44–57.51	< LOQ	NA
Ferulic acid (µg/g dry weight)	177.82 (9.98) 160.9–208.83	163.62 (9.98) 137.07–178.28	14.2 (12.64) (0.294)	111.83–248.33	159.66 (9.98) 127.1–203.72	18.16 (12.64) (0.189)
Sinapine (% dry weight)	1.00 (0.03) 0.93–1.11	0.89 (0.03) 0.85–0.96	0.11 (0.019) (< 0.001)*	0.76–1.08	0.91 (0.03) 0.84–0.97	0.096 (0.019) (< 0.001)*

NA indicates not suitable for statistical analysis.
[1] LBFLFK (sprayed) received standard herbicide treatments for weed control plus Beyond herbicide spray (35 g a.i./ha) at the 3–4 leaf stage.
[2] LBFLFK (non-sprayed) received standard herbicide treatments for weed control but no Beyond herbicide spray.
[3] Difference test p-value: * indicates p≤ 0.05; means are averages of five locations with four plot replications at each location.
[4] Obtained by calculation; sum of 4-hydroxyglucobrassicin through progoitrin.

Table 44. Antinutrients – Across-Site Summary Statistics – Spring 2015

Component (unit)	Control (Kumily)	LBFLFK (sprayed)[1]	Control minus LBFLFK (sprayed)	Reference Variety Range	LBFLFK (non-sprayed)[2]	Control minus LBFLFK (non-sprayed)
	Mean (SE) min–max	Mean (SE) min–max	Difference (SE) (p-value)[3]	min–max	Mean (SE) min–max	Difference[4] (SE) (p-value)[3]
Phytic acid (% dry weight)	2.28 (0.1) 1.99–2.58	2.31 (0.1) 2.03–2.57	-0.026 (0.043) (0.537)	1.99–3.24	2.33 (0.1) 1.96–2.63	-0.046 (0.043) (0.284)
Tannins (% dry weight)	< LOQ	< LOQ	NA	< LOQ	< LOQ	NA
4-hydroxyglucobrassicin (µmol/g dry weight)	3.47 (0.21) 2.71–4.14	3.51 (0.21) 2.65–4.27	-0.042 (0.11) (0.711)	2.14–5.21	3.33 (0.21) 2.45–3.96	0.14 (0.11) (0.223)
Epi-progoitrin (µmol/g dry weight)	0.068 (0.026) < LOQ–0.1	0.083 (0.026) < LOQ–0.12	NA	< LOQ–0.30	0.081 (0.028) < LOQ–0.12	NA
Glucoalyssin[4] (µmol/g dry weight)	1.11[4] 0.61–1.8	1.15[4] 0.68–1.82	0.97[4] (0.45)	0.093–2.65	1.11[4] 0.57–1.73	1[4] (0.9828)
Glucobrassicin[4] (µmol/g dry weight)	0.31[4] 0.16–0.8	0.67[4] 0.39–1.52	0.46[4] (< 0.001)*	0.07–1.30	0.67[4] 0.42–1.6	0.46[4] (< 0.001)*
Glucobrassicanapin[4] (µmol/g dry weight)	0.39[4] 0.19–0.63	0.40[4] 0.19–0.66	0.99[4] (0.803)	0.053–0.73	0.39[4] 0.16–0.6	1.01[4] (0.798)
Glucoiberin (µmol/g dry weight)	< LOQ	< LOQ	NA	< LOQ	< LOQ	NA
Gluconapin (µmol/g dry weight)	2.30 (0.22) 1.44–2.71	2.45 (0.22) 1.61–3.57	-0.15 (0.047) (0.002)*	0.88–5.87	2.50 (0.22) 1.25–3.61	-0.20 (0.047) (< 0.001)*

Component (unit)	Control (Kumily)	LBFLFK (sprayed)[1]	Control minus LBFLFK (sprayed)	Reference Variety Range	LBFLFK (non-sprayed)[2]	Control minus LBFLFK (non-sprayed)
	Mean (SE) min–max	Mean (SE) min–max	Difference (SE) (p-value)[3]	min–max	Mean (SE) min–max	Difference[4] (SE) (p-value)[3]
Gluconapoleiferin (µmol/g dry weight)	0.08 (0.054) < LOQ–0.17	0.083 (0.063) < LOQ–0.20	NA	< LOQ–0.57	0.089 (0.058) < LOQ–0.19	NA
Gluconasturtiin (µmol/g dry weight)	0.29 (0.023) 0.17–0.34	0.28 (0.023) 0.17–0.35	0.0096 (0.012) (0.43)	< LOQ–0.60	0.29 (0.023) 0.18–0.37	0.0061 (0.012) (0.619)
Glucoraphanin (µmol/g dry weight)	< LOQ	< LOQ	NA	< LOQ	< LOQ	NA
Neoglucobrassicin (µmol/g dry weight)	0.066 (0.025) < LOQ–0.098	0.080 (0.046) < LOQ–0.18	NA	< LOQ–0.095	0.065 (0.021) < LOQ–0.095	NA
Progoitrin[4] (µmol/g dry weight)	4.66[4] 2.60–8.03	4.99[4] 2.78–8.13	0.93[4] (0.129)	0.82–15.50	4.79[4] 2.31–8.23	0.97[4] (0.538)
Total glucosinolates (µmol/g dry weight)	11.62 (1.19) 7.16–15.48	12.78 (1.19) 7.69–17.25	-1.17 (0.34) (0.001)*	4.21–25.57	12.45 (1.19) 6.65–17.08	-0.84 (0.34) (0.019)*
Coumaric acid (µg/g dry weight)	16.89 (1.27) 13.81–21.03	< LOQ < LOQ–14.17	NA	10.22–56.50	11.85 (1.27) < LOQ–15.41	5.03 (1.42) (0.004)*
Ferulic acid (µg/g dry weight)	127.39 (3.77) 115.8–137.9	122.62 (3.77) 108.67–140.1	4.76 (2.91) (0.127)	108.97–177.60	121.14 (3.77) 102.97–130.07	6.24 (2.91) (0.053)
Sinapine (% dry weight)	1.02 (0.031) 0.90–1.20	0.95 (0.031) 0.87–1.10	0.071 (0.013) (< 0.001)*	0.79–1.09	0.95 (0.031) 0.87–1.09	0.069 (0.013) (< 0.001)*

NA indicates not suitable for statistical analysis.
[1] LBFLFK (sprayed) received standard herbicide treatments for weed control plus Beyond herbicide spray (35 g a.i./ha) at the 3–4 leaf stage.
[2] LBFLFK (non-sprayed) received standard herbicide treatments for weed control but no Beyond herbicide spray.
[3] Difference test p-value: * indicates p≤ 0.05; means are averages of seven locations with four plot replications at each location.
[4] Data were log-transformed. Means and differences were back-transformed. Difference column data are the ratio, rather than the difference, of the two means. Back-transformed SE is not provided.

Phytosterols

Phytosterols are minor components of canola and are not included in the list of recommended analytes as part of a comparative assessment as per the OECD consensus document (OECD, 2011b). However, canola has approximately twice the phytosterol content of sunflower or soybean oil, and phytosterol content has been shown to correlate to the iodine value of oil (Vlahakis and Hazebroek, 2000), a cumulative measure of the degree of unsaturation of fatty acids in oil (Unger, 2015). Therefore, phytosterol (fourteen individual species and total phytosterols) components were analysed. Of these, beta-sitosterol is predominant, with campesterol and brassicasterol being the other major species contributing to the total phytosterol content (Unger, 2015).

Winter 2014/15 season

The phytosterols brassicasterol, delta-5 avenasterol, delta-7 stigmastenol, stigmasterol, and the total phytosterols measurement showed statistically significant differences in the 2014/15 season for LBFLFK when compared to Kumily (Table 45). Delta-5 avenasterol and delta-7 stigmastenol also showed statistically significant entry-by-site interactions.

The phytosterols 24-methylene cholesterol, campestanol, cholesterol, clerosterol, delta-5,23 stigmastadienol, delta-5,24 stigmastadienol, delta-7 avenasterol, and sitostanol did not meet the criteria required for statistical analysis. All mean values of phytosterols in LBFLFK were within the reference ranges.

Spring 2015 season

The phytosterols beta-sitosterol, brassicasterol, campesterol, and total phytosterols showed statistically significant differences in the 2015 season for LBFLFK when compared to Kumily (Table 46). Brassicasterol and total phytosterols also showed statistically significant entry-by-site interactions.

Data for 24-methylene cholesterol, campestanol, cholesterol, clerosterol, delta-5 avenasterol, delta-5,23 stigmastadienol, delta-5,24 stigmastadienol, delta-7 avenasterol, delta-7 stigmastenol, sitostanol, and stigmasterol did not meet the criteria required for statistical analysis.

All mean values of phytosterols for LBFLFK were within the range of the reference varieties, except for delta-7 stigmastenol, which was slightly higher than the upper limit of the range of the reference varieties in LBFLFK (non-sprayed).

Across seasons and biological relevance

Comparing the phytosterol results of the 2014/15 and 2015 seasons, statistically significant differences were observed in 2015 between LBFLFK and Kumily for beta-sitosterol and for campesterol that were not present in 2014/15; however, the mean values for these components were within the range of the reference varieties.

Only in the 2014/15 season were delta-5 avenasterol and stigmasterol statistically significantly lower and delta-7 stigmastenol statistically significantly higher than Kumily. Only in the 2015 season were beta-sitosterol and campesterol statistically significantly lower in LBFLFK compared to Kumily. As no trends were observed across seasons for these components and

all values were within the range of the reference varieties, the observed differences in the values for these components are considered not biologically relevant.

Brassicasterol and total phytosterols were statistically significantly lower for LBFLFK compared to Kumily across both seasons. However, the means were within the range of the reference varieties and, therefore, these differences are considered not biologically relevant.

It is noted that some measurements of phytosterols across all samples did not compare well with peer-reviewed literature and ILSI Crop Composition Database values. The values for beta-sitosterol, campesterol, cholesterol, and total phytosterols were approximately 2 to 3-fold higher than the ILSI Crop Composition Database values, and brassicasterol was 1 to 2-fold higher. As all varieties tested had similar elevated results, these differences are most likely attributed to differences in the method of analysis used. The results within each season are internally consistent, and the mean contents for all measured phytosterol components and total phytosterols of LBFLFK were within the range of the reference varieties (except for one value of the minor component delta-7 stigmastenol). Additionally, the results are also consistent with available peer-reviewed literature observations that beta-sitosterol, campesterol, and brassicasterol are the predominant phytosterols in canola, making up over 90% of the relative total sterol content in this species (Reina et al., 1999).

The results across seasons for phytosterol content measurements support the conclusion that LBFLFK is compositionally equivalent to conventional canola varieties for these components and the observed differences in values are considered not biologically relevant.

Table 45. Phytosterols – Across-Site Summary Statistics – Winter 2014/15

Component (% dry weight)	Control (Kumily)	LBFLFK (sprayed)[1]	Control minus LBFLFK (sprayed)	Reference Variety Range	LBFLFK (non-sprayed)[2]	Control minus LBFLFK (non-sprayed)
	Mean (SE) min–max	Mean (SE) min–max	Difference (SE) (p-value)[3]	min–max	Mean (SE) min–max	Difference (SE) (p-value)[3]
24-methylene cholesterol	0.0038 (0.0016) 0.0027–0.0067	0.0022 (0.00041) 0.0018–0.0027	NA	0.0022–0.01	0.0022 (0.0006) 0.0018–0.0032	NA
Beta-sitosterol	0.50 (0.028) 0.43–0.58	0.49 (0.028) 0.41–0.58	0.0095 (0.0081) (0.253)	0.43–0.68	0.49 (0.028) 0.42–0.57	0.011 (0.0081) (0.173)
Brassicasterol	0.12 (0.0043) 0.11–0.13	0.078 (0.0043) 0.067–0.087	0.042 (0.0021) (< 0.001)*	0.054–0.11	0.078 (0.0043) 0.066–0.087	0.043 (0.0021) (< 0.001)*
Campestanol	< LOQ	< LOQ	NA	< LOQ–0.0014	< LOQ	NA
Campesterol	0.25 (0.0092) 0.22–0.27	0.25 (0.0092) 0.22–0.28	0.0006 (0.0058) (0.926)	0.22–0.34	0.26 (0.0092) 0.23–0.28	-0.0028 (0.0058) (0.646)
Cholesterol	0.0038 (0.00073) 0.0030–0.0047	0.0046 (0.0031) 0.0027–0.01	NA	0.002–0.006	0.0032 (0.00053) 0.0025–0.0037	NA
Clerosterol	0.0047 (0.00061) 0.0040–0.0055	0.0047 (0.00054) 0.004–0.0052	NA	0.004–0.0065	0.0046 (0.00045) 0.004–0.005	NA
Delta-5 avenasterol	0.01 (0.0015) 0.007–0.02	0.0065 (0.0015) 0.0055–0.0090	0.0039 (0.0014) (0.022)*	0.0042–0.03	0.0068 (0.0015) 0.0055–0.0100	0.0036 (0.0014) (0.032)*

Component (% dry weight)	Control (Kumily)	LBFLFK (sprayed)[1]	Control minus LBFLFK (sprayed)	Reference Variety Range	LBFLFK (non-sprayed)[2]	Control minus LBFLFK (non-sprayed)
	Mean (SE) min–max	Mean (SE) min–max	Difference (SE) (p-value)[3]	min–max	Mean (SE) min–max	Difference (SE) (p-value)[3]
Delta-5,23 stigmastadienol	< LOQ < LOQ–0.0005	< LOQ	NA	< LOQ	< LOQ	NA
Delta-5,24 stigmastadienol	0.0040 (0.001) 0.0030–0.0057	0.0044 (0.00038) 0.0040–0.0050	NA	0.0027–0.0070	0.0044 (0.00058) 0.0037–0.0052	NA
Delta-7 avenasterol	0.0011 (0.0005) 0.00082–0.0020	0.0020 (0.00011) 0.0018–0.0020	NA	0.0008–0.003	0.0018 (0.00021) 0.0015–0.0020	NA
Delta-7 stigmastenol	0.0025 (0.0008) 0.0018–0.0035	0.0068 (0.0008) 0.0042–0.0097	-0.0043 (0.0006) (< 0.001)*	0.0018–0.01	0.0064 (0.0008) 0.0047–0.0100	-0.004 (0.0006) (< 0.001)*
Sitostanol	0.0009 (0.00017) 0.0006–0.0010	0.0008 (0.00027) < LOQ–0.001	NA	0.00045–0.0018	0.00084 (0.00016) 0.00057–0.00097	NA
Stigmasterol	0.0051 (0.0005) 0.0027–0.0060	0.0041 (0.0005) 0.0022–0.0055	0.0011 (0.0003) (0.003)*	0.0015–0.0050	0.0037 (0.0005) 0.0022–0.0047	0.0015 (0.0003) (< 0.001)*
Total phytosterols	0.93 (0.039) 0.83–1.03	0.88 (0.039) 0.77–1.01	0.05 (0.015) (0.01)*	0.78–1.18	0.87 (0.039) 0.79–0.99	0.052 (0.015) (0.008)*

NA indicates not suitable for statistical analysis.
[1] LBFLFK (sprayed) received standard herbicide treatments for weed control plus Beyond herbicide spray (35 g a.i./ha) at the 3–4 leaf stage.
[2] LBFLFK (non-sprayed) received standard herbicide treatments for weed control but no Beyond herbicide spray.
[3] Difference test p-value: * indicates p≤ 0.05; means are averages of five locations with four plot replications at each location.

Table 46. Phytosterols – Across-Site Summary Statistics – Spring 2015

Component (% dry weight)	Control (Kumily)	LBFLFK (sprayed)[1]	Control minus LBFLFK (sprayed)	Reference Variety Range	LBFLFK (non-sprayed)[2]	Control minus LBFLFK (non-sprayed)
	Mean (SE) min–max	Mean (SE) min–max	Difference (SE) (p-value)[3]	min–max	Mean (SE) min–max	Difference (SE) (p-value)[3]
24-methylene cholesterol	0.0040 (0.002) 0.002–0.007	0.0019 (0.001) 0.00092–0.0032	NA	0.0015–0.0150	0.0018 (0.00085) 0.00095–0.0030	NA
Beta-sitosterol	0.47 (0.013) 0.42–0.53	0.44 (0.013) 0.40–0.49	0.026 (0.0056) (< 0.001)*	0.40–0.57	0.44 (0.013) 0.40–0.48	0.025 (0.0056) (0.001)*
Brassicasterol	0.12 (0.002) 0.10–0.13	0.072 (0.002) 0.065–0.076	0.048 (0.001) (< 0.001)*	0.052–0.110	0.072 (0.002) 0.064–0.076	0.048 (0.001) (< 0.001)*
Campestanol	< LOQ	< LOQ	NA	< LOQ–0.00057	< LOQ	NA
Campesterol	0.25 (0.012) 0.22–0.31	0.24 (0.012) 0.21–0.3	0.013 (0.0029) (0.001)*	0.21–0.35	0.24 (0.012) 0.21–0.29	0.012 (0.0029) (0.001)*
Cholesterol	0.0036 (0.00093) 0.0027–0.0055	0.0027 (0.00044) 0.0022–0.0032	NA	0.002–0.005	0.0028 (0.00044) 0.002–0.0032	NA
Clerosterol	0.0046 (0.0004) 0.0040–0.0050	0.0042 (0.00037) 0.0040–0.005	NA	0.0040–0.0052	0.0043 (0.0003) 0.0040–0.0047	NA
Delta-5 avenasterol	0.011 (0.0041) 0.0072–0.020	0.0076 (0.002) 0.005–0.010	NA	0.005–0.032	0.0076 (0.0019) 0.0052–0.010	NA

Component (% dry weight)	Control (Kumily)	LBFLFK (sprayed)[1]	Control minus LBFLFK (sprayed)	Reference Variety Range	LBFLFK (non-sprayed)[2]	Control minus LBFLFK (non-sprayed)
	Mean (SE) min–max	Mean (SE) min–max	Difference (SE) (p-value)[3]	min–max	Mean (SE) min–max	Difference (SE) (p-value)[3]
Delta-5,23 stigmastadienol	< LOQ	< LOQ	NA	< LOQ	< LOQ	NA
Delta-5,24 stigmastadienol	0.0042 (0.00051) 0.0032–0.0047	0.0042 (0.00043) 0.0037–0.0047	NA	0.0030–0.0055	0.0042 (0.00049) 0.0035–0.0050	NA
Delta-7 avenasterol	0.0011 (0.00028) 0.001–0.0018	0.0019 (0.00012) 0.0018–0.002	NA	0.00085–0.0022	0.002 (9.4e-05) 0.0018–0.0020	NA
Delta-7 stigmastenol	0.0023 (0.00037) 0.002–0.003	0.0064 (0.00069) 0.0055–0.0075	NA	0.001–0.0065	0.0066 (0.00067) 0.0057–0.0075	NA
Sitostanol	0.00060 (0.00013) 0.00042–0.00075	0.00051 (0.00012) < LOQ–0.00065	NA	< LOQ–0.00095	0.00055 (6.2e-05) 0.00050–0.00065	NA
Stigmasterol	0.0047 (0.00087) 0.0035–0.0060	0.0036 (0.00066) 0.0027–0.0045	NA	0.002–0.005	0.0037 (0.00047) 0.0030–0.0042	NA
Total phytosterols	0.89 (0.027) 0.78–1.02	0.80 (0.027) 0.71–0.91	0.089 (0.0098) (< 0.001)*	0.74–1.08	0.80 (0.027) 0.71–0.89	0.087 (0.0098) (< 0.001)*

NA indicates not suitable for statistical analysis.
[1] LBFLFK (sprayed) received standard herbicide treatments for weed control plus Beyond herbicide spray (35 g a.i./ha) at the 3–4 leaf stage.
[2] LBFLFK (non-sprayed) received standard herbicide treatments for weed control but no Beyond herbicide spray.
[3] Difference test p-value: * indicates p≤ 0.05; means are averages of seven locations with four plot replications at each location.

Conclusions on the compositional analysis of the harvested grain

As part of the food, feed, and environmental safety assessment of EPA+DHA canola event LBFLFK, a comparative assessment was performed with the parental control variety Kumily and other conventional reference canola varieties. Key compositional components were assessed for LBFLFK grain (oilseed) grown and harvested during two seasons in the United States: during the winter of 2014/15 and in the spring of 2015 as part of two randomised complete block design studies. As event LBFLFK contains a trait that confers tolerance to Beyond herbicide (active ingredient imazamox), plots treated with or without Beyond herbicide were included. Grain samples were harvested and analysed for composition, including proximates, fibres, amino acids, fatty acids, vitamins, minerals, antinutrients, and phytosterols. A total of 112 components were measured.

The EPA+DHA trait of event LBFLFK impacted the overall fatty acid composition in harvested grain as intended. For the other grain components measured, the results of the comparative approach demonstrated that EPA+DHA canola event LBFLFK (either sprayed or non-sprayed with Beyond herbicide) is compositionally equivalent to commercially available canola varieties based on comparisons to Kumily, the ranges presented for conventional reference varieties are referred to in peer-reviewed literature, as well as in the ILSI Crop Composition Database.

Nutrient composition of the processed products of LBFLFK canola

To evaluate the potential effects of processing on food and feed products derived from LBFLFK and to further establish that the nutritional components of the processed fractions were not altered in a manner that would have an adverse impact on human or animal health, a comparative assessment of nutritional components of the processed fractions was performed. Samples harvested from plots of LBFLFK sprayed with Beyond herbicide (active ingredient imazamox), the parental control Kumily, and three conventional reference varieties (IMC105, 46A65, and Wizzard) grown under commercial production conditions during the 2016 season were used for this assessment. Harvested mature seed (grain) from five field locations was used for generating processed fractions for nutrient compositional analyses. The harvested grain was processed into oil and meal fractions using conditions similar to conventional canola and representative of the expected commercial process for production of EPA+DHA canola products.

Processing was performed at [redacted] under commercial conditions, using pilot-scale equipment, which were comparable to the planned method for commercial production of oil and meal from EPA+DHA canola event LBFLFK. All equipment and reagents used were within the specifications required for commercial production of canola oil and meal. Due to sample size, the samples for the analyses were processed by a batch method whereas the standard for commercial operations is continuous processing.

Brief summary of canola processing

Several processing steps are involved in making canola oil and meal at a commercial processing facility (Unger, 2015), and these were followed to produce the samples for analysis. An overview of the processing steps is provided in Figure 82. To begin, cleaned and tempered canola grain are rolled or flaked with applied heat followed by crushing and pressing to produce the pressed oil fraction. The pressed oil and meal fractions are then processed

separately according to end-product requirements. The canola meal remaining after pressing contains between 14–20% oil (OECD, 2011b). The remaining oil in the meal is extracted using hexane to produce defatted meal and extracted oil.

A physical blend of pressed oil and extracted oil (the combination referred to as crude oil herein) was produced for refining at a ratio of approximately 83:17% of pressed oil: extracted oil. This crude oil was further processed by refining, bleaching, and deodorizing. It is noted that pressed oil alone may also be used commercially. The resulting oil product is referred to as refined, bleached, and deodorised (RBD) oil. Additional details of processing canola into commercial equivalent fractions are provided in section A.2(b).

Figure 82. Flow Diagram for Preparation of Oil and Meal from Canola

Process steps are indicated in the right most column, and resulting products of the processing are indicated to the left.

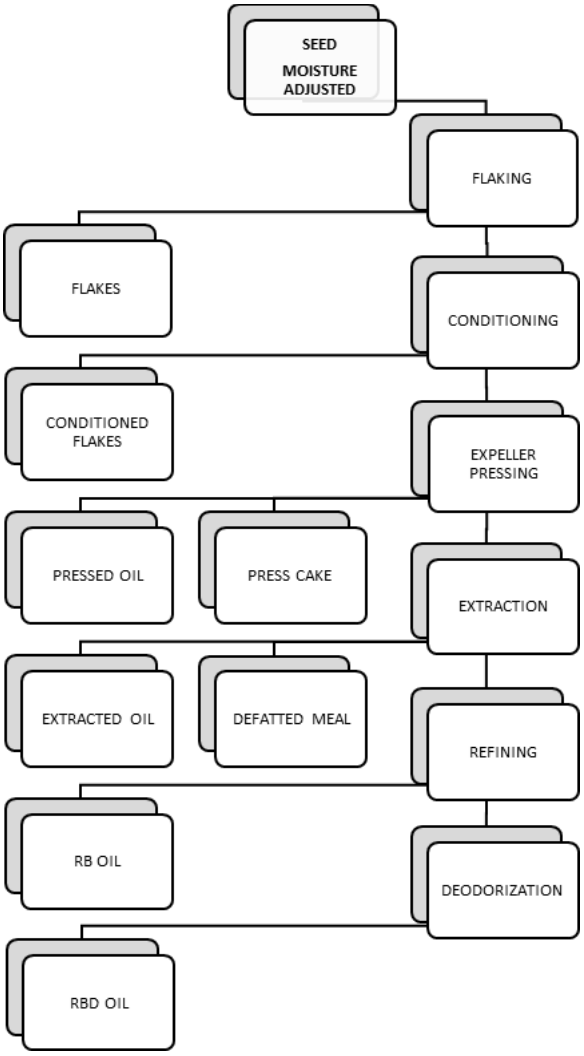

The components selected for compositional analysis were based primarily on the guidance provided in the consensus document for canola from the Organisation for Economic Co-operation and Development (OECD, 2011b). A total of 112 components were assessed, which were grouped into categories including proximates and fibres, amino acids, fatty acids, vitamins and minerals, antinutrients, phytosterols, and heavy metals. The processed fractions that were measured included defatted meal, pressed oil alone[15], pressed and extracted oil combined (crude oil), and RBD oil (Table 47). The compositional data of the milled grain (unprocessed ground grain) at each location are provided for reference in Appendix 23. The compositional data for LBFLFK, Kumily, and three reference varieties are described further as two categories of processed fractions: defatted meal and oil (crude and RBD oil).

[15] As pressed oil is the majority component of crude oil, and the data support the equivalence of the pressed oil and crude oil fractions, only crude oil (blend of pressed and extracted oil) compositional data are discussed in detail herein.

Table 47. Components Analysed per Processed Fraction

Matrix	Analyte groups
Defatted Meal	Proximates and Fibres Amino Acids Fatty Acids Vitamins and Minerals Antinutrients Heavy Metals
Pressed and Crude Oil	Moisture and Protein Amino Acids Fatty Acids Vitamins and Minerals Phytosterols Heavy Metals
RBD Oil	Fatty Acids Vitamins Phytosterols Heavy Metals

Comparisons between the across-site means for LBFLFK and Kumily were conducted using Student's paired t-Test with a two-tailed distribution (Steel and Torrie, 1976). A significance level of $\alpha = 0.05$ (confidence level = 95%) was used for all statistical tests. Means were calculated for each reference variety and are presented as a range for comparison.

Across-site mean values were compared to 1) the range of means generated from the reference varieties, 2) the International Life Sciences Institute (ILSI) Crop Composition Database data (ILSI, 2016), and 3) peer-reviewed scientific literature to provide context for the comparative analyses and assess the broader biological relevance of the results.

Additional details of the materials, processing steps, and methods for compositional and statistical analysis are given in Appendix 23. The table presenting the reference data from the ILSI Crop Composition database and peer-reviewed scientific literature is provided in Appendix 22.

Defatted meal

The final solvent-free defatted meal (containing about 1% oil and 8–10% moisture content) produced after extraction is an important by-product of canola oil production and is primarily used as an animal feed ingredient as a source of high protein feed for livestock, poultry, and fish (OECD, 2011b). Proximates, fibre, minerals, and glucosinolates in the meal are nutritionally important, and these analyses are generally used by animal nutritionists to evaluate feed ingredients and to formulate least cost rations. Protein, fat, and fibre are the key indicators of compositional differences and livestock feed quality (OECD, 2011b).

Proximates and fibre

Across sites, defatted meal from LBFLFK did not show any significant differences in proximate (moisture, crude fat, protein, ash, and carbohydrates) and fibre (crude fibre, acid detergent fibre, and neutral detergent fibre) composition compared to Kumily (Table 48). The crude fat content between both defatted meal fractions was comparable, with a mean of 1.12% for

LBFLFK versus 0.94% in Kumily. As expected, defatted meal of both LBFLFK and Kumily was reduced in total fat content and enriched in moisture, protein, carbohydrates, ash, and fibre as compared to the milled grain (OECD, 2011b).

Table 48. Defatted Meal Proximates and Fibre – Across-Site Summary Statistics

Analyte (% DW)	Control (Kumily)	LBFLFK	t-Test[2]	Reference Variety Range
	Mean[1] (SD)	Mean[1] (SD)	p-value[3]	min–max[1]
Moisture	11.66 (1.40)	10.94 (1.64)	0.3258	10.10–10.89
Crude fat	0.94 (0.08)	1.12 (0.46)	0.2425	0.77–0.91
Protein	47.32 (1.71)	46.75 (1.54)	0.4449	47.51–49.38
Ash	7.50 (0.12)	7.47 (0.25)	0.8262	7.74–7.94
Carbohydrates	44.25 (1.66)	44.65 (1.65)	0.5787	42.11–43.77
Crude fibre	11.0 (0.7)	11.6 (0.8)	0.1097	11.1–12.0
Acid detergent fibre	19.1 (1.9)	19.4 (1.7)	0.7399	18.2–19.0
Neutral detergent fibre	23.3 (1.8)	24.8 (1.7)	0.1369	23.4–24.4

Limits of quantitation (LOQ) on a dry weight basis: moisture (0.2%), crude fat (0.1%), protein (0.2%), ash (0.4%), carbohydrates (0.4%), crude fibre (0.2%), acid detergent fibre (0.3%), neutral detergent fibre (0.3%).
[1] LBFLFK and Kumily means were formed from ten replicate samples (n = 10). For reference varieties' minimum and maximum means, n = 10 except for one variety (IMC105), where n = 8.
[2] Student's paired t-Test (two-tailed distribution) was used to determine the probability of a significant difference between LBFLFK and Kumily means.
[3] * indicates $p \leq 0.05$.

Amino acids

No difference was observed for LBFLFK compared to Kumily for the across-site mean values of the amino acids aspartic acid, threonine, serine, glutamic acid, glycine, alanine, valine, isoleucine, leucine, tyrosine, phenylalanine, lysine, arginine, proline, methionine, and tryptophan (Table 49). The mean values for histidine and cystine were statistically significantly different between LBFLFK and Kumily, which were both slightly lower than the range of the reference varieties. The mean values of histidine and cystine in both LBFLFK and Kumily meal were slightly higher than the range shown in the ILSI Crop Composition Database, and histidine in Kumily meal was slightly higher than the range seen in peer-reviewed scientific literature. However, cystine was in the range seen in peer-reviewed scientific literature. Compared to milled grain, defatted meal fractions of both LBFLFK and Kumily have enriched amino acid content, as would be expected based on the higher protein content found in the proximate analysis.

Table 49. Defatted Meal Amino Acids – Across-Site Summary Statistics

Amino Acid (% DW)	Control (Kumily)	LBFLFK	t-Test[2]	Reference Variety Range
	Mean[1] (SD)	Mean[1] (SD)	p-value[3]	min–max[1]
Aspartic acid	3.71 (0.14)	3.90 (0.20)	0.0574	3.55–3.86
Threonine	2.03 (0.06)	1.99 (0.06)	0.1701	2.06–2.16
Serine	2.03 (0.07)	1.99 (0.07)	0.0964	2.06–2.16
Glutamic acid	8.48 (0.50)	8.10 (0.28)	0.0657	8.53–8.87
Glycine	2.39 (0.08)	2.37 (0.05)	0.4740	2.39–2.59
Alanine	2.00 (0.07)	1.99 (0.07)	0.7343	2.01–2.09
Valine	2.49 (0.11)	2.44 (0.10)	0.4484	2.48–2.63
Isoleucine	1.95 (0.09)	1.89 (0.08)	0.2191	1.95–2.07
Leucine	3.36 (0.13)	3.26 (0.10)	0.0767	3.40–3.58
Tyrosine	1.28 (0.03)	1.26 (0.08)	0.5431	1.26–1.38
Phenylalanine	1.94 (0.07)	1.90 (0.08)	0.2498	1.93–2.06
Lysine	2.71 (0.12)	2.66 (0.09)	0.4517	2.74–2.86
Histidine	1.26 (0.06)	1.20 (0.03)	0.0221*	1.31–1.33
Arginine	3.00 (0.13)	2.96 (0.13)	0.5409	3.01–3.26
Proline	2.87 (0.18)	2.78 (0.15)	0.2398	2.90–3.00
Cystine	1.07 (0.10)	0.98 (0.07)	0.0325*	1.11–1.15
Methionine	0.94 (0.04)	0.90 (0.04)	0.0685	0.95–0.97
Tryptophan	0.75 (0.02)	0.73 (0.03)	0.0754	0.76–0.78

Limits of quantitation (LOQ) on a dry weight basis: aspartic acid (0.02%), threonine (0.02%), serine (0.01%), glutamic acid (0.02%), glycine (0.01%), alanine (0.01%), valine (0.02%), isoleucine (0.02%), leucine (0.02%), tyrosine (0.04%), phenylalanine (0.03%), lysine (0.01%), histidine (0.01%), arginine (0.05%), proline (0.05%), cystine (0.01%), methionine (0.01%), tryptophan (0.01%).

[1] LBFLFK and Kumily means were formed from ten replicate samples (n = 10). For reference varieties' minimum and maximum means, n = 10 except for one variety (IMC105), where n = 8.

[2] Student's paired t-Test (two-tailed distribution) was used to determine the probability of a significant difference between LBFLFK and Kumily means.

[3] * indicates $p \leq 0.05$.

Fatty acids

Fatty acids are a minor proximate component of canola defatted meal (~1%). Given the very low percent of individual fatty acids, comparison of these data is not meaningful to an assessment and is not presented here. No fatty acid that was less than LOQ in LBFLFK defatted meal was above LOQ in either Kumily or the reference varieties.

Vitamins and minerals

No statistically significant differences were observed in the vitamin content of defatted meal from LBFLFK relative to Kumily (Table 50). As expected, the mean content of fat-soluble vitamins in the defatted meal fraction is reduced in both LBFLFK and Kumily compared to milled grain.

No differences were observed for phosphorus, magnesium, sodium, iron, zinc, copper, and manganese between defatted meal from LBFLFK compared to Kumily. Calcium was statistically significantly lower, and potassium was statistically significantly higher in defatted meal from LBFLFK compared to Kumily. Calcium in both LBFLFK and Kumily was less than that of the reference range but was within the range of values in the literature. Potassium in

both LBFLFK and Kumily was slightly higher than the reference range and was higher than the literature range. As calcium was lower and potassium was higher in milled grain for both LBFLFK and Kumily as compared to the reference varieties, the processing did not impact the mineral content for LBFLFK differently than for Kumily or other conventional canola varieties. The content of the primary minerals (phosphorus, potassium, calcium, and magnesium) in defatted meal of LBFLFK, Kumily, and the reference varieties is increased compared to the milled grain, which correlates with the higher ash proximate content of defatted meal.

Table 50. Defatted Meal Vitamins and Minerals – Across-Site Summary Statistics

Analyte (DW)	Control (Kumily)	LBFLFK	t-Test[2]	Reference Variety Range
	Mean[1] (SD)	Mean[1] (SD)	p-value[3]	min–max[1]
α-tocopherol (mg/100g)	1.9 (0.2)	1.6 (0.3)	0.0549	1.6–2.9
ɣ-tocopherol (mg/100g)	2.7 (0.4)	2.7 (0.8)	0.9097	0.9–1.2
β-tocopherol (mg/100g)	< LOQ (NA)	< LOQ (NA)	NA	< LOQ–< LOQ
δ-tocopherol (mg/100g)	< LOQ (NA)	< LOQ (NA)	NA	< LOQ–< LOQ
Total Tocopherols (mg/100g)	4.7 (0.6)	4.3 (1.2)	0.3822	2.5–4.1
Vitamin K1 (mg/100g)	0.04369 (0.00426)	0.03906 (0.00606)	0.1576	0.03243–0.04264
Calcium (%)	0.567 (0.038)	0.491 (0.041)	0.0079*	0.714–0.784
Phosphorus (%)	1.37 (0.06)	1.44 (0.10)	0.0936	1.41–1.48
Magnesium (%)	0.581 (0.051)	0.561 (0.035)	0.4365	0.587–0.632
Potassium (%)	1.64 (0.08)	1.69 (0.05)	0.0467*	1.31–1.58
Sodium (%)	0.003 (0.001)	0.003 (0.000)	0.1248	0.003–0.005
Iron (%)	0.0166 (0.0037)	0.0167 (0.0048)	0.9679	0.0129–0.0185
Zinc (%)	0.0063 (0.0005)	0.0065 (0.0007)	0.3407	0.0052–0.0062
Copper (%)	0.00044 (0.00004)	0.00044 (0.00007)	0.8752	0.00039–0.00054
Manganese (%)	0.0080 (0.0016)	0.0080 (0.0014)	0.9297	0.0060–0.0071

Limits of quantitation (LOQ) on a dry weight basis: α-tocopherol (0.3 mg/100g), y-tocopherol (0.3 mg/100g), ß-tocopherol (0.3 mg/100g), δ-tocopherol (0.3 mg/100g), total tocopherols (0.3 mg/100g), vitamin K1 (0.000625 mg/100g), calcium (0.004%), phosphorus (33 ppm), magnesium (0.001%), potassium (0.004%), sodium (0.002%), iron (0.0002%), zinc (0.001%), copper (0.0001%), manganese (0.00005%).

NA = Not applicable as value was not calculated.

[1] LBFLFK and Kumily means were formed from ten replicate samples (n = 10). For reference varieties' minimum and maximum means, n = 10 except for one variety (IMC105), where n = 8. Means less than the LOQ are expressed as "< LOQ."

[2] Student's paired t-Test (two-tailed distribution) was used to determine the probability of a significant difference between LBFLFK and Kumily means.

[3] * indicates p≤ 0.05.

Antinutrients

Values for phytic acid, epi-progoitrin, gluconapoleiferin, glucoalyssin, gluconapin, glucobrassicanapin, gluconasturtiin, neoglucobrassicin, and tannins were not statistically different between LBFLFK and Kumily (Table 51). Statistically significant differences were observed for progoitrin, 4-hydroxyglucobrassicin, ferulic acid, p-coumaric acid, and sinapine, with values lower in LBFLFK relative to Kumily, though values were either within or below the range of reference varieties. Glucobrassicin was statistically significantly higher in LBFLFK relative to Kumily and was higher than the reference ranges. However, glucobrassicin was within the range of ILSI Crop Composition Database values if the weight percent of meal in

seed is taken into consideration. Furthermore, the contribution of glucobrassicin to the total glucosinolates content in canola was small, and the values were within the range of natural variation. All samples contained < 30 µmol/g total glucosinolates as is expected for this antinutrient in canola meal (OECD, 2011b).

Table 51. Defatted Meal Antinutrients – Across-Site Summary Statistics

Antinutrient (DW)	Control (Kumily)	LBFLFK	t-Test[2]	Reference Variety Range
	Mean[1] (SD)	Mean[1] (SD)	p-value[3]	min–max[1]
Phytic acid (%)	3.9 (0.2)	4.1 (0.3)	0.1753	4.0–4.2
Glucoiberin (µmol/g)	< LOQ (NA)	< LOQ (NA)	NA	< LOQ–< LOQ
Progoitrin (µmol/g)	7.78 (1.97)	6.47 (0.87)	0.0265*	2.41–11.65
Epi-progoitrin (µmol/g)	0.15 (0.04)	0.12 (0.01)	0.0720	0.06–0.23
Glucoraphanin (µmol/g)	< LOQ (NA)	< LOQ (NA)	NA	< LOQ–< LOQ
Gluconapoleiferin (µmol/g)	0.17 (0.04)	0.14 (0.03)	0.1590	< LOQ–0.29
Glucoalyssin (µmol/g)	2.10 (0.91)	1.66 (0.36)	0.0952	0.47–1.02
Gluconapin (µmol/g)	3.45 (1.52)	3.13 (0.63)	0.4100	3.25–4.84
4-hydroxyglucobrassicin (µmol/g)	5.21 (0.58)	3.49 (1.18)	0.0029*	3.40–4.92
Glucobrassicanapin (µmol/g)	0.85 (0.28)	0.66 (0.14)	0.0524	0.28–0.63
Glucobrassicin (µmol/g)	0.49 (0.12)	0.87 (0.11)	0.0000*	0.30–0.68
Gluconasturtiin (µmol/g)	0.46 (0.21)	0.37 (0.11)	0.1865	0.14–0.81
Neoglucobrassicin (µmol/g)	0.14 (0.04)	0.13 (0.03)	0.5703	< LOQ–0.08
Tannins - soluble condensed (%)	0.06 (0.03)	0.07 (0.02)	0.4183	0.03–0.08
Ferulic acid (ppm)	293.1 (38.5)	236.4 (24.7)	0.0085*	293.1–310.2
p-coumaric acid (ppm)	24.4 (5.1)	12.0 (4.9)	0.0001*	31.4–72.8
Sinapine (%)	1.828 (0.229)	1.541 (0.188)	0.0020*	1.479–1.677

Limits of quantitation (LOQ) on a dry weight basis: phytic acid (0.14%), glucoiberin (0.05 µmol/g), progoitrin (0.05 µmol/g), epi-progoitrin (0.05 µmol/g), glucoraphanin (0.05 µmol/g), gluconapoleiferin (0.05 µmol/g), glucoalyssin (0.05 µmol/g), gluconapin (0.05 µmol/g), 4-hydroxyglucobrassicin (0.05 µmol/g), glucobrassicanapin (0.05 µmol/g), glucobrassicin (0.05 µmol/g), gluconasturtiin (0.05 µmol/g), neoglucobrassicin (0.05 µmol/g), tannins - soluble condensed (0.05%), ferulic acid (10 ppm), p-coumaric acid (10 ppm), sinapine (0.05%).

NA = Not applicable as value was not calculated.

[1] LBFLFK and Kumily means were formed from ten replicate samples (n = 10). For reference varieties' minimum and maximum means, n = 10 except for one variety (IMC105), where n = 8. Means less than the LOQ are expressed as "< LOQ."

[2] Student's paired t-Test (two-tailed distribution) was used to determine the probability of a significant difference between LBFLFK and Kumily means.

[3] * indicates p≤ 0.05.

Heavy metals

Canola meal contains some trace metal ions, which can act as pro-oxidants that are reduced during processing. The concentration values of the heavy metals arsenic, cadmium, lead, and mercury were not statistically different between LBFLFK and Kumily, with mercury being below the limit of quantitation (LOQ) in both cases (Table 52).

Table 52. Defatted Meal Heavy Metals – Across-Site Summary Statistics

Analyte (mg/kg DW)	Control (Kumily)	LBFLFK	t-Test[2]	Reference Variety Range
	Mean[1] (SD)	Mean[1] (SD)	p-value[3]	min–max[1]
Arsenic	0.055 (0.036)	0.033 (0.012)	0.1438	0.061–0.080
Cadmium	0.118 (0.051)	0.143 (0.067)	0.3865	0.090–0.154
Lead	0.032 (0.019)	0.023 (0.016)	0.3318	0.021–0.025
Mercury	< LOQ (NA)	< LOQ (NA)	NA	< LOQ–< LOQ

Limit of quantitation (LOQ) on a dry weight basis: 0.01 mg/kg.
NA = Not applicable as value was not calculated.
[1] LBFLFK and Kumily means were formed from ten replicate samples (n = 10). For reference varieties' minimum and maximum means, n = 10 except for one variety (IMC105), where n = 8. Means less than the LOQ are expressed as "< LOQ."
[2] Student's paired t-Test (two-tailed distribution) was used to determine the probability of a significant difference between LBFLFK and Kumily means.
[3] * indicates p≤ 0.05.

Conclusion

Overall, the composition of LBFLFK defatted meal is comparable to that of conventional canola defatted meal, and processing did not differentially alter or impact the nutritional value of LBFLFK.

Crude oil and RBD oil

Canola is principally grown for the oil that is extracted from seed for use in foods including frying and baking oils, salad oils, margarines, and shortenings. Use of EPA+DHA canola oil as a food ingredient will be limited to those categories and inclusion levels for an EPA- and DHA- containing product as those evaluated as Generally Recognised as Safe (GRAS) by the U.S. FDA (2017b). Crude oil (unrefined pressed and/or extracted oil) may also be used in some additional applications, such as a fish feed ingredient as a source of fat (Glencross et al., 2003). For human nutrition, important assessments of canola oil include fatty acid composition and content of vitamins E and K1 (OECD, 2011b).

Fatty acids

As expected, the introduction of the EPA+DHA trait and the associated enzymatic pathway in LBFLFK results in the presence of fatty acids not normally found in conventional canola as expected. In addition, the enzymatic pathway uses endogenous fatty acids as substrates to produce EPA and DHA and therefore impacts the content of some fatty acids found in conventional canola varieties.

To guide a discussion of fatty acid composition of the processed oil fractions, the fatty acids analysed are divided into three groups: canola endogenous fatty acids not impacted by the EPA+DHA trait, canola endogenous fatty acids impacted by the trait, and EPA+DHA trait-associated fatty acids.

Canola endogenous fatty acids not impacted by the trait

Based on the compositional analysis of grain across the 2014/15 and 2015 season (see Appendix 22), the fatty acids C14:0, C16:0, C16:1n-9, C17:0, C17:1, C18:1n-7, C20:2n-6, and C22:1n-9 are considered not impacted by the EPA+DHA trait because they did not show a statistically significant difference between LBFLFK and Kumily or they are minor fatty acids

with mean values within the range of natural variation based on the reference varieties, the ILSI Crop Composition Database, or peer-reviewed literature. In addition, the levels of these fatty acids are consistent across the different LBFLFK oil fractions and comparable to levels present in grain (see Table 53, Table 54, and Appendix 23).

The fatty acid C18:1n-7 did not show any statistically significant differences between LBFLFK and Kumily across all oil fractions. The fatty acids C14:0, C16-1n-9, C17:0, C17:1, and C20:2n-6 are minor fatty acids, and though statistically significant differences were seen in the oil fractions (except for C17:0 in crude oil), the mean values were just slightly outside the range of the reference varieties and well within the range presented by ILSI Crop Composition Database or peer-reviewed literature. The fatty acid C16:0 in RBD oil from LBFLFK was statistically higher than Kumily and appeared to be slightly enriched compared to the crude oil from LBFLFK. C14:0 did not show a statistically significant difference in milled grain, though differences were observed between LBFLFK and Kumily in crude oil and RBD oil fractions. These differences were small in magnitude, and the mean values were well within the range of variation presented by ILSI Crop Composition Database or peer-reviewed literature (Appendix 22). The fatty acid C22:1n-9 (erucic acid) was consistently below the LOQ across all processed fractions and milled grain for LBFLFK and Kumily, which is in line with the required level for this antinutrient of less than 2% in canola oil (OECD, 2011b).

Canola endogenous fatty acids impacted by the trait

Statistically significant differences were consistently observed for the fatty acids C16:1n-7, C18:0, C18:1n-9, C18:1 trans, C18:2n-6, C18:3n-3, C20:0, C20:1n-9, C22:0, C24:0, C24:1n-9, and total trans fatty acids between LBFLFK and Kumily based on the compositional analysis of grain harvested across the 2014/15 and 2015 seasons (see Appendix 22) and are therefore considered impacted by the introduced EPA+DHA trait. The above fatty acids also showed statistically significant differences in all of the processed fractions except for C20:0 and total trans fatty acids in RBD oil (Table 53, Table 54). The mean values for C16:1n-7, C18:3n-3, C20:1n-9, C22:0, C24:0, and C24:1n-9 were still generally within the ranges of natural variation based on the ILSI Crop Composition Database and/or peer-reviewed literature. The mean values for the fatty acids C18:0 (stearic acid, increased in LBFLFK), C18:1n-9 (oleic acid, decreased), and C18:2n-6 (linoleic acid, increased) are consistently outside the range of natural variation based on ILSI Crop Composition Database and peer-reviewed literature. Oleic acid and linoleic acid are the primary precursors for the synthesis of EPA and DHA in LBFLFK canola, and changes in these fatty acids may have a secondary effect on overall levels of stearic acid. Processing appears to lead to a slight increase of the relative percent of oleic acid and linoleic acid in RBD oil as compared to milled grain.

The refinement process also resulted in an increase in total trans fatty acids in RBD oil relative to crude oil or the milled grain. This increase was observable for both LBFLFK and Kumily such that in RBD oil, no significant difference was observed. This increase in total trans fatty acids, also seen in the reference canola varieties, is likely the result of isomerisation of fatty acids to trans fats that occurs spontaneously and, with heating, at a faster rate (Wolff, 1993; Chardigny, 1996).

EPA+DHA trait-associated fatty acids

In addition to C20:5n-3 (EPA) and C22:6n-3 (DHA), the presence of fatty acids C16:1 trans, C18:2n-9, C18:3n-6, C18:4n-3, C20:2n-9, C20:3n-3, C20:3n-6, C20:3n-9, C20:4n-3,

C20:4n-6, C22:4n-3, C22:4n-6, C22:5n-3, and C22:5n-6 are associated with the EPA+DHA trait as they were present in LBFLFK but had values consistently below the LOQ in Kumily and reference varieties based on the compositional analysis of grain harvested across the 2014/15 and 2015 seasons (see Appendix 22). The presence of these fatty acids in LBFLFK but not in the reference varieties is expected and attributed to the introduction of the EPA+DHA trait in LBFLFK (see Figure 83). The fatty acids C18:2n-9 and C20:2n-9 were not quantifiable in milled grain of Kumily or the reference varieties, though were present in the oil fractions (Table 53, Table 54). Therefore, in the context of the processed oil fractions, these could also fall into the category of endogenous fatty acids impacted, rather than introduced, by the EPA+DHA trait. Though it was quantifiable in milled grain from the 2014/15 and 2015 seasons, C16:1 trans fatty acids were below the LOQ in all processed oil fractions and in the milled grain from the 2016 season. All other fatty acids associated with the trait were consistently present across the oil fractions.

Table 53. Crude Oil Fatty Acids – Across-Site Summary Statistics

Fatty Acid (% Relative)	Control (Kumily)	LBFLFK	t-Test[2]	Reference Variety Range
	Mean[1] (SD)	Mean[1] (SD)	p-value[3]	min–max[1]
C14:0	0.056 (0.005)	0.061 (0.003)	0.0198*	0.042–0.057
C16:0	4.471 (0.140)	4.581 (0.045)	0.0211*	3.592–4.090
C16:1n-7	0.247 (0.015)	0.168 (0.007)	0.0000*	0.190–0.211
C16:1n-9	0.039 (0.004)	0.048 (0.004)	0.0001*	0.040–0.046
C16:1 trans	< LOQ (NA)	< LOQ (NA)	NA	< LOQ–< LOQ
C16:3n-3	< LOQ (NA)	< LOQ (NA)	NA	< LOQ–< LOQ
C17:0	0.048 (0.003)	0.049 (0.002)	0.3742	0.038–0.045
C17:1	0.057 (0.003)	0.025 (0.006)	0.0000*	0.052–0.058
C18:0	2.290 (0.182)	2.994 (0.276)	0.0001*	2.064–2.159
C18:1n-7	3.199 (0.084)	3.152 (0.089)	0.2767	2.749–3.000
C18:1n-9	58.417 (1.195)	27.880 (1.532)	0.0000*	61.007–62.450
C18:1 trans	0.021 (0.013)	0.042 (0.010)	0.0003*	0.022–0.024
C18:2n-6	20.003 (1.163)	28.732 (1.027)	0.0000*	18.513–23.654
C18:2n-9	0.026 (0.003)	1.321 (0.168)	0.0000*	0.022–0.026
C18:2 trans	< LOQ (NA)	0.046 (0.009)	NA	< LOQ–< LOQ
C18:3n-3	8.273 (0.470)	5.221 (0.551)	0.0000*	2.760–7.482
C18:3n-6	< LOQ (NA)	2.348 (0.361)	NA	< LOQ–< LOQ
C18:3 trans	0.067 (0.004)	0.067 (0.003)	0.8524	0.041–0.067
C18:4n-3	< LOQ (NA)	0.356 (0.041)	NA	< LOQ–< LOQ
C20:0	0.723 (0.038)	0.676 (0.028)	0.0090*	0.666–0.706
C20:1n-9	1.106 (0.042)	0.748 (0.032)	0.0000*	1.104–1.280
C20:2n-6	0.070 (0.017)	0.113 (0.011)	0.0000*	0.068–0.072
C20:2n-9	< LOQ (NA)	0.338 (0.074)	NA	< LOQ–< LOQ
C20:3n-3	< LOQ (NA)	0.065 (0.015)	NA	< LOQ–< LOQ
C20:3n-6	< LOQ (NA)	5.199 (0.438)	NA	< LOQ–< LOQ
C20:3n-9	< LOQ (NA)	0.055 (0.015)	NA	< LOQ–< LOQ
C20:4n-3	< LOQ (NA)	2.222 (0.314)	NA	< LOQ–< LOQ
C20:4n-6	< LOQ (NA)	2.057 (0.283)	NA	< LOQ–< LOQ
C20:5n-3 (EPA)	< LOQ (NA)	5.390 (0.429)	NA	< LOQ–< LOQ
C22:0	0.349 (0.013)	0.268 (0.012)	0.0000*	0.314–0.372
C22:1n-9	< LOQ (NA)	< LOQ (NA)	NA	< LOQ–< LOQ
C22:2n-6	< LOQ (NA)	< LOQ (NA)	NA	< LOQ–< LOQ
C22:4n-3	< LOQ (NA)	1.173 (0.176)	NA	< LOQ–< LOQ
C22:4n-6	< LOQ (NA)	0.599 (0.061)	NA	< LOQ–< LOQ
C22:5n-3	< LOQ (NA)	2.915 (0.328)	NA	< LOQ–< LOQ
C22:5n-6	< LOQ (NA)	0.065 (0.009)	NA	< LOQ–< LOQ
C22:6n-3 (DHA)	< LOQ (NA)	0.512 (0.069)	NA	< LOQ–< LOQ
C24:0	0.192 (0.025)	0.125 (0.010)	0.0001*	0.196–0.254
C24:1n-9	0.133 (0.013)	0.099 (0.013)	0.0004*	0.133–0.148
Total Trans Fatty Acids	0.096 (0.012)	0.155 (0.013)	0.0000*	0.066–0.094

Limits of quantitation (LOQ) on a fresh weight basis: 0.02% for all but C16:1n-7 (0.04%) and C18:1n-7 (0.03%).
NA = Not applicable as value was not calculated.

[1] LBFLFK and Kumily means were formed from ten replicate samples (n = 10). For reference varieties' minimum and maximum means, n = 10 except for one variety (IMC105), where n = 8. Means less than the LOQ are expressed as "< LOQ."

[2] Student's paired t-Test (two-tailed distribution) was used to determine the probability of a significant difference between LBFLFK and Kumily means.

[3] * indicates $p \leq 0.05$.

Table 54. RBD Oil Fatty Acids – Across-Site Summary Statistics

Fatty Acid (% Relative)	Control (Kumily)	LBFLFK	t-Test[2]	Reference Variety Range
	Mean[1] (SD)	Mean[1] (SD)	p-value[3]	min–max[1]
C14:0	0.056 (0.004)	0.063 (0.003)	0.0052*	0.042–0.056
C16:0	4.410 (0.140)	4.695 (0.046)	0.0001*	3.56–4.041
C16:1n-7	0.245 (0.012)	0.173 (0.011)	0.0000*	0.191–0.211
C16:1n-9	0.039 (0.004)	0.049 (0.004)	0.0001*	0.039–0.045
C16:1 trans	< LOQ (NA)	< LOQ (NA)	NA	< LOQ–< LOQ
C16:3n-3	< LOQ (NA)	< LOQ (NA)	NA	< LOQ–< LOQ
C17:0	0.047 (0.001)	0.052 (0.002)	0.0002*	0.037–0.045
C17:1	0.058 (0.002)	0.027 (0.003)	0.0000*	0.051–0.058
C18:0	2.280 (0.178)	3.100 (0.273)	0.0000*	2.059–2.156
C18:1n-7	3.188 (0.087)	3.250 (0.102)	0.0814	2.752–2.996
C18:1n-9	59.048 (0.979)	29.554 (1.558)	0.0000*	61.327–62.776
C18:1 trans	0.029 (0.013)	0.047 (0.007)	0.0079*	0.029–0.030
C18:2n-6	19.603 (0.882)	29.560 (1.000)	0.0000*	18.282–23.331
C18:2n-9	0.065 (0.005)	1.428 (0.165)	0.0000*	0.055–0.068
C18:2 trans	< LOQ (NA)	0.038 (0.016)	NA	< LOQ–< LOQ
C18:3n-3	7.446 (0.452)	4.916 (0.504)	0.0000*	2.538–6.886
C18:3n-6	< LOQ (NA)	2.211 (0.348)	NA	< LOQ–< LOQ
C18:3 trans	0.595 (0.038)	0.511 (0.068)	0.0079*	0.207–0.532
C18:4n-3	< LOQ (NA)	0.314 (0.037)	NA	< LOQ–< LOQ
C20:0	0.722 (0.035)	0.700 (0.028)	0.1181	0.667–0.702
C20:1n-9	1.117 (0.044)	0.795 (0.034)	0.0000*	1.112–1.281
C20:2n-6	0.058 (0.006)	0.114 (0.011)	0.0000*	0.060–0.067
C20:2n-9	0.035 (0.016)	0.373 (0.079)	0.0000*	0.027–0.033
C20:3n-3	< LOQ (NA)	0.062 (0.013)	NA	< LOQ–< LOQ
C20:3n-6	< LOQ (NA)	4.959 (0.450)	NA	< LOQ–< LOQ
C20:3n-9	< LOQ (NA)	0.047 (0.014)	NA	< LOQ–< LOQ
C20:4n-3	< LOQ (NA)	1.912 (0.283)	NA	< LOQ–< LOQ
C20:4n-6	< LOQ (NA)	1.747 (0.251)	NA	< LOQ–< LOQ
C20:5n-3 (EPA)	< LOQ (NA)	4.132 (0.321)	NA	< LOQ–< LOQ
C22:0	0.347 (0.013)	0.272 (0.012)	0.0000*	0.313–0.370
C22:1n-9	< LOQ (NA)	< LOQ (NA)	NA	< LOQ–< LOQ
C22:2n-6	< LOQ (NA)	< LOQ (NA)	NA	< LOQ–< LOQ
C22:4n-3	< LOQ (NA)	1.021 (0.156)	NA	< LOQ–< LOQ
C22:4n-6	< LOQ (NA)	0.530 (0.058)	NA	< LOQ–< LOQ
C22:5n-3	< LOQ (NA)	2.225 (0.240)	NA	< LOQ–< LOQ
C22:5n-6	< LOQ (NA)	0.052 (0.008)	NA	< LOQ–< LOQ
C22:6n-3 (DHA)	< LOQ (NA)	0.358 (0.039)	NA	< LOQ–< LOQ
C24:0	0.192 (0.021)	0.252 (0.017)	0.0000*	0.192–0.252
C24:1n-9	0.133 (0.014)	0.095 (0.013)	0.0001*	0.132–0.148
Total Trans Fatty Acids	0.626 (0.039)	0.594 (0.065)	0.2489	0.238–0.561

Limits of quantitation (LOQ) on a fresh weight basis: 0.02% for all but C16:1n-7 (0.04%) and C18:1n-7 (0.03%).
NA = Not applicable as value was not calculated.

[1] LBFLFK and Kumily means were formed from ten replicate samples (n = 10). For reference varieties' minimum and maximum means, n = 10 except for one variety (IMC105), where n = 8. Means less than the LOQ are expressed as "< LOQ."

[2] Student's paired t-Test (two-tailed distribution) was used to determine the probability of a significant difference between LBFLFK and Kumily means.

[3] * indicates $p \leq 0.05$.

Moisture and Protein

In crude oil, protein was < LOQ for LBFLFK, Kumily, and the reference varieties. There was no significant difference between LBFLFK and Kumily in the across-site means for moisture. Across site means of moisture for both LBFLFK and Kumily fell within the range of the reference varieties (Table 55).

Table 55. Crude Oil Moisture and Protein – Across-site Summary Statistics

Analyte (% FW)	Control (Kumily)	LBFLFK	t-Test[2]	Reference Variety Range
	Mean[1] (SD)	Mean[1] (SD)	p-value[3]	min–max[1]
Moisture (%)	0.38 (0.26)	0.31 (0.13)	0.5424	0.30–0.38
Protein (%)	< LOQ (NA)	< LOQ (NA)	NA	< LOQ–< LOQ

Limits of quantitation (LOQ) on a fresh weight basis: moisture (0.01%), protein (0.2%).
NA = Not applicable as value was not calculated.
[1] LBFLFK and Kumily means were formed from ten replicate samples (n = 10). For reference varieties' minimum and maximum means, n = 10 except for one variety (IMC105), where n = 8. Means less than the LOQ are expressed as "< LOQ."
[2] Student's paired t-Test (two-tailed distribution) was used to determine the probability of a significant difference between LBFLFK and Kumily means.
[3] * indicates p≤ 0.05.

Vitamins and Minerals

For both crude oil and RBD oil, the vitamins α-tocopherol, γ-tocopherol, β-tocopherol, δ-tocopherol, and total tocopherols were not statistically different between LBFLFK and Kumily (Table 56, Table 57). While vitamin K1 content in crude oil was statistically different between LBFLFK and Kumily, no difference was observed for RBD oil. The vitamin K1 values for both LBFLFK and Kumily oil fractions were higher than the range of the reference varieties but well within the range of the conventional varieties given in the literature. The processing of milled grain into crude oil led to an enrichment of vitamin content in a similar way for LBFLFK, Kumily, and the reference varieties, as would be expected for fat-soluble vitamins. However, levels of vitamin K1 in RBD oil in all sample types tested were decreased compared to crude oil.

Minerals are not a meaningful component in canola oil and were not analysed for the RBD oil fraction. For crude oil, the following minerals were < LOQ in LBFLFK, Kumily, and all reference varieties: sodium, zinc, copper, and manganese (Table 56). Iron, except for a trace amount in Kumily, was < LOQ. Calcium was not statistically significantly different in LBFLFK compared to Kumily, and both values were less than the range of the reference varieties. Phosphorus values for LBFLFK were statistically significantly higher than for Kumily and were within the range of the reference varieties, with phosphorus content in Kumily slightly lower than the range. LBFLFK was statistically significantly higher than Kumily for magnesium and potassium and was at the upper limit of the reference range (magnesium) or slightly higher (potassium).

Table 56. Crude Oil Vitamins and Minerals – Across-Site Summary Statistics

Analyte (FW)	Control (Kumily)	LBFLFK	t-Test[2]	Reference Variety Range
	Mean[1] (SD)	Mean[1] (SD)	p-value[3]	min–max[1]
α-tocopherol (mg/100g)	26.8 (5.7)	26.1 (4.4)	0.4398	26.9–31.6
γ-tocopherol (mg/100g)	58.5 (10.7)	61.1 (9.1)	0.3479	51.0–60.5
β-tocopherol (mg/100g)	0.252 (0.135)	< LOQ (NA)	NA	0.260–0.327
δ-tocopherol (mg/100g)	0.727 (0.338)	0.740 (0.263)	0.8541	0.587–0.840
Total tocopherols (mg/100g)	86.2 (13.2)	88.0 (11.0)	0.5546	79.6–91.5
Vitamin K1 (mg/100g)	0.10685 (0.02373)	0.13404 (0.03797)	0.0242*	0.06309–0.10660
Calcium (%)	0.004 (0.003)	0.006 (0.002)	0.1277	0.007–0.010
Phosphorus (ppm)	111.211 (54.962)	193.848 (34.294)	0.0087*	131.268–201.726
Magnesium (%)	0.002 (0.001)	0.003 (0.001)	0.0059*	0.002–0.003
Potassium (%)	0.003 (0.002)	0.007 (0.001)	0.0103*	0.002–0.005
Sodium (%)	< LOQ (NA)	< LOQ (NA)	NA	< LOQ–< LOQ
Iron (%)	0.0002 (0.0001)	< LOQ (NA)	NA	< LOQ–< LOQ
Zinc (%)	< LOQ (NA)	< LOQ (NA)	NA	< LOQ–< LOQ
Copper (%)	< LOQ (NA)	< LOQ (NA)	NA	< LOQ–< LOQ
Manganese (%)	< LOQ (NA)	< LOQ (NA)	NA	< LOQ–< LOQ

Limits of quantitation (LOQ) on a fresh weight basis: α-tocopherol (0.3 mg/100g), y-tocopherol (0.3 mg/100g), ß-tocopherol (0.3 mg/100g), δ-tocopherol (0.3 mg/100g), total tocopherols (0.3 mg/100g), vitamin K1 (0.000625 mg/100g), calcium (0.004%), phosphorus (33 ppm), magnesium (0.001%), potassium (0.004%), sodium (0.002%), iron (0.0002%), zinc (0.001%), copper (0.0001%), manganese (0.00005%).

NA = Not applicable as value was not calculated.

[1] LBFLFK and Kumily means were formed from ten replicate samples (n = 10). For reference varieties' minimum and maximum means, n = 10 except for one variety (IMC105), where n = 8. Means less than the LOQ expressed as "< LOQ."

[2] Student's paired t-Test (two-tailed distribution) was used to determine the probability of a significant difference between LBFLFK and Kumily means.

[3] * indicates $p \leq 0.05$.

Table 57. RBD Oil Vitamins– Across-Site Summary Statistics

Analyte (mg/100g FW)	Control (Kumily)	LBFLFK	t-Test[2]	Reference Variety Range
	Mean[1] (SD)	Mean[1] (SD)	p-value[3]	min–max[1]
α-tocopherol	27.5 (7.3)	25.8 (4.3)	0.5438	21.8–31.0
ɣ-tocopherol	55.2 (7.1)	56.1 (8.7)	0.7450	41.7–54.7
ß-tocopherol	0.515 (0.139)	0.472 (0.153)	0.2253	0.454–0.600
δ-tocopherol	0.902 (0.217)	0.843 (0.061)	0.4393	0.708–0.878
Total tocopherols	84.1 (11.9)	83.1 (10.1)	0.7996	64.7–87.0
Vitamin K1	0.08483 (0.01635)	0.09306 (0.01455)	0.1861	< LOQ–0.06195

Limits of quantitation (LOQ) on a fresh weight basis: α-tocopherol (0.3 mg/100g), y-tocopherol (0.3 mg/100g), ß-tocopherol (0.3 mg/100g), δ-tocopherol (0.3 mg/100g), total tocopherols (0.3 mg/100g), vitamin K1 (0.000625 mg/100g).

[1] LBFLFK and Kumily means were formed from ten replicate samples (n = 10). For reference varieties' minimum and maximum means, n = 10 except for one variety (IMC105), where n = 8. Means less than the LOQ are expressed as "< LOQ."

[2] Student's paired t-Test (two-tailed distribution) was used to determine the probability of a significant difference between LBFLFK and Kumily means.

[3] * indicates p≤ 0.05.

Phytosterols

Phytosterol content has been shown to correlate to the iodine value of oil (Vlahakis and Hazebroek, 2000) and is a cumulative measure of the degree of unsaturation of fatty acids in oil (Unger, 2015). Values for individual phytosterols were determined for the oil fractions, and total phytosterols were then calculated (Table 58, Table 59). The measurements of most individual phytosterols were low or below the LOQ, with only campesterol and sitosterol making a meaningful contribution to the total phytosterol value. No statistically significant differences between LBFLFK and Kumily were observed for campesterol and sitosterol in either the crude oil or RBD oil fractions. The processing and refinement steps led to slight and similar reductions in total phytosterol content for all sample types.

Table 58. Crude Oil Phytosterols – Across-Site Summary Statistics

Analyte (% FW)	Control (Kumily)	LBFLFK	t-Test[2]	Reference Variety Range
	Mean[1] (SD)	Mean[1] (SD)	p-value[3]	min–max[1]
Brassicasterol	0.1041 (0.0058)	0.0664 (0.0018)	0.0000*	0.0769–0.0918
Cholesterol	0.0035 (0.0007)	0.0029 (0.0004)	0.0198*	0.0027–0.0039
Campesterol	0.1981 (0.017)	0.2025 (0.0215)	0.6614	0.2310–0.2631
Stigmasterol	0.0033 (0.0009)	0.0026 (0.0010)	0.1224	0.0015–0.0025
Sitosterol	0.3875 (0.0248)	0.3896 (0.0171)	0.7571	0.3720–0.4363
Delta-5 avenasterol	0.009 (0.0020)	0.0068 (0.0012)	0.0235*	0.0088–0.0169
Delta-7 avenasterol	< LOQ (NA)	< LOQ (NA)	NA	< LOQ–< LOQ
24-methylene cholesterol	0.0025 (0.0012)	< LOQ (NA)	NA	0.0025–0.0070
Campestanol	< LOQ (NA)	< LOQ (NA)	NA	< LOQ–< LOQ
Delta-5,23 stigmastadienol	< LOQ (NA)	< LOQ (NA)	NA	< LOQ–< LOQ
Clerosterol	0.0058 (0.0012)	0.0060 (0.0004)	0.5608	0.0052–0.0055
Sitostanol	< LOQ (NA)	< LOQ (NA)	NA	< LOQ–< LOQ
Delta-5,24 stigmastadienol	0.0034 (0.0003)	0.0037 (0.0003)	0.0183*	0.0030–0.0044
Delta-7 stigmastenol	0.0014 (0.0008)	0.0051 (0.0019)	0.0004*	0.0013–0.0027
Total phytosterols	0.7263 (0.0407)	0.6952 (0.0371)	0.0667	0.7132–0.8250

Limits of quantitation (LOQ) on a fresh weight basis: brassicasterol (0.002%), cholesterol (0.002%), campesterol (0.002%), stigmasterol (0.002%), sitosterol (0.002%), delta-5 avenasterol (0.002%), delta-7 avenasterol (0.002%), 24-methylene cholesterol (0.002%), campestanol (0.002%), delta-5,23 stigmastadienol (0.002%), clerosterol (0.002%), sitostanol (0.002%), delta-5,24 stigmastadienol (0.002%), delta-7 stigmastenol (0.002%), total phytosterols (0.010%).

NA = Not applicable as value was not calculated.

[1] LBFLFK and Kumily means were formed from ten replicate samples (n = 10). For reference varieties' minimum and maximum means, n = 10 except for one variety (IMC105), where n = 8. Means less than the LOQ are expressed as "< LOQ."

[2] Student's paired t-Test (two-tailed distribution) was used to determine the probability of a significant difference between LBFLFK and Kumily means.

[3] * indicates $p \leq 0.05$.

Table 59. RBD Oil Phytosterols – Across-Site Summary Statistics

Analyte (% FW)	Control (Kumily)	LBFLFK	t-Test[2]	Reference Variety Range
	Mean[1] (SD)	Mean[1] (SD)	p-value[3]	min–max[1]
Brassicasterol	0.0909 (0.0068)	0.0577 (0.003)	0.0000*	0.0667–0.0813
Cholesterol	0.0029 (0.0005)	0.0022 (0.0007)	0.0255*	0.0023–0.0031
Campesterol	0.1853 (0.0198)	0.1857 (0.023)	0.9616	0.2124–0.2433
Stigmasterol	0.0027 (0.0008)	< LOQ (NA)	NA	< LOQ–0.0021
Sitosterol	0.3591 (0.0237)	0.3569 (0.0222)	0.8145	0.3426–0.4069
Delta-5 avenasterol	0.0083 (0.0017)	0.0064 (0.0013)	0.0232*	0.0076–0.0143
Delta-7 avenasterol	< LOQ (NA)	< LOQ (NA)	NA	< LOQ–< LOQ
24-methylene cholesterol	0.0023 (0.0011)	< LOQ (NA)	NA	0.0023–0.0057
Campestanol	< LOQ (NA)	< LOQ (NA)	NA	< LOQ–< LOQ
Delta-5,23 stigmastadienol	< LOQ (NA)	< LOQ (NA)	NA	< LOQ–< LOQ
Clerosterol	0.0046 (0.0006)	0.0049 (0.0005)	0.3881	0.0040–0.0046
Sitostanol	< LOQ (NA)	< LOQ (NA)	NA	< LOQ–< LOQ
Delta-5,24 stigmastadienol	0.0037 (0.0003)	0.0039 (0.0004)	0.1480	0.0036–0.0052
Delta-7 stigmastenol	< LOQ (NA)	0.0048 (0.0018)	NA	0.0023–0.0023
Total phytosterols	0.6679 (0.0486)	0.6342 (0.0469)	0.1099	0.6514–0.7623

Limits of quantitation (LOQ) on a fresh weight basis: brassicasterol (0.002%), cholesterol (0.002%), campesterol (0.002%), stigmasterol (0.002%), sitosterol (0.002%), delta-5 avenasterol (0.002%), delta-7 avenasterol (0.002%), 24-methylene cholesterol (0.002%), campestanol (0.002%), delta-5,23 stigmastadienol (0.002%), clerosterol (0.002%), sitostanol (0.002%), delta-5,24 stigmastadienol (0.002%), delta-7 stigmastenol (0.002%), total phytosterols (0.010%).

NA = Not applicable as value was not calculated.

[1] LBFLFK and Kumily means formed from ten replicate samples (n=10). For reference varieties' minimum and maximum means, n = 10 except for one variety (IMC105), where n = 8. Means less than the LOQ expressed as "< LOQ."

[2] Student's paired t-Test (two-tailed distribution) used to determine the probability of a significant difference between LBFLFK and Kumily means.

[3] * indicates p≤ 0.05.

Other Analytes

Amino acids were < LOQ in crude oil from LBFLFK, Kumily, and reference varieties. Additionally, all heavy metals were < LOQ in oil fractions of LBFLFK, Kumily, and the reference varieties. See Appendix 23 for LOQ values.

Conclusion

Processing did not alter or impact the nutritional value of oil derived from LBFLFK canola. The overall composition of the crude oil and RBD oil fractions for LBFLFK is comparable to that of conventional canola oil with the exception of the intended changes in the fatty acids resulting from the introduced EPA+DHA trait.

Summary of the impact of processing

LBFLFK canola will be grown and processed into food or feed fractions in the same manner as other commercialised canola. As part of the food and feed safety assessment, detailed analytical evaluations were performed to compare composition of processed fractions from LBFLFK, the parental variety Kumily, and three reference varieties grown at five locations and to determine any impact the processing may have on the nutritional value of LBFLFK.

The processing conditions for this assessment were similar to current commercial canola processing practices to produce defatted meal and oil fractions.

Based on the compositional analysis of the defatted meal fractions, the content of key components including proximates and fibre, amino acids, fatty acids, vitamins, minerals, antinutrients, and heavy metals in LBFLFK was comparable to that of conventional canola. Due to processing, the mean content of components including moisture, protein, carbohydrates, ash, fibre, amino acids, antinutrients, and minerals was increased in defatted meal compared to milled grain while the mean content of fat and fat-soluble vitamins was reduced. These trends were consistent between LBFLFK, Kumily, and the reference varieties.

The content of fatty acids, vitamins, and phytosterols in the LBFLFK oil fractions was comparable to that of conventional canola varieties except for those fatty acids that are related to the EPA+DHA trait. Due to processing and refining, the content of fat-soluble vitamins is increased and the content of total phytosterols is slightly reduced in the oil fractions compared to the milled grain. These trends were similar for LBFLFK, Kumily, and the reference varieties.

Based on these data, it can be concluded that processing of LBFLFK grain into defatted meal and oil fractions does not introduce or change nutritional components in a manner that might have an adverse impact on human or animal health. As intended, the EPA+DHA canola trait significantly impacted the fatty acid composition of the LBFLFK oil fractions.

Safety assessment of the fatty acids impacted by the EPA+DHA canola trait

The introduced fatty acid biosynthetic pathway in EPA+DHA canola event LBFLFK impacts the content of omega-3 long-chain polyunsaturated fatty acids (LC-PUFAs) in the seeds. Figure 83 depicts the introduced biosynthetic pathway with the endogenous canola fatty acid C18:1n-9 (oleic acid) as the starting substrate for the seven steps of desaturation and elongation to the intended final product, C22:6n-3 (DHA). In addition to the trait fatty acids C20:5n-3 (EPA) and DHA, other intermediary fatty acids of the pathway are C18:2n-6 (linoleic acid), C18:3n-6 (gamma-linolenic acid), C20:3n-6 (dihomo-gamma-linolenic acid), C20:4n-6 (arachidonic acid), and C22:5n-3 (clupanodonic acid). Further, the seven desaturase and three elongase enzymes newly expressed in LBFLFK are capable of synthesizing EPA and DHA via several different, though minor routes, resulting in an expanded fatty acid pathway that produces additional, nominal fatty acids (Figure 83).

Based on the data obtained from the compositional analysis of grain harvested in the winter 2014/15 and spring 2015 seasons (Appendix 22), as well as of the oil fractions obtained upon processing (Appendix 23), the fatty acids measured in LBFLFK are assigned to three groups to guide a safety evaluation.

The first group is comprised of endogenous canola fatty acids not impacted by the EPA+DHA trait (Table 60). Assigned to this group were those fatty acids:

1) for which no difference was observed between LBFLFK and the parental variety Kumily (C16:0, C18:1n-7), including those for which the mean values were below the limit of quantitation (LOQ) in LBFLFK, Kumily, and the conventional canola varieties (C16:3n-3, C22:1n-9, and C22:2n-6), or

2) that constituted a minor fraction of the total fatty acid content in grain, and for which the mean values in LBFLFK were not suitable for statistical analysis but

were within the ranges represented by the conventional varieties (C14:0, C16:1n-9, C17:0, C17:1, and C20:2n-6).

The fatty acids belonging to this first group will not be discussed further here as their content in LBFLFK is comparable to other conventional canola varieties.

The second group is comprised of endogenous canola fatty acids impacted by the EPA+DHA trait (Table 61). Assigned to this group were fatty acids:

1) for which consistent differences were observed between LBFLFK and the parental variety Kumily, and for which the mean values were generally within the range of natural variation presented by conventional canola varieties (C16:1n-7, C18:0, C18:3n-3, C20:0, C20:1n-9, C22:0, C24:0, and C24:1n-9), or

2) for which the mean values were consistently outside the range of natural variation presented by conventional canola varieties (C18:1n-9, C18:2n-6, and total trans fatty acids), or

3) which were minor components in LBFLFK, and for which the mean value was below the LOQ in grain of Kumily though above the LOQ in the oil fractions of Kumily and the conventional canola varieties (C18:2n-9, C20:2n-9).

Those endogenous canola fatty acids in this group with levels outside of the range of conventional canola varieties (categories 2 and 3 above) are addressed in the following safety evaluation. These fatty acids include C18:1n-9 (oleic acid) and C18:2n-6 (linoleic acid), which are the primary precursors for the production of the LC-PUFAs in LBFLFK, as well as C18:2n-9, C20:2n-9, and total trans fatty acids. The endogenous canola fatty acids in category 1 for this group, for which the content was within the range of conventional canola varieties, are not discussed further.

The third group comprises those fatty acids introduced by the EPA+DHA trait, including C20:5n-3 (EPA) and C22:6n-3 (DHA), as well as the fatty acids C18:3n-6, C18:4n-3, C20:3n-3, C20:3n-6, C20:3n-9, C20:4n-3, C20:4n-6, C22:4n-3, C22:4n-6, C22:5n-3, and C22:5n-6 (Table 62). These fatty acids are consistently quantifiable in LBFLFK and not in conventional canola.

Thus, the following safety evaluation will focus on the fatty acids that were significantly outside of the range of conventional canola varieties (as highlighted in Table 61) and the fatty acids that are only consistently quantifiable in LBFLFK and not in conventional canola (Table 62).

Figure 83. Expanded EPA+DHA Fatty Acid Pathway in LBFLFK

The primary introduced fatty acid pathway is indicated with dark grey circles. The pathway is complemented with additional reactions shown as fatty acids in light circles, which are supported by data contained in Yilmaz et al. (2017). Fatty acids endogenous to canola are presented via the underlying grey box. Canola endogenous desaturase and elongase activity is indicated via the black bold arrows. Newly expressed desaturase and elongase reactions are shown via the open arrows and are part of the introduced pathway to synthesise EPA and DHA from oleic acid (C18:1n-9).

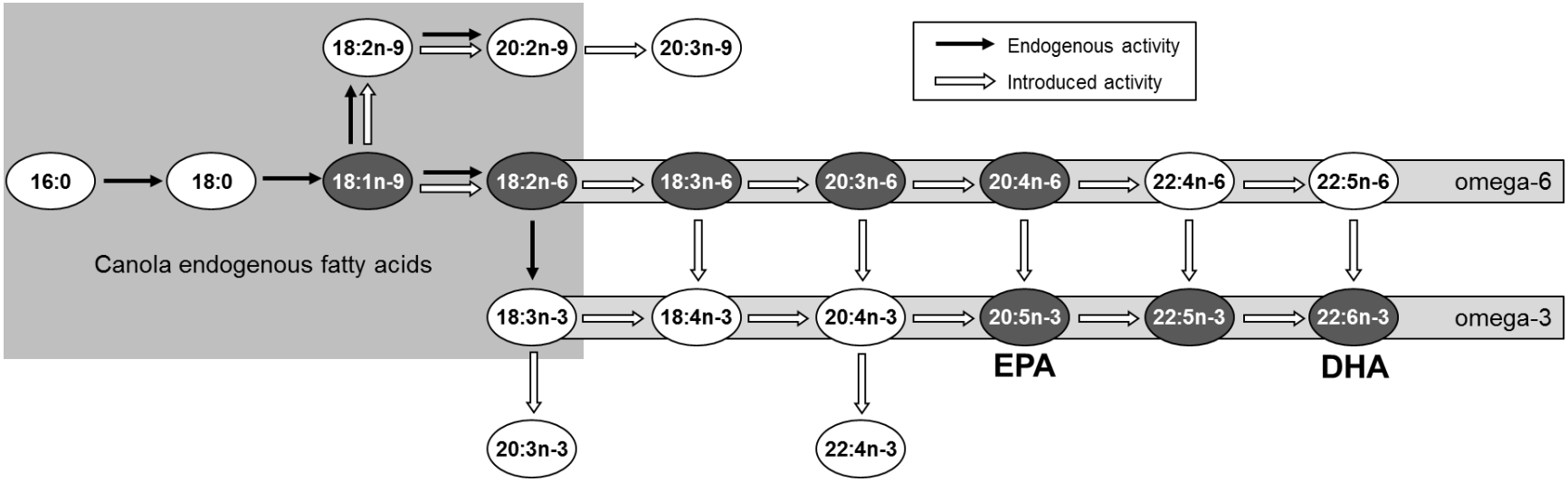

Table 60. Endogenous Canola Fatty Acids Not Impacted by the EPA+DHA Trait

Shorthand Name	Trivial or Common Name / Abbreviation
C14:0	Myristic acid
C16:0	Palmitic acid
C16:1n-9	Cis-7 hexadecenoic acid
C16:3n-3	Hexadecatrienoic acid
C17:0	Margaric acid
C17:1	Margaroleic acid
C18:1n-7	Cis-vaccenic acid
C20:2n-6	Eicosadienoic acid
C22:1n-9	Erucic acid
C22:2n-6	Docosadienoic acid

Table 61. Endogenous Canola Fatty Acids Impacted by the EPA+DHA Trait

Shorthand Name[1]	Trivial or Common Name / Abbreviation
C16:1n-7	Palmitoleic acid
C18:0	Stearic acid
C18:1n-9	Oleic acid / OA
C18:2n-6	Linoleic acid / LA
C18:2n-9	N/A
C18:3n-3	Alpha-linolenic acid / ALA
C20:0	Arachidic acid
C20:1n-9	Gondoic acid
C20:2n-9	N/A
C22:0	Behenic acid
C24:0	Lignoceric acid
C24:1n-9	Nervonic acid
Total TFA	Total trans fatty acids

N/A = Trivial or common name not available.
[1] Only fatty acids listed in bold are discussed further; the others are within the range of conventional canola values.

Table 62. Fatty Acids Introduced by the EPA+DHA Trait

Shorthand Name	Trivial or Common Name / Abbreviation
C18:3n-6	Gamma-linolenic acid / GLA
C18:4n-3	Stearidonic acid / SDA
C20:3n-3	Eicosatrienoic acid / ETrA
C20:3n-6	Dihomo-gamma-linolenic acid / DGLA
C20:3n-9	Mead acid
C20:4n-3	Bishomostearidonic acid / ETA
C20:4n-6	Arachidonic acid / ARA
C20:5n-3	Timnodonic acid / EPA
C22:4n-3	N/A
C22:4n-6	Adrenic acid / DTA
C22:5n-3	Clupanodonic acid / DPAn-3
C22:5n-6	Osbond acid / DPAn-6
C22:6n-3	Docosahexaenoic acid / DHA

N/A = Not available.

The safety of the fatty acids present in LBFLFK, including both endogenous fatty acids with altered levels outside of the range represented by conventional canola varieties and fatty acids not present in conventional canola varieties, was evaluated based on their occurrence and content in foods that are safely and routinely consumed. Two complementary approaches were pursued to support this safety evaluation, one based on a literature search and the second on experimentally determining the fatty acid composition of various edible oils and fat-containing foods. The aim of the systematic literature search was to identify peer-reviewed scientific literature stating that the fatty acids are present in food as well as to identify those stating that the fatty acids or food containing the fatty acids are considered safe for consumption. The search methodology is presented in Appendix 24. For the analysis of the fatty acid composition of fats and oil, routinely-consumed, commercially obtained edible oils and fat-containing foods were obtained by purchasing from various retailers. The food groups assessed consisted of fish oil and fish, dairy (including butter and cheese), eggs, meat, and other meat products. The results obtained were compared against the fatty acid profile of RBD oil from LBFLFK, Kumily, and the conventional canola varieties. This approach allowed quantitation of those fatty acids in edible oils and fats that are also present in LBFLFK but absent from Kumily and reference canola RBD oil samples and identification of those edible oils and fat-containing foods that are most similar in their fatty acid profile to LBFLFK RBD oil. The materials, methods, and results for this study are further described in Appendix 25.

In the following evaluation, the fatty acids in LBFLFK are first addressed individually, followed by an evaluation of the overall fatty acid profile of RBD oil derived from LBFLFK. For reference, a summary of the fatty acid contents as determined in the compositional analyses for LBFLFK grain harvested in the 2014/15 and 2015 seasons (Appendix 22), as well as for the RBD oil processed fraction (Appendix 23) are presented in Table 63.

Table 63. Summary of the Fatty Acids Impacted by the EPA+DHA Trait in LBFLFK Grain and RBD Oil

Shorthand Name	Range in 2014/15 grain compositional analysis[1] [% of total fatty acids]	Range in 2015 grain compositional analysis[2] [% of total fatty acids]	Mean in 2016 processed fraction RBD oil[3] [% of total fatty acids]	Mean in 2016 processed fraction RBD oil[4] [% of total fatty acids]
C18:1n-9	22.53–31.04	23.31–28.18	29.554	30.397
C18:2n-6	27.35–30.28	26.09–29.61	29.560	29.261
C18:2n-9	0.82–1.03	0.96–1.38	1.428	1.416
C20:2n-9	0.17–0.28	0.27–0.43	0.373	0.360
Total TFA	0.24–0.36	0.25–0.32	0.594	0.617
C20:5n-3 (EPA)	4.98–7.94	5.47–6.98	4.132	3.972
C22:6n-3 (DHA)	0.73–1.18	0.59–0.96	0.358	0.346
C18:3n-6	1.12–2.17	1.44–1.82	2.211	2.158
C18:4n-3	0.20–0.29	0.21–0.33	0.314	0.308
C20:3n-3	0.057–0.073	0.060–0.082	0.062	0.058
C20:3n-6	2.25–4.19	3.65–4.53	4.959	4.899
C20:3n-9	0.05–0.07	0.06–0.10	0.047	0.048
C20:4n-3	1.15–2.11	1.54–2.37	1.912	1.895
C20:4n-6	1.89–2.72	1.62–2.19	1.747	1.729
C22:4n-3	0.32–0.64	0.54–0.9	1.021	0.983
C22:4n-6	0.29–0.56	0.38–0.5	0.530	0.499
C22:5n-3	2.05–3.44	2.51–3.00	2.225	2.140
C22:5n-6	0.05–0.12	0.05–0.10	0.052	0.046

Fatty acids listed above the double line are those also present in other canola varieties. Fatty acids listed below the double line are those introduced by the EPA+DHA trait.
TFA = trans fatty acids
[1] Range based on five locations with four plot replications per location.
[2] Range based on seven locations with four plot replications per location.
[3] Mean of 10 replicate samples.
[4] Mean of three technical replicates for one pooled sample.

Endogenous canola fatty acids impacted by the EPA+DHA trait

Endogenous canola fatty acids with altered levels due to the introduction of the EPA+DHA trait are evaluated in this section. First, the results of the literature search are presented, followed by the experimentally obtained data for the fatty acid composition of edible oils and fat-containing foods.

C18:1n-9 (Oleic acid)

Oleic acid is a prevalent fatty acid component of many vegetable oils and present in rapeseed oil (8.0–60.0%), peanut oil (35.0–69%), maize oil (20.0–42.2%), palm oil (36.0–44.0%), and sunflower seed oil (14.0–39.4%) (Codex Alimentarius Commission, 2009a; OECD, 2011b). Oleic acid is one of the main fatty acids of olive oil, with percentages of 43.5–84.6% reported, depending on the olive cultivars analysed (León et al., 2004). Likewise, nut seed oils contain high amounts of oleic acid (Venkatachalam and Sathe, 2006; Rengel et al., 2015). Low saturated, high oleic, low linolenic soybean oil (LSHOLLSO) has obtained Generally Recognised as Safe (GRAS) status by the U.S. FDA (2009). LSHOLLSO has a fatty acid profile that is comparable to other commercial high oleic vegetable oils (e.g., high oleic canola,

high oleic safflower, high oleic sunflower) and traditional oils such as olive oil and canola oil, which have obtained GRAS status by the U.S. FDA (2009).

In the analysis of various edible oils and fat-containing foods, oleic acid was detected in all samples tested (Appendix 25). The highest concentration was in the conventional canola oil samples, ranging from 59.4–62.9% of total fatty acids, with lower concentrations in the fish and fish oil samples. Of the fish and fish oils tested, salmon from aquaculture (37.209% of total fatty acids), pangasius (34.067% of total fatty acids), and salmon oil (20.779% of total fatty acids) had concentrations in a similar range as LBFLFK RBD oil (Table 64). As oleic acid is the starting substrate for the pathway leading to EPA and DHA in LBFLFK, its level is reduced as compared to conventional canola varieties, though values are within the reported range of other vegetable oils.

C18:2n-6 (Linoleic acid)

Linoleic acid (LA) is a fatty acid component of many plant-based oils (Codex Alimentarius Commission, 2009a). Highest levels are found in grapeseed oil (58.0–78.0%), maize oil (34.0–65.6%), and safflower seed oil (67.8–83.2%) (Codex Alimentarius Commission, 2009a). Linoleic acid is also one of the main fatty acids of olive oil, with percentages from 1.6–29.2% reported (León et al., 2004). The Life Sciences Research Organization Select Committee on GRAS Substances assessed the health aspects of linoleic acid and some vegetable oils as food ingredients (SCOGS, 1977). Linoleic acid has obtained GRAS status by the U.S. FDA as a dietary supplement (U.S. FDA, 1996). LSHOLLSO also contains 8–30% linoleic acid and has obtained GRAS status by the U.S. FDA (2009).

In the analysis of various edible oils and fat-containing foods, linoleic acid was detected in all samples tested, except for the mackerel and squid samples (Appendix 25). The range in conventional canola oil samples was 18.3–23.3% of total fatty acids. Lower concentrations were found in salmon from aquaculture (16.3%) and some liver (6.9–16.5% of total fatty acids) and egg samples (15.0–15.3% of total fatty acids). Of the samples tested, LBFLFK RBD oil had the highest C18:2n-6 content, though the value is within the range of other vegetable oils as reported in the literature.

C18:2n-9

Fatty acid C18:2n-9 is a common compound found in sea foods. It was detected in blue crab meats (2.63–6.51% of total fatty acids) (Çelik et al., 2004), farmed and wild gilthead (0.27 and 1.73 weight%, respectively), farmed sea bass (0.32 weight%), mussels (1.04 weight%) (Costa et al., 2017), and various fish oils (Ando et al., 1992; Jeong et al., 1998; Izquierdo et al., 2005; Grigorakis et al., 2010; Beccaria et al., 2015).

In the analysis of various edible oils and fat-containing foods, C18:2n-9 was detected in conventional canola oil samples, in fish oil samples, butter and cheese samples, one meat sample, and in *Mortierella alpina* oil (Appendix 25). Concentrations in the fish oil samples ranged from 0.043–0.165% of total fatty acids. Of the fish oils tested, Menhaden oil had the highest concentration of C18:2n-9 at 0.165% of total fatty acids. LBFLFK RBD oil had the highest C18:2n-9 content of the samples tested, though the value is within the range reported in the literature for commonly consumed seafood.

C20:2n-9

The presence of fatty acid C20:2n-9 was determined in the context of dietary feeding studies with Gilthead bream. Levels detected for C20:2n-9 were 0.1–0.7% of the fatty acid composition of liver phospholipids (Kalogeropoulos et al., 1992) and 0.15–0.33 g/100 g fatty acids in the muscle (Izquierdo et al., 2005). C20:2n-9 was also measured in muscle meat of fryer rabbits (Forrester-Anderson et al., 2006) and melon seed oil (Hu and Ao, 2007).

In the analysis of various edible oils and fat-containing foods, C20:2n-9 was detected in fish oil samples, in one butter sample, and in *Mortierella alpina* oil (Appendix 25). Of all commercially obtained samples, the highest concentration was in the fish oil samples, ranging from 0.064–0.129% of total fatty acids. Of the fish oils, Menhaden oil had the highest concentration of C20:2n-9 at 0.129% of total fatty acids. LBFLFK RBD oil had the highest C20:2n-9 content of the samples tested, though the value is within the range reported in the literature for some consumed fish species.

Trans fatty acids

Trans fatty acids (TFA) are not a homogeneous group. The occurrence of TFA and the adverse health effects associated with their consumption are usually addressed in general without assessing individual TFA (EFSA Panel on Dietetic Products, Nutrition and Allergies, 2010). TFA occur naturally in food products or can be formed or added to foods during industrial processing and manufacture. TFA are formed when vegetable oils are partially hydrogenated during processing to produce spreads such as margarine. Some TFA are also formed during heating of oils at high temperatures. Naturally occurring TFA are found in some animal products including butter, cheese, and meat and originate from bacterial transformation of unsaturated fatty acids in the rumen of ruminant animals. Dairy and beef fat typically contain around 3–6% TFA of total fatty acids (EFSA Panel on Dietetic Products, Nutrition and Allergies, 2010). In the fat of milk and meat products from ruminant animals, the main TFA are isomers of oleic acid, with trans-vaccenic acid (C18:1n-7 trans) predominating. In foods containing partially hydrogenated vegetable oil, the main TFA is elaidic acid (C18:1n-9 trans), which is also an isomer of oleic acid (EFSA Panel on Dietetic Products, Nutrition and Allergies, 2010).

A growing body of scientific evidence indicates biological differences between TFA derived from ruminant versus industrial sources (Anadón et al., 2010). One potential factor explaining such differences is that the predominant TFA in milk fat, trans-vaccenic acid, has several bioactive properties that may be beneficial to human health. Strong evidence exists that health risks are associated with consumption of diets high in TFA from industrially-produced hydrogenated fats (Semma, 2002; Gebauer et al., 2011). It has been demonstrated that consumption of TFA increases the amount of low-density lipoprotein (LDL) cholesterol in the blood (Allen et al., 2016), a major risk factor for coronary heart disease (Fritsche and Steinhart, 1997; Liska et al., 2016). As of 2005, the Dietary Guidelines for Americans advise consumers to limit trans-fat consumption to less than 1% of calories and to keep intake of TFA as low as possible (USDA and U.S. HHS, 2010), which is similar to the recommendations by the World Health Organization (WHO, 2003; Mouratidou et al., 2014) and EFSA (EFSA, 2004; EFSA Panel on Dietetic Products, Nutrition and Allergies, 2010). In June 2015, the U.S. FDA announced that partially hydrogenated oils, which are the primary source of industrially-produced TFA, are no longer considered GRAS for any use in human food (U.S. FDA, 2015).

In the analysis of various edible oils and fat-containing foods, TFA (expressed as total trans fatty acids) were detected in all samples tested except for some fish samples and chicken liver (Appendix 25). The highest concentration of trans fatty acids was in the dairy and meat samples, ranging from 2.484–7.81% of total fatty acids, and in one fish sample (wild salmon) at 11.036% of total fatty acids. Of the fish oils, cod liver oil had the highest concentration at 5.119% of total fatty acids. Comparatively, LBFLFK RBD oil had one of the lower contents of trans fatty acids, similar to that of conventional canola oils.

Fatty acids introduced by the EPA+DHA trait

Those fatty acids that are consistently quantifiable in LBFLFK, but not in Kumily and conventional canola varieties, are evaluated in the following section to allow a conclusion on the safe consumption. First, the results of the literature search are presented, followed by the experimentally obtained data for the fatty acid composition of edible oils and fat-containing foods.

C20:5n-3 (EPA) and C22:6n-3 (DHA)

EPA and DHA are typical components of marine fish oil. Currently, they are primarily consumed through seafood, including finfish (e.g., salmon, tuna, and trout) and shellfish (e.g., crab, mussels, and oysters) (Blasbalg et al., 2011; Kitessa et al., 2014). For example, EPA is present in sardine oil at 10.1 g per 100 g edible portion (USDA, 2016), at 14.1 ± 0.5% in cultured bighead carp, and at 17.2 ± 0.7% in ridgetail white prawn (Li et al., 2011). DHA is present in, for instance, sardine oil at 10.7 g per 100 g edible portion (USDA, 2016), at 18.7 ± 0.8% of total fatty acids in chub mackerel, and at 16.0 ± 0.9% of total fatty acids in mantis shrimp (Li et al., 2011). Other sources of DHA are DHA algal oils, which contain at least 35% DHA of total fatty acids and have obtained GRAS status by the U.S. FDA (2016). Further, DHA is the major fatty acid present in oil produced from the microalgae *Schizochytrium* sp. ONC-T18, and the profile of this algal oil is similar to that found in other algal oils and fish oils that are currently used in food, including infant formula (U.S. FDA, 2000, 2014). The corresponding applications for GRAS status for the algal oil product from *Schizochytrium* sp. included acute and subchronic toxicity studies, genotoxicity studies, and developmental and reproductive toxicity studies. No evidence of toxicity was noted at the highest dose levels tested, and the FDA concluded that the intended uses described for the algal oil are safe, suitable, and GRAS based on scientific procedures (U.S. FDA, 2016). Studies indicate that oily fish consumption or dietary omega-3 long-chain PUFA supplements decrease the risk of mortality from coronary heart disease and sudden cardiac death. Numerous health organisations recommend adult intakes of 250–500 mg combined EPA and DHA per day (Yi et al., 2014; Salem and Eggersdorfer, 2015), including the U.S. Department of Health and Human Services (HHS) and the USDA via the Dietary Guidelines for Americans (U.S. HHS and USDA, 2015). Also, EFSA proposed to set an Adequate Intake of 250 mg for EPA plus DHA for adults based on cardiovascular considerations (EFSA Panel on Dietetic Products, Nutrition and Allergies, 2010).

Thus, EPA and DHA have a history of safe use and consumption as they occur in foods from marine sources commonly consumed and at levels comparable to those in LBFLFK (Table 64), with safety determined by several food safety agencies. Therefore, it can be concluded that they are safe for human and animal consumption.

C18:3n-6 (Gamma-linolenic acid)

The safety of refined buglossoides oil containing 6.2–6.4% of gamma-linolenic acid was assessed by the EFSA Panel on Dietetic Products, Nutrition and Allergies (NDA) as a novel food ingredient. It was concluded that the oil is safe for the proposed uses and use levels (EFSA Panel on Dietetic Products, Nutrition and Allergies, 2015).

In the analysis of various edible oils and fat-containing foods, C18:3n-6 was detected in one fish and most fish oil products, as well as in *Mortierella alpina* oil. *Mortierella alpina* contained C18:3n-6 at 1.778% of total fatty acids. In the fish and fish oil products where it was detected, the amount of C18:3n-6 ranged from 0.105–0.319% of total fatty acids. Of the samples tested, LBFLFK RBD oil had the highest C18:3n-6 content, though the value is similar to that of *Mortierella alpina* oil and below the range reported for buglossoides oil, which has been assessed as safe by EFSA.

C18:4n-3 (Stearidonic acid)

Stearidonic acid (SDA) is present at low levels (up to 1.8%) in the muscle tissue of marine organisms based on the analysis of triglyceride and phospholipid fractions of 21 marine species of fish, three species of cephalopods, and six species of crustaceans from the Mediterranean Sea (Passi et al., 2002). The safety of refined buglossoides oil, with 19.7–20.8% SDA, was assessed as a novel food ingredient by the EFSA NDA Panel, which concluded that the oil is safe for the proposed uses and use levels (EFSA Panel on Dietetic Products, Nutrition and Allergies, 2015).

In the analysis of various edible oils and fat-containing foods, C18:4n-3 was also detected in fish and fish oil products. The fish oil product category had samples with the most C18:4n-3, ranging from 0.099–2.973% of total fatty acids. Within the fish oil category, the algal oils had less C18:4n-3 than the oils from fish. LBFLFK RBD oil contained C18:4n-3 at a concentration about 10-fold lower than some of the fish oils analysed.

C20:3n-3 (Eicosatrienoic acid)

Eicosatrienoic acid is reported to be present in beef. Levels determined in the *longissimus thoracis* cow muscle ranged from 6.54 ± 0.41 to 9.99 ± 0.69 mg per 100 g muscle (Moreno et al., 2007).

In the analysis of various edible oils and fat-containing foods, C20:3n-3 was detected in fish and fish oil samples, ranging from 0.157–0.321% of total fatty acids. LBFLFK RBD oil contained C20:3n-3 at a concentration up to 5-fold lower than some of the fish and fish oil samples analysed.

C20:3n-6 (Dihomo-gamma-linolenic acid)

Animal tissues are a typical source of dihomo-gamma-linolenic acid (DGLA) (FAO, 2010). DGLA has anti-inflammatory and anti-allergic effects since it is metabolised to anti-inflammatory eicosanoids (Dooper et al., 2002). The toxicity of an oil containing more than 40% DGLA, produced by the oleaginous fungus *Mortierella alpina*, was assessed in acute and subchronic toxicity studies in rats. The results demonstrated that DGLA oil does not produce adverse effects in rats when orally administered for 13 weeks. Also, in an acute oral toxicity test, DGLA oil (10 g/kg) exhibited no toxicity except for light symptoms, which are generally

caused by oral administration of large amounts of oil (Kawashima et al., 2009). In certain strains of the nematode *Caenorhabditis elegans*, exposure to excess dietary DGLA caused the destruction of germ cells and lead to sterility (Webster et al., 2013), but the data do not allow a conclusion on the relevance of these findings for mammals.

In the analysis of various edible oils and fat-containing foods, C20:3n-6 was detected across many product categories, including in meat, butter, cheese, fish, fish oil, and in *Mortierella alpina* oil. The highest concentrations were found in meat, with grass-fed calf liver and corn-fed beef liver having C20:3n-6 concentrations of 4.05% and 6.77% of total fatty acids, respectively. LBFLFK RBD oil contained C20:3n-6 at lower or equal concentration to liver samples.

C20:3n-9 (Mead acid)

Mead acid is a component of duck and chicken eggs at levels of 0.742 ± 0.013% and 0.181 ± 0.015% of total fatty acids, respectively (Wang et al., 2014b). It is also found at low levels in pork liver pâté (D'Arrigo et al., 2004), lamb meat (Alves and Bessa, 2009; Nudda et al., 2013), and pasteurised cow milk (Alonso et al., 2009).

In the analysis of various edible oils and fat-containing foods, C20:3n-9 was detected in several product categories, including in fish oil, meat, and butter samples. Except for one butter sample, the fish oil product category had the highest concentration of C20:3n-9, ranging from 0.039–0.097% of total fatty acids. LBFLFK RBD oil contained C20:3n-9 at a comparable concentration to fish oil samples.

C20:4n-3 (Bishomostearidonic acid)

Bishomostearidonic acid is a minor component typically present in animal tissues (FAO, 2010). Marine fish oils can also contain minor quantities (around 1–2%) (Ghioni et al., 2002).

In the analysis of various edible oils and fat-containing foods, C20:4n-3 was present in every fish oil, including algal, and in some of the fish products, with concentrations ranging from 0.49–1.52% of total fatty acids. Of the fish oils, Menhaden oil had the highest concentration of C20:4n-3 at 1.52% of total fatty acids. LBFLFK RBD oil had the highest C20:4n-3 content of the samples tested, though at a level comparable to the Menhaden oil sample and within the range reported in the literature for some fish oils.

C20:4n-6 (Arachidonic acid)

Arachidonic acid (ARA) is a component of animal fats, liver, egg, fish (FAO, 2010), abalone (Su et al., 2004), and prawn (Li et al., 2011). The EFSA NDA Panel has assessed the safety of an arachidonic acid-rich oil (≥ 40%) obtained by fermentation from the fungus *Mortierella alpina* (EFSA, 2008). The product, referred to as Fungal Oil SUN-TGA40S, is intended for use as a source of arachidonic acid for infant formula. In two subchronic feeding studies in rats (Hempenius et al., 2000; Lina et al., 2006), administration of the arachidonic acid-rich oil did not induce toxicologically relevant effects. The Panel concluded that SUN-TGA40S is a safe source of arachidonic acid to be used in infant formula. A comparable arachidonic acid-rich oil (≥ 40%) produced by *M. alpina* has obtained GRAS status by the U.S. FDA (2010).

In the analysis of various edible oils and fat-containing foods, C20:4n-6 was present in samples from all product categories, but meat and *Mortierella alpina* oil samples contained the highest levels. Meat samples contained C20:4n-6 ranging from 0.042–9.82% of total fatty

acids, and the *Mortierella alpina* oil sample contained 33.1% of total fatty acids. LBFLFK RBD oil had similar or up to 20-fold lower concentrations of C20:4n-6 compared to the other samples.

C22:4n-3

Evaluation of the fatty acid composition in wild sea bass showed presence of low amounts of C22:4n-3 (0.6 ± 0.2% of total fatty acids) (Alasalvar et al., 2002). Mukhopadhyay and Ghosh (2003) reported a C22:4n-3 value of 2.9% of total lipids in carp eggs.

In the analysis of various edible oils and fat-containing foods, C22:4n-3 was only present in the fish oils in the range of 0.05–0.11% of total fatty acids. Of the fish oils, Menhaden oil had the highest concentration of C22:4n-3 at 0.109% of total fatty acids. LBFLFK RBD oil had the highest C22:4n-3 content of the samples tested, though within the range reported for wild fish species and below the value reported for carp eggs.

C22:4n-6 (Adrenic acid)

Adrenic acid (also called docosatetraenoic acid) is a minor component present in animal tissues (FAO, 2010) and was also detected at low levels in the edible meat of fish (Li et al., 2011).

In the analysis of various edible oils and fat-containing foods, C22:4n-6 was present in fish oil and meat products, as well as in *Mortierella alpina* oil. C22:4n-6 in the fish oil and *Mortierella alpina* products ranged from 0.073–0.364% of total fatty acids. The highest concentrations were found in meats. Corn-fed chicken and corn-fed beef livers had C22:4n-6 at 0.66% and 2.72% of total fatty acids, respectively. LBFLFK RBD oil had up to 5-fold lower concentrations of C22:4n-6 than observed in commonly consumed meat products.

C22:5n-3 (Clupanodonic acid)

Clupanodonic acid is a component of fish oil. It is present in sardine oil at 2 g per 100 g (USDA, 2016).

In the analysis of various edible oils and fat-containing foods, C22:5n-3 was detected in all the product categories, with meat and fish oil products containing the most. Meat products contained C22:5n-3 in the range of 0.029–4.75% of total fatty acids, with grass-fed calf liver containing the most. The concentration of C22:5n-3 in fish oil products ranged from 0.54–5.78% of total fatty acids, with two algal oils having the most. LBFLFK RBD oil had a concentration of C22:5n-3 of at least 2.5-fold lower than in meat or fish oil products, and at comparable levels reported in the literature for sardine oil.

C22:5n-6 (Osbond acid)

Osbond acid is a minor component present in animal tissues (FAO, 2010; Li et al., 2011).

In the analysis of various edible oils and fat-containing foods, C22:5n-6 was present in *Mortierella alpina* oil, fish oil products, and corn-fed chicken liver, ranging from 0.102–16.3% of total fatty acids. The three algal oils had the highest concentrations at 1.42%, 1.70%, and 16.3% of total fatty acids. LBFLFK RBD oil had the lowest concentration of C22:5n-6 of the samples tested and was at least 10-fold lower in concentration than chicken liver.

Comparative evaluation of fatty acids present in LBFLFK RBD oil

To allow for a comparison of the overall fatty acid profile of LBFLFK RBD oil with the commercially-available edible oils and fat-containing foods tested, the presence or absence (above or below LOQ) of individual fatty acids was used as a tool to identify those foods that were most similar to LBFLFK RBD oil. The edible oils and fat-containing foods with the fewest differences compared to LBFLFK RBD oil were the Menhaden oils, fish oil, salmon oil, and *Mortierella alpina* oil, all of which have GRAS status with the U.S. FDA (U.S. FDA, 1999, 2001, 2002, 2004, 2017a). Table 64 shows the relative fatty acid profiles of these products together with that of LBFLFK RBD oil and highlights the fatty acids that are either present or absent relative to LBFLFK RBD oil.

Compared to *Mortierella alpina* oil, LBFLFK RBD oil contained three additional fatty acids (C20:3n-3, C20:3n-9, and C22:4n-3) and lacked three other ones (C12:0, C16:1 trans, and C16:3n-3). Other than six fatty acids not present in the RBD oil, oil derived from LBFLFK very closely reflects the profile of the Menhaden oil, fish oil, and salmon oil. Therefore, the overall LBFLFK RBD oil fatty acid profile is comparable in content and distribution of fatty acids with Menhaden fish oil that is considered GRAS by the U.S. FDA.

Table 64. Relative Fatty Acid Profiles (% Total Fatty Acids) in LBFLFK RBD Oil and Other Edible Oils

Product/Sample	LBFLFK RBD Oil	Refined Menhaden Oil	Menhaden Oil	Fish Oil	Salmon Oil	*Mortierella alpina* Oil
C4:0	< LOQ	< LOQ	< LOQ	< LOQ	< LOQ	< LOQ
C6:0	< LOQ	< LOQ	< LOQ	< LOQ	< LOQ	< LOQ
C8:0	< LOQ	< LOQ	< LOQ	< LOQ	< LOQ	< LOQ
C10:0	< LOQ	< LOQ	< LOQ	< LOQ	< LOQ	< LOQ
C11:0	< LOQ	< LOQ	< LOQ	< LOQ	< LOQ	< LOQ
C12:0	< LOQ	**0.123 (0.007)**	**0.125 (0.002)**	**0.125 (0.004)**	**0.073 (0.006)**	**0.055 (0.003)**
C14:0	0.063 (0.002)	7.350 (0.037)	8.576 (0.003)	7.125 (0.013)	4.571 (0.006)	2.515 (0.076)
C14:1	< LOQ	**0.038 (0.002)**	**0.061 (0.003)**	**0.032 (0.001)**	**0.031 (0.003)**	< LOQ
C15:0	0.042 (0.003)	0.509 (0.01)	0.694 (0.003)	0.525 (0.01)	0.466 (0.006)	0.219 (0.011)
C15:1	< LOQ	< LOQ	< LOQ	< LOQ	< LOQ	< LOQ
C16:0	4.669 (0.006)	16.099 (0.048)	16.600 (0.029)	16.521 (0.02)	13.716 (0.018)	10.380 (0.266)
C16:1n-7	0.171 (0.001)	8.029 (0.044)	11.806 (0.022)	8.236 (0.025)	5.512 (0.068)	2.482 (0.07)
C16:1n-9	0.046 (0.002)	0.377 (0.001)	0.325 (0)	0.375 (0.023)	0.310 (0.01)	0.121 (0.01)
C16:1 trans	< LOQ	**0.644 (0.024)**	**0.693 (0.014)**	**0.620 (0.008)**	**0.512 (0.007)**	**0.186 (0.009)**
C16:3n-3	< LOQ	**1.501 (0.034)**	**1.581 (0.005)**	**1.375 (0.023)**	**0.601 (0.021)**	**0.397 (0.01)**
C17:0	0.053 (0.001)	0.452 (0.009)	0.649 (0.208)	0.490 (0.009)	0.462 (0.01)	0.292 (0.012)
C17:1	0.027 (0.001)	0.150 (0.004)	0.182 (0.007)	0.177 (0.013)	0.246 (0.005)	0.057 (0.001)
C18:0	3.108 (0.01)	3.234 (0.029)	2.889 (0.008)	3.445 (0.016)	3.245 (0.01)	5.905 (0.11)
C18:1n-7	3.267 (0.006)	2.928 (0.017)	3.144 (0.009)	3.076 (0.006)	2.911 (0.022)	1.020 (0.017)
C18:1n-9	30.397 (0.036)	8.526 (0.03)	6.138 (0.008)	8.241 (0.026)	20.779 (0.067)	6.994 (0.117)
C18:1 trans	0.073 (0.012)	0.267 (0.106)	0.172 (0.029)	0.295 (0.137)	0.396 (0.205)	0.115 (0.017)
C18:2n-6	29.261 (0.034)	1.193 (0.002)	1.363 (0.001)	1.145 (0.008)	5.801 (0.014)	6.962 (0.139)
C18:2n-9	1.416 (0.003)	0.165 (0.003)	0.101 (0.003)	0.164 (0.003)	0.110 (0.005)	0.158 (0.005)
C18:2 trans	0.036 (0.005)	0.191 (0.053)	0.316 (0.062)	0.224 (0.063)	0.162 (0.067)	0.099 (0.091)
C18:3n-3	4.875 (0.005)	0.766 (0.008)	1.236 (0.008)	0.670 (0.007)	2.346 (0.001)	0.245 (0.005)
C18:3n-6	2.158 (0.004)	0.232 (0.006)	0.319 (0.009)	0.228 (0.003)	0.168 (0.009)	1.778 (0.032)
C18:3 trans	0.509 (0.009)	0.238 (0.011)	0.525 (0.002)	0.348 (0.009)	0.359 (0.016)	0.092 (0.006)
C18:4n-3	0.308 (0.002)	2.787 (0.01)	2.973 (0.005)	2.373 (0.014)	1.605 (0.016)	0.783 (0.008)
C20:0	0.684 (0.001)	0.214 (0.005)	0.225 (0.007)	0.290 (0.018)	0.297 (0)	0.690 (0.018)
C20:1n-9	0.800 (0.003)	1.018 (0.006)	0.958 (0.005)	1.304 (0.005)	2.331 (0.013)	0.442 (0.007)
C20:2n-6	0.107 (0.002)	0.190 (0.01)	0.240 (0.004)	0.177 (0.002)	0.595 (0.01)	0.348 (0.006)
C20:2n-9	0.360 (0.003)	0.111 (0.003)	0.129 (0.008)	0.127 (0.005)	0.064 (0.003)	0.046 (0.022)

Product/Sample	LBFLFK RBD Oil	Refined Menhaden Oil	Menhaden Oil	Fish Oil	Salmon Oil	*Mortierella alpina* Oil
C20:3n-3	0.058 (0.002)	0.181 (0.003)	0.255 (0.008)	0.185 (0.011)	0.321 (0.009)	**< LOQ**
C20:3n-6	4.899 (0.083)	0.158 (0.008)	0.242 (0.002)	0.179 (0.003)	0.179 (0.007)	3.077 (0.031)
C20:3n-9	0.048 (0.001)	0.059 (0.01)	0.039 (0.004)	0.054 (0.006)	0.056 (0.005)	**< LOQ**
C20:4n-3	1.895 (0.002)	0.749 (0.01)	1.523 (0.004)	0.760 (0)	0.699 (0.017)	0.207 (0.004)
C20:4n-6	1.729 (0.002)	1.129 (0.006)	1.133 (0.006)	1.374 (0.006)	0.993 (0.009)	33.117 (0.586)
C20:5n-3 (EPA)	3.972 (0.021)	17.514 (0.037)	14.561 (0.036)	17.241 (0.031)	9.696 (0.041)	4.849 (0.084)
C22:0	0.275 (0.003)	0.121 (0.007)	0.155 (0.008)	0.151 (0.016)	0.144 (0.006)	1.724 (1.476)
C22:1n-9	< LOQ	**0.147 (0.007)**	**0.164 (0.005)**	**0.206 (0.016)**	**0.310 (0.015)**	< LOQ
C22:2n-6	< LOQ	**0.064 (0.003)**	**0.084 (0.001)**	**0.075 (0.008)**	**0.088 (0.011)**	< LOQ
C22:4n-3	0.983 (0.004)	0.079 (0.002)	0.109 (0.007)	0.075 (0.005)	0.049 (0.004)	**< LOQ**
C22:4n-6	0.499 (0.004)	0.098 (0.003)	0.218 (0.002)	0.133 (0.007)	0.106 (0.002)	0.261 (0.011)
C22:5n-3	2.140 (0.008)	1.959 (0.009)	2.485 (0.007)	2.145 (0.012)	1.486 (0.023)	0.539 (0.009)
C22:5n-6	0.046 (0.005)	0.464 (0.003)	0.446 (0.009)	0.475 (0.002)	0.530 (0.023)	0.102 (0.004)
C22:6n-3 (DHA)	0.346 (0.003)	13.165 (0.04)	11.408 (0.026)	11.848 (0.017)	12.564 (0.037)	3.225 (0.054)
C24:0	0.241 (0.003)	0.067 (0.006)	0.115 (0.006)	0.109 (0.007)	0.093 (0.004)	8.278 (0.135)
C24:1n-9	0.094 (0.002)	0.477 (0.018)	0.304 (0.004)	0.459 (0.016)	0.433 (0.006)	0.345 (0.011)
Total TFA	0.617 (0.025)	1.339 (0.089)	1.707 (0.08)	1.487 (0.08)	1.429 (0.119)	0.492 (0.076)
Total Saturated FA[1]	9.135	28.170	30.028	28.781	23.069	30.058
Total Monounsaturated FA[1]	34.802	21.690	23.082	22.108	32.862	11.515
Total Omega-6 FA[1]	38.697	3.527	4.044	3.785	8.462	45.645
Total Omega-3 FA[1]	14.576	38.701	36.131	36.673	29.368	9.848

< LOQ = Below limit of quantitation; FA = Fatty acids
Values are the mean of three technical replicates with standard deviation listed in parentheses. Standard deviation was not calculated for values < LOQ.
Bold text indicates fatty acids that are either present or absent relative to LBFLFK RBD oil.
[1] Total values are the sum of means and, therefore, no standard deviation is provided.

Conclusions on fatty acid safety evaluation

To establish the safety of the fatty acids in LBFLFK associated with the EPA+DHA trait and the safety of the overall fatty acid profile, a systematic literature search was conducted and complemented with a detailed comparative analysis of the fatty acid composition of various edible oils and fat-containing foods. The results of the literature search demonstrated that all fatty acids introduced or impacted by the EPA+DHA trait are already present in foods that are considered safe for consumption. A compositional analysis of commonly consumed foods confirmed the similarity of the fatty acid profile in LBFLFK RBD oil to Menhaden oil and other fish oils.

The levels of fatty acids in LBFLFK were confirmed to be similar to those in commonly consumed foods as presented in the compositional analysis and reported in the literature. All fatty acids present in LBFLFK were shown to be present in other organisms and foods, indicating repeated dietary exposure. Moreover, various oils from different sources containing the fatty acids present in LBFLFK have been assessed by regulatory authorities such as the FSANZ, U.S. FDA and EFSA, and these have concluded that the respective oils are safe for consumption for the proposed uses and use levels. None of the fatty acids present in LBFLFK have been reported to cause adverse effects in humans or animals. It is therefore concluded that no specific toxicity studies are needed to make a determination of safety for the fatty acid-containing products of LBFLFK. All fatty acids associated with the EPA+DHA trait, when compared to commonly consumed foods from marine, animal or plant sources, are present at similar levels and have a history of safe use and consumption.

(b) Information on the range of natural variation for each constituent measured to allow for assessment of biological significance should any statistically significant differences be identified

The section “Fatty acids introduced by the EPA+DHA trait” above provides information first from literature sources on the natural variation of each constituent, followed by experimentally determined contents of the key constituents within EPA+DHA canola for comparison with the natural variation of the same constituents within common food sources. Section B.5(a) discusses both the comparison and assesses the biological significance of any statistically significant differences.

(c) The levels of any other constituents that may potentially be influenced by the genetic modification, as a result, for example, of downstream metabolic effects, compared with the levels in an appropriate comparator as well as the range of natural variation

See Section B.5(a) for discussion regarding changes to levels of constituents within foods derived from EPA+DHA canola as a result of the impact of the genetic modification on downstream metabolic effects within the plant. The appropriate non-GM comparator Kumily was assessed side-by-side along with utilisation of the ILSI database to indicate the range of natural variation in the constituents compared to the GM food.

(d) The levels of any naturally occurring allergenic proteins in the GM food compared with the levels in an appropriate comparator. Particular attention must be paid to those foods that are required to be declared when present as an ingredient, and where significant alterations to protein content could be reasonably anticipated.

Canola is not considered to contain allergenic proteins. Rape seed contains glucosinolates and erucic acid, discussed earlier, which are considered anti-nutrients rather than allergens. Section B.5(a) details the safety assessment of LC-PUFAs in LBFLFK canola that differ from the fatty acid profile of conventional canola.

PART C INFORMATION RELATED TO THE NUTRITIONAL IMPACT OF THE FOOD PRODUCED USING GENE TECHNOLOGY

The application must contain the following information if the compositional analysis indicates biologically significant changes to the levels of certain nutrients in the food produced using gene technology compared to the non-GM counterpart food:

(a) Data are required on the anticipated dietary intake of the GM food in relation to the overall diet, together with any information which may indicate a change to the bioavailability of the nutrients from the GM food

For information on anticipated dietary intake, please refer to sections B.3(b) and B.3(c). In short, the introduced genetic modification will provide a sustainable alternative source of omega-3 fatty acids from canola oil.

The commercialisation of oil produced from LBFLFK will provide a new and alternative source of EPA and DHA, expanding consumer access and choice for these long-chain omega-3-fatty acids. Therefore, a general increase in the consumption of omega-3 fatty acids may occur for those consumers who select products containing oil produced from LBFLFK or other sources of EPA and DHA. Incorporation of oil from LBFLFK would be in line with what is already incorporated into food using marine and other currently available sources of EPA and DHA (U.S. FDA, 2017a). Consumers would then be able to choose foods containing EPA and DHA similar to choices that they have today.

(b) Where the GM food contains an intended nutritional change, information, such as clinical trial data, must be provided to determine the nutritional impact of the GM food.

Based on the compositional analysis data obtained from field trials performed in the U.S., the fatty acid profile of LBFLFK canola differs from conventional canola due to the intentionally introduced EPA+DHA trait (section B.5). LBFLFK canola contains fatty acids associated with the trait that are not present in conventional canola, and fatty acids with altered relative levels as compared to conventional canola, either because they are serving as substrates for the EPA+DHA biosynthetic pathway or because of shifts in relative percentage of overall fatty acids. For the other components measured, LBFLFK canola is compositionally not different from its conventional counterpart Kumily (identified differences were not found to be biologically relevant) and is equivalent to other commercially available canola varieties based on comparisons to non-GM reference varieties, taking into account natural variation. Based on the available body of evidence regarding the safety of the newly introduced fatty acids, no further nutritional studies with food derived from LBFLFK canola are considered necessary.

As discussed in section B.5(a) in the subsection “Fatty acids introduced by the EPA+DHA trait”, EPA and DHA occur in foods from marine sources. The fatty acid profile in LBFLFK canola oil is compositionally comparable to Menhaden oil and other fish oils and therefore similar to that in commonly consumed food and feed (Andre et al., 2019). In addition, based on the results of a repeated-dose 90-day oral toxicity study in Wistar rats (Appendix 26 and Part D), dietary administration of LBFLFK canola defatted meal and RBD oil had no unintended adverse effects on clinical examinations, clinical pathology, or pathology.

The primary intended use of LBFLFK canola oil as a feed ingredient will be to partially or fully replace the oil fraction of the diet for farmed marine organisms. This is possible for any farmed marine organism that currently has a source of EPA and/or DHA incorporated into the diet (e.g., those currently using fish oil as a feed ingredient). The maximum usage of oil from LBFLFK canola will always be limited by the dietary requirements of the aquatic animal being farmed. Farmed marine animals have varied dietary requirements, which include a requirement for energy from lipids and specifically for omega-3 LC-PUFAs, such as EPA and DHA, for the growth and health of the animals (for example, see the summary of the nutritional requirements of Atlantic salmon (FAO, 2019)).

Fish oil has historically provided both the requirement for energy from lipids and LC-PUFAs. Because of limited supplies of fish oil, partially or fully replacing fish oil as a feed ingredient is needed to support global aquaculture. As noted for salmon (FAO, 2019), these studies have demonstrated that it is possible to replace the major proportion of fish oil with vegetable oil and still maintain optimum growth and feed utilisation over the major part of the fish life cycle. Various vegetable oils, including canola oil, are already commonly used to supplement the lipid energy requirements of farmed marine organisms, with an increase in this usage in recent years (Ytrestøyl et al., 2014). Any replacement of oil in aquafeed diet formulations with LBFLFK canola oil is expected to have no impact on fish health and production as compared to the combinations of canola oil and fish oil used in current commercial formulations.

Therefore, it can be concluded that there is no need for nutritional studies with aquatic species to make a determination of safety, efficacy, or bioavailability for the EPA+DHA containing oil derived from LBFLFK canola. When used in feed rations in aquaculture operations, LBFLFK canola oil is considered to be as safe as conventional canola oil and as safe as comparable sources of EPA and DHA when considering the intended EPA+DHA trait.

PART D OTHER INFORMATION

There is no requirement to conduct animal feeding or whole food toxicity studies on the food produced using gene technology. However, if a 90-day (or longer) whole food toxicity study in rodents has been provided to satisfy the data and information requirements of another jurisdiction, this should also be provided to FSANZ as additional supporting information.

Therefore, a repeated-dose 90-day oral toxicity study in male and female Wistar rats that was conducted to compare rat diet containing LBFLFK canola defatted meal and RBD oil to rat diet containing defatted meal and RBD oil from the conventional counterpart Kumily, and to detect potential toxicologically relevant differences after a 3-month administration period, is provided to FSANZ as Appendix 26.

REFERENCES

Abbadi A, Domergue F, Bauer J, Napier JA, Welti R, Zähringer U, Cirpus P and Heinz E, 2004. Biosynthesis of very-long-chain polyunsaturated fatty acids in transgenic oilseeds: Constraints on their accumulation. Plant Cell 16, 2734-2748.

Agaba MK, Tocher DR, Zheng X, Dickson CA, Dick JR and Teale AJ, 2005. Cloning and functional characterisation of polyunsaturated fatty acid elongases of marine and freshwater teleost fish. Comparative Biochemistry and Physiology Part B: Biochemistry and Molecular Biology 142, 342-352.

Alasalvar C, Taylor K, Zubcov E, Shahidi F and Alexis M, 2002. Differentiation of cultured and wild sea bass (*Dicentrarchus labrax*): Total lipid content, fatty acid and trace mineral composition. Food Chemistry 79, 145-150.

Allen BC, Vincent MJ, Liska D and Haber LT, 2016. Meta-regression analysis of the effect of trans fatty acids on low-density lipoprotein cholesterol. Food and Chemical Toxicology 98, 295-307.

Alonso L, Cuesta P and Gilliland S, 2009. Effect of β-cyclodextrin on trans fats, CLA, PUFA and phospholipids of milk fat. Journal of the American Oil Chemists' Society 86, 337-342.

Altschul SF, Madden TL, Schäffer AA, Zhang J, Zhang Z, Miller W and Lipman DJ, 1997. Gapped BLAST and PSI-BLAST: A new generation of protein database search programs. Nucleic Acids Research 25, 3389-3402.

Alvarez M, Estrada J, Gozalo F, Fernandez-Rojo F and Barber D, 2001. Oilseed rape flour: Another allergen causing occupational asthma among farmers. Allergy 56, 185-188.

Alves SP and Bessa RJ, 2009. Comparison of two gas–liquid chromatograph columns for the analysis of fatty acids in ruminant meat. Journal of Chromatography A 1216, 5130-5139.

Anadón A, Martínez-Larrañaga MR, Martínez MA, Ares I, Ramos E, Gómez-Cortés P, Juárez M and Miguel A, 2010. Acute oral safety study of dairy fat rich in trans-10 C18:1 versus vaccenic plus conjugated linoleic acid in rats. Food and Chemical Toxicology 48, 591-598.

Anderson RG, Deb D, Fedkenheuer K and McDowell JM, 2015. Recent progress in RXLR effector research. Molecular Plant-Microbe Interactions 28, 1063-1072.

Ando Y, Nishimura K, Aoyanagi N and Takagi T, 1992. Stereospecific analysis of fish oil triacyl-sn-glycerols. Journal of the American Oil Chemists' Society 69, 417-424.

Andre C, Buesen R, Riffle B, Wandelt C, Sottosanto JB, Marxfeld H, Strauss V, van Ravenzwaay B and Lipscomb EA, 2019. Safety assessment of EPA+DHA canola oil by fatty acid profile comparison to various edible oils and fat-containing foods and a 28-day repeated dose toxicity study in rats. Food and Chemical Toxicology 124, 168-181.

AOF, 2004, online. Canola meal. Accessed on April 13, 2021. available at http://www.australianoilseeds.com/__data/assets/pdf_file/0011/1271/AOF_Canola_Meal_Report-Limitations__and__Opportunities_2004.pdf

AOF, 2019, online. Delivering high quality products to local and global markets. Accessed on April 13, 2021. available at http://www.australianoilseeds.com/oilseeds_industry

Aranda-Burgos JA, da Costa F, Nóvoa S, Ojea J and Martínez-Patiño D, 2014. Effects of microalgal diet on growth, survival, biochemical and fatty acid composition of *Ruditapes decussatus* larvae. Aquaculture 420, 38-48.

Armbrust EV, Berges JA, Bowler C, Green BR, Martinez D, Putnam NH, Zhou S, Allen AE, Apt KE and Bechner M, 2004. The genome of the diatom *Thalassiosira pseudonana*: Ecology, evolution, and metabolism. Science 306, 79-86.

Astwood JD, Leach JN and Fuchs RL, 1996. Stability of food allergens to digestion *in vitro*. Nature Biotechnology 14, 1269-1273.

ATCC, 2017a, online. *Pavlova lutheri*. Accessed on March 16, 2017. available at https://www.atcc.org/Products/All/50092.aspx

ATCC, 2017b, online. *Phytophthora infestans*. Accessed on March 16, 2017. available at https://www.atcc.org/Search_Results.aspx?dsNav=Ntk:PrimarySearch%7cPhytophthora+infestans%7c3%7c,Ny:True,Ro:0,N:1000552&searchTerms=Phytophthora+infestans&redir=1

ATCC, 2017c, online. *Phytophthora sojae*. Accessed on March 16, 2017. available at https://www.atcc.org/Search_Results.aspx?dsNav=Ntk:PrimarySearch%7cPhytophthora+sojae%7c3%7c,Ny:True,Ro:0,N:1000552&searchTerms=Phytophthora+sojae&redir=1

ATCC, 2017d, online. *Pythium irregulare*. Accessed on March 16, 2017. available at https://www.atcc.org/Search_Results.aspx?dsNav=Ntk:PrimarySearch%7cPythium+irregulare%7c3%7c,Ny:True,Ro:0,N:1000552&searchTerms=Pythium+irregulare&redir=1

Atienza G, Arafiles K, Carmona M, Garcia J, Macabago A, Peñacerrada B, Cordero P, Bennett R and Dedeles G, 2012. Carotenoid analysis of locally isolated Thraustochytrids and their potential as an alternative fish feed for *Oreochromis niloticus* (Nile tilapia). Mycosphere 3, 420-428.

Atkinson HJ, Morris JH, Ferrin TE and Babbitt PC, 2009. Using sequence similarity networks for visualization of relationships across diverse protein superfamilies. PLoS One 4, e4345.

Bai Y, McCoy JG, Levin EJ, Sobrado P, Rajashankar KR, Fox BG and Zhou M, 2015. X-ray structure of a mammalian stearoyl-CoA desaturase. Nature 524, 252-256.

Barker RF, Idler KB, Thompson DV and Kemp JD, 1983. Nucleotide sequence of the T-DNA region from the *Agrobacterium tumefaciens* octopine Ti plasmid pTi15955. Plant Molecular Biology 2, 335-350.

BASF, 2018, online. Clearfield® Stewardship. Accessed on August 20, 2021. available at https://www.intergrain.com/app/uploads/2018/08/BASFClearfieldStewardshipBrochure-2.pdf

Bates PD, Durrett TP, Ohlrogge JB and Pollard M, 2009. Analysis of acyl fluxes through multiple pathways of triacylglycerol synthesis in developing soybean embryos. Plant Physiology 150, 55-72.

Bauer J and Senger T, 2010. Promoters from *Brassica napus* for seed specific gene expression. Patent WO2010000708, World Intellectual Property Organization.

Bäumlein H, Boerjan W, Nagy I, Bassfüner R, Van Montagu M, Inzé D and Wobus U, 1991. A novel seed protein gene from *Vicia faba* is developmentally regulated in transgenic tobacco and Arabidopsis plants. Molecular and General Genetics 225, 459-467.

Beaudoin F, Michaelson LV, Hey SJ, Lewis MJ, Shewry PR, Sayanova O and Napier JA, 2000a. Heterologous reconstitution in yeast of the polyunsaturated fatty acid biosynthetic pathway. Proceedings of the National Academy of Sciences of the United States of America 97, 6421-6426.

Beaudoin F, Michaelson LV, Lewis MJ, Shewry PR, Sayanova O and Napier JA, 2000b. Production of C20 polyunsaturated fatty acids (PUFAs) by pathway engineering: Identification of a PUFA elongase component from *Caenorhabditis elegans*. Biochemical Society Transactions 28, 661-663.

Beccaria M, Costa R, Sullini G, Grasso E, Cacciola F, Dugo P and Mondello L, 2015. Determination of the triacylglycerol fraction in fish oil by comprehensive liquid chromatography techniques with the support of gas chromatography and mass spectrometry data. Analytical and Bioanalytical Chemistry 407, 5211-5225.

Beck E, Ludwig G, Auerswald E, Reiss B and Schaller H, 1982. Nucleotide sequence and exact localization of the neomycin phosphotransferase gene from transposon Tn5. Gene 19, 327-336.

Bergé J-P and Barnathan G, 2005. Fatty acids from lipids of marine organisms: Molecular biodiversity, roles as biomarkers, biologically active compounds, and economical aspects. In: Marine Biotechnology I. Eds Gal YL and Ulber R, Springer, Berlin, 49-125.

Birch PR, Boevink PC, Gilroy EM, Hein I, Pritchard L and Whisson SC, 2008. Oomycete RXLR effectors: Delivery, functional redundancy and durable disease resistance. Current Opinion in Plant Biology 11, 373-379.

Blasbalg TL, Hibbeln JR, Ramsden CE, Majchrzak SF and Rawlings RR, 2011. Changes in consumption of omega-3 and omega-6 fatty acids in the United States during the 20th century. American Journal of Clinical Nutrition 93, 950-962.

Braybrook SA, Stone SL, Park S, Bui AQ, Le BH, Fischer RL, Goldberg RB and Harada JJ, 2006. Genes directly regulated by LEAFY COTYLEDON2 provide insight into the control of embryo maturation and somatic embryogenesis. Proceedings of the National Academy of Sciences of the United States of America 103, 3468-3473.

Brown MR, 2002. Nutritional value and use of microalgae in aquaculture. Avances en Nutrición Acuícola VI. Memorias del VI Simposium Internacional de Nutrición Acuícola 3, 281-292.

Brugnano C, Guglielmo L and Zagami G, 2008. Food type effects on reproduction of hyperbenthic calanoid species *Pseudocyclops xiphophorus* Wells, 1967, under laboratory conditions. Chemistry and Ecology 24, 111-117.

Bushey DF, Bannon GA, Delaney BF, Graser G, Hefford M, Jiang X, Lee TC, Madduri KM, Pariza M and Privalle LS, 2014. Characteristics and safety assessment of intractable proteins in genetically modified crops. Regulatory Toxicology and Pharmacology 69, 154-170.

Buzza GC, 2007. Canola breeding in the seventies – a personal look back. Proceedings of the 15th Australian Research Assembly on Brassicas (ARAB15), Geraldton, Western Australia, 63-68.

Caers M, Coutteau P, Sorgeloos P and Gajardo G, 2003. Impact of algal diets and emulsions on the fatty acid composition and content of selected tissues of adult broodstock of the Chilean scallop *Argopecten pupuratus* (Lamarck, 1819). Aquaculture 217, 437-452.

Canola Council of Canada, 2015, online. Canola meal feeding guide. Accessed on November 30, 2016. available at http://www.canolacouncil.org/media/516716/2015_canola_meal_feed_industry_guide.pdf

Canola Council of Canada, 2016a, online. Industry overview. Accessed on October 4, 2016. available at http://www.canolacouncil.org/markets-stats/industry-overview/

Canola Council of Canada, 2016b, online. What is canola? Accessed on September 30, 2016. available at http://www.canolacouncil.org/oil-and-meal/what-is-canola/

Canola Council of Canada, 2017, online. Estimated acerage and percentage. Accessed on June 9, 2017. available at http://www.canolacouncil.org/markets-stats/statistics/estimated-acreage-and-percentage/

Carvalho AP and Malcata FX, 2005. Optimization of omega-3 fatty acid production by microalgae: Crossover effects of CO2 and light intensity under batch and continuous cultivation modes. Marine Biotechnology 7, 381-388.

Castro-Sánchez P and Martín-Villa JM, 2013. Gut immune system and oral tolerance. British Journal of Nutrition 109, S3-S11.

Çelik M, Türeli C, Çelik M, Yanar Y, Erdem Ü and Küçükgülmez A, 2004. Fatty acid composition of the blue crab (*Callinectes sapidus* Rathbun, 1896) in the northeastern Mediterranean. Food Chemistry 88, 271-273.

Centre National de Séquençage, 2017, online. Genoscope, *Brassica napus* Genome Browser. Accessed on October 24, 2017. available at http://www.genoscope.cns.fr/brassicanapus/

Chalhoub B, Denoeud F, Liu S, Parkin IAP, Tang H, Wang X, Chiquet J, Belcram H, Tong C, Samans B, Corréa M, Da Silva C, Just J, Falentin C, Koh CS, Le Clainche I, Bernard M, Bento P, Noel B, Labadie K, Alberti A, Charles M, Arnaud D, Guo H, Daviaud C, Alamery S, Jabbari K, Zhao M, Edger PP, Chelaifa H, Tack D, Lassalle G, Mestiri I, Schnel N, Le Paslier M-C, Fan G, Renault V, Bayer PE, Golicz AA, Manoli S, Lee T-H, Thi VHD, Chalabi S, Hu Q, Fan C, Tollenaere R, Lu Y, Battail C, Shen J, Sidebottom CHD, Wang X, Canaguier A, Chauveau A, Bérard A, Deniot G, Guan M, Liu Z, Sun F, Lim YP, Lyons E, Town CD, Bancroft I, Wang X, Meng J, Ma J, Pires JC, King GJ, Brunel D, Delourme R, Renard M, Aury J-M, Adams KL, Batley J, Snowdon RJ, Tost J, Edwards D, Zhou Y, Hua W, Sharpe AG, Paterson AH, Guan C and Wincker P, 2014. Early allopolyploid evolution in the post-Neolithic *Brassica napus* oilseed genome. Science 345, 950-953.

Chardigny J-M, Sébédio, J-L, and Berdeaux, O, 1996. Trans polyunsaturated fatty acids: Occurrence and nutritional implications. In: Advances in Applied Lipid Research, Volume 2. JAI Press Inc., 1-33.

Chardin H, Mayer C, Senechal H, Wal J, Poncet P, Desvaux F and Peltre G, 2003. Lipid transfer protein 1 is a possible allergen in *Arabidopsis thaliana*. International Archives of Allergy and Immunology 131, 85-90.

Chen X, Pfeil JE and Gal S, 2002. The three typical aspartic proteinase genes of *Arabidopsis thaliana* are differentially expressed. European Journal of Biochemistry 269, 4675-4684.

Cheng B, Wu G, Vrinten P, Falk K, Bauer J and Qiu X, 2010. Towards the production of high levels of eicosapentaenoic acid in transgenic plants: The effects of different host species, genes and promoters. Transgenic Research 19, 221-229.

Chilton MD, Tepfer DA, Petit A, David C, Casse-Delbart F and Tempé J, 1982. *Agrobacterium rhizogenes* inserts T-DNA into the genomes of the host plant root cells. Nature 295, 432-434.

Chukwudebe A, Privalle L, Reed A, Wandelt C, Contri D, Dammann M, Groeters S, Kaspers U, Strauss V and van Ravenzwaay B, 2012. Health and nutritional status of Wistar rats following subchronic exposure to CV127 soybeans. Food and Chemical Toxicology 50, 956-971.

Cirpus P and Bauer J, 2006. Method for producing polyunsaturated c20 and c22 fatty acids with at least four double bonds in transgenic plants. Patent WO2006100241 A2, World Intellectual Property Organization.

Codex Alimentarius Commission, 2009a. Codex standard for named vegetable oils (CODEX-STAN 210-1999). Food and Agricultural Organization of the United Nations and the World Health Organization.

Codex Alimentarius Commission, 2009b. Foods derived from modern biotechnology. Codex Alimentarius Commission, Joint FAO/WHO Food Standards Programme. Rome, Italy. 85 pp.

Codex Alimentarius Commission, 2009c. Guideline for the conduct of food safety assessment of foods derived from recombinant-DNA plants (CAC/GL 45-2003). Codex Alimentarius Commission, Joint FAO/WHO Food Standards Programme. Rome, Italy.

Cook HW and McMaster CR, 2002. Fatty acid desaturation and chain elongation in eukaryotes. New Comprehensive Biochemistry 36, 181-204.

Coruzzi G, Broglie R, Edwards C and Chua N-H, 1984. Tissue-specific and light-regulated expression of a pea nuclear gene encoding the small subunit of ribulose-1, 5-bisphosphate carboxylase. EMBO Journal 3, 1671.

Costa R, Albergamo A, Piparo M, Zaccone G, Capillo G, Manganaro A, Dugo P and Mondello L, 2017. Multidimensional gas chromatographic techniques applied to the analysis of lipids from wild-

caught and farmed marine species. European Journal of Lipid Science and Technology 119, 1600043.

Cove DJ, Perroud P-F, Charron AJ, McDaniel SF, Khandelwal A and Quatrano RS, 2009. The moss *Physcomitrella patens*: A novel model system for plant development and genomic studies. Cold Spring Harbor Protocols 2009, pdb-emo115.

Cowling WA, 2007. Genetic diversity in Australian canola and implications for crop breeding for changing future environments. Field Crops Research 104, 103-111.

Crowe J, Dobeli H, Gentz R, Hochuli E, Stiiber D and Henco K, 1994. 6xhis-Ni-NTA chromatography as a superior technique in recombinant protein expression/purification. In: Protocols for Gene Analysis. Ed Harwood AJ, Humana Press, Totowa, NJ, 371-387.

D'Arrigo M, Hoz L, Cambero I, Lopez-Bote C, Pin C and Ordóñez J, 2004. Production of n-3 fatty acid enriched pork liver pâté. LWT - Food Science and Technology 37, 585-591.

D'Souza F, Lecossois D, Heasman M, Diemar J, Jackson C and Pendrey R, 2000. Evaluation of centrifuged microalgae concentrates as diets for *Penaeus monodon* Fabricius larvae. Aquaculture 31, 661-670.

De Block M, De Brouwer D and Tenning P, 1989. Transformation of *Brassica napus* and *Brassica oleracea* using *Agrobacterium tumefaciens* and the expression of the *bar* and *neo* genes in the transgenic plants. Plant Physiology 91, 694-701.

de Groot MJA, Bundock P, Hooykaas PJ and Beijersbergen AGM, 1998. *Agrobacterium tumefaciens*-mediated transformation of filamentous fungi. Nature Biotechnology 16, 839-842.

Decker EL, Parsons J and Reski R, 2014. Glyco-engineering for biopharmaceutical production in moss bioreactors. Frontiers in Plant Science 5, 346.

Delalat B, Sheppard VC, Ghaemi SR, Rao S, Prestidge CA, McPhee G, Rogers M-L, Donoghue JF, Pillay V and Johns TG, 2015. Targeted drug delivery using genetically engineered diatom biosilica. Nature Communications 6, 8791.

Delaney B, Astwood JD, Cunny H, Conn RE, Herouet-Guicheney C, Macintosh S, Meyer LS, Privalle L, Gao Y, Mattsson J, Levine M and ILSI International Food Biotechnology Committee Task Force on Protein Safety, 2008. Evaluation of protein safety in the context of agricultural biotechnology. Food and Chemical Toxicology 46, S71-S97.

Delaunay F, Marty Y, Moal J and Samain J-F, 1993. The effect of monospecific algal diets on growth and fatty acid composition of *Pecten maximus* (L.) larvae. Journal of Experimental Marine Biology and Ecology 173, 163-179.

Denic V and Weissman JS, 2007. A molecular caliper mechanism for determining very long-chain fatty acid length. Cell 130, 663-677.

Deutsch EW, Overall CM, Van Eyk JE, Baker MS, Paik Y-K, Weintraub ST, Lane L, Martens L, Vandenbrouck Y, Kusebauch U, Hancock W, Hermjakob H, Aebersold R, Moritz R and Omenn G, 2016. Human proteome project mass spectrometry data interpretation guidelines 2.1. Journal of Proteome Research 15, 3961.

Dhammu H, Seymour M, Hashem A and Bucat J, 2020, online. Chemical weed control in canola, Bulletin Number 4907. Department of Primary Industries and Regional Development. Accessed on August 25, 2021. available at https://www.agric.wa.gov.au/sites/gateway/files/Weed%20Control%20in%20Canola.pdf

Dhert P and Sorgeloos P, 1995. Live feeds in aquaculture. In: Aquaculture Towards the 21st Century. Proceedings of the INFOFISH-AQUATECH 94 Conference, Colombo, Sri Lanka, 29-31 August 1994. Eds Nambiar K and Singh T, INFOFISH, Kuala Lumpur, 209-219.

Díaz-Perales A, Blanco C, Sánchez-Monge R, Varela J, Carrillo T and Salcedo G, 2003. Analysis of avocado allergen (Prs a 1) IgE-binding peptides generated by simulated gastric fluid digestion. Journal of Allergy and Clinical Immunology 112, 1002-1007.

Domergue F, Abbadi A, Ott C, Zank TK, Zahringer U and Heinz E, 2003. Acyl carriers used as substrates by the desaturases and elongases involved in very long-chain polyunsaturated fatty acids biosynthesis reconstituted in yeast. Journal of Biological Chemistry 278, 35115-35126.

Domergue F, Abbadi A, Zähringer U, Moreau H and Heinz E, 2005. *In vivo* characterization of the first acyl-CoA Δ6-desaturase from a member of the plant kingdom, the microalga *Ostreococcus tauri*. Biochemical Journal 389, 483-490.

Dooper MM, Wassink L, M'rabet L and Graus YM, 2002. The modulatory effects of prostaglandin-E on cytokine production by human peripheral blood mononuclear cells are independent of the prostaglandin subtype. Immunology 107, 152-159.

Doroudi M, Southgate PC and Lucas J, 2003. Variation in clearance and ingestion rates by larvae of the black-lip pearl oyster (*Pinctada margaritifera*, L.) feeding on various microalgae. Aquaculture Nutrition 9, 11-16.

Duggleby RG and Pang SS, 2000. Acetohydroxyacid synthase. Journal of Biochemistry and Molecular Biology 33, 1-36.

Duwenig E and Loyall LP, 2007. Expression cassettes for seed-preferential expression in plants. Patent WO2006089950A3, World Intellectual Property Organization.

EFSA, 2004. Opinion of the Scientific Panel on Dietetic Products, Nutrition and Allergies on a request from the Commission related to the presence of *trans* fatty acids in foods and the effect on human health of the consumption of *trans* fatty acids. EFSA Journal 81, 1-49.

EFSA, 2008. Scientific Opinion of the Panel on Dietetic Products Nutrition and Allergies on a request from the European Commission on the safety of `fungal oil from *Mortierella alpina*`. EFSA Journal 770, 1-15.

EFSA Panel on Dietetic Products, Nutrition and Allergies, 2010. Scientific Opinion on dietary reference values for fats, including saturated fatty acids, polyunsaturated fatty acids, monounsaturated fatty acids, trans fatty acids, and cholesterol. EFSA Journal 8, 1461.

EFSA Panel on Dietetic Products, Nutrition and Allergies, 2015. Scientific Opinion on the safety of refined Buglossoides oil as a novel food ingredient. EFSA Journal 13, 4029.

EFSA Panel on Genetically Modified Organisms, 2011. Scientific Opinion on Guidance for risk assessment of food and feed from genetically modified plants. EFSA Journal 9, 2150.

Ellerström M, Stålberg K, Ezcurra I and Rask L, 1996. Functional dissection of a napin gene promoter: Identification of promoter elements required for embryo and endosperm-specific transcription. Plant Molecular Biology 32, 1019-1027.

Ewing B and Green P, 1998. Base-calling of automated sequencer traces using *phred*. II. Error probabilities. Genome Research 8, 186-194.

FAO, 2010. Fats and fatty acids in human nutrition. Report of an expert consultation. Food and Agriculture Organization of the United Nations, Rome, Italy.

FAO, 2016, online. FAOSTAT. Accessed on September 21, 2017. available at http://www.fao.org/faostat/en/#home

FAO, 2019, online. Atlantic salmon - Nutritional requirements. Aquaculture Feed and Fertilizer Resources Information System. Accessed on February 28, 2019. available at www.fao.org/fishery/affris/species-profiles/atlantic-salmon/nutritional-requirements/en/

FAO, 2020. The State of Wold Fisheries and Aquaculture 2020. Sustainability in action. Rome, Italy. 224 pp.

FAO/WHO, 2001. Guidelines for the preparation of working papers on intake of food additives for the Joint FAO/WHO Expert Committee on Food Additives. Joint FAO/WHO Expert Committee on Food Additives (JECFA), World Health Organization and Food and Agriculture Organization of the United Nations. 29 pp.

Fawke S, Doumane M and Schornack S, 2015. Oomycete interactions with plants: Infection strategies and resistance principles. Microbiology and Molecular Biology Reviews 79, 263-280.

Finn RD, Coggill P, Eberhardt RY, Eddy SR, Mistry J, Mitchell AL, Potter SC, Punta M, Qureshi M, Sangrador-Vegas A, Salazar GA, Tate J and Bateman A, 2016. The Pfam protein families database: Towards a more sustainable future. Nucleic Acids Research 44, D279-D285.

Flock MR, Harris WS and Kris-Etherton PM, 2013. Long-chain omega-3 fatty acids: Time to establish a dietary reference intake. Nutrition Reviews 71, 692-707.

Focke M, Hemmer W, Hayek B, Götz M and Jarisch R, 1998. Identification of allergens in oilseed rape (*Brassica napus*) pollen. International Archives of Allergy and Immunology 117, 105-112.

Forrester-Anderson IT, McNitt J, Way R and Way M, 2006. Fatty acid content of pasture-reared fryer rabbit meat. Journal of Food Composition and Analysis 19, 715-719.

Fritsche J and Steinhart H, 1997. Contents of trans fatty acids (TFA) in German foods and estimation of daily intake. European Journal of Lipid Science and Technology 99, 314-318.

FSANZ, 2003, online. Erucic acid in food: A toxicological review and risk assessment. Accessed on October 4, 2016. available at http://www.foodstandards.gov.au/publications/documents/Erucic%20acid%20monograph.pdf

FSANZ, 2017. Supporting Document 2: Nutrition Risk Assessment Report (at Approval) – Application A1143, Food derived from DHA canola line NS-B50027-4.

Fu T-J, Abbott UR and Hatzos C, 2002. Digestibility of food allergens and nonallergenic proteins in simulated gastric fluid and simulated intestinal fluid – A comparative study. Journal of Agricultural and Food Chemistry 50, 7154-7160.

Gagné R, Tremblay R, Olivier F, Pernet F, Miner P and Samain J-F, 2012. Effect of shear velocity and flow regimes on scallop post-larval detachment feed on two different diets. Aquaculture 370, 172-178.

Gardner RC, Chonoles KR and Owens RA, 1986. Potato spindle tuber viroid infections mediated by the Ti plasmid of *Agrobacterium tumefaciens*. Plant Molecular Biology 6, 221-228.

Gavel Y and von Heijne G, 1990. Sequence differences between glycosylated and non-glycosylated Asn-X-Thr/Ser acceptor sites: Implications for protein engineering. Protein Engineering 3, 433-442.

Gebauer SK, Destaillats F, Mouloungui Z, Candy L, Bezelgues J-B, Dionisi F and Baer DJ, 2011. Effect of trans fatty acid isomers from ruminant sources on risk factors of cardiovascular disease: Study design and rationale. Contemporary Clinical Trials 32, 569-576.

Gebauer SK, Psota TL, Harris WS and Kris-Etherton PM, 2006. n-3 fatty acid dietary recommendations and food sources to achieve essentiality and cardiovascular benefits. The American Journal of Clinical Nutrition 83, S1526-1535S.

Gerdes K, Møller-Jensen J and Jensen RB, 2000. Plasmid and chromosome partitioning: Surprises from phylogeny. Molecular Microbiology 37, 455-466.

Gheysen G, Villarroel R and Van Montagu M, 1991. Illegitimate recombination in plants: A model for T-DNA integration. Genes & Development 5, 287-297.

Ghioni C, Porter AEA, Taylor GW and Tocher DR, 2002. Metabolism of 18:4n-3 (stearidonic acid) and 20:4n-3 in salmonid cells in culture and inhibition of the production of prostaglandin F2α (PGF2α) from 20:4n-6 (arachidonic acid). Fish Physiology and Biochemistry 27, 81-96.

Glencross B, Hawking W and Curnow J, 2003. Evaluation of canola oil as alternative lipid resources in diet for juvenile red seabream, *Pagrus auratus*. Aquaculture Nutrition 9, 305-315.

Glencross BD and Turchini GM, 2011. Fish oil replacement in starter, grow-out, and finishing feeds for farmed aquatic animals In: Fish Oil Replacement and Alternative Lipid Sources in Aquaculture Feeds Eds Turchini GM, Ng WK and Tocher DR, CRC Press Boca Raton, FL, 373-404.

González-Araya R, Lebrun L, Quéré C and Robert R, 2012. The selection of an ideal diet for *Ostrea edulis* (L.) broodstock conditioning (part B). Aquaculture 362, 55-66.

González-Araya R, Quéau I, Quéré C, Moal J and Robert R, 2011. A physiological and biochemical approach to selecting the ideal diet for *Ostrea edulis* (L.) broodstock conditioning (part A). Aquaculture 42, 710-726.

González-Araya R, Quillien V and Robert R, 2013. The effects of eight single microalgal diets on sex-ratio and gonad development throughout European flat oyster (*Ostrea edulis* L.) conditioning. Aquaculture 400, 1-5.

González-Rovira A, Mourente G, Zheng X, Tocher DR and Pendón C, 2009. Molecular and functional characterization and expression analysis of a Δ6 fatty acyl desaturase cDNA of European Sea Bass (*Dicentrarchus labrax* L.). Aquaculture 298, 90-100.

Goossens A, Dillen W, De Clercq J, Van Montagu M and Angenon G, 1999. The *arcelin-5* gene of *Phaseolus vulgaris* directs high seed-specific expression in transgenic *Phaseolus acutifolius* and Arabidopsis plants. Plant Physiology 120, 1095-1104.

Goossens A, Geremia R, Bauw G, Montagu M and Angenon G, 1994. Isolation and characterisation of arcelin-5 proteins and cDNAs. European Journal of Biochemistry 225, 787-795.

Gouda R, Kenchington E, Hatcher B and Vercaemer B, 2006. Effects of locally-isolated micro-phytoplankton diets on growth and survival of sea scallop (*Placopecten magellanicus*) larvae. Aquaculture 259, 169-180.

GRDC Grownotes, 2018. Canola: Weed Control. Grains Research and Development Corporation. Section 6, 1-10.

Grémare A, Amouroux J, Chaabeni Y and Charles F, 1998. Experimental study of the effect of kaolinite on the ingestion and the absorption of monospecific suspensions of *Pavlova lutheri* by the filter-feeding bivalve *Venus verrucosa*. Vie Milieu 48, 295-307.

Grigorakis K, Giogios I, Vasilaki A and Nengas I, 2010. Effect of the fish oil, oxidation status and of heat treatment temperature on the volatile compounds of the produced fish feeds. Animal Feed Science and Technology 158, 73-84.

Grimes HD, Overvoorde PJ, Ripp K, Franceschi VR and Hitz WD, 1992. A 62-kD sucrose binding protein is expressed and localized in tissues actively engaged in sucrose transport. Plant Cell 4, 1561-1574.

Guerche P, Jouanin L, Tepfer DA and Pelletier G, 1987. Genetic transformation of oilseed rape (Brassica napus) by the Ri T-DNA of *Agrobacterium rhizogenes* and analysis of inheritance of the transformed phenotype. Molecular and General Genetics 206, 382-386.

Guiry MD, 2015a. *Ostreococcus tauri* In: Guiry MD and Guiry GM, (2017). AlgaeBase. World-wide electronic publication, National University of Ireland, Galway (taxonomic information republished from AlgaeBase with permission of M.D. Guiry). Accessed through: World Register of Marine Species at http://www.marinespecies.org/aphia.php?p=taxdetails&id=345497 on September 22, 2017.

Guiry MD, 2015b. *Pavlova lutheri* (Droop) J.C.Green, 1975. In: Guiry MD and Guiry GM, (2017). AlgaeBase. World-wide electronic publication, National University of Ireland, Galway (taxonomic information republished from AlgaeBase with permission of M.D. Guiry). Accessed through: World Register of Marine Species at http://www.marinespecies.org/aphia.php?p=taxdetails&id=249732 on September 22, 2017.

Guo B, Wan X and Liang Z, 2013. Identification and heterologous expression of a Δ4-fatty acid desaturase gene from *Isochrysis sphaerica*. Journal of Microbiology and Biotechnology 23, 1413-1421.

Gylling H, 2006. Rapeseed oil does not cause allergic reactions. Allergy 61, 895.

Hajdukiewicz P, Svab Z and Maliga P, 1994. The small, versatile *pPZP* family of Agrobacterium binary vectors for plant transformation. Plant Molecular Biology 25, 989-994.

Hammond BG, 2007. *In vitro* digestibility assays. In: Food Safety of Proteins in Agricultural Biotechnology. CRC Press, Boca Raton, FL, 213-214.

Hammond BG, Mayhew DA, Naylor MW, Ruecker FA, Mast RW and Sander WJ, 2001. Safety assessment of DHA-rich microalgae from *Schizochytrium* sp.: I. Subchronic rat feeding study. Regulatory Toxicology and Pharmacology 33, 192-204.

Han J, Lühs W, Sonntag K, Zähringer U, Borchardt DS, Wolter FP, Heinz E and Frentzen M, 2001. Functional characterization of β-ketoacyl-CoA synthase genes from *Brassica napus* L. Plant Molecular Biology 46, 229-239.

Hannapel DJ, 1993. Nucleotide and deduced amino acid sequence of the 22-kilodalton cathepsin D inhibitor protein of potato (*Solanum tuberosum* L.). Plant Physiology 101, 703-704.

Harris NJ and Booth PJ, 2012. Folding and stability of membrane transport proteins *in vitro*. Biochimica et Biophysica Acta - Biomembranes 1818, 1055-1066.

Harris RP, 1977. Some aspects of the biology of the harpacticoid copepod, *Scottolana canadensis* (Willey), maintained in laboratory culture. Chesapeake Science 18, 245-252.

Haslekås C, Stacy RA, Nygaard V, Culiáñez-Macià FA and Aalen RB, 1998. The expression of a peroxiredoxin antioxidant gene, *AtPer1*, in *Arabidopsis thaliana* is seed-specific and related to dormancy. Plant Molecular Biology 36, 833-845.

Hastings N, Agaba MK, Tocher DR, Zheng X, Dickson CA, Dick JR and Teale AJ, 2004. Molecular cloning and functional characterization of fatty acyl desaturase and elongase cDNAs involved in the production of eicosapentaenoic and docosahexaenoic acids from α-linolenic acid in Atlantic salmon (*Salmo salar*). Marine Biotechnology 6, 463-474.

Haughn GW and Somerville CR, 1990. A mutation causing imidazolinone resistance maps to the *Csr1* locus of *Arabidopsis thaliana*. Plant Physiology 92, 1081-1085.

Hawkins L, Hutchinson S and Laing I, 2005. The effects of temperature and food ration on metabolite concentrations in newly settled king scallop (*Pecten maximus*) spat. Aquaculture 250, 841-848.

Health and Environmental Sciences Institute, 2017, online. COMprehensive Protein Allergen REsource (COMPARE) Database. Accessed on September 19, 2017. available at http://comparedatabase.org/

Heim U, Wang Q, Kurz T, Borisjuk L, Golombek S, Neubohn B, Adler K, Gahrtz M, Sauer N and Weber H, 2001. Expression patterns and subcellular localization of a 52 kDa sucrose-binding protein homologue of *Vicia faba* (VfSBPL) suggest different functions during development. Plant Molecular Biology 47, 461-474.

Helsberg M and Eichenlaub R, 1986. Twelve 43-base-pair repeats map in a cis-acting region essential for partition of plasmid mini-F. Journal of Bacteriology 165, 1043-1045.

Hempenius R, Lina B and Haggitt R, 2000. Evaluation of a subchronic (13-week) oral toxicity study, preceded by an *in utero* exposure phase, with arachidonic acid oil derived from *Mortierella alpina* in rats. Food and Chemical Toxicology 38, 127-139.

Heppard EP, Kinney AJ, Stecca KL and Miao G-H, 1996. Developmental and growth temperature regulation of two different microsomal [omega]-6 desaturase genes in soybeans. Plant Physiology 110, 311-319.

Hernandez-Buquer S and Blacklock BJ, 2013. Site-directed mutagenesis of a fatty acid elongase ELO-like condensing enzyme. FEBS Letters 587, 3837-3842.

Heuzé V, Tran G, Sauvant D and Lessire M, 2016, online. Rapeseeds. Feedipedia, a programme by INRA, CIRAD, AFZ and FAO. Accessed on October 13, 2016. available at http://www.feedipedia.org/node/15617

Hirokawa T, Boon-Chieng S and Mitaku S, 1998. SOSUI: Classification and secondary structure prediction system for membrane proteins. Bioinformatics 14, 378-379.

Hu B, Liu B, Liu L, Liu C, Xu L and Ruan Y, 2014. Epigenetic control of Pollen Ole e 1 allergen and extensin family gene expression in *Arabidopsis thaliana*. Acta Physiologiae Plantarum 36, 2203-2209.

Hu MH and Ao Y, 2007. Characteristics of some nutritional composition of melon (*Cucumis melo* hybrid 'ChunLi') seeds. International Journal of Food Science and Technology 42, 1397-1401.

Huang Y-Y, Liu G-M, Cai Q-F, Weng W-Y, Maleki SJ, Su W-J and Cao M-J, 2010. Stability of major allergen tropomyosin and other food proteins of mud crab (*Scylla serrata*) by *in vitro* gastrointestinal digestion. Food and Chemical Toxicology 48, 1196-1201.

Huang YS, Chaudhary S, Thurmond JM, Bobik EG, Jr., Yuan L, Chan GM, Kirchner SJ, Mukerji P and Knutzon DS, 1999. Cloning of delta 12- and delta 6-desaturases from *Mortierella alpina* and recombinant production of gamma-linolenic acid in *Saccharomyces cerevisiae*. Lipids 34, 649-659.

ILSI, 2016, online. International Life Sciences Institute Crop Composition Database, Version 6. Accessed on May 16, 2017. available at https://www.cropcomposition.org/query/index.html

ITIS, 2016, online. *Brassica napus* L. Accessed on September 30, 2016. available at http://www.itis.gov/servlet/SingleRpt/SingleRpt?search_topic=TSN&search_value=23060

Izquierdo M, Montero D, Robaina L, Caballero M, Rosenlund G and Ginés R, 2005. Alterations in fillet fatty acid profile and flesh quality in gilthead seabream (*Sparus aurata*) fed vegetable oils for a long term period. Recovery of fatty acid profiles by fish oil feeding. Aquaculture 250, 431-444.

Jakobsson A, Westerberg R and Jacobsson A, 2006. Fatty acid elongases in mammals: Their regulation and roles in metabolism. Progress in Lipid Research 45, 237-249.

Jeong B-Y, Choi B-D, Moon S-K and Lee J-S, 1998. Fatty acid composition of 72 species of Korean fish. Fisheries and Aquatic Sciences 1, 129-146.

Jiang L, Eriksson J, Lage S, Jonasson S, Shams S, Mehine M, Ilag LL and Rasmussen U, 2014. Diatoms: A novel source for the neurotoxin BMAA in aquatic environments. PloS One 9, e84578.

Jiménez-López JC, Rodríguez-García MI and de Dios Alche J, 2011. Systematic and phylogenetic analysis of the Ole e 1 pollen protein family members in plants. In: Systems and Computational Biology - Bioinformatics and Computational Modeling. Ed Yang N-S, InTech, 245-260.

Jo K-R, Kim C-J, Kim S-J, Kim T-Y, Bergervoet M, Jongsma MA, Visser RG, Jacobsen E and Vossen JH, 2014. Development of late blight resistant potatoes by cisgene stacking. BMC Biotechnology 14, 50.

Jonsson P, Berntsson K, André C and Wängberg S-Å, 1999. Larval growth and settlement of the European oyster (*Ostrea edulis*) as a function of food quality measured as fatty acid composition. Marine Biology 134, 559-570.

Jung S, Swift D, Sengoku E, Patel M, Teule F, Powell G, Moore K and Abbott A, 2000. The high oleate trait in the cultivated peanut [*Arachis hypogaea* L.]. I. Isolation and characterization of two genes encoding microsomal oleoyl-PC desaturases. Molecular and General Genetics 263, 796-805.

Kajikawa M, Yamato KT, Sakai Y, Fukuzawa H, Ohyama K and Kohchi T, 2006. Isolation and functional characterization of fatty acid Δ5-elongase gene from the liverwort *Marchantia polymorpha* L. FEBS Letters 580, 149-154.

Kalogeropoulos N, Alexis MN and Henderson RJ, 1992. Effects of dietary soybean and cod-liver oil levels on growth and body composition of gilthead bream (*Sparus aurata*). Aquaculture 104, 293-308.

Kamoun S, 2002. Basic biology: What makes *Phytophthora infestans* a pathogen? Proceedings of the Global Initiative on Late Blight, Hamburg, Germany, 11-13.

Kashenko S, 2007. Adaptive responses of embryos and larvae of the heart-shaped sea urchin *Echinocardium cordatum* to temperature and salinity changes. Russian Journal of Marine Biology 33, 381-390.

Kawalleck P, Somssich IE, Feldbrügge M, Hahlbrock K and Weisshaar B, 1993. Polyubiquitin gene expression and structural properties of the *ubi4-2* gene in *Petroselinum crispum*. Plant Molecular Biology 21, 673-684.

Kawashima H, Toyoda-Ono Y, Suwa Y and Kiso Y, 2009. Subchronic (13-week) oral toxicity study of dihomo-γ-linolenic acid (DGLA) oil in rats. Food and Chemical Toxicology 47, 1280-1286.

Keller MD, Bellows WK and Guillard RRL, 1989. Dimethyl sulfide production in marine phytoplankton. In: Biogenic Sulfur in the Environment. Eds Saltzman ES and Cooper WJ, American Chemical Society, Washington, DC, 167-182.

Khadake R, Khonde V, Mhaske V, Ranjekar P and Harsulkar A, 2011. Functional and bioinformatic characterisation of sequence variants of Fad3 gene from flax. Journal of the Science of Food and Agriculture 91, 2689-2696.

Kilara A, Sharkasi TY and Morr CV, 1986. Effects of temperature on food proteins and its implications on functional properties. Critical Reviews in Food Science & Nutrition 23, 323-395.

Kitessa SM, Abeywardena M, Wijesundera C and Nichols PD, 2014. DHA-containing oilseed: A timely solution for the sustainability issues surrounding fish oil sources of the health-benefitting long-chain omega-3 oils. Nutrients 6, 2035-2058.

Kliebenstein DJ, Kroymann J, Brown P, Figuth A, Pedersen D, Gershenzon J and Mitchell-Olds T, 2001. Genetic control of natural variation in Arabidopsis glucosinolate accumulation. Plant Physiology 126, 811-825.

Knauer J, Barrett S, Volkman J and Southgate PC, 1999. Assimilation of dietary phytosterols by Pacific oyster *Crassostrea gigas* spat. Aquaculture Nutrition 5, 257-266.

Kobayashi T, Sakaguchi K, Matsuda T, Abe E, Hama Y, Hayashi M, Honda D, Okita Y, Sugimoto S and Okino N, 2011. Increase of EPA in Thraustochytrids through expression of a fatty acid Δ5 desaturase gene driven by the Thraustochytrid ubiquitin promoter. Applied and Environmental Microbiology 77, 3870-3876.

Kolkman JM, Slabaugh MB, Bruniard JM, Berry S, Bushman BS, Olungu C, Maes N, Abratti G, Zambelli A, Miller JF, Leon A and Knapp SJ, 2004. Acetohydroxyacid synthase mutations conferring resistance to imidazolinone or sulfonylurea herbicides in sunflower. Theoretical and Applied Genetics 109, 1147-1159.

Koornneef M and Meinke D, 2010. The development of Arabidopsis as a model plant. Plant Journal 61, 909-921.

Kovalic D, Garnaat C, Guo L, Yan Y, Groat J, Silvanovich A, Ralston L, Huang M, Tian Q and Christian A, 2012. The use of next generation sequencing and junction sequence analysis bioinformatics to achieve molecular characterization of crops improved through modern biotechnology. Plant Genome 5, 149-163.

Krasowska A, Dziadkowiec D, Polinceusz A, Plonka A and Łukaszewicz M, 2007. Cloning of flax oleic fatty acid desaturase and its expression in yeast. Journal of the American Oil Chemists' Society 84, 809-816.

Kris-Etherton PM, Grieger JA and Etherton TD, 2009. Dietary reference intakes for DHA and EPA. Prostaglandins, Leukotrienes and Essential Fatty Acids 81, 99-104.

Krogh A, Larsson B, von Heijne G and Sonnhammer EL, 2001. Predicting transmembrane protein topology with a hidden Markov model: Application to complete genomes. Journal of Molecular Biology 305, 567-580.

Lage S, Annadotter H, Rasmussen U and Rydberg S, 2015. Biotransfer of β-N-methylamino-L-alanine (BMAA) in a eutrophicated freshwater lake. Marine Drugs 13, 1185-1201.

Laing I, 2000. Effect of temperature and ration on growth and condition of king scallop (*Pecten maximus*) spat. Aquaculture 183, 325-334.

Lee KR, Sohn SI, Jung JH, Kim SH, Roh KH, Kim JB, Suh MC and Kim HU, 2013. Functional analysis and tissue-differential expression of four *FAD2* genes in amphidiploid *Brassica napus* derived from *Brassica rapa* and *Brassica oleracea*. Gene 531, 253-262.

Lee S-K, Yoon S-H, Kim S-H, Choi J-H and Park H-S, 2005a. Chestnut as a food allergen: Identification of major allergens. Journal of Korean Medical Science 20, 573-578.

Lee Y-N, Chen L-K, Ma H-C, Yang H-H, Li H-P and Lo S-Y, 2005b. Thermal aggregation of SARS-CoV membrane protein. Journal of Virological Methods 129, 152-161.

León L, Uceda M, Jiménez A, Martín L and Rallo L, 2004. Variability of fatty acid composition in olive (*Olea europaea* L.) progenies. Spanish Journal of Agricultural Research 2, 353-359.

Leonard AE, Pereira SL, Sprecher H and Huang Y-S, 2004. Elongation of long-chain fatty acids. Progress in Lipid Research 43, 36-54.

Li D, Moorman R, Vanhercke T, Petrie J, Singh S and Jackson CJ, 2016. Classification and substrate head-group specificity of membrane fatty acid desaturases. Computational and Structural Biotechnology Journal 14, 341-349.

Li G, Sinclair AJ and Li D, 2011. Comparison of lipid content and fatty acid composition in the edible meat of wild and cultured freshwater and marine fish and shrimps from China. Journal of Agricultural and Food Chemistry 59, 1871-1881.

Li P-L and Farrand SK, 2000. The replicator of the nopaline-type Ti plasmid pTiC58 is a member of the *repABC* family and is influenced by the TraR-dependent quorum-sensing regulatory system. Journal of Bacteriology 182, 179-188.

Li S-C, Wang W-X and Hsieh DP, 2002. Effects of toxic dinoflagellate *Alexandrium tamarense* on the energy budgets and growth of two marine bivalves. Marine Environmental Research 53, 145-160.

Lim ZL, Senger T and Vrinten P, 2014. Four amino acid residues influence the substrate chain-length and regioselectivity of *Siganus canaliculatus* Δ4 and Δ5/6 desaturases. Lipids 49, 357-367.

Lina B, Wolterbeek A, Suwa Y, Fujikawa S, Ishikura Y, Tsuda S and Dohnalek M, 2006. Subchronic (13-week) oral toxicity study, preceded by an in utero exposure phase, with arachidonate-enriched triglyceride oil (SUNTGA40S) in rats. Food and Chemical Toxicology 44, 326-335.

Liska DJ, Cook CM, Wang DD, Gaine PC and Baer DJ, 2016. Trans fatty acids and cholesterol levels: An evidence map of the available science. Food and Chemical Toxicology 98, 269-281.

Liu Q, Singh SP, Brubaker CL, Sharp PJ, Green AG and Marshall D, 1999. Molecular cloning and expression of a cDNA encoding a microsomal w-6 fatty acid desaturase from cotton (*Gossypium hirsutum*). Australian Journal of Plant Physiology 26, 101-106.

Liu W, Pearce C, Alabi A and Gurney-Smith H, 2009. Effects of microalgal diets on the growth and survival of larvae and post-larvae of the basket cockle, *Clinocardium nuttallii*. Aquaculture 293, 248-254.

Liu W, Pearce C, McKinley R and Forster I, 2016. Nutritional value of selected species of microalgae for larvae and early post-set juveniles of the Pacific geoduck clam, *Panopea generosa*. Aquaculture 452, 326-341.

Lohner K and Esser AF, 1991. Thermal unfolding and aggregation of human complement protein C9: A differential scanning calorimetry study. Biochemistry 30, 6620-6625.

López Alonso D, García-Maroto F, Rodríguez-Ruiz J, Garrido JA and Vilches MA, 2003. Evolution of the membrane-bound fatty acid desaturases. Biochemical Systematics and Ecology 31, 1111-1124.

López Y, Nadaf H, Smith O, Connell J, Reddy A and Fritz A, 2000. Isolation and characterization of the Δ12-fatty acid desaturase in peanut (*Arachis hypogaea* L.) and search for polymorphisms for the high oleate trait in Spanish market-type lines. Theoretical and Applied Genetics 101, 1131-1138.

MacDonald MH, Mogen BD and Hunt AG, 1991. Characterization of the polyadenylation signal from the T-DNA-encoded octopine synthase gene. Nucleic Acids Research 19, 5575-5581.

Madduri KM, Schafer BW, Hasler JM, Lin G, Foster ML, Embrey SK, Sastry-Dent L, Song P, Larrinua IM, Gachotte DJ and Herman RA, 2012. Preliminary safety assessment of a membrane-bound delta 9 desaturase candidate protein for transgenic oilseed crops. Food and Chemical Toxicology 50, 3776-3784.

Mankin SL, Hill DS, Olhoft PM, Toren E, Wenck AR, Nea L, Xing L, Brown JA, Fu H and Ireland L, 2007. Disarming and sequencing of *Agrobacterium rhizogenes* strain K599 (NCPPB2659) plasmid pRi2659. In Vitro Cellular and Developmental Biology - Plant 43, 521-535.

Marx CJ and Lidstrom ME, 2001. Development of improved versatile broad-host-range vectors for use in methylotrophs and other gram-negative bacteria. Microbiology 147, 2065-2075.

Masson L and Ray DS, 1986. Mechanism of autonomous control of the *Escherichia coli* F plasmid: Different complexes of the initiator/repressor protein are bound to its operator and to an F plasmid replication origin. Nucleic Acids Research 14, 5693-5711.

Mathesius C, Barnett J, Cressman R, Ding J, Carpenter C, Ladics G, Schmidt J, Layton R, Zhang J and Appenzeller L, 2009. Safety assessment of a modified acetolactate synthase protein (GM-HRA) used as a selectable marker in genetically modified soybeans. Regulatory Toxicology and Pharmacology 55, 309-320.

Mazur BJ, Chui C-F and Smith JK, 1987. Isolation and characterization of plant genes coding for acetolactate synthase, the target enzyme for two classes of herbicides. Plant Physiology 85, 1110-1117.

Meade SJ, Reid EA and Gerrard JA, 2005. The impact of processing on the nutritional quality of food proteins. Journal of AOAC International 88, 904-922.

Meesapyodsuk D and Qiu X, 2012. The front-end desaturase: Structure, function, evolution and biotechnological use. Lipids 47, 227-237.

Metcalfe DD, Astwood JD, Townsend R, Sampson HA, Taylor SL and Fuchs RL, 1996. Assessment of the allergenic potential of foods derived from genetically engineered crop plants. Critical Reviews in Food Science & Nutrition 36, 165-186.

Meyer A, Kirsch H, Domergue F, Abbadi A, Sperling P, Bauer J, Cirpus P, Zank TK, Moreau H, Roscoe TJ, Zahringer U and Heinz E, 2004. Novel fatty acid elongases and their use for the reconstitution of docosahexaenoic acid biosynthesis. Journal of Lipid Research 45, 1899-1909.

Meyer BJ, 2016. Australians are not meeting the recommended intakes for omega-3 long chain polyunsaturated fatty acids: Results of an analysis from the 2011-2012 National Nutrition and Physical Activity Survey. Nutrients 8, 111.

Monroig Ó, Guinot D, Hontoria F, Tocher DR and Navarro JC, 2012a. Biosynthesis of essential fatty acids in *Octopus vulgaris* (Cuvier, 1797): Molecular cloning, functional characterisation and tissue distribution of a fatty acyl elongase. Aquaculture 360–361, 45-53.

Monroig Ó, Navarro JC, Dick JR, Alemany F and Tocher DR, 2012b. Identification of a Δ5-like fatty acyl desaturase from the cephalopod *Octopus vulgaris* (Cuvier 1797) involved in the biosynthesis of essential fatty acids. Marine Biotechnology 14, 411-422.

Monroig Ó, Zheng X, Morais S, Leaver MJ, Taggart JB and Tocher DR, 2010. Multiple genes for functional ∆6 fatty acyl desaturases (Fad) in Atlantic salmon (*Salmo salar* L.): Gene and cDNA characterization, functional expression, tissue distribution and nutritional regulation. Biochimica et Biophysica Acta - Molecular and Cell Biology of Lipids 1801, 1072-1081.

Moreno FJ, Mellon FA, Wickham MS, Bottrill AR and Mills E, 2005. Stability of the major allergen Brazil nut 2S albumin (Ber e 1) to physiologically relevant *in vitro* gastrointestinal digestion. FEBS Journal 272, 341-352.

Moreno T, Varela A, Portela C, Pérez N, Carballo J and Montserrat L, 2007. The effect of grazing on the fatty acid profile of *longissimus thoracis* muscle in Galician Blond calves. Animal 1, 1227-1235.

Morgan W and Kamoun S, 2007. RXLR effectors of plant pathogenic oomycetes. Current Opinion in Microbiology 10, 332-338.

Mori H, Kondo A, Ohshima A, Ogura T and Hiraga S, 1986. Structure and function of the F plasmid genes essential for partitioning. Journal of Molecular Biology 192, 1-15.

Mouratidou T, Livaniou A, Saborido C, Wollgast J and Caldeira S, 2014. Trans fatty acids in Europe: Where do we stand? A synthesis of the evidence: 2003-2013. JRC Science and Policy Reports. European Commission, Joint Research Centre.

Mukhopadhyay T and Ghosh S, 2003. Lipid profile and fatty acid composition in eggs of common carp (*Cyprinus carpio*). Journal of OLEO Science 52, 439-442.

Murotsu T, Tsutsui H and Matsubara K, 1984. Identification of the minimal essential region for the replication origin of miniF plasmid. Molecular and General Genetics 196, 373-378.

Nakabayashi K, Okamoto M, Koshiba T, Kamiya Y and Nambara E, 2005. Genome-wide profiling of stored mRNA in *Arabidopsis thaliana* seed germination: Epigenetic and genetic regulation of transcription in seed. Plant Journal 41, 697-709.

Naumovski L and Friedberg EC, 1983. Construction of plasmid vectors that facilitate subcloning and recovery of yeast and *Escherichia coli* DNA fragments. Gene 22, 203-209.

NCBI, 2017a, online. *Arabidopsis thaliana*. Accessed on January 18, 2017. available at https://www.ncbi.nlm.nih.gov/Taxonomy/Browser/wwwtax.cgi?mode=Info&id=3702&lvl=3&p=has_linkout&p=blast_url&p=genome_blast&p=mapview&lin=f&keep=1&srchmode=1&unlock

NCBI, 2017b, online. *Ostreococcus tauri*. Accessed on January 18, 2017. available at https://www.ncbi.nlm.nih.gov/Taxonomy/Browser/wwwtax.cgi?id=70448

NCBI, 2017c, online. *Pavlova lutheri*. Accessed on January 18, 2017. available at https://www.ncbi.nlm.nih.gov/Taxonomy/Browser/wwwtax.cgi

NCBI, 2017d, online. *Physcomitrella patens*. Accessed on January 18, 2017. available at https://www.ncbi.nlm.nih.gov/Taxonomy/Browser/wwwtax.cgi

NCBI, 2017e, online. *Phytophthora infestans*. Accessed on January 18, 2017. available at https://www.ncbi.nlm.nih.gov/Taxonomy/Browser/wwwtax.cgi?mode=Info&id=4787&lvl=3&lin=f&keep=1&srchmode=1&unlock

NCBI, 2017f, online. *Phytophtora sojae*. Accessed on January 18, 2017. available at https://www.ncbi.nlm.nih.gov/Taxonomy/Browser/wwwtax.cgi?mode=Info&id=67593&lvl=3&p=has_linkout&p=blast_url&p=genome_blast&p=mapview&lin=f&keep=1&srchmode=1&unlock

NCBI, 2017g, online. *Pythium irregulare*. Accessed on January 18, 2017. available at https://www.ncbi.nlm.nih.gov/Taxonomy/Browser/wwwtax.cgi?mode=Info&id=36331&lvl=3&p=has_linkout&p=blast_url&p=genome_blast&p=mapview&lin=f&keep=1&srchmode=1&unlock

NCBI, 2017h, online. *Thalassiosira pseudonana*. Accessed on January 18, 2017. available at https://www.ncbi.nlm.nih.gov/Taxonomy/Browser/wwwtax.cgi?mode=Info&id=35128&lvl=3&p=has_linkout&p=blast_url&p=genome_blast&p=mapview&lin=f&keep=1&srchmode=1&unlock

NCBI, 2017i, online. *Thraustochytrium*. Accessed on January 18, 2017. available at https://www.ncbi.nlm.nih.gov/Taxonomy/Browser/wwwtax.cgi?mode=Info&id=145168&lvl=3&p=has_linkout&p=blast_url&p=genome_blast&p=mapview&lin=f&keep=1&srchmode=1&unlock

NCBI Resource Coordinators, 2016. Database resources of the National Center for Biotechnology Information. Nucleic Acids Research 44(Database issue), D7-D19.

Nudda A, Battacone G, Boe R, Grazia Manca M, Pier Giacomo Rassu S and Pulina G, 2013. Influence of outdoor and indoor rearing system of suckling lambs on fatty acid profile and lipid oxidation of raw and cooked meat. Italian Journal of Animal Science 12, e74.

Numaguchi K, 2000. Evaluation of five microalgal species for the growth of early spat of the Japanese pearl oyster *Pinctada fucata martensii*. Journal of Shellfish Research 19, 153-157.

Nury S and Meunier J-C, 1990. Molecular mechanisms of the irreversible thermal denaturation of guinea-pig liver transglutaminase. Biochemical Journal 266, 487-490.

OECD, 1997. Consensus document on the biology of *Brassica napus* L. (oilseed rape). Series on Harmonization of Regulatory Oversight in Biotechnology No. 7.

OECD, 2002a, online. Consensus document on compositional considerations for new varieties of maize (*Zea mays*): Key food and feed nutrients, anti-nutrients and secondary plant metabolites. Accessed on October 4, 2017. available at http://www.oecd.org/env/ehs/biotrack/46815196.pdf

OECD, 2002b, online. Consensus document on compositional considerations for new varieties of sugar beet: Key food and feed nutrients and antinutrients. Accessed on October 4, 2017. available at https://www.oecd.org/science/biotrack/46815157.pdf

OECD, 2011a, online. Consensus document on compositional considerations for new varieties of sugarcane (*Saccharum* ssp. hybrids): Key food and feed nutrients, anti-nutrients and toxicants. Accessed on October 4, 2017. available at http://www.oecd.org/env/ehs/biotrack/48962816.pdf

OECD, 2011b, online. Revised consensus document on compositional considerations for new varieties of low erucic acid rapeseed (canola): Key food and feed nutrients, anti-nutrients and toxicants. Accessed on October 4, 2017. available at https://www.oecd.org/env/ehs/biotrack/49343153.pdf

OECD, 2012, online. Revised consensus document on compositional considerations for new varieties of soybean [*Glycine max* (L.) Merr.]: Key food and feed nutrients, anti-nutrients, toxicants and allergens. Accessed on October 4, 2017. available at http://www.oecd.org/officialdocuments/publicdisplaydocumentpdf/?cote=env/jm/mono(2012)24&doclanguage=en

OECD, 2016, online. Revised consensus document on compositional considerations for new varieties of rice (*Oryza sativa*): Key food and feed nutrients and anti-nutrients. Accessed on October 4, 2017. available at http://www.oecd.org/officialdocuments/publicdisplaydocumentpdf/?cote=env/jm/mono(2016)38&doclanguage=en

OGTR, 2016, online. The Biology of *Brassica napus* L. (canola) and *Brassica juncea* (L) Czern. & Coss (Indian mustard). Accessed on September 27, 2016. available at http://www.ogtr.gov.au/internet/ogtr/publishing.nsf/content/canola-3/$FILE/biologycanola08_2.pdf

Oka A, Sugisaki H and Takanami M, 1981. Nucleotide sequence of the kanamycin resistance transposon Tn*903*. Journal of Molecular Biology 147, 217-226.

Okunuki H, Teshima R, Shigeta T, Sakushima J-i, Akiyama H, Goda Y, Toyoda M and Sawada J, 2002. Increased digestibility of two products in genetically modified food (CP4-EPSPS and Cry1 Ab) after preheating. Journal of the Food Hygenic Society of Japan 43, 68-73.

Parker-Barnes JM, Das T, Bobik E, Leonard AE, Thurmond JM, Chaung L-T, Huang Y-S and Mukerji P, 2000. Identification and characterization of an enzyme involved in the elongation of n-6 and n-3 polyunsaturated fatty acids. Proceedings of the National Academy of Sciences of the United States of America 97, 8284-8289.

Parveen T and Sharma K, 2014. *Pythium* diseases, control and management strategies: A review. International Journal of Plant, Animal and Environmental Sciences 5, 244-257.

Passi S, Cataudella S, Di Marco P, De Simone F and Rastrelli L, 2002. Fatty acid composition and antioxidant levels in muscle tissue of different Mediterranean marine species of fish and shellfish. Journal of Agricultural and Food Chemistry 50, 7314-7322.

Pereira SL, Leonard A E, Huang Y-S, Chuang L-T and Mukerji P, 2004. Identification of two novel microalgal enzymes involved in the conversion of the ω3-fatty acid, eicosapentaenoic acid, into docosahexaenoic acid. Biochemical Journal 384, 357-366.

Peters C, Tsirigos KD, Shu N and Elofsson A, 2016. Improved topology prediction using the terminal hydrophobic helices rule. Bioinformatics 32, 1158-1162.

Petrie JR, Liu Q, Mackenzie AM, Shrestha P, Mansour MP, Robert SS, Frampton DF, Blackburn SI, Nichols PD and Singh SP, 2010. Isolation and characterisation of a high-efficiency desaturase and elongases from microalgae for transgenic LC-PUFA production. Marine Biotechnology 12, 430-438.

Pinto UM, Pappas KM and Winans SC, 2012. The ABCs of plasmid replication and segregation. Nature Reviews Microbiology 10, 755-765.

Pirtle IL, Kongcharoensuntorn W, Nampaisansuk M, Knesek JE, Chapman KD and Pirtle RM, 2001. Molecular cloning and functional expression of the gene for a cotton Δ-12 fatty acid desaturase (*FAD2*). Biochimica et Biophysica Acta - Gene Structure and Expression 1522, 122-129.

Poikonen S, Puumalainen T, Kautiainen H, Burri P, Palosuo T, Reunala T and Turjanmaa K, 2006. Turnip rape and oilseed rape are new potential food allergens in children with atopic dermatitis. Allergy 61, 124-127.

Ponis E, Parisi G, Zittelli GC, Lavista F, Robert R and Tredici M, 2008. *Pavlova lutheri*: Production, preservation and use as food for *Crassostrea gigas* larvae. Aquaculture 282, 97-103.

Ponis E, Probert I, Veron B, Le Coz J-R, Mathieu M and Robert R, 2006. Nutritional value of six Pavlovophyceae for *Crassostrea gigas* and *Pecten maximus* larvae. Aquaculture 254, 544-553.

Ponis E, Robert R and Parisi G, 2003a. Nutritional value of fresh and concentrated algal diets for larval and juvenile Pacific oysters (*Crassostrea gigas*). Aquaculture 221, 491-505.

Ponis E, Robert R, Parisi G and Tredici M, 2003b. Assessment of the performance of Pacific oyster (*Crassostrea* gigas) larvae fed with fresh and preserved *Pavlova lutheri* concentrates. Aquaculture International 11, 69-79.

Qiu X, Hong H and MacKenzie SL, 2001. Identification of a Δ4 fatty acid desaturase from *Thraustochytrium* sp. involved in the biosynthesis of docosahexanoic acid by heterologous expression in *Saccharomyces cerevisiae* and *Brassica juncea*. Journal of Biological Chemistry 276, 31561-31566.

Raghukumar S, 2002. Ecology of the marine protists, the Labyrinthulomycetes (Thraustochytrids and Labyrinthulids). European Journal of Protistology 38, 127-145.

Rask L, Ellerström M, Ezcurra I, Stålberg K and Wycliffe P, 1998. Seed-specific regulation of the napin promoter in *Brassica napus*. Journal of Plant Physiology 152, 595-599.

Reina RJ, White KD and Firestone D, 1999. Sterol and triterpene diol contents of vegetable oils by high-resolution capillary gas chromatography. Journal of AOAC International 82, 929-936.

Rengel A, Pérez E, Piombo G, Ricci J, Servent A, Tapia MS, Gibert O and Montet D, 2015. Lipid profile and antioxidant activity of macadamia nuts (*Macadamia integrifolia*) cultivated in Venezuela. Natural Science 7, 535-547.

Reski R, Parsons J and Decker EL, 2015. Moss-made pharmaceuticals: From bench to bedside. Plant Biotechnology Journal 13, 1191-1198.

Robert SS, Petrie JR, Zhou X-R, Mansour MP, Blackburn SI, Green AG, Singh SP and Nichols PD, 2009. Isolation and characterisation of a Δ5-fatty acid elongase from the marine microalga *Pavlova salina*. Marine Biotechnology 11, 410-418.

Rodewald J and Trognitz B, 2013. Solanum resistance genes against *Phytophthora infestans* and their corresponding avirulence genes. Molecular Plant Pathology 14, 740-757.

Roman EA and González Flecha FL, 2014. Kinetics and thermodynamics of membrane protein folding. Biomolecules 4, 354-373.

Ronquillo JD, Fraser J and McConkey A-J, 2012. Effect of mixed microalgal diets on growth and polyunsaturated fatty acid profile of European oyster (*Ostrea edulis*) juveniles. Aquaculture 360, 64-68.

Rosales-Mendoza S, Orellana-Escobedo L, Romero-Maldonado A, Decker EL and Reski R, 2014. The potential of *Physcomitrella patens* as a platform for the production of plant-based vaccines. Expert Review of Vaccines 13, 203-212.

Rossak M, Smith M and Kunst L, 2001. Expression of the *FAE1* gene and *FAE1* promoter activity in developing seeds of *Arabidopsis thaliana*. Plant Molecular Biology 46, 717-725.

Rousseaux CS and Gregg WW, 2013. Interannual variation in phytoplankton primary production at a global scale. Remote Sensing 6, 1-19.

Salem N and Eggersdorfer M, 2015. Is the world supply of omega-3 fatty acids adequate for optimal human nutrition? Current Opinion in Clinical Nutrition & Metabolic Care 18, 147-154.

Sandhu D, Schallock KG, Rivera-Velez N, Lundeen P, Cianzio S and Bhattacharyya MK, 2005. Soybean *Phytophthora* resistance gene *Rps8* maps closely to the *Rps3* region. Journal of Heredity 96, 536-541.

Sayanova O, Beaudoin F, Libisch B, Castel A, Shewry PR and Napier JA, 2001. Mutagenesis and heterologous expression in yeast of a plant delta6-fatty acid desaturase. Journal of Experimental Botany 52, 1581-1585.

SCOGS, 1977. Evaluation of the health aspects of coconut oil, peanut oil, and oleic acid as they may migrate to food from packaging materials, and linoleic acid as a food ingredient.

Semma M, 2002. Trans fatty acids: Properties, benefits and risks. Journal of Health Science 48, 7-13.

Semura H, 1995. The effect of algal species and concentration on the rates of filtering, digestion, and assimilation of the adult Japanese bay scallop *Pecten albicans*. Bulletin of the Japanese Society of Scientific Fisheries (Japan) 61, 673-678.

Senger T, Marty L, Kunze I, Haertel HA, Bremmer S, Breazeale S, Bauer J, Vrinten P, Stymne S and Lindberg YJ, 2016. Materials and methods for PUFA production, and PUFA-containing compositions. Patent WO2016075326 A2, World Intellectual Property Organization.

Shanklin J, Whittle E and Fox BG, 1994. Eight histidine residues are catalytically essential in a membrane-associated iron enzyme, stearoyl-CoA desaturase, and are conserved in alkane hydroxylase and xylene monooxygenase. Biochemistry 33, 12787-12794.

Sharma N, Cram D, Huebert T, Zhou N and Parkin IAP, 2007. Exploiting the wild crucifer *Thlaspi arvense* to identify conserved and novel genes expressed during a plant's response to cold stress. Plant Molecular Biology 63, 171-184.

Shaw B, Harrison P and Andersen R, 1994. Evaluation of the copepod *Tigriopus californicus* as a bioassay organism for the detection of chemical feeding deterrents produced by marine phytoplankton. Marine Biology 121, 89-95.

Shaw B, Harrison P and Andersen R, 1995. Feeding deterrence properties of apo-fucoxanthinoids from marine diatoms. II. Physiology of production of apo-fucoxanthinoids by the marine diatoms *Phaeodactylum tricornutum* and *Thalassiosira pseudonana*, and their feeding deterrent effects on the copepod *Tigriopus californicus*. Marine Biology 124, 473-481.

Shendure J and Ji H, 2008. Next-generation DNA sequencing. Nature Biotechnology 26, 1135-1145.

Shizuya H, Birren B, Kim U-J, Mancino V, Slepak T, Tachiiri Y and Simon M, 1992. Cloning and stable maintenance of 300-kilobase-pair fragments of human DNA in *Escherichia coli* using an F-factor-based vector. Proceedings of the National Academy of Sciences of the United States of America 89, 8794-8797.

Sijtsma L and de Swaaf ME, 2004. Biotechnological production and applications of the ω-3 polyunsaturated fatty acid docosahexaenoic acid. Applied Microbiology and Biotechnology 64, 146-153.

Silvanovich A, Bannon G and McClain S, 2009. The use of E-scores to determine the quality of protein alignments. Regulatory Toxicology and Pharmacology 54, S26-S31.

Silvanovich A, Nemeth MA, Song P, Herman R, Tagliani L and Bannon GA, 2005. The value of short amino acid sequence matches for prediction of protein allergenicity. Toxicological Sciences 90, 252-258.

Simopoulos AP, 2016. An increase in the omega-6/omega-3 fatty acid ratio increases the risk for obesity. Nutrients 8, 128.

Singh BK and Shaner DL, 1995. Biosynthesis of branched chain amino acids: From test tube to field. Plant Cell 7, 935-944.

Singh BK, Stidham MA and Shaner DL, 1988. Assay of acetohydroxyacid synthase. Analytical Biochemistry 171, 173-179.

Smigocki AC, 1991. Cytokinin content and tissue distribution in plants transformed by a reconstructed isopentenyl transferase gene. Plant Molecular Biology 16, 105-115.

Sparrow FK, 1936. Biological observations on the marine fungi of Woods Hole waters. Biological Bulletin 70.

Sperling P and Heinz E, 2001. Desaturases fused to their electron donor. European Journal of Lipid Science and Technology 103, 158-180.

Spolaore P, Joannis-Cassan C, Duran E and Isambert A, 2006. Commercial applications of microalgae. Journal of Bioscience and Bioengineering 101, 87-96.

Stachel SE and Zambryski PC, 1986. *Agrobacterium tumefaciens* and the susceptible plant cell: A novel adaptation of extracellular recognition and DNA conjugation. Cell 47, 155-157.

Steel RGD and Torrie JH, 1976. Introduction to Statistics. McGraw-Hill, New York, NY, 382 pp.

Su X, Antonas KN and Li D, 2004. Comparison of n-3 polyunsaturated fatty acid contents of wild and cultured Australian abalone. International Journal of Food Sciences and Nutrition 55, 149-154.

Tabata S, Hooykaas PJJ and Oka A, 1989. Sequence determination and characterization of the replicator region in the tumor-inducing plasmid pTiB6S3. Journal of Bacteriology 171, 1665-1672.

Tan S, Evans RR, Dahmer ML, Singh BK and Shaner DL, 2005. Imidazolinone-tolerant crops: History, current status and future. Pest Management Science 61, 246-257.

Tavares S, Grotkjær T, Obsen T, Haslam RP, Napier JA and Gunnarsson N, 2011. Metabolic engineering of *Saccharomyces cerevisiae* for production of eicosapentaenoic acid, using a novel Δ5-desaturase from *Paramecium tetraurelia*. Applied and Environmental Microbiology 77, 1854-1861.

Taylor SL, 2002. Protein allergenicity assessment of foods produced through agricultural biotechnology. Annual Review of Pharmacology and Toxicology 42, 99-112.

Thomas K, Aalbers M, Bannon G, Bartels M, Dearman R, Esdaile D, Fu T, Glatt C, Hadfield N and Hatzos C, 2004. A multi-laboratory evaluation of a common *in vitro* pepsin digestion assay protocol used in assessing the safety of novel proteins. Regulatory Toxicology and Pharmacology 39, 87-98.

Thompson JD, Higgins DG and Gibson TJ, 1994. CLUSTAL W: Improving the sensitivity of progressive multiple sequence alignment through sequence weighting, position-specific gap penalties and weight matrix choice. Nucleic Acids Research 22, 4673-4680.

Thompson PA, Guo M-x and Harrison PJ, 1996. Nutritional value of diets that vary in fatty acid composition for larval Pacific oysters (*Crassostrea gigas*). Aquaculture 143, 379-391.

Thompson PA and Harrison PJ, 1992. Effects of monospecific algal diets of varying biochemical composition on the growth and survival of Pacific oyster (*Crassostrea gigas*) larvae. Marine Biology 113, 645-654.

Thorn KS, Christensen HE, Shigeta R, Huddler D, Shalaby L, Lindberg U, Chua N-H and Schutt CE, 1997. The crystal structure of a major allergen from plants. Structure 5, 19-32.

Tocher DR, 2015. Omega-3 long-chain polyunsaturated fatty acids and aquaculture in perspective. Aquaculture 449, 94-107.

Tomaru Y, Ebisuzaki S, Kawabata Zi and Nakano Si, 2002. Respiration rates of the Japanese pearl oyster, *Pinctada fucata martensii*, feeding on *Pavlova lutheri* and *Chaetoceros gracilis*. Aquaculture 33, 33-36.

Tonon T, David H, Larson TR and Graham IA, 2003. Identification of a very long chain polyunsaturated fatty acid Δ4-desaturase from the microalga *Pavlova lutheri*. FEBS Letters 553, 440-444.

Trinidade A, Kumar S, Haji M, Shakeel M and Leong P, 2010. The prevalence of oilseed rape hypersensitivity in a mixed cereal farming population. Clinical Otolaryngology 35, 13-17.

Tripathi M and Mishra A, 2007. Glucosinolates in animal nutrition: A review. Animal Feed Science and Technology 132, 1-27.

Truksa M, MacKenzie SL and Qiu X, 2003. Molecular analysis of flax 2S storage protein conlinin and seed specific activity of its promoter. Plant Physiology and Biochemistry 41, 141-147.

Turchini G, Moretti V, Hermon K, Caprino F, Busetto M, Bellagamba F, Rankin T, Keast R and Francis D, 2013. Monola oil versus canola oil as a fish oil replacer in rainbow trout feeds: Effects on growth, fatty acid metabolism and final eating quality. Food Chemistry 141, 1335-1344.

U.S. EPA, 2017. Part 725—Reporting requirements and review processes for microorganisms. Section §725.421—Introduced genetic material. In: *U.S. Code of Federal Regulations (CFR). Title 40: Protection of Environment.* (U.S. Environmental Protection Agency). Washington (DC): U.S. Government Printing Office (GPO). available at http://www.gpo.gov/fdsys/browse/collectionCfr.action?collectionCode=CFR.

U.S. FDA, 1996. Part 582—Substances generally recognized as safe. Section §582.5065—Linoleic acid. In: *U.S. Code of Federal Regulations (CFR). Title 21: Food and Drugs. (U.S. Food and Drug Administration)*. Washington (DC): U.S. Government Printing Office (GPO). available at http://www.gpo.gov/fdsys/browse/collectionCfr.action?collectionCode=CFR.

U.S. FDA, 1999, online. GRN 16: GRAS notice for Menhaden oil. Accessed on November 15, 2017. available at https://www.fda.gov/downloads/Food/IngredientsPackagingLabeling/GRAS/NoticeInventory/ucm264566.pdf

U.S. FDA, 2000, online. GRN 41: GRAS notification for the use of DHASCO and ARASCO (single cell sources of DHA and ARA) as sources of the LCPUFAs in infant formulas. Accessed on May 15,

2017. available at https://www.fda.gov/downloads/Food/IngredientsPackagingLabeling/GRAS/NoticeInventory/ucm266169.pdf

U.S. FDA, 2001, online. GRN 80: GRAS notice for extending the level of use of ARASCO (single cell oil) as a source of arachidonic acid in infant formulas. Accessed on October 13, 2017. available at https://www.fda.gov/downloads/Food/.../GRAS/NoticeInventory/ucm266650.pdf

U.S. FDA, 2002, online. GRN 102: GRAS Notice for small planktivorous pelagic fish body oil. Accessed on November 20, 2017. available at https://www.fda.gov/downloads/Food/IngredientsPackagingLabeling/GRAS/NoticeInventory/ucm260966.pdf

U.S. FDA, 2004, online. GRN 146: GRAS Notice for salmon oil. Accessed on November 20, 2017. available at https://www.fda.gov/downloads/Food/IngredientsPackagingLabeling/GRAS/NoticeInventory/ucm263474.pdf

U.S. FDA, 2009, online. GRN 306: GRAS notice for low saturated high oleic low linolenic soybean oil (LSHOLLSO). Accessed on May 15, 2017. available at https://www.fda.gov/downloads/Food/IngredientsPackagingLabeling/GRAS/NoticeInventory/ucm269419.pdf

U.S. FDA, 2010, online. GRN 326: GRN notification for the use of refined arachidonic rich oil ("RAO") as an ingredient in infant formula. Accessed on May 15, 2017. available at https://www.fda.gov/downloads/Food/IngredientsPackagingLabeling/GRAS/NoticeInventory/ucm269507.pdf

U.S. FDA, 2012, online. Agency Response Letter GRAS Notice No. GRN 000425 Canola oil (low erucic acid rapeseed oil). Accessed on September 8, 2021. available at https://www.cfsanappsexternal.fda.gov/scripts/fdcc/index.cfm?set=GRASNotices&id=425

U.S. FDA, 2014, online. GRN 553: GRAS determination of DHA algal oil (DHASCOe-B) produced from a new production strain of *Schizochytrium* sp. for use as an ingredient in infant formula (pre-term and term). Accessed on May 15, 2017. available at https://www.fda.gov/downloads/Food/IngredientsPackagingLabeling/GRAS/NoticeInventory/ucm456952.pdf

U.S. FDA, 2015, online. Final determination regarding partially hydrogenated oils. Accessed on May 15, 2017. available at https://www.gpo.gov/fdsys/pkg/FR-2015-06-17/pdf/2015-14883.pdf

U.S. FDA, 2016, online. GRN 677: GRAS determination of DHA algal oil for use in infant formula. Accessed on May 15, 2017. available at https://www.fda.gov/downloads/Food/IngredientsPackagingLabeling/GRAS/NoticeInventory/ucm530169.pdf

U.S. FDA, 2017a. Part 184—Direct food substances affirmed as generally recognized as safe. Section §184.1472—Menhaden oil. In: *U.S. Code of Federal Regulations (CFR). Title 21: Food and Drugs. (U.S. Food and Drug Administration)*. Washington (DC): U.S. Government Printing Office (GPO). available at http://www.gpo.gov/fdsys/browse/collectionCfr.action?collectionCode=CFR.

U.S. FDA, 2017b. Part 184—Direct food substances affirmed as generally recognized as safe. Section §184.1555—Rapeseed oil. In: *U.S. Code of Federal Regulations (CFR). Title 21: Food and Drugs. (U.S. Food and Drug Administration)*. Washington (DC): U.S. Government Printing Office (GPO). available at http://www.gpo.gov/fdsys/browse/collectionCfr.action?collectionCode=CFR.

U.S. HHS, Public Health Service, Centers for Disease Control and Prevention and National Institutes of Health, 2009. Biosafety in microbiological and biomedical laboratories. 5th edition, U.S. Dept. of Health and Human Services, Washington (DC), 437 pp.

U.S. HHS and USDA, 2015, online. 2015-2020 dietary guidelines for Americans. 8th edition. Accessed on January 4, 2018. available at http://health.gov/dietaryguidelines/2015/guidelines/

Unger E, 2015. Processing. In: Canola: Chemistry, Production, Processing and Utilization. Eds Daun JK, Eskin NM and Hickling D, AOCS, Urbana, IL, 163-187.

USDA-ERS, 2017. Canola. Accessed on January 29, 2019.

USDA-FAS, 2016, online. Oilseeds, Table 12. Accessed on October 3, 2016. available at http://apps.fas.usda.gov/psdonline/

USDA, 2016, online. National Nutrient Database for Standard Reference Release 28. Full Report (All Nutrients): 04594, Fish oil, sardine. Accessed on April 4, 2018. available at https://ndb.nal.usda.gov/ndb/foods/show/730?n1=%7BQv%3D1%7D&fgcd=&man=&lfacet=&count=&max=&sort=&qlookup=&offset=&format=Full&new=&measureby=&Qv=1&ds=&qt=&qp=&qa=&qn=&q=&ing=

USDA and U.S. HHS, 2010. Dietary Guidelines for Americans, 7th edition. Washington (DC): U.S. Government Printing Office (GPO). available at https://health.gov/dietaryguidelines/dga2010/DietaryGuidelines2010.pdf.

Vassilopoulou E, Rigby N, Moreno FJ, Zuidmeer L, Akkerdaas J, Tassios I, Papadopoulos NG, Saxoni-Papageorgiou P, van Ree R and Mills C, 2006. Effect of *in vitro* gastric and duodenal digestion on the allergenicity of grape lipid transfer protein. Journal of Allergy and Clinical Immunology 118, 473-480.

Venkatachalam M and Sathe SK, 2006. Chemical composition of selected edible nut seeds. Journal of Agricultural and Food Chemistry 54, 4705-4714.

Vieths S, Reindl J, Müller U, Hoffmann A and Haustein D, 1999. Digestibility of peanut and hazelnut allergens investigated by a simple *in vitro* procedure. European Food Research and Technology 209, 379-388.

Vlahakis C and Hazebroek J, 2000. Phytosterol accumulation in canola, sunflower, and soybean oils: Effects of genetics, planting location, and temperature. Journal of the American Oil Chemists' Society 77, 49-53.

Waku K, 1992. Origins and fates of fatty acyl-CoA esters. Biochimica et Biophysica Acta - Lipids and Lipid Metabolism 1124, 101-111.

Wang H, Klein MG, Zou H, Lane W, Snell G, Levin I, Li K and Sang B-C, 2015. Crystal structure of human stearoyl-coenzyme A desaturase in complex with substrate. Nature Structural & Molecular Biology 22, 581-585.

Wang HS, Yu C, Tang XF, Zhu ZJ, Ma NN and Meng QW, 2014a. A tomato endoplasmic reticulum (ER)-type omega-3 fatty acid desaturase (LeFAD3) functions in early seedling tolerance to salinity stress. Plant Cell Reports 33, 131-142.

Wang Q, Jin G, Jin Y, Ma M, Wang N, Liu C and He L, 2014b. Discriminating eggs from different poultry species by fatty acids and volatiles profiling: Comparison of SPME-GC/MS, electronic nose, and principal component analysis method. European Journal of Lipid Science and Technology 116, 1044-1053.

Wang Y-D, Peng K-C, Wu J-L and Chen J-Y, 2014c. Transgenic expression of salmon delta-5 and delta-6 desaturase in zebrafish muscle inhibits the growth of *Vibrio alginolyticus* and affects fish immunomodulatory activity. Fish & Shellfish Immunology 39, 223-230.

Wang Y, Zhang W-Z, Song L-F, Zou J-J, Su Z and Wu W-H, 2008. Transcriptome analyses show changes in gene expression to accompany pollen germination and tube growth in Arabidopsis. Plant Physiology 148, 1201-1211.

Webster CM, Deline ML and Watts JL, 2013. Stress response pathways protect germ cells from omega-6 polyunsaturated fatty acid-mediated toxicity in *Caenorhabditis elegans*. Developmental Biology 373, 14-25.

WHO, 2003. Diet, nutrition and the prevention of chronic diseases. Joint WHO/FAO Expert Consultation. World Health Organization Technical Report Series 916.

WHO, 2004. Laboratory Biosafety Manual. 3rd edition, World Health Organization, Geneva, 178 pp.

Wolff RL, 1993. Heat-induced geometrical isomerization of α-linolenic acid: Effect of temperature and heating time on the appearance of individual isomers. Journal of the American Oil Chemists' Society 70, 425-430.

WoRMS, 2004. *Thraustochytrium* Sparrow, 1936. Accessed through: World Register of Marine Species at http://www.marinespecies.org/aphia.php?p=taxdetails&id=119095 on September 9, 2017.

WoRMS, 2015. *Thalassiosira pseudonana* Hasle & Heimdal, 1970. In: Kociolek JP, Balasubramanian K, Blanco S, Coste M, Ector L, Liu Y, Kulikovskiy M, Lundholm N, Ludwig, T , Potapova M, Rimet F, Sabbe K, Sala S, Sar E, Taylor J, Van de Vijver B, Wetzel CE, Williams DM, Witkowski A and Witkowski J, (2017) DiatomBase. Accessed through: World Register of Marine Species at http://www.marinespecies.org/aphia.php?p=taxdetails&id=148934 on September 22, 2017.

Wu G, Truksa M, Datla N, Vrinten P, Bauer J, Zank T, Cirpus P, Heinz E and Qiu X, 2005. Stepwise engineering to produce high yields of very long-chain polyunsaturated fatty acids in plants. Nature Biotechnology 23, 1013-1017.

Wu L, Roe CL and Wen Z, 2013. The safety assessment of *Pythium irregulare* as a producer of biomass and eicosapentaenoic acid for use in dietary supplements and food ingredients. Applied Microbiology and Biotechnology 97, 7579-7585.

Yagami T, Haishima Y, Nakamura A, Osuna H and Ikezawa Z, 2000. Digestibility of allergens extracted from natural rubber latex and vegetable foods. Journal of Allergy and Clinical Immunology 106, 752-762.

Yan Y-B, Wang Q, He H-W and Zhou H-M, 2004. Protein thermal aggregation involves distinct regions: sequential events in the heat-induced unfolding and aggregation of hemoglobin. Biophysical Journal 86, 1682-1690.

Yates B, De Soyza A, Harkawat R and Stenton C, 2008. Occupational asthma caused by *Arabidopsis thaliana*: A case of laboratory plant allergy. European Respiratory Journal 32, 1111-1112.

Yi T, Li S-M, Fan J-Y, Fan L-L, Zhang Z-F, Luo P, Zhang X-J, Wang J-G, Zhu L, Zhao Z-Z and Chen H-B, 2014. Comparative analysis of EPA and DHA in fish oil nutritional capsules by GC-MS. Lipids in Health and Disease 13, 190.

Yilmaz JL, Lim ZL, Beganovic M, Breazeale S, Andre C, Stymne S, Vrinten P and Senger T, 2017. Determination of substrate preferences for desaturases and elongases for production of docosahexaenoic acid from oleic acid in engineered canola. Lipids 52, 207-222.

Ytrestøyl T, Aas TS and Åsgård TE, 2014, online. Resource utilisation of Norwegian salmon farming in 2012 and 2013. Nofima. Accessed on January 27, 2017. available at https://nofima.no/wp-content/uploads/2014/11/Nofima_report_resource_utilisation_Oct_2014.pdf

Zank T, Bauer J, Cirpus P, Abbadi A, Heinz E, Qiu X, Vrinten P, Sperling P, Domergue F and Meyer A, 2005. Method for the production of multiply-unsaturated fatty acids in transgenic organisms. Patent WO2005012316 A2, World Intellectual Property Organization.

Zank TK, Zähringer U, Beckmann C, Pohnert G, Boland W, Holtorf H, Reski R, Lerchl J and Heinz E, 2002. Cloning and functional characterisation of an enzyme involved in the elongation of Δ^6-polyunsaturated fatty acids from the moss *Physcomitrella patens*. Plant Journal 31, 255-268.

Zank TK, Zähringer U, Lerchl J and Heinz E, 2000. Cloning and functional expression of the first plant fatty acid elongase specific for Δ6-polyunsaturated fatty acids. Biochemical Society Transactions 28, 654-658.

Zastrow-Hayes GM, Lin H, Sigmund AL, Hoffman JL, Alarcon CM, Hayes KR, Richmond TA, Jeddeloh JA, May GD and Beatty MK, 2015. Southern-by-sequencing: A robust screening approach for molecular characterization of genetically modified crops. Plant Genome 8, 1-15.

Zhang D, Pirtle IL, Park SJ, Nampaisansuk M, Neogi P, Wanjie SW, Pirtle RM and Chapman KD, 2009. Identification and expression of a new delta-12 fatty acid desaturase (*FAD2-4*) gene in upland cotton and its functional expression in yeast and *Arabidopsis thaliana* plants. Plant Physiology and Biochemistry 47, 462-471.

Zhang J, Chiodini R, Badr A and Zhang G, 2011. The impact of next-generation sequencing on genomics. Journal of Genetics and Genomics 38, 95-109.

Zhang S-Y, Sun G-X, Yin X-X, Rensing C and Zhu Y-G, 2013. Biomethylation and volatilization of arsenic by the marine microalgae *Ostreococcus tauri*. Chemosphere 93, 47-53.

Zielinska DF, Gnad F, Wiśniewski JR and Mann M, 2010. Precision mapping of an *in vivo* N-glycoproteome reveals rigid topological and sequence constraints. Cell 141, 897-907.

Zilberman D, Cao X and Jacobsen SE, 2003. *ARGONAUTE4* control of locus-specific siRNA accumulation and DNA and histone methylation. Science 299, 716-719.